PROGRESS IN LOW TEMPERATURE PHYSICS

I

SERIES IN PHYSICS

General Editors:

J. DE BOER, H. BRINKMAN and H. B. G. CASIMIR

L. ROSENFELD, Nuclear Forces
E. A. GUGGENHEIM, Thermodynamics
J. BOUMAN (editor), Selected Topics in X-Ray Crystallography

L. ROSENFELD, Theory of Electrons
W. ELENBAAS, The High Pressure Mercury Vapour Discharge
S. R. DE GROOT, Thermodynamics of Irreversible Processes

J. G. WILSON (editor), Progress in Cosmic Ray Physics Volume I
J. G. WILSON (editor), Progress in Cosmic Ray Physics Volume II
C. J. GORTER (editor), Progress in Low Temperature Physics
KAI SIEGBAHN (editor), Beta- and Gamma-Ray Spectroscopy

BØRGE BAK Elementary Introduction to Molecular Spectra
E. A. GUGGENHEIM and J. E. PRUE, Physicochemical Calculations
J. M. BURGERS and H. C. VAN DE HULST (editors), Gas Dynamics of Cosmic Clouds; a Symposium

PREFACE

The classic chapters of classical physics: optics, electricity, magnetism, heat, mechanics, etc., are different from those into which modern physics is usually divided: spectroscopy, metals, semiconductors, gases, liquids, nuclei, elementary particles, etc. The theoretical aspects of physics are often divided into electro-magnetism, statistical mechanics, quantum mechanics, hydrodynamics, etc. Whichever of these divisions is considered, low temperature physics is concerned with paragraphs in several of the chapters and constitutes, so to speak, a transverse section.

In certain chapters low temperatures are only used as an auxilary research tool; for example, to obtain easily a high concentration of protons, deuterons or alpha-particles or to orientate atomic nuclei. In other chapters low temperatures are found to provoke anomalous behaviour of matter. Superconductivity and liquid helium II present the most striking examples of this. The possibility of varying the absolute temperature by one order of magnitude or more is a most valuable asset of the low temperature region. Certain fields of research, e.g., para- and antiferro-magnetism, heat conduction, specific heats, thus find themselves closely linked up with low temperature research.

Before 1940 low temperature physics was concentrated within a small number of institutes. These institutes are still active, but, in addition, many other laboratories, including most leading research institutes, have acquired a modest low temperature set-up. Consequently low temperature physics is spreading out vigourously and the number of its students is increasing rapidly. In spite of that, there is a strong interaction and cooperation among the low temperature physicists, which is stimulated by frequent international conferences held under the auspices of the International Institute of Refrigeration and the Commission on very low temperatures of the International Union of Pure and Applied Physics.

In the early period specialists from several countries used to enjoy hospitality in the few low temperature laboratories, which enabled them to extend their investigations to low temperatures. At present small low temperature groups often cooperate with other groups in the same institute. Now, as before, low temperature physics comprises a large variety of themes and its senior students are apt to be actively interested in a rather wide choice of subjects.

In the present book recent research and the present status of knowledge in several fields of low temperature physics are reviewed. The three main fields: magnetism, liquid helium and superconductivity receive ample attention, while a choice is made among the most promising of other subjects. Certain subjects, however, are only discussed briefly, while others are entirely missing. On some of these subjects, a very recent review has appeared, while in a few cases the most competent authority was unable to write a review paper at short notice. It is quite possible that in a second volume the neglected fields of low temperature research may be covered in due time.

C. J. GORTER

CONTENTS

CHAPTER I

THE TWO FLUID MODEL FOR SUPERCONDUCTORS AND HELIUM II

BY

C. J. GORTER

KAMERLINGH ONNES LABORATORIUM, LEIDEN

1. Introductory Remarks

Though the experimental and theoretical investigation of caloric, magnetic, electric and mechanical properties of matter at low temperatures has led to many interesting and important conclusions, it cannot be denied that the most exciting discoveries in this field have been that of superconductivity by Kamerlingh Onnes in 1911 [1] and that of liquid helium II by Keesom 16 years later [2]. The superconductors and helium II confront us with many complicated phenomena as well as with fundamentally unsolved problems. The two fluid model has allowed us to create some order among the phenomena while the unsolved problems may be considered to concern largely the interpretation of that model.

2. Some Properties of Superconductors

Superconductivity is the frictionless motion of electrons in certain metals. It was not until 1933 when it was recognized [3] that superconductors have a second fundamental property, namely that frictionless surface currents tend to screen off external magnetic fields in such an effective way that the magnetic induction vanishes in a massive fragment of superconductive metal.

In the simplest geometrical arrangement – a thick needle shaped sample in a longitudinal external magnetic field H – this second

fundamental property leads to a magnetic term $H^2V/8\pi$ in the free energy, where V is the volume of the sample. As soon as the sum of the free energy of the superconductor and this magnetic term becomes larger than the free energy of the normal phase at the same temperature, the latter will become thermodynamically stable and superconductivity is disturbed [4].

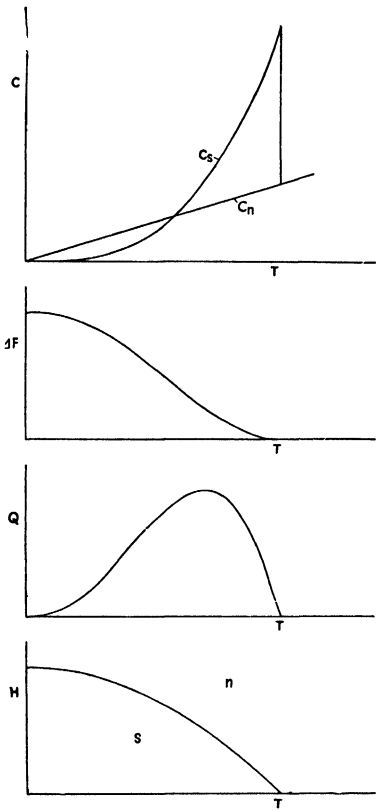

Fig. 1. Specific heats, difference in free energy, heat of transition and threshold curve

The electronic specific heat of a normal metal is given by

$$c_n = \gamma T, \tag{1}$$

where T denotes the temperature and γ a constant characteristic of the metal (cf. Ch. XI).

With a reasonable accuracy the specific heat of a superconductive metal – duly corrected for the lattice specific heat – is found to be given by

$$c_s \approx 3\gamma\, T^3/T_c^2. \tag{2}$$

This leads to the following approximate expression for the difference in free energy of the two phases [5]

$$\Delta F = F_n - F_s \approx \Delta U_o - \tfrac{1}{2}\gamma T^2 + \tfrac{1}{4}\gamma T^4/T_c^2, \tag{3}$$

where ΔU_o indicates the energy difference between the two phases at zero temperature. The condition $\Delta F = 0$ for the critical temperature T_c gives [6]

$$T_c \approx 2\left(\frac{\Delta U_o}{\gamma}\right)^{\frac{1}{2}}. \tag{4}$$

Now

$$\Delta F = H_{\text{thr}}^2 V/8\pi \tag{5}$$

gives a parabolic magnetic threshold curve (See Ch. VII)

$$H_{\text{thr}} \approx H_o \left(1 - \frac{\gamma T^2}{4\Delta U_o}\right) \tag{6}$$

with the threshold field at zero temperature

$$H_o = \left(\frac{8\pi \Delta U_o}{V}\right)^{\frac{1}{2}}$$

All superconductors obey with a reasonable accuracy the equations provided with the approximate sign. They thus obey a sort of law of corresponding states [7] and we may characterize every superconductor by one constant only. It is reasonable to choose ΔU_o, the energy difference between the normal and the superconductive phase at zero temperature, to be this constant. The critical temperature is then given by (4), where γ is a constant characteristic of the normal phase.

At T_c we have an extraordinarily well-defined transition of the second order in Ehrenfest's sense [8] and the remarkable property of such a transition is that not only the free energies, but also the energies and the entropies of the two phases are equal. In presence of an external magnetic field, however, we have a transition of the first order with a heat of transition

$$Q \approx 4\Delta U_o \frac{(H_o - H_{\text{thr}})}{H_o^2} \frac{H_{\text{thr}}}{} \tag{7}$$

Finally one may remark that the specific heats and the entropies concerned are of the order of γT_c, which amounts to only 10^{-3} R per gram atom.

Among the other properties of superconductors we might mention that the thermoelectric effects are zero and that the heat conduction (in pure metals) is smaller than in the normal phase, though at T_c there is no jump (See Ch. X).

3. Some Properties of Liquid Helium II

Liquid helium has a jump in the specific heat [9] at its so-called λ-temperature T_λ. This change is of the order of R and thus much higher than that in superconductors. Its magnitude is also less well-defined and a distinct tail extends above the λ-temperature.

The almost frictionless motion of the liquid below the λ-temperature – the so-called helium II – immediately suggests an analogy with

the motion of electrons in a superconductor. There is no apparent analogy to the action of an external magnetic field on a superconductor, so the complications connected with different shapes are lacking while alloying is only possible with the isotope ^{3}He (See Ch. VI).

But in other respects helium II exhibits more varied and curious properties than superconductors do. When almost frictionless motion occurs through a narrow slit, heat is produced in the vessel left by the liquid while an equal amount of cold is developed in the vessel into which the liquid flows [10]. This is the mechano-caloric effect and the heat or cold per unit mass of liquid passing is called the heat of transport Q^*. If we introduce a temperature gradient along the slit a very high heat flow is found. At the same time a flow of matter takes place towards the high temperature side, which may lead to a helium fountain of considerable height [11]. This fountain height or rather the pressure gradient which is able to counterbalance the flow of matter does not depend on the dimensions of a very narrow slit.

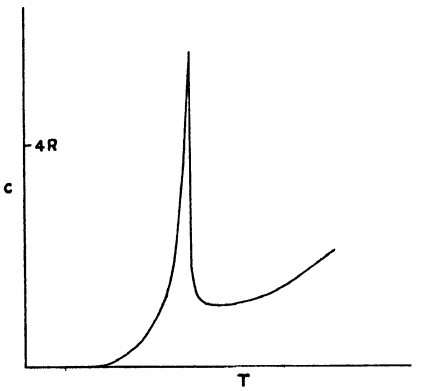

Fig. 2. Specific heat of liquid helium

With the aid of irreversible thermodynamics [12] De Groot has proved [13] that

$$\operatorname{grad} p = \frac{\varrho Q^*}{T} \operatorname{grad} T, \tag{8}$$

where ϱ is the density, as long as the transports of matter and heat are linear in the gradients of temperature and pressure.

The most remarkable property of liquid helium II is, however, its capability to propagate heat waves and heat pulses with only a slight attenuation [14]. This so-called "second sound" is generated by an alternating or pulsed supply of heat. The velocity of propagation may be measured with great accuracy and is found to be between 18½ and 20½ meters per second between 1.0°K and 1.9°K while the velocity of normal sound is more than ten times higher.

4. Behaviour near Zero Temperature

Near zero temperature superconductors and liquid helium have passed into an extraordinary state of matter which is characterized by the possibility of frictionless motion of electrons and helium atoms respectively. It is remarkable that the entropy of this state vanishes with a high power of T. The energies associated with this decrease of entropy are many times larger in helium than in superconductors. When the frictionless motion is set up the energy increases, the entropy remaining zero. The non-reversible transition to zero motion is extremely slow. Frictional processes due to scattering of electrons by impurities and friction between the helium and the walls have ceased to occur. Apparently we are not concerned with individual motion of electrons or helium atoms, but with moving systems composed of many individuals [15]. No convincing explanation has been offered on the nature of these systems and the conditions under which they may occur.

5. The Services Rendered by the Two Fluid Model

The so-called two fluid model is useful in the description of the phenomena occurring between the absolute zero and the transition temperatures T_c and T_λ. In this model an internal parameter is introduced which may vary between 0 and 1 only. In one of the two current versions [16] this parameter is called x and it is supposed to be zero at zero temperature and one at the transition temperature. In the other version [17] the parameter $\omega = 1 - x$ varies from one to zero in the same interval. The existence is assumed of two interpenetrating fluids, each possessing its own velocity field and its own enertia. There is no or at most very little exchange of momentum between the fluids. One of the fluids, the superfluid, bears the frictionless motion; its last trace disappears at the transition temperature when $\omega = 1 - x = 0$. The other fluid, the normal fluid, behaves more or less as a normal electron gas or a normal liquid: it is scattered by irregularities and heat waves or it has a normal viscosity and adheres to a wall. It rapidly disappears with decreasing temperature when $x = 1 - \omega \to 0$. The relative amounts of the fluids, whatever this may mean, are taken to be $\omega = 1 - x$ and $x = 1 - \omega$.

Without any further definition of quantitative elaboration this two fluid model can offer a simple description of many of the exceptional properties of superconductors and helium II [18].

In the frictionless motion of helium through a narrow slit it is clearly the superfluid which moves. In the vessel left by the superfluid its relative concentration $1 - x$ decreases while it increases in the vessel on the other side of the slit. Keeping the relative concentration constant requires a supply of heat and cold respectively (mechano-caloric effect).

Introduction of a temperature gradient introduces a gradient of the internal parameter x which leads to an internal force, sometimes

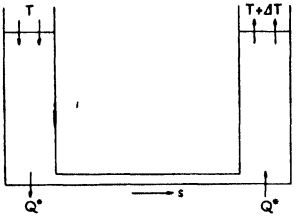

Fig. 3. Mechano-caloric effect

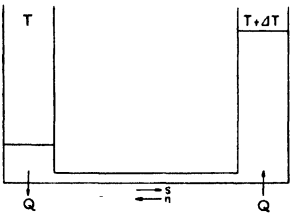

Fig. 4. Fountain effect

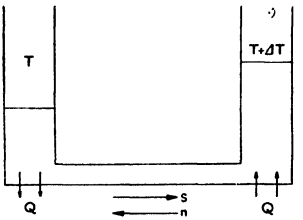

Fig. 5. Heat conduction by convection of the two fluids

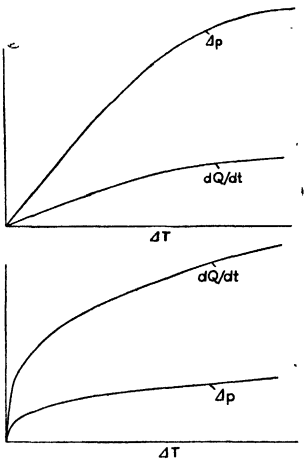

Fig. 6. Heat flow dQ/dt and fountain pressure in a narrow slit (above) and a wide slit (below)

called the diffusion force, driving the normal fluid towards the low temperature side and the superfluid to the high temperature side. The resulting convection of the fluids accounts for the heat conduction. In narrow slits the motion of the normal fluid is impeded by its adherence to the wall and its viscosity. The fountain effect then clearly demonstrates the diffussion force acting on the superfluid.

It is found that in relatively wide channels and high temperature gradients the heat flow as well as the fountain pressure increase con-

siderably slower than if they were proportional to the temperature gradient. Under high temperature gradients the heat flow and the fountain effect [19] are approximately proportional to $(\text{grad } T)^{1/3}$, while the transition from this cube root dependence to the linear dependence at very small temperature gradients is exactly similar for the two effects. (Allen and Reekie's [20] rule). This behaviour may be accounted for by assuming a mutual friction between the two fluids which is approximately proportional to the cube of the relative velocity of the two fluids [21]. The existence of such a mutual friction is corroborated by the occurrence of a pressure gradient proportional to the cube of the superfluid velocity through a slit of a few microns width.

The very simple equations of motion for the superfluid and the normal fluid:

$$-(1-x)\ \text{grad}\ P + x(1-x)\,S^*\varrho\ \text{grad}\ T - Ax(1-x)\varrho^2|v_s - v_n|^2 (\boldsymbol{v}_s - \boldsymbol{v}_n) = \varrho(1-x)d\boldsymbol{v}_s/dt \tag{9}$$

$$-x\ \text{grad}\ P - x(1-x)S^*\varrho\ \text{grad}\ T + Ax(1-x)\varrho^2|v_s - v_n|^2 (\boldsymbol{v}_s - \boldsymbol{v}_n) + \eta_n(\Delta\boldsymbol{v}_n + (1/3)\ \text{grad div}\ \boldsymbol{v}_n) = \varrho x d\boldsymbol{v}_n/dt \tag{10}$$

have often been used in the discussion of the behaviour of helium II. In these equations $\boldsymbol{v}_s$ and $\boldsymbol{v}_n$ are the velocities of superfluid and normal fluid, P is the pressure, while S^* varies only slowly as a function of temperature. It has the dimensions of entropy per unit mass and characterizes the diffusion force (cf. §§ 6 and 7). The domain of the usefulness of (9) and (10) is limited. They account satisfactorily for the the transport phenomena in slits and capillaries of widths from 5 microns upwards, at not too low velocities. There are even indications that at very low velocities, particularly in very narrow slits, no mutual friction would occur below a critical velocity [22]. Experiments with slits of the order of 1 micron suggest also a considerable decrease in the normal viscosity η_n, while on the other hand investigations with oscillating discs and rotating cylinders (See Ch. IV) reveal the existence of more forces [23] than are present in (9) and (10). We should like to point out that as a consequence of (9) the superfluid velocity $\boldsymbol{v}_s$ should in general have a curl, while usually the possibility of turbulance is not considered. The condition — perhaps not implausible on theoretical grounds [24] (See Ch. II) – that $\boldsymbol{v}_s$ should be rotation-free cannot very easily be introduced in an equation of the type (9). The most remarkable success of the two fluid model was the prediction [25] of

second sound which is interpreted as a wave in the internal parameter x, the normal and the superfluid oscillating in respect to each other, while the total density ϱ remains constant. From (9) and (10) we get for the velocity of propagation v_{II}, if we suppose that no periodic transition from superfluid to normal fluid and vice versa occurs,

$$v_{II}^2 = \frac{x(1-x)\,S^*}{dx/dT}, \tag{11}$$

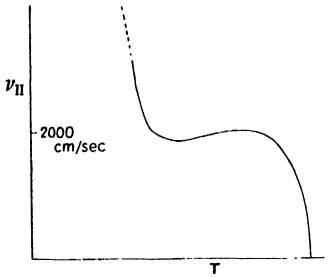

Fig. 7. Velocity of second sound v_{II} as a function of T.

while the supposition that at any moment the value of x is adjusted to the momentary value of T gives

$$v_{II}^2 = \frac{x\,(1-x)\,S^{*2}T}{c}, \tag{12}$$

where c is the specific heat per unit mass.

At low velocities the normal fluid only exchanges momentum with the walls. This gives the possibility of eliminating friction by choosing a wide channel and to observe in this way second sound and the high heat conduction. On the other hand the normal fluid may be immobilized by choosing a very narrow channel and thus the fountain effect and the mechano-caloric effect may be observed.

In the case of superconductors we do not have the possibility to vary the friction just mentioned, since the normal electrons do not exchange momentum so much with the walls as with irregularities and the heat waves of the crystalline lattice. This leads to a volume friction which would damp down second sound within a fraction of a wavelength and would also impede an energy flow by convection [26] of the fluids. Also several other effects similar to the exceptional phenomena in helium must be so small in superconductors that they are very difficult to observe. Thus the two fluid model renders less brilliant services for superconductivity than for liquid helium II.

However, the losses occurring in the surface screening layer under the influence of high frequency fields confirm the presence of normal electrons in the superconductive phase particularly at temperatures not too much below T_c. According to London's formulae [27] the thickness of the layer must be inversely proportional to the square root of the density of the superconductive electrons. It is in agreement

with the expectations from the two fluid model that this thickness is found to increase rapidly when T_c is approached [28].

6. The Free Energy as a Function of the Internal Parameter

The thermodynamician is inclined to consider the free energy as a function of the internal parameter x and to state that the value found for this parameter at each temperature must be determined by the minimum of the free energy as a function of the parameter at that temperature. The prototype of such a consideration is the case of a one component – two phase system at constant volume, e.g. of vapour and liquid enclosed in a box. The free energy of this system is the sum of the free energies of the two phases. That of the liquid (supposed to be incompressible) is proportional to its mass $1 - x$, that of the vapour contains a term proportional to $x \ln x$. At any temperature x will adjust itself according to the minimum of the non linear total free energy and consequently x will, with rising temperature, gradually increase from zero to one, which value is reached where $(\partial F/\partial x)_{x=1} = 0$. At that temperature the system as a whole exhibits a second order transition.

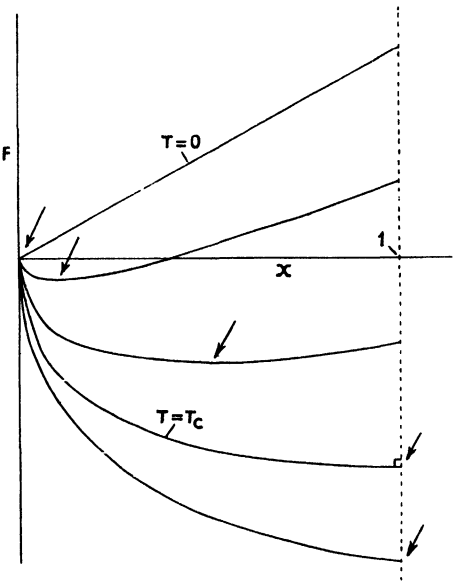

Fig. 8. Free energy of a superconductor as a function of x according to (13) for different values of T.

In 1934 the following expression was proposed [29] for the electronic free energy of a superconductor:

$$F = x\Delta U_o - \tfrac{1}{2}x^{\alpha}\gamma T^2, \qquad (13)$$

which gives the electronic free energy for the normal metal if $x=1$, and where the factor the x^{α} provides for the required non-linearity in x. If $\alpha = \frac{1}{2}$ the minimum of this free energy leads to the equations (3), (4) and (6), which approximately describe the experimental data. We also find

$$x = (T/T_c)^4, \qquad (14)$$

an expression which later was found to be in good agreement [30] with the dependence of the thickness of the surface screening layer which presumably should be proportional to $(1 - x)^{-\frac{1}{2}}$. Encouraged by this success a somewhat similar proposal [31] was made for the approximate Gibbs free energy G of liquid helium

$$G = x^{7/6} \Delta U_o - x S_\lambda T, \qquad (15)$$

which leads to

$$x = S/S_\lambda = (T/T_\lambda)^6 \qquad (16)$$

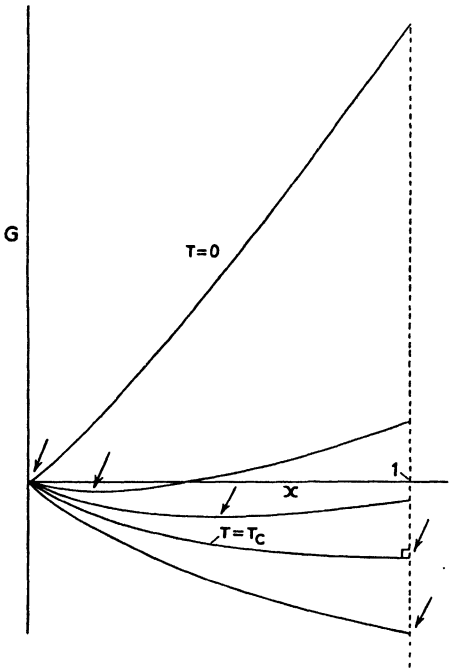

Fig. 9. Gibbs free energy of helium II as a function of x according to (15) for different temperatures

Though this expression excels because of its simplicity and has been used for several calculations aimed at obtaining a rough interpretation of data, it is unsatisfactory in that the specific heat of the normal state ($x = 1$), which is quite important above T_λ, has been suppressed. Therefore the somewhat more complicated expression

$$G = x^{7/6} \Delta U_o - \tfrac{1}{2} \frac{x^{5/6} S_\lambda T^2}{T_\lambda} \qquad (17)$$

has sometimes been used [32] and also leads to (16). The quantitative differences in the conclusions derived from (15) and (17) are remarkably small.

Following this thermodynamic line of thought the following expression has been proposed [33] for the heat of transport:

$$Q^* = Tx \left(\frac{\partial S}{\partial x}\right)_T = - Tx \left(\frac{\partial^2 G}{\partial x \partial T}\right), \qquad (18)$$

which by (8) determines the fountain effect. The corresponding expression for the diffusion force has $(\partial S/\partial x)_T$ for S^* in (9) and (10). However, the two fluid model is apparently not sufficiently sharply defined, so the validity of (18) is still a controversial matter [34].

7. The Formule of H. London and Tisza for Helium II

Quite another line of thought is followed by others, who advocate that one should derive the value of x and the magnitude of the heat of transport etc. directly from a statistical or quantum mechanical model or theory without having recourse to non equilibrium values of x and the process of minimizing the free energy.

As long as a satisfactory theory is lacking one might then not only ascribe separate velocity fields and inertia to the two fluids, but also separate thermodynamical quantities and in particular give the superfluid the entropy zero. The superfluid entering a vessel with zero entropy needs to be lifted to the entropy S appropriate to the temperature of the vessel. If this happens reversibly, we obtain (as does H. London [35])

$$Q^* = TS \tag{19}$$

which by (8) determines the fountain effect while the corresponding expression for the diffusion force has S/x for S^* in (9) and (10).

A somewhat more specialized description has been proposed by Tisza [36] who supposes that neither the normal nor the superfluid has a specific heat, so that the entropy below T_λ is entirely due to the temperature independent specific entropy of the normal fluid. Thus

$$S = xS_\lambda. \tag{20}$$

Between 1.1°K and T_λ both assumptions are, with a reasonable degree of accuracy, verified by experiments on the fountain effect, the mechano-caloric effect, the velocity of second sound [37] and experiments with stacks of oscillating discs [38] (See Ch. IV).

The expression (15) has the advantage that in connection with (18) it leads to equations (19) and (20) which have in general been confirmed by experimental results.

8. Theoretical Background in the Case of Helium II

The theoretical background of the two fluid model is still obscure. For the case of helium there are two very different proposals advanced by F. London and Tisza [39], and by Landau [40], respectively.

London and Tisza describe the separation into two fluids as a Bose-Einstein condensation while Landau considers the normal fluid to consist of excitations, of which he distinguishes two kinds: quantized

compressional waves (phonons), and excitations with a minimum energy, called rotons (See Ch. II).

In the neighbourhood of the λ-temperature both views lead to difficulties. For an ideal gas the Bose-Einstein picture predicts a jump here in the derivative of the specific heat rather than in the specific heat itself and more or less artificial additional assumptions [41] are required to adjust this discrepancy. On the other hand it is difficult to see how, in the phonon-roton picture, an assembly of those excitations can gradually approach the whole normal liquid at the λ-temperature.

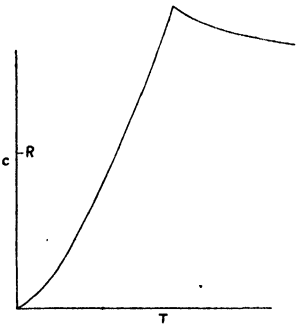

Fig. 10. Specific heat of ideal Bose-Einstein gas

Landau predicted a pronounced change in the properties of the liquid at about 1°K, below which the rotons would rapidly vanish. The confirmation of this change by the steep increase of the velocity of propagation of heat pulses in helium II was a triumph for his interpretation [42]. The formulation of his views, however, was rather vague in so far as the phonons and rotons are concerned. Kramers' and Kronig's analysis [43] would give a sound basis of the two fluid model also confirming H. London's formula (19), but unfortunately it is not sure whether their treatment is applicable at the higher temperatures too. At the lower temperatures, where the phonons apparently are dominant, there is little use for the two fluid model since direct description by means of phonons of long mean free paths seems more appropriate [44]. If one could experiment with cubic kilometers of helium instead of with cubic centimeters, this might be different. Feynman's recent analysis [45] of the rotons, however, gives hope that the Landau treatment may be worked out and confirmed for the temperatures above 1°K too (See Ch. II).

9. Theoretical Background in the Case of Superconductivity

Heisenberg and Koppe [46] have proposed a statistical background for the two fluid model for superconductors. They assume that the free electron levels just above the Fermi limit may combine into a condensed state which has the properties of the superfluid. Condensation into this state is accompanied by a decrease of energy. Supposing

that electrons may occupy free electron levels as well as enter the condensed state and that the electrons in this latter state contribute zero to the entropy, the total free energy may be obtained as a function of T and of the number of condensed electrons $\omega = 1 - x$. Not too far below T_c there is little difference with (13), but at low temperatures there are deviations which lead to lower x – values than given by (16). This latter behaviour seems to be confirmed by data on Sn, Nb and a few other superconductors [47]. Heisenberg and Koppe originally suggested that electrostatic interaction could account for the condensation phenomenon, but the isotope effect (cf. Ch. VII) made it plausible that, in agreement with views expressed by Fröhlich and Bardeen, the condensation is due to interaction through the intermediary of lattice waves.

Marcus and Maxwell [48] have recently analyzed the criteria which the statistical background must fulfill in order to lead to the two fluid model, but they were not able to establish a satisfactory connection with the theoretical treatment of Fröhlich and Bardeen.

10. Final Remarks

Several years ago Daunt, Mendelssohn and F. London [49] discussed the analogies between superconductors and liquid helium. Aside from making many remarks repeated in the present article, they stressed the analogy between the maximum transport rate occurring when a helium II film creeps on the surface of a solid and the maximum transport rate of the surface screening currents on a superconductor.

In the first case this transport is found to be of the order of 10^{-5} gr/cm sec while in the second one it amounts to $mcH_{\text{thr}}/4\pi e$. In both cases it decreases linearly to zero when the temperature approaches the transition temperature. A connection of these quantities with quantum theory was suggested by observing that the transport rates are of the order of magnitude of Planck's constant h divided by the volume per helium atom or per superconductive electron respectively.

As attractive as this suggestion was at first sight, it must be stated that no recent advance has been made in its elaboration. On the contrary, it is not easy to see why the energy difference ΔU_o, on which H_o and the transport rate of superconductors depend (cf. (5)), could be connected with h in a rather complicated way. Moreover, experimentally the values of H_o seem not to be simply connected with the number of superconductive electrons.

The connection often sought between the superfluid properties in helium II and the Bose-Einstein condensation has incidentally led to the suspicion that in superconductors one might also be concerned with even units viz. with electron pairs. This suggestion has likewise had little success so far.

In the present contribution it has been stressed that many apparently conflicting and incoherent data find an easy interpretation or at least a descritpion with the help of the two fluid model. This model has moreover rendered remarkable results in the prediction of the mechano-caloric effect and of second sound. On the other hand it must be admitted that it suffers from vagueness and ambiguity which is, for instance, reflected in the uncertainty about the equations of motion of the fluids in helium II. This vagueness will possibly remain until the theoretical foundation of the two fluid model has acquired solidity.

REFERENCES

[1] H. Kamerlingh Onnes, Versl. Kon. Ak. van Wet. Amsterdam, **20**, 81, (1911), Leiden Comm. 122*b*.

[2] W. H. Keesom and M. Wolfke, Versl. Kon. Akad. van Wet. Amsterdam, **36**, 1204, (1927), Leiden Comm. 190*b*.

[3] W. H. Meissner and R. Ochsenfeld, Naturwissenschaften, **21**, 787, (1933). C. J. Gorter, Nature, **132**, 931, (1933).

[4] C. J. Gorter, Arch. Mus. Teyler, Haarlem, **7**, 378, (1933). C. J. Gorter and H. B. G. Casimir, Physica, **1**, 306, (1933).

[5] J. A. Kok, Physica, **1**, 1103, (1933), Leiden Comm. Suppl. 77*a*.

[6] C. J. Gorter, Physica, **19**, 745, (1953), Leiden Comm. Suppl. 105*e*.

[7] E. Maxwell, Phys. Rev., **87**, 1126, (1952).

[8] P. F. Ehrenfest, Proc. Acad., Amsterdam, **36**, 153, (1933), Leiden Comm. Suppl. 75*b*.

[9] W. H. Keesom and K. Clusius, Proc. Acad., Amsterdam, **35**, 307, (1932). Leiden Comm. 219*e*.

[10] J. G. Daunt and K. Mendelssohn, Nature, **143**, 719, (1939).

[11] J. F. Allen and H. Jones, Nature, **141**, 243, (1938).

[12] H. London, Proc. Roy. Soc. A, **171**, 484, (1939) had derived this equation earlier making use of a cyclic process in which all irreversible phenomena were supposed to be negligible.

[13] S. R. de Groot, Physica, **13**, 555, (1947).

[14] V. P. Peshkov, Journ. Phys. Moscow, **18**, 389, (1946).

[15] A. B. Pippard, Physica, **19**, 765, (1953). N. Bohr, Physica, **19**, 761, (1953).

[16] C. J. Gorter and H. B. G. Casimir, Phys. Z., **35**, 963, (1934). P. L. Bender and C. J. Gorter, Physica, **18**, 597, (1951), Leiden Comm. Suppl. 104*d*.

[17] W. Heisenberg, Z. f. Naturforschung, **2a**, 185, (1947). H. Koppe, Ann. Physik (6) **1**, 405, (1947) Erg. ex. Naturwissenschaften, **23**, 283, (1950).

[18] F. London, Phys. Rev., **54**, 947, (1938); Journ. chem. Phys., **43**, 49, (1939).
L. Tisza, Journ. Phys. et Radium, **1**, 164, and 350, (1940), Phys. Rev., **72**, 838, (1947).
L. D. Landau, Journ. Phys. Moscow, **5**, 71, (1941).
[19] W. H. Keesom, B. F. Saris and L. Meyer, Physica, **7**, 817, (1940), Comm. Leiden 260*a*.
[20] J. F. Allen and J. Reekie, Proc. Cambridge Phil. Soc., **35**, 114, (1939).
[21] C. J. Gorter and J. H. Mellink, Physica, **15**, 285, (1949), Leiden Comm. Suppl. 98*a*.
[22] R. Bowers, B. S. Chandrasekar and K. Mendelssohn, Phys. Rev., **80**, 856, (1950).
C. S. Hung, B. Hunt and P. Winkel, Physica, **18**, 629, (1952); Leiden Comm. No. 289*c*.
[23] K. R. Atkins, Phil. Mag. Suppl., **1**, 169, (1952).
[24] F. London, Phys. Soc. Cambridge Conf. Rep., **1**, (1947).
[25] L. Tisza, Journ. de Phys., **1**, 350, (1940), 350.
L. D. Landau, Journ. Phys. Moscow, **5**, 71, (1941).
[26] K. Mendelssohn and J. L. Olsen, Proc. Phys. Soc. London, **A, 63**, 2, (1950).
[27] F. London, Une conception nouvelle de la supraconductibilité, Paris (1937); Superfluids, New York (1950).
M. von Laue, Supraleitung, Berlin (1949).
[28] J. G. Daunt, A. R. Miller, A. B. Pippard and D. Shoenberg, Phys. Rev., (2), **74**, 842, (1948).
[29] C. J. Gorter and H. B. G. Casimir, Phys. Z., **35**, 963, (1934).
P. L. Bender and C. J. Gorter, Physica, **18**, 597, (1951), Leiden Comm. Suppl. 104*d*.
[30] J. G. Daunt, A. R. Miller, A. B. Pippard and D. Shoenberg, Phys. Rev., (2), **74**, 842, (1948).
[31] C. J. Gorter, Physica, **15**, 523, (1949); Leiden, Comm. Suppl. 99*a*.
J. de Boer and C. J. Gorter, Physica, **18**, 565, (1952); Leiden Comm. Suppl. 104*e*.
[32] J. de Boer, Phys. Rev., **76**, 852, (1949).
J. G. Daunt, Phil. Mag. Suppl., **1**, 209, (1952).
[33] C. J. Gorter, Physica, **15**, 523, (1949); Leiden Comm. Suppl. 99*a*.
T. Usui, Physica, **17**, 694, (1951).
[34] O. K. Rice, Phys. Rev., **76**, 1701, (1949).
S. R. de Groot, L. Jansen and P. Mazur, Physica, **16**, 691, (1951).
I. Prigogine and P. Mazur, Physica, **17**, 661, (1951).
R. B. Dingle, Phil. Mag., **42**, 1080, (1951); Phil. Mag. Supplement, **1**, 111, (1952).
[35] H. London, Proc. Roy. Soc. London A, **176**, 522, (1940).
[36] L. Tisza, Phys. Rev., **72**, 838, (1947).
[37] C. J. Gorter, P. W. Kasteleyn and J. H. Mellink, Physica, **16**, 113, (1950); Leiden. Comm. Suppl. 100*b*.
[38] E. Andronikashvilli, Journ. Phys. Moscow, **10**, 201, (1946).
A. C. Hollis Hallett, Proc. Roy. Soc. A, **210**, 404, (1952).
[39] F. London, Phys. Rev., **54**, 947, (1938); Journ. chem. Phys., **43**, 49, (1939).
L. Tisza, Journ. Phys. et Radium **1**, 164 and 359, (1940); Phys. Rev., **72**, 838, (1947).
[40] L. D. Landau, Journ. Phys. Moscow, **5**, 71, (1941).
[41] A. Bijl, J. de Boer and A. Michels, Physica, **8**, 655, (1941).
F. London, Phys. Soc. Cambridge Conf. Rep., **1**, (1947).

[42] K. R. Atkins and D. V. Osborne, Phil. Mag., **41**, 1078, (1950).
[43] H. A. Kramers, Physica, **18**, 653, (1952).
R. Kronig, Physica, **19**, 535, (1953).
[44] H. C. Kramers, F. A. W. van Burg and C. J. Gorter, Phys. Rev., **90**, 1117, (1953).
[45] R. P. Feynman, Phys. Rev., **91**, 1301, (1953); **94**, 262, (1954).
[46] W. Heisenberg, Z. f. Naturforschung, **2a**, 185, (1947).
H. Koppe, Ann. Physik, (6), **1**, 405, (1947); Erg. der ex. Naturw., **23**, 283, (1950).
[47] P. L. Bender and C. J. Gorter, Physica, **18**, 597, (1951); Leiden Comm. Suppl. 104*d*.
R. D. Worley, M. W. Zemansky and H. A. Boorse, Phys. Rev., **87**, 1142, (1952).
[48] P. M. Marcus and E. Maxwell, Phys. Rev., **91**, 1035, (1953).
P. M. Marcus, Summaries 3rd Int. Conf. Low Temp. Physics, Houston, **19**, (1953).
[49] J. G. Daunt and K. Mendelssohn, Nature, **150**, 604, (1942).
K. Mendelssohn, Proc. phys. Soc., **57**, 310, (1945); F. London, Rev. mod. Physics **17**, 310 (1945); Phys. Soc. Combridge Conf. Rep., **1**, (1947).

CHAPTER II

APPLICATION OF QUANTUM MECHANICS TO LIQUID HELIUM

BY

R. P. FEYNMAN

CALIFORNIA INSTITUTE OF TECHNOLOGY, PASADENA, CALIFORNIA

1. Introduction

Liquid helium exhibits quantum mechanical properties on a large scale in a manner somewhat differently than do other substances. No other substance remains liquid to a temperature low enough to exhibit the effects. These effects have long been a puzzle. It is supposed that they can all be ultimately understood in terms of the properties of Schrödinger's equation. We cannot expect a rigorous exposition of how these properties arise. That could only come from complete solutions of the Schrödinger equation for the 10^{23} atoms in a sample of liquid. For helium, as for any other substance today we must be satisfied with some approximate understanding of how, in principle, that equation could lead to solutions which indicate behavior similar to that observed.

Since the discovery of liquid helium considerable progress has been made in understanding its behavior from first principles. Some of the properties are more easily understood than others. The most difficult of these concern the resistance to flow above critical velocity. If we permit some conjectures of Onsager [1], however, perhaps a start has been made in understanding even these. The aim of this article is to describe those physical ideas which have been suggested to explain the behavior of helium which can most easily be related to properties of the Schrödinger equation.

We shall omit references to the phenomena involved in the Rollin

film. It appears that the film can be understood as being maintained by van der Waals attraction to the wall. The flow properties of the film are interpreted as a special case of flow properties of helium in leaks in general.

The article falls naturally into two main sections. First, there are phenomena in which the superfluid velocity is irrotational. Here we can give a fairly complete picture. The second part concerns the case in which vorticity of the superfluid exists. Our position here is less satisfactory and more uncertain. It is described here in considerable detail because of the interesting problems it presents.

2. Summary of the Theoretical Viewpoint

The first striking way that helium differs from other substances is that it is liquid even down to absolute zero. Classically at absolute zero all motion stops, but quantum mechanically this is not so. In fact the most mobile substance known is one at absolute zero, where on the older concepts we should expect hard crystals. Helium stays liquid, as London [2] has shown, because the inter-atomic forces are very weak and the quantum zero point motion is large enough, since the atomic mass is small, to keep it fluid even at absolute zero. In the other inert gases the mass is so much higher that the zero-point motion is insufficient to oppose the crystalizing effect of the attractive forces. In hydrogen the intermolecular forces are very much stronger, so it, too, is solid. In liquid ^{4}He there is a further transition at 2.2°K, the λ-transition, between two liquid states of different properties. A transition is expected (at 3.2°K) for such atoms if the interatomic forces are neglected, as Einstein [3] noticed. London [4] has argued that the λ-transition corresponds to the transition which occurs even in the ideal Einstein-Bose gas. The inter-atomic forces alter the temperature and, in a way as yet only imperfectly understood [5,6] the order of the transition, but qualitatively the reason for the transition is understood. We will concern ourselves here, only with the liquid He II, below the λ-point, and shall try to elucidate the qualitative reasons for some of its strange behavior. Also we explicitly limit our considerations to a liquid made purely of ^{4}He atoms so that the wave function must be symmetric for interchange of the atoms. We do not mean to imply anything about liquid helium ^{3}He, nor about superconductors, either by analogy nor by contrast. That is, we shall use the fact that the wave function is symmetric in many arguments without

stopping to inquire whether the symmetry is necessary part of the argument.

The central feature which dominates the properties of helium II is the scarcity of available low energy excited states in the Bose liquid [7, 8]. There do exist excited states of compression (i.e.: phonons) but states involving stirring or other internal motions which do not change the density cannot be excited without expenditure of an appreciable excitation energy. This is because, for quantum energies to be low, long wave lengths or long distances are necessary. But the wave function cannot depend on large scale modifications of the liquid's configuration. For a large scale motion, or stirring, which does not alter the density, only moves some atoms away to replace them by others *. It is essentially equivalent to a permutation of one atom for another ,and the wave function must remain unchanged by a permutation of atoms, because ^{4}He obeys the symmetrical statistics. The only wave functions available are those which change when atoms move in a way which is not reproducible by permutation, and therefore either, (1) movements accompanied by change in density (phonons), (2) movements over distances less than an atomic spacing, therefore of short wave length and high energy (rotons and more complex states), or (3) movements resulting in a change in the position of the containing walls (flow). We shall discuss these states in detail presently.

The scarcity of low energy excited states is the seat of many of the phenomena in the liquid. This has been known since the work of Landau who developed a theory of the liquid on the assumption of such scarcity. The specific heat is very low at low temperature and only rises rapidly above about 1°K when enough thermal energy is available to excite an appreciable number of the higher energy states (rotons). There are so few states excited that the excitations may be localized in the fluid like wave packets. These move about, collide with each other and the walls, and imitate the appearance that in the perfect background fluid there is another fluid or gas. This "gas" of excitations carries all the entropy of the liquid, may carry waves of number den-

* In the ideal gas the low excitations are those in which one or two atoms are excited to low states. These involve density changes and are more analagous to phonon states (but are even lower in energy than in the liquid because the ideal gas has infinite compressiblity, and therefore vanishing sound velocity). The interatomic forces in the liquid make it more imperative that if atoms are moved away from one point others move in to take their place, if high repulsive energies between nearby atoms are to be avoided.

sity (second sound, analagous to sound in an ordinary gas), finds it difficult to diffuse through long thin channels, tries to even up uneven velocity distributions among its roton "molecules" (viscosity), and acts in many ways as a normal fluid. Meanwhile the background in which the rotons travel, that is, the total body of fluid itself, can flow. It flows, at low velocity, without resistance through small cracks. The reason is that to have resistance, flow energy and momentum must go into heat, that is internal excitations (eg. rotons). The energy required to form a roton is not available (at the necessary momentum change) unless the fluid velocity is very high.

Actually it appears likely that helium in flow doesn't form rotons directly at all. Resistance sets in at a relatively low velocity (critical velocity) because apparently a kind of turbulence begins in the perfect fluid *. This cannot occur at lower velocities because energy is needed to create vorticity. And, if we accept Onsager's suggestion, the vorticity is quantized, the line integral of the momentum per atom (mass of atom times fluid velocity) around a closed circuit must be a multiple of h. Below the critical velocity not enough kinetic energy is available in the fluid to produce the minimum vortex lines.

We shall discuss first the way that the scarcity of states accounts for many of the properties of the liquid. Here we are summarizing work of many others, particularly Landau. It is thought best to reemphasize this viewpoint, since it is the one which is directly supported by quantum mechanics. Furthermore, in this way we are starting over the more familiar ground. Next we discuss the quantum mechanical view of the reason for the scarcity of states. Finally in the second part of the paper we discuss the quantized vortex lines proposed by Onsager.

3. Landau's Interpretation of the Two Fluid Model

One of the most fruitful ideas in interpreting the behavior of the liquid is the two fluid model. It was developed by Tisza [9] from analogy to the structure of an ideal Bose gas. It is often spoken of as a vague association of two penetrating fluids. Landau [10] has interpreted it in a definite manner. We review his interpretation here, although an excellent review by Dingle [11] already exists. He has strongly emphasized the fact that one might picture the helium as a background fluid in which excitations move. At absolute zero one has a perfect

* The author now considers his statement (reference 7) that the reason for flow resistance "cannot very well be a kind of turbulence", to be in error.

ideal fluid which may flow frictionlessly with potential flow. If heated, the heat energy excites the liquid. This it does by creating here and there within it excitations of some sort. These excitations can make their way from one place to another, collide with the walls and with each other, and give to helium some properties associated with the so-called normal fluid component, such as viscosity. Landau as a result of his study of quantum hydrodynamicas was lead to suppose the excitations to be of two kinds. Of lowest energy are the phonons, or quantized sound waves, whose energy E equals pc where p is the momentum and c the speed of sound. Above these separated by an energy gap Δ are those of another kind, called rotons. At first he supposed the energy of these to be given by $\Delta + p^2/2\mu$ if they have momentum p, where μ is an effective mass. Later he found that this did not agree with the experiments of Peskhov on second sound, and he proposed instead the formula

$$E_{\text{rot}} = \Delta + (p - p_0)^2/2\mu \tag{1}$$

where p_0 is some constant. He went further and suggested that all these excitations really are of the same class and differ only in momen-

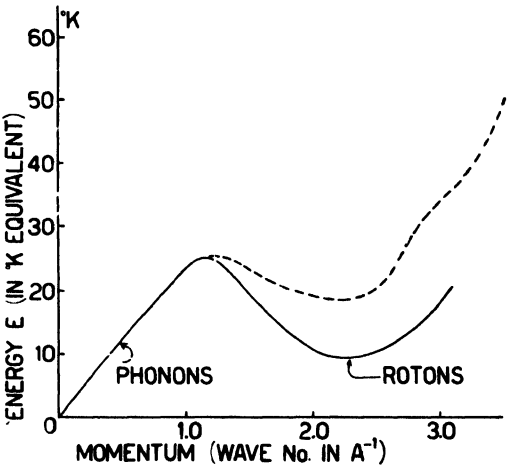

Fig. 1. The energy of excitations as a function of their momentum. Solid line as envisaged by Landau with parameters set to fit specific heat data; dotted line, an approximate curve derived from quantum mechanics.
Excitations in linear section for low momentum correspond to phonons. Those near the minimum of the curve are called rotons.

tum. The energy $E(p)$ of those of momentum p, depends only on the magnitude of p, rising at first linearly as pc, but later falling to a minimum at p_0 and rising again, as in Fig. 1, solid curve. The curve in the vicinity of the minimum is given by (1). At the low temperatures encountered in He II only the states near $p = 0$, and those close to the minimum are excited. Therefore we do not have to know the rest of the curve accurately. Furthermore, the only important excitations are one of the two classes, phonons and rotons.

Supposing the excitations to obey Bose statistics the number, at temperature T, of momentum in the range $d^3\boldsymbol{p}$ is, according to statistical mechanics,

$$n_{\boldsymbol{p}} = (\exp \beta E - 1)^{-1} d^3\boldsymbol{p}(2\pi\hbar)^3 \tag{2}$$

with $\beta = (kT)^{-1}$ and $E = E(p)$. From this the average energy $E(p)$ and the specific heat can be calculated. In agreement with experiment it begins at low temperature as T^{+3} as expected, according to Debye, since only phonons are excited. At higher temperatures the higher energy roton excitations become excited, and the specific heat rises much more rapidly. The thermodynamic properties are in excellent agreement with the theory if [12]

$$\begin{aligned} c &= 240 \text{ meters/sec} \\ \Delta/k &= 9.6^\circ\text{K} \\ p_0/\hbar &= 2.0 \text{ Å}^{-1} \\ \mu &= 0.77\, m \end{aligned}$$

where m is the atomic mass of helium.

The hydrodynamic equations of the two fluid model arise as follows. Suppose the fluid at absolute zero has density ϱ_0 and velocity $\boldsymbol{v}_s$. In the first part of this paper we shall take $\boldsymbol{v}_s$ to be irrotational $\nabla \times \boldsymbol{v}_s = 0$. Later we discuss the problem of local circulation. The mass current density is $\varrho_0\boldsymbol{v}_s$ and the kinetic energy is $\frac{1}{2}\varrho_0\boldsymbol{v}_s^2$. Suppose that as a result of a rise in temperature a limited number of excitations are formed in the fluid. Landau has shown that the energy to form excitations in a moving fluid is not $E(p)$ but is

$$E = E(p) + \boldsymbol{p} \cdot \boldsymbol{v}_s \tag{3}$$

This results from simple considerations of the relations in moving and still frames of reference. The mass current density equals the momentum density of the fluid since all of the atoms have the same mass. It now is

$$\boldsymbol{j} = \varrho_o \boldsymbol{v}_s + \langle \boldsymbol{p} \rangle \tag{4}$$

where $\langle \boldsymbol{p} \rangle$ is the mean momentum of the excitations per unit volume. Now the mean $\langle \boldsymbol{p} \rangle$ depends on how the excitations drift. If they are in equilibrium with the fixed walls of the vessel the mean $\boldsymbol{p}$ is *not* zero. The energy is $E(p) + \boldsymbol{p} \cdot \boldsymbol{v}_s$. It is lower than $E(p)$ for those excitations, whose momentum is directed oppositely to $\boldsymbol{v}_s$. Therefore in equilibrium more excitations align oppositely to $\boldsymbol{v}_s$ than parallel to it. For this reason the mean $\boldsymbol{p}$ is directed oppositely to $\boldsymbol{v}_s$ and for small $\boldsymbol{v}_s$ is proportional to it, let us say $\langle \boldsymbol{p} \rangle = -\varrho_n \boldsymbol{v}_s$. This defines ϱ_n. If ϱ_s is defined as $\varrho_o - \varrho_n$ we have a total current $\varrho_s \boldsymbol{v}_s$ in a situation in which the excitations are in equilibrium with fixed walls. The equilibrium is established by collisions of the excitations with the walls and with each other.

The number of excitations of momentum $\boldsymbol{p}$ is again determined by (2) but now with E given by (3) so that the average $\boldsymbol{p}$ is

$$\langle \boldsymbol{p} \rangle = \int \boldsymbol{p} (\exp \beta(E(\boldsymbol{p}) + \boldsymbol{p} \cdot \boldsymbol{v}_s) - 1)^{-1} \, d^3\boldsymbol{p} (2\pi\hbar)^{-3}$$

or expanding to first order in $\boldsymbol{v}_s$, find $\langle \boldsymbol{p} \rangle = -\varrho_n \boldsymbol{v}_s$ where

$$\varrho_n = -\frac{\beta}{3} \int p^2 (\exp(\beta E(p)) - 1)^{-2} \exp \beta E(p) \, d^3\boldsymbol{p} \, (2\pi\hbar)^{-3} \tag{5}$$

The density ϱ_n determined from experiments in second sound is in reasonable agreement with this expression (evaluated with the constants given above it fits above 1°K, but below 1°K the values $p_o/\hbar = 2.3$ Å^{-1} and $\mu = 0.40\, m$ fit better, and do not alter the good fit to the thermodynamic data). This explicitly shows that ϱ_n is a derived concept, and does not represent the density of anything which has microscopic meaning.

The excitations can drift also. The distribution for equilibrium in a drifting gas is, according to statistical mechanics,

$$n(E) = (\exp \beta(E - \boldsymbol{p} \cdot \boldsymbol{u}) - 1)^{-1} \tag{6}$$

where $\boldsymbol{u}$ is a parameter. In this case the mean momentum is

$$\langle \boldsymbol{p} \rangle = -\varrho_n (\boldsymbol{v}_s - \boldsymbol{u}).$$

If we write $\boldsymbol{u} = \boldsymbol{v}_n$ we have for the current

$$\boldsymbol{j} = \varrho_o \boldsymbol{v}_s - \varrho_n (\boldsymbol{v}_s - \boldsymbol{u}) = \varrho_s \boldsymbol{v}_s + \varrho_n \boldsymbol{v}_n \tag{7}$$

This can be interpreted macroscopically as saying that the current is like that in a mixture of two fluids, one of density ϱ_s moving at velocity $\boldsymbol{v}_s$, the other of density ϱ_n and velocity $\boldsymbol{v}_n$.

Actually (6) is not an equilibrium distribution unless the walls move at velocity $\boldsymbol{u}$, and furthermore $\boldsymbol{u}$ is constant throughout the liquid. It is generally taken as a good approximation in the case that $\boldsymbol{u}$, that is, $\boldsymbol{v}_n$, is not constant. The lack of equilibrium in this case produces irreversible effects, such as viscosity, which can be associated with the "normal fluid component". The distribution is in equilibrium even if $\boldsymbol{v}_s$ is not constant.

The entropy of the system is that of the excitations. It is easily verified that the mean group velocity of the excitations (the mean of $\delta(E(p) + \boldsymbol{p} \cdot \boldsymbol{v}_s)/\delta \boldsymbol{p}$) is just $\boldsymbol{v}_n$. The entropy can therefore be considered as flowing with the "normal fluid".

It is also possible to work out the expected value of the energy of the system. If one calculates the internal energy and subtracts the internal energy the system would have at the same entropy but with $\boldsymbol{v}_s = \boldsymbol{v}_n = 0$ the excess expanded to the second order in the velocities can be written $\frac{1}{2}\varrho_s \boldsymbol{v}_s^2 + \frac{1}{2}\varrho_n \boldsymbol{v}_n^2$. This is just what the two fluid model would expect.

Therefore Landau shows that a liquid system with excitations as described will behave in many ways like a mixture of two fluids.

Furthermore, considerable progress has been made by Landau and Khalatnikov [13] in the interpretation of many irreversible phenomena, such as viscosity, attenuation of second sound, etc. from the kinetic theory implied by such excitations. It is not possible as yet to find the crosssection for collision, say between two rotons, from first principles. But if a few such quantities are considered as unknown parameters, a great deal can be said. The number of rotons varies very rapidly with temperature, in the manner given by (2). For this reason the mean free path for collision and the resultant viscosity resulting from roton-roton collisions has a known temperature dependence. In a similar way the contribution of collisions between rotons and phonons or between phonons can be worked out. There are also collisions in which the number of excitations change. The results are often in excellent agreement with experiment.

There is, therefore, little doubt that in liquid helium there are such excitations, with the energy spectrum that Landau suggests, and that this picture supplies the complete interpretation of the two fluid model for helium II.

4. The Reason for the Scarcity of Low Energy States

The next question that concerns us is to try to see from first principles why the excitations of the helium fluid have these characteristics.

Landau has, in fact, tried to obtain some justification for the spectrum from a study of quantum hydrodynamics. This is not a completely detailed atomic approach. One attempts to describe the liquid by a few quantities such as density and current, or velocity. Then one makes these quantities operators with reasonable commutation relations, and tries to find the excitation energies of the fluid. The problem has not been analyzed in sufficient detail to establish the energy spectrum (1). Such an approach cannot give us an ultimate detailed understanding for two reasons. First, the numerical values of Δ, p_0, μ show these quantities to be characteristic of the atomic structure of the liquid. A theory which describes the fluid simply by average variables and which therefore cannot represent the fact that the liquid does in fact have atomic structure cannot lead to definite values for excitation energy. A more serious problem is this. It is necessary to show not only that the excitations $E(p)$ exist, but that there are not a host of other possible excitations lying lower. If we describe the liquid with average variables we have no assurance that there are no excitations at a level below the coarsness of our averages. Possibly excitations exist which represent no gross density variation and no mean current. If many other lower excitations exist they dominate the specific heat curve and the properties of the fluid. (Perhaps in ^{3}He we have an example of a system capable of excitations at an atomic level which are not describable by the variables used in quantum hydrodynamics).

However it is possible from first principles to see why there are no other excitations but those supposed by Landau and why the energy spectrum of these excitations has, qualitatively, the form which he supposed. [7, 8]

In order to do so, we should, rigorously, have to solve the Schrödinger equation for the system.

$$H\psi = -\frac{\hbar^2}{2m} \Sigma_i \nabla_i^2 \psi + \Sigma_{ij} V(\boldsymbol{R}_{ij})\psi = E\psi$$

where m is the atomic mass, $V(\boldsymbol{R}_{ij})$ is the mutual potential of two atoms separated by the distance $\boldsymbol{R}_{ij} = \boldsymbol{R}_i - \boldsymbol{R}_j$, and ∇_i^2 represents the Laplacian with respect to the coordinates $\boldsymbol{R}_i$ of the i^{th} atom.

The sums must be taken over all of the N atoms in the liquid. We cannot solve this equation directly but we can make surprising headway in guessing the characteristics of the wave functions ψ which satisfy it.

We shall have to picture the wave function ψ. It differs from one state to another. But we will consider its value for only one state at a time. Then it is a definite but complicated function $\psi(\boldsymbol{R}_1, \boldsymbol{R}_2 \ldots \boldsymbol{R}_N)$ of the $3N$ variables $\boldsymbol{R}_i$. To picture it we must have a scheme by which we clearly represent it in our minds. Now such a function is a number associated with every set $\boldsymbol{R}^N$ of values $\boldsymbol{R}_i$, or, as we shall say, with every configuration of the atoms. We can represent a configuration $\boldsymbol{R}^N$ by imagining each of the N atoms in the vessel containing the liquid to be located with its center at one of the $\boldsymbol{R}_i$. That is, each configuration is represented, as classically, as a particular definite location for each of the atoms. Then $\psi(\boldsymbol{R}^N)$ is a number associated with each such arrangement of the atoms. We can call it the amplitude of the configuration. For a given state, this amplitude for some atomic arrangements is large – these arrangements then have large probability – for others small and the configuration is unlikely. When we wish to speak of how the amplitude changes as the values of $\boldsymbol{R}_i$ change, we shall use the more vivid language of asking how the amplitude changes as the atoms are "moved" about. Such motions are not directly related to any real classical motions, of course. In fact we cannot describe classical motions directly. All such classical ideas must be interpreted in terms of the mathematical behavior of ψ, if we are to be consistent with quantum mechanical principles. Most of our task, therefore, is trying to describe the ψ functions which correspond to the various kinds of states of energy, or motion, of which the liquid is capable.

Start by considering the ground state wave function which we shall call Φ .We use the intuition which we have acquired from knowing the solutions of the Schrödinger equations for simpler systems. For stationary states, ψ can be taken to be a real number. The lowest state always has no nodes (except for the exclusion principle, which does not operate here). Therefore Φ is everywhere positive. It is symmetrical, that is, Φ depends only on where atoms are, not on which is which. The energy $V(\boldsymbol{R})$ of interaction of two helium atoms, as worked out by Slater and Kirkwood,[14] for example, consists of a very weak attraction at large distances, but a powerful repulsion inside of 2.7 Å (see Fig. 2). The atoms in liquid helium at the normal density have

a volume of 45 cubic Ångströms each so they are not tightly squeezed together. If one wishes a rough approximation, consider the atoms as impenetrable spheres of 2.7 Å diameter, and forget the attraction, whose effect is, after all, mainly just to hold the liquid together at the normal density even if the external pressure falls to zero. Then configurations of atoms in which some overlap each other, that is, are closer than about 2.7 Å, are of very small amplitude. In the most likely configurations the atoms are well spaced. As for a particle in a box whose wave function bows highest in the center and falls gradually to zero at the walls, we may imagine the amplitude highest for good separation and falling toward zero if a pair of atoms approach

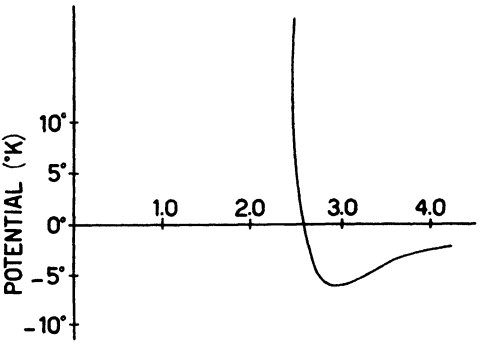

Fig. 2. The potential of interaction of two helium atoms as function of their separation as worked out from quantum mechanics by Slater and Kirkwood.

too closely. Our structure is a liquid, as a consequence of the zero-point energy, so that no particular lattice arrangement is strongly preferred. All configurations for which the spacing is ample have high probability. We can get from one arrangement to another without ever crossing a forbidden configuration of overlapping atoms because of the large spacing (cube root of atomic volume is 3.6 Å). Although not crystalline, there is a little local order induced by the tendency of atoms to stay apart, so that X-ray or neutron scattering experiments show a structure very similar to that of other simple liquids like liquid argon.

For the configurations of high amplitude the density is fairly uniform, at least until we look over such small volumes that we can see the fine grain atomic structure. If the density in a region is raised the atoms come closer together so that the "bow" on the wave function

which occurs as one atom is moved from contact with a neighbour on one side to one of the other side, is confined to a smaller space. The increased curvature represents increased kinetic energy and it is not as likely to find a configuration in which such an energy barrier is penetrated. As a matter of fact, this feature is easily analyzed quantitatively. Long range density fluctuations are sound waves. The rise of energy on compression is described by the compressibility coefficient, or equivalently by the speed of sound. Classically, standing density waves oscillating as a normal mode behave as an harmonic oscillator. Likewise, in quantum mechanics these are quantum oscillators and have zero point motions, although the most likely configuration is that of uniform constant density. The wave function for the zero-point motion of an oscillator is a gaussian so that the amplitude Φ for a given kind of density fluctuation falls off exponentially with the square of the fluctuation. To summarize, the ground state function is large for any configuration in which the atoms are well spaced from one another at nearly constant average density. If falls off if these conditions are violated.

Next we turn to the excited states. Right away one obvious excitation is that of the standing sound wave. If the classical frequency is ω the quantum excitation energy of such a mode is $\hbar\omega$. Usually one prefers by linear combinations to make states of running waves, or phonons. If the wave number is k, the energy is $\hbar kc$ if c is the sound velocity.

We may readily obtain the wave function for such a phonon excitation. If the density is $\varrho(\boldsymbol{R})$ the classical normal coordinate going with such a mode is

$$q_{\boldsymbol{k}} = \int \varrho(\boldsymbol{R}) \exp(i\boldsymbol{k} \cdot \boldsymbol{R})\, d^3\boldsymbol{R} \tag{8}$$

Quantum mechanically for an oscillator the wave function for the ground state is a gaussian, and the first excited state is just the coordinate times this gaussian (the first hermite polynomial $H_1(x)$ is just x). Hence the wave function is

$$\psi_{\text{phonon}} = q_{\boldsymbol{k}}\Phi \tag{9}$$

if Φ is the ground state wave function of the system, which we have described in the preceding paragraphs. We have not bothered to normalize our function. The liquid consists of many atoms so if $\boldsymbol{R}_i$ is the position of the i^{th}, the density in any configuration is

$$\varrho(\boldsymbol{R}) = \Sigma_i \delta(\boldsymbol{R} - \boldsymbol{R}_i) \tag{10}$$

the sum extending over all the atoms. Putting this in (8) and then (9) we find

$$\psi_{\text{phonon}} = (\Sigma_i \exp. i\boldsymbol{k} \cdot \boldsymbol{R}_i)\, \Phi \tag{11}$$

This is valid if the wave length $(2\pi/k)$ is much larger than the atomic spacing, for then our description by compressional waves is adequate. The state energy is $\hbar kc$. Since $\hbar\boldsymbol{k}$ is the momentum $\boldsymbol{p}$ of the state, this means $E = pc$. Since the wave length can be very long this energy can be exceedingly low.

The central problem is to see why no states other than these phonons can have such low energies. We try to construct the wave function ψ of an excitation which should be as low in energy as possible and yet not represent a phonon. We must associate a number which may now be positive or negative with each configuration. In fact, since ψ must be orthogonal to the ground state Φ which is everywhere plus, ψ must be plus for half the configurations and minus for the other half. Furthermore, ψ must be orthogonal to all the phonon states. This simply means that ψ must vary from plus to minus for changes in the configurations which do not appreciably alter the large scale density. Configurations can alter without variation of mean density by simply stirring the atoms about. Of course, since ψ must represent as low an energy as possible we must give low amplitude to configurations in which atoms seriously overlap, just as in the ground state Φ.

The function ψ takes on its maximum positive value for some configuration of the atoms. Let us call this configuration A, and the particular locations of the atoms α-positions. We said that the α-positions must be well spaced so that the atoms do not overlap, and further that they are, on a large scale, at roughly uniform density. Equally, call configuration B, with atomic positions β, that for which ψ has its largest negative value. Now we want B to be as different as possible from A. We want it to require as much readjustment over as long distances as possible to change A to B. Otherwise ψ changes too rapidly and easily from plus to minus, our wave function has a high gradient, and the energy of the state is not as low as possible.

Try to arrange things so that A *requires* a large displacement to be turned into B. At first you might suppose it is easy. For example (see Fig. 3) in A take some atom in the left side of the box containing the liquid and move it way over to the other side of the vessel, and

call the resulting configuration B. One objection to this is that an atom is moved from one side to another, so a hole remains at the left and an extra atom is at the right. This represents a density variation. To avoid this we may imagine that another atom has been moved at the same time from right to left, and the various holes and tight squeezes have been ironed out by some minor adjustments of several of the neighbouring atoms. This movement of two atoms each a distance of the size of the vessel, one from left to right and the other from right to left, is certainly a long displacement, so B and A are very different. But they are not.

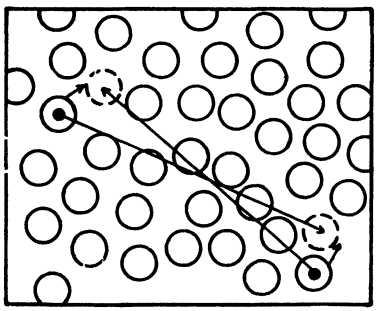

Fig. 3. Two configurations (solid and dotted) that result from large displacements (long arrows) of the atoms, can actually be accomplished by much smaller adjustments (short arrows) because of the identity of the atoms

The atoms must be considered as identical, the amplitude must not depend on which atom is which. One cannot allow ψ to change if one simply permutes atoms. The long displacements can be accomplished in two steps. In the first step permute the atoms you wish to move to those α-positions closest to the ultimate position they are to occupy in the final configuration B. This step does not change ψ because all the atoms are still in the same configuration of α-positions. Then the change to the B configuration is made by small readjustments, no atom moving more than half the atomic separation. In this minor motion ψ must change quickly from plus to minus and the energy cannot be low. For the reason that the wave function is unchanged by permutation of the atoms it is imposible to get a B configuration very far from the A configuration. No very low energy excitations can appear (other than phonons) at all.

In the phonon case we consider configurations in which, as ψ changes sign, the density distribution changes. A change in density cannot be accomplished by permuting atoms. That is why the Bose statistics does not affect phonon states. But it leaves them isolated as the lowest states of the system, so the specific heat approaches zero as T approaches zero according to Debyes T^3 law. This is the key argument for the understanding of the properties of liquid helium. It is given in

somewhat more detail in reference 7. Since it is a negative argument, attempting to prove that a low energy state does *not* exist, it is difficult to convey conviction in a few words. The reader should try to invent wave functions of low energy for himself. After a few attempts he will see much more clearly what we have tried to explain here.

5. Rotons

The qualitative argument is complete in itself. Nevertheless it is gratifying that it may be pushed even further to produce a quantitative estimate of the energy of these other excited states. We give only a summary of the considerations here (see reference 8 for details). We try to clarify our picture of the wave function ψ, until we can write a mathematical expression for it. This expression put into the energy integral $\int \psi^* H \psi d^N V / \int \psi^* \psi d^N V$ will give us an estimate for the energy.

As we said, in order to get the energy as low as possible we wish the gradients of ψ to be small. Therefore the configuration B (where ψ is maximum negative) must be as far as possible from configuration A. Yet we noted that no β-site is more than half the atomic spacing from an α-site. The two configurations are generally nearly the same. They are furthest from each other if as many atoms as possible must be moved. That is accomplished when, as illustrated in Fig. 4, all the β-sites are between α-sites, so every atom must move. To completely specify ψ, of course, we must give its value for all configurations, not only for A and B when all atoms are on α-sites, or all on β-sites. The lowest energy results if the transition from plus to minus (hence A to B) is as gradual as possible. First for configurations in which each of the atoms is either on an α or on a β-position, this is most naturally accomplished if ψ is proportional to the number on α-sites minus the number on β-sites. This difference passes smoothly from plus to minus. It can be expressed mathematically this way: Consider a function, $f(\boldsymbol{R})$, of position, which is $+1$ if $\boldsymbol{R}$ is at an α-

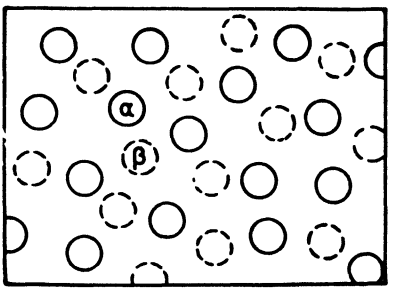

Fig. 4. The excited state wave function must be positive for one configuration, solid circles (α-positions) and negative for another. They are separated as far as possible if the negative configuration leaves no atom unmoved, dotted circles (β-positions)

site and — 1 if $\boldsymbol{R}$ is at a β-site. Then $\Sigma_i f(\boldsymbol{R}_i)$ summed on all the atoms is just the desired number on α-sites minus number on β-sites. For intermediate positions ψ will vary as smoothly as possible if $f(\boldsymbol{R})$ is taken to vary in some smooth way between its extreme values of + 1 and — 1, which it takes on at α and β-sites. This suggests that we take ψ to be of the form

$$\psi = \Sigma_i f(\boldsymbol{R}_i).$$

But this is incomplete for we tacitly assumed that in all the configurations the atoms did not overlap, the mean density did not vary very much and so on, just as in the ground state. This feature can be taken into account if we take instead

$$\psi_{\text{roton}} = \Sigma_i f(\boldsymbol{R}_i)\, \Phi \tag{12}$$

where Φ is the ground state function. [15] Then ψ will fall rapidly if the atoms overlap, etc. We actually do not know what the function $f(\boldsymbol{R})$ is but we expect it to vary rapidly, so that if expanded in a fourier integral the dominant wave lengths would be the atomic spacing.

According to the variational principle the best wave function is that which minimizes the energy integral. In this way, by variation of $f(\boldsymbol{R})$ it is readily found (see reference 8) that the minimum results if the function is

$$f(\boldsymbol{R}) = \exp(i\boldsymbol{k} \cdot \boldsymbol{R}) \tag{13}$$

and that the corresponding energy is

$$E(k) = \hbar^2 k^2 / 2mS(k) \tag{14}$$

where m is the atomic mass. The function $S(k)$ is the form factor for the scattering of neutrons from the liquid. That is, it is the Fourier transform of the function $p(R)$ which gives the probability per unit volume of finding an atom at a distance R from a given atom in the liquid in the ground state.

The local partial order of the liquid in the ground state shows up as in other liquids as a ring in the diffraction pattern (of neutrons, or X-rays). That is to say, there is a maximum in the function $S(k)$, which occurs when k represents a wavelength near the nearest neighbour spacing. The maximum in $S(k)$ represents a minimum in $E(k)$ here. This confirms the expectation that the low excitation would have wave numbers in this vicinity.

The state (12) and (13) has the momentum $\boldsymbol{p} = \hbar\boldsymbol{k}$. Ordinarily not

every value of a parameter in a wave function has significance in the variational method. But states of different momenta are orthogonal, and the energies (14) are significant not only for k near the minimum, but also in the neighbourhood of this value. The range of values for which (14) is useful is limited only by the range for which (12) can be expected to be a good wave function. For small k, (12) is identical to the wave function (11) representing phonon excitation, and (14) can be shown to give $\hbar kc$ in that region. Therefore the expression should be reasonable not only for k near the reciprocal atomic spacing, but for low k as well. It predicts a spectrum at first linear in p $(= \hbar k)$ then falling to a minimum, just as anticipated by Landau, and in agreement with experiment.

The curve $S(k)$ taken from neutron data of Henshaw and Hurst [16], or from the X-ray scattering data of Reekie [17] agree. The $E(k)$ which results is shown in Fig. 1 by the dashed line. The general behavior and minimum are clearly shown.

The actual value of the energy at the minimum is twice too high to agree with the experimental value (solid line) for Δ. The theoretical value lies above the true value, as it should according to the variational principle.

The inaccuracy of the wave function (12) prevents us from giving a complete description of what the roton wave function must look like. The function (12) does not satisfy the conservation of current. It appears as though a more accurate function would represent a current distribution large and unidirectional in one region, with a field of return currents surrounding it, somewhat in the nature of a smoke ring. These and other arguments suggest a trial function of the type

$$\psi = \Sigma_i \exp i\boldsymbol{k} \,.\, \boldsymbol{R}_i \,.\, \exp i \Sigma_j g(\boldsymbol{R}_j - \boldsymbol{R}_i)\, \Phi \qquad (15)$$

with the g, representing the back flow, to be determined. It is very hard to perform the integrals required in the variation problem with (15), so it has not been verified whether (15) represents a substantial improvement.

One way to understand the low energy for k near the reciprocal atomic spacing is this. One might consider these as sound waves of very short wave length. To obtain a density variation of long wave length is hard. To make the compression work must be done against opposing forces. For wave lengths closer to atomic spacing, however,

such density variations are easier to arrange. In fact, one can create variations of wave length equal to the atomic spacing simply by arranging the atoms, doing no appreciable work against repulsions, the energy being purely kinetic $\hbar^2k^2/2m$. Actually the energy is even lower ($S(k)$ at maximum is 1.3) for there is a positive tendency in the liquid to have such variations; if some atoms are correctly arranged the others are more likely to be also satisfactory because of the local order. Therefore the energy does not continue to rise as $\hbar kc$ but falls lower for wave lengths near the atomic separation.

It is easy to verify that these excitations behave in just the way that has been assumed in developing the statistical mechanics and the two fluid model. To represent a state with two excitations, say with momenta $\boldsymbol{k}_1$ and $\boldsymbol{k}_2$ one has the approximate wave function

$$\psi = (\Sigma_i \exp i\boldsymbol{k}_1 \cdot \boldsymbol{R}_i)\ (\Sigma_j \exp (i\boldsymbol{k}_2 \cdot \boldsymbol{R}_j))\ \Phi$$

and so on. Since the order of the factors is irrelevant this is the same state if $\boldsymbol{k}_1$ and $\boldsymbol{k}_2$ are reversed.The excitations obey the Bose statistics. In moving fluid the energy of the excitations can be shown to be (3).

6. Irrotational Superfluid Flow

So far we have only described the wave function for states representing internal excitation. We turn next to a description of the wave function which represents the state of the fluid when macroscopically we say it is flowing. We will assume that the flow velocity does not vary appreciably over distances of the order of an atomic spacing.

It is not dfficult to represent by wave functions states which represent the motion of the superfluid. Suppose the system is at absolute zero so there are no excitations. If the entire system moves forward as a body, since the center of gravity coordinate can bc separated out from Schrödinger's equation, the wave function is

$$\psi = (\exp i\boldsymbol{k} \cdot (\Sigma_i \boldsymbol{R}_i))\ \Phi$$

where $N\hbar\boldsymbol{k}$ is the momentum of the system, if there are N atoms. In case the velocity is not uniform we can construct a wave function somewhat as follows: If the velocity varies only slowly from place to place, those atoms temporarily in a macroscopic region where the velocity is, say, $\boldsymbol{v}$ must surely have a wave function very much the same as though the liquid in the region were isolated and moving at a uniform velocity. This suggests that the phase contains a term

$\hbar^{-1}m\boldsymbol{v} \cdot \Sigma_i \boldsymbol{R}_i$, the sum being taken only over those atoms in the region. Other regions where $\boldsymbol{v}$ differs make similar contributions to the phase so the total phase is $m\Sigma_i \boldsymbol{v}(\boldsymbol{R}_i) \cdot \boldsymbol{R}_i$ where $\boldsymbol{v}(\boldsymbol{R})$ is the velocity at $\boldsymbol{R}$. This suggests a wave function of the form

$$\psi_{\text{flow}} = [\exp i(\Sigma_i s(\boldsymbol{R}_i))]\, \Phi \tag{16}$$

where $s(\boldsymbol{R})$ is a function which varies only very little over distances as small as the atomic spacing. We have suggested that it is $\hbar^{-1}m\boldsymbol{v}(\boldsymbol{R}) \cdot \boldsymbol{R}$, but as is usual for waves whose wave length varies with position, the momentum is the gradient of the phase, not the coefficient of $\boldsymbol{R}$. Thus (16) does represent the helium flowing, but the velocity is given by

$$\boldsymbol{v} = \hbar m^{-1} \nabla s. \tag{17}$$

It is readily verified that the current density is $\varrho_0 \boldsymbol{v}$, and the energy (from the variational integral) is $\frac{1}{2}\varrho_0 \boldsymbol{v}^2$, as expected classically. There is no change in density, as in (16) we have not allowed these small effects to be represented.

If excitations exist in the moving fluid the wave function is (16) multiplied by the factor $\Sigma_i f(\boldsymbol{R}_i)$ in (12). The excitation energy turns out to be (3) as expected, interpreting $\boldsymbol{v}$ as the superfluid velocity $\boldsymbol{v}_s$.

Equation (17) implies that the motion is irrotational, that is, $\nabla \times \boldsymbol{v}_s = 0$. In a simply connected region this has only one solution for given motion of the boundaries. For fixed boundaries it is $\boldsymbol{v}_s = 0$. In a multiply connected region the situation is different. Since $\nabla \times \boldsymbol{v}_s = 0$, the circulation about any closed curve which can be shrunk to a point is zero. On the other hand, in the case of a toroidal region, if the curve encloses the hole the circulation need not vanish. Although the wave function must be single valued, s may be of the nature of the azimuthal angle, increasing by 2π, or a multiple thereof if one goes around the hole. That is, for a circuit enclosing a hole (into which liquid may not freely flow) the circulation must be an integral multiple n of a quantized unit $2\pi\hbar/m$,

$$\oint \boldsymbol{v}_s \cdot d\boldsymbol{s} = 2\pi\hbar m^{-1} \cdot n = 2\pi n \cdot 1.5 \times 10^{-4}\ \text{cm}^2/\text{sec} \tag{18}$$

These states do not influence the previous statistical mechanical argument. There are too few of them. The velocity may be considered as a macroscopic variable, such as density. For a macroscopic torus even the lowest of the states given by (18) is very much higher than

a roton energy Δ. Thus if the torus area is A, radius R, the mass moving is $mA \cdot (2\pi R)/d^3$ where d^3 is the atomic volume. It moves at velocity given by $v_s \cdot 2\pi R = 2\pi\hbar m^{-1}$, from (18), so the kinetic energy is $(\hbar^2/2md^2) \cdot (2\pi A/Rd)$. The factor $\hbar^2/2md^2$ is an energy of the order of a roton, but the second factor is very large, being the torus dimension over the atomic spacing. Incidentally the total angular momentum is $\hbar$ per atom.

If the fluid must flow irrotationally, at first sight, it cannot lose energy, unless it is moving very rapidly. This has been pointed out by Landau. If a body of fluid is moving at velocity v, and loses a small energy δE, it must do so (to keep the flow irrotational) by the entire fluid changing its velocity. Let the change in v be δv. If M is the effective fluid mass the momentum change δp is $M\delta v$ and $\delta E = Mv\delta v = v\delta p$. Now this energy loss must go into heat; that is, into internal excitations of rotons. But if the momentum transferred to excitations is δp the energy cannot be small. It must be at least about $(\delta p/p_0)\Delta$ where Δ and p_0 are the energy and momentum of an individual roton. That is, δE must be at least $(\Delta/p_0)\delta p$ and energy cannot be lost unless v exceeds Δ/p_0, about 70 meters per second. (More accurately v must be high enough that a line drawn from the origin at slope v can cut the $E(p)$ *vs* p curve). This suggests the reason for the frictionless flow of superfluid. But we have proved too much, for in actuality the resistance sets in at velocities a few hundred times smaller.

The only way that gross slowing down can occur for lower velocities is for small parts of the fluid to stop or slow down without the entire fluid having to slow down at once. That is, energy loss must be accompanied by flow which is not irrotational; that is, flow which involves local circulation. To understand such effects we must add a new element to our picture of phonons, rotons and potential flow. These are the quantized vortex lines suggested by Onsager. [1] We proceed to describe them.

7. Rotation of the Superfluid

The problem which now faces us is to extend (16) so that we can also represent states for which $\nabla \times \boldsymbol{v}$ does not vanish, or at least where there is circulation in the superfluid. We analyze the situation at absolute zero for simplicity. We must present ourselves a problem in which such circulation is necessary and try to find the lowest energy state. The situation first considered by the author was the slip-stream

between two regions of fluid moving at different velocity, but it is easier to arrive at the result by considering the problem of helium with high angular momentum in a cylindrical vessel. Suppose, for example, the helium at absolute zero is initially under such pressure that it is solid and is set into rotation, then the pressure is released so that it liquifies. What is the final state of the helium? We ask then for the lowest state of a quantity of helium which has a definite, macroscopically high, total angular momentum.

For a system of given angular momentum the kinetic energy is least if the angular velocity ω is a constant throughout the liquid. This motion is not rotation free for $\nabla \times \boldsymbol{v} = 2\omega$. But it is very difficult for helium to manage a state of local circulation. In fact, without high excitation energy, local circulation is impossible. At first one might find it hard to see why the liquid cannot simply rotate as a rigid body. The energy is then low. But a liquid is not a rigid body. A part of it can turn independently of the whole. In a rough way of speaking the liquid may be thought of as made up of many quasi-independent units of nearly atomic dimensions. Any motion of the body can be compounded of motions of the tiny parts. But to set any small part into a rotational state requires a high energy because the moment of inertia is so small. If only a limited energy is available nearly all the "parts" must be frozen out in their ground states.That is, nearly everywhere the local angular momentum is zero, i.e., $\nabla \times \boldsymbol{v}_s = 0$. It takes energy to create circulation and, furthermore, we can expect this circulation not to be distributed uniformly throughout the fluid. The rigid body type of rotation where $\nabla \times \boldsymbol{v}_s \neq 0$ everywhere is not possible, or if at all, only with an enormous expenditure of energy, an expenditure far higher than that gained by the uniform distribution of angular velocity.

Another possibility that suggests itself is that the liquid, if the angular momentum is high, is not free of excitations like rotons and phonons even though the temperature is at absolute zero. These excitations could carry the angular momentum. That is, in the language of the two fluid model, perhaps there is at $T = 0$ a mixture of superfluid and normal fluid, with the superfluid component not rotating, and with the normal fluid carrying all of the angular momentum. The energy to maintain the normal fluid being sustained by the fact that if less normal fluid were present, for given angular momentum the kinetic energy would have to be larger. This turns out, for vessels of

centimeter dimensions turning at about one radian per second, to be a state of nearly 10^4 times the energy of a rigid body rotating at the same angular velocity. Surely nature can find some lower state for the helium.

We know (see 18) that if there is a hole in the liquid, circulation can exist. Therefore another solution suggests itself. The liquid circulates around a hole with constant circulation as in a free vortex (familiar from rotation of water around an emptying drain). The velocity varies inversely as the radius, rising to such heights near the center as to be able to maintain the hole free of liquid by centrifugal force. Such a solution would be easy to verify in a striking manner by looking at the surface of the liquid. Instead of the usual parabola it would be the curve of the surface of a free vortex. The energy is still quite a bit higher than the rigid body case, because the velocity instead of being distributed proportionally to the radius, actually falls as the radius increases. Nevertheless it is orders of magnitude below the mixture of normal fluid suggested above.

However, this is still not the lowest possible energy state, and the striking experiment will not succeed. To show this we construct a lower state. Suppose that the liquid has not only one vortex at the center, but several vortices. For example, suppose beside the central one there were a number distributed about the circle of radius $R/2$, half that of the vessel R, and all turning the same way. Viewed grossly this is like a vortex sheet so the tangential velocity can jump as we pass from inside $R/2$ to outside. Then the velocity can be arranged a little more like the linear curve by two sections, each of which is a $1/r$ curve. The gain in energy resulting from this improved distribution may more than compensate the energy needed to make the additional holes (and, further, the central vortex need not now be so large and energetic).

Continuing in this way with ever more vortices it soon becomes apparent that the energy can always be reduced if more vortices form. However there is a limit. Due to the quantization (18) of the vortex strength the smallest vortex has circulation $2\pi\hbar m^{-1}$. The lowest energy results if a large number of minimum strength vortex lines (which we shall call unit lines) form throughout the fluid at nearly uniform density. The lines are all parallel to the axis of rotation. Since the curl of the velocity is the circulation per unit area, and the curl is 2ω, there will be

$$2m\omega/2\pi\hbar = 2.1 \times 10^3\omega \text{ lines per cm}^2 \tag{19}$$

with ω in radians per second. For $\omega = 1$ rad per second the lines are about 0.2 mm apart so that the velocity distribution is practically uniform.

Such weak lines will not form actual macroscopic holes. In fact, if one neglects atomic structure and assumes a classical continuous liquid with surface tension, a unit line makes a hole opposed by surface tension which figures out to be only 0.4 Å in radians. That means that there is no real hole in the liquid. Around such a unit line, for example a straight one along the z-axis, the wave function off the axis is roughly

$$\psi = (\exp i\Sigma_i\varphi_i)\,\Phi \tag{20}$$

where φ_i is the angle about the z-axis. This does not hold close to the axis. On the axis $\exp i\varphi$ is meaningless, and close to it has enormous gradients. A particle on the axis cannot have angular momentum, yet (20) implies that each atom has angular momentum $\hbar$, nor can there be exceptions because the Bose statistics implies that they are equivalent. Therefore a more accurate expression than (20) would be this expression multiplied by a factor which is unity except if any one of the atoms comes very close to the axis, in which case it falls rapidly to zero. The density of fluid falls to zero on the axis. This is the remnant of the classical hole. Actually quantum mechanically the line will not remain perfectly straight in one spot but will have some zero point motion of wandering and waving to and fro.

It is not hard to get a reasonable estimate of the energy contained in these lines. First consider an isolated unit line along the axis of a cylinder of length L, radius b. The velocity at radius r is $\hbar/mr$ and if ϱ_o is the fluid density in atoms per cc ($\varrho_o = 1/45$ Å^3) the kinetic energy is the integral

$$K.\,E. = \tfrac{1}{2}\int \varrho_o m(\hbar/mr)^2 \,.\, 2\pi r\, dr \,.\, L.$$

The upper limit of the integral is b. It diverges at the lower limit, but within about the atom spacing the velocity formula is meaningless. Furthermore, inside this radius some of the energy is potential, required to keep to density down near the axis (that is, to make the partial "hole"). Therefore the energy needed to form such a line, per unit length, is

$$\begin{aligned}\text{Line energy per unit length} &= \varrho_o\pi\hbar^2m^{-1}ln(b/a)\\ &= 10^{-8}ln(b/a) \text{ ergs/cm.}\end{aligned} \tag{21}$$

Here a is a length of order of the atomic spacing. Its exact determination would require solving the difficult quantum mechanical problem. In almost all applications the ratio b/a will be very large, and the logarithm large enough to be insensitive to the exact value of a. For this reason we will not attempt a detailed evaluation, but simply choose a to be close to the atomic spacing. We arbitrarily take $a =$ 1.0 Å. In more complicated geometrical situations the lower limit will be the same, but the upper limit b will be some other characteristic dimension of the apparatus, or more usually the spacing between vortex lines, etc. It can be found by integrating the velocity distribution as determined for the given distriubution of singular vortex lines.

For a cylinder of liquid rotating at angular velocity $\omega = 1$ rad/sec the vortices are about 0.02 cm apart. This is 0.5×10^6 times a if $a = 4$ Å, so we can take the $ln(b/a)$ in this case to be about $ln(0.5 \times 10^6)$ or 14. Neglecting the variation of this logarithm with ω we find for the energy of all of the lines:

Total line energy per unit volume $= \varrho_s \omega \hbar \, . \, ln(b/a)$

where we have estimated $ln(b/a)$ as 14. The ratio of this to the kinetic energy for a rigid body is $4\hbar m^{-1} R^{-2} \omega^{-1} ln(b/a)$ if the cylinder radius is R. For $R = 1$ cm, $\omega = 1$ rad/sec this ratio is 10^{-2}. For macroscopic laboratory dimensions the excess energy to form the lines is small. They would form if rotating solid helium is melted by releasing the pressure, the angular velocity distribution would differ imperceptibly from uniformity, and the surface should appear parabolic.

It is not self-evident that there is no state of appreciably lower energy, and that the energy of the rotating liquid is correctly estimated. This subject has not yet been analyzed any more deeply than is reported here. Therefore this part of the paper is not on as firm a foundation as the rest. We must therefore still consider it conjectural whether the considerations on rotational flow reported here are actually correct. It is interesting that all the conclusions were arrived at independently by the author without knowledge of Onsager's previous work (with which they are in exact concordance).

3. Properties of Vortex Lines

In a situation more general than uniform rotation, in which the curl of the velocity is not constant, we can imagine a similar situation. We have a situation instantaneously with many vortex lines. Some are

closed on themselves in rings, and others terminate with their ends on the fluid boundaries. Viewed from a continuum approximation in which atomic structure is neglected, a velocity $\boldsymbol{v}_s$ can be defined at every point. The curl of this is zero everywhere, except at one of the vortex lines where it is infinite. These lines are real quantized vortex lines. The circulation around a small circuit surrounding only one line is $2\pi\hbar m^{-1}$. The lines have a sense depending on the direction of rotation. The circulation about any curve whatosever is given by

$$\oint \boldsymbol{v}_s \cdot ds = 2\pi\hbar m^{-1} n$$

where n is always an integer, being the net number of lines linked by the circuit, account being taken to the sign of each.

If $\nabla \times \boldsymbol{v}_s$ is averaged over a large enough region that many lines are included, the number of lines per cm^2 must be at least $<\nabla \times \boldsymbol{v}_s> m/2\pi\hbar$ and the energy of these lines per unit volume is at least

$$\tfrac{1}{2} |<\nabla \times \boldsymbol{v}_s>| \varrho_0 \hbar . ln(b/a) \tag{22}$$

where b is the spacing between lines, $1/b^2 = <\nabla \times \boldsymbol{v}_s> m/2\pi\hbar$. This shows that in our liquid it takes energy to create circulation. Actually in real, complex situations the energy might exceed greatly the value in (22). There may be great complex activity with many lines twisting and turning so that several lines of opposite senses are close together. In this case, the case of developed turbulence, the number of lines present may be bigger than the average $\nabla \times \boldsymbol{v}_s$ would indicate. (Probably in such a case it would be hard to define the average $\nabla \times \boldsymbol{v}_s$ because the result may depend on the size of the region over which the average is taken).

The discussion of the rotating cylinder of liquid with which we introduced the lines is rather special. We shall try to give a more complete and general description of the state of the superfluid with circulation. We continue to study the case at absolute zero. Let us try to characterize the state of a fluid in which we desire two things (which, it will turn out, are mutually incompatable). We want (a) the liquid to be flowing with a velocity $\boldsymbol{v}_s$ which is a smooth function of position without singularities (on a scale of distances large compared to atomic dimensions) and (b) we want $\nabla \times \boldsymbol{v}_s$ not to vanish.

Suppose the liquid in an element of volume ΔV (large compared to the atomic volume) is moving at velocity $\boldsymbol{v}$. Then as we have seen the wave function should depend on the position of the atoms, if they are

within ΔV as exp $(im\boldsymbol{v} \cdot \Sigma_i \boldsymbol{R}_i)\ \Phi$. That is, if a number of atoms in the region are displaced, each by $\Delta \boldsymbol{R}_i$ from one allowed (by Φ) configuration to another allowed one, the main effect is that the wave function must change phase by

$$\Sigma_i (m\boldsymbol{v} \cdot \Delta \boldsymbol{R}_i)\hbar^{-1} \tag{23}$$

This can also be seen in another way. If a region of fluid can be considered to have a velocity $\boldsymbol{v}$ it has a momentum density $\varrho_0 m\boldsymbol{v}$. It is characteristic of momentum in quantum mechanics, that if the center of mass is changed the wave function changes phase by an amount proportional to the momentum and to the displacement of the center of mass. Now if the atoms are displaced by $\Delta \boldsymbol{R}_i$ the center of mass moves so the phase change (23) results. This is true at least if the displacement makes no other important change in the wave function. We will suppose that both before and after the displacement the atoms are well spaced and there are no gross density fluctuations, etc. such that in case the liquid were not in motion both configurations would have essentially the same amplitude.

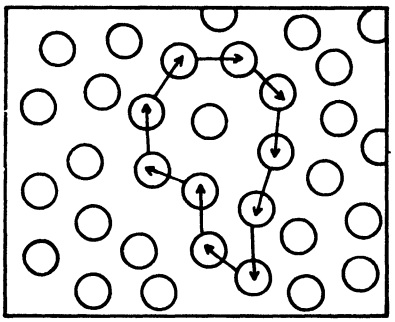

Fig. 5. The wave function must not change as a result of a permutation. If all the atoms are displaced around a ring, as shown, the phase change must be a multiple of 2π

The same argument goes for atoms in other regions, etc. so the phase shifts accumulate to a sum in (23) over displacements of atoms all over the liquid, if $\boldsymbol{v}$ is now considered as a function of $\boldsymbol{R}_i$. The displacements $\Delta \boldsymbol{R}$ must be small compared to the distances over which $\boldsymbol{v}$ varies. We shall apply the formula in a case in which $\Delta \boldsymbol{R}$ is the separation between atoms.

Select, in a given configuration, a very long closed chain of atoms each of which is a nearest neighbor of the next in line (see Fig. 5). The last should have the first as nearest neighbor. The chain may consist of very large numbers of atoms and may even be so long that it passes through regions of varying velocity. Consider a displacement of each atom to its nearest neighbor next in line. The wave function cannot change, for it is simply a special permutation of the atoms. Further we will suppose that if all the displacements are made together

a little at a time, each intermediate configuration is allowed. This sliding of the chain along itself is not prevented by potential barriers, especially if we allow small temporary displacement of other atoms adjacent to the ring to permit passage in tight places. In the final configuration all atoms have returned to their original positions, except those of the ring which have moved one over. We suppose, because of the ease in which the displacement can be made that we can assume the wave function does not vanish for any intermediate position during the displacement. Then its phase shift is given by (23), but this must represent no change in the wave function. It is therefore necessarily an integral multiple of 2π. We conclude that

$$\oint \boldsymbol{v}_s \cdot \boldsymbol{ds} = 2\pi\hbar m^{-1} n \tag{24}$$

where n is an integer and the integral is taken over any path which goes from one atom to the next neighbor, etc. If $\boldsymbol{v}_s$ is now assumed continuous at an atomic scale, the path can be smoothed out to any continuous curve. Of course, it is impossible that (24) holds for all continuous paths if n is an integer (depending on the path) if $\boldsymbol{v}_s$ is free of singularities and continuous unless $n = 0$ (in a simply connected region). Because any path can be deformed continuously into an infinitesimal path, the left side changing continuously to zero. The right side cannot change continuously so it must be zero for all paths. Likewise for a toroidal region n must be the same for all paths which surround the hole.

We see therefore that $\boldsymbol{v}_s$ cannot be continuous if we are to have circulation. There must be places where $\boldsymbol{v}_s$ is discontinuous, and places in the fluid where a displacement of an atom to its neighbor may not be possible without passing through a node in wave function. In the neighborhood of such a node the probability of finding an atom is reduced. This decrease in density requires energy to maintain it. We shall therefore try to arrange conditions so that such places are as infrequent as possible. Under those conditions, for nearly every conceivable ring of atoms the atoms can be moved over to the next adjacent atom without the wave function vanishing. Its phase change must be a multiple of 2π. If two adjacent rings have a phase change which is different, differing by 2π say, then between them somewhere must lie a very small ring of three or four atoms for which the circulation is $2\pi\hbar/m$. For example, suppose for a certain ring A the phase is zero, but for a nearby ring B it is 2π. Then shift ring B by a few

atoms at a time until it gets as close to ring A as possible, but still has phase shift 2π. Likewise shift A until it is as close to B as possible but so that it has still shift 0. Then A and B will contain many atoms in common and only differ by a few, as illustrated in Fig. 6. Then

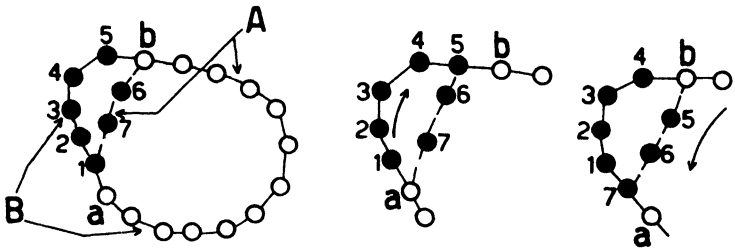

Fig. 6. A displacement along ring B followed by a reverse displacement along an adjacent ring A with many atoms in common is equivalent to a displacement around the ring C, indicated by black circles (except for an inconsequential permutation 5–b).

consider a permutation consisting of shifting B forward, then shifting A backward. It is readily verified that this change is the same as a shift of atoms around the very small ring C consisting of those parts of A and B which are not common, plus one of the common atoms. But the change in phase is 2π when B shifts and 0 when A shifts back, so that it must be 2π for the very small ring C. * This represents a highly concentrated angular momentum. Somewhere in the middle of ring C is a nodal point. It is readily appreciated geometrically that these nodal points must essentially form lines through the fluid. They are quantized vortex lines. It must be admitted that this argument is far from complete. We should consider states in which the location of the vortex line is uncertain, that is, a superposition of states with various locations for the line. Such a state would have a lower energy. Possibly we make a serious error in imagining that the velocity can be defined right up to atomic distance from the axes, if this axis itself does not have a definite location. Onsager has remarked, in private communication, on the possibility that these quantum effects might lower the energy to such an extent that the logarithm in (24) should

* The change in phase cannot be determined only from the initial and final configuration, but requires a description of the amplitude for intermediate configurations as well. Therefore this argument is not complete unless it is also assumed that partial rotations of C consisting of displacements of less than one atom spacing can also be roughly imitated by partial displacements of B and A.

be absent. At any rate, although our energy estimates may be incorrect, quantized vortex lines probably exist. We continue our discussion of the consequences of this assumption.

On a large scale according to the theorem of Helmholtz, vorticity moves with the fluid in such a way that the strength of a vortex filament remains constant. This means that if the fluid drifts the lines drift with it, maintaining their quantized strength. This is true, at least, if no forces act directly on the vortex line. In general the force per unit length on a vortex line equals the density, $\varrho_0 m$, times the vector cross product of the circulation, $2\pi\hbar m^{-1}$, and the velocity of fluid where the vortex is.

9. Critical Velocity and Flow Resistance

We next turn to the role such vortex lines may play in the resistance to flow found at sufficiently high velocities. We have suggested that this resistance cannot be understood in terms of a direct creation of rotons, the superfluid otherwise being in perfect flow. Let us consider what would happen if liquid is flowing out of an orifice, or tube, into a reservoir of fluid at rest. In Fig. 7 is illustrated the distribution of flow for irrotational motion. A very high velocity develops near the corners and large accelerations develop there. An ordinary fluid, such as water, flows in a complicated manner such as illustrated in Fig. 8 (a few moments after flow starts). The water shoots out straight into the nearly still fluid in the reservoir, forming a vortex sheet, which is unstable and curls around, eventually in an extremely complex manner. Let us see how helium might try to imitate some of the features of the type of flow illustrated in Fig. 8. Just for rough orientation and estimate suppose the fluid tries to go out in a jet, let us say at first of the same width and velocity as in the tube. Take the case that the tube is a long slot perpendicular to the paper, and the flow is roughly two dimensional.

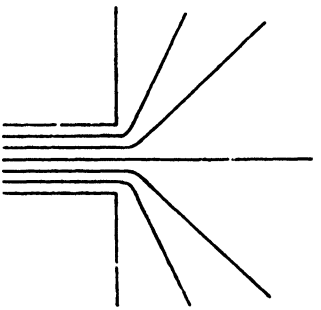

Fig. 7. Ideal potential flow from an orfice

Then circulation is implied for the velocity is v in the jet and 0 outside. This requires the formation of vortex lines, perhaps as illustrated in Fig. 9. The spacing is x and if this is small compared to d,

the slot width, the velocity distribution is roughly uniform inside the the jet. Taking a line integral along the jet for unit distance, and returning outside the jet, the circulation is v so the number of lines per centimeter is

$$\frac{1}{x} = v/2\pi\hbar m^{-1}.$$

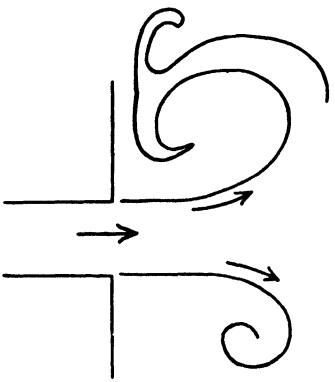

Fig. 8. Real flow from an orfice for ordinary liquids, producing an unstable vortex sheet

It takes energy to form these lines. If there is not enough kinetic energy in the fluid to supply the energy to make the lines, no resistance will appear. Once the lines can be formed they are, in a manner we shall soon discuss, ultimately dissipated as heat and a resistance appears. Let us see what order of critical velocity we would estimate in this way. The lines move out at the velocity of the fluid at their own location, which is $v/2$. Another way to see the necessity for this is to realize that as the fluid passes from inside to outside the pipe vorticity is created, so new lines must continually come rolling out of the ends of the orifice. In our case v/x lines are created per second. The energy needed to create these is (per unit length of slot)

$$\frac{v^2}{2\pi\hbar m^{-1}} \varrho_0 \pi\hbar^2 m^{-1} ln(d/a)$$

where the argument in the logarithm is only approximate. The total kinetic energy available per cc of fluid is $\frac{m\varrho_0 v^2}{2}$, so that per second $vd\,\frac{m\varrho_0 v^2}{2}$ is available. If we define v_0 as that velocity for which the energy available is just large enough to create the vortices we find

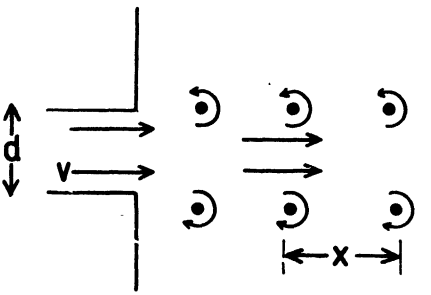

Fig. 9. Idealization of supposed vortex rings formed when superfluid helium issues at high speed from an orfice.

$$v_0 d = \hbar m^{-1} ln(d/a).$$

For example, for a slit of width $d = 10^{-5}$ cm, (which is about three

times the width of a Rollin film at a height of 1 cm) this gives $v_o =$ 100 cm/sec, if $ln(d/a)$ is taken as 6. This is somewhat higher than the critical velocities observed. The calculation is only meant as an estimate because the actual situation must be complicated. For one thing, near the critical condition x comes out about $3d$ so our picture of a uniform jet is poor. Further, the velocity in the jet must of course be reduced as a result of the energy needed to form the vortex line. Actually probably the situation near the critical point must be very complicated and irregular. The flow for short momentary periods may be much like Fig. 7 but irregularly vortex lines peel off of the edges of the slit, probably starting at one point along the slit and progressing to other places, or perhaps if the hole is circular, one or two vortex lines is fed out continuously in a form roughly like a helix. It is predicted that very close to the critical velocity when loss just begins, the resistance will be irregular and show fluctuations. These fluctuations are very small however and would be hard to detect. Possibly some sound may be generated by the flow irregularities. It is difficult to estimate its intensity. When helium is driven, just above critical velocity, through an emery powder superleak, some noise should be generated as the various vortex lines suddenly form and pass into the stream. The irregularities are a result of the unpredictable quantum transitions between states of no vortex line and one with a section of line.

Another possible source of vortex lines is the contact between flowing liquid and the walls. It is not necessary that all the loss occurs at the exit end of the tube. The walls of the pipe are irregular. Vortex lines may be created inside the pipe also.

It is difficult to go beyond this order of magnitude calculation in describing the conditions controlling the production of vortex lines. For example, if one studies the example given there are serious difficulties. As a particular vortex line leaves the end of the tube there are very great forces trying to pull it back resulting from its image in the tube wall. Let us imagine a line a distance b above the wall in a tube in which the velocity of flow is v_o. It is readily shown that the forces acting on the line are these. First a force pulling away from the surface of strength $2\pi\hbar\varrho_o v_o$. Second, from the image, an attraction to the wall of strength $\pi\hbar^2\varrho_o/mb$. A vortex line responds to forces by moving through the liquid to reduce the net force to zero. In this case it would drift upstream if the attraction is highest. But a vortex line

will interact with the wall, especially at its ends which go into the wall surface. Suppose this results in a frictional force which keeps the line from moving upstream. Then the response is to move closer to the wall. The vortex only moves away from the wall if $2\pi\hbar\varrho_0 v$ exceeds $\pi\hbar^2\varrho_0/mb$. Even if v is 100 cm/sec this requires b to exceed 10^{-6} cm or 20 atomic spacings. We might expect a vortex line to fluctuate away from the surface by a few atomic diameters. But how can we expect to penetrate the enormous potential barrier, to create a line so far away from the surface that the flow velocity can pull it further out and create eventual vorticity and energy loss?

More likely a line gets started somehow and has its ends tied on the wall. Then the forces of the fluid on the rest of the line cause it to wander about in such a way that more and more vortex line is fed out. It is not necessary to create bodily at one instant a complete section of line. For example, for the case of liquid issuing from a tube perhaps the vortex lines are helices with contact points at the edge of the hole which turn round and round while the helix moves outward. Similar things could happen inside tubes. If the tubes are very narrow the line will hit the other surface easily and be attracted by the walls. It can never get very far from a wall. Even if started somehow it will fall back into the tube walls unless the velocity v_0 suffices to keep it in the stream. Therefore the smallest tubes have the highest critical velocities.

10. Turbulence

The patterns of vortex lines which we have studied are well known to be unstable. In the case of the rotating cylinder this is not true if the cylindrical vessel containing the helium rotates also. But if the container is stopped the situation is altered. There are forces between the wall and vortex lines. (This is because the fluid density is altered near the line axis, so the interaction with the wall is not the same as the average for the rest of the helium). The lines at the outside drag past the stationary wall and as a result get distorted from their original vertical line position. This twists others, etc. Lines fall into the wall and others twist about each other in a complex way. It would be interesting to study this experimentally, to see how fast, and in what manner, the liquid eventually slows down.

In ordinary fluids flowing rapidly and with very low viscosity the phenomena of turbulence sets in. A motion involving vorticity is

unstable. The vortex lines twist about in an ever more complex fashion, increasing their length at the expense of the kinetic energy of the main stream. That is, if a liquid is flowing at a uniform velocity and a vortex line is started somewhere upstream, this line is twisted into a long complex tangle further down stream. To the uniform velocity is added a complex irregular velocity field. The energy for this is supplied by pressure head.

We may imagine that similar things happen in the helium. Except for distances of a few ångstroms from the core of the vortex, the laws obeyed are those of classical hydrodynamics. A single line playing out from points in the wall upstream (both ends of the line terminate on the wall, of course) can soon fill the tube with a tangle of line. The energy needed to form the extra length of line is supplied by a pressure head. (The force that the pressure head exerts on the lines acts eventually on the walls through the interaction of the lines with the walls). The resistance to flow somewhat above critical velocity must be the analogue in superfluid helium of turbulence, and a close analogue at that.

There are some ways, however, in which the two cases differ. In a classical fluid there is a thin boundary layer near the wall of the pipe in which viscosity controls the situation. In this boundary layer there is a large vorticity, but it escapes into the stream to be amplified, only from the edge of the layer. Inside it is damped by viscosity. As the stream velocity falls the boundary layer thickens, for the amplification is less and the damping overpowers it ever further from the wall. Below a critical velocity the turbulence ceases altogether and the flow is laminar, but with vorticity, the viscosity keeping the vorticity from amplifying itself. That is, viscosity is the mechanism which determines whether vorticity will be amplified or not, and therefore whether turbulence is produced. If the viscosity goes to zero as a limit (and no other physical phenomena are added) a classical ideal liquid would exhibit turbulence at any velocity, no matter how small.

Superfluid helium is an ideal fluid of zero viscosity. It does not exhibit turbulence at low velocity because of another, quantum mechanical, effect. The vorticity is quantized and cannot begin at as low amount as desired. One must supply energy enough to get the first one or two vortex lines started before the amplification process of turbulence can take over. There will not be a boundary layer with a structure analogous to that in classical flow (although near the walls the flow will

be somewhat different because of the dragging forces between the moving vortex lines and the wall).

In a classical fluid ,if the turbulent stream empties into a reservoir, the turbulent motion continues for a while, but as a result of the viscosity, it gradually slows up and dies out, the energy appearing eventually as heat.

What happens to a turbulent mass of superfluid left to itself? If there is normal fluid present the rotons and phonons will collide with the vortex lines and take energy from them, gradually turning this energy gain into more rotons and phonons (as a result of collisions among rotons the number of these may change). But an interesting question arises if the experiment is imagined at absolute zero. What can eventually become of the kinetic energy of the vortex lines?

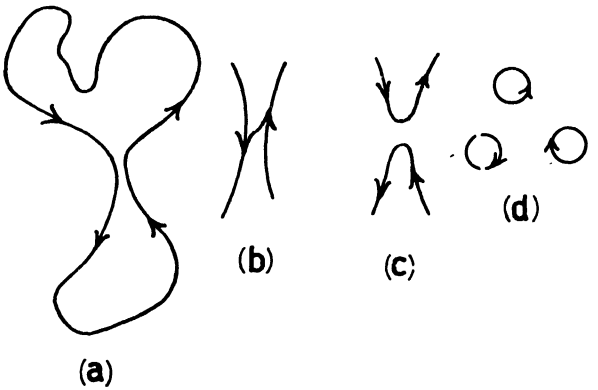

Fig. 10. A vortex ring (a) can break up into smaller rings if the transition between states (b) and (c) is allowed when the separation of vortex lines becomes of atomic dimensions. The eventual small rings (d) may be identical to rotons.

One possibility that suggests itself is this. Consider a large distorted ring vortex (Fig. 10a). If, in a place, two oppositely directed sections of line approach closely, the situation is unstable, and the lines twist about each other in a complicated fashion, eventually coming very close; in places, nearly within an atomic spacing. Consider two such lines (Fig. 10b). With a small rearrangement, the lines (which are under tension) may snap together and join connections a new way to form two loops (Fig. 10c). Energy released this way goes into further twisting and winding of the new loops. This continues until the single loop has become chopped into a very large number of small loops (Fig. 10d).

The smallest ring vortex that can exist must have a radius about half the atomic spacing. Let us guess that this is in fact a roton. Then all the energy of the vortex will eventually end by forming large numbers of rotons, that is, heat. Perhaps eventually it will be easier to understand the details of the complete transformation of organized flow energy into disorganized heat energy for liquid helium than for other substances.

11. Rotons as Ring Vortices

It is not unreasonable to guess that these smallest vortices are rotons. The velocity distribution around a roton, which is found by analytic means (ref. 8) is similar to that around a vortex ring. It is quite reasonable that a vortex ring can be only so small. To increase the curvature of a vortex line beyond that of radius roughly a may take energy. Let us imagine a roton to be the circular quantized vortex of lowest energy. A large circular vortex has (from (21)) energy $E = 2\pi R \cdot \frac{\pi\hbar^2}{m} \varrho_0 ln\, R/a$. It carries momentum $p = \pi R^2 \cdot 2\pi\hbar\varrho_0$. This momentum is that of a roton, p_0, if $R = 2.2$ Å. The energy is the right order (it corresponds to replacing ln by 1.6).

One might object that such a vortex drifts through the fluid, at velocity $v = (\hbar/2mR) ln\, R/a$, so one would expect rotons not to have a zero group velocity. Actually this drift, of a large vortex, has its seat in the force tending to shrink the vortex to decrease the energy of the line. The response to the radially directed force is a perpendicular motion. It is analagous to the ornery response of a gyroscope. In fact, if a vortex line were a thin flexible mechanical tube with inertia, and were started with zero forward motion, it would first fall in a bit and then move forward in a halting fashion, like the nutation of a gyroscopic, or the motion of an electron in crossed magnetic and electric fields. In a roton we imagine that the forces tending to contract the ring are already opposed by a kind of stiffness of the ring. It is already as small as possible. No drift motion results. In fact forward drift would expand it and raise the energy, while reverse drift would try to compress it to smaller size, again raising the energy. The lowest energy is at zero drift velocity. We may notice in passing that they can only drift in a direction perpendicular to their plane, that is, along, or opposite, the direction of the momentum. This agrees with a property derived for rotons from their energy-momentum relation

(1), that the group velocity $\delta E(p)/\delta p$ is in the direction of the momentum, (or opposite).

Having travelled so far making one unverified conjecture upon another we may have strayed very far from the truth. However imprudent it may be, there is one further observation we would like to make. A detailed picture is not available which describes physically just what goes on as the transition is approached from below. The free energy expression arising from (6) does not of itself describe the transition. The transition occurs when the number of rotons is very large. Some sort of interaction may occur between them, or there may be some limitation to the degrees of freedom. [18] There is no doubt that it is the analogue of the transition in the ideal gas, but it would be nice if we could get a less mathematical and formal description of the events. Of the following I am not sure, but it does seem to be an interesting possibility.

If rotons are the smallest ring vortices, and those of lowest energy, Δ, then there are states of higher energy corresponding to larger rings. For example, a ring of twice the diameter may have twice the energy more or less. The relative number of these will be expected to be very low, however. Since Δ is 9.6°K, at the transition $\exp(-\Delta/kT)$ is 10^{-2}, so very few larger vortices will be expected in equilibrium. Certainly none whose length is 10^2 or 10^3 atoms! This neglects an important feature, however. For a long line there are an enormous number of shapes and orientations available. Such a line is not infinitely flexible, of course, for the curvature cannot well exceed a^{-1}. It may be likened to a chain of a finite number of links. Adding one link requires an energy ε, say of order Δ, but increases the number of orientations by some factor, asymptotically, say s. In equilibrium then, the number of chains of $n+1$ links is a factor $s \exp(-\varepsilon/kT)$ times the number with n links. For low temperatures this is less than unity. No long chains are important. The excitations consist of rotons and a few other rings of slightly larger size. As the temperature rises, however, there comes a time when the factor $s \exp(-\varepsilon/kT)$ exceeds unity. Then suddenly the rings of very largest length are of importance. The state with one vortex line (or a very few) which winds and winds throughout the liquid like a near approximation to a Jordon curve, is no longer of negligible weight. The superfluid is pierced through and through with vortex line. We are describing the disorder of Helium I. At first the curve doesn't make full use of all of its orientations and higher

entropy. But as the temperature rises a little more it squeezes into the last corners and pockets of superfluid until it has no more degrees of flexibility available. The specific heat curve drops off from the transition to a smooth curve and the memory of the possiblity the helium can exhibit quantum properties in a unique way is lost in the perfusion of states and in disorder, as it is for more usual liquids.

REFERENCES

[1] L. Onsager, Nuov. Cim., **6**, Supp., **2**, 249, (1949).
[2] F. London, Nature, **141**, 643, (1938).
[3] A. Einstein, Ber. Berl Akad., **3**, (1925).
[4] F. London, Phys. Rev., **54**, 947, (1938).
[5] R. P. Feynman, Phys. Rev., **91**, 1291, (1953).
[6] G. V. Chester, Phys. Rev., **94**, 246, (1954).
[7] R. P. Feynman, Phys. Rev., **91**, 1301, (1953).
[8] R. P. Feynman, Phys. Rev., **94**, 262, (1954).
[9] L. Tisza, Phys. Rev., **72**, 838, (1947).
[10] L. Landau, J. Phys. U.S.S.R., **5**, 71, (1941).
[11] R. B. Dingle, Advances in Phys., **1**, 112, (1952).
[12] D. de Klerk, R. P. Hudson and J. R. Pellam, Phys. Rev., **93**, 28, (1954).
[13] L. Landau and I. Khalatnikov, J. Exper. Theor. Phys. (U.S.S.R.), **19**, 637, 709, (1949).
[14] J. C. Slater and J. G. Kirkwood, Phys. Rev., **37**, 682, (1932).
[15] A. Bijl, Leiden, Comm. Suppl., **90a**, Physica, **7**, 869, (1940).
[16] D. G. Henshaw and D. G. Hurst, Phys. Rev., **91**, 1222, (1953).
[17] J. Reekie and T. S. Hutchison, Phys. Rev., **92**, 827, (1953). We are grateful to Dr. Reekie for sending us the curve of S(k) derived from his data.
[18] R. P. Feynman, Phys. Rev. **94**, 262, (1954), especially the discussion preceding expression (28). There is a typographical error there. The relation (28) should read as an inequality, the left side not greater than the right side.

CHAPTER III

RAYLEIGH DISKS IN LIQUID HELIUM II

BY

J. R. PELLAM *

NATIONAL BUREAU OF STANDARDS, WASHINGTON D. C.

1. Introduction

While more modern versions of a quantum liquid are very likely to replace the two-fluid model as an exact description, the concept of the two interpenetrating fluids (see Ch. I) should always provide a convenient method for visualizing and anticipating the properties of liquid helium II. Second sound propagation was originally predicted [1] on the basis of this concept and interpreted as a thermal wave phenomenon, i.e. a 'concentration wave' between the normal fluid and superfluid components. Although visualized as a mass transport mechanism, the internal convection of the components through each other was early recognized as precluding application of normal acoustic techniques. Thus, the condition of zero total momentum (1)

$$x v_n + (1 - x) v_s = 0 \tag{1}$$

excludes the classical vibrating diaphragm as a generator of second sound. Such a device drives the two fluid components indiscriminately, so that $v_n = v_s$, resulting in generating first sound rather than second sound. The same condition neutralizes the ordinary velocity and pressure microphones as detectors, since both the net fluid flow and the net momentum change (and therefore pressure fluctuations) are held zero by this constraint, (1).

Therefore the early efforts to observe these temperature waves were based on thermal methods both for excitation and detection. In Peshkov's [2] original experiments demonstrating the existence of second sound, the waves were generated by periodic current flow in an electric heater element and detected by a temperature sensitive element, or

* Now at California Institute of Technology, Pasadena, California.

bolometer, which responded to the temperature variations accompanying the concentration waves. Most subsequent investigations of second sound, both with the standing wave and the pulse method, have relied entirely on these thermal characteristics of the waves. Although experimentally convenient, such strictly thermal techniques actually require direct cognizance of neither the two-fluid viewpoint nor the thermomechanical properties of the liquid. In fact second sound might equally well have been discovered experimentally as a pure thermal phenomenon without any prior association with the two-fluid or thermomechanical notions.

A direct method for detecting and measuring temperature waves by mechanical means was essential to the mass transport concept of second sound propagation. Clearly such an experiment, dependent in principle on the internal convection between the two fluid components of liquid helium II would (a) if negative, open serious doubt to the mass-transport notion, or (b) if positive, establish the internal consistency of the theory. Since the latter proved true, the propagation of second sound waves may evidently be at least visualized as a self-maintained internal vibration between the two fluid components. Although for easy visualization the two-fluid model fulfills an important function, it should be realized that the final quantum mechanical treatment may well provide a quite different interpretation along the line of recent advances [3] (See Ch. II).

The device which detects the mechanical energy content of second sound waves is an adapted version of the disk apparatus which Lord Rayleigh [4] employed in 1882 for the first quantitative measurement of ordinary sound intensity. This *Rayleigh disk* responds to the kinetic energy density of a mechanical wave, without regard to the direction of particle migration, so that the counterflowing nature of the mass transport within liquid helium II in no way affects its performance. It is interesting that this device, developed by Rayleigh in the century before the advent of microphones, is capable of detecting the internal counterflow of quantum hydrodynamics to which microphones are insensitive.

2. Operation of the Classical Rayleigh Disk

The tendency of a flat obstacle to align itself crosswise to the direction of particle velocity in a fluid field was first discussed by Thompson and Tait [5] in 1867 and employed by Rayleigh some fifteen years later

for sound intensity measurements. In 1891 König [6] gave an exact mathematical expression for the torque τ exerted on a disk of radius (a) suspended within an incompressible fluid at an angle φ to the direction of undisturbed particle velocity v,

$$\tau = (4/3)\, \varrho a^3 v^2 \sin 2\varphi \tag{2}$$

This result was obtained by integrating the Bernouilli pressure over the surface of the disk.

How the unbalanced Bernoulli pressures exert a net couple tending to align the disk crosswise to the fluid may be seen by considering the highly variable velocity distribution over the surface resulting from the distortion of the velocity field. In Fig. 1 the fluid flow of initial

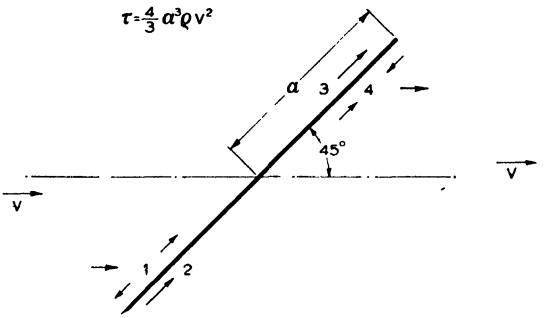

Fig. 1.

undisturbed velocity v encounters the disk at 45°, the angle of maximum effect. For example, the Bernoulli pressure at point 1, where stagnation occurs, exceeds that at point 2 where tangential flow persists. Similarly, fluid flow continues past the front face at point 3, even though stagnation occurs at point 4 where streamlines reconverge behind the disk. The direction of these unbalanced pressures is such as to produce a net torque acting in the counterclockwise direction. Applied to an ordinary sound field in a classical fluid the same torque is seen to exist for the opposite half of the cycle, when the particle motion occurs in the opposite direction. This is evident from figure 1, where it may be seen that the same stagnation points, and flow regions, would occur for flow in the reverse direction. Or, because of the quadratic form of the König expression, the sense of the resultant torque is independent of the direction of particle flow.

Since the disk tends to swing crosswise to the direction of the propagation axis regardless of the instantaneous direction (sign) of particle flow, both halves contribute constructively. The resulting rectifying action enables the device to detect and measure ordinary sound intensity.

3. The Thermal Rayleigh Disk

Thus far we have been considering the operation of the disk in its classical application as a detector of ordinary acoustical energy. This same property of responding to a particle flow irrespective of its actual direction enables the Rayleigh disk also to detect the internal counterflow associated with the heat flow in liquid helium II. The fact that the opposing fluid fields exist simultaneously in opposite directions about the disk is without consequence, as the torque responds strictly to net kinetic energy density rather than to net mass flow. Since this situation holds for both halves of the cycle, a rectifying action occurs as before, and the thermal Rayleigh disk constitutes a detector of second sound.

Assuming that normal fluid interaction with the disk conforms to the classical formula (2) we have for the normal fluid contribution to the torque τ_n when $\varphi = \pi/4$

$$\tau_n = (4/3)\, a^3 \varrho x \, <v_n^2> av \tag{3}$$

Clearly the disk measures only time-average values of the torques, so that the mean square value of particle velocity $<v_n^2>_{av}$ is introduced; the ac term in the expression for torque contributes no net rotation to the disk, and is too high in frequency (hundreds of cycles/sec) to produce any periodic motion. By using the relationship for entropy flow

$$\dot{H}/T = \varrho \, x \, S^* v_n \tag{4}$$

the observed torque may be related directly to heat current density $\dot{H}$ (cal/sec.cm^2) as follows,

$$\tau_n = (4/3)\, (a^3 \varrho/x) \, <\dot{H}^2>_{AV}/(\varrho S^* T)^2 \tag{5}$$

Similarly for the torque resulting from superfluid flow about the disk one obtains

$$\tau_s = (4/3) a^3 \varrho_s v_s^2 = (4/3)\, (a^3 \varrho/(1 - x)) \, <\dot{H}^2>_{AV}/(\varrho S^* T)^2 \tag{6}$$

where the zero momentum relationship (1) has been employed. Finally,

combining these two component torques additively, the net resultant torque τ exerted on the disk by the heat current density $\dot{H}$ becomes

$$\tau = \tau_n + \tau_s = (4/3)\,(a^3\varrho/x\,(1 - x))\,\langle H^2\rangle_{AV}/(\varrho S^* T)^2 \qquad (7)$$

4. Arrangement

A typical assembly [7] employed for conducting measurements with the thermal Rayleigh disk is illustrated in the diagram of Fig. 2. The disk

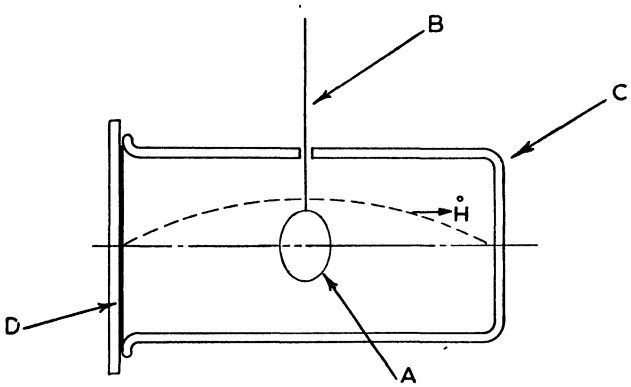

Fig. 2.

A can conveniently consist of a circular mirror (such as a galvanometer mirror) and thus fulfill the dual function of responding to the second sound field and deflecting a beam of light as a measure of the angular displacement produced. Knowledge of the restoring constant of the supporting fiber B provides a direct determination of the torque exerted on the disk A by the second sound field. The disk can be suspended at the midpoint of a horizontally oriented cylindrical glass cavity C, within which resonant second sound waves are set up between the end walls. These temperature waves are generated within the cavity by introducing periodic heating at the proper frequency over the surface of one of the end-walls D. Such heating is produced electrically by means of a uniform a-c current flow through a thin carbon layer comprising the surface of this thermal driving element D.

By tuning this imposed driving frequency for maximum deflection of the disk from equilibrium, the condition of half-wave resonance for the heat waves along the axis of the cavity is attained. For this situation the heat current density $\dot{H}$ is a maximum at the center of the

cavity and decreases cosinusoidally to (nearly) zero at the end walls, as indicated in Fig. 2. The heat current density at the end-wall of the driving element D is not quite zero, being in fact precisely the known heating rate introduced. The actual (undisturbed) heat current density $\dot{H}$ encountered by the disk at the midpoint of the cavity under conditions of resonance is then just this input heating multiplied by the resonance reenforcement factor $(2/\pi)Q$ for the system.

Typical resonance curves for the thermal Rayleigh disk are illustrated in Fig. 3 where torque τ (dyne.cm) is plotted versus frequency for

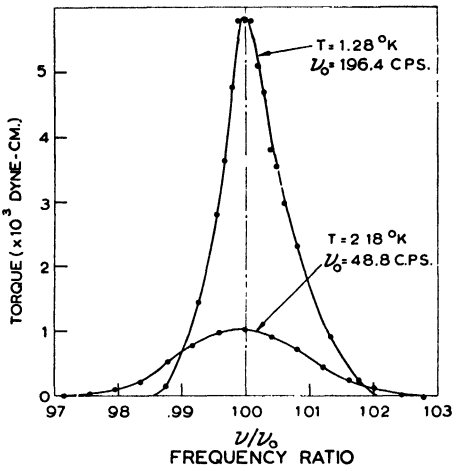

Fig. 3.

two characteristic temperatures. The same value of heat current driving input is maintained at the generator surface D and, in order further to compare the resultant resonance response, torque τ is plotted versus relative frequency ν/ν_o. That is, the system must be retuned for each temperature (because of temperature dependence of wave-velocity) so that resonant frequency ν_o is different for each response curve (as indicated, see Fig. 3). Clearly both the shape and magnitude of the resonance response curves (for constant heat input density) vary with temperature, and two essential criteria are provided by this data. One is the maximum torque τ_{max} exerted by the second sound field on the disk, observable from the resonance peak. The other criterion is the Q of the system specified in the usual manner as $\nu_o/\Delta\nu$, where $\Delta\nu$ here is band-width for half maximum deflection

(which for the case under consideration also represents half-maximum kinetic energy content). Since the input heat current density is amplified at the position of the disk by the resonance reinforcement factor $(2/\pi)Q$, this leads directly to the effective heat current density $\dot{H}$.

5. Performance

The comparison with theoretical values of the torque exerted by the second sound field on the thermal Rayleigh disk is given in Fig. 4, where the ratio $\tau/<\dot{H}^2>_{av}$ is plotted versus temperature (for a disk

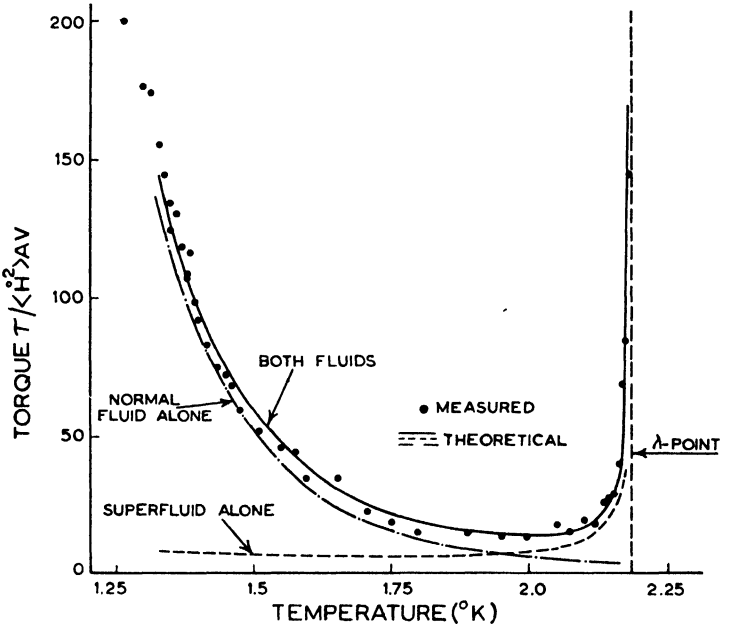

Fig. 4.

of $\frac{1}{2}''$ diam.). Experimental determinations are represented by the solid circles. Theoretical values of this torque ratio for the same disk are indicated by dashed curves for the contribution expected from normal fluid alone, Eq. (5), and also for the contribution expected from superfluid alone, Eq. (6). The torque ratio for the combined effects of both fluids simultaneously is given by the solid curve, Eq. (7), representing the sum of the two. The agreement between this composite curve and the measurements is regarded as confirming the relationship of Eq. (7).

As may be seen from Eq. (7) the variation of torque ratio with temperature depends primarily on the concentration x of normal fluid component; i.e. S^* is relatively temperature insensitive. The torque rises rapidly both near the λ-point, where $(1 - x)$ vanishes, and at very low temperatures, where x decreases. Reference to the theoretical curves for the separate component fluids shows that the normal fluid is responsible for the rise at the lower temperatures, whereas the superfluid component causes the increased torque near the λ-point. In either case the minority component contributes the greater torque, a consequence of the dependence of torque on kinetic energy density plus the zero momentum constraint of Eq. (1). This momentum condition requires the low concentration component to possess the greater particle velocity and accordingly the greater energy density (by virtue of the quadratic dependence on particle velocity).

With the aid of Eq. (12) of Chapter I for the thermodynamic expression for second sound wave velocity v_{II}, the relationship of Eq. (7) for the composite torque on the disk may be given in the alternative form

$$\tau = (4a^3/3)\ (1/\varrho cT)\ (\dot{H}/v_{II})^2 \tag{8}$$

The essential feature of Eq. (8) is its dependence solely on the overall properties of liquid helium II, rather than those related to the separate fluid components. This situation is related to the earlier statement that, whereas the response of the Rayleigh disk to temperature waves is highly consistent with the two-fluid concept, eventual quantum mechanical treatments may proceed quite independently of such a model. Already [3] heat transport in liquid helium II has been described in terms of 'polarized' rotons aligning themselves upstream against the background fluid. An extension of this approach to account for the torque exerted by an oriented roton migration about the disk, plus interaction with the background fluid, should lead to Eq. (8). The form of Eq. (8) allows a measurement of specific heat capacity c by means of the thermal Rayleigh disk. Such determinations are shown in Fig. 5 where c (cal/gm . deg) measured by this means is plotted versus temperature. The points represent values determined using the disk and are compared with measurements by earlier investigators [8] employing conventional methods (See also Ch. VI).

The action of the thermal Rayleigh disk constitutes but a single example of a general type of experiment applicable to liquid helium II,

in which the Bernoulli pressure differences associated with heat current may be utilized. Actually the Bernoulli principle must be extended to include an additional pressure term

$$p = -(\varrho/2x\,(1-x))\,\langle \dot{H}^2 \rangle_{AV}/(\varrho S^* T)^2 = -(\tfrac{1}{2}\varrho CT)\,(\dot{H}/v_{II})^2 \quad (9)$$

to account for the decrease in hydrostatic pressure produced by the counterflowing fluids. This contribution exists independently of the

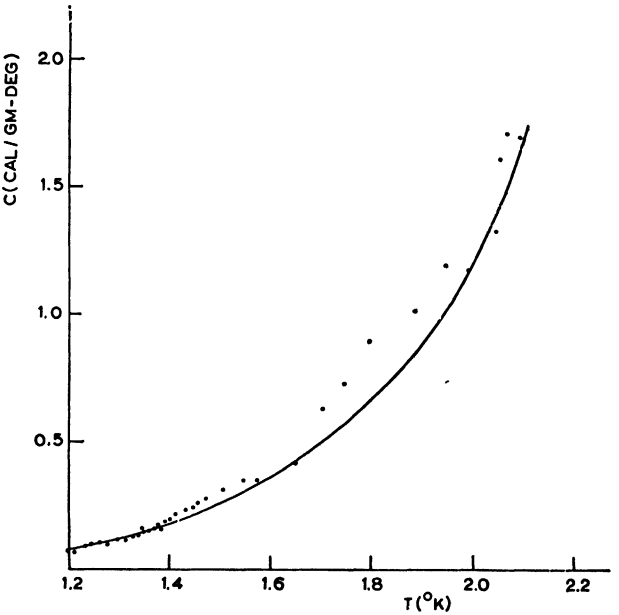

Fig. 5.

usual Bernoulli pressure term $-\frac{1}{2}\varrho v^2$ related to total current flow (which in the present case is repressed).

6. Remarks

The thermal Rayleigh disk provides a direct method for detecting and measuring second sound waves by purely mechanical means, dependent solely upon such fundamentals as kinetic energy density and the geometry. While not necessarily confirming the two-fluid hypothesis, the operation of the disk is consistent with conditions based on that model.

Future applications of the Rayleigh disk include such possibilities as

observing the torque exerted by superfluid alone. This could be accomplished by suspending the disk within a region of steady-state flow of pure superfluid through a background of stationary normal fluid, produced by combining a heat source with a suitable combination of semi-permeable barriers.

REFERENCES

[1] L. Tisza, J. de Phys. et rad., **1**, 165, 350, (1940).
L. Landau, J. Phys. U.S.S.R., **5**, 71, (1941).
[2] V. P. Peshkov, J. Phys., **8**, 381, (1944); **10**, 389, (1946).
[3] R. Feynman, Phys. Rev., **94**, 262, (1954).
[4] Lord Raleigh, Phil. Mag., **14**, 186, (1882).
[5] Lord Kelvin and P. Tait, Natural Philosophy (Oxford University Press, London, 1867), p. 336.
[6] W. König, Wied. Ann. t., **43**, 15, (1891).
[7] J. Pellam and P. Morse, Phys. Rev., **78**, 474, (1950).
J. Pellam and W. Hanson, Phys. Rev., **85**, 216, (1952).
[8] H. C. Kramers, J. D. Wasscher and C. J. Gorter, Physica, **18**, 361, (1952); Leiden Comm. 288*d*.

CHAPTER IV

OSCILLATING DISKS AND ROTATING CYLINDERS IN LIQUID HELIUM II

BY

A. C. HOLLIS HALLETT
DEPARTMENT OF PHYSICS, UNIVERSITY OF TORONTO

1. Introduction

Of the many peculiar properties of liquid helium below its transition temperature (lambda-point), perhaps the most striking is its superfluidity. The liquid will flow through very narrow channels with such large velocities that it is only possible to deduce an upper limit for the viscosity which is of the order of $10^{-5}\,\mu$ poise. Yet the liquid will cause considerable damping of the oscillations of a disk or cylinder suspended in it as if the viscosity of the liquid was about a million times larger than this upper limit.

It was to explain this discrepancy in the value of the viscosity deduced from the results of two different types of experiment that the two fluid model for liquid helium was originally conceived. Liquid helium below the lambda-point (usually known as liquid helium II) is considered to be a homogeneous mixture of a superfluid (zero viscosity) component and a normal (finite viscosity) component. It is the superfluid which flows without friction through the finest of channels, while the finite viscosity of the normal component is responsible for the observed damping of an oscillating disk or cylinder. At any temperature below the lambda-point, the normal component is said to be a fraction x of the whole, or is said to have a density $\varrho_n = x\varrho$ where ϱ is the total density of the liquid. The superfluid is the remaining fraction $(1 - x)$ of the liquid, or may be said to have a density $\varrho_s = (1 - x)\varrho$.

2. Viscous Behaviour of liquid Helium II

Observations of the damping of an oscillating cylinder were first made in 1935 at Toronto by the late Dr Wilhelm in collaboration with Misener and Clark [1]. They lacked an adequate solution of the Navier-Stokes equation for motion of a viscous fluid caused by the oscillations of their cylinder, and were consequently unable to deduce the values of the viscosity from the observed damping with any certainty. In 1938 MacWood [2, 3] of Leiden obtained a solution of the Navier-Stokes equation (subsequently corrected by Hollis Hallett [4] in 1952) which gave the motion of a viscous fluid in the neighbourhood of an oscillating disk, and deduced values of the viscosity from the results of a detailed investigation of the damping of an oscillating disk at various temperatures between 1.2°K and 4°K (Keesom and MacWood [5]).

The physical mechanism which is responsible for the damping of an oscillating system is important because, as it will be shown below, the density of the viscous fluid enters into any calculations, and the relevant density is not the total density of helium II, but the density of the normal component alone. The damping force on an oscillating disk is proportional to the product of the coefficient of viscosity, η, and the velocity gradient at the disk surface. The motion of the disk is propagated outwards in the form of an exponentially damped viscous wave which falls to $(1/e)$ of its initial amplitude at a distance from the disk equal to $\sqrt{(2\eta/\omega\varrho)}$ (where $\omega = 2\pi/T$ if T is the period of oscillation) known as the penetration depth. The velocity gradient is therefore proportional to $v/\sqrt{(2\eta/\omega\varrho)}$, if v is the velocity of the disk, and consequently the damping force is proportional to $\eta/\sqrt{(2\eta/\omega\varrho)}$, i.e. proportional to $\sqrt{\eta\varrho}$. As a result, the damping of the disk gives not a measure of η alone, but a measure of $\sqrt{\eta\varrho}$.

It should be noted that from this argument the fluid extending to a distance $\sqrt{(2\eta/\omega\varrho)}$ from the disk is dragged into motion with the disk by means of the coupling effect of viscosity between the disk and the liquid. But since only the normal component of helium II possesses viscosity, only the normal fluid will be dragged; the superfluid component with zero viscosity cannot be dragged into motion with the disk and therefore remains at rest, assuming that there is no interaction between the two components. Consequently the relevant value of the density is the density of the normal component, and therefore the square of the damping of the disk gives a measure of $\eta_n\varrho_n$. In Fig. 1 is plotted the variation of the square of the damping of a disk in

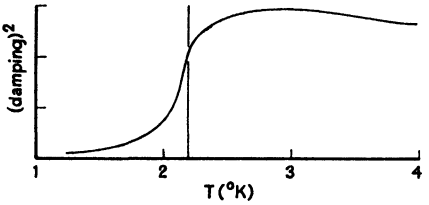

Fig. 1. The variation with temperature of the square of the damping of an oscillating disk.

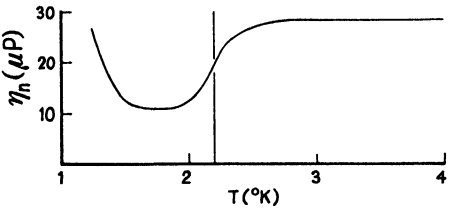

Fig. 2. The variation with temperature of η_n deduced from the results of figure 1.

arbitrary units with temperature, and in Fig. 2, the temperature variation of η_n calculated from the results of Fig. 1 using accepted values of ϱ_n [6]. The striking difference between the shape of the two curves below the lambda-point is due to the fact that ϱ_n decreases very rapidly as the temperature is reduced. At the lambda-point itself, de Troyer, van Itterbeek and van den Berg [7] from whose paper the data for Fig. 1 and 2 are taken, have found no evidence of any discontinuity in the damping.

The normal component which is dragged into oscillation with an oscillating disk will add a moment of inertia to the moment of inertia of the disk itself, and this increased moment of inertia will be observed as an increased period of oscillation of the system. This principle has been used by Andronikashvili [8, 9] in his design of an apparatus which gives values of ϱ_n directly. The apparatus consisted of a pile of 50 thin aluminium disks separated by spacers whose thickness was less than the penetration depth. The normal component between the disks was therefore completely dragged with the apparatus, and the moment of inertia of the system is equal to the moment of inertia of the apparatus plus the moment of inertia of 50 disks of liquid of density ϱ_n whose radius and thickness are known from the measured geometry of the apparatus. Variation of the period of oscillation with temperature can then be interpreted as the variation with temperature of the density of the dragged fluid. The density ϱ_n calculated from these results is shown in Fig. 3.

As it can be seen from Fig. 3, the density of the dragged fluid decreases very rapidly as the temperature is lowered. Consequently at about 1.5°K where $x = 0.1$, the moment of inertia of the dragged fluid is only about 4% of the moment of inertia of the apparatus, and the

experimental errors are correspondingly large. It has therefore been the practice to use data for $\varrho_n = x\varrho$ which can be calculated from the observed values of the velocity of second sound

$$v_{II}^2 = \frac{x(1-x)S^{*2}T}{c} \qquad (1)$$

(Eq. (12) of Ch. I) assuming that values of S^* (see Ch. I) and specific heat c are known. The wisdom of this practice is doubtful, for not only are S^* and c known to only 10%, it has been shown in Ch. I that the specific assumptions which lead to the above equation may not be correct. The correct equation may be

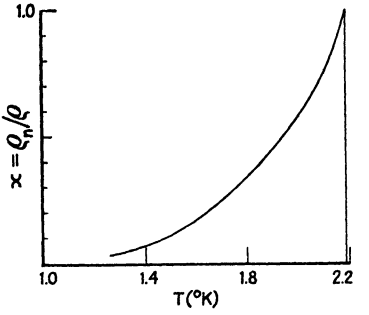

Fig. 3. The variation of $x = \rho_n/\rho$ with temperature. The total density $\rho = 0.145$ g cm^{-3} and is practically independent of temperature.

$$v_{II}^2 = \frac{x(1-x)\,S^*}{(\partial x/\partial T)}, \qquad (2)$$

which is Eq. (11) of Ch. I.

Clearly an experiment which will give unequivocal values of either η_n or ϱ_n with good accuracy over the whole temperature range is extremely desirable. One such experiment designed to give η_n directly has been carried out by Heikkila and Hollis Hallett, and it is possible to give the preliminary results although they have not yet been published elswhere. They have used a rotating cylinder viscometer of the type used by Kellström [10] and Bearden [11] in their determinations of the viscosity of air. The liquid is contained in a hollow vertical cylinder which can be rotated at various constant velocities. Within this cylinder is situated a smaller cylinder which is suspended by a very fine torsion fibre. As the fluid rotates with the outer cylinder, it exerts a viscous torque on the inner cylinder which can be measured by measuring the angular deflection of the inner cylinder from its rest position. Theory shows that the torque exerted upon the inner cylinder is directly proportional to the velocity of rotation of the outer; the constant of proportionality involves the dimensions of the two cylinders and is also proportional to the viscosity. The density of the moving fluid does not enter into the theory at all, with the result that this method has the great advantage that η_n may be determined directly without

using any data other than the dimensions of the apparatus. Working with velocities of rotation in the range 0.01 to 0.05 cm/sec, they found proportionality between torque and rotational velocity and deduced values of the viscosity. The values of η_n so deduced are plotted against temperature in Fig. 4 (full curve) and compared with the oscillating disk values of η_n [4, 7, 12] (dashed curve).

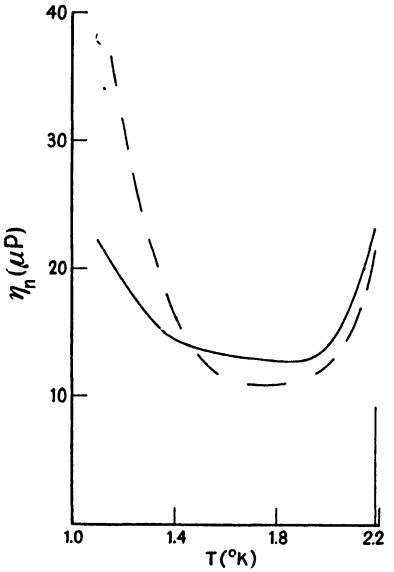

Fig. 4. The variation of η_n with temperature as deduced from the results of the rotating cylinder (full curve) and the oscillating disk (dashed curve).

The discrepancies between the two curves at temperatures less than 1.7°K may well be ascribed to errors in the values of ϱ_n used to obtain values of η_n from the damping of the oscillating disks since these values of ϱ_n were calculated from the velocity of second sound using Eq. (1). In fact, ϱ_n could be deduced from the damping of an oscillating disk if η_n is assumed to be known from the results of the rotating cylinder experiment. But in view of the discrepancies at higher temperatus where values of ϱ_n are known with much greater certainty, one hesitates to ascribe all the low temperature discrepancies to errors in ϱ_n alone. Above 1.8°K, there is almost a constant 12% difference between the two curves, and this rather suggests some constant error in one or both experiments such as might arise from neglect of thermal contraction or error in calibration. Until the reason for the discrepancy at high temperatures is known exactly, it is impossible to use these experiments to decide which theoretical relationship between ϱ_n and v_{II}^2 is correct.

3. Theory of the Viscosity of Liquid Helium II

A theory which predicts the rise of viscosity at low temperatures has been published by Landau and Khalatnikov [13, 14] and is based on Landau's [15] system of quantum hydrodynamics. The assumed energy spectrum of the liquid is shown in Fig. 5 [16]. The elementary excitations have energy ε and are regarded as particles of momentum p.

Initially the energy is proportional to the momentum, $\varepsilon = cp$ where c is the velocity of ordinary sound, and the corresponding excitations are sound quanta or 'phonons'. Near the minimum of the curve there are excitations called 'rotons' which have momentum in the neighbourhood of p_0, and energy $\varepsilon = \Delta + \frac{1}{2}(p - p_0)^2/\mu$ where μ is the effective mass of the roton. Phonons are regarded as excitations of long wavelength, and the rotons as excitations of short wavelength, and the liquid is considered as a mixture of an ideal gas of phonons and an ideal gas of rotons. For this ideal gas assumption to be valid, the number of phonons and rotons must not be large. Consequently the predictions of the theory will not be valid near the lambda-point.

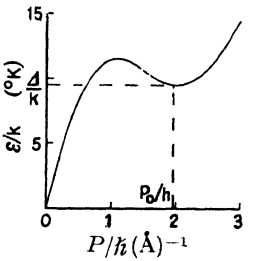

Fig. 5. The energy spectrum of liquid helium II after Landau.

If liquid helium II flows over a plane surface in the $x - y$ plane, viscosity is considered to arise from a transfer of momentum in the z-direction ~~much in the same way that the viscosity of a gas is considered in Kinetic Theory~~. Consideration of the scattering of rotons both by rotons and by phonons, shows that the roton behaves as a massive particle and the phonon as a light particle. Consequently collision of a roton with a phonon leaves the roton momentum practically unchanged and this process gives a negligible contribution to the momentum transfer. Collision of a roton with another roton leads to the roton contribution to the viscosity of the form.

$$\eta_{\text{rot}} = (1/15)\, t_r N_r (p_0^2/\mu)$$

Here t_r is the mean time between collisions, and N_r represents the number of rotons. As the temperature decreases, the number of rotons decreases, and consequently the mean time between collisions must increase. As a result $t_r N_r$ is independent of temperature, and therefore η_{rot} is a constant, independent of temperature.

Scattering of phonons by rotons and by phonons leads to the phonon contribution to the viscosity, η_{ph}. Above 0.9°K the density of rotons is considerably greater than the density of phonons, and therefore scattering of phonons by rotons will be the most important mechanism of momentum transfer. This leads to the phonon contribution to the viscosity which varies with temperature as $T^{-\frac{1}{2}} \exp(\Delta/kT)$. The total viscosity is therefore

$$\eta = \eta_{\text{rot}} + \eta_{\text{ph}}$$

which may be written as

$$\eta = A + B\,T^{-\frac{1}{2}} \exp\,(\Delta/kT)$$

where A and B are constants independent of temperature. It should be pointed out that the constants A and B contain many parameters which are not known with any degree of accuracy, so that for a comparison with experimental data it is necessary to choose suitable values which best fit the experimental curve at some point.

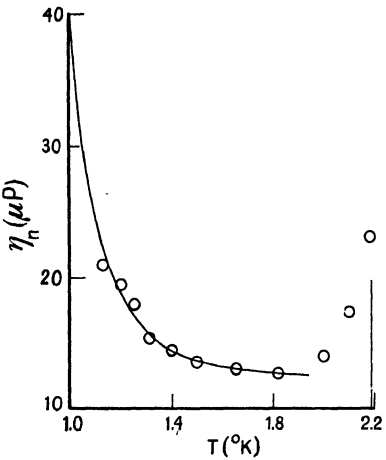

Fig. 6. Comparison of the theory of Landau and Khalatnikov (full curve) with the results of the rotating cylinder viscometer (open circles).

The full curve which is drawn in Fig. 6 has been calculated from the Landau-Khalatnikov theory with suitably chosen values of A and B and shows good agreement with the experimental results obtained with the rotating cylinder viscometer. The value of Δ/k used for this curve was 8° as deduced by Kramers, Wasscher and Gorter [17], from their specific heat measurements. As it was pointed out earlier, the theory does not hold near the lambda-point, and therefore no agreement between experiment and theory above 1.8°K can be expected. It should also be pointed out that even with Δ/k chosen, there still remain two constants which are fitted to the experimental data, with the result that the agreement between the theory and experiment shown in Fig. 6 may be to some extent a result of good curve fitting; the temperature range covered by the experiment is scarcely large enough to decide definitely whether the viscosity increases as $T^{-\frac{1}{2}} \exp\,(\Delta/kT)$ or as some other function of temperature. However, in spite of this, the Landau-Khalatnikov theory does have the great merit in that it predicts the experimental observation that the viscosity increases as the temperature is lowered; a similar prediction has not yet come from any other theory.

4. Non-viscous Behaviour of Liquid Helium II

In Ch. I it was shown that the flow of liquid helium II through relatively wide channels under the conditions of large temperature gradients could be explained by the assumption of a force of mutual friction [18] between the normal and superfluid components which increased as the cube of their relative velocity. The equations of motion of normal and superfluid components were then formed and these are Eq. (9) and (10) of Ch. I. For the experiments described here, the pressure and temperature gradients are assumed to be negligible, and the term (1/3) grad div $\boldsymbol{v}_n$ is assumed to be very much less than $\Delta \boldsymbol{v}_n$. Consequently the equations become

$$-Ax\,(1-x)\,\varrho^2|\boldsymbol{v}_s-\boldsymbol{v}_n|^2\,(\boldsymbol{v}_s-\boldsymbol{v}_n)=\varrho\,(1-x)\,d\boldsymbol{v}_s/dt \tag{3}$$

for the superfluid component, and

$$+Ax\,(1-x)\,\varrho^2|\boldsymbol{v}_s-\boldsymbol{v}_n|^2\,(\boldsymbol{v}_s-\boldsymbol{v}_n)+\eta_n\Delta\boldsymbol{v}_n=\varrho x\,d\boldsymbol{v}_n/dt \tag{4}$$

for the normal component.

For viscosity determinations it has always been assumed that the damping of an oscillating disk results from a motion of the liquid given by

$$\eta_n\Delta\boldsymbol{v}_n=\varrho x\,d\boldsymbol{v}_n/dt. \tag{5}$$

This assumption has been justified by the experimental result that there is no observable dependence of the damping upon the amplitude of swing of the disk or upon its velocity. If the term giving the effect of mutual friction is taken into account, it is found that the damping should increase as the velocity increases. Since this increase of damping with velocity has never been observed, it is presumed that the velocities have been too small for the mutual friction to be important.

Experiments were carried out by Smith [19] at Leiden and by Hollis Hallett [4, 20] at Cambridge to observe the damping at larger velocities, and to see if such an increase in the damping could be found. Smith found no such increase up to an amplitude of 0.2 radian, or a velocity of 0.25 cm/sec. Hallett had, however, investigated amplitudes up to 1 radian and had found striking variation of damping with amplitude in the range 0.2 to 1 radian as shown in Fig. 7. It will be observed from this figure that as the amplitude of oscillation, Φ, increases, the damping is initially independent of amplitude until a certain amplitude Φ_m is reached. Further increase of amplitude causes the damping to increase, quickly at first, but more slowly as Φ increases further, and

it tends to level off to some extent in the region of $\Phi = 1$ radian. It can be further observed that the damping varies more with amplitude as the temperature is reduced, and no such variation of the damping

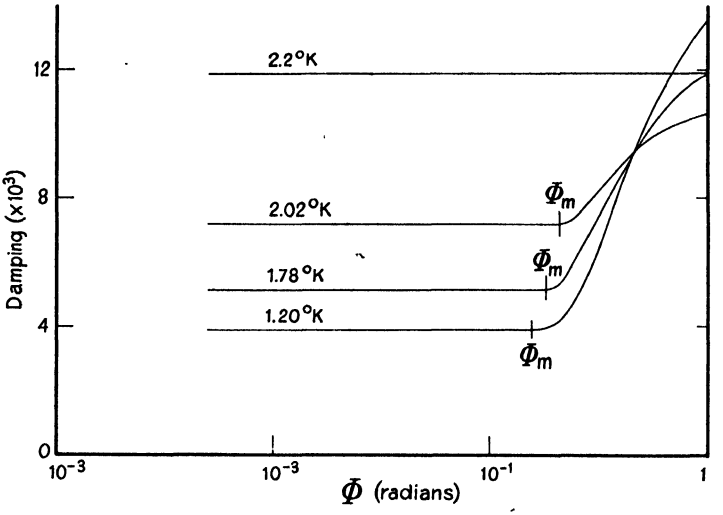

Fig. 7. The variation with amplitude of the damping of a disk oscillating with a period of 11 sec.

is observed in helium I at 2.2°K. The damping at amplitudes less than Φ is controlled by the viscosity and density of the normal component as shown in § 2; the variation of the damping with amplitude at amplitudes greater than Φ_m is apparently due to some non-linear friction which is more important that viscosity.

Similar variation of damping with amplitude had also been observed with a pile of disks which was similar to Andronikashvili's apparatus for the determination of ϱ_n. It was also observed with this apparatus that the period of oscillation increased with amplitude as shown in

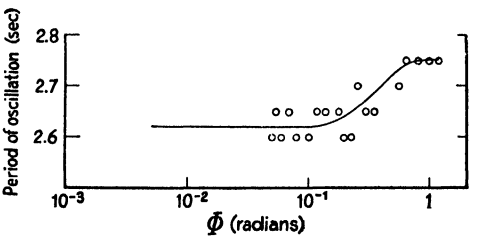

Fig. 8. The variation with amplitude of the period of oscillation of a pile of disks.

Fig. 8. In general, the period seemed to begin to increase at about the same Φ_m at which the damping increased; at short periods (i.e. large velocities) the period seemed to flatten off at a constant value at large amplitudes. This increase of period was interpreted as the result of an increased moment of inertia of the fluid dragged between the disks which could only arise from an increase in the density of the dragged fluid. Estimations of the density of this dragged fluid at the largest amplitudes showed that at large velocities where the period had increased to a constant value, the density of the carried fluid had changed from ϱ_n at small amplitudes to ϱ at large amplitudes. Evidently the non-linear frictional forces which cause the increase in damping are also responsible for the dragging of the superfluid component into motion with the normal.

It should be pointed out that a variation of damping with amplitude similar to that illustrated in Fig. 7 would result from the assumption of turbulence in the normal component. The constant damping at small amplitudes is certainly the result of laminar motion of the normal component but this may well become unstable at the amplitude Φ_m for which the Reynolds Number $(v_m R\varrho_n/\eta_n)$ (where $v_m = 2\pi R\Phi_m/T$ if R and T are respectively the radius and period of oscillation of the disk) reaches a critical value. The increase of damping at larger amplitudes could well be ascribed to the added dissipative effects of turbulence in the motion of the normal component. Calculation of the Reynolds Numbers using the observed values of Φ_m at various temperatures, leads to values which decrease from about 6000 at 2.17°K to about 20 at 1.2°K. Even if these values were considered large enough as measures of the limit of stability, it should be pointed out that in helium I, Φ_m is greater than 1 radian, and the corresponding Reynolds Number is greater than 50000. Since the motion is not turbulent for a Reynolds Number of 50000, it is most unlikely to be turbulent for the lower Numbers encountered in liquid helium II.

It has often been suggested that because the viscosity of the superfluid component is zero, the Reynolds Number corresponding to its motion is infinite, no matter what the velocity of the superfluid component. Thus, if the superfluid component moves at all, its motion is turbulent. This may possibly account for the excessive damping once Φ_m has been exceeded, because the superfluid component is evidently moving, but this gives no mechanism whatsoever which can possibly cause the superfluid to begin to move in the first instance.

The mutual friction of Gorter and Mellink, however, provides an interaction between the two components and does certainly give a mechanism which will cause the superfluid component to be dragged into motion with the normal. It also provides additional dissipative forces which will cause the damping of a disk to exceed the value which the viscous damping has at small amplitudes. Consequently the predictions of the Gorter-Mellink theory agree well in a qualitative manner with the experimental results. However, when put to numerical test, the mutual frictional force is inadequate; it predicts values of the damping which are considerably less than the dampings actually observed.

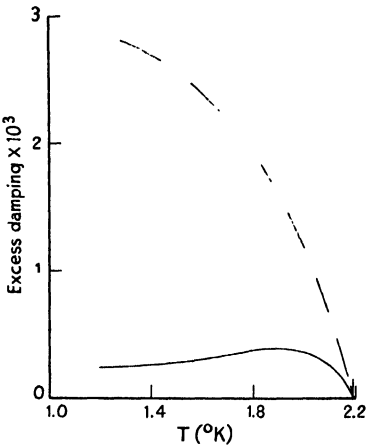

Fig. 9. The variation with temperature of the damping of a single disk which is in excess of the viscous damping at an amplitude of 0.2 radian. The full curve shows the excess damping predicted by the Gorter-Mellink theory; the dashed curve shows the actual experimental results.

The damping in excess of the viscous damping, which results from the action of the Gorter-Mellink mutual friction, has been calculated by Zwanikken [21] for a single disk. The comparison between the theory (full curve) and experiment (dashed curve) is shown in Fig. 9 which is drawn from the results obtained at an amplitude just above Φ_m with a single disk oscillating with a period of 3.8 sec. From these curves it can be seen that the Gorter-Mellink mutual friction does not agree in magnitude with the observed excess damping, particularly at low temperatures, nor does it predict the correct temperature dependence.

Another attack on the problem was made by Hollis Hallett [22] using the rotating cylinder viscometer described in § 2. For this apparatus there is a further simplification of the hydrodynamical Eq. (3) and (4), for the velocities are constant and independent of time. Consequently the equations become

$$-Ax\,(1-x)\,\varrho^2|\boldsymbol{v}_s-\boldsymbol{v}_n|^2\,(\boldsymbol{v}_s-\boldsymbol{v}_n)=0 \tag{6}$$

$$+Ax\,(1-x)\,\varrho^2|v_s-v_n|^2\,(\boldsymbol{v}_s-\boldsymbol{v}_n)+\eta_n\Delta_n=0 \tag{7}$$

with the net result that the force of mutual friction is zero, and the equation of motion of the fluid is

$$\eta_n \Delta \boldsymbol{v}_n = 0. \tag{8}$$

The solution of this equation with the appropriate boundary conditions leads directly to the result that the torque upon the inner cylinder is directly proportional to the velocity of rotation of the outer, and that the constant of proportionality is itself proportional to η_n.

The variation of torque with velocity which was actually observed in helium II is illustrated by the full curve of Fig. 10. The straight dashed line of this figure represents the variation of torque with velocity which would have been expected had the torque been a result of the viscous forces of the normal component alone. It can be readily seen that the observed torque is considerably larger than that due to viscosity and that the qualitative result seems to be the same as that found with the oscillating disk. At small velocities the torque exerted upon the inner cylinder is the result of the viscous drag produced by laminar motion of the normal component. As the velocity increases, there comes a certain velocity above which the torque increases above the value due to viscosity as if non-linear frictional forces are becoming important.

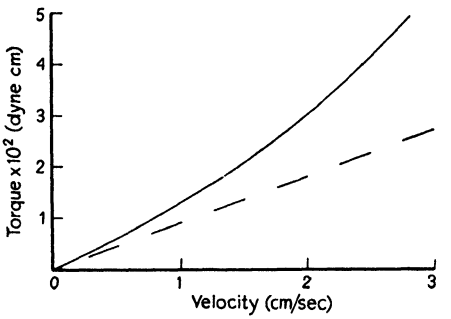

Fig. 10. The variation with velocity at 1.84°K of the torque exerted upon the inner cylinder of the rotating cylinder viscometer. The full curve shows the experimental results; the dashed curve shows the expected variation due to viscosity alone.

The results of the rotating cylinder viscometer give more definite confirmation of the conclusions reached in the discussion of the results of the oscillating disk experiment. The excessive torques observed cannot be due to the Gorter-Mellink mutual friction alone, because this force vanishes from the equations of motion of the liquid. Also, the results cannot be due to turbulence, for, as Taylor [23] has shown both by theory and experiment, the geometrical arrangement in which the outer cylinder rotates while the inner is at rest, gives a motion of the fluid which is stable against fluctuations due to turbulence at all velocities.

Evidently the Gorter-Mellink mutual friction by itself does not explain the results of these types of experiment, and it is necessary to postulate the existence of some new type of frictional force. Hallett

has suggested that possibly this force may have the character of a frictional force within the superfluid component itself, capable of exerting a tangential force on a solid boundary. Certainly the observed excess dampings of a disk (Fig. 9) increase rapidly as the temperature is lowered and, in fact, appear to have the same temperature dependence as ϱ_s, the density of the superfluid component. This does rather suggest that this new type of frictional force is in some way dependent upon the amount of the superfluid component present. Also, the rapidity with which the damping of a disk (Fig. 7) increases with amplitudes for amplitudes greater than Φ_m, does rather suggest that Φ_m is in some way a critical amplitude, and that the non-linear frictional forces act only when Φ_m is exceeded and do not act at all fluid velocities. It is, however, important to note that these experiments do not prove that the Gorter-Mellink mutual friction does not exist; they merely prove that by itself the Gorter-Mellink mutual friction is inadequate. Perhaps the superfluid component relies upon a mutual friction to bring it into motion, but once in motion, it is able to exert a tangential retarding force on a moving solid boundary.

REFERENCES

[1] J. O. Wilhelm, A. D. Misener and A. R. Clark, Proc. Roy. Soc. A, **151**, 342, (1935).
[2] G. E. MacWood, Physica, **5**, 374, (1938).
[3] G. E. MacWood, Physica, **5**, 763, (1938).
[4] A. C. Hollis Hallett, Proc. Roy. Soc. A., **210**, 404, (1952).
[5] W. H. Keesom and G. E. MacWood, Physica, **5**, 737, (1938).
[6] V. P. Peshkov, Phys. Soc. Camb. Int. Conf. Report on Low Temp. p. 19, (1946).
[7] A. de Troyer, A. van Itterbeek and G. J. van den Berg, Physica, **17**, 50, (1951).
[8] E. L. Andronikashvili, Jour. Phys. U.S.S.R., **10**, 201, (1946).
[9] E. L. Andronikashvili, Jour. Exp. Theor. Phys., **18**, 424, (1948).
[10] G. Kellström, Phil. Mag., **23**, 313, (1937).
[11] J. A. Bearden, Phys. Rev., **56**, 1023, (1939).
[12] E. L. Andronikashvili, Jour. Exp. Theor. Phys., **18**, 429, (1948).
[13] L. D. Landau and I. M. Khalatnikov, Jour. Exp. Theor. Phys., **19**, 637, (1949).
[14] L. D. Landau and I. M. Khalatnikov, Jour. Exp. Theor. Phys., **19**, 709, (1949).
[15] L. D. Landau, Jour. Phys. U.S.S.R., **5**, 71, (1941).
[16] L. D. Landau, Jour. Phys. U.S.S.R., **11**, 91, (1941).
[17] H. C. Kramers, J. D. Wasscher and C. J. Gorter, Physica, **18**, 329, (1952).
[18] C. J. Gorter and J. H. Mellink, Physica, **15**, 285, (1949).

[19] P. L. Smith, Physica, **16,** 808, (1950).
[20] A. C. Hollis Hallett, Proc. Phys. Soc. Lond. A, **63,** 1367, (1950).
[21] G. C. J. Zwanikken, Physica, **16,** 805, (1950).
[22] A. C. Hollis Hallett, Proc. Camb. Phil. Soc., **49,** 717, (1953).
[23] G. I. Taylor, Phil. Trans. Roy. Soc. A., **223,** 289, (1923).

CHAPTER V

THE LOW TEMPERATURE PROPERTIES OF HELIUM THREE

BY

E. F. HAMMEL
LOS ALAMOS SCIENTIFIC LABORATORY

1. Introduction

During the year 1948, sufficient pure ^{3}He became available from United States Atomic Energy Commission sources [1] to permit liquefaction of the gas and the determination of a few physical properties[2], [3]. Increasing amounts of the isotope have since been prepared so that at the present time small quantities for research purposes are now generally available from the Isotopes Division US AEC [4]. Prior to 1948 speculations regarding the possibility of liquefying ^{3}He under its own vapor pressure were generally unfavorable [5] with the exception of a paper by de Boer and Lunbeck [6], based upon the former's quantum statistical theory of corresponding states [7], in which probable values of the critical constants, vapor pressure, molar volume and internal energy at 0°K were presented. The experimental values for most of these quantities became available a few months later and agreed with the predictions to within a few percent, thus providing a striking confirmation of de Boer's theory.

The properties of ^{3}He, besides having an intrinsic value of their own, were anticipated with particular interest since they were expected to help explain the apparently more complicated behavior of liquid ^{4}He. It is well known that the two most successful theories for ^{4}He, the London-Tisza [8] and the Landau [9] theory, differ in the relative importance assigned the role of statistics. It was therefore believed that the behavior of pure ^{3}He would provide a critical test of these two theoretical approaches. To date the evidence is inconclusive. Since recent theoretical treatments [10], recognizing the contribution of both theories

in different temperature regions have sought to embrace both viewpoints, future experiments on ^{3}He may be expected to complement those on ^{4}He rather than provide support for one theory or another.

2. Theory of Liquid ^{3}He

2.1. Introduction

The success of the London [8] interpretation of the behavior of liquid ^{4}He in terms of the condensation of an ideal Bose-Einstein gas clearly suggested a similar approach to the problem of liquid ^{3}He. Possibly because there was no evidence to the contrary, this idea seems generally to have been accepted, with the result that, to date, almost all theoretical discussions of liquid ^{3}He have been based upon the statistical mechanics of an ideal Fermi-Dirac gas. It was of course understood that such a model was a very crude approximation at best, since it neglected all molecular interactions.

In contrast to the behavior of a B.E. gas no condensation phenomenon is possible for an ideal Fermi-Dirac fluid, although the latter will definitely exhibit a unique set of properties which may be compared with experiment. As will be apparent later, the experimental results have so far failed to support this theoretical approximation. This means (a) that the degeneracy temperature is much lower than previously suspected, e.g., the mass of the 'particles' comprising the assembly may be greater than that of a single ^{3}He atom, (b) that the ideal gas is an unsatisfactory limiting model, or (c) that the statistics play a relatively minor role in the behavior of the liquid. For comparison with experimental data and to illustrate the above conclusion, the results of the ideal F.D. gas treatment shall nevertheless be briefly presented.

2.2. Ideal Fermi-Dirac Gas Approximation

For an ideal F.D. gas the various thermodynamic quantities are given in terms of the well known F.D. functions,

$$\frac{U}{R} = \frac{3}{2} T \frac{F_{3/2}(\eta)}{F_{1/2}(\eta)}$$

$$\frac{S}{R} = \frac{5}{2} \frac{F_{3/2}(\eta)}{F_{1/2}(\eta)} - \eta$$

$$\frac{c_v}{R} = \frac{15}{4} \frac{F_{3/2}(\eta)}{F_{1/2}(\eta)} - \frac{9}{4} \frac{F_{1/2}(\eta)}{F_{1/2}'(\eta)}$$

where

$$F_k(\eta) = \frac{1}{k!}\int_0^\infty \frac{x^k}{e^{x-\eta}+1}\,dx.$$

For $T < T_0/10$ (large values of η) the above equations reduce to

$$\frac{U}{R} \approx \frac{3\,\varepsilon_0}{5\,k}\left\{1 + {}^5/_{12}\,\pi^2\left(\frac{kT}{\varepsilon_0}\right)^2 + \ldots\right\} \tag{1}$$

$$\frac{c_v}{R} \approx \frac{S}{R} \approx 4.93\left(\frac{kT}{\varepsilon_0}\right)$$

where

$$\varepsilon_0 = kT_0 = \frac{h^2}{8}\left(\frac{3\varrho}{\pi}\right)^{2/3}\left(\frac{1}{m}\right)^{5/3}.$$

Introducing the appropriate values for the mass and density of liquid ^{3}He, Singwi [11] and Goldstein [12] have computed values of the specific heat and entropy for the corresponding ideal F. D. gas model for which the degeneracy temperature is $T_0 \approx 5°$K. Their results will be compared with experiment in § 4.6.

Heer and Daunt [13] have modified the above treatment by the introduction of a smooth potential well throughout the whole volume of the liquid. Although their theory is applied primarily to the interpretation of mixtures, the authors derive a semi-theoretical vapor pressure equation for pure ^{3}He (applicable for temperatures below one quarter of the assumed degeneracy temperature) which agrees with the experimental data within 2.5% between 1° and 1.8°K,but diverges both above and below these limits.

Pomeranchuk [14] has also employed an ideal F.D. gas approximation in the development of a theory of liquid ^{3}He which differs from the above treatments primarily in that the system is described in terms of the Landau [9] model of liquid ^{4}He and certain consequences of the rigorous ideal gas F.D. theory are introduced as assumptions. It is assumed that the 'quasi particles' or more properly the 'elementary excitations' in liquid ^{3}He obey F.D. statistics. For temperatures much less than T_0 the momenta of the excitations will be close to p_0, the momentum at the top of the Fermi surface. Hence the 'excitation' energy will be given by

$$\varepsilon = \frac{(p_0 + \Delta p)^2 - p_0^2}{2\mu} = v\Delta p$$

where μ is the excitation mass and v is the velocity of the excited particle. The number of 'excitations' per cm^3 is

$$n(\varepsilon) \sim p_0^2 \Delta p \hbar^{-3} \sim p_0^2\, \varepsilon \hbar^{-3} v^{-1}.$$

The internal energy is given by

$$\begin{aligned} U &= U_0 + n(\varepsilon) \times \varepsilon \\ &= U_0 + \tfrac{1}{2} a' \varepsilon^2 \end{aligned}$$

where

$$a' = p_0^2 v^{-1} \hbar^{-3} \pi^{-2}.$$

Since under these conditions ($T << T_0$), $\varepsilon \approx kT$, then

$$n(\varepsilon) \approx N\, T/T_0$$

assuming the occupation probability of the first few excited states is approximately unity. From this it follows that

$$U = U_0 + \tfrac{1}{2}\, a\, T^2 \text{ and } c_v = a\, T$$

a is here approximately equal to the coefficient of T^2 in Eq. (1). Since the results are essentially identical with those of the ideal F.D. gas treatment, Pomeranchuk's use of the fact that the excitation energy distribution is approximately classical while a valid and interesting physical interpretation of the $T << T_0$ approximation of the ideal F.D. gas, in reality adds nothing new to the discussion. Furthermore, his estimate of $T_0 = 5°$K implies that the 'quasi particles' are actually treated as single ^{3}He atoms.

2.3. Other Theoretical Discussions of Liquid ^{3}He

A number of theories of liquid helium have been proposed [15] which are sufficiently general to be applied both to liquid ^{3}He and liquid ^{4}He. Many of these endeavor to account for interactions between the particles. The lack of a satisfactory theory of liquids has, however, prevented the development along these lines of even a moderately comprehensive and satisfactory explanation of the properties of liquid ^{3}He.

Other recent theories [16] of liquid ^{4}He consider the ^{3}He case sufficiently different to warrant a new and separate approach.

3. The State Properties of ^{3}He

3.1. Density

The densities of the liquid and saturated vapor derived from measurements of $\varrho_l - \varrho_v$ by Grilly, Hammel and Sydoriak [3] have recently been redetermined by Kerr [17], using a technique which permitted direct measurement of ϱ_l and ϱ_v. His results are reported in Tab. 1 and Fig. 1. The critical density was found to be 0.0413 g/cm^3. The

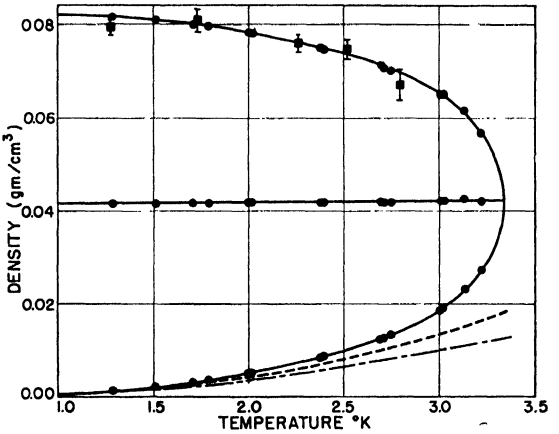

Fig. 1. Orthobaric densities of ^{3}He
Legend: ● Kerr. ⊣ Grilly, Hammel and Sydoriak.
— — — — pressure virial. — · — · — · ideal gas.

extrapolated liquid density at absolute zero is 0.082 g/cm^3. From Kerr's data the rectilinear diameter equation is $\varrho_m = 0.0412 + 4.14 \times 10^{-5}\, T$.

Since the coefficient of T is almost equal to zero, the rectilinear diameter is effectively parallel to the temperature axis and ^{3}He is thus the only substance for which the critical density is half the liquid

TABLE 1. ^{3}He Orthobaric Densities
(Smoothed values)

T_K °K*	ρ_l gm/cm^3	ρ_v gm/cm^3	T_K °K*	ρ_l gm/cm^3	ρ_v gm/cm^3
0.0	0.08235	0	2.4	0.07448	0.00806
1.0	0.08185	0.00058	2.6	0.07200	0.01056
1.2	0.08147	0.00098	2.8	0.06882	0.01376
1.4	0.08093	0.00154	3.0	0.06462	0.01798
1.6	0.08020	0.00228	3.1	0.06193	0.02067
1.8	0.07924	0.00325	3.2	0.05861	0.02400
2.0	0.07801	0.00450	3.3	0.05416	0.02845
2.2	0.07645	0.00608	3.34	0.04131	0.04131

* Kistemaker Scale

density at absolute zero. The saturated vapor density is accurately represented by use of the calculated [18], [19] second virial coefficients using the inverse volume expansion up to 2.8°K, beyond which the calculated densities become imaginary. Use of the corresponding pressure expansion requires the use of higher virals than the second to achieve the same accuracy (see Fig. 1).

3.2. Critical Constants

The critical constants of ^{3}He are given in Tab. 2.

TABLE 2

T_c °K	P_c mmHg	V_c cm^3/mol
3.35 ± 0.02[1a]	890 ± 20[1a]	73.23[17]

3.3. The Equation of State of the Gas

The second virial coefficient for gaseous ^{3}He at low temperatures was first computed by de Boer, van Kranendonk and Compaan [18], using a Lennard-Jones 6—12 potential with constants fitted by de Boer and Michels [20] to the high temperature experimental virial coefficient data of ^{4}He. These calculations have recently been repeated and extended by Kilpatrick, Keller, Hammel and Metropolis [19] for ^{3}He, using the same potential function. Since experimetal data on ^{3}He are not yet available* the theoretical results are presented in Tab. 3 and are contrasted with those for ^{4}He in Fig. 2.

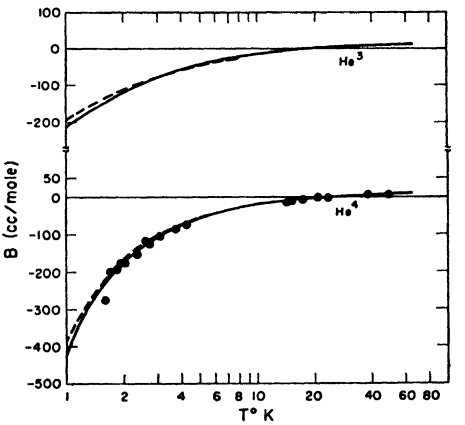

Fig. 2. Second Virial Coefficients of ^{3}He and ^{4}He
Legend: ——— Calculated, Kilpatrick *et al.* — — — — Calculated, de Boer *et al.* ● Experimental values

The calculations of Kilpatrick *et al.* demonstrated that practically all of the difference between the second virial coeffi-

* Recent experimental measurements by Keller [60] have yielded second virial coefficients of ^{3}He at 1.51 and 2.15°K of —169.5 and — 117.9 cm^3/mole respectively. These data lie about midway between the calculated values reported above [19] and a new calculation by Kilpatrick, Keller, and Hammel[56] of the second virial coefficient of ^{3}He using an exp. — 6 potential.

cients for ^{3}He and ^{4}He above 4°K is attributable to the difference in mass rather than the difference in statistics.

TABLE 3. Second Virial Coefficients of ^{3}He (Lennard-Jones Potential) [19]

T°K	B_{33} cc/mole	T°K	B_{33} cc/mole
0.5	— 320	5.0	— 43.49
1.0	— 214.4	6.0	— 34.11
1.2	— 187.08	7.0	— 27.29
1.4	— 165.13	8.0	— 22.11
1.6	— 147.21	9.0	— 18.04
1.8	— 132.36	10.0	— 14.75
2.0	— 119.89	15.0	— 4.77
2.2	— 109.29	20.0	0.28
2.4	— 100.18	25.0	3.29
2.6	— 92.28	30.0	5.28
2.8	— 85.38	35.0	6.67
3.0	— 79.29	40.0	7.70
3.2	— 73.88	50.0	9.07
3.4	— 69.05	60.0	9.93
4.0	— 57.25		

4. Thermal Properties

4.1. The Vapor Pressure of Liquid ^{3}He

The vapor pressure of liquid ^{3}He has been determined over the temperature range 0.5 — 3.3°K [14, 2, 21]. The most accurate results are represented by the following empirical vapor pressure equations (to which no theoretical significance is attached).

Sydoriak and Roberts:

$$\log_{10} p_{mm} = -\frac{1.0343}{T} + 2.5 \log_{10} T - 0.0426\, T + 2.0160 \text{ for } 0.4 < T < 1.5\text{°K} \tag{1}$$

Abraham, Osborne and Weinstock:

$$\log_{10} p_{mm} = -\frac{0.97796}{T} + 2.5 \log_{10} T + 0.000302\, T^2 + 1.91594 \text{ for } 1.0 < T < 3.3\text{°K} \tag{2}$$

Values at selected temperatures are given in Tab. 4.

4.2. The Specific Heat of Liquid ^{3}He

The specific heat of liquid ^{3}He has been measured by de Vries and

TABLE 4. The Vapor Pressure of Liquid ^{3}He

T°K†	P mmHg[21]	T_K°K*	P mmHg[1a]
0.5	0.149	1.0	8.68
0.55	0.290	1.2	19.93
0.6	0.515	1.4	38.33
0.65	0.850	1.6	65.50
0.7	1.322	1.8	102.94
0.75	1.962	2.0	152.04
0.8	2.80	2.5	334.44
0.85	3.86	3.0	617.89
0.9	5.18	3.195	760.0
0.95	6.78	3.3	844.74

† Temperature scale based on susceptibility measurements using chrome methyl amine alum. Calibration based on ^{3}He vapor pressure (T_K scale Ref. 1a) in temperature range 1.0 – 2.9°K.

* Kistemaker scale as employed in Ref. 1a.

TABLE 5. The Specific Heat of Liquid ^{3}He

T°K	c_{sat} cal/deg mole		
	Ref. 22†	Ref. 23*	Ref. 24*
0.4	—	0.79	—
0.5	0.92	0.82	0.77
0.6	0.92	0.86	0.82
0.7	0.93	0.90	0.87
0.8	0.94	0.94	0.91
0.9	0.96	0.98	0.96
1.0	1.00	1.03	1.01
1.2	1.17	1.15	—
1.4	1.41	1.29	—
1.6	1.77	1.45	—
1.8	2.16	1.64	—
2.0	2.58	1.87	—
2.2	3.04	2.14	—
2.4	—	2.44	—

† Numerical values from personal communication from de Vries based on work reported in Ref. 22. Equation suggested by the authors giving a fair fit to data over range indicated is:

$$c_{sat} = 3.72\,T - 4.74\,T^2 + 1.72\,T^3 + 0.565\,T^4 - 0.263\,T^5 \text{ cal/deg. mole. } 0.5 < T < 2.25.$$

* Specific heats were obtained from the following empirical equations representing the best fit to the experimental data obtained by each investigator.
Roberts and Sydoriak: $c_{sat} = 0.667 + 0.290\,T + 0.078\,T^3$ cal/deg mole, $0.4 < T < 2.4$.
Osborne, Abraham and Weinstock: $c_{sat} = 0.53 + 0.48\,T$ cal/deg mole, $0.42 < T < 1.06$.

Daunt [22], Roberts and Sydoriak [23], and Osborne, Abraham and Weinstock [24]. Smoothed experimental results are presented in Tab. 5.

4.3. The Melting Curve for ^{3}He*

The melting curve for ^{3}He has been determined by Osborne, Abraham and Weinstock [25] from 0.16°K to 1.51°K. From 0.5°K to 1.5°K the data are represented by the equation

$$P = 26.8 + 13.1\ T^2 \text{ atmos}$$

Below 0.5°K the results diverge from the equation and approach a constant value of $P = 29.3$ atmospheres as shown in Fig. 3. The ob-

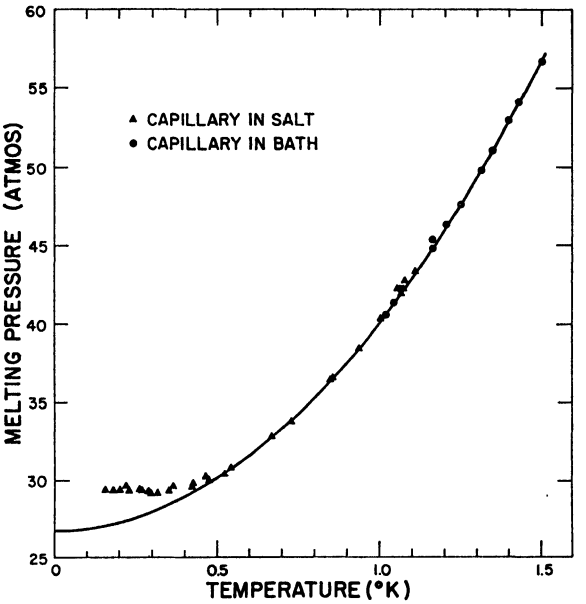

Fig. 3. Melting Curve of ^{3}He

served experimental behavior below 0.5°K may be due to lack of thermal equilibrium between the ^{3}He capillary and the paramagnetic salt, or a peculiarity of the blocked capillary technique pointed out by Sydoriak [26] which, in the event that the slope of the melting line changed sign, would continue to record the minimum of the melting

* The pressure – temperature curve of melting ^{3}He has been measured in the region 75 – 3525 kg/cm^2 and 1.95 – 30°K with an accuracy of at least 0.1% in pressure and 0.1°K in temperature by Grilly and Mills [58]. A provisional equation for the melting line is: $P(\text{kg/cm}^2) = 24.15 + 20.099\ T^{1.5168}$.

curve, *i.e.*, when the bath temperature is reduced below that of the minimum in a melting curve, the block will form higher up in the capillary at the temperature of the minimum.

Pomeranchuk [14] was the first to point out that in solid helium the amplitude of the zero point energy oscillations will probably be small in comparison with the internuclear distances. Under these conditions the exchange forces leading to spin alignment will be very small until the temperature is so reduced that kT is of the order of the magnetic coupling energy of neighboring dipoles ($T \approx 10^{-7}$°K). Since the thermal entropy of the solid is negligible between this temperature and a few degrees K, the total solid entropy within this temperature range should be $R \ln 2$.

For the liquid, on the other hand, ordering of the spins may be expected to occur at physically accessible temperatures, since the ex-

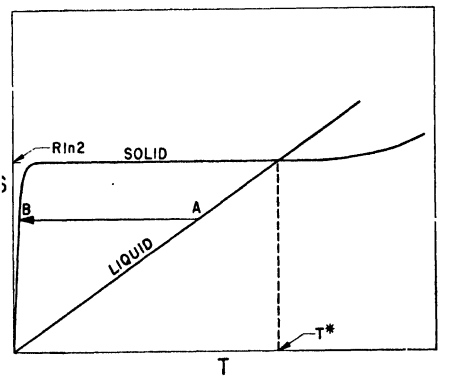

Fig. 4. Entropy of solid and liquid ^{3}He. (Schematic).

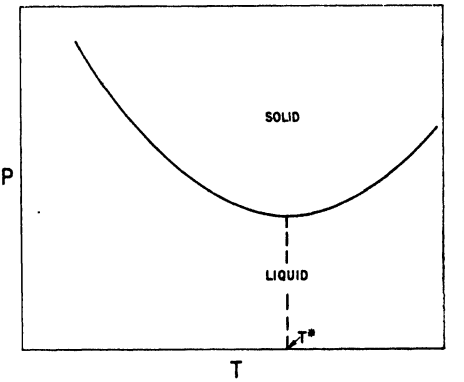

Fig. 5. Melting line of ^{3}He. (Schematic).

change energy leading to spin alignment should comprise a sizable fraction of the interaction energy. Consequently when the entropy of the liquid (spin plus thermal) decreases below $R \ln 2$, ($T = T^*$) the slope of the melting line should change sign (assuming $V_l - V_s$ remains positive) as shown in Figs. 4 and 5.

In consequence, below T^*, the heat of fusion, $\Delta H_f = T(S_l - S_s)$ will be negative. Furthermore an adiabatic solidification of the liquid below T^* by compression, process A → B in Fig. 4, should yield in principle extremely low temperatures (of the order of 10^{-7}°K.)

An examination of the experimental melting curve of ^{3}He (Fig. 3) shows that T^* cannot be greater than 0.5°K, assuming as Pomeran-

chuk does that no nuclear alignment occurs in the solid. The observed leveling off of the melting curve below 0.5°K rather than passing through a minimum is not inconsistent with the specification of $T^* = 0.5$°K, as pointed out above. If the thermal entropy of the liquid is not trivial at this temperature, as seems probable, some alignment of spins must have occurred at temperatures above T^*. Thus there is no basis for assuming that a temperature, identified as T^* from the behavior of the melting curve, is in any way related to the onset of spin alignment in the liquid [24, 32]. Chen and London [27] point out in this connection that the assumption of no spin alignment in the solid, though probable, is not yet verified. The gradual or discontinuous elimination of any spin alignment in the liquid as the pressure increases toward the freezing pressure, is also not inconsistent with the experimental results [27].

4.4 Theoretical Considerations

The quantities discussed above are related thermodynamically, and these relationships provide internal checks or constraints on the data. The thermodynamic equilibrium condition for the co-existence of two phases at any given temperature and pressure is:

$$G_1 = G_2 \tag{1}$$

where G is the Gibbs free energy for the system. If the subscript v refers to vapor, and l to liquid, we have

$$G_v = RT \ln \left(\frac{P}{T^{5/2}} \times \frac{h^3 \sigma}{(2\pi m)^{3/2} k^{5/2}} \right) + BP + \tfrac{1}{2} CP^2 \tag{2a}$$

where σ is the nuclear spin degeneracy, and B and C are the second and third pressure virial coefficients. If the equation of state is assumed to be $PV = RT(1 + B/V)$, the value of C in the pressure expansion is $-B^2/RT$. For the liquid, the Gibbs free energy is

$$G_l = -\int_0^T S_l \, dT + \int_0^T V_l \left(\frac{dP}{dT} \right)_{\text{sat.}} dT + G_l^\circ. \tag{2b}$$

Along the saturation line, Eq. (1) holds and yields after rearrangement the following vapor pressure equation with which any equation purporting to represent experimental data must be consistent:

$$\ln P = -\frac{\Delta H_0}{RT} + \frac{5}{2}\ln T - \frac{BP}{RT} - \frac{1}{2}\frac{CP^2}{RT} - \frac{1}{RT}\int_0^T S_l\, dT + \frac{1}{RT}\int_0^T V_l \left(\frac{dP}{dT}\right)_{\text{sat.}} dT - \ln \frac{h^3\sigma}{(2\pi m)^{3/2} k^{5/2}}, \tag{3}$$

where $\Delta H_0 = -G^\circ_l$ is the heat of vaporization at absolute zero. Satisfactory values exist for the second virial coefficients [18, 19], the density of the liquid is known as a function of temperature, and vapor pressures have been measured over a considerable temperature range as indicated in § 4.1. Hence the two remaining quantities ΔH_0 and the entropy integral

$$\int_0^T S_l\, dT = \int_0^T dT' \int_0^{T'} c_{\text{sat.}}\, d\ln T''$$

remain undetermined. If specific heat data were available from sufficiently low temperatures that the extrapolation to zero could be accurately made, the integral could be evaluated and ΔH_0 obtained from Eq. (3). Alternatively if a satisfactory theoretical expression for c_{sat} existed, this could be employed in the usual manner to compute the entropy up to the temperature at which experimental specific heat values are available. Lacking both types of information, it will be shown below that experimental determinations of the vapor pressure curve place certain restrictions on the values of ΔH_0 and the integral of the entropy from absolute zero to the lowest temperature of measurement but cannot define either uniquely.

4.5. The Heat of Vaporization of Liquid ^{3}He

From Eq. (1) of § 4.4., one may obtain the Clapeyron-Clausius equation which, with the help of vapor pressure, virial and liquid density data, permits a computation of the heat of vaporization as a function of temperature. Accurate calculations of this quantity have been reported by Abraham, Osborne and Weinstock [1a] and more recently by Sydoriak and Roberts [28] and by Kerr [17]. Their results are shown in Fig. 6, and in Tab. 6. It is apparent that calculated values of $\Delta H_{\text{vap.}}$ will be quite dependent upon the choice of the vapor pressure equation used to compute $(dP/dT)_{\text{sat}}$ and, as mentioned in § 4.4, until the contribution of the entropy integral can be obtained from ab-

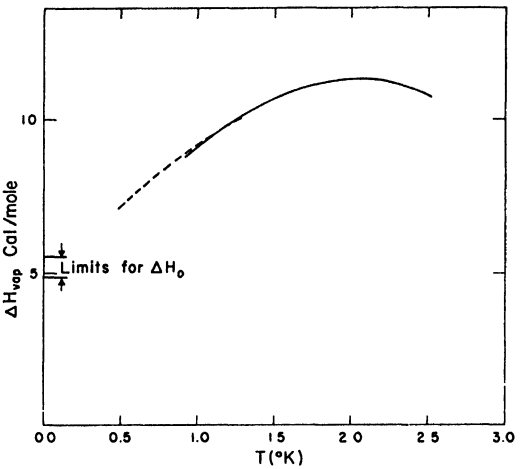

Fig. 6. Heat of vaporization of liquid ^{3}He.
Legend: — — — Sydoriak and Roberts[28].
——— Abraham, Osborne, and Weinstock.[1a]

solute zero, the value of $\Delta H_{vap.}$ at $T = 0°K$ (*i.e.*, ΔH_0) cannot be uniquely determined from vapor pressure measurements [29].

4.6. The Entropy of Liquid ^{3}He

The entropy of liquid ^{3}He is discussed in this section separately for

TABLE 6. Heat of Vaporization of Liquid ^{3}He

$T°K$	$\Delta H_{vap.}$ (cal mole^{-1})		
	Ref. 1a	Ref. 28	Ref. 17
0	(4.47)	5.05 ± 0.25	—
0.5	(6.95)	7.15	—
1.0	9.12 ± 0.12	9.16	9.10
1.5	10.65 ± 0.24	—	10.53
2.0	11.34 ± 0.41	—	11.15
2.5	10.81 ± 0.69	—	10.44
3.0	—	—	7.88

each laboratory in which such measurements have been carried out. This is done because the different treatments developed at these three centers have prompted additional discussion and elaboration of the subject which, by this method of presentation, can be related directly to the measurements themselves.

4.6.1. The Argonne Entropy Measurements

Re-arranging the Clapeyron-Clausius equation, using the data of § 4.5 and the Sackür-Tetrode equation the entropy of the liquid may be determined from

$$S_l = S_v - (V_v - V_l)\left(\frac{dP}{dT}\right)_{sat}$$
$$= S_v - \frac{\Delta H_{vap.}}{T}. \qquad (1)$$

Abraham, Osborne and Weinstock [1a] used this method to compute the entropy of liquid ^{3}He. In their computations, Abraham *et. al.* [1a] neglected nuclear spin contributions to the entropy on the assumption that over the temperature range investigated, the spin system was classical. On this basis, there still remained in addition to the spin entropy at absolute zero a residual entropy of 0.42 e.u., which would have to be removed in some unspecified fashion below 1°K. Although this proposition has received support from ter Haar [30] and Singwi [11], it is now recognized that this residual entropy is not a necessary consequence of the vapor pressure measurements (*vide infra*).

Computation of the entropy of the liquid by the above method is open to some criticism on the grounds that the derivative of the vapor pressure with temperature is required, and this becomes less reliable at the low temperature terminus of the measurements. Also in this temperature region the entropy of vaporization approaches the entropy of the vapor, yielding a liquid entropy which is the difference of two large numbers. A small error in $(dP/dT)_{sat}$ is thus magnified in the value of S_l. Finally this method is unsuited for extrapolation to $T = 0$, because it requires that the coefficient of the $1/T$ term in the vapor pressure equation be interpreted as ΔH_0. Consequently besides questionable entropy values in the vicinity of $T = 0$, the extrapolated heat of vaporization values (enclosed in brackets in Tab. 6) are almost certainly not valid.* It will be seen later that an alternative method is available for estimating this quantity.

The fact that the vapor pressure measurements cannot be used to extrapolate the liquid entropy was pointed out by Lifshitz [31] and by Chen and London [27]. Lifshitz showed that the vapor pressure data of Abraham *et al* [1a] could be used to compute the Gibbs free energy of

* This method is quite satisfactory in that temperature region where the slope of the vapor pressure curve is accurately known.

the liquid along the saturation line, including the nuclear spin contribution, from Eq. (2a) § 4.4. Assuming the ideal F.D. gas approximation (which is probably not justified) it follows that G_l should be proportional to T^2. Upon plotting G_l *vs* T^2, Lifshitz found that G_l could be satisfactorily represented by:

$$G_l/R = -2.82 - 0.38\,T^2 + 0.017\,T^4$$

and

$$S_l/R = 0.76\,T - 0.068\,T^3.$$

From these relationships ΔH_0 is found to be 5.5 cal/mole (compare 4.47 cal/mole, Ref. 1a), and the specific heat along the saturation line to be 0.76 RT. This method has been re-examined by Weinstock, Abraham and Osborne [32], who included corrections for nonideality, etc., with the following results:

$$G_l/R = -2.715 - 0.489\,T^2 + 0.0133\,T^4 + R^{-1}\int_0^T V_l\left(\frac{dP}{dT}\right)_{sat} dT$$

and

$$S_l/R = 0.978\,T - 0.053\,T^3.$$

This corrected entropy expression is almost identical with that for the ideal F.D. fluid as calculated by Singwi [11] and Goldstein [12], but the agreement is probably fortuitous.

Adopting only the requirement that the entropy of the liquid vanish at 0°K in accordance with Nernst's heat theorem, Chen and London [27] obtained the following equations (also fitting the experimental data [1a]) for the vapor pressure and liquid entropy.

$$\log_{10}(P_{mm}/T^{5/2}) = 2.3126 - 1.1561/T - 0.25254\,T - 0.00667\,T^2 + 0.05266\,T^3 - 0.01210\,T^4$$

$$S_l/R = 1.1630\,T + 0.04608\,T^2 - 0.4850\,T^3 + 0.1393\,T^4 - R^{-1}\frac{d}{dT}\left[BP - \frac{(BP)^2}{2RT}\right] + R^{-1}\,V_l\left(\frac{dP}{dT}\right)_{sat}.$$

Assuming that the coefficient of $1/T$ in the vapor pressure equation is equal to $\Delta H_0/R$ ln 10, we find the Chen and London value of ΔH_0 to be 5.29 cal/mole (cf. 5.5 cal/mole Ref. 31 and 4.47 cal/mole Ref. 1a).

Acknowledging that the extrapolated entropy of the liquid is not uniquely determined by vapor pressure data, Weinstock, Abraham

and Osborne [32] derived a second vapor pressure equation equally consistent with the data which implied no residual entropy other than the spin entropy at absolute zero. This latter vapor pressure equation was not developed as a convenient expansion in log T and powers of T, since the experimental data were adequately represented by Eq. (2) § 4.1. From their second vapor pressure equation, Weinstock *et al*, [32] obtained the following expressions for the entropy and specific heat of the liquid,

$$S_l/R = \ln 2 + 0.344\,T + 0.013\,T^3$$
$$c_l/R = 0.344\,T + 0.039\,T^3.$$

These equations are intended to represent the behavior of the liquid only down to that temperature at which nuclear alignment begins. They yield results differing from previously published values by the same authors only below 1°K.

Since the slope of the melting curve is positive to 0.5°K, then above that temperature the entropy of the liquid must be greater than that of the solid. Assuming the solid entropy to be only the value for randomly oriented spins, *i.e.*, R ln 2, and assuming no thermal entropy for the liquid (which appears questionable), the authors conclude that the above equations are valid to 0.5°K and that no nuclear alignment has occurred in the liquid above this temperature.*

The recent heat capacity measurements, cf. § 4.2, of Osborne, Abraham and Weinstock [24] have provided another expression, valid over a larger temperature range for the entropy of liquid ^{3}He. Their equation [24], normalized to yield their previously determined [1a, 32] value of the liquid entropy at 1°K, is

$$S_l = 2.09 + 0.53 \ln T + 0.48\,(T - 1) \text{ cal deg}^{-1} \text{ mole}^{-1}.$$

Since the slope of the melting curve becomes zero near 0.42°K, the entropy change between solid and liquid also becomes zero, whence the entropy of the solid at 0.42 degrees is computed to be 1.35 ± 0.15 cal deg^{-1} mole^{-1}, subject to the qualification that the entropy of the liquid does not change significantly as the freezing pressure is approached. Since this value of the entropy corresponds almost exactly to R ln 2, and since it may be presumed that the thermal entropy of

* Recent measurements by Fairbank *et al* [57], of the nuclear magnetic susceptibility of liquid ^{3}He indicate that at 0.5°K, the nuclear spins are about 20% aligned.

the solid is negligible at this temperature, its follows that in the solid (but not necessarily in the liquid) the spins are randomly oriented.

4.6.2. The Los Alamos Entropy Measurements

In order to avoid the magnification of experimental error introduced into the estimation of the liquid entropy by differentiating the vapor pressure data and using Eq. (1) § 4.6.1, Roberts and Sydoriak [21] have treated their vapor pressure and specific heat [21, 26] data in the following manner: From actual specific heat measurements beginning at 0.5°K, it is possible to determine the difference in entropy between this temperature and any higher temperature T. The absolute entropy of the liquid is then

$$S_l(T) = S_{0.5} + \int_{0.5}^{T} c_{sat}\, d \ln T \tag{2}$$

(Using specific heat functions derived from the data § 4.2. to determine $S_{0.5}$ is of course useless, since the form of the function may change radically below 0.5°K). The theoretical vapor pressure equation (Eq. (3), § 4.4) containing the integral $\int_{0.5}^{T} S_l\, dT$, may be written as follows:

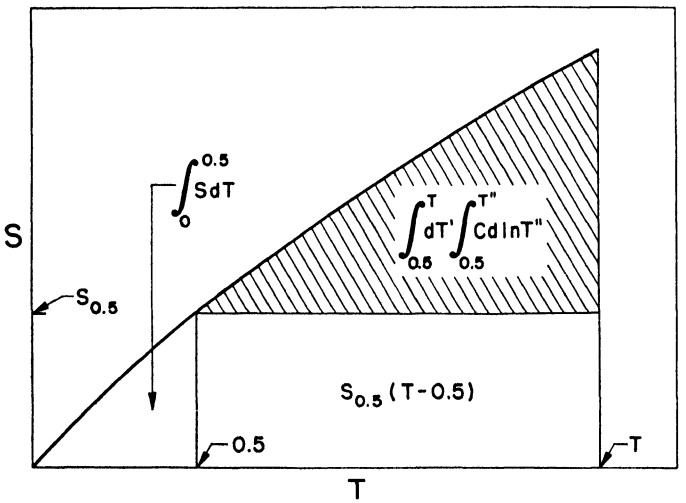

Fig. 7. Separation of the entropy integral.*

* Note added in proof: The upper limit of the second integral in the shaded section should be T^1 rather than T''.

$$\ln P/T^{5/2} + \frac{BP}{RT} - \frac{1}{2}\left(\frac{BP}{RT}\right)^2 - \frac{1}{RT}\int_0^T V_l \left(\frac{dP}{dT}\right)_{sat} dT +$$

$$+ \frac{1}{RT}\int_{0.5}^{T} dT' \int_{0.5}^{T'} c_{sat}\, d \ln T'' = \frac{-\Delta H_0 - \int_0^{0.5} S_l\, dT + 0.5\, S_{0.5}}{RT} - S_{0.5}/R + i, \quad (3)$$

where i is the chemical constant, *i.e.* the negative of the last term in Eq. (3) § 4.4.

The separation of the entropy integral is shown more clearly in Fig. 7, where the shaded area represents the portion determined experimentally. Using all of the available vapor pressure data, virial coefficients, liquid density, etc., the left hand side of the above equation can be evaluated, and if plotted *vs* $1/T$, one will obtain the quantity

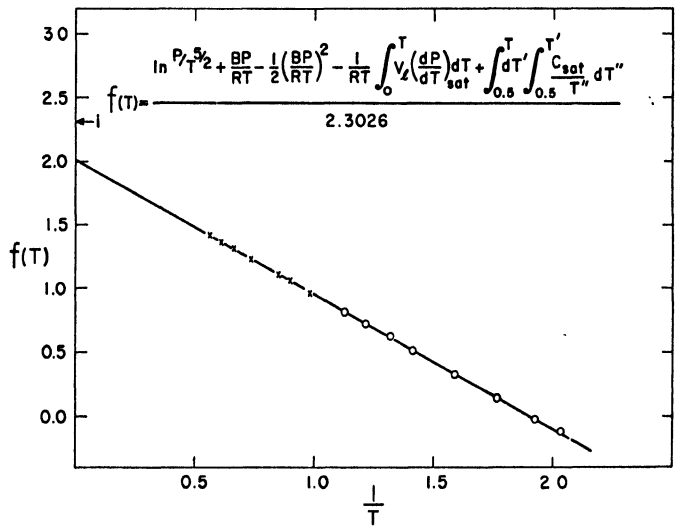

Fig. 8. Plot of left hand side of Eq. (3) *vs* $1/T$. Slope is equal to *

$$(-\Delta H_0 - \int_0^{0.5} S_l dT + 0.5 S_{0.5})\ (2.3026\ R)^{-1}$$

Legend: × Argonne vapor pressure data. ○ Los Alamos vapor pressure data.

* Note added in proof: The coefficient of the last term of the numerator shown in Fig. 8 should be $(RT)^{-1}$.

$$\left(-\Delta H_0 - \int_0^{0.5} S_l \, dT + 0.5 \, S_{0.5}\right) R^{-1}$$

from the slope and $i - S_{0.5}R^{-1}$ from the intercept as shown in Fig. 8. Within the accuracy of the experimental data, therefore, $S_{0.5}$ may be determined uniquely whence S_l (T) for $T > 0.5°K$ may be obtained from Eq. (2). Using this technique, Roberts and Sydoriak computed the absolute entropy of liquid ^3He to be 1.46 cal mole^{-1} deg^{-1} at 0.5°K. Their results are shown in Fig. 9 together with the most recent Argonne (Osborne, Abraham and Weinstock [24]) and the de Vries and Daunt [22] entropy data. Also included are the results of the Chen and London [27], and ideal Fermi-Dirac calculations. In Tab. 7 the entropy of liquid ^3He derived from the specific heat data of Tab. 5, is reported for each of the three laboratories.

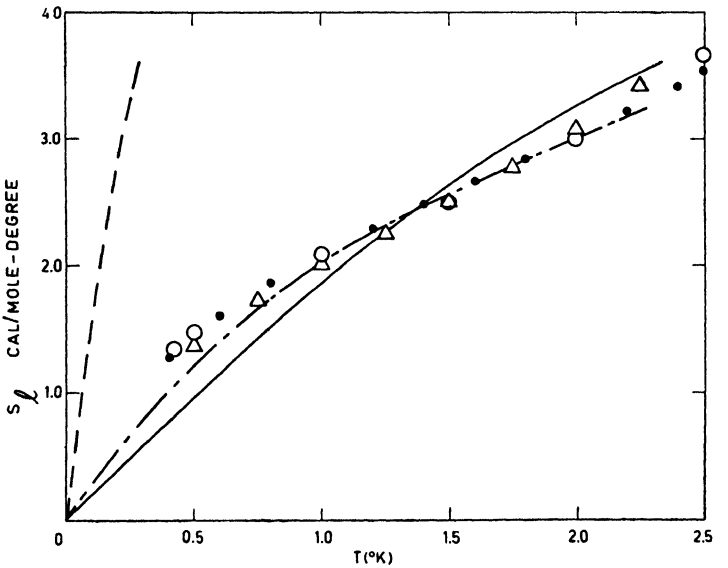

Fig. 9. Entropy of liquid ^3He.

Legend: ● Roberts and Sydoriak [21]. ○ Osborne *et al* [24]. △ de Vries and Daunt [22]. — — — Ideal F.D. gas $T_0 = 0.6°K$ ——— Ideal F.D. gas $T_0 = 5.0°K$ — · — · — Chen and London [21].

TABLE 7. The Entropy of Liquid ^{3}He

T°K	S_l (cal/deg mole) Ref. 24 & 32	Ref. 22	Ref. 21 & 26
0.4	—	—	1.28
0.42	1.35	—	—
0.5	1.48	1.37	1.46
1.0	2.09 ± 0.14	2.02	2.09
1.5	2.50 ± 0.17	2.50	2.56
2.0	3.00 ± 0.22	3.08	3.01
2.5	3.66 ± 0.29	—	3.51

4.6.3. The Ohio State Entropy Measurements

The experiments of de Vries and Daunt [22] summarized in graphical form in their most recent publication, indicate a leveling off of the specific heat between 0.6°K and 1°K. Since no extrapolation of the specific heat curve is justified, only entropy differences throughout the measured temperature range may be computed. By assigning the value of the liquid entropy derived by Abraham *et al* [32, 1a] at 1.5°K an absolute representation of the entropy temperature curve was obtained, as shown in Fig. 9. The results are reproduced with reasonable precision by the formula:

$S_l = 3.72\,T - 2.37\,T^2 + 0.573\,T^3 + 0.141\,T^4 - 0.053\,T^5$ cal/deg mole for $0.5 < T < 2.25$.

4.6.4. General Discussion of Entropy Measurements

It should be clear from the preceding sections that knowledge of the entropy of liquid ^{3}He by itself provides insufficient evidence for a decision regarding either the degree of spin alignment in the liquid, or the role played by statistics in the behavior of the liquid. When the entropy of the liquid falls below R ln 2, however, some alignment of the spins must have occurred. Although ΔH_0, the heat of vaporization at absolute zero, should in principle be obtainable from a vapor pressure equation which accurately represents the data over the entire temperature range, this condition has not been met and no theoretical significance can be attached to any vapor pressure equation so far reported. Thus, lacking a satisfactory extrapolation of the entropy to absolute zero, experimental measurements can only yield

$$\left(-\Delta H_0 - \int_0^{0.5} S_l \, dT\right)$$

assuming 0.5° the lowest measured temperature. An upper limit to the value of the integral can easily be obtained however since the entropy must increase with temperature, whence

$$\int_0^{0.5} S_l \, dT \leqslant 0.5 \, S_{0.5},$$

from which a lower limit for ΔH_0 may be derived. As the measurements are extended to lower temperatures, it will be possible to arrive at a more precise knowledge of ΔH_0. Roberts' and Sydoriak's [21] 'best' value for ΔH_0 so obtained is $4.80 < \Delta H_0 < 5.31$ cal/mole. The mean value of 5.05 given in Tab. 6 corresponds to the assumption $S \sim T$.

The general resemblance of the experimental entropy curves given in Fig. 9 to that for the ideal F.D. liquid appears to favor an interpretation of liquid ^{3}He behavior in terms of the ideal F.D. gas model. The remarkably high specific heat (for liquid ^{4}He, for example, the specific heat is lower by a factor of about 250 at 0.5°K) and entropy values at these low temperatures seem to require either a F.D. type gas model or a solid model with a very low Debye Θ similar to that discussed by Singwi [11]. On the other hand, the magnetic measurements of Fairbank, Ard, Dehmelt, Gordy and Williams [33] to be discussed in the next section indicate that the F.D. degeneration temperature (5.0°K) used in the above comparisons is much too high, and, as will be seen in § 5, the agreement between the experimental results and the ideal F.D. gas model as exhibited in Fig. 9, then becomes entirely fortuitous.

5. Magnetic Properties of Liquid ^{3}He

The magnetic properties of liquid ^{3}He were first discussed by Goldstein and Goldstein [34] and subsequently by Pomeranchuk [14]. The former authors considered first the possibility of nuclear ferromagnetism in liquid ^{3}He. Assuming an ideal F.D. gas model, and free particle wave functions, the quantum mechanical exchange energy was computed as a function of the internuclear distance for two interaction potential functions, the Slater-Kirkwood and the Margenau. It was shown that at absolute zero, subject to the above approximations, the total energy of the system in the anti-ferromagnetic case was lower than the ferromagnetic configuration throughout the physically acceptable range of internuclear distances. These predictions were con-

firmed by Hammel, Laquer, Sydoriak and McGee [35], who showed that the volume magnetic susceptibility of liquid ^{3}He was less than 5×10^{-6} down to 0.9°K.

Goldstein and Goldstein also computed the nuclear paramagnetic susceptibility of liquid ^{3}He, again based on an ideal F.D. gas model. This paramagnetic volume susceptibility is given by

$$\varkappa_p = \frac{n\mu^2}{kT} \times \frac{-F_{1/2}'(\eta)}{F_{1/2}(\eta)}$$

where $F_{1/2}(\eta)$ is the Fermi Dirac function described previously (§ 2), n is the atomic concentration, and μ is the nuclear magnetic moment of ^{3}He. At temperatures very much less than the degeneracy temperature T_0,

$$\lim_{T \ll T_0} \varkappa_p = \frac{3n\mu^2}{2kT_0},$$

$\varkappa$ reduces to the temperature independent Pauli paramagnetic susceptibility. At temperatures very much greater than T_0, the susceptibility is given by the usual Curie law.

$$\lim_{T \gg T_0} \varkappa_p = \frac{n\mu^2}{kT}$$

The total susceptibility is equal to the sum of the diamagnetic and paramagnetic susceptibilities,

$$\varkappa_T = \varkappa_p + \varkappa_d$$

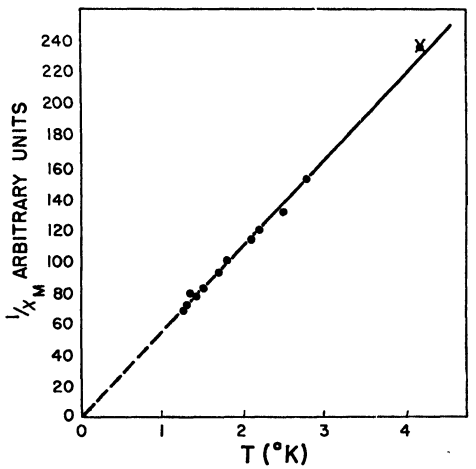

Fig. 10. Inverse molar nuclear susceptibility of liquid ^{3}He.

where $\varkappa_d$ is the diamagnetic susceptibility of ^{4}He properly corrected for the density of liquid ^{3}He. Unfortunately, due to the very small nuclear magnetic moment, the paramagnetic volume susceptibility turns out to be only 6—8% of the total, which is itself approximately minus 5×10^{-8}. Consequently a definitive experimental investigation of the susceptibility by classical techniques would require measurements of a very high degree of precision. Nuclear resonance techniques permit a direct measurement of the nuclear susceptibility, however, and these have been applied to the liquid ^{3}He problem by Fairbank *et al* [33] in the temperature range 1.2—2.8°K. Their results shown in Fig. 10 demonstrate that within the experimental accuracy of $\pm$ 10%, liquid ^{3}He in this range shows purely classical behavior, *e.g.*, $1/\chi_M \sim T$. In Fig. 11 the ratio of the Pauli (temperature independent) susceptibility $\varkappa_0$, to the calculated susceptibility $\varkappa$, is plotted as a function of T/T_0, for both the classical and ideal Fermi Dirac fluid. A degeneracy temperature of 5°K, based upon the liquid density and mass of ^{3}He would have clearly required inverse susceptibilities more than double the observed values in the lower temperature range. Since the error of the measurements is, as mentioned above, estimated at $\pm$ 10%, a T_0 of about 0.6°K is the maximum possible value of T_0 that the ideal F.D. model can permit *. Given this as an upper

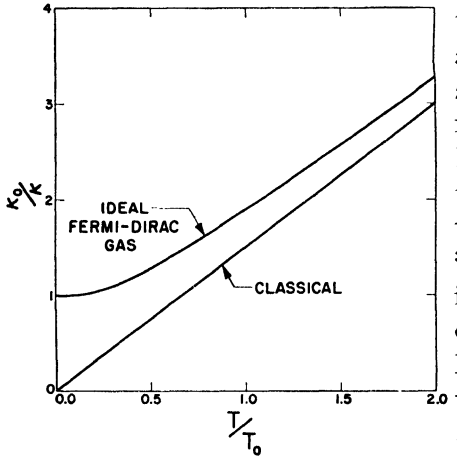

Fig. 11. Ratio of the temperature independent Pauli susceptibility to the calculated susceptibility for an ideal F.D. gas and a classical gas *vs* T/T_0.

* Measurements of the nuclear susceptibility of liquid ^{3}He from 0.23° K by Fairbank, *et al*, were reported as a post deadline paper at the Washington Meeting, Am. Phys. Soc., May 1, 1954. It was demonstrated that the susceptibility followed closely that predicted for an ideal Fermi-Dirac gas with a degeneracy temperature of 0.45°K. This corresponds to an effective mass per 'particle' of about 10 times the mass of a free ^{3}He atom if the ideal F.D. formalism is preserved. Since, however, the thermal properties are completely at variance with those predicted for an ideal F.D. gas with T_0 less than about 5°K, it appears that this simple theory is quite incompatible with the experimental data. These results of Fairbank, Ard, and Walters [57] have been discussed by Goldstein [59] who shows that the entropy of ^{3}He at very low temperatures is primarily the entropy of spin disorder.

limit for the degeneracy, any resemblance between the observed thermodynamic functions for liquid ^{3}He and that for an ideal F.D. gas with the particle density of liquid ^{3}He disappears completely (cf. the plot in Fig. 9 of the entropy of an ideal F.D. gas with $T_0 = 0.6°K$). Consequently there appears to be no basis for relating the ideal F.D. gas model to liquid ^{3}He behavior unless major modifications of this limiting theory are simultaneously introduced.

6. Transport Properties

6.1. The Viscosity of Gaseous ^{3}He

A theoretical calculation of the viscosity of gaseous ^{3}He at low temperatures was first made by de Boer and Cohen [36], using the appropriate quantum mechanical expression for the viscosity and employing the Lennard-Jones interaction potential used previously for calculation of the equation of state and transport properties of ^{4}He (cf. Chap. XVIII). An experimental determination of the viscosity of gaseous ^{3}He presented in Fig. 12 by Becker, Misenta and Schmeissner [37] agrees well with the theoretical predictions and would seem effectively to confirm both the choice of the intermolecular potential as well as the general theoretical foundations of the theory. Simultaneously, with these measurements, however, the viscosity ^{4}He gas was determined at Leiden over the same temperature range by van Itterbeek, Schapink, van den Berg and van Beek [38]. Their viscosity data is higher by about 10% than that of Becker *et al.* Furthermore the high temperature viscosity, heat conductivity, and second virial coefficients computed using the Lennard-Jones potential are not in agreement with experimental values [39]. Consequently further improvement in the form of the He—He interaction potential appears desirable.

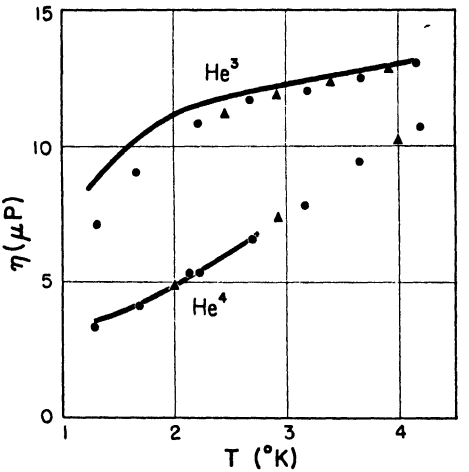

Fig. 12. Viscosity of gaseous ^{3}He and ^{4}He at low temperature.
(Solid lines are calculations of de Boer and Cohen [36]).

6.2. The Viscosity and Heat Conductivity of Liquid ^{3}He

Measurements of the viscosity of liquid ^{3}He reported by Weinstock, Osborne and Abraham [40] showed that the viscosity increased with decreasing temperature from 22μ poise at 2.79°K to 30.4μ poise at 1.04°K. The viscosity was determined by forcing the liquid to flow through an annulus, approximate corrections being made for the fact that evaporation occurred within the channel.

Theoretical discussions of the viscosity of liquid ^{3}He based essentially upon the ideal F.D. gas model have been published by ter Haar and Wergeland [41], Singwi and Kothari [42], Pomeranchuk [14] and by Buckingham and Temperley [43]. It is shown that for temperatures well below T_0, the viscosity according to this model must vary inversely at T^2 due to the increase of the collision mean free path with decreasing temperature. The possibility of a decrease in the effective cross section at low velocities (Ramsauer effect) was also considered by Buckingham and Temperley [43] and found to be insufficient in magnitude to account for the observed trend of viscosity with temperature. Although the measured rise in viscosity with decreasing temperature is not inconsistent with the requirements of an ideal F.D. gas model, the experiments certainly do not support this model, since the condition of $T << T_0$ is clearly not fulfilled in the reported temperature range. One may therefore conclude only that the temperature dependence of the viscosity of liquid ^{3}He resembles that of an ordinary liquid.

No measurements of the heat conductivity of liquid ^{3}He have been reported. Singwi and Kothari [42] and Pomeranchuk [14] both suggest that the property should vary inversely as T, provided the ideal F.D. gas model is applicable and $T << T_0$. As mentioned previously there appears to be no valid basis for this assumption.

6.3. The Flow Properties of Liquid ^{3}He

Since the statistical arguments of the London-Tisza theory of liquid helium would deny the possibility of superfluidity in liquid ^{3}He while this phenomenon was definitely allowed in any pure quantum liquid according to the Landau theory, an investigation of this property was considered a highly critical experiment. Studies of the flow of liquid ^{3}He were first reported by Osborne, Weinstock and Abraham [44] through super leaks down to 1.05°K and subsequently by Daunt and Heer [45] to 0.25°K using a method involving film flow and its associated heat conductivity along the walls of

the containing vessel. In each case no evidence for the superfluidity of ^{3}He was observed. These results have been interpreted quite generally as supporting the London-Tisza theory of liquid ^{4}He and, by analogy, the corresponding statistical (Ideal F.D. gas) model for liquid ^{3}He. Since the latter theory no longer appears tenable in view of the susceptibility measurements of Fairbank *et al* [33], it would appear that these experiments have not clarified the question of whether or not B.E. statistics are essential for superfluidity. In this connection it is interesting to note that Landau's theory (which appears more accurate the lower the temperature, for ^{4}He) makes no specification of the temperature at which superfluidity should appear in a quantum liquid. Consequently it does not appear impossible that liquid ^{3}He might exhibit superfluidity below 0.25°K *.

7. Miscellaneous Low Temperature Properties of ^{3}He

7.1. Adsorption

The adsorption of pure ^{3}He on activated charcoal has been studied

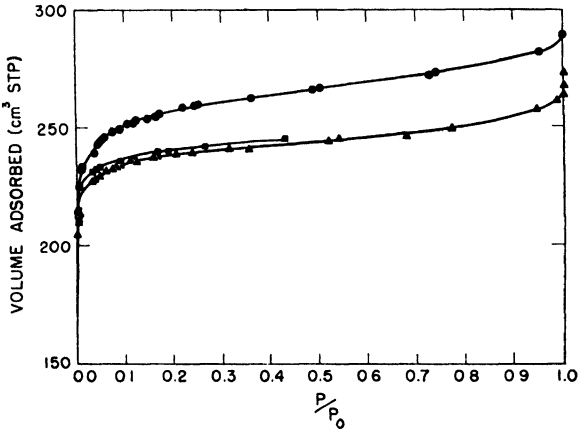

Fig. 13. Adsorption of ^{3}He and ^{4}He on activated charcoal
Legend: ● ^{4}He at 4°K. ■ ^{3}He at 2.5°K. ▲ ^{4}He at 3°K.

experimentally by Hoffman and Hammel [47]. The results are presented and compared with ^{4}He in Fig. 13. It is apparent that the adsorption

* Recent experiments on ^{3}He—^{4}He solution flow properties by A. F. Schuch and E. F. Hammel indicate that the ^{3}He component flows through a superleak at a rate independent of the driving pressure and, in the immediate vicinity of the solution λ-point it flows at a rate in excess of that exhibited by the ^{4}He component. There is no indication of superfluidity in pure liquid ^{3}He however, in agreement with other experiments [46].

isotherm is of the Langmuir type, rather than multilayer, on this adsorbent and that the volume of gas necessary to form a monolayer is about the same for the two isotopes, namely, 0.45 cm^3 STP/m^2 for ^{4}He and 0.43 cm^3 STP/m^2 for ^{3}He. It would appear from these results that if the high packing density of the monolayer is due to the balancing of the zero point energy of the adsorbed state by the attractive forces of the wall, as suggested by Long and Meyer [48], then the zero point energy in a monolayer is approximately the same for the two isotopes. In this connection it is interesting to note that application of the Bennewitz and Simon [49] modification for quantum liquids of Trouton's rule yields, probably fortuitously, a zero point energy for liquid ^{3}He within a few percent of the value calculated in like manner for liquid ^{4}He [50].

7.2. Low Temperature Neutron Studies of ^{3}He

In 1948, L. Goldstein [51] discussed the possibility of using neutron transmission techniques to investigate certain properties of liquid ^{3}He and ^{3}He—^{4}He mixtures. In particular, isotope analysis of ^{3}He-^{4}He mixtures *in situ* and in completely closed systems becomes feasible in view of the large cross section of ^{3}He, 5000 barns [52] for thermal (300°K) neutrons, compared with the corresponding cross section of 0.72 barns for ^{4}He. Also absolute measurement of ^{3}He densities in the liquid and vapor phases is feasible using neutron absorption techniques. Goldstein, Sweeney and Goldstein [53] have also discussed the theory of slow neutron scattering by liquid ^{3}He and liquid ^{4}He in terms of the ideal statistical model in each case. Recognizing that such models can represent only possible approximations to the actual structure of the liquid, the angular neutron scattering differs decidedly for the two idealized liquids. Although the experimental difficulties appear formidable for the last mentioned study and there is now considerable doubt regarding the adequacy of this model, there is no question that neutron techniques will in the future contribute considerably to our understanding of the liquid helium problem.

7.3. Thermomolecular Pressure Ratios

Sydoriak and Roberts [28] have measured ^{3}He thermomolecular pressure ratios by the single tube method [54], the tube temperature being 298°K at the top and 2.15°K at the bottom. The observed cold-to-warm pressure ratios, which ranged from 0.997 to 0.481 with varation

of the total pressure, agreed with ratios calculated from the Weber-Schmidt equation [55] with a standard deviation of $\pm$ 0.004.

8. Conclusion

The problem of ^{3}He behavior at low temperatures may be summarized as follows:

a The properties of the gas may be satisfactorily treated theoretically by straightforward quantum statistical methods. There appears to be some possibility for improvement of the intermolecular potential.

b Very little is known about the properties of solid ^{3}He. It seems probable however that its nuclear spins are randomly oriented down to 0.5°K.

c The properties of the liquid conform to no theoretical model, so far advanced. Although there is some *a priori* basis for believing that liquid helium should approximate an ideal F.D. gas assembly of particles, it now seems apparent that the actual interaction forces between the particles invalidate the applicability of this simple limiting model. There is also no definite evidence so far that statistics play any part in the non-superfluidity of ^{3}He. Thus although a considerable number of properties of ^{3}He have now been measured, it appears that the intriguing problem of liquid helium has been extended rather than resolved by this new information.

ACKNOWLEDGMENT

The author gratefully acknowledges his indebtedness to the staff of the Los Alamos Scientific Laboratory Cryogenic group and especially to Drs. L. Goldstein, T. R. Roberts, S. G. Sydoriak, W. E. Keller and E. C. Kerr for many helpful discussions on the subject matter of this report.

REFERENCES:

[1] The method of production of pure ^{3}He is described by B. M. Abraham, D. W. Osborne and B. Weinstock in (*a*) Phys. Rev., **80**, 366, 1950 and (*b*) Science, **117**, 121, (1953).

[2] S. G. Sydoriak, E. R. Grilly and E. F. Hammel, Phys. Rev., **75**, 303, (1949).

[3] E. R. Grilly, E. F. Hammel and S. G. Sydoriak, Phys. Rev., **75**, 1103, (1949).

[4] See catalog, 'Isotopes – Radioactive and Stable,' published by Oak Ridge National Laboratory, Oak Ridge, Tennessee, U.S.A.

[5] (*a*) F. Simon, Trans. Faraday Soc., **33**, 65, (1937); (*b*) F. London and O. K. Rice, Phys. Rev., **73**, 1188, (1948); (*c*) L. Tisza, Physics Today, **1**, 26, (1948); (*d*) H. A. Fairbank, C. A. Reynolds, C. T. Lane, B. B. McInteer, L. T. Aldrich

and A. O. Nier, Phys. Rev., **74**, 345, (1948) derived a possible boiling point of 2.9° K based on dilute solution studies.

[6] J. de Boer and R. J. Lunbeck, Physica, **14**, 510, (1948).

[7] J. de Boer, Physica, **14**, 139, (1948).

[8] (*a*) F. London, Phys. Rev., **54**, 947, (1938); (*b*) L. Tisza, Phys. Rev. **72**, 838, (1947); (*c*) L. Tisza, Phys. Rev., **75**, 885, (1949).

[9] L. Landau, J. of Physics (U.S.S.R.), **5**, 71, (1941); **8**, 1, (1941); **11**, 91, (1941); Phys. Rev., **75**, 884, (1949).

[10] H. N. V. Temperley, Proc. Phys. Soc., **65A**, 490, 619, (1952); **66A**, 995, (1953); R. P. Feynman, Phys. Rev., **91**, 1291, 1307, (1953).

[11] K. S. Singwi, Phys. Rev., **87**, 540, (1952).

[12] L. Goldstein (1948, unpublished). Goldstein has also recently applied the ideal gas approximation to the study of mixtures. This asymptotic theory gives a semi-quantitative description of a number of properties of mixtures. Phys. Rev. **95**, 869, (1954).

[13] C. V. Heer and J. G. Daunt, Phys. Rev., **81**, 447, (1951).

[14] I. Pomeranchuk, J. Exptl. Theor. Phys. (U.S.S.R.), **20**, 1919, (1950).

[15] I. Prigogine and J. Philippot, Physica, **18**, 729, (1952); **19**, 235, (1953); H. N. V. Temperley, Proc. Phys. Soc., **65A**, 490, 619, (1952); **66A**, 995, (1953); **67A**, 495, (1954); M. Toda and A. Isihara, Prog. Theoret. Phys. (Japan), **6**, 480, (1951); O. K. Rice, Phys. Rev., **93**, 1161, (1954); N. F. Mott, Phil. Mag., **40**, 61, (1949); M. Born and H. S. Green, 'A General Kinetic Theory of Liquids,' Cambridge, (1949); H. S. Green, 'The Molecular Theory of Fluids,' Chap. IX, North-Holland Publishing Co., (1952).
See also M. Toda and F. Takano, J. Phys. Soc. (Japan), **9**, 14, (1954).

[16] R. P. Feynman, Phys. Rev. Rev., **91**, 1291, 1301, (1953); S. F. B. Tyabji, Nature, **172**, 849, (1953); J. M. Ziman, Proc. Roy. Soc., **219A**, 257, (1953).

[17] E. C. Kerr, Phys. Rev. **96**, (1954).

[18] J. de Boer, J. van Kranendonk and K. Compaan, Physica, **16**, 545, (1950).

[19] J. E. Kilpatrick, W. E. Keller and E. F. Hammel, N. Metropolis, Phys. Rev. **94**, 1103, (1954).

[20] J. de Boer and A. Michels, Physica, **5**, 945, (1938).

[21] T. R. Roberts and S. G. Sydoriak. To be published.

[22] G. de Vries and J. G. Daunt, Phys. Rev., **92**, 1572, (1953); **93**, 631, (1954).

[23] T. R. Roberts and S. G. Sydoriak, Phys. Rev., **93**, 1418, (1954). Modified by use of latent heats calculated from Eq. (1) § 4.1.

[24] D. W. Osborn, B. M. Abraham and B. Weinstock, Phys. Rev., **94**, 202, (1954).

[25] D. W. Osborne, B. M. Abraham and B. Weinstock, Phys. Rev., **82**, 263, (1951); B. Weinstock, B. M. Abraham and D. W. Osborne, Phys. Rev., **85**, 158, (1952).

[26] T. R. Roberts and S. G. Sydoriak, Phys. Rev., **93**, 1418, (1954).

[27] T. Chen and F. London, Phys. Rev., **89**, 1038, (1953).

[28] S. G. Sydoriak and T. R. Roberts (To be published).

[29] Cf. B. Blaeney and F. Simon, Trans. Faraday Soc., **35**, 1205, (1939); J. Kistemaker, Physica, **12**, 281, (1946); R. Berman and J. Poulter, Phil. Mag., **43**, 1047, (1952); R. A. Erickson and L. D. Roberts, Phys. Rev., **93**, 957, (1954).

[30] D. ter Haar, Phys. Rev., **91**, 1018, (1953).

[31] E. M. Lifshitz, J. Exptl. Theoret. Phys. (U.S.S.R.), **21**, 659, (1951).

[32] B. Weinstock, B. M. Abraham and D. W. Osborne, Phys. Rev., **89**, 787, (1953).

[33] W. M. Fairbank, W. B. Ard, H. G. Dehmelt, W. Gordy and S. R. Williams, Phys. Rev., **92,** 208, (1953).
[34] L. Goldstein and M. Goldstein, J. Chem. Phys., **18,** 538, (1950).
[35] E. F. Hammel, H. L. Laquer, S. G. Sydoriak and W. E. McGee, Phys. Rev., **86,** 432, (1952).
[36] J. de Boer and E. G. D. Cohen, Physica, **17,** 993, (1951).
[37] E. W. Becker, R. Misenta and F. Schmeissner, Phys. Rev., **93,** 244, (1954).
[38] A. van Itterbeek, F. W. Schapink, G. J. van den Berg, and H. J. M. van Beek, Physica, **19,** 1158, (1953).
[39] E. A. Mason and W. E. Rice, J. Chem. Phys., **22,** 522, (1954).
[40] B. Weinstock, D. W. Osborne and B. M. Abraham, Proc. Int. Conf. Phys. of Very Low Temp., Cambridge, Mass., M.I.T., **47,** (1949).
[41] D. ter Haar and H. Wergeland, Phys. Rev., **75,** 886, (1949).
[42] K. S. Singwi and L. S. Kothari, Phys. Rev., **76,** 305, (1949).
[43] R. A. Buckingham and H. N. V. Temperley, Phys. Rev., **78,** 482, (1950).
[44] D. W. Osborne, B. Weinstock, and B. M. Abraham, Phys. Rev., **75,** 988, (1949).
[45] J. G. Daunt and C. V. Heer, Phys. Rev., **79,** 46, (1950).
[46] A. F. Schuch and E. F. Hammel (to be published); cf. Phys. Rev., **87,** 154, (1952).
[47] C. J. Hoffman and E. F. Hammel (To be published).
[48] E. Long and L. Meyer, Phil. Mag. Sup., **2,** 1, (1953).
[49] K. Bennewitz and F. Simon, Z. Phys., **17,** 183, (1923).
[50] See I. Prigogine and J. Philippot, Physica, **18,** 729, (1952).
[51] L. Goldstein, Declassified Los Alamos Report, LADC, 546, June, 1948.
[52] L. D. P. King and L. Goldstein, Phys. Rev., **75,** 1366, (1949); J. H. Coon and R. A. Nobles, *ibid.* 1358.
[53] L. Goldstein, D. Sweeney, and M. Goldstein, Phys. Rev., **77,** 319, (1950); *ibid.*, **80,** 141, (1950).
[54] S. Weber and W. H. Keesom, Commun. Kamerlingh Onnes Lab., Leiden, No. 223*b*.
[55] S. Weber and G. Schmidt, Commun. Kamerlingh Onnes Lab., Leiden, No. 246*c*.
[56] J. E. Kilpatrick, W. E. Keller, and E. F. Hammel, Phys. Rev. **97,** (1955).
[57] W. M. Fairbank, W. B. Ard, and G. K. Walters, Phys. Rev. **95,** 566 (1954).
[58] E. R. Grilly and R. L. Mills (To be published).
[59] L. Goldstein, Phys. Rev. **96** (1954).
[60] W. E. Keller (To be published).

CHAPTER VI

LIQUID MIXTURES OF HELIUM THREE AND FOUR

BY

J. J. M. BEENAKKER AND K. W. TACONIS
KAMERLINGH ONNES LABORATORY, LEIDEN

1. Introduction

The discovery of the isotope ^{3}He by Alvarez and Cornog [1] in 1939 created prospects for new research after the war.

In the preceding chapter Hammel reported the great amount of work done on pure liquid helium 3. Here we will discuss the results obtained with mixtures of the two isotopes which are especially of importance with respect to the interesting lambda transition phenomenon in the liquid phase. Several authors [2] had pointed out before any ^{3}He was prepared that it would be very important to study the behaviour of ^{3}He in liquid helium in order to verify the interpretation of the lambda point by F. London as a Bose Einstein degeneracy.

Indeed, ^{3}He having an even particle structure should obey Fermi statistics, hence only the ^{4}He atom could demonstrate superfluid properties. The first confirmation of this conclusion came from Daunt, Probst and Johnston [3], who showed that ^{3}He did neither partake in the helium film transfer nor in the flow through very narrow slits, which forms a direct subsurface connection between two vessels. In both cases only the superfluid could move from the main vessel to a second one and it was proven that all the ^{3}He remained in the main vessel thus that the ^{3}He is absent in the superfluid flow. The experiments indicate methods for separation of mixtures which can be used to enrich to an appreciable extent the ^{3}He concentration starting from

well helium or atmosferic helium which contain ^{3}He in amounts of about 10^{-5}% and 1.4×10^{-4}% as is known from work by Aldrich and Nier [4].

Besides these methods thermal diffusion [5] was also used initially to prepare mixtures containing about 1% ^{3}He. Later on in the U.S. the production of pure ^{3}He by nuclear processes superseded the above methods as the handling of large quantities was very laborious. Moreover Lane, Fairbank and Nier [6] developed another separation method in the liquid phase below the λ point which is very useful and effective. This method called heat flush is still in use in some laboratories and is connected to the heat conduction mechanism in He II. Since in the heat conduction process normal fluid flows away from the heater and superfluid in the opposite direction, the ^{3}He atoms – having only interaction with the normal fraction – are carried away from the heater in the direction of the heat current. The heat flush method was used in Leiden [7] in a double separation column as shown in Fig. 1. From the heater W a heat current flows through the container A (200cc) filled with atmosferic liquid helium and through an annular tube B to the cold region formed by a thin walled platinum tube P_1 surrounded by the helium bath. The heat current was strong enough to maintain a temperature difference over the platinum wall of more than 0,002°, hence also in the capillary C a heat current will flow to the second platinum contact P_2 with the bath. The helium vapour pumped off through D by means of a Toepler pump showed an increase of the ^{3}He concentration by a factor of about 4000.

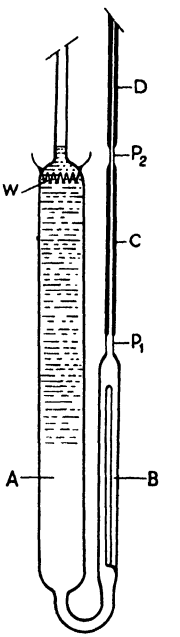

Fig. 1. Leiden ^{3}He separator

Separation on still larger scale was obtained by Soller, Fairbank and Crowell [8]. Their apparatus was suspended below the liquefier. Through the valves V_1 and V_2 the vessels A (700cc) and B (1000cc) were filled with liquid helium. The temperature in B could be reduced by pumping through tube T_4 and the liquid in A was simultaneously cooled because of the good thermal contact afforded by the copper cup C. Now below the λ point heat is applied in A by the heater H_1. The heat flush carries the ^{3}He to the small tube D which is the coldest part of vessel A. Through T_1 the mixture containing ^{3}He can be removed. After the sample has been drawn off the liquid helium in A

is drained into B which is by that time sufficiently emptied by continuous pumping. Vessel A may finally be refilled from the liquefier and the previous process repeated. Starting with well helium the enrichment factor was 30000. In the following, the experimental data on mixtures will be reviewed, whereas in § 3 a survey will be given concerning several theoretical descriptions of the behaviour of mixtures.

2. The Equilibrium between Liquid and Vapour

In the first experiments performed to study the distribution of ^{3}He between the liquid and vapour of a mixture the so called static method was used: From a known condensed mixture samples of liquid and vapour were taken off and analysed by means of a mass spectrometer. In an ideal mixture the partial vapour pressure of ^{3}He should be $p_3 = p_3^\circ X$ where p_3° is the saturated vapour pressure of pure ^{3}He and X the concentration in the liquid and similarly $p_4 = p_4^\circ(1 - X)$. The concentration ratio in the vapour $C_V = p_3/p_4$ divided by that in the liquid $C_L = X/(1 - X)$ gives the distribution coefficient

$$C_V/C_L = p^\circ_3/p^\circ_4 \qquad (1)$$

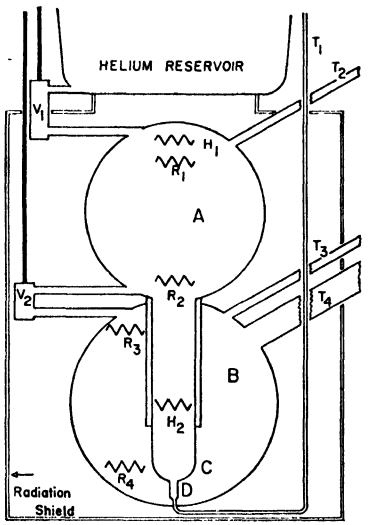

Fig. 2. ^{3}He separator used by Soller *et al.*

From this equation it was expected that the concentration in the vapour would be much higher than in the liquid as p_3° is much greater than p_4°, especially at low temperatures. From the data published by Fairbank *et al.* [9] and Daunt *et al.* [10], it could be concluded that in He I the behaviour of the mixture is quite normal, i.e. in agreement with the Henry-Raoult equation (1).

Below the λ point, however, almost no ^{3}He was found in the vapour. The reason for this discrepancy was obvious because two different but associated effects could explain the observed behaviour. This first effect is caused by the helium film which creeps up in the connection tube to the analysing system, evaporates somewhere in this tube, whereupon the helium gas flows back and condenses again. This gas

flow -- originating from the film – contains only ^{4}He and therefore prevents the ^{3}He from entering the tube and thus the analysing apparatus. The second effect is due to the condensation of the helium vapour flowing back to the liquid surface as this will create in the liquid a heat current directed to the wall of the vessel and this heat flow will carry the ^{3}He towards the wall thus decreasing the liquid concentration at the surface and consequently in the vapour.

In the Leiden experiments [11] performed on dilute mixtures of about 0.1% only the excess pressure of the mixture above that of the surrounding helium bath was measured while the liquid was kept homogeneous (by agitating). According to Henry-Raoult $\Delta p = X\,(p_3^\circ - p_4^\circ)$. From this equation the concentration in the liquid, X, could be calculated and compared with the known concentration of the condensed gas. It appeared that the calculated X was much higher than the actual one, indicating that the vapour concentration C_V is much higher than classically should be expected, a result contrary to the previous investigations. The values of C_V/C_L derived from the experiment, having a rather low accuracy were: 35 at 1.75°K, 16 at 1.9° K and 10 at 2.0° K. To explain these results Taconis and Beenakker assumed that the ^{3}He would mix only with the normal fraction, x, of the ^{4}He and in this way they obtained a rather satisfactory agreement with the modified Henry-Raoult equation (1) which becomes

$$C_V/C_L = p_3^\circ/p_4^\circ x \tag{2}$$

More data concerning the vapour liquid equilibrium were later obtained by Weinstock *et al.* [12], Eselsohn *et al.* [13] and Heer *et al.* [14] and finally in 1952 by Sommers. [15] Sommers measured the dew point pressure of a gas mixture at a known temperature and also the excess pressure in the vapour when the vessel was completely filled with the liquid mixture. The derived distribution function plotted versus temperature for different values of liquid concentration is shown in Fig. 3. The C_V/C_L data are dependent on the concentration at higher temperatures, the lower concentration giving the highest values, at low temperatures, however, the dependence is not clear but seems to be reversed. As this result seemed doubtful because especially at low temperature the above mentioned heat flush effect in the liquid might introduce an important systematic error and as it was interesting to measure at still lower temperature because formula (2) predicts much higher values of C_V/C_L, new investigations were undertaken in this

region at Leiden. [16] Care was taken to avoid concentration differences in the liquid. Fig. 4 shows the apparatus used by the Leiden group. In a small vessel A a certain amount of a known mixture was condensed

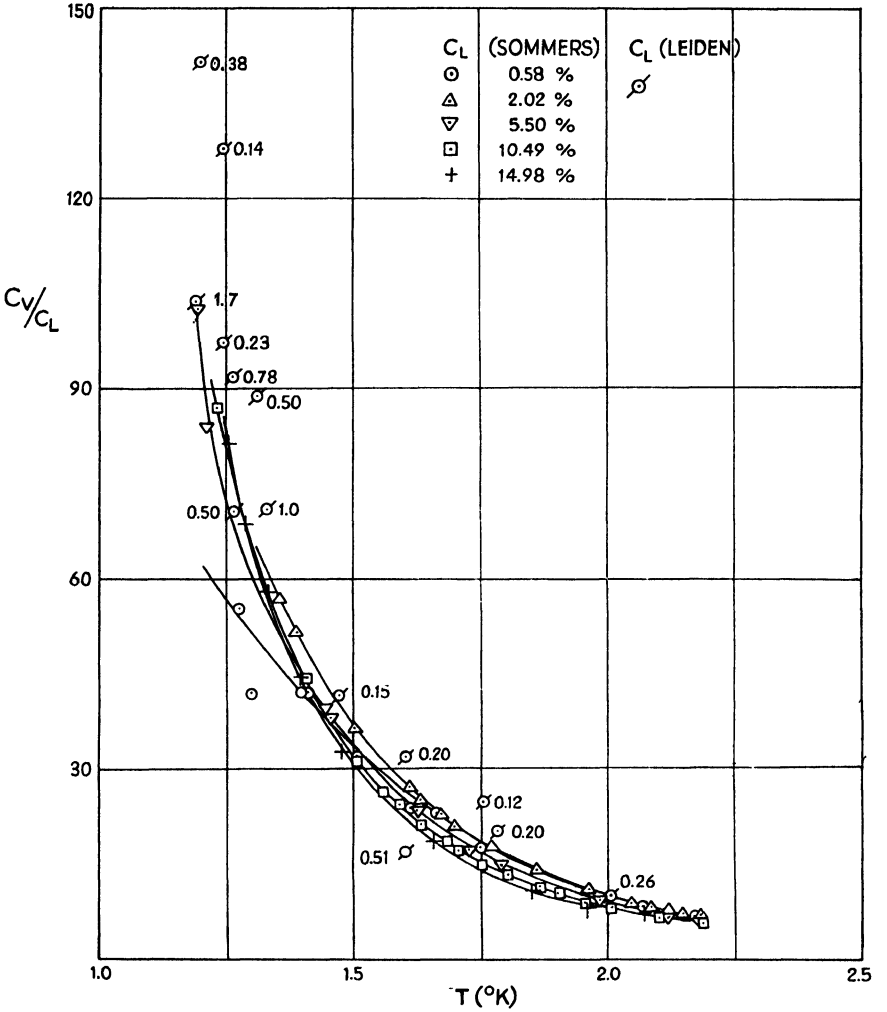

Fig. 3. The distribution function versus temperature

just sufficient to fill volume B plus the calibrated capillary C. By creating heat in the second vessel B, connected with A through a superleak formed between gold wires and soft glass in which they are sealed, the ^{4}He could be drawn by filmcreep into vessel B. During heating

the concentration in A is continually increased as is observed by measuring the increasing excess pressure in A above the bath pressure with an oil manometer. The heating is continued till finally all the liquid has disappeared from vessel A. The excess pressure Δp has then reached its maximum. Moreover the height of the liquid level in the capillary C is observed during the last period of the process. From the rise of Δp versus time, knowing the volume of A and assuming that the vapour is an ideal gas, the amount of ^{3}He evaporating from the liquid can be calculated rather accurately, whereas the quantity of liquid in A is derived from the reading of the height of the liquid in the capillary C. The concentration of ^{3}He in the liquid C_L is thus calculated starting from the empty position, with respect to which all the preceding situations are determined i.e. the quantity of liquid and the number of mols ^{3}He dissolved in this liquid are known. The values of C_V/C_L can be derived in this way with rather good accuracy and are plotted in Fig. 3 marked by ⊙ provided by the concentration in %. Since very small quantities of liquid were used concentration gradients in these small drops were almost impossible. The points in the graph lie higher than the Sommers data. At higher temperatures this may be explained by the lower concentrations used, at lower temperatures the explanation must be found in the heat flush effect in the experiments by Sommers.

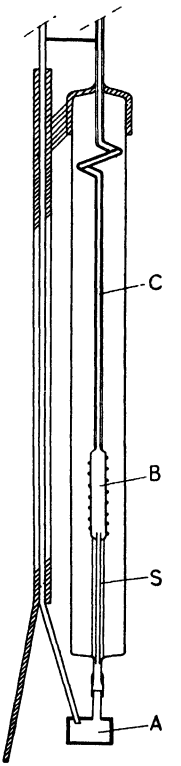

Fig. 4. Superleak apparatus

A comparison of the results for dilute mixtures with Eq. (2) shows rather large deviations at low temperature the experimental value being smaller. The agreement with the theories reviewed in the next paragraph is better. De Boer and Gorter, working out the hypothesis of Taconis and Beenakker, showed that x is concentration dependent and replaced Eq. (2) by a more correct one. For higher concentrations the theoretical curves then approach the experimental data although of course the results of this theory are far more dependent for dilute mixtures on the concentration than the experimental data. It seems, however, possible to introduce an extra heat of mixing which enables a better adaption to the experiments. The calculations by Mikura based on the ideas of Daunt

and Heer demonstrate that a very nice correspondance can be obtained when more adjustable parameters are available. For details we refer the reader to the next paragraph and especially to the work of Mikura. From the Leiden experiments described here more data concerning the behaviour of ^{3}He in mixtures can be obtained. (1) The helium transfer through the superleak in mixtures is measured as a function of the concentration by observing the velocity with which the level in the capillary C rises and (2) The influence of ^{3}He on the fountain effect can be studied by observing the equilibrium position of the level in the capillary C as a function of the measured temperature differences between A and B. The temperature difference has to be smaller of course than that which empties the vessel completely from liquid. Data on these two investigations will be given in paragraphs 10 and 8 respectively.

3. Theoretical Description of the Behaviour of Mixtures of ^{3}He and He II

The behaviour of mixtures of ^{3}He and He II can be described following two different lines of thought. The thermodynamical description based on the properties of He II can be extended to mixtures by making an ad hoc assumption about the entropy of mixing, or, starting from a more fundamental theory of the lambda transition in liquid helium one can try to compute the influence of ^{3}He on the properties of He II.

The first method was chosen by De Boer and Gorter [17], Rice *et al.* [18], Stout [19] and Koide and Usui [20], using the assumption of Taconis and Beenakker [11, 21] that ^{3}He forms an ideal mixture with the normal fluid. The second line was followed in the theories of Harasima [22], Heer and Daunt [14, 23] later refined by Mikura [24], and of Toda and Isihara [25] starting from an interpretation of the lambda point in liquid helium as a consequence of the Bose-Einstein condensation, and of Pomeranchuk [26] starting from Landau's excitation theory. In this section we will give a brief account of the most important of these theories, the results of which will be compared with experimental data in subsequent paragraphs.

As was already mentioned De Boer and Gorter made use of the assumption that ^{3}He forms an ideal mixture with the normal fluid. In this case the Gibbs' function, G, for one mole of the mixture is of the form:

$$G = XG_3 + (1-X)G_4 + RTX/X_e.\ [X_e \ln X_e + (1 - X_e) \ln (1 - X_e)] \quad (3)$$

where G_3 and G_4 are the Gibbs' functions for the pure components, X the

mole fraction of ^{3}He, and $X_e = X/(X + x\,(1 - X))$ the concentration of ^{3}He relative to the normal fluid only, whose fraction is given by x.

Using a definite expression for the Gibbs' function of He II, one can calculate the different thermodynamical quantities, if one assumes that in equilibrium G is minimum with respect to variations of x at constant T and X.

For the sake of illustration we will give the results for the dependence of x on X and T, using for G_4 the expression suggested by Gorter (cf. Ch. I:)

$$G_4 = -E_0\,(1 - x^{7/6}) - x\,S_\lambda\,T \tag{4}$$

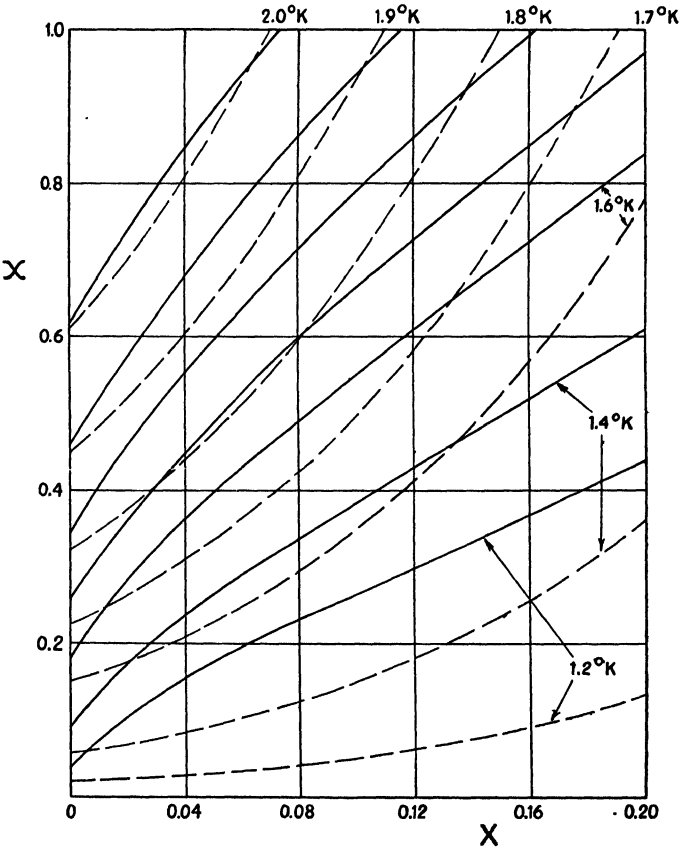

Fig. 5. The fraction x of the normal fluid, as a function of the ^{3}He-concentration X, at different temperatures.
———— De Boer and Gorter
— — — — — — Mikura

Substituting (2) in (1) and making use of the equilibrium condition, one obtains the following relation between these quantities:

$$7/6\, E_0\, x^{1/6} - T\, S_\lambda = RT \ln [(X + x - xX)/X\,(1 - X)],$$

which can be solved numerically. The results are plotted in Fig. 5.

It is of interest to remark that $(\partial x/\partial X)_T$ has, in this model, the same limit for low concentrations, a value of about 7, for all temperatures. Hence at low concentrations each atom of ^{3}He will create about seven "normal atoms", resulting e.g. in an increase of the specific heat at low concentrations of $6\,X\,(R - x_0\, S_\lambda)$.

As is well known F. London [27] suggested that the lambda transition in liquid helium is a consequence of the degeneracy that occurs at low temperatures in a gas composed of particles that obey Bose-Einstein statistics. In such a gas the number of atoms in the state of zero momentum is no longer negligible below a certain temperature as was shown by Einstein [28]. The atoms in the lowest state form the superfluid of the two fluid model, the excited atoms the normal fluid.

The difficulty in this treatment is that the helium liquid is certainly not an ideal gas, hence rather large discrepancies may be expected. In fact the transition in an ideal Bose-Einstein gas is of the third rather than of the second order as is the case in liquid helium, i.e. there is no discontinuity in the specific heat at the transition temperature.

Bijl, De Boer and Michels [29] showed that this difficulty could be overcome by assuming an energy spectrum with a gap between the zero state and the first excited one.

Heer and Daunt put forward the idea that the behaviour of ^{3}He mixtures could be described as an ideal mixture of a degenerate Bose-Einstein gas and a non-degenerate Fermi-Dirac gas. This theory was criticized by De Boer and Gorter [30], who showed that the distribution function C_V/C_L must have a discontinuity at the lambda point as a consequence of the finite jump in the specific heat of liquid helium at this temperature without regard to the model used, in opposition to the results of Heer and Daunt. Recently Mikura made a refinement of the treatment by introducing a Bose-Einstein liquid model for He II slightly different from that of Bijl et al. In this model He II is composed of Bose-Einstein particles in a smoothed potential well. Between the zero state and the first excited state there is an energy gap $k\Delta$, k being the Boltzmann constant, and the particles are clustered

together in groups of ν atoms, the total number of particles being given by N_4.

In this case the free energy of the system is given by:

$$F = -kTZ + \frac{N_4}{\nu} kT \ln \lambda_4 \tag{5}$$

Z being the sum of states for a Bose-Einstein assembly under the specified conditions and λ_4 a normalizing parameter, the normalizing condition being given by $(\partial F/\partial \lambda_4)_{T,V} = 0$. In this way one gets for the number of noncondensed particles

$$N_4 \, x/\nu = (2\pi \nu m_4 \, kT/h^2)^{3/2} \, N_4 \, V_4^\circ \exp(-\Delta/T) \tag{6}$$

V_4° being the molar volume of ^{4}He.

Introducing ^{3}He in this system as an ideal Fermi-Dirac gas in a smoothed potential well, one obtains expressions for the free energy of the mixture.

In the same way as with pure ^{4}He, one finds for the fraction of normal fluid:

$$N_4 \, x/\nu = (2\pi \nu m_4 \, kT/h^2)^{3/2} \, (N_4 \, V_4^\circ + N_3 \, V_3^\circ) \exp(-\Delta/T) \tag{7}$$

It appeared necessary to introduce still another assumption regarding the dependence of Δ on ^{3}He-concentration to get agreement with experimental data on the lambda temperature of mixtures (cf. § 5). Mikura suggested the following expression:

$$\Delta = \Delta_0 \, N_4 \, V_4^\circ / (N_3 \, V_3^\circ + N_4 \, V_4^\circ) \tag{8}$$

A comparison with experiments will be given below.

Pomeranchuk confines his considerations to very dilute mixtures and has made some calculations regarding the equations of motion valid for the mixture. As in Landau's theory the excitations in He II are composed of phonons and rotons, ^{3}He behaves as an ideal gas that contributes only to the roton spectrum, with an effective mass μ_3 which must be determined from experiment. Hence the density of the normal fluid, ϱ_n, is increased by an amount: $\mu_3 X \, \varrho/m_4$. For the entropy, S, per gram he obtains:

$$S = S_0 + (R \, X/4) \ln (1.5 \, T^{3/2}/X) \cdot \tag{9}$$

the index 0 designing the value in pure ^{4}He. Hence in this model there

is a temperature independent increase of the specific heat with a value: (3/8) RX.

Pomeranchuk's treatment has been rather succesful in explaining the behaviour of second sound. For the velocity of second sound v_{II} he gets the following expression:

$$v_{II}^2 = (T/C)\,(\varrho_s/\varrho_n)\,[(S_0 + RX/4)^2 + RXC/4] \qquad (10)$$

C being the specific heat per gram of the mixture. At low temperatures the impurity atoms become predominant and (10) reduces to:

$$v_{II}^2 = (5\,k\,T)/(3\,\mu_3) \qquad (11)$$

4. The Specific Heat

Important informations on the behaviour of mixtures can be obtained from measurements of the specific heat as a function of concentration and temperature. Since the amount of ^{3}He available is rather small, several experimental difficulties had to be overcome before such measurements could be performed. Recently the Leiden group developed a method to determine rather accurately the specific heat of about 200 mm^3 of such mixtures. To avoid heat leak to the calorimeter along the filling tube of the liquid reservoir and to eliminate corrections for the heat of evaporation the reservoir was first almost completely filled with the liquid mixture by means of a very narrow capillary. The end of this capillary was subsequently closed by silver soldering. After warming up the reservoir to room temperature – the pressure inside becoming about 1200 atm – the filling capillary was spiralled and the reservoir mounted in a standard calorimeter set up. Control measurements of the specific heat of He II gave results that were in excellent agreement with those of Kramers *et al.* [31].

The experimental data for a 2.5% mixture of ^{3}He are given in Fig. 6. The accuracy of the specific heat measurements above 1.8°K was rather small, as one was mostly interested in the determination of the lambda shift, which was — 0.037 degree. A theoretical interpretation of the results is still rather difficult as up to now only measurements at one concentration are available. So far one can only say that the increase in the specific heat is considerably greater at higher temperatures than for an ideal ^{3}He gas given by Pomeranchuk.

The predictions of the theory of Mikura are of the right order of magnitude but the uncertainty in the specific heat of ^{3}He that enters in the expressions makes a numerical comparison of little value.

The theory of De Boer and Gorter gives an increase of the specific heat that is rather much too high in the low temperature region but it seems possible to obtain better agreement by adapting the form of

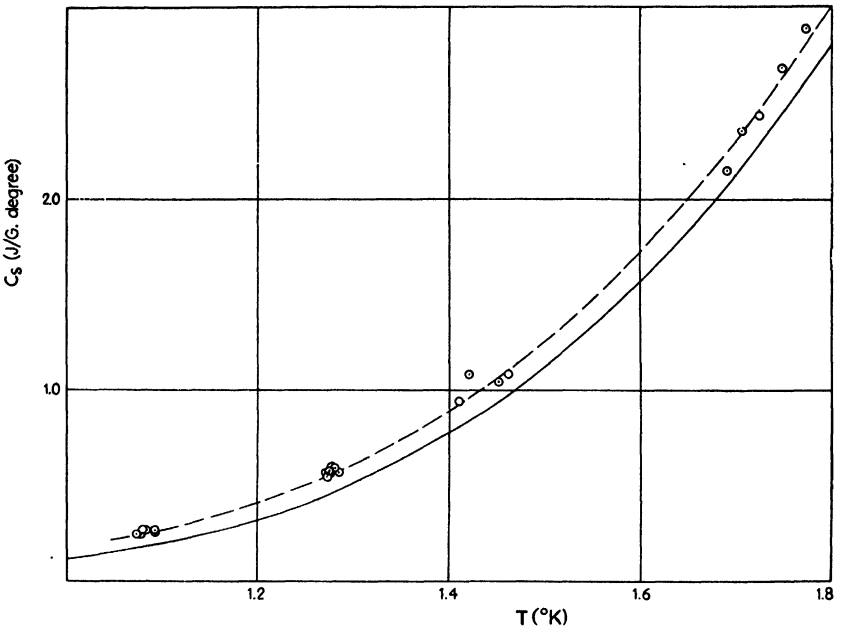

Fig. 6. The specific heat C_s plotted versus temperature
——— pure ^{4}He ⊙ 2.5% ^{3}He mixture.

the Gibbs function for pure ^{4}He, a modification that is also suggested by the results of other experiments. Pending further experimental results a detailed discussion must be postponed.

5. The Influence of ^{3}He on the Lambdapoint

The presence of ^{3}He has a pronounced effect on the value of the lambda point, which is shifted towards lower temperatures as was first shown by Abraham, Weinstock and Osborne [32] for mixtures with ^{3}He concentrations varying between 2% and 25%. Similar experiments were performed by Eselsohn and Lazarev [33] for a mixture with a concentration of about 1.5% and by Daunt and Heer [34] for mixtures with higher concentration of 40% to 90%.

To detect the lambda point Abraham *et al.* made use of a so called "superleak" made by sealing a platinum wire in a glass capillary.

Because of the difference between the expansion coefficients of the glass and the platinum in cooling a narrow annular channel is formed that is nearly gas-tight but open to the filmcreep. A reservoir with the mixture is connected by means of this superleak with a glass vessel outside the cryostat. By measuring the pressure increase in this vessel per unit of time as a function of the temperature of the mixture, the lambda point could be determined with an accuray of about 0.05°K. We remark that a systematic error may be caused by a concentration gradient in the liquid due to the heat flush effect.

Eselsohn and Lazarev also made use of the film creep to determine the Lambda point of the mixture. Their apparatus consisted of two reservoirs connected by a narrow capillary, one of the vessels being mounted higher than the other. They determined the temperature at which the fluid started to flow from the higher to the lower vessel. As the concentration of their mixture is rather uncertain, the value they give for the depression of the lambda point is not very accurate.

Daunt and Heer performed experiments with mixtures having a much higher concentration the lambda point being depressed below 1°K. For the highest concentration they found a value of 0.38°K. These temperatures were reached by adiabatic demagnetization of chromium potassium alum. Fig. 7 gives a schematic diagram of the

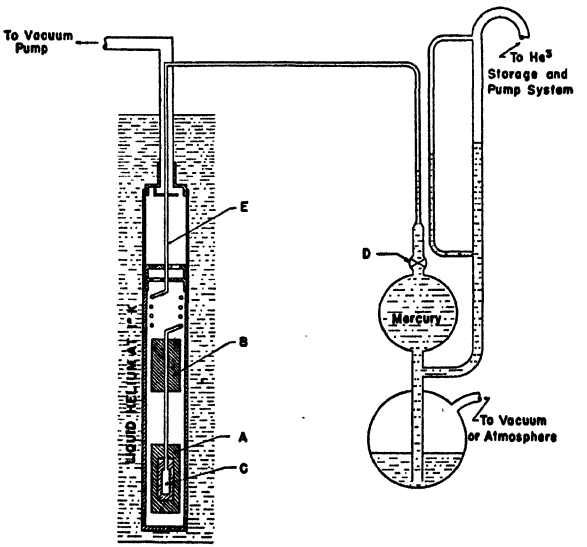

Fig. 7. Experimental apparatus used by Daunt and Heer

apparatus used. By means of a Toepler pump, D, the mixture of known concentration is condensed via a fine bore stainless steel capillary E, into a copper reservoir C. This reservoir is pressed inside a cylindrical pill A, of chromium potassium alum. In order to reduce the heat influx along the capillary a second salt cylinder B, was mounted higher up this tube so as to serve as a heat barrier to flow of heat from the helium bath. For the same purpose the whole arrangement was mounted in a vacuum jacket. The lambda point was found by measuring the warming up curve of the vessel. On passing the lambda point the heat leak decreases due to the disappearance of the creeping film.

Recently King and Fairbank [35] made experiments close to the lambda point. For the determination of the lambda temperature of the mixture, they used the disappearance of second sound at this temperature. They found that for concentrations below 4% the lambda temperature decreases linearly with ^{3}He concentration with a slope of — 1.5 degree per mol.

From the Leiden specific heat measurements we conclude also to a shift of the λ point of — 1,5 degree per mol. There exist a considerable number of theoretical calculations on the dependence of the lambda point on ^{3}He concentration. Most of the authors mentioned in section 3 have made numerical evaluations of this dependence. Nearly all theories give roughly the correct behaviour of this quantity, differing mostly in the initial slope of the curve of T_λ versus X, as is shown in Table 1. Although Pomeranchuk made no calculations on

TABLE 1

Theoretical initial slope of the curve of T_λ versus X

Authors	$(\partial T_\lambda/\partial X)$ in degrees per mol.
Stout [19]	— 3.4
De Boer and Gorter [17] G_4 linear in T.	— 2.7
G_4 quadratic in T. [23]	— 3.2
Rice [18]	— 3.2
Heer and Daunt [14]	— 1.9
Harasima [22]	— 2.6
Mikura [24]	— 2.7
Pomeranchuk [26]	— 0.8

the shift of the lambda point one can estimate this quantity taking for the lambda point the temperature at which the mass of the excited

particles becomes equal to the total mass. With an effective mass derived from experiments on second sound one obtaines a shift of about 0.8 degree per mol.

For the sake of simplicity we will give only the final expression of two of the theories, i.e. those of De Boer and Gorter and of Mikura.

The former authors give the following expression:

$$1 - X = \exp\left[-(\partial G/\partial x)_{T_\lambda}/RT_\lambda\right]_{x=1} \tag{12}$$

In the theory of Mikura one obtains:

$$T_\lambda = T_\lambda^\circ \left[1 - X \Big/ \left\{1 + \left(\frac{V_3^\circ}{V_4^\circ} - 1\right) X\right\}\right]^{2/3}$$
$$\exp\left[\tfrac{2}{3}(\Delta_0/T_\lambda^\circ)\left\{1 - X \Big/ \left\{1 + \left(\frac{V_3^\circ}{V_3^\circ} - 1\right) X\right\}\left(\frac{T_\lambda^\circ}{T_\lambda}\right) - 1\right\}\right]. \tag{13}$$

T_λ° being the lambda point in pure ^{4}He. The results of both formulae are shown in Fig. 8.

As Daunt [23] has drawn attention to the influence of the form of the Gibbs function on the dependence of the lambda point on ^{3}He concentration, we give in Fig. 8 also the results of the Gibbs function as suggested by De Boer [36]:

$$G_4 = E_0\,(1 - x^{7/6}) - \tfrac{1}{2}\,(S_\lambda/T_\lambda)\,x^{5/6}\,T^2 \text{ (cf. eq. 4)} \tag{14}$$

6. The Heat of Mixing in ^{3}He—^{4}He Mixtures

Before the heat of mixing was actually measured Sommers made some estimates of the order of magnitude [15].

There are various possible ways to derive the thermodynamical quantities of a mixture from the measured values of the vapour pressure as a function of liquid and vapour concentration at different temperatures. Morrow [37], for instance, calculated the values of the so-called excess potentials, i.e. the differences between the partial thermodynamical potentials for a classical ideal mixture and the values derived from the vapour pressure measurements of Sommers. Although from a mathematical point of view the different thermodynamical quantities are fully determined, the uncertainty of the experimental data limits the accuracy of such computations to a rather low degree. Sommers calculated the latent heat of evaporation for different concentrations with the aid of the Clapeyron equation for a mixture. His results show that this quantity is not given by a linear combination

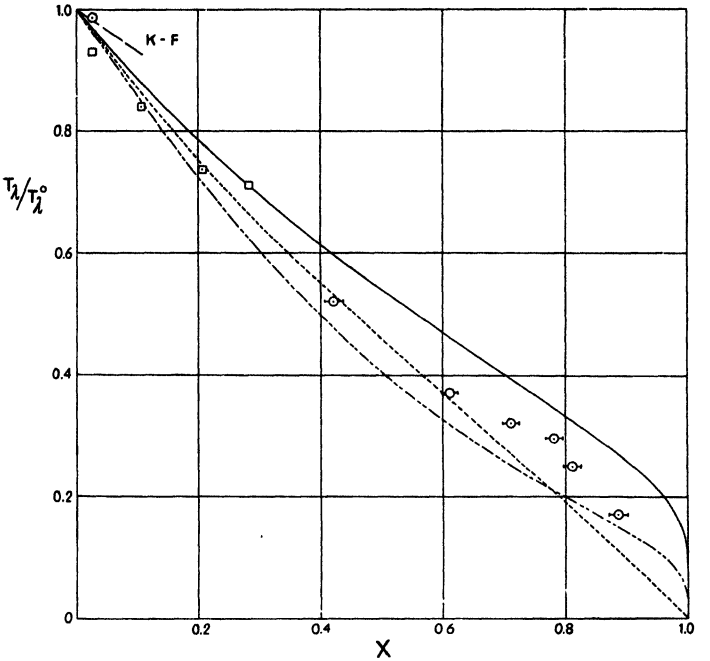

Fig. 8. The ratio of the lambda temperature of a mixture $T\lambda$, to that of pure ^{4}He, $T\lambda^\circ$, as a function of the concentration X.
——— - - ——— - - de Boer and Gorter (quadratic in T)
——————— de Boer (linear in T)
- - - - - - - - - - - Mikura
□ Experimental results of Abraham, Osborne and Weinstock.
-⊙- ,, ,, ,, Heer and Daunt.
K-F Experimental results of King and Fairbank.
⊙ Leiden specific heat result.

of the corresponding values for the pure components as in the case of an ideal classical solution, but indicate a heat of mixing of the order of 3 cal. per mol at 1.5°K.

Up to now only one direct experimental result is available.

Sommers, Keller and Dash [38] measured the integral heat of mixing at constant temperature for a 8.6% mixture at 1.02°K in the following way: A known amount of liquid ^{3}He is separated from a reservoir containing pure ^{4}He by a thin wall. By breaking this diafragm the two liquids are mixed. The temperature drop that would occur by the mixing process is compensated by the condensation of a certain amount of helium gas which is subsequently determined. Knowing the heat of evaporation one is able to calculate a lower limit for the integral

heat of mixing at constant temperature, ΔH. Their result was a positive heat of mixing of 1.98 cal. per mol ^{3}He. They compared this value with that derived from a classical regular solution as given by Van Laar: 3.02 cal. per mol [15, 39].

As this theory is purely classical, the character of the heat of mixing is still rather obscure. More light is shed on its nature by the expression that follows from the theory of De Boer and Gorter:

$$\Delta H_{mol} = (1 - X)\,(x^{7/6} - x_0^{7/6})\,E_0 \tag{15}$$

Using a Taylor expansion for low concentrations one gets:

$$\Delta H_{mol} = (1 - X)\,\Delta x\, S_\lambda\, T \tag{16}$$

Δx being the amount of normal fluid induced by the ^{3}He. From eq. (16) it is clear that in this model the heat of mixing is entirely due to the excitation of an extra amount of normal fluid. As $(\partial x/\partial X)_T$ is in dilute mixtures independent of concentration, the same will be true for the molar heat of mixing.

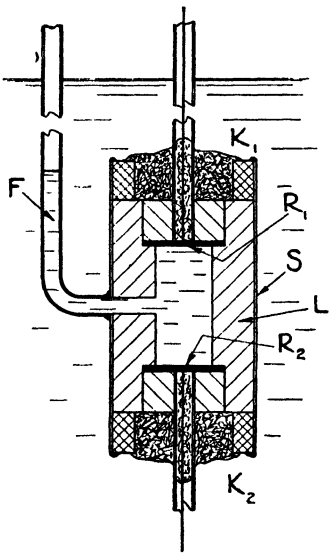

Fig. 9. The low temperature apparatus for the determination of the velocity of second sound as used by Lynton and Faibank.

Similar considerations are approximately valid in the case of the theories of Heer and Daunt and of Mikura. As in these theories x is not so strongly influenced by the presence of ^{3}He (cf. Fig. 5) the molar heat of mixing will be smaller than that given by Eq. (16). In the model of Mikura the value will be partly compensated by the decrease of the energy gap $k\Delta$ by the presence of ^{3}He.

Nanda [40] made some computations of ΔH for the theories of De Boer and Gorter and of Heer and Daunt. For the experiment of Sommers *et al.* he derives the values: 3.35 cal per mol (De Boer and Gorter, G_4 quadratic in T) and 0.68 cal per mol (Heer and Daunt) as compared with the lower limit given by Sommers c.s. of 1.98 cal per mol.

7. The Influence of ^{3}He on the Velocity of Second Sound

Lynton and Fairbank [41] showed that the velocity of second sound is influenced considerably by small amounts of ^{3}He. They measured this quantity in mixtures ranging in concentration between 0.09% and 0.8%. The velocity of second sound was measured using the pulse method, whereby the time of flight of a single heat pulse between the transmitter and the receiver a known distance apart is measured from the photograph of an oscilloscope trace using standard radar techniques. The error in the determination of the velocity is not greater than 1%. Fig. 9 gives a schematic diagram of the low temperature part of the apparatus, It consisted of a set of closely fitting lucite parts, L, holding

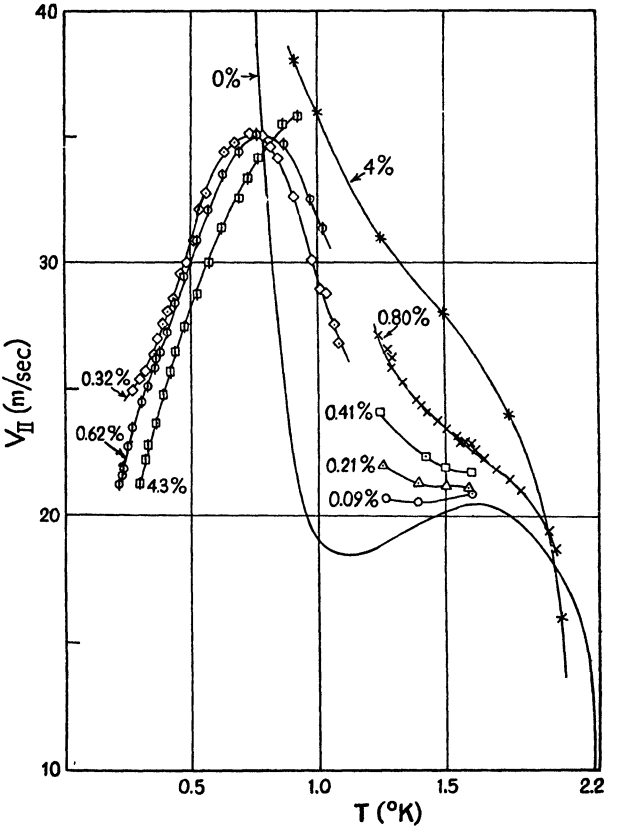

Fig. 10. The velocity of second sound, v_{II}, plotted as a function of temperature at different liquid concentrations. ⊙, Δ, □ and × Lynton and Fairbank. * Weinstock and Pellam. ◇, ⊕ and ⊏⊐ King and Fairbank ———— pure ^{4}He.

two circular carbon strip resistors, R_1 and R_2, at either end of a cavity. To each resistor were soldered two Kovar wires, one of which was connected to a Kovar tube, which together with the wire formed a coaxial lead. The whole assembly was made vacuum tight by means of a stainless steel sleeve, S. The cavity was filled via a copper tube F. The diameter of the cavity was smaller than that of the resistors; this difference insured that the second sound propagation was essentially one-dimensional.

As is shown in Fig. 10 they found a strong increase in the velocity of second sound; this increase being more pronounced at the lower temperatures.

Weinstock and Pellam [42] used for the determination of the velocity a thermal Rayleigh disk (cf. Ch. III). With a 4% mixture they got results that are in good agreement with those of Lynton and Fairbank (Fig. 9). Furthermore they found that the directing force acting on the disk decreased strongly in the presence of ^{3}He. At the lowest temperature, 0.9°K, the value was only a few tenths percent of that in pure ^{4}He.

Recently King and Fairbank [43] performed experiments below 1°K with a method similar to that of Lynton and Fairbank in mixtures with concentrations between 0.0017% and 4.3%. They found that the velocity of second sound has a maximum at about 0.8°K and below that temperature is nearly independent of ^{3}He-concentration, while the value decreases with the square root of temperature (Fig. 10). In contrast to the results [44] in pure ^{4}He at these temperatures the heat pulse shows no dispersion.

We will now compare the different experimental results with those of theory. Expressions for the velocity of second sound in mixtures are given by Pomeranchuk, [26] Koide and Usui, [20] Mikura [24] and by Price [45].

Koide and Usui consider two different cases, namely that, in second sound, ^{3}He moves with the normal fluid, and the case in which it remains at rest. Using for the Gibbs' function of the mixture a form similar to that of De Boer and Gorter (cf. Eq. (3)), they find that agreement with experiment can only be reached if one assumes that ^{3}He remains at rest. Their considerations are restricted to temperatures above 1°K.

Mikura on the contrary shows that if one assumes a Bose-Einstein liquid model, agreement can only be reached in the case that ^{3}He moves with the normal fluid.

These results are an argument against the theory of De Boer and Gorter, as from other experiments (cf. § 1) it is clear that in a stationary flow of He II, ^{3}He takes part in the motion of the normal fluid. There still remains, however, the possibility that in an oscillating movement of rather high frequency the ^{3}He remains at rest.

A more general treatment of this problem is given by Price, who considers in detail the consequences of the various assumptions regarding the behaviour of ^{3}He in the equations of motion. In the case that ^{3}He moves with the velocity of the normal component his results are for low concentrations identical with those derived by Pomeranchuk (cf. section 3, Eq. 10 and Eq. 11).

Lynton and Fairbank, [46] Khalatnikov [47] and King and Fairbank [35] compared the experimental results with this theory. It appeared that good agreement could be reached if one assumes for μ_3 a value that varies slightly in linear way with temperature from 3.6 m_3 at 1.8°K to 2 m_3 at 0.2°K, m_3 being the atomic mass of ^{3}He. The behaviour in the low temperature region is in good agreement with the prediction of Eq. (11).

Finally Koide and Usui [48] derive expressions for the torque exerted on the thermal Rayleigh disk in a mixture. With the above mentioned assumption on the behaviour of ^{3}He, their results are qualitatively in good agreement with those of experiments by Weinstock and Pellam. Mikura [49] obtains the same result for his Bose-Einstein liquid model if he assumes that the ^{3}He moves with the normal fluid.

8. The Influence of ^{3}He on the Fountain Effect

In their experiments on dilute mixtures of ^{3}He and He II Daunt, Probst and Johnston [3] found a kind of osmotic effect. Their apparatus consisted essentially of two reservoirs connected at the upper side by a narrow slit (cf. Fig. 11). When a mixture was condensed in one of the vessels the slit acted as a semipermeable wall. The ^{4}He can pass through the slit by means of the creeping film, but the ^{3}He is stopped as it does not take part in the film flow and the slit is almost gas tight. It appeared that contrary to the behaviour of pure He II the liquid levels in both reservoirs were not at the same height, the level of the mixture being always higher than that of the pure ^{4}He.

Quantitative data were provided by Taconis, Beenakker and Dokoupil [50]. Figure 11 gives a schematic diagram of their apparatus. Two reservoirs A and B are connected by a narrow slit S. In the vessel A

a heater is placed to create a temperature difference between A and B, the latter always being at the temperature of the surrounding helium bath. This temperature difference can be determined by the vapour pressure difference between the liquid in A and the bath as measured by a differential oil manometer. In the same way the difference in pressure between B and the bath was measured.

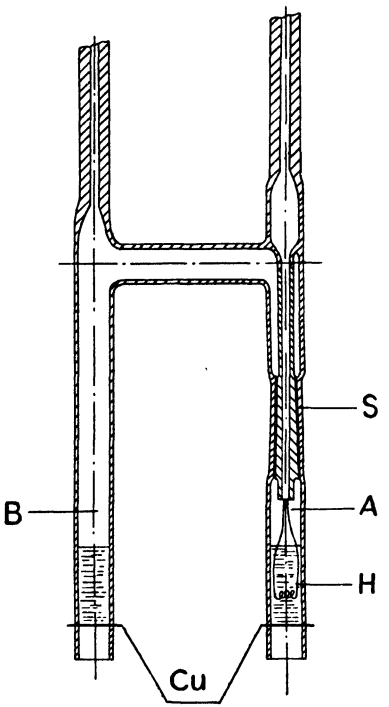

Fig. 11. Apparatus for studying the fountain effect in mixtures.

In B a known amount of a ^{3}He—^{4}He mixture with a concentration of about 10^{-3} was condensed and the excess pressure of the mixture with respect to the bath was measured. This pressure difference is almost entirely due to the ^{3}He-atoms in the vapour. Hence knowing the volumes of the gas and the liquid, the concentration of the ^{3}He in the liquid can be calculated by a mass balance.

By heating in A a temperature difference between both reservoirs was created and it was found that a certain amount of the liquid flowed from B over to A so that for each temperature difference there was a well defined equilibrium position of the levels in A and B. These results can be interpreted in the following way: In a stationary situation the force acting on the superfluid due to the temperature difference – the fountain pressure – was counterbalanced by a force in the opposite direction due to difference in the^3 He concentration: the osmotic pressure.

The results of Taconis *et al.* [50] were in agreement with the relation:

$$\varrho\, RT\, X/M = f\, \Delta T \tag{17}$$

where ϱ and M are the density and the molecular weight of the ^{4}He, X the concentration of the ^{3}He in B, f the fountain pressure per degree temperature difference and ΔT the temperature difference between A and B. So according to these experiments the osmotic force is given by the law of Van 't Hoff as in ordinary liquids.

More light is shed on these results by a derivation of Eq. (17) due to Gorter, Taconis and Beenakker [51] starting from the equations of motion for the superfluid. When we assume that for very dilute mixtures, in a first approximation the relation.

$$(1 - x) \operatorname{grad} p + x (1 - x) \varrho (\partial^2 G/\partial x^2) \operatorname{grad} x = 0 \tag{18}$$

remains valid, we get for a stationary situation neglecting outside forces:

$$\operatorname{grad} x = 0 \tag{19}$$

In this equation the presence of the ^{3}He can easily be introduced by putting:

$$\operatorname{grad} x = (\partial x/\partial X)_T \operatorname{grad} X + (\partial x/\partial T)_X \operatorname{grad} T \tag{20}$$

Hence we see that in this case a gradient in the concentration of the normal fluid due to a temperature gradient must be balanced by an opposite gradient in the same concentration due to a gradient in the concentration of the ^{3}He. Substituting in (20) for $(\partial x/\partial X)_T$ and $(\partial x/\partial T)_X$ the values valid under the assumption that the ^{3}He forms an ideal mixture with the normal fluid (de Boer and Gorter [17b]) we get $\varrho RT/M = f \Delta T$ in agreement with Eq. (17). This result was later substantiated by calculations with the aid of the thermodynamics of irreversible processes by Mazur [52]. The same relation can also be derived with the aid of the equations of motion given by Pomeranchuk [26] for a dilute mixture of ^{3}He and ^{4}He. For a stationary case he gets:

$$\operatorname{grad} \mu_4 = 0 \tag{21}$$

where μ_4 is the partial thermodynamic potential of the ^{4}He in the mixture, which is identical to the common derivation of Van 't Hoffs law. A similar result for small concentrations of ^{3}He is given by Mikura [24].

With the apparatus described in § 2 measurements were made on higher concentrations (to about 3%) and correspondingly larger temperature differences (of a few tenths of a degree) were used. In the stationary state, to each temperature difference between vessel A and B, corresponds a well defined value for the liquid concentration X, and this is adjusted by the helium film creep through the superleak until the equilibrium is reached. The results are shown in Fig. 12. The liquid concentration X is derived from the measurements as indicated in § 2, x_B is the value for the normal fraction in the pure ^{4}He

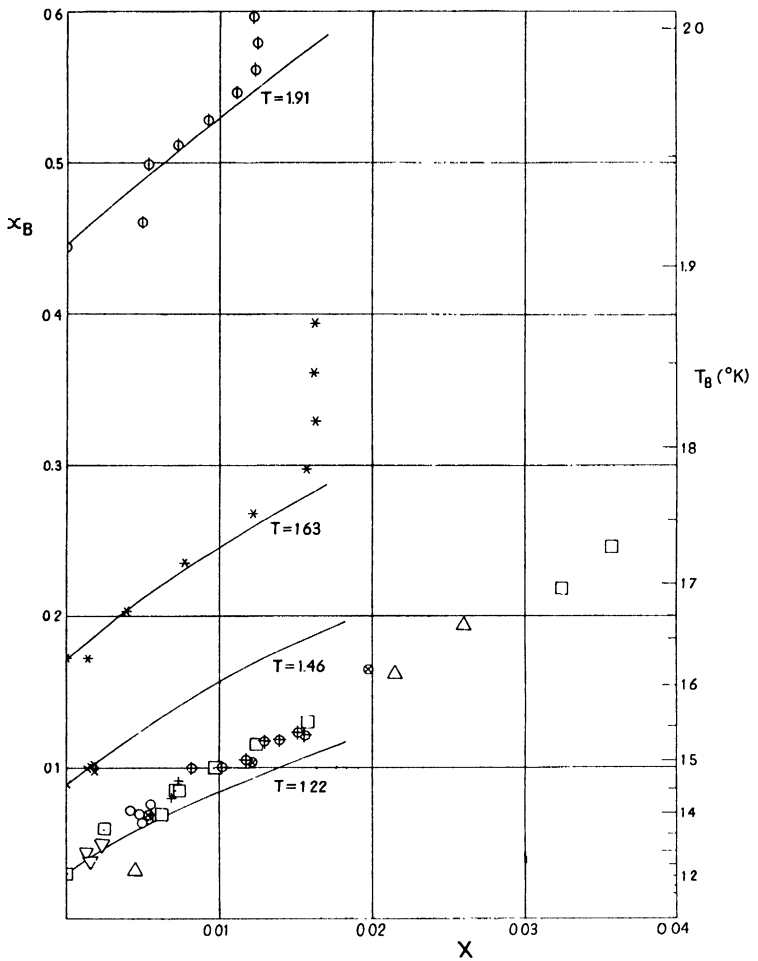

Fig. 12. Measurement of the fountain effect.
x_B versus X (left ordinate) T_B versus X (right ordinate).

in vessel B at the temperature created by heating. As in the theory of de Boer and Gorter (see also Gorter, Taconis and Beenakker) the value of x in vessel A is approximately the same as in vessel B, i.e. grad $x \approx 0$ over the superleak, one can compare the so found dependence of x on X with the results of this theory. In the graph the de Boer and Gorter values are drawn using the Gibbs function quadratic in T. The linear dependence of x in vessel B on the ^{3}He concentration in vessel A can also be derived in a good approximation by integrating Eq. (17) after introducing for f the value $\varrho\, x\, S_\lambda$.

9. The Influence of ^{3}He on the Heat Transport in He II

In § 1 we saw that a very good separation of ^{3}He and ^{4}He can be achieved by creating a stationary heat current in He II. This heat current carries the ^{3}He to that part of the apparatus which is artificially kept cold. Taconis and Mellink [7], who obtained in this way a separation factor of about 4000, estimated that in the stationary situation there was an enrichment of the concentration by about a factor two for each millimeter of heat current path. Such a pronounced gradient in the concentration of the ^{3}He has an influence on the heat conductivity of the mixture, as was measured by Beenakker, Taconis, Lynton, Dokoupil and Van Soest [53].

Fig. 13 is a schematic diagram of their apparatus. R is the reservoir for the mixture with a height of 1 mm. This reservoir is connected by means of a narrow capillary and a glass tube, c, with a differential oil manometer to measure the pressure difference between the liquid in c and the surrounding helium bath. Reservoir and capillary are surrounded by a vacuum jacket. At the bottom of the reservoir a heater, H, is mounted.

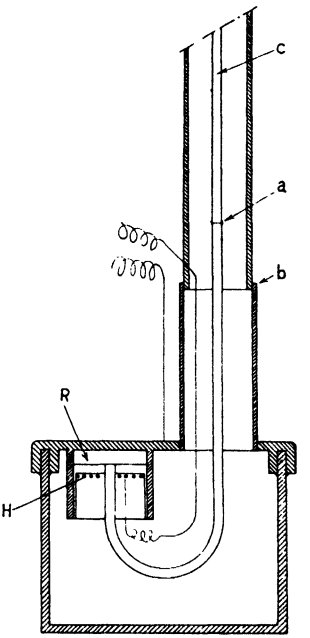

Fig. 13. Apparatus for measuring the influence of ^{3}He on the heat transport in He II.

With a Toepler pump a certain amount of a ^{3}He—^{4}He mixture from a known concentration ranging between 0.6 and 2.8×10^{-4} was condensed in the reservoir until the liquid level became visible in the glass tube at a. As the concentration of the ^{3}He is rather small, the vapour pressure of the liquid at a can be used as a thermometer for the temperature of this place. The difference in temperature between a and the helium bath was measured as a function of the amount of heat supplied by the heater at different temperatures and concentrations.

There exists a linear relation between the heat supplied, Q, and the temperature difference, ΔT. The slope of the curves for ΔT versus Q gives the heat resistance of the mixture in degrees per watt.

Fig. 14 gives a graphical representation of the measured resistances as a function of temperature at different concentrations. For the inter-

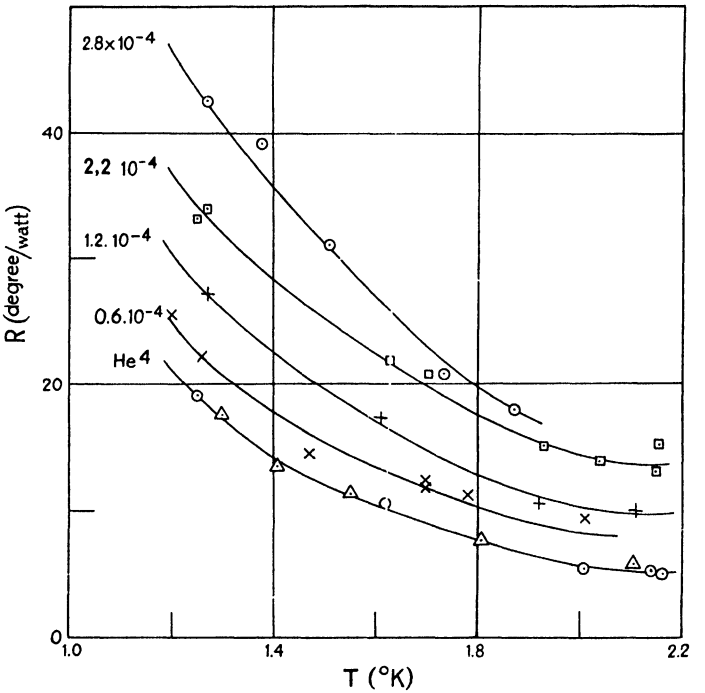

Fig. 14. The heat resistance, R, as a function of temperature at different concentrations.

pretation of these results, the heat resistance of the apparatus if filled with pure He II was measured.

As was shown by Kapitza [54] there is a finite heat resistance between a wall and the He II liquid. This resistance is confined to the immediate surroundings of the wall [51, 55, 56, 57].

Since the extra resistance is caused by a gradient in the ^{3}He concentration which exists in the bulk liquid, one can assume that the influence of the ^{3}He and the so-called Kapitza resistance are additive effects. For small concentrations the value of the Kapitza resistance will not alter very much, hence the heat resistance due to the presence of the ^{3}He can be found by subtracting from the measured value for the mixture the corresponding value for pure He II. The resistances derived in this way are proportional to the concentration of the ^{3}He as is shown in Fig. 15.

These results can be interpreted in the following way. The heat current in the reservoir takes place by a stream of normal fluid that

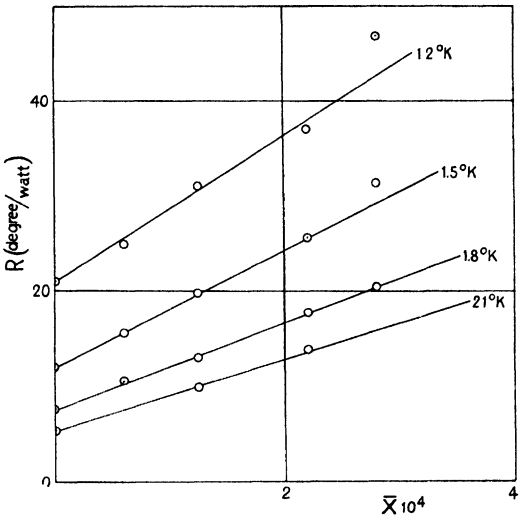

Fig. 15. The heat resistance, R, as a function of the concentration, $\bar{X}$, at different temperatures.

drives the ^{3}He atoms to the cold wall. Hence there is established a gradient of the ^{3}He concentration which will give rise to a back diffusion of the ^{3}He. In a stationary situation, assuming that there is no slip between the normal and the ^{3}He atoms and that no stirring occurs – the higher concentration and hence the lighter part of the liquid is at the upper side of the reservoir (Fig. 1) – we obtain:

$$D \frac{dX}{dz} + v_n X = 0, \tag{22}$$

where D is the diffusion coefficient of ^{3}He in He II, v_n the velocity of the normal fluid. Using the balance of mass for the ^{3}He, we get for the difference in concentration over the reservoir, ΔX:

$$\Delta X = - v_n X \, h/D, \tag{23}$$

where h is the height of the reservoir. This difference in concentration is related to a temperature difference according to

$$\varrho \, R \, T \, \Delta X/M = f \, \Delta T \text{ (cf. Eq. 17).}$$

Hence we get for the resistance R_3 of the mixture:

$$R_3 = (R \, \varrho h/f^2 O) \, X/D, \tag{24}$$

where O is the surface across which the heat current takes place and X the mean concentration in the reservoir. From this equation the diffusion constant can be calculated, when a correction for the influence of the capillary is applied *.

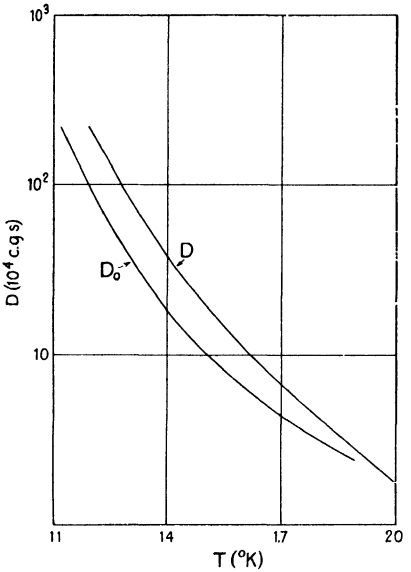

Fig. 16. The diffusion constant, D, as a function of temperature; for comparison the value of $D_0 = 1.4\,\eta/\varrho_n$ is given.

The results of this calculation are shown in Fig. 16 where D is plotted as a function of temperature. As at temperatures far enough from the lambda point the density of the normal fluid becomes rather small, one may try to describe the diffusion process as the self diffusion of normal ^{4}He atoms. For a gas of hard elastic spheres one gets

$$D_0 = 3\,A\,\eta/\varrho_n, \qquad (25)$$

where A is a constant with a value of about 0.46, η the viscosity of He II and ϱ_n the density of the normal fluid.

Fig. 16 shows that there is a good qualitative agreement between both values. This might suggest that the diffusion process of ^{3}He in He II shows a gas-like behaviour. Since according to this result the extra heat resistance is proportional to the concentration of the ^{3}He, it is possible in this way to determine the concentrations of a given mixture relative to a standard.

10. The Influence of ^{3}He on the Helium Transfer through Superleaks

The apparatus described in § 2 (Fig. 4) opens the possibility to study the helium transfer through the superleak as a function of the temperature difference over the superleak and the ^{3}He concentration in the lower vessel A. It was thought that in this way it would be possible to measure the influence of the ^{3}He on the filmtransfer over the wall immediately below the entrance of the slit and to be able to compare the results with those of Hammel and Schuch [58]). These authors mea-

* This correction was erroneously omitted in the original publication of Beenakker *et al* [53].

sured the quantity of ^{4}He flowing through a superleak from a vessel containing a ^{3}He—^{4}He mixture in equilibrium with its saturated vapour to a vessel that was evacuated and kept at the same temperature. The superleak was located above the liquid level. They found that the transport was considerably influenced by the presence of ^{3}He having a much lower value at higher ^{3}He concentrations. Moreover it was found that also some ^{3}He was transported through the superleak.

A closer examination of this phenomenon by Wansink *et al.*[59] revealed, however, that the helium transfer was determined by the flow through a superleak that is completely filled with liquid instead of by filmtransfer, as it appeared that the transfer rate depended not only on the ^{3}He concentration, but also on the temperature difference over the slit and the width of this slit which was altered during the experiments. As was found by Winkel[60] such a liquid helium transfer is strongly dependent on the temperature difference and the width of the slit. From his experiments can be concluded that the transfer velocity is given by $v^m = A/\Delta T$, where A is a constant of the apparatus and $/$ the value of the fountain pressure per degree. The value of m is dependent on the width of the slit being equal to 3 for wider slits and increasing to values of 5 or even 6 for narrow slits. The much smaller transfer rate in the presence of ^{3}He can be explained by a decrease of the fountain pressure due to the osmotic pressure of the ^{3}He. Using the apparatus described in § 2 Wansink *et al.* found values of m as high as 7 corresponding to the very narrow slit used in this apparatus. Their experiments give as a preliminary result the same kind of curves of transfer velocity versus the effective fountain pressure, as in the case of pure ^{4}He, provided that an effective fountain pressure is used, which is equal to the fountain pressure in pure ^{4}He diminished by the osmotic pressure of the ^{3}He as given by Van 't Hoffs relation.

It seems to us that the same explanation is also valid for the experiments of Hammel and Schuch as also in their case the slit would be filled with liquid. This assumption is strengthened by their result that some ^{3}He is also transferred through the slit. In the Leiden apparatus the ^{3}He did not pass through the superleak due to a heat flow created by the difference in the temperature between the two vessels. The flow of normal fluid will drive the ^{3}He back to the vessel A.

In conclusion we should like to remark that although experimental data are available over the whole field of properties of these mixtures, they are far from complete enough to decide between the different

theoretical descriptions and only more and accurate data will make it possible to give a satisfactory interpretation to the entire behaviour of mixtures.

REFERENCES

[1] L. W. Alvarez and R. Cornog, Phys. Rev., **56**, 379 613, (1939).
[2] B. F. Saris, Thesis, Leiden, (1941); J. Franck, Phys. Rev., **70**, 561, (1946).
[3] J. G. Daunt, R. E. Probst and H. L. Johnston, Phys. Rev., **73**, 638, (1948); J. Chem. Phys., **15**, 759, (1947.)
[4] L. T. Aldrich and A. O. Nier, Phys. Rev., **70**, 983, (1946); Phys. Rev., **74**, 1590, (1950).
[5] R. C. Jones and W. A. Furry, Rev. Mod. Phys., **18**, 151, (1946); B. B. Mc.Inteer, L. T. Aldrich and A. O. Nier, Phys. Rev., **74**, 946, (1948).
[6] C. T. Lane, H. A. Fairbank, L. T. Aldrich and A. O. Nier, Phys. Rev., **73**, 256, (1948); Phys. Rev., **75**, 46, (1949).
[7] K. W. Taconis, Ned. Tijd. Nat., **16**, 101, (1950).
[8] T. Soller, W. M. Fairbank and A. D. Crowell, Phys. Rev., **91**, 1058, (1953).
[9] H. A. Fairbank, C. T. Lane, L. T. Aldrich and A. O. Nier, Phys. Rev., **71**, 911, (1947); Phys. Rev., **73**, 729, (1948).
[10] J. G. Daunt, R. E. Probst and S. R. Smith, Phys. Rev., **74**, 494, (1948).
[11] K. W. Taconis, J. J. M. Beenakker, L. T. Aldrich and A. O. C. Nier, Physica, **15**, 733, (1949); Leiden Comm., 279a.
[12] B. Weinstock, D. V. Osborne and B. M. Abraham Phys. Rev., **77**, 400, (1950).
[13] B. N. Eselsohn and B. G. Lazarev, J. exp. theor. Phys. U.S.S.R., **20**, 1055, (1950).
[14] C. V. Heer and J. G. Daunt, Phys. Rev., **81**, 447, (1951).
[15] H. S. Sommers, Phys. Rev., **88**, 113, (1952).
[16] To be published in Physica before long.
[17a] J. de Boer and C. J. Gorter, Phys. Rev., **77**, 569, (1950);
[b] Physica, **16**, 225, 667, (1950); Leiden Comm. Suppl. 101a.
[18] O. K. Rice, Phys. Rev., **76**, 1701, (1949); **77**, 142, (1950); **79**, 1024, (1950).
O. K. Rice and O. G. Engel, Phys. Rev., **78**, 183, (1950).
O. G. Engel and O. K. Rice, Phys. Rev., **77**, 55, (1950).
[19] J. W. Stout, Phys. Rev., **76**, 864, (1949).
[20] S. Koide and T. Usui, Prog. Theor. Phys. Japan, **6**, 506, 622, (1951).
S. Koide, N. Matsudaira and T. Usui, Sc. Pap. Coll. Educ. Tokyo, **2**, 129, (1952).
[21] K. W. Taconis, J. J. M. Beenakker, L. T. Aldrich and A. O. C. Nier, Phys. Rev., **75**, 1966, (1949).
[22] A. Harasima, J. Phys. Soc. Japan, **6**, 271 (1951).
[23a] J. G. Daunt, T. P. Tseng and C. V. Heer, Phys. Rev., **86**, 911, (1952).
[23b] J. G. Daunt, Phil. Mag. Suppl., **1**, 209, (1952).
[24] Z. Mikura, Prog. Theor. Phys. Japan, **11**, 25, (1954).
[25] M. Toda and A. Isihara, Prog. Theor. Phys. Japan, **6**, 480, (1951).
[26] J. Pomeranchuk, J. Exp. Theor. Phys. U.S.S.R. **19**, 42, (1949).
[27] F. D. London, Nature, **141**, 643, (1938); Phys. Rev., **54**, 947, (1938); J. Phys. Chem., **43**, 49, (1939).
[28] A. Einstein, Sb. Preuss. Akad. Berlin, 261, (1924); 3 (1925).
[29] A. Bijl, J. de Boer and A. Michels, Physica **8**, 655, (1941).
[30] J. de Boer and C. J. Gorter, Physica, **18**, 565, (1952): Leiden Comm. Suppl. 104e.

[31] H. C. Kramers, J. D. Wascher and C. J. Gorter, Physica, **18**, 329, (1952); Leiden Comm. 288c.
[32] B. M. Abraham, B. Weinstock and D. V. Osborne, Phys. Rev., **76**, 864, (1949).
[33] B. N. Eselsohn and B. G. Lazarev, Dok. Akad. Sc. U.S.S.R. **72**, 265, (1950).
[34] J. G. Daunt and C. V. Heer, Phys. Rev., **79**, 46, (1950).
[35] J. C. King and H. A. Fairbank, Bull. Am. Phys. Soc. (3) **28**, 65, (1953).
[36] J. de Boer, Phys. Rev., **76**, 852, (1949).
[37] J. C. Morrow, Phys. Rev., **89**, 1034, (1953).
[38] H. S. Sommers, W. E. Keller and J. G. Dash, Phys. Rev., **91**, 489, (1953); **92**, 1345, (1953).
[39] J. H. Hildebrand and R. L. Scott, Solubility in non-electrolytes, Reinhold Publ. Comp. New York, 1950, Chap. 2, 3, 7 and 8.
[40] V. S. Nanda, Phys. Rev., **94**, 241, (1954).
[41] E. A. Lynton and H. A. Fairbank, Phys. Rev., **80**, 1043, (1950).
[42] B. Weinstock and J. R. Pellam, Phys. Rev., **89**, 521, (1953).
[43] J. C. King and H. A. Fairbank, Phys. Rev., **93**, 21, (1953).
[44] K. R. Atkins and D. V. Osborne, Phil. Mag. **41**, 1078 (1950). H. C. Kramers, F. A. W. v. d. Burg and C. J. Gorter, Phys. Rev., **90**, 1117 (1953). D. de Klerk, R. P. Hudson and J. R. Pellam, Phys. Rev., **93**, 28 (1953).
[45] P. J. Price, Phys. Rev., **89**, 1209, (1953).
[46] E. A. Lynton and H. A. Fairbank, Proc. Int. Conf. Low Temp. Phys. Oxford, 88 (1951).
[47] I. M. Khalatnikov, Dok. Akad. Sci. U.S.S.R., **79**, 57 (1951).
[48] S. Koide and T. Usui, Prog. Theor. Phys. Japan, **6**, 622, (1951).
[49] Z. Mikura, Prog. Theor. Phys. Japan, in print.
[50] K. W. Taconis, J. J. M. Beenakker and Z. Dokoupil, Phys., Rev. 78, 171 (1950).
[51] C. J. Gorter, K. W. Taconis and J. J. M. Beenakker, Physica, **17**, 841, (1951) Leiden Comm. Suppl. 103d.
[52] P. Mazur, Thesis, Utrecht 1951.
[53] J. J. M. Beenakker, K. W. Taconis, E. A. Lynton, Z. Dokoupil and G. van Soest, Physica, **18**, 433 (1953), Leiden, Comm. 289a.
[54] P. L. Kapitza, J. Phys. U.S.S.R., **4**, 181 (1941).
[55] R. Kronig and A. Thellung, Physica, **16**, 678 (1950).
[56] R. Kronig, A. Thellung and P. Woldringh, Physica, **18**, 21 (1952).
[57] I. M. Khalatnikov, J. Exp. Theor. Phys., **22**, 687 (1952).
[58] E. F. Hammel and A. F. Schuch, Phys. Rev., **87**, 154 (1952).
[59] D. H. N. Wansink et. al. To be published in Physica.
[60] P. Winkel, Thesis, Leiden 69, (1954).

CHAPTER VII

THE MAGNETIC THRESHOLD CURVE OF SUPERCONDUCTORS

BY

B. SERIN

RUTGERS UNIVERSITY, NEW BRUNSWICK, N.J.

1. Introduction

In 1914, three years after his discovery of superconductivity, Kamerlingh Onnes [1] observed that the perfect conductivity property is destroyed and the normal resistivity restored by the application of a large magnetic field. Several years later, Tuyn and Kamerlingh Onnes [2] showed that when the applied magnetic field is parallel to the length of a wire, the field value which restores resistance is quite precisely defined at each temperature. This field value is termed the threshold field or critical field. The experiments indicated clearly that the threshold field value increases approximately proportionally to $(T_c^2-T^2)$, as the temperature T is reduced below the transition temperature T_c.

The suggestion that thermodynamics could be applied profitably to this magnetically induced transition from the superconducting state to the normal resistance state came from several quarters. However, the theoretical position was obscure so long as a superconductor was regarded merely as a perfect conductor. From this viewpoint, the currents induced in the superconductor as the magnetic field is increased to the threshold value must necessarily be dissipated with the evolution of Joule heat upon the transition into the normal state. Thus the transition must be regarded as essentially irreversible.

Clarification came with the discovery by Meissner [3] that the magnetic induction is always zero inside a reasonably large specimen of superconductive metal. The experiments, for example, showed that in order to achieve this state of perfect magnetic shielding, superconducting surface currents appear in a sphere cooled below the transition

temperature in a constant field, and then disappear in a reversible manner as the applied magnetic field is decreased to zero. These observations cannot be explained by assuming perfect conductivity [4]. It therefore may be inferred that superconducting currents differ in an essential way from usual conduction currents, and that in principle the former can disappear reversibly in the magnetic transition to the normal state. A complete thermodynamic theory of the transition was worked out by Gorter and Casimir [5] in 1934.

2. Thermodynamic Discussion

According to the thermodynamic treatment (see Ch. I), superconductive metal and normal metal are two phases of the same substance at any temperature below the transition temperature. In the absence of a magnetic field, the superconductive phase is stable and has the smaller free energy, $F_s(T)$. An applied magnetic field increases the total free energy of the superconductive phase, until the threshold field value is reached. At this point the total superconductive free energy equals the free energy of the normal phase, $F_n(T)$, and the two phases exist in equilibrium. At fields exceeding the threshold value, the normal phase is stable. The curve of threshold field values H_{th} as a function of temperature T, (see Ch. I), therefore divides the H_{th}-T plane into two regions, one corresponding to states of the superconductive phase, the other to states of the normal phase; the curve itself defines the unique values of H_{th} and T for which the two phases are in equilibrium.

For the equilibrium condition we have [5]

$$F_n(T) - F_s(T) = [H_{th}(T)]^2 V/8\pi,$$

where V is the volume of the specimen. The entropy difference and the difference in the specific heats, respectively, are determined from this relation to be

$$S_n(T) - S_s(T) = -(V H_{th}/4\pi)\, \mathrm{d}H_{th}/\mathrm{d}T, \tag{1}$$

$$c_n(T) - c_s(T) = -(VT/4\pi)\,[H_{th}\, \mathrm{d}^2 H_{th}/\mathrm{d}T^2 + (\mathrm{d}H_{th}/\mathrm{d}T)^2], \tag{2}$$

where S is the entropy and c the specific heat.

From the shape of the curve of threshold field as a function of temperature, we can deduce many facts about the thermodynamic properties of the two phases. Several of these deductions are independent of the finer details of the shape. For example, at the transition temperature, the threshold field is zero and the slope of the curve is finite. Thus

we see from (1) that the entropy difference is zero at this temperature, and there is no latent heat of transition. For the same reasons, it follows from (2) that there is a discontinuous increase in the specific heat on passing from the normal phase to the superconductive phase at the transition temperature. Both of these facts were observed [6] before the status of the thermodynamic theory became clear. Furthermore, since the slope of the curve is negative at all temperatures above the absolute zero, the entropy of the superconductive phase is always less than the entropy of the normal phase, establishing that the former phase is a state of greater order than the latter. As the absolute zero is approached, the slope of the threshold field curve approaches zero, and the entropies of both phases tend toward zero, in agreement with the Nernst theorem. Thus the quantity $H_0^2 V/8\pi$, where H_0 is the threshold field at absolute zero, equals the difference in the internal energy of the two phases at this temperature.

We now pass to more particular considerations. Kok [7] showed that if one assumes that the specific heat of the superconductive phase varies as the cube of the temperature, and also uses the well established relation for the specific heat of the normal phase

$$c_n = \gamma T + A\,(T/\Theta)^3, \tag{3}$$

it follows from (2) that the threshold field curve is a parabola (see Ch. I, Eqs. 2 through 6). γT is the electronic specific heat and $A(T/\Theta)^3$ the lattice contribution; (Θ is the Debye temperature). Since all threshold field curves approximate parabolas, Eq. (4) of Ch. I,

$$T_c \approx 2\,(\Delta U_0/\gamma)^{1/2} = 2\,(H_0^2 V/8\pi\gamma)^{1/2}, \tag{4}$$

is approximately verified for tin, indium and thallium [7], when the magnetic data and the calorimetric data are compared.

Daunt and Mendelssohn [8] first used accurate determinations of the threshold field curve as a means of determining thermodynamic quantities; in particular γ, the coefficient of the electronic specific heat term. They did this without making the special assumptions of Kok. It is assumed only that the entropy of the superconductive phase goes to zero more rapidly than T as the temperature approaches the absolute zero. Under these conditions, the dominant term in the entropy difference comes from the electrons of the normal phase and (1) may be written

$$-\,(V H_{th}/4\pi)\,\mathrm{d}H_{th}/\mathrm{d}T \approx \gamma T.$$

Thus, Daunt and Mendelssohn differentiated their low temperature

threshold field data, substituted in the left hand side of the above equation, and plotted the result as a function of temperature. At low temperatures, the curves are linear and pass through the origin so that the slope equals γ. Actually, it is unnecessary to differentiate the data. Under the same assumptions, as $T \to 0$, the free energy of the normal phase is very much greater than the free energy of the superconductive phase, so that Eq. (5), Ch. I., becomes

$$H_{th}^2 V/8\pi = \Delta F \approx F_n = H_0^2 V/8\pi - \gamma T^2/2,$$
$$H_{th} = H_0(1 - 4\pi\gamma T^2/H_0^2/V)^{1/2} \approx H_0 (1 - 2\pi\gamma T^2/H_0^2 V). \quad (5)$$

Since $H_0^2 V/2\pi\gamma$ is of the order of the square of the critical temperature, we have neglected terms of order $(T/T_c)^4$ in expanding the square root. The terms we have neglected in the free energy are of the same order (see Ch. I, Eq. 3 and 4), so that the approximation is self-consistent. We conclude that the threshold field curve is, in general, parabolic at sufficiently low temperatures, so that a plot of H_{th} as a function of T^2 can be used to evaluate γ according to (5). However, it is essential to use only the low temperature data. One cannot use data obtained near the critical temperature, as suggested in a recent publication [9], unless he is certain that the threshold field curve is exactly parabolic over the complete temperature range. Finally we remark that Daunt, Horseman and Mendelssohn [10] used (2) to calculate the specific heat difference from the threshold field data for tin and found excellent agreement with the careful calorimetric measurements of Keesom and van Laer [11]. In § 5, we shall re-examine these calorimetric data. A table of the values of γ obtained from magnetic measurements on superconductors is given in Ch. XI.

Despite the good agreement between the magnetic threshold data and the calorimetric data for tin mentioned above (and also for indium [12] and lead [13]), there exist some metals for which it is most difficult in practice to get meaningful magnetic data. These metals are some of the elements in groups IVa and Va of the periodic table (e.g., vanadium [14], niobium [15] and tantalum [16]) which are noted for their high melting temperatures. The magnetic properties of these substances are more characteristic of superconductive alloys [17] than of the other pure superconductive metals. Generally speaking, the applied field must be increased over a range of several hundred oersteds before the transition to the normal state is complete; and furthermore, the magnetic transition is irreversible. Thus, it is difficult to arrive at a mea-

ningful definition of the threshold field for these substances, and the application of the thermodynamic theory to the interpretation of the data is of dubious validity. We will not discuss them further.

So far we have used, for the most part, only the formal thermodynamic theory of the magnetic phase transition. However, all the results of this theory are implicitly contained at least qualitatively in the two-fluid model discussed in Ch. I. The model has the advantages of providing a crude picture of the superconductive phase and of being formulated directly in terms of the important physical variable γ and ΔU_0. In the next sections we hope to illustrate the usefulness of the two fluid model in the discussion of experimental results.

3. The Isotope Effect

In 1950, Maxwell [18] and Reynolds, Serin and co-workers [19] observed that the transition temperature of a superconductive element depends on the isotopic mass. For a given substance, the relationship is approximately $M^{1/2} T_c = \text{const.}$, (where M is the isotopic mass) for all the elements that have been measured to date. This discovery stimulated several workers to obtain extremely precise threshold field data and also revived interest in the two-fluid model for superconductors.

The early measurements were made near the transition temperature. At a given temperature, the threshold field was determined by noting the field value at which the magnetic induction in the metal abruptly changed from zero to the value of the applied field. Since the threshold field is proportional to $(T_c - T)$ near T_c, the transition temperature was determined by extrapolating to zero threshold field. The threshold field curves of samples (of the same element) of different average isotopic masses all have the same initial slope, but differ in the values of the transition temperature according to the relation $M^{1/2} T_c = \text{const.}$

The measurements were soon extended to low temperatures. Reynolds, Serin and Nesbitt [20] found that the threshold field curves of mercury are parabolic over the whole temperature range. Parabolas were fitted to the data for the different isotopes by the method of least squares. From these curves the parameters γ and K in Kok's relation $c_n - c_s = \gamma T - K T^3$ were determined. It was found that γ was independent of isotopic mass, whereas K varied as the mass. Since Eq. (4) is exact when the threshold field curve is parabolic, it follows that H_0/T_c is a constant for the isotopes of mercury. Thus H_0 also varies as $M^{-\frac{1}{2}}$. The range of isotopic mass available in mercury is only

about two percent, so that all the changes produced by the changes in atomic mass are small and the measurements present considerable difficulties. (For example, the difference in transition temperatures between $^{199.5}$Hg and $^{203.4}$Hg is 0.04°K). Thus the conclusions about γ and K stated above are just within the experimental error.

At about the same time, Lock, Pippard and Shoenberg [21] determined the threshold field curves of tin. The range of isotopic mass available is about ten percent. Thus the isotopic effects are relatively large, and it is possible to arrive at accurate conclusions concerning the thermodynamic parameters.

The threshold field curves of tin are *not* parabolic. Despite this fact, the ratio H_0/T_c is a constant for the isotopes. Furthermore, the reduced field $h = H_{th}/H_0$ is the same function of the reduced temperature $t = T/T_c$ for all the masses. Lock *et al.* pointed out that these two facts constituted a quite general proof that γ is independent of isotopic mass. We can see this by rewriting our expression (5) as

$$h = H/H_0 = 1 - 2\pi\,\gamma\,t^2\,(T_c^2/H_0^2 V),\ t \to 0.$$

Thus if h is a universal function of t and H_0/T_c is a constant, γ too must be a constant. From their data, Lock *et al.* estimated that the difference in γ between $^{116.2}$Sn and $^{123.8}$Sn is such that $\Delta\gamma/\gamma < 1.4 \times 10^{-3}$. They also found that the relation between transition temperature and mass is $M^{0.46}\,T_c = \text{const.}$ in this element. All these results were adequately confirmed by Serin, Reynolds and Lohman [22] and by Maxwell [23]. The isotope effect has also been observed in lead [24] and thallium [25].

In Fig. 1 we show the threshold field data of Serin *et. al.* for tin isotopes. The universality of the relationship between the reduced field and reduced temperature is evident, as is the deviation from parabolic behavior.

The most important conclusion to emerge from these investigations is that the field H_0 varies approximately as $M^{-\frac{1}{2}}$, so that the energy gap in the two-fluid model varies inversely as the isotopic mass. (Elementary reflection indicates that γ should be independent of mass.) Thus it would appear that the energy gap separating the superconductive phase from the normal phase results from some strong interaction between the electrons in the metal and the crystalline lattice. This conclusion seems inevitable, since the frictionless currents are clearly associated only with the electrons and the isotopic mass is a property only of the lattice. In fact, Fröhlich [26], before hearing of

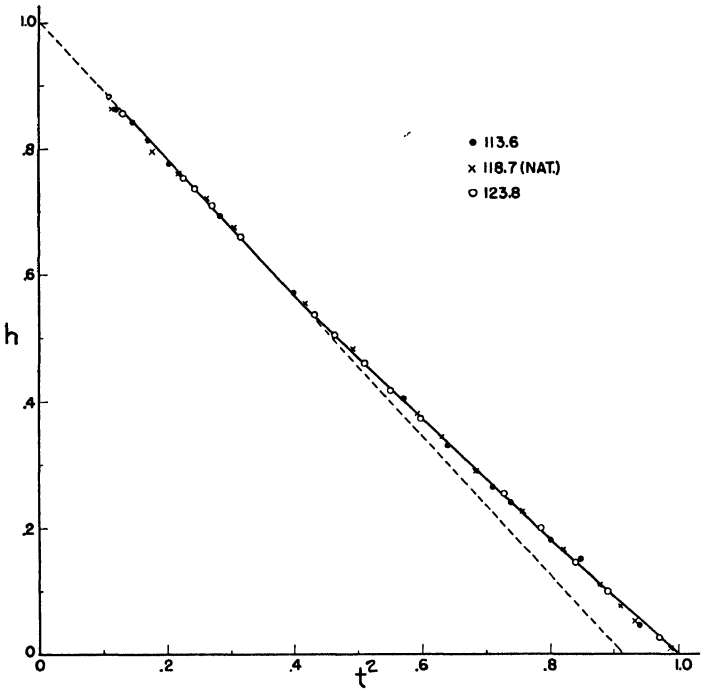

Fig. 1. The reduced threshold field is plotted as a function of the square of the reduced temperature for two tin isotopes and natural tin.

the experimental investigations, had suggested that superconductivity comes about as the result of just such an interaction. (Conversely, the experimentalists were unaware of Fröhlich's theory.) Soon after the discovery of the isotope effect, Bardeen [27] proposed a similar theory These theories are essentially concerned with demonstrating that the electron-lattice interaction results in an energy gap of the right order of magnitude and with the correct dependence on the lattice mass. Careful examination of the calculations by Bardeen [28] has revealed that they rest on very insecure theoretical foundations. From our point of view the theories suffer from an even more fundamental failing because they do not demonstrate the cooperative nature of the superconductive transition as described in Ch. I. So, for example, they cannot give a physical picture of the order parameter in the two-fluid model. Thus, although the experiments have provided an essential clue to the interaction which brings about superconductivity, a satisfactory fundamental theory of the phenomenon has not yet been derived.

4. Comparisons with the Two-Fluid Model

Bender and Gorter [29] recently reopened the question of interpreting the threshold field curves in terms of the two-fluid model. Since the curve for tin is not parabolic, it cannot be explained in detail in terms of the simple model outlined in Ch. I. Bender and Gorter pointed out, however, that the data fit reasonably well to a more complicated model given by Koppe [30]. This model is ostensibly derived from a theory of superconductivity due to Heisenberg -- a theory which attempts to explain the phenomenon on the the basis of electronic interactions only. Such a theory clearly cannot contain within itself an explanation of the isotope effect. However, since Koppe's derivation seems to be only loosely related to Heisenberg's basic assumptions, this last fact does not constitute a fundamental objection to the use of the model.

Koppe's model is identical in form to the model given in Ch. I, but all the detailed relationships are quite complicated. However, the model predicts a unique non-parabolic relationship between the reduced threshold field and the reduced temperature with which the data for all superconductors are presumed to agree. This matter has been investigated most carefully by Marcus and Maxwell [31], who find that while the threshold field data of several superconductors come reasonably close to Koppe's form, the data do deviate from this form in a systematic way. Furthermore, they verified the observation of Reynolds, Serin and Nesbitt that the threshold field curve of mercury is strictly parabolic, and so provides a glaring exception to Koppe's universal curve.

Probably because of this last circumstance, Marcus and Maxwell, attempted to fit the data with the form of the two-fluid model given in Ch. I, Eq. 13, in which the free energy of the superconductive phase is taken as

$$F_s = X \Delta U_0 - X^\alpha \gamma T^2/2.$$

They proposed further that α be taken as an adjustable parameter which can have different values for various superconductive metals. Clearly, the data for mercury are fitted or $\alpha = 0.5$. However, it is impossible to find individual values of α which give complete agreement with the data for tin, indium and thallium.

At this point we question whether much is to be gained from attempts to extend the two-fluid model to describe the detailed behavior of individual superconductors. It is no doubt conceivable that a sufficiently

ingenious model could accomplish this end. However, it seems that so long as the fundamental physical nature of the order parameter X is obscure, little can be gained by introducing still another parameter such as α, whose nature must necessarily be more obscure. The explanation of the two-fluid model itself as well as the properties of individual superconductors must come from a fundamental theory. No model, however detailed, can substitute for this. Thus, until such a theory is forthcoming, little is lost by confining our attention to the simple version of the two-fluid model given in Ch. I.

5. The Specific Heat of Superconductive Tin

As a result of the investigations of the isotope effect, we have available quite precise threshold field data for tin. To impart an idea of the precision, we give in Table 1 the averages of the values of several quantities measured independently in three different laboratories [21,22,23] along with the mean deviations from these averages. The measurements were made on different samples of various isotopic masses which were prepared according to the individual practice of each laboratory. Moreover, the detailed technique for determining the threshold field value was different in each case, although all were based on the reappearance of the induction upon the transition into the normal phase.

TABLE 1

Constants for tin

T_c (°K)	H_0/T_c (oersteds/°K)	$(dH_{th}/dT)_{T_c}$ (oersteds/°K)	γ (cal/deg² mole)
3.740 ± 0.009	81.8 ± 0.3	147 ± 2	$(4.43 \pm 0.02) \times 10^{-4}$

Each group has derived an analytic expression for the reduced threshold field h as a function of the reduced temperature t, which was obtained by fitting the expression to their data. We have calculated the values of h yielded by each expression at ten different values of t. The r.m.s. deviation of the h-values given by two of the expressions from those given by the third is 0.005, corresponding to about a 1.5 oersted deviation in the actual threshold field.

It seems to us that examination of Table 1 and consideration of the r.m.s. deviation of the threshold field lead to the conclusion that the internal consistency of the tin data is extraordinary. We feel, therefore, that we can use the data with some impunity to infer the specific heat of the superconductive phase.

Since the threshold field curve for tin is not parabolic, the specific heat of the superconductive phase must deviate from a strict T^3-dependence. It has been pointed out [29] that the calorimetric data of Keesom and van Laer [11] show evidences of such deviation. To clarify this matter, we took the analytic expression of Serin, Reynolds and Lohman [22] for the reduced threshold field and differentiated it according to (2) to obtain $c_n - c_s$. c_n can be substracted formally from both sides of the result to obtain c_s. The curve marked h in Fig. 2 is the value obtained in this way plotted so that the deviation from the T^3-dependence is emphasized.

In arriving at this result it is not necessary to use explicit values of γ or of the Debye temperature. The points in Fig. 2 are the data of Keesom and van Laer. In order to plot the calorimetric data in the same way, it was neccessary to use values for the Debye temperature and for γ; we used the value [11] 185°K for the Debye temperature and took $\gamma = 4.43 \times 10^{-4}$ cal/deg^2 mole. The dashed curve is judged to be the best one that can be drawn through the data points. The curve marked k is the deviation predicted by Koppe's model [30].

It seems to us that the agreement between the deviation $\Delta(t)$ calculated from magnetic data and the deviation exhibited by the calori-

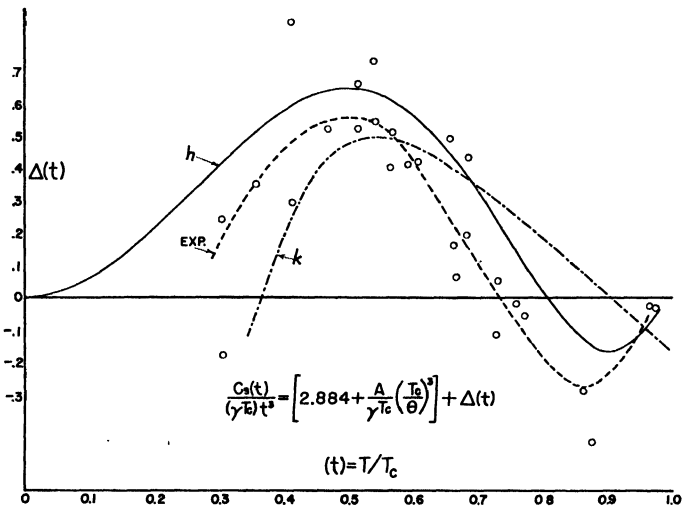

Fig. 2. The deviation from the T^3-dependence of the specific heat of superconductive tin is plotted as a function of the reduced temperature. h is calculated from the magnetic data; the points and dashed curve are the calorimetric data [11]; k is from Koppe's theory.

metric data cannot possibly be fortuitous, despite the great scatter of the data. In fact we are convinced that these deviations are essentially correct both as regards magnitude and temperature dependence, whereas the deviation predicted by Koppe's model does not agree too well with experiment. Finally, we note that recently Brown, Zemansky and Boorse [32] measured the specific heat of niobium and found that the data did not agree in detail with Koppe's theory.

6. The Effect of Impurities

Recently, Lohman and Serin have determined the effect of impurities on the magnetic properties of superconductive tin. Samples were prepared by melting various small amounts (never exceeding one percent) of each of seven different metals with tin, and then casting the solution in glass tubes and cooling slowly. Small concentrations were used for two reasons: to insure that a homogeneous solid solution of the impurity in tin resulted, and to avoid, if possible, the irreversible magnetic behavior typical of more concentrated alloys.

Thus far, the observations have consisted of determinations of the threshold field values as a function of temperature at temperatures near the transition point. The initial slopes of the threshold field curves of the impure samples are all about equal to that of pure tin. However, the transition temperatures depend on the nature of the impurity.This dependence shows several surprising regularities, which we now discuss.

The transition temperature is always initially reduced upon the addition of impurity. There is also a correlation between the change in the transition temperature and the residual electrical resistivity of the samples. This is shown in Fig. 3, where the change in transition temperature ΔT_c is plotted as a function of ϱ, the ratio of the residual resistivity of the impure sample to the resistivity of pure tin. The other fact that can be seen from Fig. 3 is that there is some correlation between the value of ΔT_c and the number of valence electrons of the impurity atom. The tin atom has four valence electrons and lead (upper curve) has the same number; whereas antimony and bismuth (middle curve) have five, indium three and zinc, cadmium and mercury each have two electrons. The points for the latter four elements fall on the lowest curve in Fig. 3. Lastly, it appears that the initial decrease in transition temperature is independent of the nature of the impurity.

The magnetic behavior of all of our samples was essentially that of a pure metal, and we feel confident that the thermodynamic theory can

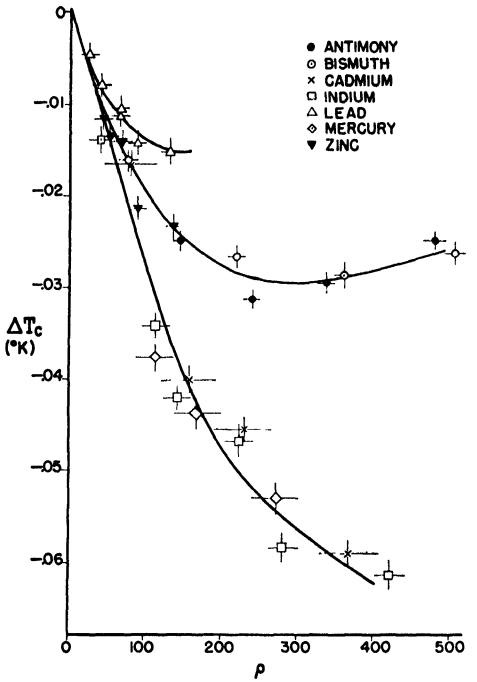

Fig. 3. The change in transition temperature is plotted as a function of the residual electrical resistivity for various impure tin samples.

be used to analyze the data. Thus in the light of (4) we tentatively interpret these results as indicating that very small amounts of impurity affect only the energy gap ΔU_0 (or H_0) in the two-fluid model. However, for impurity concentrations greater than a few tenths of a percent, we must surprisingly conclude that γ is changed, since the transition temperature depends on the nature of the impurity. Our results are not in contradiction to those obtained by Love [33] for quenched tin-bismuth and tin-antimony alloys having much greater concentrations of bismuth and antimony.

In concluding, I wish to thank Dr. E. A. Lynton for many helpful discussions during the preparation of this review.

Notes added in proof: § 3 The existence of the isotope effect in thallium has been verified [34, 35]. § 4 On the basis of further measurements, Maxwell and Lutes [35] conclude that neither Koppe's model nor the two-fluid model with adjustable α are adequate to fit the threshold field curves. § 6 Lee and Raynor [36] have determined the effect of the impurities on the lattice parameters of tin. There are no regularities of behavior, so that the observed changes in the superconductive behavior cannot simply be attributed to changes in these parameters.

REFERENCES

[1] H. Kamerlingh Onnes, Leiden Comm., 139f (1914).
[2] W. Tuyn and H. Kamerlingh Onnes, Leiden Comm., 174a (1925).
[3] W. H. Meissner and R. Ochsenfeld, Naturwiss., **21,** 787 (1933).
[4] D. Shoenberg, *Superconductivity*, Ch. II, University Press, Cambridge (1952).
[5] C. J. Gorter and H. G. B. Casimir, Physica, **1,** 306 (1934).
[6] W. H. Keesom and J. N. van Ende, Leiden Comm., 219b (1932).
W. H. Keesom and J. A. Kok, Leiden Comm., 221e (1932).
[7] J. A. Kok, Physica, **1,** 1103 (1934).
[8] J. G. Daunt and K. Mendelssohn, Proc. Roy. Soc. A, **160,** 127 (1937).
[9] A. Wexler and W. S. Corak, Phys. Rev., **85,** 85 (1952).
[10] J. G. Daunt, A. Horseman and K. Mendelssohn, Phil. Mag., **27,** 754 (1939).
[11] W. H. Keesom and P. H. van Laer, Physica, **5,** 193 (1938).
[12] J. R. Clement and E. H. Quinnell, Phys. Rev., **92,** 258 (1953).
[13] M. Horowitz, A. A. Silvidi, S. F. Malaker and J. G. Daunt, Phys. Rev., **88,** 1182 (1952).
[14] Ref. 9; also R. T. Webber, J. M. Reynolds and T. R. McGuire, Phys. Rev., **76,** 293 (1949).
[15] L. C. Jackson and H. Preston-Thomas, Phil. Mag., **41,** 1284 (1950).
[16] H. Preston-Thomas, Phys. Rev., **88,** 325 (1952).
[17] D. Shoenberg, *op. cit.*, pp. 37—47; see also Ch. VIII this volume.
[18] E. Maxwell, Phys. Rev., **78,** 477 (1950).
[19] C. A. Reynolds, B. Serin, W. H. Wright and L. B. Nesbitt, Phys. Rev., **78,** 487 (1950).
[20] C. A. Reynolds, B. Serin and L. B. Nesbitt, Phys. Rev., **84,** 691 (1951).
[21] J. M. Lock, A. B. Pippard and D. Shoenberg, Proc. Camb. Phil. Soc., **47,** 811 (1951).
[22] B. Serin, C. A. Reynolds and C. Lohman, Phys. Rev., **86,** 162 (1952).
[23] E. Maxwell, Phys. Rev., **86,** 235 (1952).
[24] M. Olsen-Bär, Nature, **168,** 245 (1951); also Ref. 22.
[25] E. Maxwell, *Low-Temperature Physics*, Nat. Bur. Stands., Circular 519 (1952), p. 29.
[26] H. Fröhlich, Phys. Rev., **79,** 845 (1950).
[27] J. Bardeen, Phys. Rev., **80,** 567 (1950).
[28] J. Bardeen, Rev. Mod. Phys., **23,** 261 (1951).
[29] P. L. Bender and C. J. Gorter, Physica, **18,** 597 (1952).
[30] H. Koppe, Ann. Phys., **6,** 405 (1947).
[31] P. M. Marcus and E. Maxwell, Phys. Rev., **91,** 1035 (1953).
[32] A. Brown, M. W. Zemansky and H. A. Boorse, Phys. Rev., **92,** 52 (1953).
[33] W. F. Love, Phys. Rev., **92,** 238 (1953); see also J. W. Stout and L. Guttman, Phys. Rev., **88,** 703 (1952).
[34] N. E. Alekseevski, Zh. eksper. teor. Fiz., **24,** No. 2, 240 (1953).
[35] E. Maxwell and O. S. Lutes, Phys. Rev., **95,** 333 (1954).
[36] J. A. Lee and G. V. Raynor, Proc. Phys. Soc. B, **67,** 737 (1954).

CHAPTER VIII

THE EFFECT OF PRESSURE AND OF STRESS ON SUPERCONDUCTIVITY

BY

C. F. SQUIRE

THE RICE INSTITUTE, HOUSTON, TEXAS

1. Introduction

The discovery [1, 2] that for a given metal the heavier isotope caused the superconducting transition temperature, T_c, for that metal to be slightly lower, has given support to the idea that the interaction of conducting electrons with the lattice vibrations is important to the detailed description of the superconducting transition [3, 4]. Concurrently, a phenomological theory [5] describes the new electronic state in terms of a two electron fluid such that for $T < T_c$ one of the fluids is separated from the other by an energy gap and possesses superfluid properties. The effects of pressure and of stress on T_c and on the critical field, H_c, could bring additional evidence to support these concepts. Pressure may alter the elastic constants and hence change the amplitude of lattice vibration. Pressure may alter the energy gap between the two electron fluids. Volume changes may be brought about with pressure which affect electron density and alter the positions of allowed energy bands. These pressure effects may be competing in their effect on T_c and on H_c.

2. Experimental

The first studies of the effect of pressure and of stress on superconductors were by Kamerlingh Onnes and Sizoo [6] at Leiden and it was clearly demonstrated that pressure would lower the transition temperature, T_c, for a given metal. Simple one dimensional tension caused the value of T_c to be higher.

During World War II, the physicists Lasarev and Kan [7] worked on the problem of producing much higher pressures on superconductors

and on measuring the effects produced. That work has continued in Russia and most interesting results were obtained. Their experimental technique involved the enormous expansion of ice upon its solid – liquid phase transition. The phase diagram of ice is well known [8] and the authors found the pressure within the constant volume chamber followed the phase line separating the solid and liquid and then with lower temperatures gave pressures between ice types I and III and into the region of ice type II of 1700 atmospheres. The "ice bomb" shown in Fig. 1 allowed the superconducting specimen to be cooled into the liquid helium region with the pressure having been established at the much higher temperature, 250°K. To do this the bomb was filled at 285°K with water all the way up into the capillary region marked "6" in the figure. This capillary was then frozen such that the ice would block the entrance to the bomb. The entire bomb was then chilled to approximately 250°K under nearly constant volume conditions. Strain gauges were fastened to the walls of the bomb to observed the swelling of the walls and so to measure the pressure. Further cooling to liquid helium caused both a contraction of the phosphor-bronze metal of the bomb as well as of the ice within the bomb. Thus there was left some uncertainty – about 3% – as to the pressure on the superconductor.

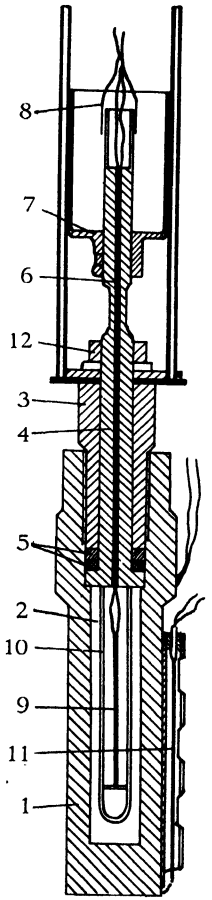

Fig. 1. Equipment for producing all sides predsure on superconducting metal (9) by freezing water to ice in a thick walled bomb (1) under nearly constant volume conditions. Lasarev and Kan, J. Exp. Th. Phys. **14**, 439 (1944).

Studies on the superconducting transition in pure metallic In and Sn with use of the ice bomb were published by Kan, Lasarev and Sudovstov [9] and their results are shown in Fig. 2 and 3. In Fig. 2 the resistance of the specimen in liquid helium just before the transition is the symbol R_0. Pressure lowers the transition temperature for In such that $dT_c/dP = -4.6 \times 10^{-5}$ deg/Kg/cm^2. The effect was a little greater on Sn and

the authors give the slope as -5.7×10^{-5}. They point out that the compressibility at constant temperature (at 285°K) is actually smaller for Sn than for In.

Now Sizoo and Kamerlingh Onnes[6] had shown that simple one dimensional tension on a superconductor would tend to raise the transition temperature and these results have been confirmed by Alekseevski [10] as well as more recently by Grenier, Spondlin, and Squire [11]. All these results suggest that the critical temperature increases when interatomic distance increases and lowers with decreasing the distance. But in 1949, Kan, Lasarev and Sudovstov [12] measured a number of other metals and whereas Hg, Ta, and Pb behaved in a manner similar to Sn and In, the metal Tl was found to have an opposite sign of dT_c/dP. The changes in temperature are small for Thallium and one might worry about the effect being in some way complicated with two crystalline forms of the metal (c.p.h. and f.c.c.). The studies by Fiske [13] confirm the studies by Kan et al. whereas the results by Chester and Jones [14] show that with the pressure of 13000 atm. the T_c is lowered by 0.06°K which is again the customary sign for the slope.

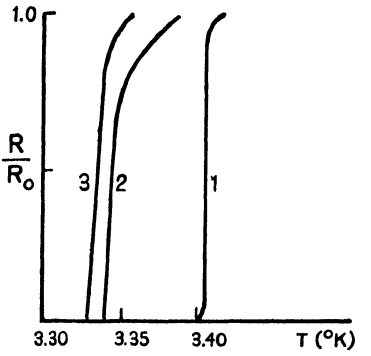

Fig. 2. Superconducting transition in In showing resistance ratio vs. temperature for the following pressures: 1 = 1 Kgm/cm²
2 = 1370 Kgm/cm²
3 = 1730 Kgm/cm²
Kan, Lasarev and Sudovstov, J. Exp. Th. Phys. **18**, 875 (1948).

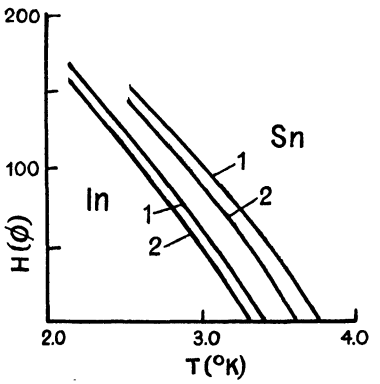

Fig. 3. Magnetic control field vs. temperature for In and Sn at pressures: 1 = 1 Kgm/cm²
2 = 1730 Kgm/cm²
Kan, Lasarev and Sudovstov, J. Exp. Th. Phys. **18**, 825 (1948).

One might assume these matters to be unsettled and feel that Tl could be made to fall in line but probably this is not to be so. Recently Alekseevski and Brandt [15] have studied the effect of pressure on two intermetallic compounds; Au_2Bi and Bi_2K – both of which become superconductors. It was found that the transition

temperature increases when Bi_2K was compressed on all sides and this result had also been found for Bi_3Ni by Alekseevski in an earlier work [16]. Thus two more cases have been reported which behave like Tl. These authors reported that dT_c/dP was negative for Au_2Bi and that since it has the same cubic lattice as Bi_3K for which the slope is positive, the observed effects can not be attributed to changes in the angles of the lattice. Alekseevski and Brandt assert that the shift of T_c with pressure is related to the electron concentration and that there may be a certain optimum concentration such that above that value dT_c/dP will be negative.

The recent discovery by Chester and Jones [14] showed that pure Bi becomes superconducting at 20000 atmospheres and above with T_c of about 7°K. They produced high pressures by the Bridgman technique and their adaption is shown in Fig. 4. A large press exerts the high pressure on the two faces of a cone shaped vise and then these forces are locked in by the heavy screws. The relatively small equipment is then lowered into the liquid helium cryostat. Bridgman [8] had shown that at room temperature the Bi underwent a crystalline change with 25500 atm. and so Chester and Jones assert that more than likely this is the reason for the appearance of superconductivity in Bi.

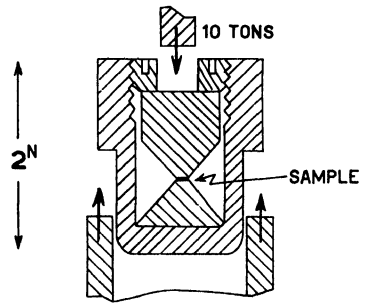

Fig. 4. Schematic Drawing of high pressure "press" used for studies at liquid helium temperature on superconducting Bi. Chester and Jones, Phil. Mag. 44, 1281 (1953).

Fiske [13] recently summarized the pressure data on Sn and Tl, see Table I. He has compared the values of dT_c/dP taken from one dimensional tension by asserting that the hydrostatic stress was one-third the tensile stress. The rather good agreement brought about in this way with the pressure experiments suggests that shear components have a small or negligible effect on T_c of tin. Indeed, Fiske [17] now reports the effect of pure shear stress is less than 5×10^{-7} deg/atm. In the one dimensional stress experiments of Grenier, Spondlin and Squire [11] the authors kept the forces within the elastic limits and worked with a pure single crystal. They pointed out that to a first approximation there was no volume change responsible for the shift of the temperature, T_c. The magnetic critical field, H_c, as a function

TABLE I *

Summary of Data on the Effect of Hydrostatic Pressure on the Superconducting Transition of Tin and Thallium.

Authors	Pressure (atm.)	ΔT_c (°K)	$\Delta T_c/\Delta P$ (deg. atm.$^{-1}\times 10^5$)
	For Tin		
Sizoo & Onnes	95	— 0.0027	— 3
	82**	— 0.007	— 8.6**
Alekseyevsky	21**	— 0.001	— 5
Kan, Lazarev & Sudovstov	1730	— 0.10	— 5.8
Chester & Jones	11500	— 0.52	— 4.3
	17500	— 0.8	— 4.5
Grenier, Spondlin & Squire	60**	— 0.0034	— 5.5**
Present Work	<115		— 4.9 ± 0.5
	For Thallium		
Kan, Lazarev & Sudovstov	1370	0.008	0.6
	1730	0.025	1.4
Chester & Jones	13400	— 0.06	— 0.4
Present Work	<48		1.3 ± 0.2

* Presented at the Third International Conference on Low Temperature Physics and Chemistry, Houston, Texas, Dec. 17, 1953 by M. D. Fiske.

** Hydrostatic value deduced from tensile stress.

of temperature gave a series of parallel curves to the zero stress curve. Thus, it was argued, the stress caused a change in the energy gap between the two-fluid electron model. As is well known, the value of the energy density of H_c at the temperature 0°K is a measure of the energy gap.

The effect of superconductivity on the velocity and attenuation of pressure waves (sound) has been the subject of considerable speculation and experimentation. Early efforts at the Rice Institute by Overton [18] with pulsed 10 Mc/sec sound were unsatisfactory because the quartz crystal transducer would not adhere properly to such superconductors as tin and lead owing to a large thermal contraction. Sound pulses through Ta were sharper but the interpretation and precision made difficult because the sintered specimen lacked physical homogeneity. Sound velocity did not change (± 0.3 percent). Standing wave methods at 1 Mc/sec by Olsen and Bommel [19] confirm these results to 1 part in 20000. The matter of attenuation is still obscure.***

*** H. E. Bommel, Phys. Rev. **96, 220, 1954** has found a drop in attenuation of sound waves at high ultrasonic frequencies for single lead crystals. Working at lower frequencies and with polycrystalline tin Squire did not observe the small change (Phys. Rev. **95, 1126, 1954**).

We would complete our survey of the experimental facts by indicating that both Shalnikov [20] and Hilsch [21] examined superconduction in thin metal films which had been formed by evaporating onto a glass surface whose temperature was held at 4.2°K. The amorphous like metal so deposited had a higher T_c and a much higher critical magnetic field curve. Hilsch [22] had made a Bi film exhibit superconductivity at 5°K. Annealing at room temperature destroys this property of the film. Zavaritski [23] has recently shown the effect of annealing evaporated films prepared at very low temperatures is to remove the anomalous behavior and bring the superconductor properties close to the bulk metal. Even at 80°K some annealing may take place. The effect of plastic deformation on superconductivity was studied by Lasarev and Galkin [24] during the war. These authors showed that plastic deformation could cause greatly increased values of T_c, H_c, and dH_c/dT. For Sn they produced $T_c = 9$°K and a critical field of 15000 gauss at 2°K compared to 210 gauss for the pure single crystal in the non deformed condition. As in the amorphous films just discussed, the critical current I_c needed to destroy the superconducting phase is greatly reduced. Recently Khotkevich [25] and Golik have systematically studied the effect of plastic deformation on the superconductivity of Sn, In, Tl, and Hg. The degree of plastic deformation was taken as the ratio R'/R at the temperature 4.2°K where R' is the resistance of the distorted specimen and R is the undeformed. The deformation carried out at 4.2°K produced great changes in the T_c as found earlier by Lasarev and Galkin.

3. Discussion of Theory and Experiment

The theoretical aspects of the effect of pressure and of stress on superconductivity require some discussion. The effect of pressure on lattice vibration may be understood in quite an elementary way. On compression the volume diminishes and the velocity of elastic waves increases. Unless one has high compression the bulk modulus will remain constant. The energy in the modes of lattice vibration may remain constant during the isothermal compression by simply lowering the amplitude of each mode of motion to offset the increase in wave velocity [26]. The energy is the sum of the energy in each mode:

$$E = \sum_{n=1}^{\infty} \left(\frac{\pi n c}{L}\right)^2 A_n^2$$

when the elastic waves have velocity c and amplitude A_n as in a continuum of length L. The interaction term in the Fröhlich-Bardeen [3, 4] theory of superconductivity is then reduced by the amplitude decrease of lattice motion. One must, therefore, go to lower temperatures before the interaction may produce the special superconducting energy state. What is needed for a more quantitative understanding of the pressure shift in T_c for, say Sn, is the effect of pressure on the velocity of elastic waves at that temperature.

One is keenly aware that not all metals are superconductors and an important criterion for superconductivity has been shown by Born and Chang [27] to be those metals whose electrons have a radius in momentum space which is nearly as large as the boundary plane of the first Brillouin zone. Another way [28] of putting this requirement is that the effective mass of the superconducting electrons shall be small in order to account for the observed Meissner effect, etc. The effect of pressure on the allowed energy zones then is of great importance to superconducting character of the metal. Saxon and Hutner [29] have shown that we may expect the width of the first allowed energy band to be smaller with deepening of the potential well between atoms and this would be just the effect caused by pushing the atomic centers closer together. One would then expect that the superconducting state would exist at a higher temperature, T_c, for the compressed solid than for the uncompressed one. For the majority of superconducting elements this is not the case and we must conclude that for these metals the small shift in width of the energy bands is of no importance.

REFERENCES

[1] E. Maxwell, Phys. Rev. **78,** 477 (1950); ibid. **86,** 235 (1952).
[2] B. Serin *et al.*, Phys. Rev., **78,** 487 (1950); ibid, **86,** 162 (1952).
[3] J. Bardeen, Phys. Rev. **79,** 167/(1950); Rev. Mod. Phys. **23,** 261 (1951).
[4] H. Fröhlich, Phys. Rev. **79,** 845 (1950); Proc. Roy. Soc. **64,** 129 (1951).
[5] P. L. Bender and C. J. Gorter, Physica **18,** 597 (1952).
[6] G. J. Sizoo and H. Kamerlingh Onnes, Leiden Comm. No 180b (1925).
[7] B. Lasarev and L. Kan, Journal of Exp. and Theoret. Phys. USSR, **14,** 439 and **463,** 1944.
[8] P. W. Bridgman, "The Physics of High Pressure" MacMillan Co., New York, 1950.
[9] L. C. Kan, B. G. Lazarev and A. I. Sudovstov, J. Exp. Theoret. Phys. **18,** 825 (1948).
[10] N. E. Alekseevski, J. Exp. Th. Phys. **10,** 244 and 746 (1940).
[11] C. Grenier, R. Spondlin and C. Squire, Physica **19,** 833 (1953).
[12] L. C. Kan, B. G. Lasarev and A. I. Sudovstov, Doklady Akad. **69,** 173 (1949).
[13] M. D. Fiske, Third Int. Conf. Low Temperatures, Rice Institute, 1953.

[14] P. F. Chester and G. O. Jones, Phil. Mag. **44**, 1281 (1953).
[15] N. E. Alekseevski and N. B. Brandt, J. Exp. Th. Phys. **22**, 200 (1952).
[16] N. E. Alekseevski, J. Exp. Th. Phys. **19**, 358 (1949).
[17] M. D. Fiske, private communication – to be published.
[18] W. C. Overton, Jr., Thesis, The Rice Institute, 1950.
[19] H. Bommel and J. L. Olsen, Phys. Rev. **91**, 1017 (1953).
[20] A. Shalnikov, Nature **142**, 74 (1938).
[21] R. Hilsch, Phys. Zeit. **9**, 592 (1939).
[22] R. Hilsch, Proc. Int. Conf. Low Temperatures, Oxford, 1951.
[23] N. V. Zavaritski, Doklady Akad. **86**, 501 (1952).
[24] B. Lazarev and A. Galkin, J. Exp. The. Phys. **14**, 747 (1944).
[25] V. I. Kotkevich and V. P. Golik, J. Exp. Th. Phys. **20**, 427 (1950).
[26] C. F. Squire, Low Temperature Physics, 187, McGraw-Hill Book Company, New York, 1953.
[27] M. Born and K. C. Chang, Nature **161**, 968 (1948); J. Phys. Radium **9**, 249 (1948).
[28] J. Bardeen, Phys. Rev., **81**, 829 (1951).
[29] D. S. Saxon and R. A. Hutner, Philips Research Repts. **4**, 81 (1949).

CHAPTER IX

KINETICS OF THE PHASE TRANSITION IN SUPERCONDUCTORS

BY

T. E. FABER AND A. B. PIPPARD

THE ROYAL SOCIETY MOND LABORATORY, CAMBRIDGE, ENGLAND

1. Introduction

The fact that the superconducting state of a metal may be destroyed by the application of a moderate magnetic field has been known almost as long as the phenomenon of superconductivity itself, and there have been many precise determinations of the strength of field required and its dependence on temperature for different superconductors (see for example, Shoenberg [1]). This information is of great importance in establishing the thermodynamic functions of the superconducting and normal states, but it gives no indication of the mechanisms which are involved in the change of phase, of which until recently very little has been known. Within the last few years, however, a systematic attack on the kinetic problem has been begun, and it is now possible to give an account of some of the general processes which operate, although much of the detailed behaviour is still obscure.

The magnetic behaviour of a superconductor may be best outlined with reference to a particular metal, tin, which is typical of the so-called "soft" superconductors and which has been more intensively investigated than any other. If a long rod of superconducting tin be subjected to a magnetic field parallel to its length, no penetration of the field occurs except in a thin layer at the surface which carries a current sufficient to prevent entry of flux into the interior; as the field is increased so the screening current increases until at the critical value, H_c, the metal reverts to its normal resistive state, the current decays and the flux enters. The variation of H_c with temperature is very nearly parabolic, according to the law $H_c = H_0 (1 - (T/T_c)^2)$, in which for tin H_0 is 306 gauss, and T_c (the transition temperature above which

the superconducting state does not exist) is 3.740°K. Under ideal conditions the transition between the superconducting and normal states in a magnetic field is reversible; if the field is reduced below H_c all flux is expelled from the superconductor and the screening current is re-established in the surface layer. This important result enables simple thermodynamical arguments to be applied to the phase transition, (see Ch. I), and it may be easily deduced that $H_c^2/8\pi = f_n - f_s$, in which f_n and f_s are the free energies per unit volume of the normal and superconducting phases respectively in zero magnetic field (it should be noted that although the normal phase does not exist in zero field the concept of f_n is not meaningless, since the free energy of a normal metal is virtually independent of magnetic field).

Now although we have referred to the reversibility of the transition as characteristic of the behaviour of ideal superconductors, marked irreversibilities do in fact commonly occur. These effects are analogous to the supercooling and superheating that are often noticed during the phase transition between, say, a liquid and a vapour. One finds, for example, that as the field is lowered past the critical value the specimen remains normal, apparently in a metastable condition, and only when H is well below H_c does the transition to the superconducting state take place. The phenomenon, which is especially marked in pure homogeneous specimens, is due to the difficulty of forming a nucleus of the stable phase, a difficulty which arises, just as it does with liquids and vapours, from the existence of a surface energy at an interphase boundary. It is usual to describe it as a "supercooling", though this is somewhat imprecise since generally the temperature is kept constant throughout and only H is varied (one can observe the same effect, though less conveniently, by keeping H constant and lowering the temperature instead). The converse phenomenon, which is not so easy to observe and has been less intensively studied, is described as a "superheating".

The nature of the nucleation process is the first problem which must be solved if the kinetics of the transition are to be understood. When this is satisfactorily elucidated there still remain many others, as for example the manner in which the nucleus expands to fill the whole volume of the specimen. There have been many experiments [2] which show that the establishment of stable equilibrium may be a comparatively slow process, times of the order of minutes being sometimes required. We shall not attempt here to provide an explanation of all

the early observations, some of which are indeed very puzzling to interpret, but we shall discuss a particularly simple case in sufficient detail to show why such time effects occur and what may be deduced from a study of them.

So long as the specimen is a rod parallel to the field the ideal behaviour, in the sense used above, is straightforward – the specimen is either wholly superconducting or wholly normal according as the field is less or greater than H_c. If, however, the specimen has any other shape new complications arise, since when it is wholly superconducting its diamagnetism causes the field at the surface to vary from point to point. For example, an ellipsoid for which the demagnetizing coefficient is n has, in an external field H, a field at the surface which varies between $H/(1-n)$ at the equator and zero at the poles. Thus it is to be expected that a sphere, having $n = {}^1/_3$, can be neither wholly superconducting nor wholly normal in fields between ${}^2/_3\, H_c$ and H_c, since in the former case the field at some points would exceed H_c and in the latter the field at all points would be less than H_c, both contingencies being inconsistent with the phase diagram. It is found that under these conditions the specimen is composed of regions of alternately normal and superconducting material in the form of thin rods or laminae lying parallel to the field. The proportion of each phase present adjusts itself in this so-called Intermediate State so that the field within the specimen is everywhere close to H_c. A number of attempts [3] have been made to develop a thermodynamic theory of the intermediate state on the basis of simple models of the structure, and all agree in one important respect, that in order to account for the details of the magnetization curves of small ellipsoidal specimens it is necessary to postulate a surface energy at the interface between normal and superconducting regions, of the same nature as that needed to account for the phenomenon of supercooling already referred to. If, as is customary, the surface energy is expressed as $\Delta \times H_c^2/8\pi$, Δ has the dimensions of length and is of the order of magnitude of 3×10^{-5} cm in pure tin It may readily be shown that this is far too large to be accounted for by any effect localized within a few atomic layers at the interface, and in the next section we shall develop a model which permits an alternative explanation of the origin of Δ.

2. A Model of the Superconducting State

When discussing the experimental results which will be presented

we shall find it convenient to have in mind a model of the superconducting state. It is not to be expected, in the absence of a satisfactory fundamental theory, that any wholly correct model can be devised, but what we now develop appears to account adequately for most of the observed behaviour, and there are grounds for hope that it represents a basically correct view of the nature of a superconductor, even though the detailed interpretation of it is still unknown.

The thermodynamic properties of a superconductor, in particular the second-order transition to the normal state at the critical temperature, recall the behaviour of alloys exhibiting an order-disorder transition, and it seems reasonable to think of the superconducting transition as occurring between a disordered (normal) and more or less ordered (superconducting) state of the conduction electrons. We may characterized the degree of order formally by a parameter, ω, which has the property of taking the value zero in the normal metal and of varying continuously from 0 to 1 as the temperature is lowered from T_c to absolute zero. It was shown by Gorter and Casimir [4] that the observed thermodynamical behaviour can be reproduced adequately by the assumption that the free energy per unit volume in the absence of a magnetic field takes the form

$$f = -\beta\,(\omega + 2\,t^2\sqrt{1-\omega}), \tag{1}$$

in which β is a constant, $H_0^2/8\pi$, and t is the reduced temperature, T/T_c. In this expression contributions from lattice vibrations are neglected, as they are assumed to be the same in both states at the same temperature. Thus for example in the normal state, for which $\omega = 0$, $f_n = -2\beta t^2$, so that the specific heat varies proportionately to the temperature, in agreement with the observed electronic specific heat in normal metals. For all temperatures below T_c (i.e. for $t < 1$), there is a non-zero value of ω, say ω_0, which minimizes f and which defines the equilibrium value of ω; it is readily found that $\omega_0 = 1 - t^4$, so that $f_s = -\beta\,(1 + t^4)$ and the specific heat of the superconductor varies at t^3, in satisfactory agreement with experiment.

In order to describe the magnetic properties of a superconductor it is necessary to include in the model an equation relating the current density, $\boldsymbol{J}$, at any point to the field applied, and we shall here assume the correctness of the London [5] theory, which sums up the property of diamagnetism in the equation

$$\operatorname{curl} \Lambda \boldsymbol{J} + \boldsymbol{H} = 0, \tag{2}$$

in which Λ is a function of temperature, but is otherwise constant in a uniform specimen. This equation combined with Maxwell's equation, Curl $\boldsymbol{H} = 4\pi\boldsymbol{J}$, yields a differential equation for the field

$$\nabla^2\boldsymbol{H} = \frac{4\pi}{\Lambda}\boldsymbol{H}, \tag{3}$$

whose solutions have the property of confining $\boldsymbol{H}$ to a thin layer at the surface of the metal. For example the solution for a semi-infinite plane slab has the form,

$$H = H\,(0)\,\mathrm{e}^{-x/\lambda} \tag{4}$$

where $H(0)$ is the field at the surface, H is the field at a depth x below the surface, and $\lambda = \sqrt{(\Lambda/4\pi)}$. The penetration of field is thus confined to a depth of order λ, which by experiment is found to be about 10^{-5} cm. To be more precise, λ varies with temperature very nearly according to the law [6]

$$\lambda = \lambda_o\,(1 - t^4)^{-\frac{1}{2}} \tag{5}$$

rising from λ_o at 0°K (about 5×10^{-6} cm in pure tin) towards infinity as t tends to unity. Comparison of this experimental result with the temperature variation of ω shows that Λ must be assumed to vary inversely as ω, $\Lambda = \Lambda_o/\omega$, where Λ_o is a constant of the metal. It is now possible to make a tentative generalization of the London equation so that it may be applied to a situation in which ω varies from point to point, as at a phase boundary, by writing it in the form

$$\mathrm{curl}\left(\frac{\Lambda_o\boldsymbol{J}}{\omega}\right) + \boldsymbol{H} = 0. \tag{6}$$

It should be pointed out that there is some evidence[7] that the London equation is not the final solution to the electrodynamical problem in superconductors, but in the absence of any more certain solution and in view of its analytical simplicity we shall not attempt a more refined model.

In a great deal of what follows we shall be concerned with situations in which ω does vary, and it is of fundamental importance to know what restrictions there are on the abruptness of its variation. From a number of experiments it is fairly clear that ω can only change slowly in space, for instance in pure tin a significant change appears to be possible only over a distance of 10^{-4} cm at least, much greater than the

penetration depth. There are different views as to the origin of this phenomenon of Coherence [8], and the formulation of its influence on the thermodynamic properties depends on the point of view taken. Here we shall adopt the crudest assumption, that provided ω does not vary more rapidly than a certain limiting rate the equation of Gorter and Casimir holds unmodified. We therefore place a restrictive condition, roughly of the form $|\text{ grad } \omega| < \omega/\xi$, on the possible spatial variations of ω; the quantity ξ so introduced is known as the Range of Coherence.

The interphase surface energy owes its origin to coherence, and a discussion [9] of the magnitude of Δ will serve to illustrate this concept. Since ω cannot change abruptly it is to be expected that the phase boundary will be extended, perhaps as shown in Fig. 1, with ω dropping

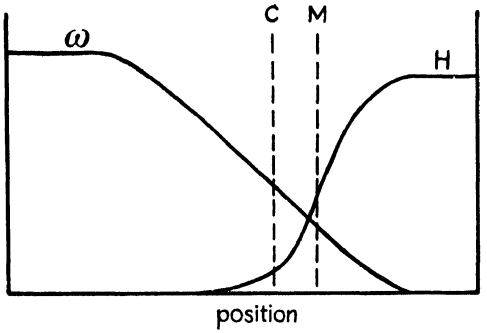

Fig. 1. Variation of ω and H at a phase boundary

gradually to zero over a distance of about ξ. Given the form of the variation of ω we can calculate the manner in which the magnetic field falls from H_c in the normal phase to zero in the superconducting phase, and from this result compute the magnetic Gibbs function of the specimen. In the present case the local density of the Gibbs function, g, is $f - H_cB/8\pi$, where f is the free energy density in zero field and B is the local value of the field, and the condition of phase equilibrium is that g shall take the same value, g_e, far enough from the boundary in both phases. The division of g into two parts, f and $-H_cB/8\pi$, enables us to define two effective boundaries – the configuration boundary C such that if ω took its equilibrium value up to C and then dropped abruptly to zero the integrated value of f would be the same as for the smooth variation of ω, and the magnetic boundary M defined so that if $B = H_c$ up to M the integrated value of $H_cB/8\pi$ would be

the same as in practice. It is easy to show that the Gibbs function of the whole sample is equal to g_s per unit volume, plus $H_c^2/8\pi$ times the separation between C and M per unit area of interface. Thus the separation of C and M is just the parameter Δ defining the surface energy, and is positive if C lies towards the superconducting side and M towards the normal side of the boundary.

It is now understandable how, since ξ is about 10^{-4} cm in tin, Δ should be a few times 10^{-5} cm. The temperature variation of Δ gives valuable information about the variation of ξ; an experimental curve for Δ is shown in Fig. 2, together with a curve for λ. It will be

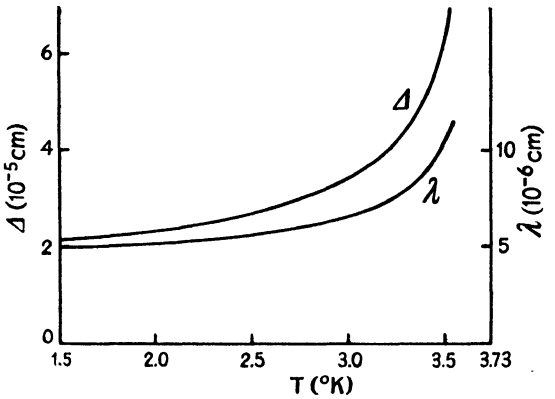

Fig. 2. Temperature-variation of penetration depth, λ, and surface energy parameter, Δ.

seen that they are very similar in shape though not in magnitude, and as Δ can be regarded as the difference between a quantity proportional to ξ and one proportional to λ we may suppose that ξ has also a variation roughly as $\omega^{-\frac{1}{2}}$. The reason for this is not understood, but there is evidence from other experiments to support it.

In concluding this account of our model of a superconductor it must be mentioned that there is strong evidence [10] to show that ξ depends on the purity of the material, and it is probably linked to the mean free path, l, of the electrons in the normal state. It seems that if progressively increasing quantities of a soluble impurity such as indium are added to tin, ξ remains constant as long as l is considerably greater than 10^{-4} cm, but that when l gets smaller than 10^{-4} cm ξ begins to decrease also, probably in such a way that its value at 0°K becomes something like l itself. The temperature variation of ξ appears to remain the same as in the pure metal. Thus by adding

impurity the range of coherence may easily be reduced below 10^{-5} cm. This has the effect of narrowing the phase boundary and of reducing the surface energy parameter Δ, and indeed it is thought that with indium concentrations greater than about 3% Δ passes through zero and becomes negative.

3. Nucleation

Our knowledge of the processes of nucleation in superconductors derives from a study of supercooling and superheating, so this section must begin with a summary of the evidence concerning these two phenomena.

We described in § 1 how a specimen of a superconducting metal may remain below the critical field in a metastable normal state. It is a simple matter to measure [11] the sharp limiting field, H_l, at which this supercooling eventually breaks down, and with pure tin it is commonly found to be around $0.9H_c$. However, if a number of similar tin specimens are studied one after the other, their limiting fields are never by any means identical, and this suggests that the values of H_l measured are not really characteristic of the pure homogeneous metal, but are determined for each specimen by some particular inhomogeneity or flaw in its structure where nucleation occurs with greater ease than elsewhere. The same conclusion is reached if, instead of taking a series of separate specimens, measurements are made on different parts of a single long rod of tin; this can readily be done, if the rod is surrounded by a number of small independent solenoids which can be used to vary the field locally. One observes that H_l varies markedly from point to point along the rod; no part of it, in fact, is free from flaws, some of them promoting nucleation more effectively than others.

It is possible to locate some of these flaws roughly, using simple methods which need not be described here [11].

There is no evidence that they are associated with obvious macroscopic faults in the metal, nor with crystal boundaries. They usually lie at the surface, or at any rate within a surface layer whose depth is about 5×10^{-4} cm (which rather suggests that they tend to be about 5×10^{-4} cm thick themselves); but removing this layer by electropolishing merely allows new flaws underneath to come into play. Many flaws are extremely stable, remaining unaffected even by warming the metal to room temperature and re-cooling, so that the supercooling behaviour can be remarkably reproducible. Any handling of the specimen, how-

ever, seems invariably to change their characteristics completely. Judging from these meagre clues, we imagine them to be regions where the crystal lattice of the metal is distorted over a rather large volume by the presence of a network of dislocations.

The lowest value of H_l that has been reported in tin is about $0.5H_c$, but there is little doubt that if a specimen could be prepared really free from flaw it would supercool considerably further. In aluminium large supercoolings are quite common [12] (for a reason we shall mention later), and recently values of H_l as low as $0.05H_c$ have been observed in this metal. These really low limiting fields do at last appear to be unconnected with flaws, and are believed to be characteristic of the pure undistorted material.

So long as H_l is fixed by a single, stable flaw, the ratio H_l/H_c seems to vary with temperature in a characteristic manner – whether its magnitude is large or small. This is illustrated by some typical results

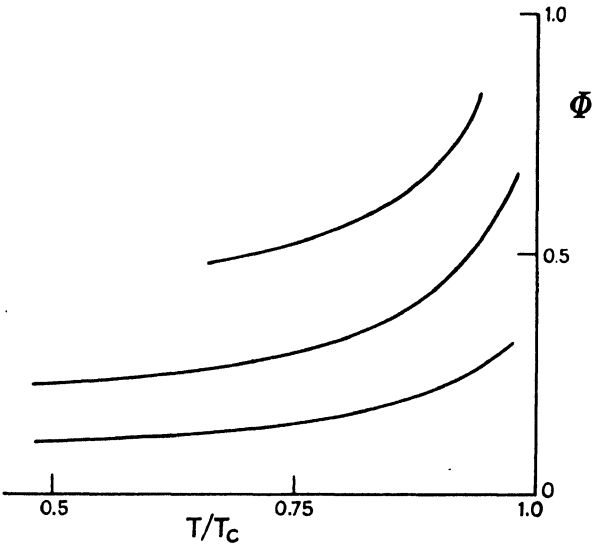

Fig. 3. Temperature-variation of supercooling. The lower two curves refer to two specimens of tin, the top curve to aluminium.

in Fig. 3, though for later convenience we have plotted a quantity Φ, defined as $(1 - H_l^2/H_c^2)$.

We may mention that the degree of supercooling attainable is sometimes affected by the strength of the maximum magnetic field to which the specimen has previously been subjected. This phenomenon has

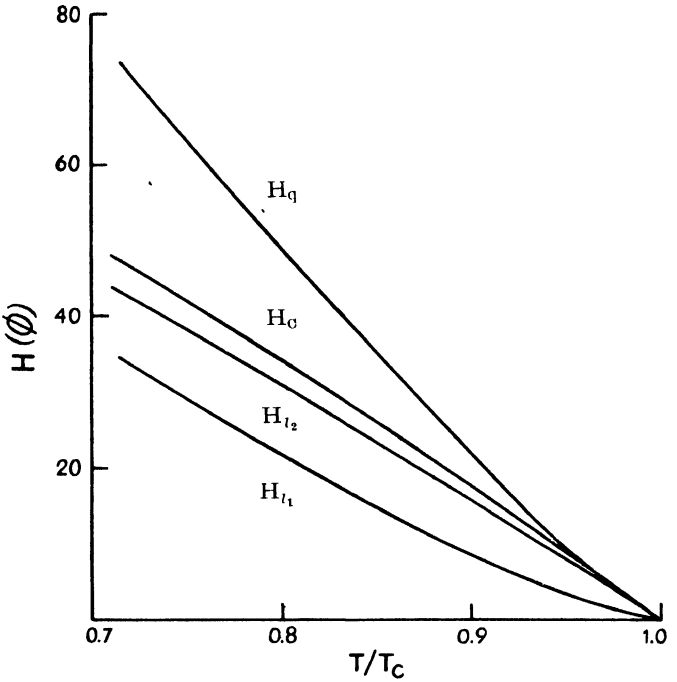

Fig. 4. Illustrating the quenching phenomenon in aluminium

been found with both tin and aluminium, and a particularly clear example of it is illustrated in Fig. 4 (reproduced by kind permission of Dr. Mapother). There are four curves on this figure, one of which is the ordinary critical curve, labelled H_c. Suppose a specimen to be placed first in a very high field, which is then steadily reduced while the temperature is kept constant. It supercools in the usual way, and only becomes superconducting when it reaches some point on the lowest curve labelled H_{l_1}. If the field is now increased again, above H_c but *not* beyond the top curve, the specimen will be able to supercool once more, but only as far as the perfectly definite and reproducible curve labelled H_{l_2}. To restore the supercooling to its original value it is necessary to exceed, though only by a minute margin, what is called the quenching field H_q. It appears that in a case like this a trace of the superconducting phase persists above the critical field, probably in the neighbourhood of some flaw of unusual configuration, and below H_q serves as a centre of nucleation; but that once the quenching field is reached this trace is irreversibly destroyed.

The phenomenon can therefore be regarded in a way as an example of superheating in one very small domain. Superheating of a specimen as a whole is rare, and indeed has never been observed to more than one or two per cent of H_c. At first sight there seems no fundamental reason why it should be easier to form a normal nucleus in a superconducting matrix than to do the converse, but one must remember that when the specimen is initially in the superconducting state the lines of magnetic force are distorted outside it and the field strength may in some places be considerably greater than at others. It is probably in these places that nucleation of the normal phase occurs with such apparent ease. This belief is supported by experiments [13] which prove that the middle parts of tin rods can by themselves suffer substantial superheating, and that it is only its relatively blunt ends that make it difficult to superheat a rod as a whole. Quantitative experimental data on the subject of superheating are scanty, and we shall not discuss the problem further.

It only remains to mention that though small additions of impurity make little difference to the behaviour we have described, a specimen which contains so much that its surface tension is negative – i.e. more than about 3% of indium in the case of tin – will naturally not superheat or supercool at all. Indeed, far from there being any difficulty in creating a superconducting nucleus below H_c, many such nuclei will exist already above H_c [14]. The same can be said of pure specimens which are unevenly strained. The transition is complicated in these cases, but we have no space here to discuss the problems that arise (see Ch. VIII).

This concludes our summary of the experimental data, and we may now examine theoretically the question of how a nucleus of the superconducting phase manages to establish itself in a specimen initially normal. We shall make use of the model proposed in § 2.

Let us assume first that we do have to deal with a homogeneous specimen, in which ξ and Δ are uniform throughout, unrealistic though this attitude may be in most circumstances. According to the concept of coherence we are to picture ω building up, as the superconducting phase develops, not in one narrowly localized region, but over a domain whose radius is at least ξ; Fig. 5(a) shows in cross-section successive stages of the process envisaged. Ultimately, the value of ω at the centre will reach the equilibrium value ω_0, and the nucleus will then presumably start expanding radially, after the manner shown in Fig. 5(b);

indeed, it might have already begun to swell radially at an earlier period. However, we need only consider for the moment the very first stage of its development, because there is little doubt that if once this can be surmounted further growth will be possible somehow, and the nucleation will be effective.

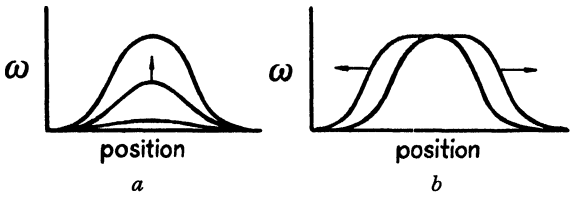

Fig. 5. Growth of a superconducting nucleus

At fields not far below the critical the process is prevented from ever starting by a potential barrier; the cost, in terms of free energy, of beginning to expel flux outweighs the advantage gained from the initial stage of condensation among the electrons. As the field is reduced the former becomes less while the latter stays constant, and eventually at a certain field strength the barrier vanishes. It is true that potential barriers can sometimes be overcome by fluctuations, but it is not difficult to show that in this instance the height of the barrier is so large compared with kT that the probability of a sufficient fluctuation is negligible – at any rate until the field has been reduced very close to the value at which the barrier disappears altogether.

This value, which should accordingly represent the limiting field H_l, can readily be deduced, provided certain simplifying assumptions are made: e.g. that the nucleus is spherically symmetrical to begin with, and that ω is small and varies according to a specified law, e.g. $\omega\ (r) = \omega(0) \exp\ (-r^2/\xi^2)$. The two terms in the free energy of the nucleus, positive and negative, may be deduced from Eq. (6) and (1). Since the calculation is similar to one that has been published already[15], we shall only quote the result here:

$$\frac{H_l}{H_c} = \frac{2\lambda}{\xi}\sqrt{1+t^2}. \tag{7}$$

This equation cannot be expected to describe the behaviour of the average, non-homogeneous specimen, but it should be applicable to the examples of particularly high supercooling noted in aluminium.

Unfortunately, this high supercooling is only observed close to T_c, over too small a range to allow the predicted temperature variation of H_l/H_c to be checked. Its magnitude, however, agrees well with the formula, if we take λ/ξ to be about 1/50 for aluminium, which is what one expects from other evidence [16]. It may be noted that in tin λ/ξ is only about 1/10. The difference reflects the considerably larger range of coherence shown by aluminium, which is probably the factor responsible for its larger supercooling. To be effective in promoting nucleation a flaw must have dimensions several times greater than ξ; i.e. it would have to be at least 2×10^{-3} cm thick in aluminium, and presumably a reasonably good specimen contains few irregularities as extensive as this.

We must now consider how it is that the presence of flaws makes nucleation easier than Eq. (7) would suggest. It was stated in § 2 that if the mean free path, l, is reduced this has the effect of reducing ξ and also Δ. It seems reasonable to suppose that flaws are regions where l is small due to lattice distortion, and hence where the surface energy is less than it should be, possibly even negative. In our previous analysis we made no use of the concept of surface energy, because it is scarcely applicable when the radius of the nucleus is much the same as the thickness of the interphase boundary; but the nuclei that develop inside flaws are a good deal bigger, and it is now helpful to bring in the parameter Δ.

Imagine, then, that a flaw consists of a spherical region inside which Δ is negative, surrounded by a shell across which Δ increases to its full positive value. In the kernel of this flaw there can, of course, be no supercooling, and a seed of the superconducting phase will exist there even in fields greater than H_c. But it will be unable to grow outwards, against the constraints of an increasing surface tension, until H has been reduced far enough for the potential barrier to disappear. Adopting some such crude model as this it is possible to calculate [17] a value for H_l, and the most general form of result obtained is

$$\Phi \doteqdot \frac{\Delta}{D} + n, \tag{8}$$

where D is a length characteristic of the flaw's dimensions, and n is a constant determined by its shape, in some cases simply its demagnetising factor.

If the typical results for Φ shown in Fig. 3 are compared with the curve for Δ in Fig. 2, it will be seen that Eq. (8) is promising, and in fact it fits the results very well, provided reasonable values are chosen for D and n, different ones, naturally, for each flaw.

To explain the quenching effect it is necessary to postulate a more complicated type of flaw. For example, a region of positive Δ surrounded by a shell in which Δ falls to a minimum without actually becoming negative, could give rise to the behaviour described above: a trace of superconductivity would superheat inside it because the interphase boundary would be unwilling to collapse into regions of larger Δ, but once this trace had been eliminated the flaw would cease to provide a centre for nucleation below H_c. Many such models can be devised, but no attempt will be made here to analyse one and to explain quantitatively the results plotted in Fig. 4.

We may sum up the conclusions of this section by saying that, although it is possible to link up measurements on supercooling with the range of coherence ξ or the surface energy parameter Δ, they do not as yet provide a reliable method for estimating these quantities. The experiments clearly show that Δ must not be regarded as absolutely uniform throughout a specimen, and this may very well have repercussions on other aspects of the transition and in particular on the detailed structure of the intermediate state.

4. Propagation

When a nucleus of the phase has formed successfully, it starts spreading into the rest of the specimen, and, judging by the delays of many seconds that are often observed before the attainment of final equilibrium, this is a surprisingly slow process. Let us consider what factors could be responsible for retarding so effectively the propagation of phase boundaries through superconductors.

Perhaps the most obvious possibility is that it requires an appreciable time simply to establish the state of order among the electrons which characterizes the superconducting phase, and equally to break down this order. If these processes are governed by a relaxation time τ, for example, one would guess, very crudely, that the rate of propagation might be limited to a value of about ξ/τ. Now high frequency experiments [18] suggest that if τ exists it is probably between 10^{-8} and 10^{-11} sec, in which case ξ/τ is at least 10^4 cm sec^{-1} in tin. We shall be concerned with rates which are mostly much slower than this, and

we shall therefore assume that some retarding agent other than the relaxation effect is dominant.

Two factors to consider next are the latent heat of the transition and the electromagnetic effects associated with eddy currents, and since these act in a rather similar way they may be discussed simultaneously. Whenever the superconducting phase advances latent heat is steadily generated at the boundary and magnetic flux steadily displaced in front of it. Both the heat and the flux must escape from the specimen and in doing so establish gradients of temperature and field strength, the latter by the induction of eddy currents in the normal metal. This results in both H and T being higher on the phase boundary than at the surface of the specimen, by an amount roughly proportional to the speed of advance. In the absence of any other factors, such as the relaxation effect already discussed, the speed will adjust itself so that the conditions all along the boundary are the phase equilibrium conditions, i.e. so that $H = H_c(T)$. Similar arguments apply to the converse case of the retreating superconducting phase.

For most practical purposes it is legitimate to ignore the latent heat and to take account only of the eddy current effect. This is because the thermal diffusivity in pure metals at low temperatures is much greater than the electromagnetic diffusivity, so that the latent heat escapes much more easily than the displaced flux, and the temperature difference established between the moving phase boundary and the surface of the specimen is infinitesimal. Thermal effects could be significant in very impure metals, and in specimens in poor contact with the surrounding helium bath, but we may neglect them here.

A quantitative eddy current theory [19] has been worked out which allows the rate of propagation to be calculated in certain simple cases. The answer naturally depends on the strength of the external field, and if this is already equal to H_c the propagation can only take place infinitely slowly. It also depends on the electrical conductivity of the normal phase (σ) and on the specimen's dimensions. For example, if a cylindrical core of the superconducting phase is contracting radially in a long rod of radius r, under the influence of an external longitudinal field H ($> H_c$), the time it takes to collapse completely should be equal to $\pi\sigma r^2 H/(H - H_c)$. This particular prediction has been checked experimentally [20] with tin specimens of varying conductivity and radius. The results were in excellent agreement with theory, apart from some minor discrepancies which suggested that the contraction was never

quite so perfectly symmetrical in practice as the theory is forced to assume.

If the superconducting core were persuaded to expand radially instead of contracting, the process would not be symmetrical at all; indeed, the interphase boundary would not even remain a smooth surface, let alone a cylindrical one. The reason for this lies in the general principle that the closer a boundary is to the outside surface of a specimen, the less difficulty it experiences in displacing flux through the intervening normal phase, and hence the faster it is able to travel. This principle ensures that the boundary is stable so long as it is moving inwards; if some part of it lags behind it is immediately encouraged to catch up, while any part that gets ahead is automatically slowed down, so that all irregularities which appear are soon eliminated. But when the boundary is moving outwards irregularities will magnify rapidly, and a tortuous arrangement of superconducting filaments, each expanding separately, is likely to result.

Because of this inherent instability of the boundary, phase propagation below the critical field must always be a devious process, and at first sight there seems little possibility of treating it theoretically. Nevertheless, some detailed experiments [21] on the subject have been done, and interesting conclusions have emerged.

Once again, cylindrical rods of tin were used as specimens, and a uniform magnetic field was applied longitudinally. The procedure was to supercool a rod first, and then to create a superconducting nucleus deliberately at one end, by lowering the field locally with the aid of a separate small solenoid. The subsequent expansion of the nucleus was followed by watching the response of a series of search coils, wound round the rod at intervals along it. In a typical experiment two of the coils might be selected, say 10 cm apart, and connected in series to a suitable recording instrument. During the transition, a voltage pulse with two sharp peaks, one from each coil, would be observed, as shown in Fig. 6. The separation between the peaks indicates that the foremost filament of the superconducting phase travels down the rod with an easily measurable velocity. In the experiments this velocity, v, was uniform and reproducible; its magnitude depended on the conditions, a typical value being 20 cm $\sec^{-1}$.

There is much evidence that the foremost filament invariably travels along the surface of the specimen; for example, etching the metal was found to reduce the apparent value of v drastically, presumably be-

cause the filament had to travel a longer path on account of the etch-pits. Of course the original nucleus is known to lie at the surface (see § 3), and it would be surprising if it began by growing inwards, because in that direction it has to displace flux through a greater bulk of normal metal and the eddy current restraints must be more severe. An initial phase of relatively rapid growth along the surface is therefore just what one would expect.

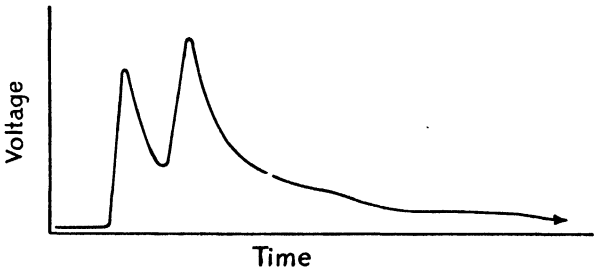

Fig. 6. Voltage pulses due to expanding superconducting filament.

In fact it appears that this growth continues until a complete, or almost complete, superconducting sheath has formed around the specimen. The flux ejected from the metal up to this stage is responsible for the main peak of the voltage pulse generated in each search coil, and from the area of these peaks the thickness of the sheath may be roughly estimated. Again, it depends on the conditions but is generally about 0.2 mm.

Finally the sheath must spread inwards, probably in a complex and irregular manner, until the last traces of flux have been expelled from the specimen. We shall discuss possible mechanisms for this expulsion in the next section, but it is clear that it must be a slow and difficult business, for the tail which invariably follows the initial peak of a voltage pulse (see Fig. 6) is liable to last 10 sec. or more.

The most important part of the experiments is the determination of the velocity v as a function of all the experimental variables. Eddy current effects are quite unable by themselves to account for the low values of v observed, and it is necessary to invoke the interphase surface energy as well. If it were not for surface energy, (or in other words for coherence), there would be nothing to stop a filament becoming thin compared with the penetration depth λ, in which case it would advance without displacing any flux and therefore with no electro-

magnetic effects to retard it. To see how surface energy affects the issue, consider the crude model illustrated by Fig. 7. This shows a cross-section through a filament of thickness d advancing along the

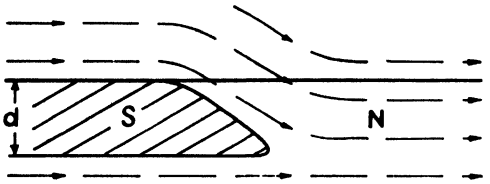

Fig. 7. Schematic cross-section of a superconducting filament.

surface and pushing magnetic lines of force out of the metal in front of it. Now the eddy currents that flow around the tip of the filament are continually dissipating in the form of heat free energy which ultimately derives from the conversion of a fresh volume of metal to the superconducting phase. An equation for the energy balance may be written down as follows:

$$d\,(H_c^2 - H^2)/(8\pi) - (\Delta - \lambda)\,H_c^2/(8\pi) = C\,\sigma_{eff}\,v\,d^2H^2. \qquad (9)$$

Here the first term on the left hand side represents the free energy released when a filament of unit breadth advances unit distance, the second term allows for the increase of surface area (both on the inside and outside of the filament), and the term on the right-hand side is the eddy current dissipation. This last expression includes an unspecified constant C, and also an "effective" conductivity, σ_{eff}.

It is necessary to write σ_{eff} instead of the usual σ, because d is often comparable with the electronic mean free path l, so that the eddy currents flow under what we may call "anomalous" conditions. There is no point in discussing this complication in any detail here, and we shall simply state that in pure tin l is so large that conditions are completely anomalous, and σ_{eff} is proportional to $\sigma d/l$. After a number of simplifications (9) then reduces to the form:

$$2\,(H_c - H)/(H_c d^2) - (\Delta - \lambda)/d^3 = C'\sigma v/l, \qquad (10)$$

where C' is a new constant which can be roughly estimated. It may be seen from this formula that there is an optimum thickness for a filament, $d_{opt} = \frac{3}{4}\,(\Delta - \lambda)\,H_c/(H_c - H)$, which allows it to travel with a maximum velocity; if it is any thinner than this it is hampered

too much by surface energy, and if it is any thicker the eddy current restraints become large. It may be assumed that a filament adopts this optimum thickness in practice, with a consequent propagation velocity:

$$v = \frac{32}{27C'}\left(\frac{l}{\sigma}\right)(\Delta - \lambda)^{-2}\left(\frac{H_c - H}{H_c}\right)^3. \tag{11}$$

This result is in good agreement with experiment.

We have reproduced this analysis at some length, partly because it illustrates the conflicting roles of surface energy and electromagnetic damping during a fairly complex example of propagation, and partly because it shows how values of $(\Delta - \lambda)$ can be extracted from the measurements. In fact the figures for Δ in tin which were used in plotting Fig. 2 were originally obtained from experiments of the type we have been describing, and the same method has been successfully applied to aluminium. The only known alternative way of deducing the surface energy is to study the intermediate state (see § 1) but this is probably a less convenient and less reliable technique and it has not been very widely applied; the results it has yielded for tin [22], so far as they go, support those in Fig. 2.

5. Elimination of Trapped Flux

The growth of a superconducting sheath along the surface of a rod involves quite a small fraction (say 1/5) of its total volume, and we must now return to consider the later, rather slow, stages of the transition, during which flux is expelled from the interior. It is known that the majority of it does eventually emerge, though specimens sometimes retain a small frozen-in magnetic moment even in zero field, indicating that a few channels of the normal phase have still not been eliminated.

It is a familiar property of a superconducting ring that the flux it encloses is unable to escape, and the same would be true of the flux inside a rod if the sheath ever closed up to form a complete and indestructible layer of the superconducting phase stretching continuously round the surface. We must therefore assume either that the sheath does not close, or that it is able from time to time to break open. There are in fact grounds for adopting the first attitude, in that a potential barrier is likely to prevent two superconducting domains (such as the opposite jaws of a closing sheath) from ever coalescing until the field

is reduced to quite a low value. In order to understand the origin of the potential barrier we must invoke the phenomenon of coherence. In Fig. 8 is shown a sketch of the presumed variation of ω across a gap in the sheath; as drawn the normal region is about as narrow as it can be without direct interaction of the superconducting regions, and we may suppose that the next stage of closure of the gap involves a non-vanishing ω everywhere, as indicated by the broken curve. Whether this stage is thermodynamically possible depends on arguments similar to those advanced in our discussion of nucleation (§ 3); if, as a result of a long range of coherence, the gap is necessarily wide, the increase of the Gibbs function due to expulsion of flux may outweigh the decrease due to electronic condensation, and coalescence will be prevented. This situation may be expected to arise in pure tin, for which $\xi >> \lambda$, though not necessarily in impure tin for which ξ is smaller. For the moment we shall concern ourselves only with pure tin.

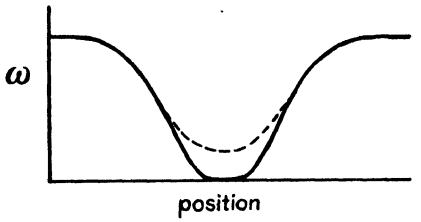

Fig. 8. Coalescence of neighbouring superconducting regions.

The final stages of the transition of a rod in a parallel field may then be idealized somewhat as follows. After the sheath, with one or more gaps, has grown along the rod the superconducting phase expands inwards so as to maintain the field in the normal regions at a value H_c while the flux leaks away. It is probable that the inward expansion is not regular since, as we have already seen, a growing superconducting region presents an unstable boundary. We therefore presume that a number of fine superconducting sheets, parallel to H, grow inwards in an irregular manner, perhaps as in Fig. 9, always leaving paths by which flux may continue to escape. At the exit of an escape route, such as A, the field is H_c within the rod and less than H_c outside, since we are dealing with the transition in a supercooled specimen, and the difference in field strength across the

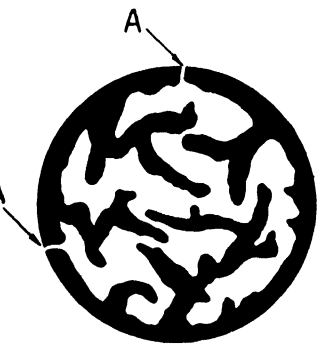

Fig. 9. Cross-section of rod in longitudinal field, showing escape routes, A. The dark regions are superconducting.

gap is associated with eddy currents flowing in the normal metal. These currents are maintained by an electric field induced by escaping flux, and it will be seen that in principle the rate of escape can be calculated in any particular case. In fact, on account of uncertainty concerning mean free path effects in the normal metal and possible resistive processes at the phase boundary, a detailed calculation is not feasible at present, but order of magnitude estimations show that there is nothing unreasonable about the time of escape observed experimentally, if the gaps are little greater than 10^{-4} cm wide.

There is no difficulty in understanding how virtually all the flux escapes, so long as coalescence is forbidden. We must bear in mind, however, that the same flaws which promote nucleation at the surface of a specimen (see § 3) may act in a similar manner to aid coalescence, and thus if H is low enough they may allow the superconducting sheath to become continuous. If this does ever happen, then presumably another mechanism for flux expulsion comes into play; we must suppose that the normal channels, which are now completely surrounded by superconducting material, begin to migrate sideways towards the surface and are able to break through the sheath and reach the outside. The tendency of lines of force to contract could provide the driving force for such a process.

There is really no evidence from the experiments on rods in longitudinal fields to determine whether migration plays a significant role or not. The question has been rather more fully studied, however, in a series of experiments involving transverse fields [23]. Transverse fields were deliberately chosen because they compel the transition to take place by way of the intermediate state, which should afford every opportunity for coalescence and consequent flux trapping. Before describing the results of the experiments, we must digress a little to discuss the nature of this intermediate state.

The intimate mixture of normal and superconducting regions which is stable in fields between H_c and $(1 - n)\, H_c$ (n is $\frac{1}{2}$ for a cylindrical rod in a transverse field) has been observed directly by Meshkovsky and Shalnikov [24] and found to be of highly complex structure. Attempts have been made to deduce the equilibrium form of this structure theoretically [3], but the manner in which it is set up has not been the subject of any detailed consideration. We can only offer here an unsubstantiated speculation which may apply to the case when the field is decreased from a value greater than H_c. Initially the specimen is

wholly normal and, in pure superconductors at any rate, a certain amount of supercooling usually occurs. At some field strength, however, a superconducting nucleus forms and immediately starts to expand, probably first as a thin spindle parallel to the field since this involves only a small displacement of flux. The next stage of growth will be sideways, but here the inherent instability of the growing superconducting phase asserts itself – growth into a thin lamina is more rapid than overall thickening of the spindle. The lamina will not be stable, since the surrounding field is less than H_c, and so it will send out laminar offshoots from itself, which will in their turn further proliferate until the whole specimen is a labyrinth of superconducting laminae. The situation is similar to that discussed earlier in this section in connexion with the rod parallel to the field, except that here demagnetization effects stop the process before the whole specimen is superconducting. We have considered the growth of only one nucleus, but of course it is possible that multiple nucleation occurs and each nucleus expands in a similar manner.

In the experiments a transverse field greater than H_c was applied to a tin rod and then removed, and the amount of trapped flux was determined from the resulting magnetic moment. It was found that in pure tin the trapped flux may be as little at 0.1% of what was contained within the specimen when the applied field was H_c, and even less than this at temperatures near T_c. It is clear that either there is no coalescence until the superconducting regions are very close together (there is evidence from these experiments that even then it occurs only through the presence of flaws), or that the normal regions can migrate very easily. But the latter hypothesis does not seem likely in view of the fact that the small amount of flux trapped is very firmly bound, so firmly indeed that application of a field in the reverse direction (which should greatly aid migration) causes no further flux leakage. We are therefore of the opinion that the expulsion of flux arises through absence of coalescence rather than through migration. It is not obvious why migration does not occur, but it may perhaps be a result of the intricate nature of the channels in which the flux is trapped. Because of the complexity of the intermediate state and the difficulty of coalescence the distribution of normal and superconducting material after the field has been removed may be something like that shown in Fig. 10. At points such as X the tendency of the flux trapped in the normal channels will be to pull the boundary of the

channel to the edge and allow leakage, but this will be resisted by the surface tension at the interface tending to draw the boundary inwards. Thus it may well be that a balance of the forces resists any attempt at migration. But although this may be the correct explanation of the behaviour in a transverse field, it would be unwise to assume that the same arguments apply in a longitudinal field; the general question of the relative importance of migration and absence of coalescence in allowing flux leakage is one which at present must remain unanswered.

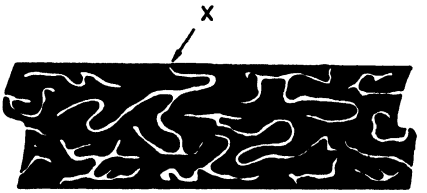

Fig. 10. Longitudinal section, in plane perpendicular to H, of rod having normal inclusions which trap flux.

If we adopt the view that the absence of coalescence, arising from coherence, is responsible for flux leakage, we should expect that by adding sufficient impurity to reduce ξ to a value comparable with λ we might eliminate the barrier preventing coalescence and thus enable flux to be trapped. Accordingly a series of experiments was performed on tin-indium alloys. These specimens were very carefully annealed single crystals, and every precaution was taken to make them as homogeneous as possible; this was necessary in order to avoid confusion of any observed effect with the flux-trapping known to occur in inhomogeneous alloys [25], resulting probably from the immobilization of phase boundaries at regions of rapidly varying critical field and surface energy. In the homogeneous alloys it was found that a dramatic change of behaviour occurred between 2.3% and 2.5% of indium, the percen-

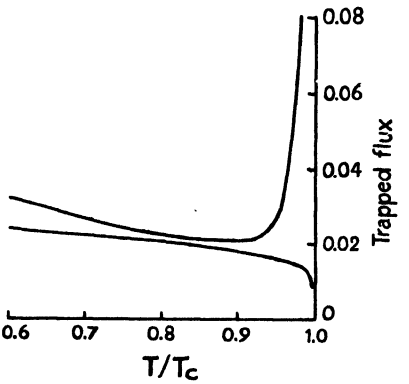

Fig. 11. Temperature-variation of trapped flux in tin-indium alloys. Lower curve 2.3% indium, upper curve 2.5% indium.

tage of trapped flux just below T_c rising from practically zero to something like 50%, as shown in Fig. 11. It is at about this concentration of indium that the mean free path of the conduction electrons and the penetration depth become comparable, and also that Doidge [14] has observed the persistence of fine superconducting threads in fields greater than H_c. It seems likely then that this change in behaviour is associated with the overcoming of the barrier to coalescence. It is beyond the scope of this article to elaborate the theory of the precise shapes of the curves in Fig. 11, but we may mention that the appearance of coalescence first in the neighbourhood of T_c may be accounted for without any extra hypotheses.

We have been unable to consider in detail all the evidence relating to this stage of the transition, or indeed to earlier stages, and may perhaps have left the impression that the phenomena are understood better than they are in reality. There are in fact still many unexplained observations and inconsistencies which call for further study, but it is, we feel, not too much to hope that a sound beginning has been made towards the clarification of this complex field.

REFERENCES

[1] D. Shoenberg, Superconductivity, Cambridge, Univ. Press, (1952).

[2] K. Mendelssohn and R. B. Pontius, Physica, **3**, 327, (1936); W. H. Keesom and P. H. van Laer, Physica, **3**, 173, (1936), Physica, **4**, 499, (1937), Physica, **5**, 986, (1938); J. G. Daunt, Phil. Mag., **24**, 361, (1937); H. Grayson Smith and K. C. Mann, Phys. Rev., **54**, 766, (1938); N. E. Alexeyevsky, J. Phys. U.S.S.R., **9**, 217, (1945), Doklady, Acad. Nauk S.S.S.R., **60**, 37, (1948); J. Babiskin, Phys. Rev., **85**, 104, (1952).

[3] F. London, Physica, **3**, 450, (1936); R. Peierls, Proc. Roy. Soc. A, **155**, 613, (1936); L. D. Landau, Phys. Z. Sowjet, **11**, 129, (1937), J. Phys. U.S.S.R. **7**, 99, (1943); E. R. Andrew, Proc. Roy. Soc. A, **194**, 98, (1948); E. M. Lifshitz and Yu. V. Sharvin, Dokl. Acad. Nauk S.S.S.R. **79**, 783, (1951).

[4] C. J. Gorter and H. B. G. Casimir, Phys. Z., **35**, 963, (1934); Z. Techn. Phys. **15**, 539, (1934). See also Ch. I.

[5] F. and H. London, Proc. Roy. Soc. A, **149**, 71, (1935).

[6] J. G. Daunt, A. R. Miller, A. B. Pippard and D. Shoenberg, Phys. Rev., **74**, 842, (1948).

[7] A. B. Pippard, Proc. Roy Soc. A, **216**, 547, (1953).

[8] V. L. Ginsburg and L. D. Landau, J. Exp. Theor. Phys., **20**, 1064, (1950); J. Bardeen, Phys. Rev. **81**, 1070, (1951); A. B. Pippard, Physica **19**, 765, (1953).

[9] A. B. Pippard, Proc. Camb. Phil. Soc., **47**, 617, (1951).

[10] A. B. Pippard, Physica, **19**, 765, (1953).

[11] T. E. Faber, Proc. Roy. Soc. A., **214**, 392, (1952).

[12] D. Shoenberg, Proc. Camb. Phil. Soc., **36**, 84, (1939); T. E. Faber, Int. Conf. Low Temp. Phys., (Houston, 1953); D. E. Mapother, J. F. Cochran and R. E. Mould, Int. Conf. Low Temp. Phys., (Houston, 1953).

[13] M. P. Garfunkel and B. Serin, Phys. Rev., **85**, 834, (1952).
[14] P. R. Doidge, Unpublished.
[15] A. B. Pippard, Phil. Mag., **63**, 273, (1952).
[16] T. E. Faber, Int. Conf. Low. Temp. Phys., (Houston, 1953).
[17] T. E. Faber, Proc. Roy. Soc. A., **214**, 392, (1952).
[18] B. G. Lazarew, A. A. Galkin and V. A. Khotkevich, Dokl. Acad. Nauk, S.S.S.R., **55**, 817, (1947); A. B. Pippard, Unpublished.
[19] A. B. Pippard, Phil. Mag., **41**, 243, (1950); E. M. Lifshitz, J. Exp. Theor. Phys., **20**, 834, (1950).
[20] T. E. Faber, Proc. Roy. Soc. A, **219**, 75, (1953).
[21] T. E. Faber, Proc. Roy. Soc. A., **223**, 174, (1954).
[22] M. Désirant and D. Shoenberg, Proc. Roy. Soc. A, **194**, 63, (1948); E. R. Andrew and J. M. Lock, Proc. Phys. Soc. A, **63**, 13, (1950).
[23] A. B. Pippard, to be published.
[24] A. G. Meshkovsky and A. I. Shalnikov, J. Phys. U.S.S.R., **11**, 1, (1947), J. Exp. Theor. Phys. U.S.S.R., **17**, 851, (1947); A. G. Meshkovsky, J. Exp. Theor. Phys. U.S.S.R., **19**, 15 (1949).
[25] K. Mendelssohn, Proc. Roy. Soc. A, **152**, 34, (1935).

CHAPTER X

HEAT CONDUCTION IN SUPERCONDUCTORS

BY

K. MENDELSSOHN
OXFORD

1. Introduction

Kamerlingh Onnes discovered the phenomenon of superconductivity in 1911 and in the following year, together with Holst he began to investigate the effect of superconductivity on the heat transport. At that time cryogenic technique was in its infancy and this preliminary work only yielded results of a qualitative nature [1]. However, it could be shown that, on passing the transition temperature T_c, the heat flow did not exhibit the same abrupt change which occurs in the electrical conductivity.

No further work was done in this particular field until in the decade following 1930 de Haas with Aoyama, Bremmer and Rademakers carried out systematic investigations [2] on superconductive pure metals and alloys. The only other contribution during this period was made on a much more modest scale in Oxford [3]. Out of this work there emerged a reasonably clear picture of the phenomena in pure metals down to temperatures of about 2°K while the behaviour of alloys suggested great complexity. It was found that as the temperature is lowered below T_c, in pure metals the heat conductivity K_s of the superconductor, without becoming discontinuous, falls *below* that of the metal in its normal state K_n. A comparison of the two values K_s and K_n at the same temperature can always be made by applying to the metal a magnetic field higher than the critical field H_c. The work on alloys was not so conclusive since it appeared that in their case K_s may be lower or higher than K_n.

After the second war the heat conductivity experiments in Oxford

were resumed on a rather larger scale and work in this field was started in Cambridge and in a number of American laboratories. In particular the effect of adding to a pure metal impurities in controlled amounts was studied in some detail [4, 5] and the range of pure metals under investigation was extended. Quite recently heat conductivity measurements on superconductors have been carried out at temperatures well below 1°K and these now allow us to form a fairly consistent model of the whole process in a pure metal. The work on alloys, on the other hand, is still far from being complete.

2. Experimental Technique

In nearly all the investigations the conventional method of measuring the temperature gradient along a rod-shaped specimen has been employed. The rod which is attached at its cold end to a heat sink is heated at the other end by means of an electric heater, permitting easy and accurate measurement of the dissipated power. The heat sink is usually provided by a bath of liquid helium, boiling under constant vapour pressure. For investigation at temperatures above 5°K an additional heater is sometimes used between the cold end of the rod and the heat sink. This permits the specimen to be kept at a temperature well above the critical point of helium. In experiments in which a Simon expansion liquefier has been used, the expansion chamber, filled with helium gas under high pressure has been found to act as a very efficient heat sink [6]. In order to avoid lateral heat loss the space around the specimen is evacuated. Radiation losses can be neglected at these low absolute temperatures.

In most determinations the temperature has been measured at two places along the rod. In the work on superconductors, gas thermometers have been given preference because they are uninfluenced by a magnetic field. In the cases were resistance thermometers have been employed, carbon resistors, having a very small magneto-resistance, have been found useful. The techniques used below 1°K have to be adapted to the special conditions obtaining at these very low temperatures and will be discussed separately.

3. Theory

In the consideration of the scattering mechanisms which limit the energy transport in a metal, the onset of superconductivity creates an added complication. It is therefore necessary, before one can deal

with the heat conduction in the superconductive state, to make a brief survey of the effects occuring in the normal metal [7].

There are two conduction mechanisms in a metal, that due to the lattice vibrations and that by the free electrons. While it has to be kept in mind that these two processes are not independent of each other, it is nevertheless convenient for an analysis of the phenomena to split up the total heat conduction of the normal metal K_n into an electronic contribution K_{en} and one due to the crystal lattice K_{gn}:

$$K_n = K_{en} + K_{gn} \tag{1}$$

Theoretical considerations suggest that in a pure metal K_{gn} is very small in comparison with K_{en} and that it can usually be neglected. Indeed experiments on cadmium [8] in which K_{en} at helium temperatures had been reduced by a high magnetic field to one thousandth of its original value have shown no saturation effect. The result indicates that, at least in this case, K_{gn} must have been as small or smaller than $10^{-3}K_{en}$. The scattering processes to be considered are therefore only those acting on the free electrons. Such scattering will be caused by the thermal vibration of the crystal lattice and by imperfections of the lattice.

Even for the simplified case of quasi-free electrons, the theoretical evaluation of the temperature dependence of the scatter of electrons by phonons meets with appreciable difficulties. In the region of low temperatures where superconductivity makes its appearance, conditions are, however, rather less complex. Below 1/10 of the Debye characteristic temperature, where the specific heat of the metal follows a T^3 law, the thermal resistance $1/K_n$ may be expected to be proportional to the square of the absolute temperature. Theory yields for the factor of proportionality

$$\alpha = \frac{A\,N^{2/3}}{K_\infty \Theta^2} \tag{2}$$

where N is the number of free electrons per atom and K_∞ is the limiting heat conduction for very high temperatures. Agreement of the numerical value for α with the experimental data is, however, poor. This may be due to uncertainties in ascribing correct values to A as well as to N. The thermal resistance due to the scattering of electrons by impurities is closely connected with the well known residual electrical resistance which is independent of temperature and which at low

enough temperatures is always the predominant term in the electrical resistivity. In fact the thermal conductivity allowed by this process is given by

$$\frac{1}{3}\left(\frac{\pi k}{\varepsilon}\right)^2 \frac{T}{r_0} = \frac{LT}{r_0} \tag{3}$$

where r_0 is the residual electrical resistance and L the Lorenz number.

Adding the influence of impurity and phonon scattering of the electrons, we therefore arrive for the electronic heat resistance of a normal metal at

$$W_e = 1/K_e = \beta/T + \alpha T^2, \tag{4}$$

where

$$\beta = r_c/L \tag{5}$$

and α has the theoretical value given by (2). The heat conduction of the metal at low temperatures therefore will rise at absolute zero linearly in accordance with the first term in (4) and then drop again as the second term becomes predominant. As Fig. 1 shows, these general features are indeed well exhibited by the experimental results. Assuming that N will not vary greatly from metal to metal, the position of the heat conductivity maximum is determined by the values for r_0 and Θ. Thus, in the same metal, as the purity is increased and r_0 becomes consequently smaller, the maximum is shifted to lower temperatures. This can, for instance, be seen in the curves of Fig. 6.

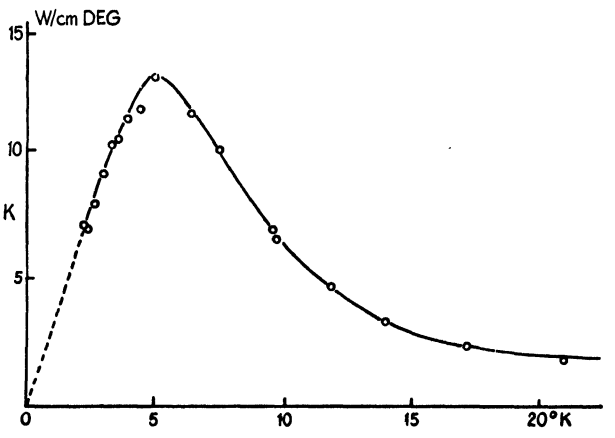

Fig. 1.
Typical heat conductivity curve of a metal (cadmium) at low temperatures.

The position of this maximum and our ability to displace it by the addition of impurities is of importance in the study of the superconductive phenomena, since below this temperature the normal electrons are mainly scattered by lattice defects whereas above it scatter by lattice vibrations is the more important process.

Re-writing equation (4) as

$$TW_e = \beta + \alpha T^3 \tag{4a}$$

and plotting TW_e against T^3, we should obtain straight lines from which the constants α and β can be evaluated. Specimens of fairly high purity, in which the lattice conduction K_g can be neglected, give indeed curves close to this linear form, showing that equation (4) represents a tolerably good approximation, at least in the domain of low temperatures where superconductivity occurs.

While, thus, the heat conduction of a normal metal at temperatures below $\Theta/10$ can be understood moderately well, the absence of a rigorous theory of superconductivity makes it extremely difficult to account for its influence in a quantitative manner. An indication of the trend of this influence is provided by the behaviour of the Thomson heat. From dimensional considerations the heat conductivity can be expressed quite generally as,

$$K = \tfrac{1}{3}\, dvc, \tag{6}$$

where d is the mean free path of the carriers, v their velocity, and c their specific heat. It has been found that, even at finite temperatures, the Thomson heat of the persistent current in a superconductive lead ring is zero, which leads to the conclusion that the specific heat of the electrons carrying this current, too, is zero [9]. Having regard to equation (6), it may be postulated that the heat conduction by these electrons, likewise, must disappear. This is clearly in agreement with the salient fact, discovered in the early experiments, that in a pure metal the heat conduction is lower in the superconductive than in the normal state.

This kind of reasoning, and even more any attempt at its quantitative application, pre-supposes the existence in the metal of two electron fluids which, to some extent, can be treated independently. This two fluid model which has been discussed in detail in Ch. I of this book has proved extremely useful in providing purely descriptive explanations of the complex and unusual phenomena encountered in super-

conductivity and liquid helium. The concept of interpenetrating fluids made up of identical particles is necessarily an artificial construction, lacking physical reality. However, as long as the strictly phenomenological character of the model is kept in mind, it is a most useful aid for a consistent interpretation of the observed facts.

Applying the two fluid concept to the observation of zero Thomson heat, leads to a model in which at the transition temperature T_c a fluid of "superconductive electrons" will begin to make its appearance and in which this fluid has zero entropy. As the temperature is lowered, the concentration of superconductive electrons ω increases at the expense of the normal ones until at the absolute zero no fluid of "normal electrons" is left. The latter postulate could be made from a comparison of the total electronic entropy S of the metal with that amount of entropy ΔS which disappears at the transition from the normal to the superconductive state. It could be shown that as absolute zero is approached $\Delta S \to S \to \gamma T$, where γ is the constant in the Sommerfeld electronic specific heat [10] (See Ch. I and Ch. XI).

For an interpretation of the heat conductivity, the variation of ω with temperature is clearly the most important function. It can only be obtained either by a rigorous theory of superconductivity or, semi-empirically, through derivation from other, experimentally determined, temperature dependent parameters such as the threshold curve or the specific heat. The latter method must again involve separate assumptions. The only attempt at a rigorous theory providing this function is that by Heisenberg [11] and Koppe [12]. In view of the later discovery of the isotope effect postulated by Fröhlich [13] and Bardeen[14], the fundamental basis of the Heisenberg theory must appear doubtful. However, it seems that this theory was sufficiently well adjusted to the observed temperature dependent parameters to make the derivation of the heat conductivity not unreasonable.

Using Eq. (6) one has then first a gradual disappearance of carriers from the conduction process. The remaining "normal electrons" will have roughly the same velocity v as those in the normal state of the metal but their mean free path and the specific heat will be affected. For the former an increase by $1/(1 - \omega/2)$ against the normal state is postulated. Calculation on these lines leads to a formula for the ratio between the electronic heat conductivity in the superconductive state, K_{es} to that in the normal one, K_{en} in terms of a reduced temperature $t = T/T_c$ which reads

$$\frac{K_{es}}{K_{en}} = \frac{2t^2}{1 + t^4} \tag{7}$$

This function is estimated to hold for $T/T_c > 0.3$, while for lower temperatures an exponential drop of this ratio with temperature is predicted.

While in the normal metal, provided that it is of sufficient purity, K_g is insignificant in comparison with K_e, the lattice conduction cannot always be neglected in the superconductive state. Firstly, as with falling temperature $(1 - \omega)$ tends towards zero, K_{es} becomes very small. Secondly, a new effect might be expected which will greatly increase K_{gs}. The small part played by lattice conduction in metals is due to the very efficient scattering of phonons by electrons. It is now possible that the "superconductive electrons" which can move through the lattice without friction are also unable to scatter phonons and the fact that these electrons carry no entropy makes this inability probable. Thus, the gradual disappearance of "normal electrons" may not only decrease K_{es} but at the same time enhance K_{gs} which at very low temperatures should give the superconductor a heat conduction similar to that of an insulator.

4. Results at Helium Temperatures

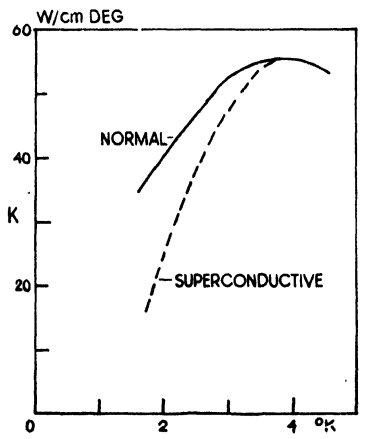

Fig. 2. Heat conductivity of tin in the superconductive and normal states.

Most of the work on superconductors has been concerned with the temperature dependence of heat conduction in the normal and superconductive stases between 2°K and T_c. The lower limit of this range was usually determined by the use of helium gas thermometers employed in the investigations. In some cases the thermal resistance in the normal state was noticeably increased by the magnetic field used to destroy superconductivity, making an extrapolation to zero field necessary.

Fig. 2 shows the curves for K_n and K_s of a spectroscopically pure tin specimen. Here the onset of superconductivity occurs just below the maximum, causing a gradual departure of

K_s to lower values. This is a case to which the Heisenberg-Koppe formula (7) should be applicable and comparison of the ratio K_s/K_n as derived from Fig. 2 is indeed in moderately good agreement with the theoretical value of K_{es}/K_{en} shown in Fig. 7.

The results obtained on a lead single crystal which are represented in Fig. 3, while being qualitatively similar, differ quantitatively from those of Fig. 2 in a marked way. Lead has a lower Θ than tin and a higher value of T_c. These factors combine to bring the onset of superconductivity to a temperature

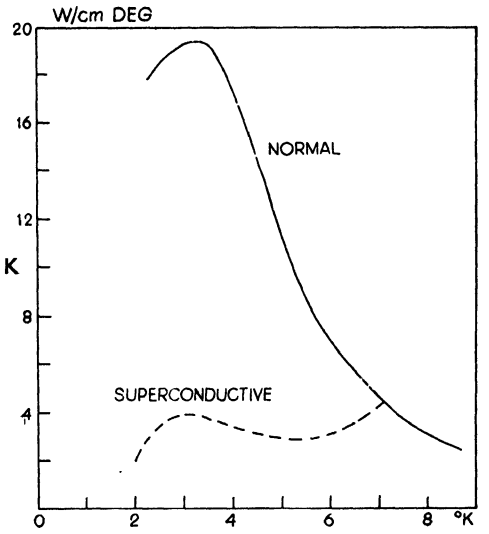

Fig. 3. Heat conductivity of a lead single crystal in the superconductive and normal states.

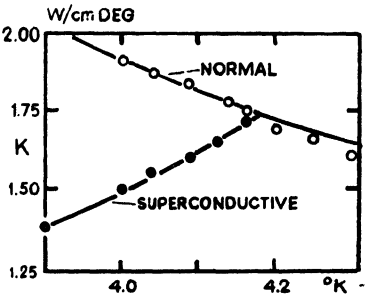

Fig. 4. Heat conductivity of mercury in the immediate neighbourhood of the transition temperature.

well above the heat conductivity maximum. As in the tin specimen K_s is again lower than K_n but the departure of the K_s is not gradual. The K_s-curve leaves that for K_n almost at right angles and the possibility of an abrupt change, somewhat similar to that taking place in electrical conduction, could not be ruled out in the first experiments. The problem was carefully investigated by Hulm [4] on mercury which also has a low Θ. However, as Fig. 4 shows, K_s, while changing fast below T_c, shows no discontinuity at this point. Moreover, the results on lead and mercury demonstrate far clearer than those on tin that the break at T_c is in K_s and not in K_n. It is already apparent from Fig. 3 and 4 that in these metals the ratio K_s/K_n will not have the form postulated by Eq. (7) and this discrepancy is well illustrated in Fig. 7 where the ratio for the lead specimen has been

inserted. The discrepancy is, however, not surprising since the heat resistance above the maximum is caused by scatter of electrons on phonons for which no provision is made in the Heisenberg – Koppe formula. It is interesting to note that the maximum, which marks the transition from predominant scatter by phonons to scatter by impurities, occurs, in a less marked degree, also in the superconductive state. This shows that even at $\frac{1}{2}\ T_c$ the heat conduction mechanism in the superconductor, while modified, is still essentially similar to that of the normal metal.

The heat conduction of pure indium, thallium, tantalum and niobium has been investigated in addition to the three metals mentioned above and the results fit tolerably well into the general pattern.

As mentioned in § 1, the behaviour of superconductive alloys is rather more complex than that of pure metals and differs from it in a number of aspects. However, this need not always be the case [15] and the curves for K_s and K_n of a lead alloy containing as much as 30%

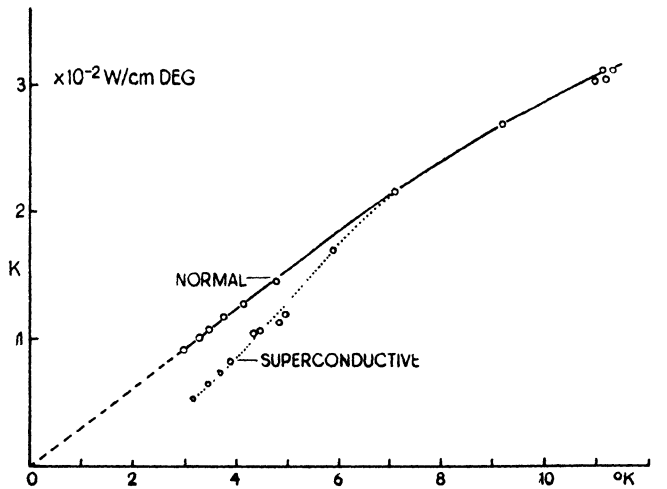

Fig. 5. Heat conductivity of an alloy of lead with 30% tin in the superconductive and normal states.

of tin, shown in Fig. 5, are similar to those found in a pure metal. When the ratio K_s/K_n for this specimen is plotted (see Fig. 7) it is found to agree with Eq. (7) rather better than lead. This is, no doubt, due to the fact that, as indicated by the almost linear form of K_n in Fig. 5, the heat resistance is due to electrons being scattered by impurities. Systematic investigations have been made on the effect of

controlled addition of mercury to tin, cadmium and indium to mercury [4], and bismuth to lead [5].

The results of the latter series which has yielded the most striking deviations from the behaviour of pure metals are given in Fig. 6.

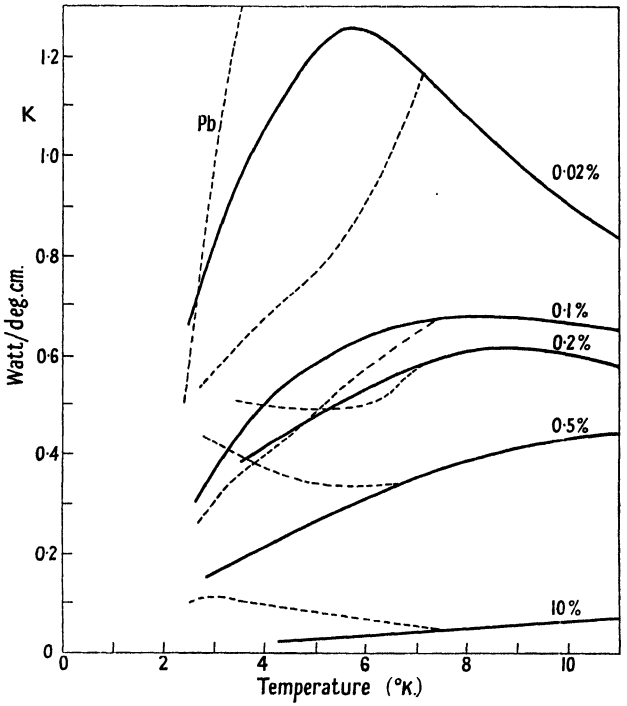

Fig. 6. Heat conductivities of the alloy series of lead with 0.02%, 0.1%, 0.2%, 0.5% and 10% bismuth. ———— normal and – – – – superconductive state.

Except for the lowest part of the K_s-curve, the data on pure lead cannot be accomodated in the figure because of the very much higher values of the thermal conductivity. First of all, the K_n-curves show well the effect, mentioned earlier, of the displacement of the maximum to higher temperatures with increasing impurity. The increase of impurity scatter is at the same time apparent in the progressive decrease of the absolute value of K_n. Turning to the behaviour of K_s, we see that in the specimen with the smallest (0.02%) impurity the general shape and the departure from K_n is still similar to that in pure lead (see Fig. 3). For the specimen with 0.1% bismuth the maximum rough-

ly coincides with T_c, and here the departure is more gradual, as in tin and the lead-tin alloy (Fig. 2 and 5). At the other end of the concentration scale, the alloy with 10% bismuth exhibits a quite anomalous behaviour, K_s, instead of falling below K_n, rises well above it. The ratio K_s/K_n is, as Fig. 7 shows, over the whole measured range, larger than one, increasing at 0.4 T_c to a value of 6. The alloys with 0.2% and 0.5% bismuth illustrate the transition from the behaviour characteristic of a pure metal to the anomalous effect obtained with 10% bismuth. In particular the 0.2% alloy is interesting as it shows a crossing over of K_s over K_n below T_c.

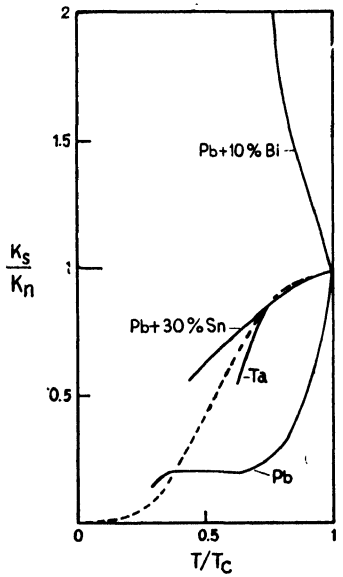

Fig. 7. The ratio K_s/K_n for two pure metals and two alloys. The broken curve represents the Heisenberg-Koppe formula.

The unsatisfactory state of the theory of superconductivity to which have to be added the complications inherent in the structure of an alloy must make any attempt at interpretation of these anomalous phenomena highly problematic. It has been suggested that the rise in K_s may be due to an enhanced lattice conduction [4] or, alternatively, that it may be caused by a circulation process [15] similar to the heat conduction in liquid helium. For the first explanation the almost identical value of K_s for pure lead and the alloy with 0.5% bismuth presents a certain difficulty, while objections, which have been discussed recently [16], have been raised against the possibility of a circulation mechanism. Altogether, it seems clear that an answer to these questions can only be obtained from further experiments, particularly in the temperature range between 1°K and 2°K and on more alloy systems.

5. Results below 1°K

The considerations mentioned at the end of § 3 emphasize the importance of measurements of the heat conductivity at very low temperatures. However, while determinations of K_s and K_n down to 2°K are comparatively simple, the experimental difficulties increase very much in work at still lower temperatures. Instead of using a vessel

filled with liquid helium as heat sink, adiabatic demagnetization of a paramagnetic salt has to be employed for the cooling process and the salt, which itself is a poor heat conductor, has to serve as heat sink.

Attempts have been made [17, 18] to use a simple technique in which two pills of compressed paramagnetic salts were connected by a wire of the metal under investigation. The two salt samples were then demagnetized to different final temperatures and their susceptibilities were measured as they warmed up. From these warming-up rates the heat conduction of the wire was calculated under the assumption that the measured susceptibilities corresponded to the temperatures at the ends of the wire. In some of this work the main object was to explore the feasibility of multi-stage cooling rather than to investigate in detail the dependence of K on T. For these, more qualitative purposes the simple method is quite sufficient and it yielded the essential information that below 1°K the ratio K_s/K_n becomes very small.

In investigations requiring greater accuracy, the arrangement of two magnetic thermometers of relatively enormous heat capacity at the ends of the specimen which moreover act as heat sink and heater must be regarded as a serious drawback. Coupled with these features are frequently unreliable thermal contacts between salt and specimen as well as poor thermal equilibrium in the salt itself which all introduce a considerable degree of uncertainty.

In recent years a method has been developed [19, 20] which avoids these undesirable features. The salt, as shown in Fig. 8, merely acts as cooling agent and heat sink. It is in thermal contact with one end of the specimen while the other end carries an electric heater. On to the specimen are painted two narrow rings of carbon black which form conducting bridges between the specimen and the leads. These carbon bridges act as thermometers which, since they are directly deposited on the specimen, are in excellent thermal contact with it. Calibration of the carbon thermometers against the susceptibility of the salt is carried out when no heat is supplied to the specimen and the whole assembly is therefore in thermal equilibrium. During the actual determination of the heat conduction knowledge of the temperature of the salt is not required since the temperature gradient is measured solely with the carbon resistors. Corrections in this method are small since the heat influx through the thermometer and heater leads amounts to less than 1% of the power dissipated in the heater and energy dissipated by the measuring current in the thermometers

is still smaller. Warming-up rates of the heat sink were found to be so slow that magnetic cycles for the destruction and re-establishment of superconductivity, containing up to 15 measured points could be carried out under practically isothermal conditions.

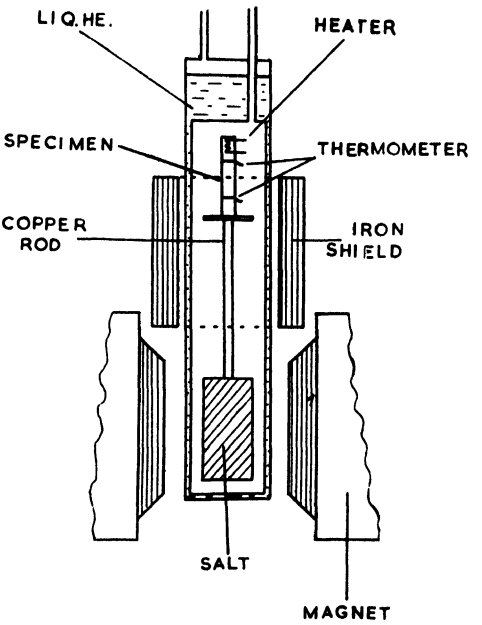

Fig. 8. Diagrammatic sketch of an apparatus for measuring heat conductivities of superconductors below 1°K in zero magnetic field.

At these low temperatures the ratio K_s/K_n in pure metals may become as small as 10^{-3} or even 10^{-4} which makes it impossible to measure on the same specimen both K_s and K_n accurately. However, there is little doubt that in these cases the heat conduction of the normal metal is given by T/β, and since β can easily be obtained from measurements on the same specimens in the helium range, the work below 1°K has been concentrated on the accurate determination of K_s.

A peculiar difficulty arises in work using paramagnetic cooling. Prior to the actual cooling process a strong magnetic field is applied to the salt and also to the superconductive specimen. The specimen is therefore rendered temporarily non-superconductive. It is essential that at the subsequent demagnetization no residual magnetic flux should become trapped in the metal when it returns to the supercon-

ductive state. In view of the high heat conduction of the normal phase and also because of the peculiar effect to be discussed in the next paragraph, any retained non-superconductive inclusions are likely to falsify the results for K_s appreciably. In none of the early work below 1°K have attempts been made to exclude the demagnetization field from the specimen and the first experiments with the new method suffered from the same drawback. While it appeared unlikely that any flux had been trapped in the purest specimens, some of the polycrystalline samples showed features indicative of normal inclusions. The method was therefore modified by separating the specimen from the salt by a long copper rod and by surrounding the specimen with a soft iron cylinder while the magnetic field was applied.

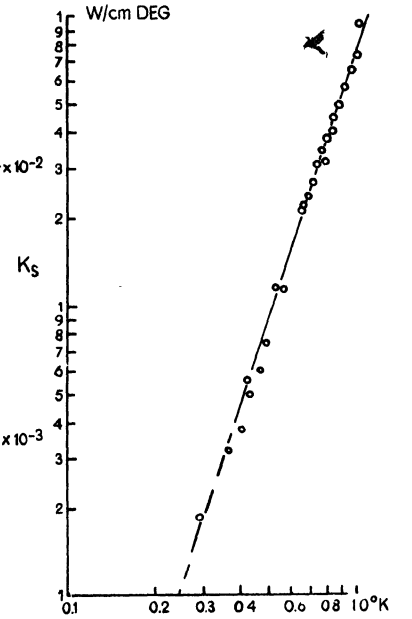

Fig. 9. Logarithmic plot of the heat conductivity of a lead single crystal in the superconductive state below 1°K. The straight line represents a third power law.

A typical result obtained in this way is shown in Fig. 9 which gives the heat conduction of a superconductive lead single crystal of high purity between 0.3° and 1°K. The value of K_s increases in this range proportional to the third power of the absolute temperature, as can be seen from the logarithmic plot in which the measured points are well represented by a straight line. Such T^3 dependencies of K_s were also found for tin and indium and for a polycrystalline specimen of niobium. The results on tin, given in Fig. 10, while being in accordance with a T^3 law at the lowest temperatures rise more steeply above 0.55°K and the same is true for indium above 0.7°K. The lead single crystal, too, shows a more rapid rise of K_s above 1° K.

The cubic form of the K_s-curve found in all these specimens strongly suggests that the region has been reached where, as discussed in § 3, the heat conduction of the metal should become similar to that of an insulator. The theory [31] for an insulator postulates a variation of the heat conduction with T^3 and the numerical values obtained from

the experiments are compatible with those predicted by the theory. It therefore seems reasonable to regard the T^3 region of the heat conductivity as that temperature range, close to absolute zero, in which the concentration of the normal electron fluid has become so small that it can be neglected. Expressing the onset of this range as a fraction of the transition temperature, we obtain for lead and tin 0.15 T_c and for indium $0.2T_c$. The concept of the T^3 range as being pure lattice conduction is further strengthened by the results on niobium. This metal is a "hard" superconductor whose superconductive properties approximate those of alloys. Indications of such anomalous behaviour were indeed found in K_s at helium temperatures. The agreement with a simple T^3 law at the lowest temperatures therefore suggests that electronic conduction, which must be regarded as the cause of the anomalous behaviour, has completely ceased to be of importance.

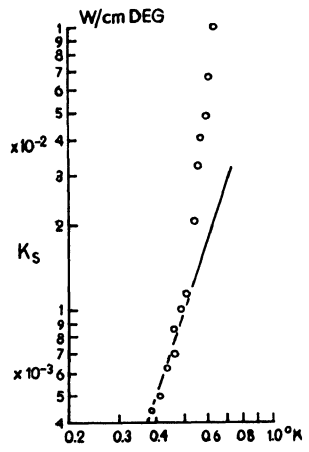

Fig. 10. Logarithmic plot of the heat conductivity of a tin single crystal in the superconductive state below 1°K. The straight line represents a third power law.

The beginning of electron conduction, as the temperature is raised, is evidently marked by the deviation of K_s to values which are always higher than would correspond to the T^3 law. Whether the excess conductivity corresponds to the exponential rise postulated by the Heisenberg-Koppe theory cannot as yet be decided with certainty. It has to be remembered that at the same temperature where electronic conduction sets in, and for the same reason, the lattice conduction will be impaired by the scatter of phonons on electrons. This process is not considered in the theory which only deals with conditions where K_g can be neglected in comparison with K_e.

In addition to these results a more complex behaviour has been observed in specimens of less satisfactory physical and chemical purity. While a detailed analysis is not possible in these cases, they can nevertheless be roughly represented as lattice conduction at the lowest temperatures with electronic conduction making itself felt over the whole region of investigation.

6. Heat Conduction in the Intermediate State

When superconductivity in a long cylindrical rod is destroyed by a transverse magnetic field, the first penetration of magnetic flux occurs when the value of the undistorted field is $\frac{1}{2}H_c$. Under these conditions the field at the surface of the cylinder has reached the value H_c. As the undistorted field is increased from $\frac{1}{2}H_c$ to H_c, the surface field remains at H_c while the material of the rod is gradually transformed from the superconductive into the normal state. There are theoretical and experimental reasons to believe that this transformation consists in the growth of normal laminae, at the expense of superconductive ones, all being directed at right angles to the cylinder axis.

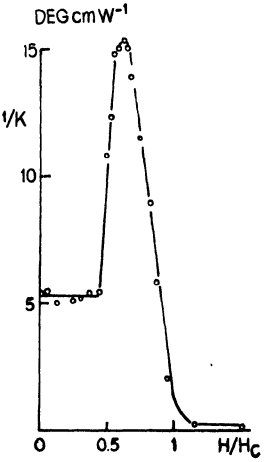

Fig. 11. Thermal resistivity of a lead single crystal in dependence on a transverse magnetic field. As the specimen passes into the intermediate state at $\frac{1}{2}H_c$, the heat resistance rises sharply before dropping to the low value in the normal state at H_c. Temperature 1.5°K.

In a pure metal where the heat conduction in the superconductive state is smaller than in the normal, one should expect a gradual increase from K_s to K_n as the transverse field is increased from $\frac{1}{2}H_c$ to H_c. This was indeed observed in the first experiments of this kind. However, a new and entirely unexpected effect was observed in samples of niobium [15] and slightly impure lead [21]. These specimens showed a pronounced *minimum* in the heat conduction between $\frac{1}{2}H_c$ and H_c. In the lead specimens K_s was smaller than K_n whereas in the niobium sample K_n was smaller than K_s but in either case the heat conduction in the intermediate state was smaller than K_s or K_n. The existence of this effect, which is illustrated by the graph shown in Fig. 11, has since been confirmed by a number of workers on pure lead [22], tin and indium [23].

In all these observations it was noted that the effect only appeared at temperatures well below T_c and that it increased with falling temperature. However, magnetic cylces on a lead single crystal taken at 1.5°K, 0.59°K and 0.43°K show a falling off as absolute zero is approached. Too little is as yet known about this effect to allow a satisfactory explanation, but it must be clear that the assumption of an enhanced lattice conduction, which has been invoked to explain the effect, is not in itself sufficient. This can only lead to a heat conduction

which is intermediate between K_s and K_n and additional assumptions, such as scatter on the phase boundaries [22, 23] or some other interaction [24, 25] between the size of the laminae and the mean free path of the carriers, have to be made in order to allow for a heat conduction minimum. The experiments below 1°K in which the effect was very marked [19] in a region where K_s is entirely due to lattice waves, strongly suggest that it must be scatter of these rather than of the electrons which is responsible for the minimum. At first sight it must seem difficult to postulate scatter of lattice vibrations on the superconductive-normal phase boundary which is of a purely electronic nature. However, it has recently been pointed out [26] that there will exist a strong secondary effect due to lattice waves entering a medium of thermal opacity when they pass from the superconductive into the normal metal.

7. The Thermal Switch

The difference between K_s and K_n, particularly in the region of very low temperatures, has led to an interesting development in cryogenic technique. One of the chief difficulties in the development of multistage cooling below 1°K is to provide for thermal make and break contacts. A number of authors [15, 16, 27] have suggested the construction of a thermal switch, consisting of a wire of superconductive material, which owing to the small value of K_s would be "open" when superconductive and "closed" when brought into the normal state by a magnetic field. Such a device has in fact been operated very successfully in double stage demagnetisation of paramagnetic salts [28]. Since at the lowest temperatures K_s is proportional to T^3 while K_n varies linearly with temperature, the ratio K_s/K_n becomes T^2/c, where c is a material constant which for a pure single crystal wire is of the order of 200. Thus, at 0.1°K the open switch will pass less than 1/10000 of the heat which it transmits in the normal state at the same temperature. A suggestion which goes even further is that of a continuously working heat pump [29] which also has been operated. In this device a sample of paramagnetic salt is connected alternately with the substance which is to be cooled and a heat sink at a higher temperature which receives the heat of magnetisation. These switching operations are performed by superconductive thermal switches of the type mentioned above and by using a bath of liquid helium as the heat sink, a temperature of 0.3°K could be maintained indefinitely [30]. The requirements in such a device are, however, more rigorous than in a straightforward

thermal switch with a starting temperature of well below 1°K. In the time interval when the switch between salt and cooled specimen is "closed", the "open" switch has to tolerate the temperature of the heat sink at its warm end. Using lead, which is probably the best metal for this purpose, the sink temperature has still to be kept very close to 1°K.

REFERENCES

[1] H. Kamerlingh Onnes and H. G. Holst, Comm. Leiden 142c (1914).
[2] W. J. de Haas, S. Aoyama and H. Bremmer, Comm. Leiden 214a (1931); W. J. de Haas and H. Bremmer, Comm. Leiden 214d (1931); Comm. Leiden 220b, c (1932); Physica **3** (1936) 687; H. Bremmer and W. J. de Haas, Physica **3**, (1936) 672, 692; W. J. de Haas and A. Rademakers, Physica, **7** (1940) 992.
[3] K. Mendelssohn and R. B. Pontius, Phil. Mag., **24** (1937) 777.
[4] J. K. Hulm, Proc. Roy Soc. A, **204** (1950) 98.
[5] K. Mendelssohn and J. L. Olsen, Proc. Phys. Soc. A, **63** (1950) 1182.
[6] H. M. Rosenberg, Thesis, Oxford (1952).
[7] cf. J. L. Olsen and H. M. Rosenberg, Phil. Mag. Suppl., **2** (1953) 28.
[8] K. Mendelssohn and H. M. Rosenberg, Proc. Roy. Soc. A, **281** (1953) 190.
[9] J. G. Daunt and K. Mendelssohn, Proc. Roy. Soc. A, **185** (1946) 225.
[10] J. G. Daunt, A. Horseman and K. Mendelssohn, Phil. Mag., **27** (1939) 754.
[11] W. Heisenberg, Z. Naturforsch., 3a (1948) 65.
[12] H. Koppe, Ann. Physik, **1** (1947) 405.
[13] H. Fröhlich, Phys. Rev., **79** (1950) 845.
[14] J. Bardeen, Phys. Rev., **80**, (1950) 567.
[15] K. Mendelssohn and J. L. Olsen, Proc. Phys. Soc. A, **63** (1950) 2.
[16] K. Mendelssohn, Physica, **19** (1953) 775.
[17] C. V. Heer and J. G. Daunt, Phys. Rev., **76**, (1949) 854.
[18] B. B. Goodman, Proc. Phys. Soc. A, **66** (1953) 217.
[19] J. L. Olsen and C. A. Renton, Phil. Mag., **43** (1952) 946.
[20] K. Mendelssohn and C. A. Renton, Proc. Roy. Soc. A, in print.
[21] K. Mendelssohn and J. L. Olsen, Phys. Rev., **80** (1950) 859.
[22] R. T. Webber and D. A. Spohr, Phys. Rev., **84** (1951) 384.
[23] D. P. Detwiler and H. A. Fairbank, Phys. Rev., **88** (1952) 1049.
[24] F. H. J. Cornish and J. L. Olsen, Helv. Phys. Acta, **26** (1953) 369.
[25] J. K. Hulm, Phys. Rev., **90** (1953) 1116.
[26] C. A. Renton, Phil. Mag. in print.
[27] C. J. Gorter, Les Phénomènes Cryomagnétiques, Paris (1948) **76**.
[28] J. Darby, J. Hatton and B. V. Rollin, Proc. Phys. Soc. A, **63** (1950) 1179.
[29] J. G. Daunt, and C. V. Heer, Phys. Rev., **76** (1949) 985.
[30] C. V. Heer, C. B. Barnes, and J. G. Daunt, Phys. Rev. **91** (1953) 412.
[31] H. B. G. Casimir, Physica, **5** (1938) 595.

CHAPTER XI

THE ELECTRONIC SPECIFIC HEATS IN METALS

BY

J. G. DAUNT

DEPARTMENT OF PHYSICS AND ASTRONOMY, OHIO STATE UNIVERSITY

1. Introduction

The primary interest in measurement of the electronic specific heat in metals stems from the fact that it allows an evaluation to be made of the density of states, $N(E^*)$, at the Fermi energy, E^*, in the energy band. The relation between the electronic specific heat, c_e, per mole of metal and $N(E^*)$ for a highly degenerate electronic system, such as in a metal, is:

$$c_e = \gamma T = \tfrac{2}{3}\pi^2 k^2 N(E^*)\, T \text{ cal/mole-deg.} \tag{1}$$

where $N(E^*)$ is the number of energy states per unit energy range per mole at the Fermi level. This result was first obtained by Sommerfeld [1].

It is to be noted that Eq. (1) is quite generally valid, independently of the condition of binding of the electronic system, as for example has been shown by Bloch [2], Sommerfeld and Bethe [3], and later again by Sommerfeld himself [1a].

For a free electronic system, such as might be assumed to be approximately represented by the s-electrons in the monovalent metals, $N(E^*)$ is given by:

$$N(E^*) = \frac{2\pi m V}{h^2}\left(\frac{3n}{\pi}\right)^{1/3} \tag{2}$$

where m is the free electronic mass, n the number of electrons per cm^3 and V the molar volume of the metal.

This gives the electronic specific heat per mole of metal to be:

$$c_e = \frac{4\pi^3 mk^2 V}{3h^2}\left(\frac{3n}{\pi}\right)^{1/3} T$$
$$= 3.26 \times 10^{-5}\, V^{2/3} n_a^{1/3}\, T \text{ cal/mole-deg} \qquad (3)$$

where n_a is the number of electrons per atom.

For a ferromagnetic metal, the right hand side of Eq. (3) must be divided by $2^{2/3}$, owing to the splitting of the d-band for electrons of opposite spin (See for example Seitz [4]).

The modification to the above formulation of c_e necessary in considering partially bound electrons is discussed in section 5 below.

As was first pointed out by Mott [5] contributions to c_e must be made not only by the s-electrons but also by the electrons in the unfilled d-band in the transition metals. Indeed in the transition metals the latter contribution is predominant, since due to their tighter binding the d-electrons show a much narrower band than the s-electrons and so have a greater number of energy levels per unit energy range. Measurements of c_e and hence of $N(E^*)$ for each series of transition metals is of interest therefore in order to obtain some estimate of the filling of the d bands.

2. Method of Evaluation of the Electronic Specific Heat from Calorimetric Measurements

At room temperature, (circa 300°K), c_e is only a few percent of the total specific heat of a metal. At sufficiently low temperatures, c_e, due to its *linear* dependence on T must dominate over the lattice specific heat, c_l, since the latter eventually diminishes proportionally to T^3. In general the temperature range in which c_e becomes a significant fraction of the total observed specific heat, c_p, of a metal is that obtainable with liquid helium, at which temperature in general also c_l is proportional to T^3. In such a temperature range it is generally assumed that the total specific heat of a pure metal may be written as the sum of c_l and c_e, namely:

$$c_p = c_v = a\, T^3 + \gamma\, T \text{ cal/mole-deg} \qquad (4)$$

Direct calorimetric determinations of c_p therefore allow γ to be eva-

luated from the intercept on the ordinate axis on a c_p/T versus T^2 plot of the experimental data (See for example Silvidi and Daunt [6]). In addition the observation of linearity of the plot of c_p/T versus T^2 serves to support the assumptions involved in Eq. (4); and the slope of the curve gives the coefficient a of the lattice specific heat. A typical plot of this kind for Zn, as observed by Silvidi and Daunt [6], is shown in Fig. 1.

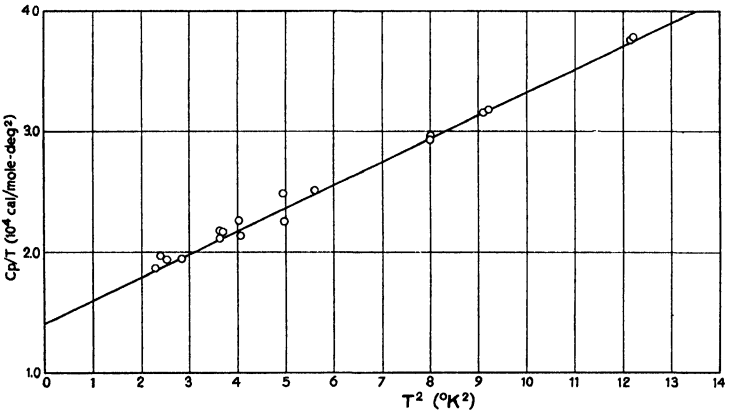

Fig. 1. Plot of c_p/T versus T^2 from calorimetric observations on Zn by Silvidi and Daunt [6], showing the linearity of the curve. The intercept on the ordinate axis gives the value of γ.

The validity of Eq. (4) depends on the following assumptions:

(a) The equality of c_p and c_v. At liquid helium temperatures this equality holds with high accuracy. Even at liquid nitrogen temperatures the difference between c_p and c_v is generally small: for example, recent calorimetric measurements on Pb, which gives the greatest effect, by Horowitz *et al.* [7] showed that at 75°K the difference only amounted to 1.4% of c_p. This shows up one of the advantages of making the measurements at very low temperatures.

(b) The proportionality of the lattice specific heat to T^3. Provided T is much less than the Debye characteristic temperature, Θ_D, one has $c_l = a\,T^3$ quite generally, as was pointed out by Blackman [8, 9]. This is so because for acoustic waves of sufficiently long wavelength, such as obtain at sufficiently low temperatures, the continuum approximation of Debye [10], must be valid. The practical, as well as the theoretical,

problem however is how low the temperature should be. On the Debye theory the T^3 region holds well for $T < \Theta_D/12$; whereas Blackman suggests that for real crystals one must have $T < \Theta_D/50$ before the T^3 region is sure.

(c) The absence of further terms contributing to c_v. For this assumption to be valid clearly there must be no magnetic effects, as occur in ferromagnetics or antiferromagnetics near respectively their Curie or Néel temperatures, and care must be taken to note the possibility of phase transitions. Another possibility of the existence of a further anomalous term in addition to those presented in Eq. (4) has been suggested by Simon [11, 12]. He proposed that an excitation process of the Schottky type [13a], should be included for some substances, for example for Li, Na, K, Be and for diamond structures such as Si, Ge, gray Sn and diamond, in order to account for the marked deviations of the observed c_v values from Debye's theory. In general these deviations, however, do not reveal maxima in the c_v versus T curves. Instead, as is shown by the most recent calorimetric observations to be made over an extended temperature range for Li by Simon and Swain [13], for K by Simon and Zeidler [14], for Be by Hill and Smith [15], for Si by Pearlman and Keesom [16], for Ge by Hill and Parkinson [17], Estermann and Weertmann [18], for gray Sn by Hill and Parkinson [17], and for diamond by Pitzer [19], De Sorbo [20] and Berman and Poulter [21], the observed c_v increases monotonically with T. Since the Debye theory uses a continuum approximation, it may not be surprising that experiment reveals deviations from the theory and it is to be expected that a more detailed investigation of the proper modes of vibration of the lattice would yield results closer to experimental observation, as was first pointed out by Born and von Karman [22]. Such vibrational theories have recently been extensively developed by Blackman [23] and many others [24] and indeed Smith [25] has given a detailed explanation of the diamond lattice specific heat using this theoretical approach. One might note parenthetically here the close agreement found by Horowitz and co-workers [7] between their observed lattice specific heat in Pb (normally conducting) and the lattice vibrational theory for fcc structures of Leighton [26]. One must conclude therefore, as Blackman has emphasized, that so long as there is not an actual maximum in the specific heat curve, lattice vibrational theory should be adequate and the introduction of an anomalous Schottky term should be superfluous. It would appear therefore that at low temperatures Eq. (4) should

be adequate in general to describe the specific heat of metals. * It seems, however, appropriate to mention here the observations of Parkinson *et al* [27] on the rare earth metals, La, Ce, Pr and Nd, which for Ce and Nd revealed maxima in the specific heat curves. These metals on the other hand are unusual in having deep unfilled 4*f*-electronic shells and it is possible that the anomalous specific heats observed are in fact Schottky type produced by changes in electronic configuration.

3. Method of Evaluation of the "Normal" Electronic Specific Heat from Magnetic Observations on Superconductors

For metals which become superconducting it is possible in principle to evaluate the electronic specific heat in the normally conducting state from magnetic measurements only. If the metal can be obtained sufficiently pure both physically and chemically, the transition normal $\rightleftarrows$ super state in a magnetic field should be thermodynamically reversible, as was first shown by Meissner and Ochsenfeld [30]. For such reversible transitions, which are obtainable only for pure specimens of simple shape, as was shown by Mendelssohn and co-workers [31, 32], the threshold magnetic field, H_c, represents the equilibrium boundary between the normal and super states, and hence from thermodynamics it was shown by Gorter and Casimir [33], that:

$$\Delta S = S_n - S_s = -\frac{V}{8\pi}\frac{\partial H_c^2}{\partial T} \tag{5}$$

where S_s and S_n are the entropies of the electrons in the super and normal states respectively per mole of metal, and where V is the atomic volume. Typical evaluations of ΔS obtained by Daunt, Horseman and Mendelssohn [34] from their magnetic measurements are shown in Fig. 2. As will be seen in this figure (especially for Pb) and as can be concluded from other considerations, ΔS is a *linear* function of T at sufficiently low temperatures and, moreover, as is demanded by the Third Law of thermodynamics, ΔS tends to zero at 0°K. If, therefore, S_s contains

* There remains however the curious and unrepeated observations on the specific heat of Na by Pickard and Simon [28], which showed a definite maximum at about 7°K. In this connection one might note that the older measurements on Ge and Be by Cristescu and Simon [29], which showed a pronounced maximum in each specific heat curve, have not been reproduced by the more recent workers. Rayne [102] has found recently an anomalous maximum at 0.87°K in the specific heat of Na and has tentatively attributed it to a martensitic transformation.

no linear term in T, ΔS must tend to the value S_n as T tends to 0°K, or symbolically:

$$\gamma = \left(\frac{\partial \Delta S}{\partial T}\right)_{T\to 0} \tag{6}$$

From (5) and (6) therefore:

$$c_e = \gamma T = -\frac{VT}{8\pi}\left(\frac{\partial^2 H_c^2}{\partial T^2}\right)_{T\to 0}. \tag{7}$$

The value of γ for the normally conducting state can therefore be obtained from magnetic measurements of H_c on superconductors, provided H_c represents the equilibrium magnetic boundary for *reversible* super⇄normal transitions.

The basic assumptions underlying the validity of Eq. (7), namely that the super ⇄ normal transition is of electronic character only and that S_s contains no linear term in T, are well supported by comparisons that can be made between the calorimetrically observed γ values and those obtained from magnetic measurements of H_c, as was done by Daunt, Horseman and Mendelssohn [34] for Sn. A detailed comparison of the results of the two methods of evaluation of γ is given in Table 2. The evident general agreement between the two methods for Cd, Zn, In, Sn and Pb gives considerable confidence in the validity of Eq. (7).

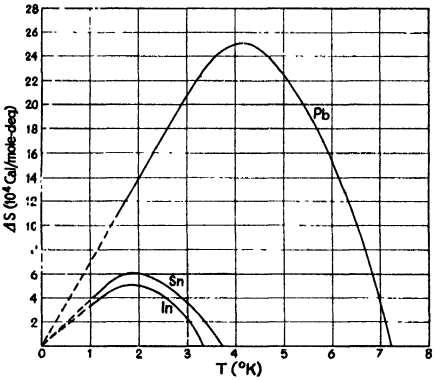

Fig. 2. The difference in entropy, ΔS, per mole between the normal and superconducting states in Pb, Sn and In obtained from magnetic threshold field measurements by Daunt, Horseman and Mendelssohn [34]. The slope of the linear part of the curve near $T = 0$°K gives the value of γ.

In evaluating γ from Eq. (7) either graphical methods must be used or H_c must be computed as a function of T from the experimental results. (See Ch. VII for a detailed discussion of the relation between H_c and T). However, as a first approximation Tuyn [35, 35a, 35b], suggested a parabolic relation, namely:

$$H_c = H_o\,[1 - (T/T_c)^2] \tag{8}$$

from which one can show that:

$$c_e = \gamma T = \frac{VT}{8\pi}\left(\frac{\partial H_c}{\partial T}\right)^2_{T=T_c}. \tag{9}$$

Although H_c is not exactly a parabolic function of T, the deviations therefrom for many superconductors are small enough to allow Eq. (9) to yield a good first approximation for γ. In many exploratory observations this is of value since in Eq. (9) it is necessary to known only the slope of the H_c versus T curve near T_c. However, as for example has been done for Sn, In, Tl [36] and for Cd [37], it is necesary to include cubic and quartic terms in T for the description of the H_c versus T curve in order to obtain accurate evaluations of γ.

4. The Observed Values of the Electronic Specific Heat in Pure Metals

A collection of the values obtained for γ experimentally for pure metals, either from magnetic measurements on the superconducting metals (Method (a)) or from calorimetric observations at low temperatures (Method (b)), is presented in Tables 1, 2 and 3. Table 1 gives the γ values for non-superconducting non-transition metals, Table 2 for superconducting non-transition metals and Table 3 for transition metals. Comments on each table are presented below. In each table the values of γ which are doubtful are inserted in parentheses.

TABLE 1

Calorimetrically observed γ values for *non-superconducting non-transition* metals

Metal	$\gamma \times 10^4$ cal/mole-deg^2	n_a	m^*/m	Reference
Cu	1.78	1	1.5	Keesom and Kok [38]
,,	1.80	1	1.5	Friedberg *et al.* [39]
Ag	1.6	1	1.0	Keesom and Kok [40]
,,	1.54	1	0.95	Keesom and Pearlman [41]
Be	0.54	2	0.46	Hill and Smith [15]
Mg	3.25	2	1.33	Friedberg *et al.* [39]
Ca	(2.9 ± 1.4)	2	0.8	Clusius and Vaughen [42]
Bi	<0.5	–	–	Armstrong and G. Smith [43]

(a) Table 1. It is to be noted that relatively few pure metals falling into this category of non-superconducting non-transition metals have had their electronic specific heats experimentally evaluated. Notably the γ values for the alkali metals are as yet unknown. Considering the fact that these would theoretically approach most nearly the free electron model of Sommerfeld, this lack of information is unfortunate The only alkali metal calorimetrically investigated to liquid helium temperatures is Na by Pickard and Simon [28] and their observed c_v values, as noted in section 2 above, proved anomalous.

The value of γ for Ca is doubtful since the measurements of Clusius and Vaughen [42] did not extend to liquid helium temperatures, the value quoted here being obtained by an extrapolation due toShiffman[79].

Many measurements have been made recently on the electronic specific heats at very low temperatures of Ge an Si; but the results obtained are not included here since they are dependent greatly on the state of physical or chemical purity of the samples.

For a discussion of the m^*/m values given in Tables 1 and 2 see section 5 below.

(b) Table 2. In this table the published results of all measurements on non-transition superconducting metals at present known to the author are included. In general the most recent observations are the more accurate and reliable. It appears in general also, probably fortuitously, that the more recent the observation the higher is the value of γ. The accuracy of the measurement of the γ values varies considerably from one result to another and no attempt has been made to assess the probable limits of error. For the calorimetric measurements, as has been pointed out by Keesom and van Laer [49] and by Horowitz and Daunt [76], the simultaneous evaluations of both the lattice and electronic specific heats from Eq. (4) may in some instances lead to an appreciable range of possible choices of the values of γ and Θ_D, owing to the scatter in the results. The original papers therefore should be consulted on this question. For the magnetic measurements on the superconductors, in general those metals with transition temperatures near or below 1°K yield less accurate γ values than those with higher T_c. This is due to the greater technical difficulties involved in measurement below 1°K, which is approximately the lowest temperature conveniently attainable with a liquid helium bath. The metals listed in Table 2 all showed a tolerable approach to reversibility in the super $\rightleftarrows$ normal transitions in a magnetic field; and hence, as discussed in section 2 above, the γ values obtained by method (a) are reliable, except for Th*. As pointed out earlier, the γ values which have been measured in this category (i.e. for Cd, Zn, In, Sn and Pb) by *both* methods show excellent agreement, except in the case of Al. Although the γ values by the two methods for Al do not differ widely, they do nevertheless represent a discrepancy.

* The γ value for Th was computed by the writer using Shoenberg's [54] magnetic data from Eq. (9), which may not be applicable, since it is unknown whether the theshold field is truly parabolic.

TABLE 2

Observed γ values for superconducting non-transition metals in their normal states, obtained from (a) magnetic measurements and (b) calorimetric measurements

Metal	$\gamma \times 10^4$ cal/mole-deg^2 Method (a)	Reference	$\gamma \times 10^4$ cal/mole-deg^2 Method (b)	n_a	m^*/m	Reference
Cd	1.28	Goodman and Mendoza [50]	1.7	2	0.75	Samoilov [44]
,,	1.54	Smith and Daunt [51]				
,,	1.70	Clement [37]				
Zn	1.36	Daunt and Heer [52]	1.25	2	0.9	Keesom and v. d. Ende [45]
,,	1.16	Goodman and Mendoza [50]	1.42	2	0.8	Silvidi and Daunt [6]
Ga	0.8–1.5	Daunt [53]				
	0.91	Goodman and Mendoza [50]		3	0.4	
Al	2.59	Daunt and Heer [52]	3.48	3	1.6	Kok and Keesom [46]
	2.95	Goodman and Mendoza [50]				
Th	(7.1)	Shoenberg [54]				
Tl	2.8	Daunt *et al.* [34]				
	3.4	Misener [55]				
	3.65	Maxwell and Lutes [36]		3	1.15	
In	3.5	Daunt *et al.* [34]	4.0	3	1.3	Clement and Quinnell [47]
	3.6	Misener [55]	4.33	3	1.4	Clement and Quinnell [48]
	4.3	Stout and Guttman [56]				
	4.0	Maxwell and Lutes [36]				
Sn	3.5	Daunt and Mendelssohn [57]	4.0	4	1.2	Keesom and v. Laer [49]
	3.95	Daunt *et al.* [34]				
	4.41	Lock *et al.* [58]				
	4.43	Serin *et al.* [59]				
	4.46	Maxwell [60]				
Hg	3.75	Daunt and Mendelssohn [57]	—			
	4.5	Misener [55]		2	1.8	
	5.33	Reynolds *et al.* [61]				
	5.3	Maxwell and Lutes [36]		2	2.2	
La	—	—	16	3	4.3	Parkinson *et al.* [27]
Pb	7.1	Daunt and Mendelssohn [57]	7.5	4	2.1	Horowitz *et al* [7]
	7.0	Daunt *et al.* [34]				

TABLE 3

γ values for the *transition* metals, obtained from (a) magnetic measurements on those which become superconducting, (b) calorimetric measurements and (c) band theory

Metal	$\gamma \times 10^4$ cal/mole-deg^2 Method (a)	Reference	$\gamma \times 10^4$ cal/mole-deg^2 Method (b)	Reference	$\gamma \times 10^4$ cal/mole-deg^2 Method (c)
Ti	(1.1)	Smith *et al.* [62]	8.0	Friedberg *et al.* [39]	—
V	15	Wexler and Corak[63]	22	Worley *et al.* [68]	—
Cr		not superconducting	3.80	Friedberg *et al.* [39]	—
Mn		not superconducting	(42)	Elson *et al.* [69]	—
,,		,, ,,	(35)	Armstrong and G. Smith [43]	
Fe(α)		not superconducting	12	Duyckaerts [70]	4.6
,,		,, ,,	12	Keesom and Kurrelmeyer [71]	
Co		not superconducting	12	Duyckaerts [72]	—
Ni		not superconducting	17.4	Keesom and Clark[73]	11.0
Zr	3.9	Smith and Daunt[51]	6.9	Friedberg *et al.* [39]	—
Nb	(60)	Daunt and Mendelssohn [57]	21	Brown *et al.* [74]	—
,,	(375)	Cook *et al.* [64]	20.4	Brown *et al.* [75]	
Mo		not superconducting	5.1	Horowitz and Daunt [76]	—
Tc	(20)	Daunt and Cobble[65]	—	—	—
Ru	(3)	Goodman [66]	—	—	—
Rh		not superconducting	—	—	—
Pd		not superconducting	31	Pickard [77a]	—
Hf		—	—	—	—
Ta	19.4	Daunt and Mendelssohn [57]	14.1	Keesom and Desirant [78]	—
W		not superconducting	1.8–2.5	Horowitz and Daunt [76]	4.8
Re	(4.6)	Daunt and Smith[67]	—	—	—
Os	(2.7)	Goodman [66]	—	—	—
Ir		not superconducting	—	—	—
Pt		not superconducting	16.0	Keesom and Kok[38]	—

Concerning the absence of calorimetric data for Ga, Tl, Hg and Th, it is to be noted that only Tl and Hg have been measured in the normally conducting state at liquid helium temperatures by Keesom and Kok [77] and by Pickard and Simon [28] respectively. The former measurements were over too small a temperature range and the latter were too anomalous to allow a γ evaluation to be made.

(c) Table 3. In general those transition metals which become superconducting show marked irreversibilities in their super $\rightleftarrows$ normal

transition in a magnetic field, due largely to the difficulty in obtaining specimens in a sufficiently pure chemical or physical condition. In addition, as in the measurements on Tc, Ru, Re and Os, irreversibilities due to irregularities in the shape of the specimens have unavoidably been present in some instances. In consequence many of the γ values obtained with method (a) are doubtful, as are indicated in Table 3 by the figures in parentheses. This doubt is particularly evident for example in Nb, where a comparison can be made with the relatively reliable γ value obtained calorimetrically; the comparison shows that γ by method (a) is far too large. Such comparisons moreover, even for those metals for which the method (a) is more certain, i.e. for V, Zr and Ta, also indicate a lack of agreement. More work clearly remains to be done on this problem. Meanwhile it is safer to regard the calorimetric observations as the more reliable.

All the calorimetric results given in Table 3 are obtained from measurements at liquid helium temperatures except those for Mn. In general if measurements are not made at liquid helium temperatures, the value of c_e is much smaller than c_l and consequently difficulty is is encountered in an accurate evaluation of γ. Moreover if the temperature is too high the assumptions implicit in Eq. (4) may not be valid. Calorimetric measurments at liquid helium temperatures would be of value not only for Mn but also for those metals which have not yet been investigated, namely: Tc, Ru, Rh, Hf, Re, Os and Ir.

Any discussion of the theoretical evaluations of γ (Method (c)) given in Table 3 is left to section 7.

5. Discussion of the Effective Mass Values

The concept of the effective electronic mass, m^*, in describing approximately the behavior of partially bound electronic systems is of general usage; the value of m^* being dependent on the curvature of the Bloch band at the Fermi level m^*, however, only has an exact meaning for electrons in a single non-overlapping band, a situation approximated by the s-electrons in the monovalent metals or by the positive holes of those transition metals with nearly filled d-bands. For most metals considerable overlapping of the bands takes place and in consequence a computation of the effective mass for such materials is of little significance.

The electronic effective mass is computed from the electronic specific heat by a formulation identical with that of Eq. (3) with however

m^* replacing m. The ratio m^*/m therefore would be given by the ratio of the observed value of γ to the value of γ obtained theoretically from Eq. (3) as it stands. (For a ferromagnetic, as pointed out above, the right hand side of Eq. (3) must be divided by $2^{2/3}$)*. It should be noted therefore that a determination of m^*/m from the observed γ values is dependent on an assignment of the numerical value of n_a, the number of electrons or positive holes per atom.

In the monovalent metals n_a can be taken rather confidently to be unity and for Ni and Pt Mott [80, 81] has assessed from diverse considerations n_a to be 0.6 positive holes per atom and for Pd n_a to be 0.55. For Fe (α) and Co one might arbitrarily take n_a to be given by the measured saturation magnetic moment per atom (expressed in Bohr magnetons); this gives for Fe (α) n_a equal to 2.22 and for Co 1.72. The determination of m^*/m from these latter two assignments however will not have the exactitude as that for the metals Ni, Pd and Pt, which have nearly filled bands. Using these assignments for n_a, m^*/m has been computed from the experimental data and the values are given in Table 1 for Cu and Ag and in Table 4 for the metals cited from Group 8. It is noteworthy that, whereas Ag approximates closely to the free electron picture, having m^*/m approximately unity, Cu shows a clear indication of a divergence from it. The metals listed in Table 4 all show very high effective masses, reffecting the tight binding of the electrons in the d-band.

TABLE 4

The effective mass, given by m^*/m, of the positive holes in the d-band of the transition metals of Group 8

Metal	$\gamma \times 10^4$ cal/mole-deg^2	n_a	m^*/m
Fe(α)	12	2.22	12
Co	12	1.72	14
Ni	17.4	0.6	28
Pd	31	0.55	27
Pt	16.0	0.6	13.3

An assignment of n_a values to the other metals listed in Tables 1, 2 and 3 is quite arbitrary and in consequence calculation of m^*/m is of no exact significance, quite apart from the question of their overlapping bands. However, since the m^*/m values may be at least somewhat suggestive, n_a has been assumed to be given by the valency and

* This number is obtained assuming that the half band with positive spin is completely filled. This may not be so for Fe (α) [82].

m^*/m has been computed for the metals listed in Tables 1 and 2. In Table 2 it is evident that all the so-called "soft" superconductors have relatively small effective masses. ($m^*/m \leqslant 2.2$).

It should again be stressed however that the significance of these evaluations is very doubtful, it being necessary to compute the real (overlapping) band structure to deduce theoretically the expected observable behavior of each metal. No attempt therefore has been made to make similar computations for the transition metals, except for those of Group 8.

6. An Apparent Correlation Among "Soft" Superconductors

For a free electronic system the quantity γ/V is proportional to the cube root of the number of electrons per cm³ (i.e. inversely proportional to the mean distance between electrons) and $\gamma/V^{2/3}$ is proportional to the cube root of the number of electrons per atom. For the "soft" superconductors, having $m^*/m \leqslant 2.2$, (see Table 2), the electronic systems are not free, but nevertheless it would seem that the above quantities would give some crude guide to their electronic densities. Since the interaction energy responsible for the appearance of superconductivity is in some way dependent on the electronic density, it interested the writer [53, 67] to plot γ/V and $\gamma/V^{2/3}$ as a function of the energy associated with the superconducting transition, namely kT_c. A plot giving the observed values of γ/V versus T_c for the soft superconductors is given in Fig. 3, (a plot of $\gamma/V^{2/3}$ presents also a picture similar to that of Fig. 3) from which it is evident that within the rather broad errors of the known data γ/V or $\gamma/V^{2/3}$ increases monotonically with T_c. In Fig. 3. also the value of γ/V for Al is inserted, which clearly does not fit the rest of the data. Al, however, was already noted to be anamalous in its divergence between the γ values obtained by methods (a) and (b).

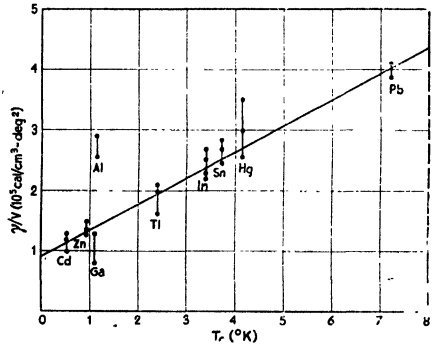

Fig. 3. Variation of γ/V with the transition temperature, T_c, for the so-called "soft" superconductors. The circles mark the individual measurements of different observers.

No data are inserted for the "hard" superconductors, since it is considered that many of their γ values and/or T_c values are insuffi-

ciently accurately known and since also their more complex band structure do not allow γ/V or $\gamma/V^{2/3}$ to represent even crudely their electronic densities.

Nevertheless the same general trend, namely high γ values correspond to high T_c values and vice versa, is quite evident also for the transitional superconductors, as was shown earlier by the writer [53]. As evidence of this and as is discussed in section 7 below, it is remarkable not only that the γ values and, not unnaturally, the paramagnetic susceptibilities go through regular alternations of maxima and minima as one goes through each series of transition elements (maxima at $n_v = 5, 7, 10$) but also that the superconducting transition temperatures, T_c, for those metals which show superconductivity also go through similar alternations, with pronounced maxima at $n_v = 5$ and 7. Indeed at the minimum where $n_v = 6$ superconductivity is suppressed entirely. Similar conclusions have been arrived at from work on superconducting alloys by Matthias and co-workers [93, 103, 104].

The straight line drawn through the data of Fig. 3 is not meant to indicate that γ/V (or $\gamma/V^{2/3}$) should be a linear function of T_c, but only to point up the general monotonic increase of γ/V with T_c. No detailed theoretical explanation of this correlation among the soft superconductors has yet been advanced, the correlation being noted here perhaps to stimulate an inquiry into it.

7. The Density of States in the d-Band in the Transition Metals

Theoretical computations of the d-band structure have been made by Krutter [83] and Slater [84] for the 3d band in Cu, from which Slater obtained the theoretical value of $\gamma = 11.0 \times 10^{-4}$ cal/mole-deg^2 for Ni, as indicated in Table 3 (Method (c)). Subsequent theoretical investigation have been made by Manning and Chodorow [85] for W, Manning [86] for Fe(α) and by Fletcher and Wohlfarth [87] and Fletcher [88] for Ni, the γ values obtained by them being given under Method (c) Table 3. (The work of Fletcher and Wohlfarth presented a γ value for Ni of 11.3×10^{-4} cal/mole-deg^2. and that of Fletcher 16.9×10^{-4}). It should be noted that for Fe(α) and Ni the theoretical evaluations of γ are much smaller than those experimentally observed; whereas for W this position is reversed. The reasons for these discrepancies are at present not understood.

The structure obtained by Slater for the 3d band in Cu is presented in Fig. 4 which plots $N(E)$ as a function of the number of electrons,

n_v, outside the closed shell as the band is filled up. Such a plot in fact gives also $N(E)$ as a function of E. It will be noted that there is a marked maximum in the d-band at the highest energy (i.e. when the band is nearly filled) and another smaller maximum at lower energy for $n_v \approx 5$. The other theoretical investigations cited also indicate the existence of a secondary maximum at the lower energies, this being especially marked in the work of Fletcher and Wohlfarth.

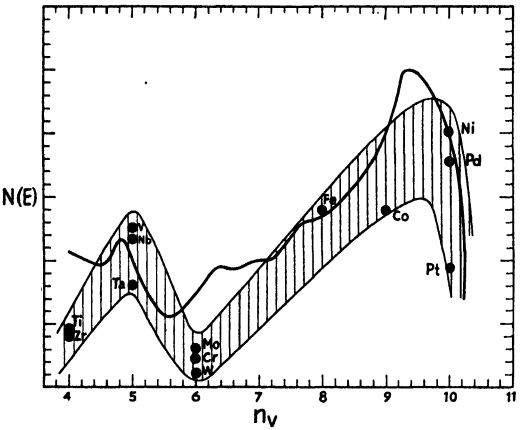

Fig. 4. Full curve gives the density of states, $N(E)$, for the 3d band in Cu plotted against the total number of electrons outside closed shells due to Krutter [83] and Slater [84]. The circles give density of states, $N(E^*)$, at the Fermi level as deduced from the observed electronic specific heats for the metals as marked. The shaded path indicates the possible region in which the $N(E^*)$ values for the other, as yet unmeasured, transition metals may fall.

Since from Eq. (1) $N(E)$ at the Fermi level is proportional to the observed γ we have inserted in the $N(E)$ versus n_v plot of Fig. 4 points corresponding to all the observed (and reliable) γ values of the three series of transition metals. We have arbitrarily normalized to Slater's curve by taking Fe(α) as on the curve and allowed for the splitting of the d-band in the ferromagnetics. It will be seen that not only for the first (3d) transition series, but also for the 4d and 5d series there are clear indications that the density of states, $N(E^*)$, at the Fermi level show two distinct maxima, one at the top of the band at $n_v \approx 10$ and the other at $n_v \approx 5$. The shaded path on the plot indicates the possible region in which the $N(E^*)$ values for the other, as yet unmeasured, transition metals may fall. The existance of such maxima at $n_v = 10$ and 5 (and at 3 and 7 also) is also evident from the paramagnetic susceptibility data [94]. It should be added parenthetically

here that the very high value of γ for Mn (at $n_v = 7$) has not been included in the plot of Fig. 4, as it is considered unreliable, due to the very high temperature (liquid hydrogen temperatures) of measurement. It is possible, however, as is discussed below, that there may yet be a third maximum at $n_v \approx 7$. Of course it is not possible to interpret the results presented in Fig. 4 as giving the overall band shape, since this must change not only in going from one crystal structure to another along each series but also in going from one series to another. Moreover it is possible that there may be band splitting, as for example in antiferromagnetism, for the elements near the centre of each series. However the marked regularities in the experimental results evident in Fig. 4 may indicate a possibility of explaining some general features of the band structures of these metals.

The low minimum for $N(E^*)$ at $n_v \approx 6$ is noteworthy, particularly as the observed γ value for W is about one half the theoretical estimate [85]. It has been suggested by Friedberg, Estermann and Goldman [39] that the very low γ value in Cr, also at $n_v = 6$, observed by them is due to effects of antiferromagnetism, which Zener [89] previously suggested should occur in Cr and which was observed by Shull and Wilkinson [90] using neutron diffraction methods with a Neel temperature of about 425°K. In an antiferromagnetic, as in a ferromagnetic, the d-band is split into a filled half and an unfilled half for electrons of opposite spins, a feature recently noted by Slater [84a]. In consequence the filled half does not contribute to the electronic specific heat and the total contribution, now from the unfilled half only, would be smaller than for a similar non-antiferromagnetic. Although this explanation for the small γ value in Cr is an interesting one, it may not be applicable to the other transition metals with $n_v=6$, namely W and Mo, although these also have relatively small γ values. Its probable in-applicability is based on the fact that W and Mo have not any observable antiferromagnetic properties, although such were sought for by Shull and Wilkinson (*loc. cit.*) to temperatures as low as 20°K.* It is possible therefore that there may be a deep minimum in the d-bands for the three transition series at about $n_v \approx 6$ and this may account for the low γ values in Mo, Cr and W. Support for this view comes from consideration of the temperature dependence of the paramagnetic susceptibility.

* It is possible however for antiferromagnetism to escape observation by this method if the exchange frequency is high compared with the reciprocal of the time of flight of the neutrons between atoms.

The temperature dependence of the paramagnetic susceptibility of a degenerate electronic system is given by:

$$\chi = \chi_o (1 + \alpha T^2)$$
$$\alpha = A \left[\frac{\partial^2 ln\, N(E)}{\partial E^2} \right]_{E=E^*} \tag{10}$$

where A is a positive constant.

For the usual forms of the $N(E)$ versus curves, e.g. $N(E) \propto E^z$ (z positive), α is negative and hence the magnetic susceptibility diminishes with rising temperature. Such a behavior occurs in a free electron gas, ($z = \frac{1}{2}$). However, if E^* is close to or at a minimum in the $N(E)$ versus E curve, α can be positive and hence the magnetic susceptibility can increase with increasing temperature. Attention to this fact has recently been drawn by Kriessman [91] and he has measured the temperature dependence of the paramagnetic susceptibility of many transition metals. In Table 5 the sign of α is set out for the three

TABLE 5

The sign of the temperature coefficient of the paramagnetic susceptibility of the transition metals

n_v	4	5	6	7
Metal	Ti	V	Cr	Mn
Sign.	+	—	+	—
Metal	Zr	Nb	Mo	Tc
Sign.	+	—	+	—
Metal	Hf	Ta	W	Re
Sign.	+	—	+	—

series of transition metals. The data for this largely comes from Kriessman, except that more recent information concerning α comes from the work of Nelson [92] for Tc and Re and of McGuire for Hf.* The table shows a regular alternation of positive and negative values of α as one goes along each series. Moreover the positive values correspond to those metals with low γ values, and the negative values to those with high γ values. (cf Table 3 and Fig. 4). This suggests that the sign of α is determined, as in Eq. (10), by the shape of the d-band and supports the contention that the low γ values at $n_v = 4$, (Ti and Zr), and at $n_v = 6$, (Mo, Cr and W), are due to real minima existing in the d-band structure.

The negative values of α at $n_v = 7$ suggest that possibly there may

* I am indebted to Drs Nelson and McGuire for informing me of their results prior to publication.

be another maximum here and gives further interest in obtaining reliable γ values for Mn, Tc and Re. The, as yet unreliable, data given in Table 3 for Mn and Tc do show high γ values; but a definitive answer to this question must await further experimental observations. However further information on this point comes from a recent observation by Matthias and Corenzwit [93] who have found a compound of Mo and Ru, having the same crystal structure (hpc) and the same n_v value as Tc, to be superconducting with T_c about 10°K. This result, combined with Daunt and Cobble's [65] on pure T_c and combined with Daunt's correlation [53] associating high T_c values with high γ values, lends further support to the belief in a maximum in the $N(E^*)$ values at $n_v \approx 7$. It is of interest to note here parenthetically that Matthias (*loc. cit.*) finds no compounds with $n_v \approx 6$ to be superconducting (Note. Cr, Mo and W also are non-superconducting) and that the pure metals with $n_v = 6$ are also those, excluding those of Group 8, which have an abnormally high contribution to their paramagnetic susceptibilities from interaction forces. (See Stoner's [94] Table 3, in which however in the light of recent measurements [76] the Θ'/q value for W should be 29100 and that for Mo 8690). This may well be a further reflection of the well-known fact, discussed some time ago by Mendelssohn and Daunt [95], that strong magnetic interactions inhibit the appearance of superconductivity.

8. Possible Influence of Inter-electronic Interactions

The theoretical background leading to the equations quoted in section 1 for the electronic specific heat omitted any treatment of the possible effects of exchange interaction on the energy of the electrons. Such an omission seems inconsistent with the usual inclusion of exchange terms in the treatment of cohesion and ferromagnetism. However when such terms are included it is found theoretically that the electronic specific heat is greatly reduced and no longer shows the linear temperature dependence which is characteristically observed in all metals. Theoretical computations of c_e in the presence of exchange interaction have successfully been carried out by Bardeen [96] Wohlfarth [97] and Lidiard [98]; and Wohlfarth has shown, for example, that:

$$c_e = \gamma T/(a - b \ln T) \tag{11}$$

where a and b are positive constants, and γ has its previous significance. For Na at liquid helium temperatures, for example, Wohlfarth

estimated that marked deviation sfrom the linear function of T should occur and that c_e should be about 9 times smaller than the Sommerfeld value. Similar results were obtained by the other workers, all stressing the great reduction in the absolute value of c_e due to the exchange forces.

In fact, as is evident from Tables 1 and 2, the observed γ values for the metals of Groups 1 to 4 all lie relatively near (within about a factor of 2) the Sommerfeld values and even the transition metals, which yield very high rather than very low γ values in general, show no indication of deviation from the linear law of temperature dependence. In order to see if a further reduction of temperature well below 1°K would show up deviations from this linear law, Nicol and Tseng [99] carried out observations on the heat conductivity of pure Cu down to 0.25°K. The heat conductivity rather than the specific heat was measured at this time for reasons of technical simplicity. However, since at these low temperatures the heat conductivity in Cu is electronic and limited by impurity scattering only, the heat conductivity and specific heat are linearly proportional to one another. The relation between heat conductivity and temperature was found to be strictly linear between 0.25°K and 4°K, indicating no deviation from the linear law for the electronic specific heats.

This conclusion has been verified by recent direct calorimetric measurements down to 0.2°K by Rayne [102] on six metals. His observed γ values are in fair agreement with those given in Tables 1 and 3 above and are as follows: (the number in parenthesis following each element denotes his observed γ value $\times$ 10^4 cal/mole-deg^2), Cu (1.73); Ag (1.60); Mo (5.25); Pd (25.6); W (3.53); Pt (16.5).

The suggestion has been put forward by Wigner [100] that the inclusion of the effects of correlation forces would result in an increase in the density of states and so increase the value of c_e. Furthermore he suggested that this increase was sufficient to compensate approximately for the decrease due to exchange interaction. The computation of the effects of correlation, which demands assessing the effects on the initial wave function of the interelectronic distances, is clearly much more complex than the usual one-electron approximations used in the other computations, as is shown by the original work of Wigner [101]. However recently Pines [105] has applied to the problem of electrons in metals a new collective description which describes the long range correlations in electronic positions in terms of the collective oscillations of the system as a whole, which general method was developed by Bohm and Pines[106].

He has found that at least for the alkali metals the effects of exchange terms and correlation terms do cancel approximately as far as the specific heat evaluation is concerned, leaving γ values approximately the same as the free electron values. It may be inferred therefore that the experimental electronic specific heat data on more complex elements can probably be explained in the same way by an approximate cancelation of these correction terms as was suggested by Wigner. It is of interest to note that when similar corrections are made to the free electron evaluation of the electronic paramagnetic susceptibility, it is found by Pines [107] that there is *not* a similar cancelation. Pines showed, again for the alkali metals, that the contribution to the susceptibility due to exchange interaction is greater than that due to correlation forces and hence one may expect the susceptibilities to be larger than those obtained on the free electron model. This result is in good agreement with experiment [108] and confirms at least qualitatively the considerations put forward by Mott and Jones [80] in their explanation of the high paramagnetic susceptibilities of the transition elements, particularly of Pd and Pt.

REFERENCES

[1] A. Sommerfeld, Z.f. Phys. **47,** 1, (1928).
[1a] A. Sommerfeld, Ann. d. Physik, **28,** 1 (1937).
[2] F. Bloch, Z.f. Phys, **52.,** 555 (1928).
[3] A. Sommerfeld and H. Bethe, Handb. d. Phys., **24/2,** 430 (1933).
[4] F. Seitz, "Modern Theory of Solids", McGraw Hill, NYC, (1940).
[5] N. F. Mott, Proc. Phys. Soc., **47,** 571, (1935); Proc. Roy. Soc. A, **152,** 42, (1936).
[6] A. A. Silvidi and J. G. Daunt, Phys. Rev., **77,** 125 (1950).
[7] M. Horowitz, A. A. Silvidi, S. F. Malaker and J. G. Daunt, Phys. Rev., **88,** 1182 (1952).
[8] M. Blackman, Proc. Roy. Soc. A, **159,** 416 (1937).
[9] M. Blackman, Rep. Progr. Phys., **8,** 11 (1941).
[10] P. Debye, Ann. d. Physik, **39,** 789 (1912).
[11] F. E. Simon, S. B. preuss. Akad. Wiss., **33,** 471 (1926).
[12] F. E. Simon, Ergebn. exakt. Naturw., **9,** 222 (1930).
[13] F. E. Simon and R. C. Swain, Z. phys. Chem., B**28,** 189 (1935).
[13a] W. Schottky, Phys. Zeit., **22,** 1, (1921); *ibid.* **23,** 9 and 448 (1922).
[14] F. E. Simon and W. Zeidler, Z. phys. Chem., **123,** 383 (1926).
[15] R. W. Hill and P. L. Smith, Phil. Mag., **44,** 636 (1953).
[16] N. Pearlman and P. H. Keesom, Phys. Rev., **88,** 398 (1952).
[17] R. W. Hill and D. H. Parkinson, Phil. Mag., **43,** 309 (1952).
[18] I. Estermann and J. R. Weertmann, J. Chem. Phys., **20,** 972 (1952).
[19] K. S. Pitzer, J. Chem. Phys., **6,** 68 (1938).
[20] W. DeSorbo, J. Chem. Phys., **21,** 876, (1953).
[21] R. Berman and J. Poulter, J. Chem. Phys., **21,** 876 (1953).
[22] M. Born and T. von Karman, Phys. Zeit., **13,** 297 (1912); *ibid.* **14,** 15 (1913).
[23] M. Blackman, Proc. Roy. Soc. A, **148,** 365 and 384 (1935); *ibid.* **149,** 117 and

128 (1935); *ibid.* **159,** 431, (1937). See also Proc. Phys. Soc., **54,** 377 (1942).
[24] For simple cubic lattices see [23] and W. V. Houston, Rev. Mod. Phys., **20,** 165 (1948). For NaCl see E. W. Kellerman, Proc. Roy. Soc. A, **178,** 23 (1941). For bcc lattices see J. Fine, Phys. Rev., **56,** 355 (1939) and E. Bauer, Phys. Rev., **92,** 58, (1953) and J. de Launay, J. Chem. Phys., **21,** 1975 (1953). For fcc lattices see [26] and J. de Launay, (*loc. cit.*) and for diamond see [25].
[25] H. M. J. Smith, Phil. Trans. Roy. Soc., **241,** 130 (1948).
[26] R. B. Leighton, Rev. Mod. Phys., **20,** 165, (1948).
[27] D. H. Parkinson, F. E. Simon and F. H. Spedding, Proc. Roy. Soc. A, **207,** 137 (1951).
[28] G. L. Pickard and F. E. Simon, Proc. Phys. Soc., **61,** 1 (1948).
[29] S. Cristescu and F. Simon, Z. phys. Chem., B**25,** 273 (1952).
[30] W. H. Meissner and R. Ochsenfeld, Naturwiss., **21,** 787 (1933).
[31] T. C. Keeley and K. Mendelssohn, Proc. Roy. Soc. A, **154,** 378 (1936).
[32] K. Mendelssohn, J. G. Daunt and R. B. Pontius, Proc. VII. Intern. Congr. Refrig., **1,** 445 (1936).
[33] C. J. Gorter and H. B. G. Casimir, Physica, **1,** 306 (1933).
[34] J. G. Daunt, A. Horseman and K. Mendelssohn, Phil. Mag., **27,** 764 (1939).
[35] W. Tuyn, Thesis, Leiden, 1924.
[35a] W. Tuyn and H. Kamerlingh Onnes, J. Franklin Inst. **201,** 379 (1926); Leiden Comm. 174a.
[35b] J. A. Kok, Physica, **1,** 1103 (1934).
[36] E. Maxwell and O. S. Lutes, U. S. Natl. Bur. Stand. Reprt., 3146, Feb. 1954.
[37] J. R. Clement, Phys. Rev., **92,** 1578 (1953).
[38] W. H. Keesom and J. A. Kok, Physica, **3,** 1035 (1936).
[39] Friedberg, Estermann and Goldman, Phys. Rev., **85,** 375 (1952); *ibid.* **87,** 582 (1952).
[40] W. H. Keesom and J. A. Kok, Physica, **1,** 770 (1934).
[41] P. H. Keesom and N. Pearlman, Phys. Rev., **88,** 141 (1952).
[42] K. Clusius and J. V. Vaughen, J. Amer. Chem. Soc., **52,** 4686 (1930).
[43] L. D. Armstrong and H. Grayson-Smith, Can. J. Res., **27,** 9 (1947).
[44] B. N. Samoilov, Dok. Akad. Nauk. SSSR., **86,** 281 (1952).
[45] W. H. Keesom and J. N. van den Ende, Proc. Amst. Akad. Sci., **35,** 143 (1932).
[46] J. A. Kok and W. H. Keesom, Physica, **4,** 835 (1937).
[47] J. R. Clement and E. H. Quinnell, Phys. Rev., **79,** 1028 (1950).
[48] J. R. Clement and E. H. Quinnell, Phys. Rev., **92,** 258 (1952).
[49] W. H. Keesom and P. H. van Laer, Physica, **5,** 193 (1938).
[50] B. B. Goodman and E. Mendoza, Phil. Mag., **42,** 594, (1951).
[51] T. S. Smith and J. G. Daunt, Phys. Rev., **88,** 1172, (1952).
[52] J. G. Daunt and C. V. Heer, Phys. Rev., **76,** 1324 (1949).
[53] J. G. Daunt, Phys. Rev., **80,** 911 (1950).
[54] D. Shoenberg, Proc. Camb. Phil. Soc., **36,** 84 (1940).
[55] A. D. Misener, Proc. Roy. Soc. A., **174,** 262 (1940).
[56] J. W. Stout and L. Guttman, Phys. Rev., **88,** 703 (1952).
[57] J. G. Daunt and K. Mendelssohn, Proc. Roy. Soc. A., **160,** 127 (1937).
[58] J. M. Lock, A. B. Pippard and D. Shoenberg, Proc. Camb. Phil. Soc., **47,** 811 (1951).
[59] B. Serin, C. A. Reynolds and A. Lohman, Phys. Rev., **86,** 162 (1952); and private communication from Dr. B. Serin.
[60] E. Maxwell, Phys. Rev., **86,** 235 (1952).
[61] C. A. Reynolds, B. Serin and L. B. Nesbitt, Phys. Rev., **84,** 691 (1951); and private communication from Dr. B. Serin.

[62] T. S. Smith, W. B. Gager and J. G. Daunt, Phys. Rev., **89**, 654 (1953).
[63] A. Wexler and W. S. Corak, Phys., Rev. **85**, 85 (1952).
[64] D. B. Cook, M. W. Zemansky and H. A. Boorse, Phys. Rev., **80**, 737 (1950).
[65] J. G. Daunt and J. W. Cobble, Phys. Rev., **92**, 507 (1953).
[66] B. B. Goodman, Nature, **167**, 111 (1951).
[67] J. G. Daunt and T. S. Smith, Phys. Rev., **88**, 309 (1952).
[68] R. D. Worley, M. W. Zemansky and H. A. Boorse, Phys. Rev., **87**, 1142 (1952).
[69] Elson, H. Grayson-Smith and J. O. Wilhelm, Can. J. Res. A., **27**, 9 (1940).
[70] G. Duyckaerts, Physica, **6**, 401 (1939).
[71] W. H. Keesom and B. Kurrelmeyer, Physica, **6**, 663 (1939).
[72] G. Duyckaerts, Physica, **6**, 817 (1939).
[73] W. H. Keesom and C. W. Clark, Physica, **2**, 513 (1935).
[74] A. Brown, M. W. Zemansky and H. A. Boorse, Phys. Rev., **86**, 134 (1952).
[75] A. Brown, M. W. Zemansky and H. A. Boorse, Phys. Rev., **92**, 52 (1953).
[76] M. Horowitz and J. G. Daunt, Phys. Rev., **91**, 1099 (1953).
[77] W. H. Keesom and J. A. Kok, Physica, **1**, 595 (1934).
[77a] G. L. Pickard, Nature, **138**, 123 (1936).
[78] W. H. Keesom and M. C. Desirant, Physica, **8**, 273 (1941).
[79] C. A. Shiffman, "The heat capacities of the elements below room temperature", Pub. G. E. Schenectady, N.Y., (1952).
[80] N. F. Mott and H. Jones, "The Theory of the Properties of Metals and Alloys", Oxford Univ. Press., London, (1936).
[81] N. F. Mott, Phil. Mag., **44**, 187 (1953).
[82] W. Hume-Rothery and B. R. Coles, Phil. Mag. Suppl., **3**, 177 (1954).
[83] H. M. Krutter, Phys. Rev., **48**, 664 (1935).
[84] J. C. Slater, Phys. Rev., **49**, 537 (1936).
[84a] J. C. Slater, Phys. Rev., **82**, 538 (1951).
[85] M. F. Manning and M. I. Chodorow, Phys. Rev., **56**, 787 (1939).
[86] M. F. Manning, Phys. Rev., **63**, 190 (1943).
[87] G. C. Fletcher and E. P. Wohlfarth, Phil. Mag., **42**, 106 (1951).
[88] G. C. Fletcher, Proc. Phys. Soc. A., **65**, 192 (1951).
[89] C. Zener, Phys. Rev., **81**, 440 (1951).
[90] C. G. Shull and M. K. Wilkinson, Phys. Rev., **86**, 599 (1952).
[91] C. J. Kriessman, Rev. Mod. Phys., **25**, 122 (1953).
[92] C. M. Nelson, Ph. D. Dissertation, Univ. of Tenn., (1952).
[93] B. T. Matthias and E. Corenzwit, Phys. Rev., **94**, 1069 (1954).
[94] E. C. Stoner, Acta Metullurgica, **2**, 259 (1954).
[95] K. Mendelssohn and J. G. Daunt, Nature, **139**, 473 (1937).
[96] J. Bardeen, Phys. Rev., **50**, 1098 (1936).
[97] E. P. Wohlfarth, Phil. Mag., **41**, 534, (1950).
[98] A. B. Lidiard, Phil. Mag., **42**, 1325 (1951).
[99] J. Nicol and T. P. Tseng, Phys. Rev., **92**, 1062 (1953).
[100] E. Wigner, Trans. Faraday Soc., **34**, 678 (1938).
[101] E. Wigner, Phys. Rev., **46**, 1002 (1934).
[102] J. Rayne, Phys. Rev., **95**, 1428 (1954).
[103] B. T. Matthias, Phys. Rev., **92**, 874 (1953).
[104] Matthias, Corenzwit and Miller, Phys. Rev., **93**, 1415 (1954).
[105] D. Pines, Phys. Rev., **92**, 626 (1953).
[106] D. Bohm and D. Pines, Phys. Rev., **92**, 609 (1953).
[107] D. Pines, Phys. Rev., **95**, 1090 (1954).
[108] Schumacher, Carver and Slichter, Phys. Rev., **95**, 1089 (1954).

CHAPTER XII

PARAMAGNETIC CRYSTALS IN USE FOR LOW TEMPERATURE RESEARCH

BY

A. H. COOKE

CLARENDON LABORATORY, OXFORD

1. Introduction

Though paramagnetic salts have been studied at low temperatures for many years, interest in them was greatly stimulated by the suggestion of Debye [1] and Giauque [2] that temperatures very much below 1°K could be reached by the adiabatic demagnetization of suitable paramagnetic salts. In the years following the first successful experiments by this method by de Haas, Wiersma and Kramers [3], and by Giauque and MacDougall [4], attention centred on a small number of salts, notably gadolinium sulphate, chromium potassium alum, ferric ammonium alum, and manganous ammonium sulphate. Recently however our knowledge of paramagnetics has been greatly increased by the development of the paramagnetic relaxation method of measuring their specific heats, and still more by the very powerful paramagnetic resonance method of investigation, by which a spectroscopic technique is applied to the study of paramagnetism. As a result we have now a rather detailed knowledge, not only of the substances mentioned above, but also of a wide range of others. In this chapter we propose to review this new information, and especially to consider the light it throws on salts useful for demagnetization work.

From this point of view we are interested in salts which at the

lowest temperatures attainable by the evaporation of liquid helium possess a considerable entropy, which can be reduced by an isothermal magnetization; that is, they behave like an assembly of weakly interacting magnetic dipoles, whose orientation in the absence of a magnetic field is completely random. As is well known, the magnetic moment M of such an assembly in a field H at a temperature T is a function of H/T and in weak fields the magnetic susceptibility $\chi = M/H$ is inversely proportional to the temperature (Curie's law). Susceptibility measurements show that there are many salts of elements of the iron and rare earth transition groups whose susceptibilities in the helium range of temperatures (4.2°K to 1°K) closely follow Curie's law. If the extraction of entropy were the only consideration, the best of them would be the one having the highest susceptibility, since the rate of extraction of entropy S is given by $(\partial S/\partial H)_T = (\partial M/\partial T)_H$. It was on this ground that Giauque and MacDougall selected gadolinium sulphate for their first experiments. However at temperatures below 1°K the specific heat of a paramagnetic salt is principally due to the anomaly arising from interaction of the magnetic ions with their surroundings and one another, the lattice specific heat being negligible in comparison. For gadolinium sulphate this magnetic specific heat is particularly large. While in one respect this is an advantage, in that the temperature rises comparatively slowly after demagnetization, lower temperatures may be reached by using a salt of lower specific heat, such as chrome alum, even though the susceptibility is smaller. We shall assume that the maximum of this specific heat anomaly lies at a temperature well below 1°K, so that at temperatures above 1°K its contribution to the specific heat is given by $c = b/T^2$ in zero magnetic field. We also assume that the susceptibility at temperatures above 1°K obeys a Curie-Weiss law $\chi = C/(T - \Theta)$, where the Curie constant C and the Weiss constant Θ may depend on the inclination of the magnetic field to the crystal axes. The magnetic properties can then be expressed in terms of the constants C, Θ, and b. Essentially this implies that the magnetic ions of the salt are in a ground state which to a first approximation can be considered completely degenerate. The Curie constant C then depends on the nature of this ground state. In higher approximation, interaction effects split the ground state by energy differences which are small compared with thermal energies at 1°K. The specific heat constant b and the Weiss constant Θ are determined by these interactions.

2. Energy Levels of a Magnetic Ion

The ground state of a free magnetic ion is characterized by the quantum numbers L, S, and J. This $(2J + 1)$-fold degenerate state is the lowest state of the multiplet formed by the L and S vectors. In a crystal however the ion is not free, but is subject to the electric field due to the other constituents of the crystal. If the ion is in an S state, for example Fe^{+++} or Mn^{++}, whose ground state is ^6S, or Gd^{+++}, whose ground state is ^8S, it is not altered by the crystalline electric field, as there is no direct interaction between the electric field and the spin, but if the ground state has orbital momentum the Stark effect of the electric field produces a re-arrangement of the energy levels of the multiplet. In salts of the iron group this effect is so great as to disturb the spin-orbit coupling, so that the vector $\boldsymbol{J}$ never appears. The orbital energy levels are split by energy differences of the order 10^3 to 10^4 cm^{-1}, so that at ordinary temperatures only a single orbital level is populated and there remains a $(2S + 1)$-fold degeneracy due to the spin. There results the well-known 'spin-only' paramagnetism of the iron group salts. The susceptibility is given by

$$\chi = Ng^2 \beta^2 S(S + 1)/3kT = C/T \qquad (1)$$

where χ is the molar susceptibility, N is Avogadro's number, β is the Bohr magneton, k is Boltzmann's constant, and S is the spin of the ground state of the free ion. The spectroscopic splitting factor g has a value close to 2, the free spin value, but may be modified by perturbations due to higher orbital levels.[5] This situation was clearly established by susceptibility measurements, which could be interpreted in terms of the magnetic moment of the single populated level.[6] Recent work has not altered this picture, though some details have been filled in. The values of g have been determined very accurately by paramagnetic resonance [7], and the anomalous behaviour of cobaltous salts has been accounted for.[8]

The rare earths present a more complicated problem than the iron group. The Stark effect ofthe crystalline field is insufficient to disturb the spin-orbit coupling, but splits the $(2J + 1)$-fold ground state of the free ion into a number of sub-states, with energy differences of the order of 100 cm^{-1}. At room temperature sufficient of these levels are populated to give a magnetic susceptibility comparable with the 'free ion' value, but Curie's law is not obeyed, since the effective magnetic moment of the ion changes as the temperature is lowered

and fewer levels are populated. In this situation paramagnetic resonance measurements have been especially valuable in determining the magnetic properties of the different levels, which could not be distinguished by susceptibility measurements alone.

An important limitation on the Stark splitting is imposed by Kramers' theorem [9], that for an ion having an odd number of electrons (half-integral spin) there must remain at least a two-fold degeneracy of the energy levels, which can be raised only by an applied magnetic field. On the other hand if the ion has an even number of electrons the crystalline electric field may (and according to a theorem of Jahn and Teller [10] will) completely resolve the degeneracy. Since a singlet level can have no paramagnetic properties, it follows that at low temperatures where only the lowest level is populated, salts of ions having an odd number of electrons generally approximate much more closely to ideal paramagnetics. Confining our attention to this class of salt, the magnetic properties at low temperatures will be due to the Kramers doublet (apart from temperature-independent susceptibility due to second order effects of the higher levels). The magnetic moment and entropy of the salt in a magnetic field can be calculated from the Brillouin function for a doublet state $S = 1/2$. The magnetic susceptibility is given by eqn (1), putting $S = 1/2$ to fit the multiplicity of the state, taking account of the anisotropy of the susceptibility by the variation of g with the direction of the magnetic field relative to the crystal axes; that is, g is regarded as a tensor. Usually the electric field at the ion has an axis of symmetry. The g-tensor then transforms according to the equation

$$g^2 = g_{\parallel}^2 \cos^2 \Theta + g_{\perp}^2 \sin^2 \Theta, \tag{2}$$

where Θ is the angle between the magnetic field and the symmetry axis, and $g_{\parallel}$ and $g_{\perp}$ are the values of g with the field respectively parallel and perpendicular to the axis. The g-values may be highly anisotropic. For example the ground state of the free Ce^{+++} ion has $J = 5/2$, and so is sixfold degenerate, with a Landé factor $g_L = 6/7$. Suppose a crystalline electric field splits this into three doublets, characterized by the component of angular momentum along the crystal axis, i.e. $J_z = \pm 1/2$, $J_z = \pm 3/2$, and $J_z = \pm 5/2$. Then it can be shown that $g_{\parallel} = g_L$ and $g_{\perp} = 3g_L$ for the doublet $J_z = \pm 1/2$; $g_{\parallel} = 3g_L$ and $g_{\perp} = 0$ for the doublet $J_z = \pm 3/2$; and $g_{\parallel} = 5g_L$ and $g_{\perp} = 0$ for the doublet $J_z = \pm 5/2$. If say the $J_z = \pm 5/2$ doublet

were the lowest in energy, the susceptibility at low temperatures would be completely anisotropic. The high g-value parallel to the axis arises because the description of each doublet as a state with $S = 1/2$, ascribes too little angular momentum to the $\pm 3/2$ and $\pm 5/2$ states; on the other hand a field perpendicular to the axis cannot split the doublets $J_z = \pm 5/2$ and $J_z = \pm 3/2$, giving $g = 0$ in this direction. While the above example is of course oversimplified, it affords some approximation to the action of the crystalline field in cerium ethylsulphate. The lowest level in this salt is a Kramers doublet with $g_{\parallel} = 3.72$ and $g_{\perp} = 0.2$, which may be compared with 4.3 and 0 for a pure $J_z = \pm 5/2$ state, while the first excited level has $g_{\parallel} = 0.95$ and $g_{\perp} = 2.18$, compared with 0.86 and 2.57 for a pure $J_z = \pm 1/2$ state. [11] At low temperatures the magnetic susceptibility parallel to the crystal axis is over a hundred times greater than perpendicular to the axis. The behaviour of other rare earth salts may be analysed in a similar way.

3. Interactions Splitting the Ground State

3.1. STARK EFFECT

Having established what is the ground state of the ion in the crystal, we must next consider how its magnetic properties are modified by the raising of its degeneracy by Stark effect, by nuclear effects, and by interactions with other paramagnetic ions. If the ground state is a doublet, the Stark effect can produce no further splitting, and therefore no contribution to the specific heat or departure from Curie's law. If however the ground state has fourfold (e.g. Cr^{+++}), sixfold (e.g. Fe^{+++}, Mn^{++}), or eightfold spin degeneracy (Gd^{+++}), it will be split into a number of doublets, of very small separation in energy, generally about 0.1 cm^{-1}.

In most of the salts used in demagnetization work the paramagnetic ion is surrounded by six oxygen atoms, producing an electric field at the ion of approximately cubic symmetry, but with a small component of tetragonal or trigonal symmetry. Van Vleck and Penney [12] showed that a six-fold spin degeneracy could be raised by a field of cubic symmetry, but that a fifth order perturbation is required. Abragam and Pryce [13] remarked that in a field of tetragonal or trigonal symmetry the energy of interaction between the spins comprising S would depend on the orientation of S relative to the axis of symmetry. Since this involves a lower order perturbation, this effect may be the

more important even when the departure from cubic symmetry is small. The energy of the different states of the multiplet is then given by

$$W = D\,[S_z^2 - \tfrac{1}{3}\,S\,(S+1)] \tag{3}$$

where D is a constant and S_z is the component of S along the symmetry axis. This splitting gives rise to a Schottky anomaly in the specific heat, whose maximum lies below 1°K, at a temperature of the order of D/k. When $D/kT << 1$, its contribution to the specific heat c is given by [14]

$$c/R = D^2\,S(S+1)\,(2S-1)\,(2S+3)/45\,k^2\,T^2. \tag{4}$$

Gorter [15] has pointed out that any departure from Curie's law expressible as a power series in $1/T$ may be represented to a first approximation by a Curie-Weiss law for the susceptibility. Van Vleck and Penney showed that for a powdered specimen, or for a crystal of cubic symmetry such as the alums, the Stark splitting neither changes the Curie constant nor introduces a Weiss constant. For a single crystal in which all the ions have the same symmetry axis the form of splitting given above results in a Weiss constant parallel to the crystal axis $\Theta_{\parallel} = -D\,(2S-1)\,(2S+3)/15k$, and a Weiss constant perpendicular to the axis $\Theta_{\perp} = D\,(2S-1)\,(2S+3)/30k$. If the crystal has more than one ion per unit cell, with different symmetry axes, the Weiss constants are obtained by averaging over the different classes of ion. The effect may be used to determine the sign of D. It will be seen that for a powdered specimen the Weiss constant averages to zero, in agreement with the general result of Van Vleck and Penney.

3.2 NUCLEAR EFFECTS

If the nucleus of the paramagnetic ion possesses a spin I there will be a hyperfine splitting of the ground state on account of interaction between the nucleus and the electronic shell. The most important effect is magnetic interaction between the nuclear and electronic magnetic moments. The splitting of the electronic energy levels from this effect can be represented to a fair approximation by an interaction energy $S.A.I$, where A is a tensor transforming in a similar way to the g-tensor. If as is usual we have axial symmetry, we can write $A_z = A$, $A_x = A_y = B$, and the interaction energy is given by

$$\mathfrak{H} = AS_zI_z + B(S_xI_x + S_yI_y) \tag{5}$$

The constants A and B are determined very directly by paramagnetic resonance experiments. Bleaney has shown that this splitting produces a Schottky anomaly in the specific heat, whose maximum lies well below 1°K. At high temperatures ($A^2 + 2\,B^2 << k\,T^2$) the contribution to the specific heat is

$$c/R = (A^2 + 2\,B^2)S\,(S + 1)\,I\,(I + 1)/9\,k^2\,T^2. \tag{6}$$

The specific heat of some rare earth salts arises chiefly from this effect[16].

The second effect which may occur is the interaction of the electric quadrupole moment of the nucleus with the gradient of the electric field at the nucleus produced by the electronic shell. The splitting of the electronic energy levels may be represented by $P[(I_z^2 - \frac{1}{3}\,I\,(I + 1)]$, and its contribution to the specific heat is

$$c/R = P^2I(I + 1)\,(2\,I - 1)\,(2\,I + 3)/45\,k^2\,T^2. \tag{7}$$

This effect is generally small compared with that due to nuclear magnetic interaction.

The nuclear magnetic interaction has a very small effect on the magnetic susceptibility. Even for a single crystal it has no effect on the Curie constant, and introduces no Weiss constant. For $S = \frac{1}{2}$, its effect in a direction Ox is given by

$$\chi_x = \frac{C}{T}\,[1 - (A_y^2 + A_z^2)\,I\,(I + 1)/36\,k^2T^2], \tag{8}$$

where C is given by eqn (1).

Since this correction seldom exceeds $10^{-4}/T^2$, we shall not consider it further, nor do we consider the effect of the quadrupole splitting on the susceptibility.

3.3 MAGNETIC AND EXCHANGE INTERACTION

Besides these effects which split the energy levels of the individual ions, there are the interactions of the magnetic ions with one another. In anhydrous salts, in which the magnetic ions are relatively close together, these interactions may strongly affect the susceptibility at temperatures of 10°K. or higher. Hydrated salts, in which the ions are 6 to 8 Å apart, are used for demagnetization work, the alums or Tutton salts for the iron group, and the hydrated sulphates or ethyl sulphates for the rare earth group. In such salts the magnetic field at any one

ion due to its neighbours is of the order of a few hundred oersted, giving an interaction energy of a few hundredths of a degree. At temperatures of this order there will be an ordering of the magnetic ions, with a consequent anomaly of the co-operative type in the specific heat. Van Vleck [17] expressed the partition function due to interaction as a power series in $1/T$, and calculated the first few terms. Of the two types of interaction to be considered, magnetic dipole interaction is well understood, but the quantum-mechanical exchange interaction still presents a difficult problem. Van Vleck considered salts whose ions have isotropic magnetic properties, for example salts of Mn^{++}, Fe^{+++}, Cr^{+++}, and Gd^{+++}. For such salts the contribution of magnetic interaction to the specific heat at high temperatures may conveniently be expressed as

$$c/R = f\,\lambda^2/T^2. \tag{9}$$

Here λ is the Curie constant for the susceptibility per unit volume, and f is a factor dependent on the lattice arrangement of the magnetic ions, for example 21.6 for the alums, and 26.5 for the Tutton salts. The calculation may be extended to anisotropic materials [18].

The effect of magnetic dipole interaction on the magnetic susceptibility was first considered by Lorentz [19], who showed that for an isotropic material in which the dipoles are arranged either at random, or on a simple cubic lattice, the interaction may be represented as an internal field in the direction of magnetization, equal to $4\pi I/3$, where I is the intensity of magnetization per unit volume. For a spherical specimen this internal field exactly cancels the demagnetizing field. The magnetic moment of such a specimen is then unaffected by magnetic interaction. Van Vleck's calculation, which gives the susceptibility as a power series in $1/T$, agrees with the Lorentz formula as far as $1/T^2$, as does a refinement of the internal field theory due to Onsager [20]. All three calculations then agree that the effective susceptibility of a spherical specimen of an isotropic material will obey Curie's law down to very low temperatures, departures due to magnetic interaction becoming appreciable only when the volume susceptibility is comparable with unity. Daniels has pointed out that this is not necessarily true for an anisotropic material, even if powdered, but in practice the corrections involved are very small.

In most detailed applications of the theory to particular salts [21] it has been assumed that in magnetically dilute salts such as the alums

and Tutton salts exchange effects are negligible on account of the great distances separating the magnetic ions. Experimental evidence for this view was afforded by the very small Weiss constants in the susceptibilities of these salts. It was shown by de Klerk [22] however that exchange effects may be comparable in magnitude with magnetic interaction. The simplest representation of exchange interaction is to suppose that two magnetic ions, of magnetic moments μ_i and μ_j have an energy of interaction $-B\mu_i.\mu_j$, where the constant B, (which may be positive or negative), depends only on the distance r separating μ_i and μ_j and not on their orientations relative to r. Further it is supposed that B diminishes so rapidly with distance that only interaction of nearest neighbours need be considered. If there are z of these neighbours, the exchange interaction results in a contribution to the specific heat which at high temperatures is given by

$$c/R = z\, B^2\, g^4\, \beta^4\, S^2\, (S+1)^2/6\, k^2\, T^2. \tag{10}$$

Moreover the specific heat contributions due to exchange and magnetic interactions are additive. The susceptibility is also affected, and at high temperatures follows a Curie-Weiss law, with a Weiss constant Θ, independent of the shape of the specimen, given by $\Theta = z\, B\, g^2\, \beta^2 S\, (S+1)/3\, k$. The Weiss constant and the specific eat contribution are thus related [23]

$$c\, T^2/R = 3\, \Theta^2/2\, z. \tag{11}$$

It would follow from this "isotropic exchange" theory that for a powdered spherical specimen the only effect giving rise to a Weiss constant is exchange interaction. From the Weiss Θ the exchange coupling and its contribution to the specific heat should be calculable. Experiment shows however that this simple picture is not correct. It frequently happens that the susceptibility obeys Curie's law with no detectable Weiss Θ, while the specific heat is much too large to be accounted for by magnetic interaction [24].

The discrepancy arises from the oversimplification in the isotropic exchange theory. If for example the exchange energy between two ions varied with the position of the ions in a manner similar to magnetic dipole interaction:

$$W = -B\, [\mu_i \,.\, \mu_j - 3\, (\mu_i \,.\, \mathbf{r})\, (\mu_j \,.\, \mathbf{r})/r^2], \tag{12}$$

the interaction would contribute to the specific heat without introducing any Weiss Θ in the susceptibility formula [25]. Such interaction

could not be considered independently of the magnetic interaction. The isotropic and dipole-dipole formulae represent extremes between which intermediate cases can arise. Exchange effects will always contribute to the specific heat of the salt, but the Weiss Θ may have any value between zero and the isotropic exchange value. The matter is complicated by the fact that exchange of different signs appears to occur between different kinds of neighbours. Kramers [26] suggested that in magnetically dilute salts exchange effects come about via excited states of intervening diamagnetic atoms. Such indirect exchange would clearly not be isotropic.

4. Methods of Experiment

The chief methods of investigation are the measurement of magnetic susceptibility, the measurement of magnetic contributions to the specific heat of a substance, usually by the paramagnetic relaxation method, and finally the investigation of paramagnetic resonance spectra.

4.1 SUSCEPTIBILITY MEASUREMENTS

Most low temperature measurements of susceptibility have been made by the Faraday method, the vertical force on a specimen in an inhomogeneous field being compared with that on a standard specimen. Of the methods of measuring the force, the simplest is the Sucksmith ring balance [27], in which the specimen is supported from a phosphor-bronze ring which is distorted by the movement of the specimen, the deflexion being magnified optically. The Leiden apparatus [28] uses a common balance, the force on the specimen being balanced by the forces between two coils carrying an electric current. This null method has the advantage over the ring balance that a much greater range of sensitivity is possible, and that the weight of the specimen is readily counterbalanced. The Leiden measurements [29], which cover the principal salts of the iron and rare earth groups, extend in general to 14°K and in some cases to 1.5°K. At temperatures near 1°K demagnetizing effects may be appreciable. It is then desirable to make measurements in a uniform field, the susceptibility being measured for example by its effect on the mutual inductance of a pair of coils surrounding the specimen. An A.C. bridge method of measurement is usually employed, the mutual inductance being balanced against that of a decade mutual inductance system. Suitable bridges for measuring very small mutual

inductances have been described by Casimir, de Haas and de Klerk, [30] and by Erickson, Roberts and Dabbs [31].

Another method which has been applied at Leiden by Becquerel, de Haas and van den Handel [29] is the measurement of the rotation of the plane of polarization of light passing through the crystal parallel to the direction of the magnetic field. To convert the measurements into absolute values of susceptibility either the rotation must be measured at some temperature where the susceptibility has been found by conventional methods, or else the measurements must be carried to fields at which saturation occurs. By fitting the curve of rotation against field to a Brillouin function, the susceptibility can be deduced. This method, which is limited to measurements along the symmetry axis, has been used down to 1.3°K.

4.2 SPECIFIC HEAT MEASUREMENTS

Specific heat measurements have the advantage of giving a direct measure of interaction effects, since in zero magnetic field an ideal paramagnetic would have no specific heat arising from magnetic effects. As has already been shown, the magnetic contributions to the specific heats of paramagnetic salts are of the order $c = R\,\tau^2/T^2$, where τ is the splitting of the ground state due to the interactions divided by Boltzmann's constant k. As we are interested in salts for which τ is a small fraction of a degree, the magnetic contribution to the specific heat will be very small compared with the lattice specific heat of the salt. The difficulty of separating this small contribution is met by the paramagnetic relaxation method of measurement, developed by Gorter [32] and his co-workers. The possibility of applying this to the determination of magnetic contributions to the specific heat was first remarked by Casimir and Du Pré [33]. A thermodynamic relation connects the isothermal and adiabatic susceptibilities of a substance with the specific heat at constant magnetization. (We consider the specific heat at constant magnetization rather than at constant field, since the former is to a first approximation independent of the magnetic field). If a magnetic field is applied to a paramagnetic salt, the energy of the various magnetic dipoles will be changed. It is found [34] that the time for the transfer of the heat of magnetization from the dipoles to the crystal lattice (the "spin-lattice relaxation time") is much longer than the time for the establishment of thermal equilibrium among the dipoles themselves (the "spin-spin relaxation time".) If then the mag-

netic field is varied by a small amount, the period of the oscillation being long compared to the spin-spin relaxation time but short compared to the spin-lattice relaxation time, we can ascribe to the spins, which are always in thermal equilibrium with one another, a temperature which differs from that of the lattice, and in fact oscillates about the lattice temperature. A measurement of variation of magnetic moment then gives the adiabatic susceptibility of the spin system, from which we can calculate the specific heat of the spin system, i.e. the magnetic contributions to the specific heat. The lattice temperature does not vary, and the lattice specific heat does not enter into the result. By this technique it is possible to measure magnetic contributions to the specific heat at liquid air temperatures where they may contribute only 10^{-7} of the total specific heat of the salt. Since the spin-lattice relaxation time is of the order 10^{-6} sec. at these temperatures, the susceptibility must be determined at radio frequencies in order to observe the transition from isothermal to adiabatic conditions. At liquid helium temperatures the spin-lattice time is usually of the order 10^{-3} sec., and measurements at audio frequencies suffice.

A few measurements [35] have been made by direct calorimetry in the helium range.

4.3. PARAMAGNETIC RESONANCE

This method of investigation was discovered only in 1945 [36], but has already given very valuable results, especially in elucidating the part played by nuclear effects. We shall discuss only the principle of the method. A detailed survey has recently been given by Bleaney and Stevens [7, 37].

If we consider a salt whose ions have a doublet ground state, for instance Cu^{++}, the application of a magnetic field H will split the doublet by $g\beta H$, where g is the spectroscopic splitting factor, as in eqn. (1) and eqn. (2). In thermal equilibrium, more ions will be in the lower state of the doublet than the higher. If now a weak oscillatory field of frequency ν is applied perpendicular to H, resonant transitions will be induced between the two states if $h\nu = g\beta H$, and energy will be absorbed from the oscillatory field. By enclosing the crystal in a cavity tuned to the frequency ν, the resonance can be detected by observing the extra damping of the cavity when the magnetic field H is brought to the resonance value. In practice, the resonance is broadened by the interaction field at each ion due to its neighbours, which may amount

to a few hundred oersted. It is therefore necessary to work with an applied field which is large compared with the interaction field. For example, using an oscillatory field of frequency 10^{10}c/sec ($\lambda = 3$ cm), resonance occurs at approximately 3570 oersted, if $g = 2$.

Interaction between the electronic magnetic moment and the nucleus imposes a hyperfine structure on the spectrum.[38] For example examination of say copper potassium sulphate under high resolution shows that the resonance lines each consist of four components, due to the spin of 3/2 of the copper nuclei; under still higher resolution each hyperfine line is seen to be double, on account of the differing magnetic moments of ^{63}Cu and ^{65}Cu. The constants A and B in Eq. (5) are determined by measuring the hyperfine splittings with the magnetic field respectively parallel and perpendicular to the crystal axis.

Again, if the ground state of the ion in the crystal has a Stark splitting, for example the Cr^{+++} ion, whose ground state is split into two doublets separated by about 0.2 cm^{-1}, one doublet gives rise to a resonance line, but in addition resonant transitions can be induced between one of the levels of the upper doublet and one of the levels of the lower. The splitting of the two doublets in zero field can be deduced from the separation of the three resonance lines [39]. Alternatively one can make use of the fact that the frequency of resonance for a transition spanning the two doublets will not be proportional to the magnetic field. By making observations at several different frequencies, it is possible to extrapolate back to zero field, and so find the Stark splitting directly.

To achieve the high resolution required to observe these fine structure and hyperfine structure effects, it is usually necessary to reduce the broadening of the resonance due to the internal field by working with a mixed crystal of the paramagnetic salt with an isomorphous diamagnetic salt. It appears that this dilution has little effect on the hyperfine splitting, but in some cases the Stark splitting is profoundly affected, and it is necessary to exercise caution in applying the results of measurements on diluted salts to the pure salts. The Stark splittings in the alums, which often depend on quite small departures from cubic symmetry, are particularly sensitive.

The great power of the method is that it gives direct information on the g-values and their variation with direction relative to the crystal axes. The measurements can be made in the presence of impurities, and if the crystal has more than one ion per unit cell, the different clas-

ses of ion can be studied separately, whereas susceptibility measurements give only a mean of the effects due to all ions. On the other hand, it is necessary to use single crystals, and the method may fail altogether, either because the transition probability for the resonance is too low, or because the line is to broad to be perceptible – for example if the life time of the two states is very short because of spontaneous transitions.

5. Some Experimental Results

CHROMIUM POTASSIUM ALUM, $CrK(SO_4)_2 \cdot 12H_2O$.

This salt has been extensively used for demagnetization work. The ground state of the free Cr^{+++} ion, $^4F_{3/2}$, is split by the crystalline electric field to give an orbital singlet with 4-fold spin degeneracy. The susceptibility [40] closely follows Curie's law, with a Curie constant of 1.83 per mole, corresponding to $g = 1.97$. The specific heat was measured at 77°K by Broer [41], who found $c/R = 0.0141/T^2$, in agreement with measurements by Starr [3] at the same temperature. Measurements between 1.3°K and 4.0°K by Kramers, Bijl and Gorter [43] gave $c/R = 0.0165/T^2$. Since the only isotope with nuclear spin, ^{53}Cr, is only 9.4% abundant, the specific heat should be due chiefly to interaction between the ions together with the single splitting of the 4-fold ground state allowed by Kramers' theorem. Unfortunately paramagnetic resonance measurements at low temperatures can only be interpreted by assuming that different ions in the same specimen undergo different splittings [44]. The effect appears to be connected with the shattering of the crystal which occurs below 160°K.

In view of this unsatisfactory state of affairs, attention has recently been given to chromium caesium alum and chromium methylamine alum. These salts exhibit only a single Stark splitting at low temperatures, [44] and the measured specific heats [45] can be accounted for almost completely by Stark and magnetic interactions.

FERRIC AMMONIUM ALUM, $FeNH_4(SO_4)_2 \cdot 12H_2O$

The ground state of the ferric ion is $^6S_{5/2}$. The susceptibility of the alum closely follows Curie's law [46], with a Curie constant of 4.37 per mole, appropriate to a free spin of 5/2. Paramagnetic resonance measurements give $g = 2.00$. The most recent measurements of the specific heat are by Broer [41] at 77°K, who finds $c/R = 0.014/T^2$, and by Kramers, Bijl and Gorter [43], in the helium range, who find $c/R =$

$0.013/T^2$, in agreement with the measurements of Benzie and Cooke [45] at the same temperatures. The demagnetization measurements of Kurti and Simon [47] gave $c/R = 0.014/T^2$. As the only isotope with nuclear spin, ^{57}Fe, is only 2.2% abundant, nuclear effects are negligible, and the specific heat is due to Stark splitting and interactions between the ions. Meyer [48] has shown that a satisfactory account of the splitting [49] observed in paramagnetic resonance measurements on a diluted salt can be obtained by supposing that it is due to an electric field of cubic symmetry with a trigonal component in addition. The zero-field splittings he calculates lead to a Stark contribution to the specific heat of $cT^2/R = 0.008$ to 0.009. As the magnetic interaction contribution to the specific heat is calculated to be $cT^2/R = 0.005$, the specific heat is accounted for, always provided the splittings in the pure salt are comparable with those in the dilute salt [50].

MANGANOUS AMMONIUM SULPHATE. $Mn(NH_4)_2(SO_4)_2 \cdot 6H_2O$.

Neglecting nuclear effects the ground state is $^6S_{5/2}$. The susceptibility is isotropic, and down to 1°K. follows Curie's law accurately [51] with a Curie constant of 4.375 per mole. Paramagnetic resonance measurements [52] give $g = 2.000$. The specific heat has been measured at temperatures from 90° to 290° by Broer [41], who finds $c/R = 0.034/T^2$, in agreement with measurements by Bijl [53], from 4°K to 20°K, and demagnetization measurements by Cooke and Hull [47]. The only isotope, ^{55}Mn, has a nuclear spin of 5/2. Bleaney, and Ingram [2]) found that under the combined effect of Stark splitting and nuclear hyperfine splitting, the ground state of the ion comprises 21 levels spread over 0.283 cm^{-1}, and calculated that this would contribute to the specific heat above 1°K an amount $c/R = 0.0154/T^2$. From relaxation measurements on the pure salt and on various mixed crystals with zinc ammonium sulphate, Benzie, Cooke and Whitley found that the specific heat varied linearly with concentration from $c/R = 0.032/T^2$ for the pure salt to $c/R = 0.017/T^2$ at infinite dilution. The calculated contribution from magnetic dipole interaction is $c/R = 0.011/T^2$.

CUPRIC POTASSIUM SULPHATE, $CuK_2(SO_4)_2 \cdot 6H_2O$.

The crystalline electric field splits the $^2D_{5/2}$ ground state of the free Cu^{++} ion to give a single orbital ground level with doublet spin degeneracy. The specific heat [54] arises from nuclear hyperfine splitting and interactions between the ions, and at high temperatures is given by

$cT^2/R=6.0\times10^{-4}$. Paramagnetic resonance studies [55], and specific heat measurements on diluted salts [24] show that the nuclear contribution to the specific heat is practically the same for all the cupric double sulphates, as $c/R = 1.1 \times 10^{-4}/T^2$, but that the interaction contribution varies considerably, from $1.4 \times 10^{-4}/T^2$ for the caesium salt to $7.0 \times 10^{-4}/T^2$ for the ammonium salt. The variation must be attributed to differing anisotropic exchange.

The susceptibility of cupric potassium sulphate is anisotropic [56], with a mean Curie constant, as measured on a powder [57] of 0.445 per mole. There are two ions per unit cell; the magnetic properties of the individual ions [2]) have axial symmetry with $g_{\parallel} = 2.45$ and $g_{\perp} = 2.14$. Demagnetization measurements show that the susceptibility follows a Curie-Weiss law, with a Weiss constant of 0.034°, according to Garrett [58], or 0.052°, according to de Klerk [22].

CUPRIC SULPHATE, $CuSO_4 . 5H_2O$.

In this relatively concentrated material the susceptibility follows a Curie-Weiss law [59] with an anisotropic Curie constant and an isotropic Weiss constant of $-0.7°$. Paramagnetic resonance measurements [60] show the importance of exchange effects. As a result the specific heat in the helium range is very large [61].

CERIUM MAGNESIUM NITRATE $Ce_2Mg_3(NO_3)_{12} . 24H_2O$.

With one ion per unit cell, the magnetic properties are symmetrical about the trigonal axis of the crystal. The $^2F_{5/2}$ state of the cerium ion is split by the crystalline electric field into a series of doublets. For the ground doublet the g-factors (Eq. 2) are $g_{\parallel} = 0.25$ and $g_{\perp} = 1.84$ [62]. According to Daniels and Robinson [63], the susceptibility perpendicular to the axis obeys Curie's law down to 0.01°K. The Curie constant per half mole is 0.318. Since the stable isotopes have no nuclear spin, the specific heat arises entirely from interaction between the ions. The value found, $c/R = 7.5 \times 10^{-6}/T^2$, can be accounted for by magnetic dipole interaction.

CERIUM ETHYL SULPHATE, $Ce(C_2H_5SO_4)_3 . 9H_2O$.

With one ion per unit cell, the magnetic properties are symmetrical about the hexagonal axis of the crystal. The g-values [11] for the lowest doublet are $g_{\parallel} = 3.72$, $g_{\perp} = 0.2$, but the next lowest doublet, with

$g_{\parallel} = 0.95$, $g_{\perp} = 2.18$, lies only 6.6° above it. As a result the susceptibility in the helium range departs markedly from Curie's law [64], and the specific heat is very large. Below 1°K only the lowest doublet is appreciably populated. Demagnetization measurements [65] show that the specific heat is then $c/R = 1.1 \times 10^{-3}/T^2$. Finkelstein and Mencher [66] have suggested that electronic quadrupole interaction may contribute to this specific heat, which is far too large to be accounted for by magnetic interaction alone.

GADOLINIUM SULPHATE, $Gd_2(SO_4)_3 \cdot 8H_2O$.

The ground state of the Gd^{+++} ion is ${}^8S_{7/2}$. Down to about 2°K the susceptibility follows Curie's law with a Curie constant of 7.82 per half-mole [67]. Paramagnetic resonance measurements on the ethyl sulphate give $g = 1.992$ [68]. The specific heat has been measured by relaxation methods between 77°K and 290°K by Broer and Gorter [69], who find $c/R = 0.37/T^2$, in agreement with demagnetization measurements by Giauque and MacDougall [70], and calorimetrically by van Dijk and Auer [71], whose result gives $c/R = 0.37/T^2$. Paramagnetic resonance measurements by Bogle and Heine [72] show that the Stark splitting of the ground state is primarily due to an electric field of axial symmetry (Eq. 3). No hyperfine splitting of the ground state occurs, in spite of the presence of isotopes of odd mass number. The overall Stark splitting at room temperature found by Bogle and Heine in gadolinium sulphate diluted with samarium sulphate was 0.82 cm^{-1}, from which the calculated Stark contribution to the specific heat is $c/R = 0.194/T^2$. As the calculated magnetic interaction contribution is $0.10/T^2$ [21], the measured specific heat is not accounted for. However, thermal contraction may change the splitting at low temperatures.

TITANIUM CAESIUM ALUM, $TiCs(SO_4)_2 \cdot 12H_2O$

This substance was used by de Haas and Wiersma [73] for some of their earliest demagnetization experiments. It has often been taken as a model of a simple paramagnetic substance [21, 74], in theoretical calculations. Unfortunately it is chemically very unstable, oxidizing readily in air. The ${}^2D_{3/2}$ ground state of the free Ti^{+++} ion is split by an electric field of cubic symmetry into an orbital doublet and triplet, the triplet lying lower. In the alum, this triplet is further split into three spin doublets. The susceptibility measurements of van den Handel [29]

indicate that the energy separations of these doublets are rather small (of the order 100 cm^{-1}). At low temperatures only the lowest doublet is populated, and the susceptibility then obeys Curie's law. Second-order effects from higher levels depress the g-values below 2. Paramagnetic resonance measurements by Bogle and Cooke (unpublished) gave $g_{\parallel} = 1.25$ and $g_{\perp} = 1.14$. On account of the overall cubic symmetry of the crystal, the magnetic susceptibility is isotropic, with a Curie constant $C = 0.130$ per mole. Specific heat measurements by Benzie and Cooke [75] gave $c/R = 4 \times 10^{-5}/T^2$, one-tenth being due to nuclear effects and the remainder to interaction between the ions.

COBALT AMMONIUM SULPHATE, $Co(NH_4)_2(SO_4)_2 . 6H O$.

The magnetic behaviour of cobalt salts differs markedly from that of other iron group salts. The magnetic susceptibility is highly anisotropic, and is far from obeying Curie's law [76]. The behaviour of cobalt ammonium sulphate is typical. In this salt each cobalt ion is subject to an electric field of approximately cubic symmetry, but with a tetragonal component. The ${}^4F_{9/2}$ ground state of the free ion is split by the cubic field to give an orbital triplet some 10^4 cm^{-1} below the next orbital level. Under the combined action of the spin-orbit coupling and the tetragonal field this is further split into a number of Kramers doublets of comparatively small separation [77]. At low temperatures only the lowest doublet is populated. The susceptibility then obeys Curie's law (apart from temperature independent effects), but with a highly anisotropic Curie constant. The Curie constant in any direction may be calculated from the paramagnetic resonance data of Bleaney and Ingram [8]. There are two ions per unit cell, each having magnetic properties of axial symmetry, with $g_{\parallel} = 6.45$ and $g_{\perp} = 3.06$.

Cobalt has only one stable isotope, ^{59}Co, with a nuclear spin of 7/2. The specific heat arises from nuclear hyperfine splitting of the ground electronic doublet, and from interaction between the ions. It has been measured by Malaker, and by Garrett, who find [78] $c/R = 4.2 \times 10^{-3}/T^2$. From measurements on mixed crystals of cobalt and zinc ammonium sulphates, Malaker concluded that the nuclear contribution to the specific heat is $c/R = 1.6 \times 10^{-3}/T^2$, in agreement with the value calculated from the resonance measurements of Bleaney and Ingram. The contribution due to the anisotropic magnetic dipole interaction is calculated to be $2.1 \times 10^{-3}/T^2$.

OTHER COBALT SALTS

Bleaney and Ingram also investigated cobalt potassium sulphate, cobalt sulphate, and cobalt fluosilicate, finding in each case a doublet ground state. The magnetic properties of cobalt sulphate at temperatures down to 0.25°K. have been investigated by Fritz and Giauque [79], who, however, interpreted their results in terms of a fourfold degenerate ground state. Cobalt fluosilicate has a certain interest, since almost all its specific heat appears to be due to exchange interaction, There is one ion per unit cell, with g-values $g_{\parallel} = 5.80$ and $g_{\perp} = 3.45$. The specific heat has been measured by Benzie, Cooke and Whitley, who find $c/R = 15 \times 10^{-3}/T^2$, of which the nuclear contribution is $1.1 \times 10^{-3}/T^2$, and the magnetic dipole interaction is calculated to be $1.2 \times 10^{-3}/T^2$.

REFERENCES.

[1] P. Debye, Ann. d. Phys., **81**, 1184 (1926).
[2] W. F. Giauque, J. Am. Chem. Soc., **49**, 1864, 1870 (1927).
[3] W. J. de Haas, E. C. Wiersma and H. A. Kramers, Nature, **131**, 719 (1933); Physica, **1**, 1 (1933).
[4] W. F. Giauque and D. P. MacDougall, Phys. Rev., **43**, 768 (1933); ibid. **44**, 235 (1933).
[5] See e.g. D. Polder, Physica, **9**, 709 (1942).
[6] C. J. Gorter, Arch. Mus. Teyler, **7**, 183 (1932); J. H. van Vleck, The Theory of Electric and Magnetic Susceptibilities, Oxford, 1932.
[7] B. Bleaney and K. W. H. Stevens, Rep. Prog. in Phys. **16**, 108 (1953).
[8] B. Bleaney and D. J. E. Ingram, Proc. Roy. Soc. Lond. A, **208**, 143 (1951); M. H. L. Pryce, Nature, Lond., **164**, 117 (1949).
[9] H. A. Kramers, Proc. Acad. Sci. Amst., **33**, 959 (1930).
[10] H. A. Jahn and E. Teller, Proc. Roy. Soc. Lond. A, **161**, 220 (1937).
[11] G. S. Bogle, A. H. Cooke and S. Whitley Proc. Phys. Soc. A, **64**, 931 (1951).
[12] J. H. Van Vleck and W. G. Penney, Phil. Mag. **17**, 961 (1934).
[13] A. Abragam and M. H. L. Pryce, Proc. Roy. Soc. Lond. A, **205**, 135 (1951).
[14] B. Bleaney, Phys. Rev. **78**, 214 (1950).
[15] C. J. Gorter, Phys. Z., **33**, 546 (1932).
[16] L. D. Roberts, S. C. Sartain and W. T. Dabbs, Rev. Mod. Phys., **25**, 170 (1953).
[17] J. H. Van Vleck, J. Chem. Phys., **5**, 320 (1937).
[18] J. M. Daniels, Proc. Phys. Soc. A., **66**, 673 (1953); A. H. Cooke, H. J. Duffus and W. P. Wolf, Phil. Mag., **44**, 623 (1953).
[19] H. A. Lorentz, The Theory of Electrons, Leipzig, 1916.
[20] L. Onsager, J. Am. Chem. Soc., **58**, 1486 (1936).
[21] M. H. Hebb and E. M. Purcell, J. Chem. Phys., **5**, 338 (1937); A. H. Cooke, Proc. Phys. Soc., **62**, 269 (1949).
[22] D. de Klerk, Physica, **12**, 513 (1946).
[23] W. Opechowski, Physica, **4**, 181 (1937); J. H. van Vleck, J. Chem. Phys. **5**, 320 (1937).
[24] R. J. Benzie and A. H. Cooke, Nature, Lond., **164**, 837 (1949); C. G. B. Garrett, Proc. Roy. Soc. Lond., **203**, 392 (1950).

[25] W. Opechowski, Physica, **14**, 237 (1948); J. F. Ollom and J. H. van Vleck, Physica, **17**, 205 (1951).
[26] H. A. Kramers, Physica, **1**, 182 (1934).
[27] e.g. L. C. Jackson, Proc. Roy. Soc. A, **140**, 695 (1933).
[28] C. J. Gorter, W. J. de Haas and J. van den Handel, Leiden Comm. No. 222d.
[29] See e.g. J. van den Handel, Thesis, Leiden 1940.
[30] H. B. G. Casimir, W. J. de Haas and D. de Klerk, Physica, **6**, 241 (1939).
[31] R. A. Erickson, L. D. Roberts and W. T. Dabbs, Rev. Sci. Inst. (in course of publication 1954).
[32] The work in this field is summarized by C. J. Gorter, Paramagnetic Relaxation, Elsevier Publishing Co., Amsterdam, 1947. See also A. H. Cooke, Rep. Prog. in Phys., **13**, 276 (1950).
[33] H. B. G. Casimir and F. K. Du Pré, Physica, **5**, 507 (1938).
[34] C. J. Gorter, Physica, **3**, 503 (1936); C. J. Gorter and F. Brons, Physica, **4**, 579 (1937).
[35] G. Duyckaerts, Mem. Soc. Roy. Sci. de Liége, **6**, 195 (1942); H. van Dijk and W. U. Auer, Physica, **9**, 785 (1942).
[36] E. Zavoisky, J. Phys. U.S.S.R., **9**, 211 (1945); ibid., **10**, 197 (1946).
[37] B. Bleaney, J. Phys. Chem., **57**, 508 (1953).
[38] R. P. Penrose, Nature, Lond., **163**, 992 (1949).
[39] D. M. S. Bagguley and J. H. E. Griffiths, Nature, Lond., **160**, 532 (1947).
[40] W. J. de Haas and C. J. Gorter, Leiden Comm. 208c (1930).
[41] L. J. F. Broer, Physica, **13**, 353 (1947).
[42] C. Starr, Phys. Rev., **60**, 241 (1941).
[43] H. C. Kramers, D. Bijl and C. J. Gorter, Physica, **16**, 65 (1950).
[44] B. Bleaney, Proc. Roy. Soc. Lond. A, **204**, 203 (1950).
[45] R. J. Benzie and A. H. Cooke, Proc. Phys. Soc. A, **63**, 213 (1950); W. E. Gardner and N. Kurti, Proc. Roy. Soc. A, **223**, 542 (1954).
[46] H. Kamerlingh Onnes and E. Oosterhuis, Leiden Comm. 129b; R. A. Erickson and L. D. Roberts, Phys. Rev., **93**, 957 (1954).
[47] A. H. Cooke, Proc. Phys. Soc. A, **62**, 269 (1949).
[48] P. H. E. Meyer, Physica, **17**, 899 (1951); ibid. **18**, 723 (1952).
[49] J. Ubbink, J. A. Poulis and C. J. Gorter, Physica, **17**, 213 (1951).
[50] H. B. G. Casimir, Magnetism and Very Low Temperatures, p. 78, Cambridge (1940).
[51] L. C. Jackson and H. Kamerlingh Onnes, Proc. Roy. Soc. Lond. A, **104**, 671 (1923); K. S. Krishnan, A. Mookherji and A. Bose, Phil. Trans. A, **238**, 125 (1939); R. A. Erickson and L. D. Roberts, Phys. Rev., **93**, 957 (1954).
[52] B. Bleaney and D. J. E. Ingram, Proc. Roy. Soc. Lond. A, **205**, 336 (1951).
[53] D. Bijl, Physica, **16**, 269 (1950).
[54] L. J. F. Broer and J. Kemperman, Physica, **13**, 465, (1947); R. J. Benzie and A. H. Cooke, Proc. Phys. Soc. A, **63**, 213, (1950); D. Bijl, Physica, **16**, 269 (1950).
[55] B. Bleaney, K. D. Bowers and D. J. E. Ingram, Proc. Phys. Soc., A, **64**, 758 (1951).
[56] J. C. Hupse, Physica, **9**, 633, (1942); D. Polder, Physica, **9**, 709 (1942).
[57] J. Reekie, Proc. Roy. Soc. Lond., A, **173**, 367 (1939).
[58] C. G. B. Garrett, Proc. Roy. Soc. Lond., A **203**, 375, 392 (1950).
[59] W. J. de Haas and C. J. Gorter, Leiden Comm., 210d (1930); R. J. Benzie and A. H. Cooke, Proc. Phys. Soc. A, **64**, 124 (1951).
[60] D. M. S. Bagguley and J. H. E. Griffiths, Proc. Roy. Soc. A, **201**, 366 (1950).
[61] J. Ashmead, Nature, Lond., **143**, 853 (1939).

[62] A. H. Cooke, H. J. Duffus and W. P. Wolf, Phil. Mag., **44**, 623 (1953).
[63] J. M. Daniels and F. N. H. Robinson, Phil. Mag., **44**, 630 (1953).
[64] J. Becquerel, W. J. de Haas and J. van den Handel, Physica, **5**, 857 (1938); R. A. Fereday and E. C. Wiersma, Physica, **2**, 575 (1935).
[65] W. J. de Haas and E. C. Wiersma, Physica, **2**, 335 (1935); A. H. Cooke, S. Whitley and W. P. Wolf, to be published.
[66] R. Finkelstein and A. Mencher, J. Chem. Phys., **21**, 472 (1953).
[67] H. R. Woltjer and H. Kamerlingh Onnes, Leiden Comm. 167c.
[68] B. Bleaney, H. E. D. Scovil and R. S. Trenam, Proc. Roy. Soc. A, **223**, 15 (1954).
[69] L. J. F. Broer and C. J. Gorter, Physica, **10**, 621 (1943).
[70] W. F. Giauque and D. P. MacDougall, J. Am. Chem. Soc., **57**, 1175 (1935).
[71] H. van Dijk and W. U. Auer, Physica, **9**, 785 (1942).
[72] G. S. Bogle and V. Heine, Proc. Phys. Soc. A, **67**, 734 (1954).
[73] W. J. de Haas and E. C. Wiersma, Physica, **2**, 438 (1935); ibid., **3**, 491 (1936).
[74] R. de L. Kronig, Physica, **6**, 33 (1939); J. H. van Vleck, Phys. Rev., **57**, 426 (1940).
[75] R. J. Benzie and A. H. Cooke, Proc. Roy. Soc. A, **209**, 269 (1951).
[76] B. Bartlett, Phys. Rev., **41**, 818 (1932); A. Bose, Indian J. Phys., **22**, 276 (1948).
[77] J. H. Van Vleck, Phys. Rev. **41**, 208 (1932); A. Abragam and M. H. L. Pryce, Proc. Roy. Soc. A, **206**, 173 (1951).
[78] S. F. Malaker, Phys. Rev., **84**, 133 (1951); C. G. B. Garrett, Proc. Roy. Soc. A, **206**, 242 (1951).
[79] J. J. Fritz and W. F. Giauque, J. Am. Chem. Soc., **71**, 2168 (1949).

CHAPTER XIII

ANTIFERROMAGNETIC CRYSTALS

BY

N. J. POULIS AND C. J. GORTER
KAMERLINGH ONNES LABORATORIUM, LEIDEN

1. Introduction

Weiss' molecular field theory [1] of ferromagnetism explained in a very simple way the disappearance of the spontaneous magnetization, and thus of ferromagnetism, at a well defined Curie temperature Θ above which paramagnetism sets in. The rapid variation of the spontaneous magnetization below the Curie temperature would be accompanied by an extra contribution to the specific heat which would be absent above that temperature. Above Θ the field-independent susceptibility would be given by the Curie-Weiss law

$$\chi = \frac{C}{T - \Theta} \tag{1}$$

where T is the absolute temperature.

The mysterious molecular Weiss field αM, where M indicates the average magnetization, which field has to be added to the external field H, was later by Heisenberg [2] brought into relation with a positive exchange interaction between the elementary magnetic moments. Though at present Heisenberg's view is generally accepted to be correct, the Weiss molecular field model, though amended in several respects, remains the basis of the discussion of the various ferromagnetic properties of different materials. In the so-called normally paramagnetic substances, in which the elementary magnetic moments are situated at relatively large distances, Θ is very small compared to room temperature so that Curie's law $\chi = C/T$ is approximately valid. It was supposed for a long time that, upon decreasing the temperature con-

siderably, those normally paramagnetic substances would also become ferromagnetic. As a matter of fact Théodorides in Strasbourg [3] and Woltjer and Kamerlingh Onnes in Leiden [4] observed that the susceptibilities of certain oxides and anhydrous salts have a rather sharp maximum. Below the temperature of this maximum the susceptibilities vary only slowly with temperature, they are slightly field dependent and very small hysteresis effects occur. Schubnikow [5] detected a jump in the specific heat near the temperature of maximum susceptibility while later researches showed that indeed most normally paramagnetic substances behave more or less similarly upon drastic reduction of the temperature. It was found that the properties below the temperature of maximum susceptibility are usually rather different from those found in ferromagnetics, while the Θ characterizing the deviation from Curie's law in the paramagnetic region is usually not positive, but negative, indicating that the interaction favours opposite rather than parallel alinement of the elementary magnetic moments.

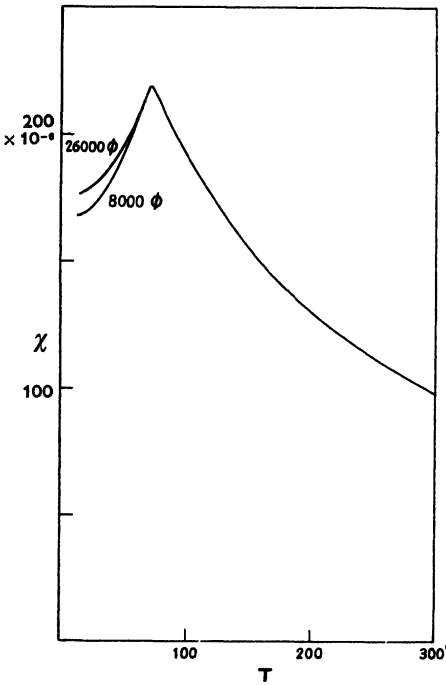

Fig. 1. The susceptibility χ for a powder of MnF_2 as a function of the temperature T and field strengths of 8000 ø and 26.000 ø according to Bizette, Thèses 1946, Paris.

At present many of the properties appearing when normally paramagnetic substances are cooled down drastically are explained by assuming the occurence of antiferromagnetism below a transition temperature T_N, the Néel temperature of the substance.

The first theory of antiferromagnetism was proposed by Néel in 1932 and 1936,[6] curiously enough not in order to explain the properties of the salts and oxides mentioned, but in connection with the magnetic properties of certain metals. Néel divided the crystalline lattice of the magnetic atoms into two sublattices supposing that each magnetic atom in one of the lattices experiences a molecular field proportional

to the opposite of the average magnetization of the other sublattice. An essential and simple conclusion of this theory was the existence of the transition temperature T_N, which is linked with the negative Θ, determined in the paramagnetic region above T , by the relation

$$T_N = -\Theta \tag{2}$$

Independently Kramers and Hulthén [7] investigated the consequences of a negative exchange interaction between nearest neighbours in a crystalline lattice. Though their quantum mechanical analysis led to the expectation that at very low temperatures an arrangement of the spins in sublattices could occur, only part of the moments in each sublattice should be alined. The later development of the spin wave method by Anderson [8], Kubo [9], Tessman [10] *et al.* led to interesting predictions on the magnetic and caloric behaviour of antiferromagnetics near the absolute zero of temperature.

A third type of theory links up with the statistical treatment of order-disorder transitions. Making use of the cluster method, Li [11] has made predictions pertaining to the neighbourhood of the Néel temperature.

Of these theories the Néel molecular field theory is by far the simplest and it is the only one which considers the whole range of temperatures from zero to above T_N. For this reason it is chiefly the molecular field treatment that has been used until now in the discussion of the various properties of antiferromagnetic crystals. Néel's original theory has been extended in several respects by Bitter [12], Van Vleck [13], Anderson [14], Nagamiya [15], Yosida [16], Gorter and Haantjes [17], as well as by Néel himself [18]. A number of these extensions will be mentioned in the later sections. Here we shall only mention a few points.

Néel has extended his original theory somewhat by presuming that the molecular field acting on each atom may contain a term proportional to the magnetization of the own sublattice in addition to the term proportional to the opposite of the magnetization of the other sublattice. If this term has the tendency to line up the spins of each sublattice, it decreases the value of $-\Theta$, while it increases T_N. Thus the ratio of $-\Theta$ and T_N becomes smaller than 1 and it gives a measure of the ratio of the two kinds of interaction.

Van Vleck has pointed out that the antiferromagnetic interaction should be supposed to occur only between certain near neighbours in the crystalline lattice and has suggested that the molecular field

picture might nevertheless remain applicable in some respects.

Along these lines of thought Anderson has remarked that in a crystalline lattice several choices of sublattices are in general possible and he has discussed how the exchange interactions of neighbours and nearest neighbours may influence the choice of sublattice structure and the parameter — Θ/T_N just mentioned.

In general — even in cubic crystals — the properties of antiferromagnetics will depend on the angles between the magnetic field and the crystalline axes. Measurements on powders therefore allow a much less detailed study of these properties than do investigations on single crystals. Unfortunately the (hydrated) crystals which may be grown easily usually have Néel temperatures below 0.1°K and their antiferromagnetism is thus confined to a temperature region which can only be reached by adiabatic demagnetization.

The first susceptibility measurements on antiferromagnetic crystals were carried out by Stout and Griffel on MnF_2[19]. Similar researches were later made on CoF_2 and $FeCl_2$ [20]. By far the greatest amount of information, however, was obtained in Leiden on $CuCl_2 . 2H_2O$. The antiferromagnetism of this salt was discovered by investigating the magnetic resonance of its protons [21]. Later on the susceptibilities were also investigated [22]. Antiferromagnetic resonance was discovered and studied with microwaves [23], while the specific heat of the powder was also measured [24]. A few similar researches were carried out on $MnCl_2 . 4H_2O$ [25], and in the adiabatic demagnetization region observations have been made on $Co(NH_4)_2(SO_4)_2 . 6H_2O$ [26] and on $CrCH_3 NH_3(SO_4)_2 . 12H_2O$.

A few other investigations will be mentioned in § 7.

2. Molecular field theory for anisotropic crystals

Let us place ourselves on the basis of Néel's original molecular field theory and distinguish between the two sublattices which we shall indicate by a single and by a double dash.

We then may put for the energy per atom

$$U = -\tfrac{1}{2} \sum_k \mu_k (p_k' + p_k'') H_k + \tfrac{1}{2} \sum_k \alpha_k \mu_k^2 p_k' p_k''. \qquad (3)$$

where k indicates the three coordinate directions, μ and H are the magnetic moment of one atom and the magnetic field and $\mu p'$ and $\mu p''$ indicate the magnetizations per atom of the sublattices, normalized

in such a way that $|p| = 1$ corresponds to complete alinement of the spins in a sublattice. The first sum gives the magnetic energy with respect to the field H, while the second sum gives the interaction energy between the two sublattices. One may also, with Yosida [16; 27], separate the interaction energy into an isotropic term and an anisotropic one which does not depend on the product of p' and p'', but on each of them:

$$U = -\tfrac{1}{2}\sum_k \mu_k (p_k' + p_k'') H_k + \tfrac{1}{2}\alpha\mu^2 \sum_k p_k' p_k'' + \tfrac{1}{2}\sum_k \beta_k (p_k'^2 + p_k''^2) \quad (3a)$$

with $\sum_k \beta_k = 0$.

As long as the directions p' and p'' may be considered opposite ($p' = -p''$) the formulations (3) and (3a) give identical results.

Making use of the usual statistical formulations one may also write down the entropy S connected with the values of p' and p''. Minimizing then the free energy $F = U - TS$ at given values of H and T leads to rather complicated solutions for the p's. We shall now consider a few special cases, confining ourselves to a Kramers degeneracy for the lowest energy level of each magnetic atom (sometimes described by putting $S = \frac{1}{2}$). Let us further put

$$\alpha_x \mu_x^2 > \alpha_y \mu_y^2 > \alpha_z \mu_z^2.$$

If now the external field is zero it is possible to obtain for $p_x' = -p_x''$ the expression

$$p_x' = \operatorname{tgh} \frac{\alpha \mu_x^2 p_x'}{kT} \quad (4)$$

We thus have two opposite spontaneous magnetizations $\mu_x p_x'$ and $\mu_x p_x''$ which may be found (see Fig. 2) from the implicit Eq. (4) which incidentally is identical with that determining the spontaneous magnetization in the Weiss theory of ferromagnetism. The two spontaneous magnetizations disappear when

$$\alpha_x \mu_x^2 = kT$$

which gives for the Néel-temperature

$$T_N = \frac{\alpha_x \mu_x^2}{k} \quad (5)$$

If now we introduce a small magnetic field in the (preferred) x-direction we get for the susceptibility per magnetic atom [28]

$$\chi_x = \frac{M_x}{H_x} = \frac{\mu_x^2}{k\left(T_N + T\cosh^2\left(\frac{T_N p_x'}{T}\right)\right)} \tag{6}$$

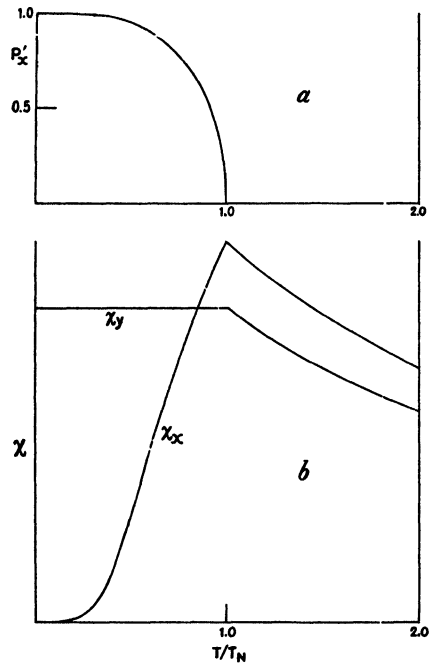

Fig. 2. a. The magnetization of the sublattices p_x' as a function of the temperature T according to (4).
b. The susceptibilities χ_x and χ_y as a function of the temperature T, assuming $\mu_x = 1.1 \times \mu_y$.

while, if we introduce a small magnetic field parallel to the y-direction, we get (see Fig. 2).

$$\chi_y = \frac{M_y}{H_y} = \frac{\mu_y^2}{(\alpha_x \mu_x^2 + \alpha_y \mu_y^2)} \tag{7}$$

The analogous expression applies for χ_z (7a).

Above the Néel temperature we finally obtain

$$\chi = \frac{\mu^2}{kT + \alpha\,\mu^2} \tag{8}$$

Figures 2 gives χ_x and χ_y as a function of T where it is supposed that $\mu_x = 1.1 \times \mu_y$ while $\alpha_x \mu_x^2 \approx \alpha_y \mu_y^2$.

In a powder we get

$$\chi = \tfrac{1}{3}(\chi_x + \chi_y + \chi_z) \tag{9}$$

which at $T = 0$ is approximately equal to $\frac{2}{3}\chi_y$.

The susceptibility in the antiferromagnetic state is usually smaller in the preferred x direction than in the other directions. This is particularly pronounced at the the very lowest temperatures, where $p_x' = -p_x'' \approx 1$. The reason is that while a small field in the x direction hardly changes p' and p'', a field in the y or z direction forces them slightly parallel to itself. Thus the magnetic energy (the first term in (3)) is lower in the latter cases. As was pointed out at an early date by Néel [29] this has the remarkable consequence that, if one increases an outside field, the p's have the tendency to place themselves perpendicular to that field. In general this will go gradually, but, for instance, if we choose the field in the x direction, a discontinuous switchover of the p's towards the $\pm y$

direction occurs at a threshold field which at $T = 0$ is given by the expression,

$$H_c^2 = \frac{\alpha_x^2 \mu_x^4 - \alpha_y^2 \mu_y^4}{\mu_x^2} \tag{10}$$

Yosida [16] and Ubbink [30] have remarked that if the α's of (3) (or the α's and β's of of (3a)) are independent of the temperature, the temperature dependence of the threshold field H_{th} is given by

$$H_{th}^2 = H_c^2 \frac{p_x'^2}{1 - (\mu_y^2 \chi_x / \mu_x^2 \chi_y)} \tag{11}$$

This formula is somewhat more general than (4) . . . .(7) but if we accept those formulae we find that H_{th} should increase by a factor $\sqrt{3}$ upon approaching T_N (Fig. 3). However, (11) only applies when $H_{th} << \alpha \mu p'$ and therefore is not valid in the immediate vicinity of T_N.

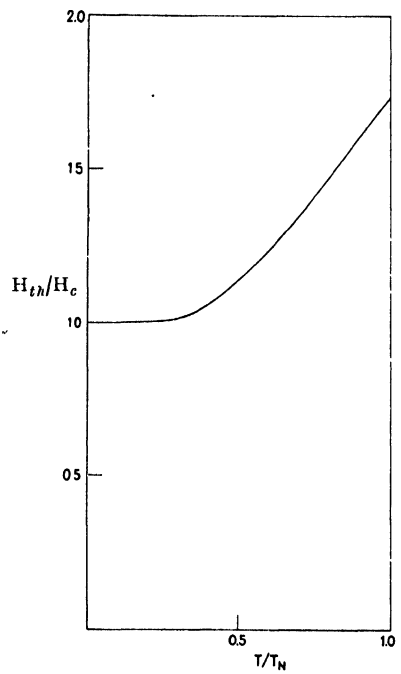

Fig. 3. The threshold field H_{th}/H_c as a function of T/T_N according to (11).

A sharp threshold field may also be found when the field is parallel to the xz-plane. In the space of the magnetic field vectors a characteristic hyperbola should occur in the xz-plane (Fig. 4) whose equation is at $T = 0$

$$\frac{H_x^2}{H_c^2} - \frac{H_z^2}{H_a^2} = 1 \tag{12}$$

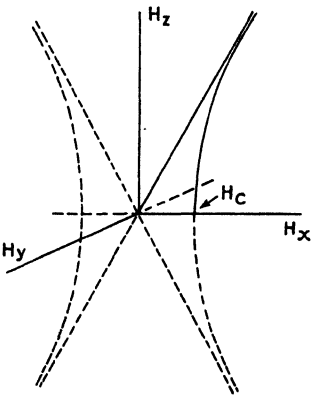

Fig. 4. The critical hyperbola in the xz-plane in the space of H-vectors.

with $$H_a^2 = \frac{\alpha_y^2 \mu_y^4 - \alpha_z^2 \mu_z^4}{\mu_z^2} \qquad (13)$$

If the field in the xz-plane hits the hyperbola the p's jump from a direction in the xz-plane to the y direction or vice versa. If the field has another direction the p's rotate gradually, but the relevant formulae are complicated and we shall not give them here.

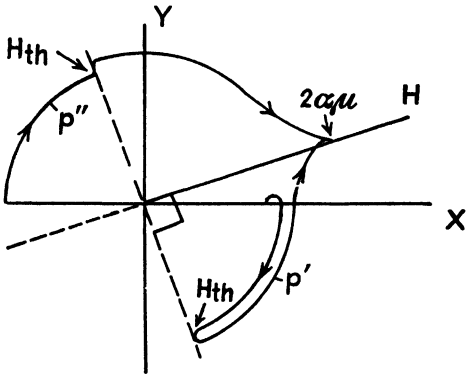

Fig. 5. Directions of p' and p'' when a magnetic field in a direction near that of the x-axis increases gradually.

If the anisotropy Δ $(\alpha \mu^2)$ is relatively small the threshold field is of the order of

$$(2 \alpha \Delta (\alpha \mu^2))^{\frac{1}{2}}.$$

Another interesting region occurs when the field becomes of the order of $2 \alpha \mu p'$. Unless we are in the immediate vicinity of T_N, where $p' << 1$, this second region occurs at much higher fields. It occurs when the angle between p' and p'' differs considerably from π since both are forced towards the external field. The angle will become zero when $H = 2 \alpha \mu p' = 2 \alpha \mu p''$ and then antiferromagnetism goes over into paramagnetism. Fig. 5 illustrates the behaviour of p' and p'' if we gradually increase a field whose direction is near that of the x-axis. Fig. 6 gives the susceptibilities $\chi_x = \mathrm{d}M_x/\mathrm{d}H_x$ and $\chi_y = \mathrm{d}M_y/\mathrm{d}H_y$ at $T = 0$, as a function of an external field in the x direction. The validity of (3) was assumed which in this case gives results differing from those obtained from (3a). If we have a cubic symmetry we can use different expressions instead of (3); Fig. 7 gives the result of a calculation with the constant external field in one of the three perpendicular directions of preference [31].

In low fields the shifts of walls between domains orientated in different directions of preference will, as Néel [32] recently remarked, give rise to hysteresis phenomena.

3. The Magnetization as a Function of the Field

In § 1 we mentioned that numerous researches have been carried out on the susceptibilities of powdered substances and that the similari-

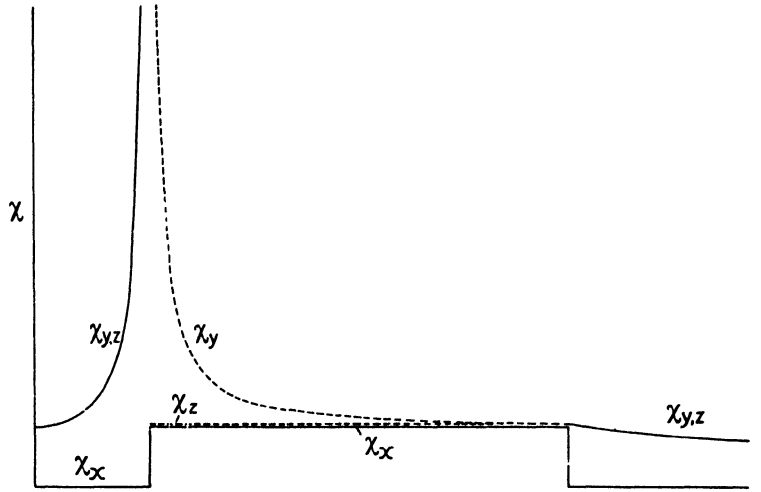

Fig. 6. The susceptibilities χ_x, χ_y and χ_z as a function of a field H_x in the x-direction for zero temperature. μ_x, μ_y and μ_z are supposed to be approximately equal, the same applies to α_y and α_z.

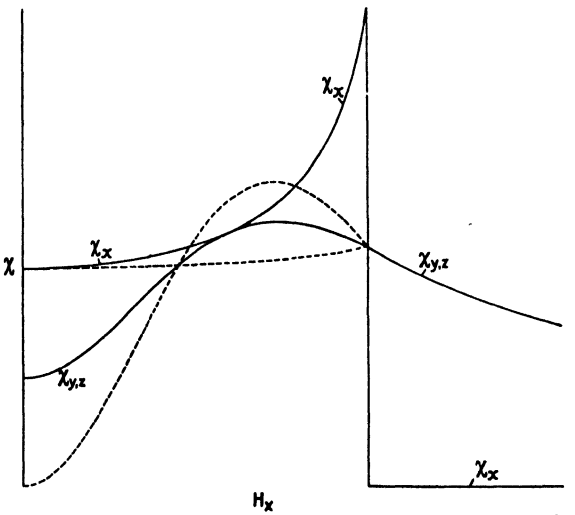

Fig. 7. The susceptibilities χ_x and $\chi_{y,z}$ as a function of a field H in the x-direction for zero temperature in a case of cubic symmetry according to [31].

ties and differences found between different substances sometimes have given rise to interesting theoretical comment (see § 7). We shall not go into this matter nor shall we concentrate our attention on Stout's [20] investigation of the magnetic anisotropy of the anhydrous fluorides of Mn, Co and Fe. Those latter investigations were the first to show a considerable magnetic anisotropy in the antiferromagnetic state, which agrees quite well with Van Vleck's formulae (6) and (7), but since their discussion necessitates the use of data obtained on the susceptibilities of powders, obtained elsewhere on different samples, there may be some doubt about certain conclusions, for instance on the apparent dependence of χ_v on the temperature.

In Leiden the magnetization of a single crystal of $CuCl_2 . 2H_2O$ was measured as a function of the field and the temperature by the balance method [33].

Fig. 8 gives the magnetization as a function of a field oriented in directions of the crystallographic *a*- and *b*-axis, for three temperatures.

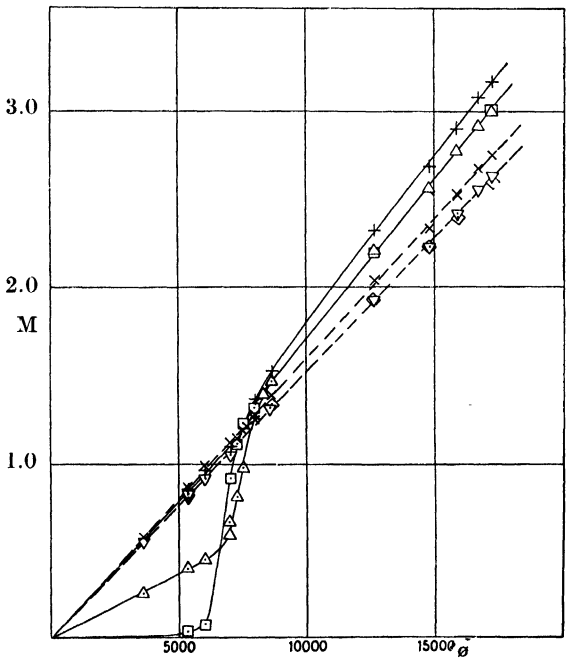

Fig. 8. The magnetization M along the *a*- and *b*-axes as a function of the field strength H. + *a*-axis, × *b*-axis } 4.1°K Δ *a*-axis, ▽ *b*-axis } 3.02°K □ *a*-axis, ◇ *b*-axis } 1.59°K

It is seen that at 1.59°K the magnetization in the *a* direction is practically zero up to a field of 6500 Ø where it makes a jump. Above that field the magnetization increases in proportion to H_a and thus the susceptibility is there a constant. In the *b* direction we have a susceptibility which is about 14% lower than that in the *a* direction at high fields. We have obviously to do with the threshold phenomenon described in § 2 and the *x*-direction of preference is the crystallographic *a* direction. When the temperature increases the magnetization in weak fields in the *a* direction increases also in qualitative agreement with (6). The threshold field increases somewhat in agreement with (11). We may remark, however, that in these measurements the crystal is placed in an inhomogeneous field which tends to blur the threshold. In § 4 we shall mention a more accurate method to study the threshold field and its dependence on temperature.

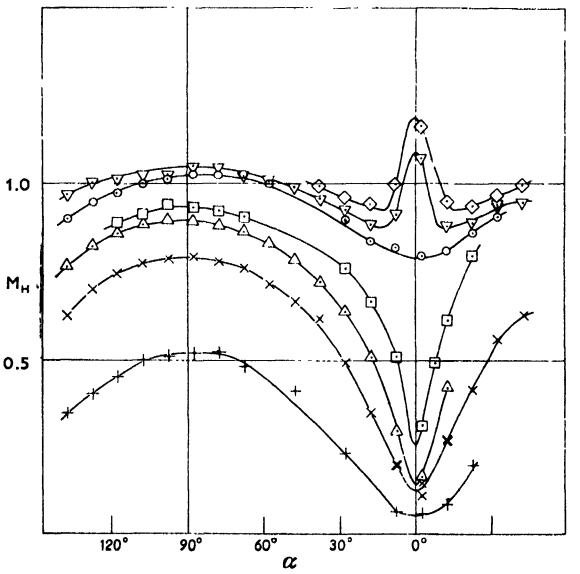

Fig. 9. Magnetization M_H in the *ab*-plane as a function of the angle α, of the magnetic field *H* with the *a*-axis, at a temperature of 2.1°K

+ 3600 ø	△ 6000 ø	○ 7000 ø	◈ 7450 ø
× 5300 ø	□ 6300 ø	▽ 7250 ø	

Fig. 9 gives the magnetization at low temperature as a function of the angle between the *a*-axis and the field in the *ab*-plane. It is seen that above the threshold field the minimum in the *a* direction is replaced by a sharp maximum. The curves are in perfect agreement with

the theoretical formulae. This is also true of Fig. 10 in which the magnetic field has different orientations in the *ac*-plane. In low fields there is no qualitative difference with the *ab*-plane, but at high fields a plateau occurs near the *a*-axis. On this plateau the field is apparently above the threshold field, while the crossing of the threshold hyper-

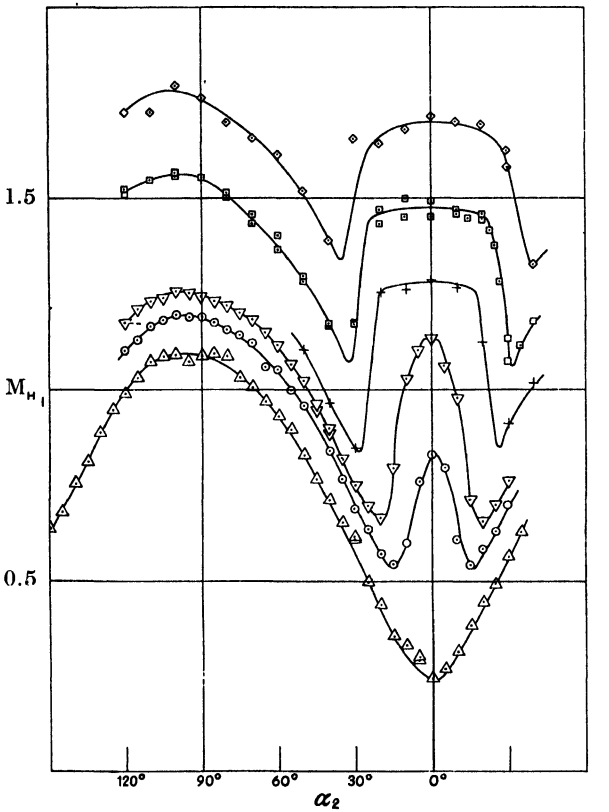

Fig. 10. Magnetization M in the *ac*-plane as a function of the angle α_2 of the magnetic field with the *a*-axis, at a temperature of 2.1°K.

△ 5660 ø ▽ 6880 ø □ 8175 ø
○ 6640 ø + 7560 ø ◇ 9225 ø

bola, which obviously is situated in this plane, is clearly marked by a sharp fall in the magnetization. Combining the data obtained at the lower temperatures (< 2°K) with the equations (7), (7a), (10), (12) and (13), and accepting the values of μ_a, μ_b and μ_c derived from measurements at liquid hydrogen temperatures with the aid of (8) (which agree with those observed in paramagnetic resonance) one calculates:

$\alpha_x \mu_x^2 = 104.6 \times 10^{-17}$ ergs; $\alpha_y \mu_y^2 = 104.4 \times 10^{-17}$ ergs; $\alpha_z \mu_z^2 = 103.8 \times 10^{-17}$ ergs.

The absolute precision of these numbers is about 3% but their differences, which are connected with H_c and H_a, are much more accurate (see (10) and (13)).

From (5) we may then evaluate T_N which turns out to be 7.6°K using $k = 13.8 \times 10^{-17}$ erg/degree. Experimentally the Néel temperature is about 60% of this value, so we are confronted with a serious quantitative discrepancy between the data and Néel's molecular field picture. An anomalous behaviour of the paramagnetic susceptibility between liquid hydrogen temperatures must be connected with this discrepancy. While at high temperatures the paramagnetic $-\Theta \approx$ 5°K, which is not very different from T_N, one should expect at the Néel temperature a susceptibility $\chi_y = \mu_y^2/2\,kT_N$. The discrepancy mentioned means that χ_y has, in the antiferromagnetic state, only 60% of this value. Since no jump of χ_y is ever found at T_N, one must expect serious deviations from the Curie-Weiss law between that temperature and the liquid hydrogen temperatures.

Now the Néel temperature lies above the boiling point of helium and so this region is not very accessible for accurate magnetic measurements. But recent unpublished results indicate that the maximum of the susceptibility lies considerably (of the order of a few tenths of a degree) higher than the T_N found in the investigation of the specific heat and of the proton magnetic resonance (see §§ 4 and 5).

So we conclude that the behaviour at and just above T_N is not yet quite clear.

We finally wish to mention that unpublished investigations have been carried out with $MnCl_2 \cdot 4H_2O$ crystals which apparently have a Néel point at about 1.6°K. Since the crystal is not rhombic and since it is not easy to work at temperatures sufficiently below T_N the results so far obtained are not very easily assayable.

4. Data on the Proton magnetic Resonance

Nuclear magnetic resonance occurs when the resonance condition

$$2\pi\nu = \gamma H \tag{14}$$

is fulfilled, where H is the constant field acting on the nucleus and ν is the frequency of an oscillating magnetic field orientated at right angles to H_o, and γ is the ratio of the magnetic spin μ_o to the mechanical spin $Sh/2\pi$ of the nucleus concerned.

If we have a single proton there are only two energy levels with a separation $2\mu_o H$, which, since the mechanical spin is $h/4\pi$, may be written $\gamma Hh/2\pi$. Equating this to $h\nu$ immediately leads to the resonance condition (14).

If (14) is fulfilled the energy absorption by a sample containing protons (e.g. in water) can be made visible on an oscillograph as a peak in a plot which represents the absorption vs. H. The width and structure of this absorption peak are due to the magnetic interactions of each proton magnetic moment with all the surrounding moments (nuclear as well as ionic) which change the effective magnetic field. Pake [34] found a fine structure in the proton magnetic resonance line in single crystals of gypsum ($CaSO_4 \cdot 2H_2O$), which could be explained by the magnetic proton-proton interaction in a water molecule of hydration. Experiments on single crystals of $CuSO_4 \cdot 5H_2O$ [35] showed that, in addition to the proton-proton interaction, the temperature dependent interaction between paramagnetic ions and the protons is important. Theoretically one can expect 4 resonance lines for a crystalline water if both interactions occur. The resonance diagrams for $CuSO_4 \cdot 5H_2O$, in which the position of the resonance frequencies are plotted for different orientations of the magnetic field, show a very complicated structure due to the overlapping of many lines. The resonance diagrams found in the case of single crystals of $CuCl_2 \cdot 2H_2O$ show a much simpler structure. Due to the symmetric position of the crystalline water molecules with respect to the Cu^{++} ion one should expect four resonance lines only. The resonance frequency for each proton may be given by:

$$2\pi\nu = \gamma (H_o + H_d) \tag{15}$$

where H_o is the externally applied field and H_d is the local field due to the magnetic proton-proton interaction and to the Cu^{++}-proton interaction. In the low temperature experiments with antiferromagnetic $CuCl_2 \cdot 2H_2O$ discussed hereafter, the local field due to the Cu^{++}-proton interaction is the most important addition to the field H_o. The field due to the Cu ions is given by

$$H_d = \mu_o^{-1} \sum_c \left\{ \frac{3(\mu_c \cdot r)(\mu_o \cdot r)}{r^5} - \frac{(\mu_c \cdot \mu_o)}{r^3} \right\} \tag{16}$$

$\mu_c = \mu p'$ is the average magnetic moment of the c^{th} Cu ion, μ_o the nuclear magnetic moment of the proton and r the distance between the c^{th} Cu ion and the proton considered. The nuclear resonance ex-

periments on $CuCl_2 . 2H_2O$ [36] show that this salt is normally paramagnetic at liquid hydrogen temperatures (Fig. 11). In this temperature region the magnetic moment of the Cu-ion can be given in a reasonable approximation by the Curie-Weiss law:

$$\mu_c = \frac{\mu^2 H_0}{k(T - \Theta)} \tag{17}$$

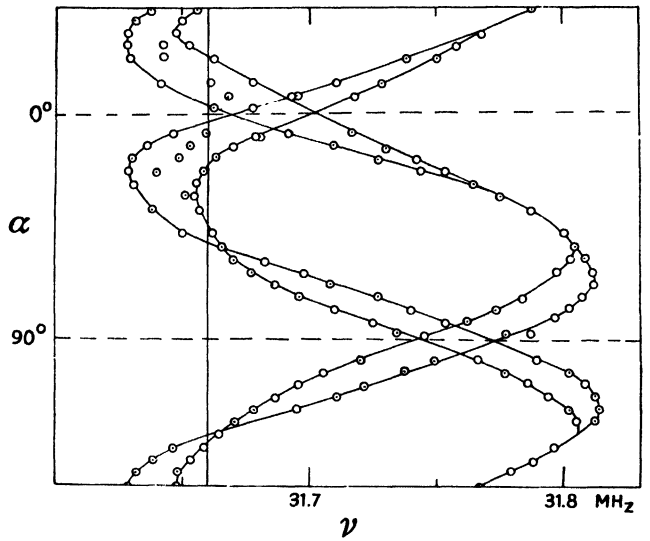

Fig. 11. Resonance diagram for H_0 in the *ab*-plane. $T = 14.3°K$. The resonance line for the protons in water is found at $\nu_0 = 31.66$ MHz. The *a*-and *b*-axes are shown by the dashed lines at $\alpha = 0°$ and $\alpha = 90°$.

Below the Néel temperature the number of lines in the resonance diagrams is doubled (eight) and these diagrams have a striking symmetry about the central proton resonance line in water (see Fig. 12). The symmetry of the resonance diagram of Fig. 12 can be understood by assuming that the Cu-ions are devided in two sublattices with antiparallel spin directions. The resonance diagram shown in Fig. 12 is for the case when the field H_0 of about 1700 Ø is rotated in the *ab*-plane of the crystal. In this relatively weak field, the Cu spins remain directed along the + or — *a*-axes regardless of the direction of the magnetic field. This leads to resonance diagrams with a period of 360°. In Fig. 13 is shown the resonance diagram for $H_0 \doteq 9000$ Ø also for the *ab*-plane of the crystal. This field is above the threshold field in the

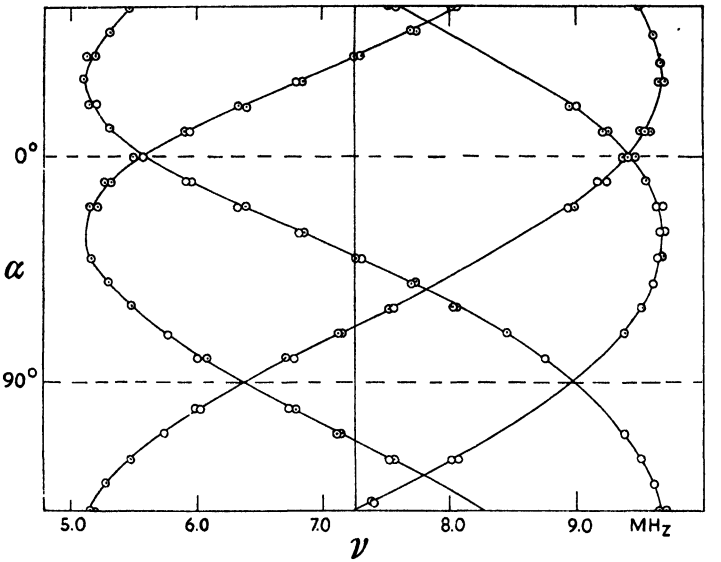

Fig. 12. Resonance diagram for H_0 rotating in the ab-plane. $T = 3.44°K$. The resonance line for the protons in water is found at $\nu_0 = 7.26$ MHz. In the diagrams the a- and b-axes are shown by the dashed lines at $\alpha = 0°$ and $\alpha = 90°$.

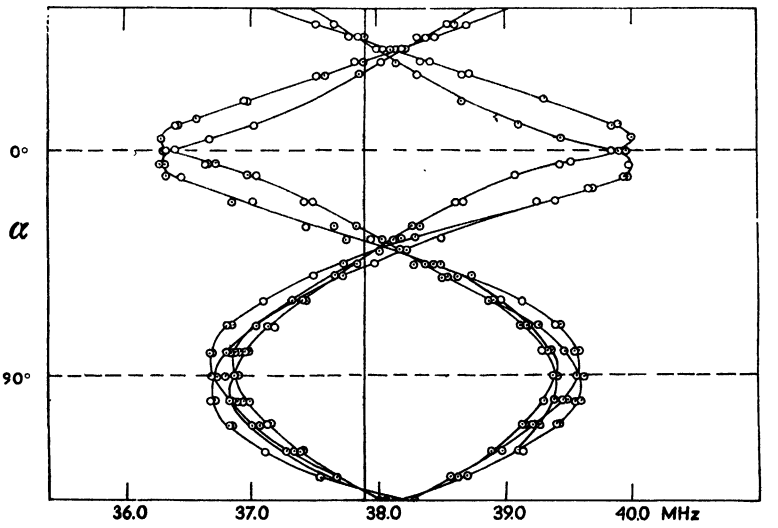

Fig. 13. Resonance diagrams for H_0 rotating in the ab-plane. $T = 3.69°K$. The resonance line for the protons in water is found at $\nu_0 = 37.91$ MHz. In the diagram the a- and b-axes are shown by the dashed lines at $\alpha = 0°$ and $\alpha = 90°$.

a direction and the period of the resonance curves has changed to 180°. This double period is caused by the fact that in these stronger fields the antiparallel Cu magnetic moments rotate with the external magnetic field H_0, but remain approximately perpendicular to it.

In § 2 we have mentioned that the gradual rotation of the spins in the neighbourhood of the threshold field may be calculated and then, making use of (15) and (16), it is possible to calculate the resonance diagram if the spatial arrangement of the magnetic ions and the nuclei is known.

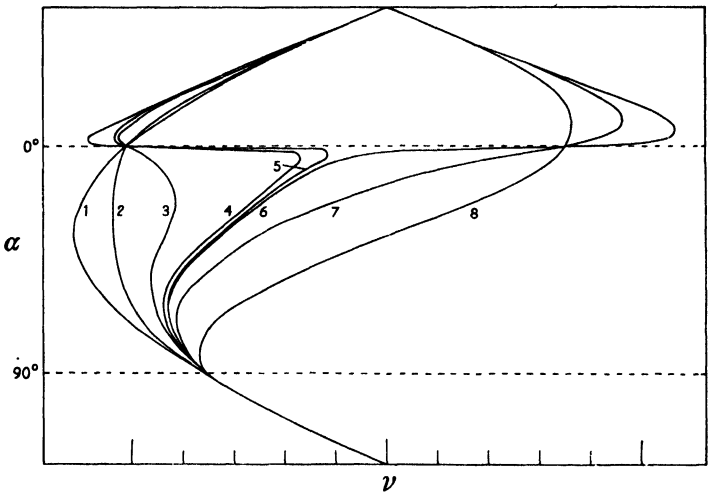

Fig. 14. Shape of the calculated resonance diagrams, for different values of the magnetic field H_0. 1: $H_0 = 0$ ø; 2: $H_0 = 4170$ ø; 3: $H_0 = 5970$ ø; 4: $H_0 = 7400$ ø; 5: $H_0 = 7440$ ø; 6: $H_0 = 7480$ ø; 7: $H_0 = 8900$ ø; 8: $H_0 = \infty$.

Fig. 14 shows the calculated curves for different values of H_0 for a threshold field of about 7460Ø. The experimental curves just behave as shown in this figure. The change in character of the curves takes place over a certain region about the threshold field, which reduces the accuracy in the determination of H_{th} to about 7 Ø. The experiments [37] show that this threshold field increases with temperature (Fig. 15).

In order to test equation (11) one should like to know p_x' as a function of temperature. It is also possible to derive this quantity from proton resonance observations [38].

The splitting Δ of the lines is proportional to H_d and, in a given spatial arrangement and orientation of the spins, H_d is proportional to

μ_c and thus to the p's. The splitting Δ is thus proportional to p' and p''. In Fig. 16 we plot Δ, which is thus proportional to p', as a function of T for two directions of T for two directions of the field and for $H_0 =$ 1640 Ø. ($H_0 // a$-axis and $H_0 // b$-axis). Apart from a multiplicative factor the two curves are found to be identical. Fig. 2 determined by (4) gives the dependence of p' on T according to the molecular field theory for $H_0 = 0$. The relatively small value of H_0 used must influence the curve only little. Nevertheless the two curves differ considerably. The most striking difference is found near the Néel temperature and can be more clearly seen in Fig. 17, where p'^2 is given as a function of T. The experimental curve approaches the temperature axis perpendicularly at a Néel temperature of 4.33°K, while according to (4) one should find a finite slope. However, in this region H_0 is no longer very large compared to the molecular field $2 \alpha \mu$, so that the interpretation of this result is rather unsure.

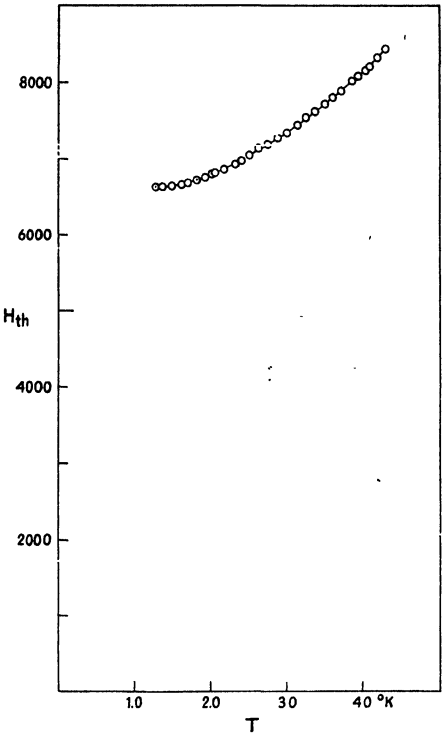

Fig. 15. The measured threshold field strength H_{th} versus temperature T.

On the low temperature side the curve approaches saturation more rapidly than the spontaneous magnetization in ferromagnetism. While in ferromagnetism the approach goes $\sim T^{3/2}$, we find here at least a fourth power of T or even an exponential approach. This seems to be in agreement with the spin wave theory for an anisotropic exchange [39].

An attempt to calculate the absolute value of Δ at $T \to 0$ has led to an average moment of the Cu ion of the order of 1 Bohr magneton. The calculation of this value of $\mu p'$ is only possible with the knowledge of a) the position of the protons in the elementary cell and b) the spin orientations of the various surrounding Cu ions. This knowledge can be obtained from the positions of the maxima of the different resonance

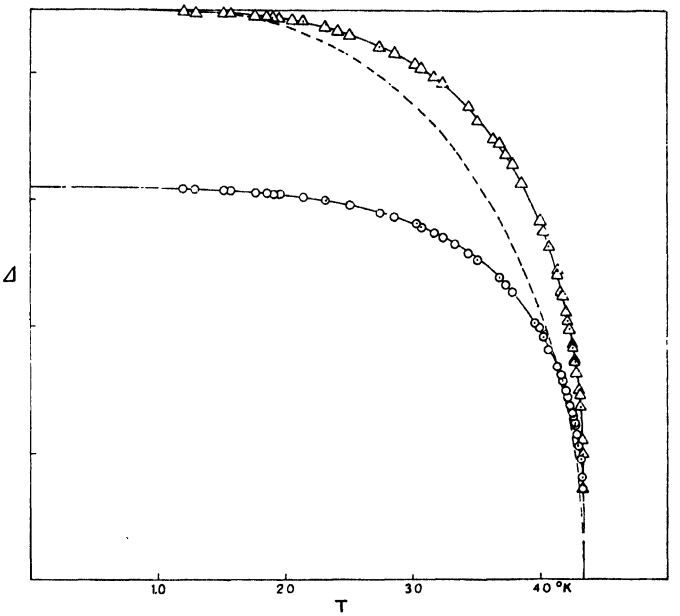

Fig. 16. The splitting △ between the extreme resonance lines as a function of the temperature T. △ Curve for H_0 parallel to the a-axis ○ Curve for H_0 parallel to the b-axis. The dashed line shows the curve according to (4) as shown in fig. 2a, fitted at $T = 0°K$ and $T = T_N°K$ to the curve with H_0 parallel to the a-axis.

diagrams with H_0 rotating in the ab- and the bc-planes of the crystal, for the paramagnetic as well as the antiferromagnetic state. It was deduced that in each layer parallel to the ab-plane the Cu ions have their spins parallel, while in adjacent layers they are oppositely oriented.

The insertion of H_{th} and p' in (11) leads to a reasonable dependence of the χ 's on temperature which also agrees with the preliminary measurements.

5. Specific Heat

According to the molecular field theory the decrease of the spontaneous magnetization with temperature should be accompanied by an extra contribution to the specific heat which should vanish at the Néel temperature, thus giving rise to a jump in the specific heat at that temperature. If we accept the equation (3) for the energy we obtain for this extra contribution to the specific heat per gramatom:

$$c_e = RT_N p_k' (dp_x'/dT) \tag{18}$$

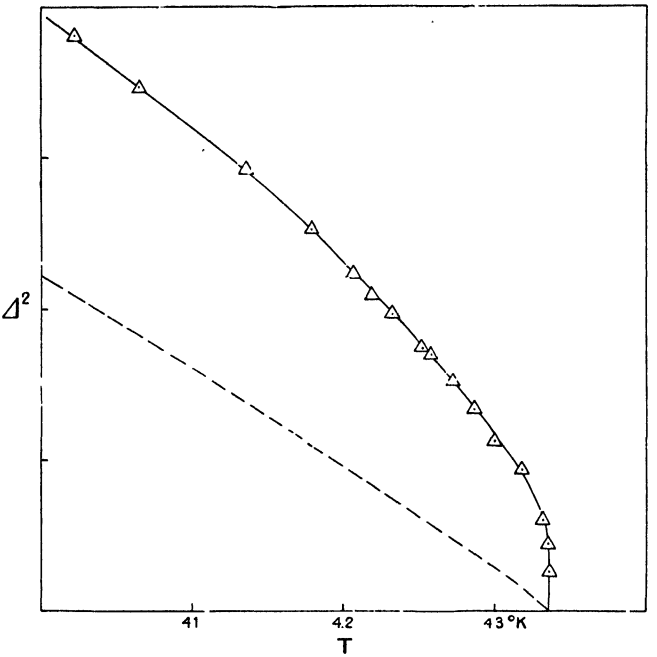

Fig. 17. Δ^2 as a function of the temperature T for H_o parallel to the α-axis. The dashed line shows the curve according to (4) for $\hat{p}'^2$ fitted at $T = 0$°K and $T = T_N$°K.

which in fact is a function of T/T_N (see Fig. 18). The total entropy content of the extra contribution should be R ln 2. The jump in c_e at T_N should be $\frac{3}{2}R = 12.4$ joule/mol, which value, of course, should increase if the lowest energy has a higher than two-fold degeneracy ($S > \frac{1}{2}$).

Experimentally this anomaly in the specific heat has been observed in a number of cases and the order of magnitude of the jump agrees in general with that expected [40]. Since the specific heat is not a crystalline property in the restricted sense of the word, we shall not go into a discussion of many data, but will confine ourselves to some remarks on the $CuCl_2 \cdot 2H_2O$ data [24] reproduced in Fig. 18, which have the advantage that because of the low temperatures used, the specific heat of the grating is only a small correction.

It is seen that at temperatures above T_N a tail of the specific heat is observed which approximately is inversely proportional to T^2 and which contains presumably about 35% of the entropy R ln 2. A somewhat similar tail was found in $MnCl_2 \cdot 4H_2O$. This tail must be due to

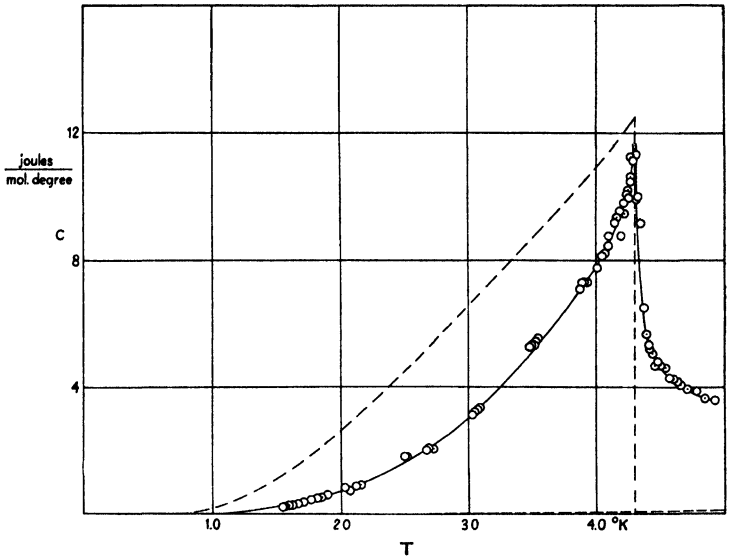

Fig. 18. Specific heat of $CuCl_2 \cdot 2H_2O$ as a function of temperature in comparison with the theoretical curve derived from (18) using p_x' derived from (4). The dashed line near the temperature axis gives an evaluation of the lattice contribution to the specific heat.

a persistance of a short range order above the Néel temperature, a persistance which we should expect in all order-disorder transformations, but which is neglected by the formalism of the molecular field theory. According to Van Vleck [41] we should find in the paramagnetic state a specific heat, due to exchange interaction, which approximately corresponds to the high temperature part of the tail mentioned.

6. Antiferromagnetic Resonance

Paramagnetic resonance is quite analogous to nuclear magnetic resonance which, in the investigations described in § 4, is used as a tool to investigate antiferromagnetism. The nuclear spins have merely been replaced by electronic spins and the nuclear γ by the electronic γ whose order of magnitude is 10^3 times larger. For separate spins the quantum condition, fixing the component of the spin in the direction of the field, defines a small number of equidistant energy levels.

Equating the difference between adjacent levels to $h\nu$ gives again the resonance condition (14). According to the usual selection rules only the component of the high frequency field which is perpendicular

to the constant field provokes transitions between the adjacent energy levels.

Now Bloch [42] has emphasized that classical treatment of the same problem does not only lead to the same resonance condition, but also gives the phases of the magnetizations induced by the high frequency magnetic field. In this treatment the equations of motion are written down for a magnetic top in a magnetic field which may have oscillating as well as constant components. It is valid for a large number of equal independent spins and it is the basis for the understanding of many details in the investigation of nuclear magnetic resonance and paramagnetic resonance. Kittel [43] and Van Vleck [44] have emphasized that it may easily be extended to the case of a strong interaction between the spins. In ferromagnetism the average interaction between the spins and their neighbours is described by the introduction of a molecular field, which acts like a magnetic field. But this molecular field, oriented exactly opposite to the average spin, does not contribute to the vector product of spin and field which occurs in the equation of motion. In the antiferromagnetic case on the other hand, the influence of the molecular field is not zero since it is determined by the spins of the other sublattice.

On the basis of the treatments of Gorter and Haantjes [17] applicable at all external fields at $T = 0$ and of Yosida [16, 45] applicable at relatively small fields and up to the Néel temperature, Ubbink [23, 30] and Yosida [16] have discussed antiferromagnetic resonance in a rhombic crystal. They replace the constant field by a magnetic field containing an oscillating term and calculate the resonance frequencies.

The results are rather complicated. Ubbink [3] has described the surface in the space of the magnetic field vectors on which the resonance condition is fulfilled for several frequencies. Fig. 19 gives four stages at relatively low frequencies while Fig. 20 gives the resonance frequency as a function of a magnetic field oriented in the direction of preference. At a relatively low frequency we expect resonance at magnetic fields somewhat below and above the threshold field H_c and moreover at a field somewhat below $2\alpha\mu$. Above $2\alpha\mu$ we have only resonance at a very high frequency near the normal paramagnetic resonance frequency. Attempts to calculate the intensity and polarization of the absorption lines recently also led to success.

Experimentally the magnetic resonances at microwave frequencies are usually studied by observing the quality (Q) factor of a cavity in

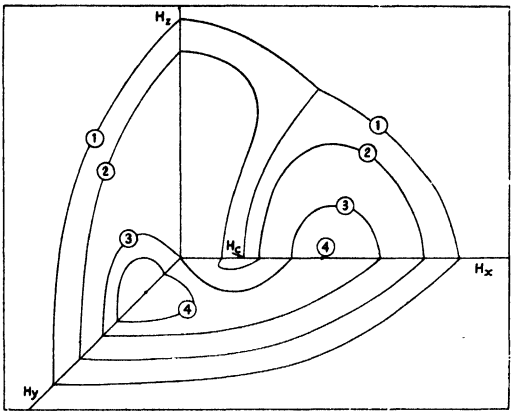

Fig. 19. The resonance surfaces in the H vector space for four different frequencies according to Ubbink.

which a small crystal has been inserted. This Q factor is then measured either by transmission or by reflection of a signal of constant frequency as a function of a magnetic field which is slowly varied.

Apart from the case of $CuCl_2 . 2H_2O$ no resonances have been observed in antiferromagnetic substances. It is clear that this negative result should be expected in powders in view of the strong dependence on the orientation of the field with respect to the crystalline axes. That no results were obtained in single crystals as e.g. MnF_2 is pro-

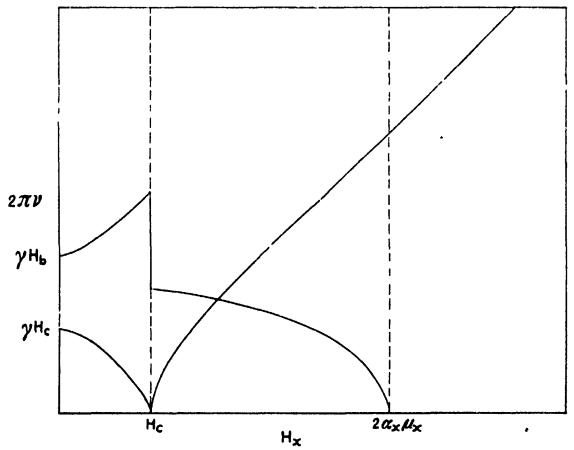

Fig. 20. Resonance frequency as a function of the field H_x in the x-direction.

bably due to the fact that neither frequencies nor the fields could be made sufficiently large.

The experimental results on $CuCl_2 . 2H_2O$ [46] are in excellent agreement with the theories. Fig. 21 shows the resonance fields at 9400

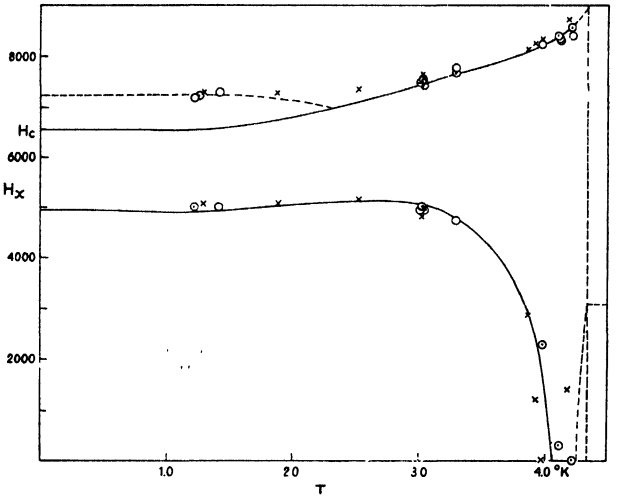

Fig. 21. Position of the resonance fields in the x-direction versus temperature for two different crystals. $\nu = 9400$ MHz.

megahertz as a function of T which are in good agreement with Yosida's formulae. In the immediate neighbourhood of the Néel temperature the phenomena are quite complicated and we shall not dwell upon them. Provisional data obtained at 4300 and recently also 34000 megahertz also agree with the theoretical expectations.

7. A Few Other Data

In this section we shall mention a few other aspects of antiferromagnetism. Since their experimental study has usually been carried out on powdered samples and not particularly at low temperatures we shall refrain from going into great detail.

In § 1 we mentioned that Néel [18] introduced interactions between different sublattices. In particular Anderson [14] has stressed that this is connected with the different – often even opposite – character of the interactions between neighbouring ions and between next nearest neighbours in the crystalline lattice. The ratio $-\Theta/T_N$ must be expected to depend greatly on the way in which the lattice of the mag-

netic ions is split into sublattices. However, the analysis of $-\Theta/T_N$ values is only a rough and unsure way to determine antiferromagnetic structure.

In § 4 we stated that the antiferromagnetic structure of $CuCl_2 . 2H_2O$ had been deduced from the proton magnetic resonance data. However, a method of more general application makes use of neutron diffraction.

In neutron diffraction experiments the very intense neutron beams emanating from fission piles are used. A monochromatic beam – with a wavelength of the order of 1 Å — may be obtained by diffraction on a suitable single crystal. This beam then falls on the antiferromagnetic powder to be studied. The scattering of the neutrons in this powder is partly due to short range interaction with atomic nuclei and partly to interaction between the neutron spin and the magnetic spins of the atoms. This latter interaction is dependent on the orientation of the atomic or ionic spins. It is for this reason that the existence of magnetic sublattices gives rise to extra lines in the Debije-Scherrer diagram of the neutrons. From the character and intensities of those lines one may derive the structure of the antiferromagnetic sublattices, the orientations of the spins in the sublattices and finally also the degree of order. A considerable number of antiferromagnetic substances have already been investigated by this new method and important conclusions have been drawn from them [47]. The method is not particularly successful in the determination of the Néel-point at which the last trace of long range order disappears. As a matter of fact short range order persisting above the Néel point also gives rise to diffuse diffraction bands.

Upon the appearance of an antiferromagnetic sub-structure the crystalline lattice changes its symmetry properties and this may have several consequences. By means of X-ray diffraction Rooksby and Tombs [48] have shown that tetragonal or rhombohedral symmetries may occur at substances as MnO, FeO and NiO which have a cubic face centred arrangement above the Néel temperature. Also anomalous changes of the crystalline parameters without change of lattice type [49] and changes in the elastic constants [50] have been observed. These effects are small and therefore not of great precision. Also their theoretical analysis is thus far lacking.

8. Final Remarks

The number of pure antiferromagnetic substances is much larger

than the corresponding number of ferromagnetics. Since moreover, antiferromagnetism is a new domain of research and has many different aspects one has the impression that very much work remains to be done. In particular antiferromagnetic resonance has just been discovered and studied in one substance only. Magnetic relaxation phenomena have not yet been studied at all while the different small elastic and mechanical effects and the hysteresis have also received little attention so far. The transition to paramagnetism under the influence of a strong field is an interesting subject for low temperature research.

The fact that the interaction energies $\propto \mu^2$ in $CuCl_2 . 2H\,O$ differ relatively so very much less than the magnetic moments μ for different directions, seems to confirm the opinion that the interaction is due to nearly isotropic exchange between spins, the description of which using a molecular magnetic field concept is only formal.

The sharpness of the proton resonance lines indicates that the sublattices do not interchange positions within less than 10^{-4} seconds, a result which is not self-evident and which cannot easily be obtained in another way. It appears, however, that in the antiferromagnetic state, the magnetic moments of each of the Cu-ions reverse in a much shorter time than the nuclear relaxation time t_2.

The problem of determining the completeness of saturation at $T = 0$ and in which way this saturation is approached is also not yet solved. The exact behaviour at the Néel point T_N where the long range order changes into short range order is experimentally as well as theoretically unclear. The behaviour in the region above T_N where we find a tail in the specific heat and marked deviations from the Curie-Weiss law deserves thorough investigation. This is apparently connected with the 40% difference between the Néel temperature, as derived by the molecular field picture from the susceptibility at $T = 0$, and the real Néel temperature though the discrepancy may be decreased somewhat if we suppose that we do not have complete saturation at $T = 0$. The problem here is to find a satisfactory description of an order-disorder transition which is complicated by the desire to establish a connection with the spin wave picture on the low temperature side. Anyhow one may assert that $CuCl_2 . 2H_2O$ presents so far the most intensively studied order-disorder transition.

REFERENCES

[1] P. Weiss, J. Phys., (4), **4**, 661 (1907); Ann. Phys., (10), **17**, 97 (1932).
[2] W. Heisenberg, Phys. Z., **49**, 619 (1928).
[3] Théoridès, J. de Phys. et le Rad., **3**, 1 (1922).
[4] H. R. Woltjer, Comm. Leiden, No. 173b; Proc. kon. Akad. Wet. Amsterdam, **28**, 536 (1935). H. R. Woltjer and H. Kamerlingh Onnes, Comm. Leiden, No. 173c; Proc. kon. Ak. Wet. Amsterdam, **28**, 544 (1925); Cf. H. Bizette, Thèses, 1946, Paris.
[5] O. N. Trapeznikowa and L. W. Schubnikow, Phys. Z. Sow. Union Charkow, **7**, 66 and 255 (1935); O. Trapeznikowa, L. W. Schubnikow and G. Miljutin, Phys. Z. Sow. Union Charkow, **9**, 237 (1936).
[6] L. Néel, Ann. Physique, (10), **18**, 5, (1932); (11), **5**, 232 (1936).
[7] H. A. Kramers, Physica, **1**, 182 (1933) and **18**, 101 (1952); L. Hulthén, Proc. kon. Akad. Wet. Amsterdam, **39**, 190, (1936) and Arkiv Mat. Astron. Fysik, A **26**, No. 11 (1938).
[8] P. W. Anderson, Phys. Rev., **86**, 694 (1952).
[9] R. Kubo, Phys. Rev., **86**, 929 (1952); R. Kubo, Rev. Mod. Phys., **25**, 344 (1953).
[10] J. R. Tessman, Phys. Rev., **88**, 1132 (1952).
[11] Yin Yuang Li, Phys. Rev., **84**, 72 (1951); cf. B. S. Gourary, R. W. Hart, Phys. Rev. **95**, 676, (1954).
[12] F. Bitter, Phys. Rev., (2), **54**, 79 (1937).
[13] J. H. Van Vleck, J. chem. Phys., **9**, 85 (1941).
[14] P. W. Anderson, Phys. Rev., (2), **79**, 705 (1950).
[15] T. Nagamiya, Prog. theor. Phys., **6**, 342 (1951).
[16] K. Yosida, Prog. theor. Phys., **7**, 25 (1952).
[17] C. J. Gorter and J. Haantjes, Comm. Leiden Suppl., No. 104b; Physica, **18**, 285 (1952).
[18] L. Néel, Ann. Physique, (12), **3**, 137 (1948).
[19] M. Griffel and J. W. Stout, J. Am. chem. Soc., **72**, 351 (1950).
[20] J. W. Stout and L. M. Matarrese, Rev. Mod. Phys., **25**, 338 (1953).
[21] N. J. Poulis, Proc. int. Conf. Low. Temp. Phys. Oxford, 162 (1951); Thesis, 1952, Leiden; N. J. Poulis, J. v. d. Handel, J. Ubbink, J. A. Poulis and C. J. Gorter, Phys. Rev., **82**, 552 (1951).
[22] J. v. d. Handel, Proc. int. Conf. low Temp. Phys., Oxford, 161 (1951).
[23] J. Ubbink, Proc. int. Conf. low Temp. Phys., Oxford, 163 (1951); Thesis, 1953, Leiden.
[24] S. A. Friedberg, Comm. Leiden, No. 289d; Physica, **18**, 714 (1952); ibid **18**, 320 (1937).
[25] cf. S. A. Friedberg and J. D. Wasscher, Comm. Leiden, No. 293c; Physica, **19**, 1972 (1953).
[26] C. G. B. Garrett, Proc. Phys. Soc. A, **63**, 1042 (1950); Proc. Roy. Soc. A., **206**, 242 (1951).
[27] K. Yosida, Prog. theor. Phys., **6**, 342 (1951).
[28] J. H. Van Vleck, J. chem. Phys., **9**, (1941), 85.
[29] L. Néel, Ann. Phys., (11), **5**, 232 (1936).
[30] J. Ubbink, Comm. Leiden Suppl. 105c; Physica, **19**, 919 (1953).
[31] T. van Peski-Tinbergen and C. J. Gorter, Comm. Leiden, no. 109a; Physica **20**, 592 (1954).
[32] L. Néel, Proc. Kyoto Conf. on theor. Physics, 1953.
[33] J. van den Handel, H. M. Gijsman and N. J. Poulis, Comm. Leiden, 290c; Physica, **18**, 862 (1952).

[34] G. E. Pake, J. chem. Phys., **16**, 327 (1948).
[35] N. Bloembergen, Comm. Leiden, No. 280c; Physica, **16**, 95 (1950), N. J. Poulis, Comm. Leiden, No. 283a; Physica, **17**, 392 (1951).
[36] N. J. Poulis and G. E. G. Hardeman, Comm. Leiden, No. 287a; Physica **18**, 201 (1952); Commun. 288b; Physica, **18**, 315 (1952).
[37] N. J. Poulis and G. E. G. Hardeman, Comm. Leiden, No. 294a; Physica, **20**, 7, (1954).
[38] N. J. Poulis and G. E. G. Hardeman, Comm. Leiden, No. 291d; Physica, **19**, 391 (1953).
[39] J. R. Tessmann, Phys. Rev., **88**, 1132 (1952).
[40] J. W. Stout and E. Catalano, Phys. Rev., 92, 1575 (1953).
[41] J. H. van Vleck, J. chem. Phys., **5**, 320 (1937).
[42] F. Bloch, Phys. Rev., (2), **70**, 460 (1946).
[43] C. Kittel, Phys. Rev., (2) **71**, 270 (1947); **73**, 155 (1948).
[44] J. H. van Vleck, Phys. Rev., **78**, 266 (1950); Physica, **17**, 234 (1951).
[45] K. Yosida, Progr. theor. Phys., **6**, 691 (1951).
[46] J. Ubbink, J. A. Poulis, H. J. Gerritsen and C. J. Gorter, Comm. Leiden, No. 288d; Physica, **18**, 361 (1952).
[47] C. G. Shull and J. S. Smart, Phys. Rev., **76**, 1256 (1949); C. G. Shull, E. O. Wollan and W. C. Koehler, Phys. Rev., **84**, 912 (1951).
[48] N. C. Tombs and H. P. Rooksby, Nature, **165**, 442 (1950).
[49] A. I. Snow, Rev. Mod. Phys., **25**, 127 (1953).
M. Foëx, Comptes Rendus, **227**, 193 (1948).
[50] R. Street and B. Lewis, Nature, **168**, 1036 (1951).

CHAPTER XIV

ADIABATIC DEMAGNETIZATION

BY

D. DE KLERK AND M. J. STEENLAND
KAMERLINGH ONNES LABORATORIUM, LEIDEN

1. Introduction

The technical methods of low temperature physics applied in the region below 1°K are widely different from those used above 1°K. The technique for the region above 1°K has been standardized many years ago: A liquefied gas is used as thermostat liquid. Different liquids are in use for different regions of temperatures (e.g. methylchloride, ethylene, methane, pentane, nitrogen, oxygen, hydrogen, neon, helium). The temperature is kept constant to a desired value by adjusting the vapour pressure over the liquid and the measurement of temperature is based on the gas thermometer.

For the region below 1°K completely different methods had to be developed. No suitable liquid is available and since the vapour pressures of all gases are too low for accurate measurements it is impossible to use a gas thermometer.

Though there are other methods of penetrating into this region (adiabatic magnetization of a superconductor, forcing liquid helium II through very narrow slits or holes) the method used in practice is the adiabatic demagnetization of a suitable paramagnetic salt. This method was proposed independently by Debije [1] and Giauque [2] in 1926 and the first experimental results were obtained in 1933 and 1934 by De Haas and Wiersma [3] in Leiden, by Giauque and McDougall [4] in Berkeley and by Kurti and Simon [5] in Oxford. By now it is used as a standard technique in many European and American low temperature laboratories. Temperatures down to 0.01°K can be easily obtained and even temperatures of the order of 0.001°K have been reached.

The method of adiabatic demagnetization consists of two stages: First an isothermal magnetization of the paramagnetic salt at the lowest temperature that can be obtained with liquid helium (referred to here as the "high" or "initial" temperature); then an adiabatic demagnetization of the salt. During the isothermal magnetization the paramagnetic ions of the crystalline lattice (which in the absence of a magnetic field are considered as free and independent so that their spatial orientation is random) are partly oriented parallel to the field. In this way the amount of order in the salt is increased, hence the entropy is diminished and a flow of heat from the sample to the surrounding liquid helium bath results. During the subsequent adiabatic demagnetization the entropy of the salt remains constant at the low value (assuming that the demagnetization is a reversible process) and a final state is obtained where the entropy is lower than at the initial temperature in zero field and hence the temperature is lower.

A first estimation of the temperatures that can be reached by the method can be obtained from the following considerations: If the angular momentum of the paramagnetic ions is $J\hbar$ (and hence the magnetic moment is $g\,J\,\mu_B$ where μ_B is the Bohr magneton and g the Landé factor) the ground level, in the absence of a magnetic field, is $(2\,J\,+\,1)$-fold degenerate and the entropy of the salt is R ln $(2\,J\,+\,1)$ per mole (here the entropy due to the lattice vibrations is neglected, but in most practical cases this gives rise to only a small correction.) When the field is switched on isothermally the ground level is split up into $2\,J\,+\,1$ equidistant levels and the ions are distributed over them according to Boltzmann's law with a consequent decrease of entropy.

It is obvious that the $(2\,J\,+\,1)$-fold degeneracy in the absence of an external field cannot persist until the absolute zero of temperature. Some kind of interaction force must act on the magnetic ions by which the entropy is reduced to zero at zero degree K. In other words the $(2\,J\,+\,1)$-fold degeneracy cannot be complete, but a small splitting due to the interaction forces will remain, even in the absence of a magnetic field. If, however, the remaining overall splitting is small as compared with kT at the initial temperature the levels are still equally populated in zero field, and the influence on the entropy is small.

If after the isothermal magnetization the field is decreased adiabatically and if the distances between the levels remain proportional

to the field, then the Boltzmann distribution of the ions over the levels remains the same, the magnetic moment is constant, and the temperature falls proportionally to the field. In low fields the interaction forces become of the same order as the external field strength, the level distances are no longer proportional to the field, and the ions are redistributed over the levels in such a way that the entropy is kept constant. The temperature in zero field depends finally on the ion distribution in zero field, hence on the level scheme which in turn is determined by the interaction forces. In general the level splitting is the smaller (and the final temperature the lower) the weaker the interactions are. For this reason it is obvious that the knowledge of the exact position of the energy levels of a paramagnetic salt is of prime importance and has been a subject of thorough investigation for many years. The interactions occurring in a paramagnetic salt can have different origins: Stark splitting caused by electric fields due to usually non-magnetic surrounding atoms; magnetic coupling between the ions (either dipole or exchange interaction); or hyperfine structure splitting. For further discussion we refer to Chap. XII.

If a relaxation time of finite length should be involved in the above mentioned level transitions the entropy cannot be constant. The demagnetization is no more a reversible (quasistatic) process and the final temperature is higher than in the case of a strictly isentropic demagnetization. Throughout this chapter we will assume that the demagnetization is purely reversible.

If the level splitting in zero field is small compared with kT so that the levels are equally occupied the magnetic moment of the salt, for not too large values of H/T, obeys Curie's law:

$$M = C\,H/T.$$

If kT becomes of the order of the level splitting this is no longer true. Hence one can say, generally speaking, that the process of adiabatic demagnetization can reduce the temperature of a salt down to a region where the deviations from Curie's law become appreciable. Thus the salts most suitable for adiabatic demagnetization are those which obey Curie's law down to as low a temperature as possible.

Let us finally consider the demagnetization process from a thermodynamic point of view. The laws of thermodynamics applied to a substance in a magnetic field may be expressed in two ways:

$$TdS = dU + MdH, \tag{1}$$

$$TdS = dU' - HdM, \tag{2}$$

where $U' = U + HM.$

Here T is the temperature, S the entropy, M the magnetic moment and H the field. It is completely arbitrary whether U or U' is considered as the internal energy of the salt; this depends only on whether one wants to include MH (the energy due to the simultaneous presence of sample and magnet) into the energy of the salt or of the magnet. If one calls one of them the energy, the other one may be considered the magnetic analog of the enthalpy.

Something similar is true about the exact definition of H. We define the external field, H_E, as the field of the magnet in the absence of the paramagnetic salt, and the internal field, H_I, as the field inside the sample, hence:

$$H_I = H_E - \varepsilon M/V.$$

Here M/V is the magnetic moment per cubic centimeter and ε the demagnetizing factor of the sample. Both H_I and H_E may be inserted in (1) or (2) the difference being a term $\frac{1}{2}\varepsilon M^2/V$ in the internal energy. H_E is used in most practical cases for reasons of convenience.

The susceptibility χ can be defined in several ways: as M/H, as $(\partial M/\partial H)_T$ or as $(\partial M/\partial H)_S$ where, again, H_I as well as H_E can be used for the magnetic field. Unless specified separately the definition of the susceptibility in this chapter is M/H_E.

The Eq. (1) and (2) are completely equivalent and it only depends on the problem under investigation which of the two is the more convenient. If we introduce the specific heats:

$$c_H = \left(\frac{\partial U}{\partial T}\right)_H = T\left(\frac{\partial S}{\partial T}\right)_H,$$

$$c_M = \left(\frac{\partial U'}{\partial T}\right)_M = T\left(\frac{\partial S}{\partial T}\right)_M,$$

application of the second law of thermodynamics to (1) and (2) gives:

$$TdS = c_H dT + T\left(\frac{\partial M}{\partial T}\right)_H dH, \tag{3}$$

$$TdS = c_M dT - T\left(\frac{\partial H}{\partial T}\right)_M dM. \tag{4}$$

A proof that adiabatic demagnetization produces a decrease of temperature follows most easily from (3). For a process at constant entropy we have:

$$c_H dT = -T\left(\frac{\partial M}{\partial T}\right)_H dH. \tag{5}$$

Since in ordinary paramagnetism $(\partial M/\partial T)_H$ is negative a negative dH entails a negative dT. (In some special cases, e.g. antiferromagnetism, $(\partial M/\partial T)_H$ may become positive and then demagnetization causes a heating effect.)

The course of temperature with the field during the demagnetization process follows from the integration of (5):

$$T - T_o = -\int_{H_o}^{H} \frac{T}{c_H}\left(\frac{\partial M}{\partial T}\right)_H dH$$

and since $T/c_H = (\partial T/\partial S)_H$ (see above) we have:

$$T - T_o = -\int_{H_o}^{H} \left(\frac{\partial M}{\partial S}\right)_H dH. \tag{6}$$

In many cases for relatively high fields this is equivalent to $H/T =$ constant, and for low fields to $T - T_{H=0} = \alpha H^2$.

The decrease of entropy during the isothermal magnetization can be derived from (4). It gives:

$$S(H = 0, T = T_i) - S(H = H_i, T = T_i) = \int_0^{M(H_i, T_i)} \left(\frac{\partial H}{\partial T}\right)_M dM, \tag{7}$$

where T_i and H_i are the initial temperature and field of the demagnetization. This entropy difference is equal to the difference in entropies at zero field between T_i and the final temperature T_f for which we may also write:

$$S\,(H = 0, T = T_i) - S\,(H = 0, T = T_f) = \int_{T_f}^{T_i} \frac{c_o}{T}\, dT, \tag{8}$$

where c_o is the specific heat in zero magnetic field. From (7) and (8) we have:

$$\int_0^{M(H_i,T_i)} \left(\frac{\partial H}{\partial T}\right)_M dM = \int_{T_f}^{T_i} \frac{c_o}{T} dT. \tag{9}$$

If the relations between M, H and T at the high temperature and between c_o and T in the low region are known we may calculate T_f for given values of H_i and T_i. The first relation is the magnetic equation of state at the initial temperature, which may be known from experiments at this temperature; the second relation depends on the scheme of energy levels of the salt mentioned before.

At the initial temperature we may often consider the magnetic ions of the lattice as free and independent. This proves to be equivalent to the condition that M is a function of H/T alone. In this case we have $(\partial H/\partial T)_M = H/T$, so that (9) can be written:

$$\int_0^{M(H_i,T_i)} \frac{H}{T} dM = \int_{T_f}^{T_i} \frac{c_o}{T} dT. \tag{10}$$

2. Description of Experimental Methods

As was mentioned in § 1 the technique of research in the demagnetization region meets some inherent difficulties not occurring in ordinary low temperature work.

The aim of research in this region is to cool down all kinds of materials to a well defined temperature below 1°K and to keep them there for a time long enough to allow investigations of their properties. Hence the apparatus for an adiabatic demagnetization experiment consists, generally speaking, of two fundamental parts: First the equipment necessary for the production, conservation and determination of the low temperature itself, and secondly that needed for cooling down the material under investigation with the paramagnetic salt and for making measurements on it. In some cases, for instance when the material under investigation is the salt itself, the apparatus can be relatively simple, but in other cases the typical difficulties in the region below 1°K may lead to a rather complicated set-up.

In this chapter we will treat the two parts of the apparatus separately. In the present section we deal only with the cooling of the paramagnetic salt and the determination of its temperature and magnetic properties; in § 5 we will discuss the cooling down of the other materials with the salt.

Let us first consider some of the technical requirements of the region below 1°K. The salt must be magnetized in thermal contact with a bath of liquid helium of as low a temperature as possible, it must then be demagnetized under adiabatic conditions, finally its temperature must be determined.

The heat capacity of a piece of paramagnetic salt of reasonable dimensions (e.g. 25 cm^3) is much smaller than that of a cryostat filled with liquid helium. Hence much more care must be given to the thermal insulation. Moreover when a liquid boiling under constant pressure is used as a thermal reservoir a heat leak causes only an evaporation at constant temperature and measurements on an immersed subject are not influenced. But in the case of a demagnetized sample a heat leak causes a rise of temperature. At relatively high temperatures the heat leaking in is distributed homogeneously over the sample, but at the lower temperatures (e.g. below 0.1°K) the heat conductivity of a salt becomes very low, hence considerable inhomogeneities in the temperature may be created within a short time. So it may happen that the heating up from the lowest temperature to that of the surrounding liquid helium takes many hours but that, due to an inhomogeneous heat leak, the time usable for investigations is only some minutes. It is often possible to eliminate the influence of the heat leak on the measurements by determining the course with time and extrapolating backwards to the moment of the demagnetization.

The temperature determination depends in most cases on the measurement of some magnetic property of the paramagnetic salt. Since this is usually carried out with an induction bridge which may be influenced by the presence of the magnet, this leads to the desirability that after the demagnetization the magnet and the cryostat should be separated and this usually entails some problems in the construction of the demagnetization set-up as a whole. This is certainly true if an iron magnet is used. In the case of an iron free coil magnet it was pointed out by Giauque [6]) that the separation is not strictly necessary. But even then the eddy currents in the magnet (both in the metal tubing and in the winding itself) may influence the bridge coils surrounding the salt. Since these eddy currents depend on the susceptibility of the salt itself sufficient elimination is difficult, especially if an a.c. bridge is used. Most investigators prefer separation also in the case of a coil magnet.

Now we will discuss the different parts of a demagnetization apparatus in some detail. An apparatus for the adiabatic demagnetization of a paramagnetic salt consists of the following essential parts:

(a) a cryostat filled with liquid helium, connected to a vacuum pump of high capacity so that the temperature of the helium can be kept as low as possible.

(b) a paramagnetic salt mounted in the cryostat in such a way that the thermal contact between the salt and the helium can be made and broken at will.

(c) a powerful electromagnet.

(d) a bridge network for the determination of the temperature.

a. CRYOSTATS

The technique of cryostats is different in different laboratories. In many places silvered glass dewars ase used, but some laboratories have metal cryostats. Since the starting temperature of the demagnetization must be as low as possible much care should be given to the protection of the helium against heat influx. Inserting radiation screens in the dewar or keeping the cap at nitrogen temperature is often desirable. Moreover, a powerful pumping installation is needed. A nice combination is a large rotary pump together with a high capacity oil ejector ("booster") pump.

The separation of the magnet and cryostat after the demagnetization presents a technical problem. If a relatively small Weiss magnet is used it is often mounted on rails and wheeled away after the demagnetization. If the magnet is large it is better to work with a movable cryostat. In Leiden and the Bureau of Standards the cryostat is suspended from a rotating arm. In this case the connections to the vacuum pump should be either flexible (e.g. with the help of ground joints or wide rubber tubing) or the pumps should move with the cryostat. Coil magnets are often mounted in such a way that they can be moved vertically.

b. SAMPLE TUBES

The thermal contact between the salt and the liquid helium is usually made and broken with the help of exchange gas. The salt is mounted in a sample tube in such a way that radiation from room temperature and heat conduction along the suspension are eliminated as well as possible. Isothermal conditions are achieved by admitting some helium

gas into the tube; for adiabatic conditions the gas is removed with a high vacuum pump.

The paramagnetic salt is usually in the shape of a sphere or a prolate spheroid, since only in these cases it is possible to account in a reasonable way for the influence of the demagnetizing field of the sample on the results of the magnetic measurements. The salt can be used as a single crystal ground in the desired shape, as a powder compressed to approximately the crystalline density, or as small crystals loosely packed in a container. It depends on the particular experiment which of the methods is the more useful: If the magnetic properties of the salt itself are investigated a single crystal may be advisable; if liquid helium must be cooled with the salt small crystals should be preferred; in the case of a heat contact between the salt and a metal a compressed pill is better. The salt should be protected against deterioration between subsequent helium runs. Covering a single crystal or a compressed pill with a thin layer of celluloid or glyptal is not absolutely effective. It is better to keep the sample at liquid nitrogen temperature between runs. It is not advisable to evacuate the sample tube at room temperature.

The sample tube may be made either of metal or of glass. A metal tube has the advantage that it can be easily dismantled if low melting solder is used, but the advantage of a glass container is that it shows no eddy currents and hence does not influence the magnetic measurements with an a.c. bridge. Glass containers must be well silvered or painted black with a material not cracking at low temperatures. This is important since even little holes in the silvering or painting may cause a serious heat leak due to radiation. It is possible to make a ground joint in a glass or metal sample tube. If they are carefully made and the proper grease is used they may be vacuum tight even when immersed in liquid helium II.

The sample inside the container may be mounted on a thin walled glass pedestal or suspended between taut fibres. Under extremely good conditions heat leaks of the order of one erg per minute have been found [7], but in general 50 ergs per minute must be considered as satisfactory. The heat conduction along the glass or fibres can be decreased by interrupting the suspension and mounting a piece of paramagnetic salt in between. Conduction through residual gas may be decreased by "baking out" the sample tube [7]. Sometimes an important source of heat influx is the vibration of the sample in the con-

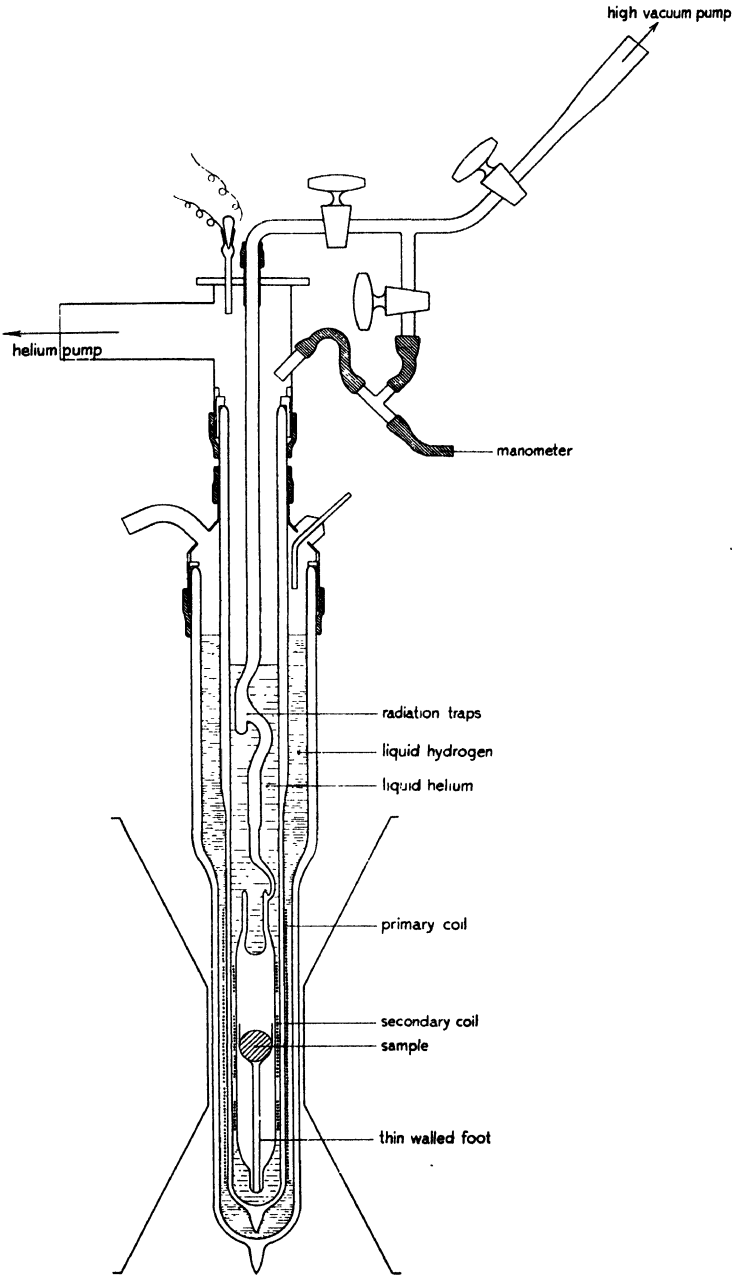

Fig. 1. Typical Leiden demagnetization cryostat, one fifth of real size.

tainer [8] especially if fibre suspension is used. It was found that even the vibrations due to the boiling of the mercury in a small diffusion pump may give a noticeable heat influx [9]. Increasing the number of fibres may sometimes decrease the heat leak [10].

In principle it is possible to make and break the thermal contact with the help of a superconductor. This method for the contact between a paramagnetic sample and the helium bath has only been used by Steele and Hein [91] so far. The method will be discussed in § 5.

c. MAGNETS

Two types of magnets are in use for adiabatic demagnetization experiments: (1) U-shaped iron core electromagnets, (2) iron free coil magnets. The fields easily obtained in ironmagnets are limited by the saturation to about 20 kilo oersteds. With a compactly wound iron free coil magnet the maximum field depends on the available energy and the cooling capacity of the installation. Fields of 100 kilo oersteds and more have been obtained.

In the case of an iron magnet the magnet itself is the expensive piece of equipment, since a motor generator is available in most laboratories and the cooling can be performed directly from the mains' water supply. In the case of a high energy coil magnet the coil can be constructed in the workshop of the laboratory, but now the power supply and the cooling installation are the complicated parts of the set-up.

The standard type iron magnet is the Weiss magnet, developed as long ago as 1907 [11]. With a magnet of moderate size consisting of about two tons of iron a field of 15 kilo oersteds can be easily obtained in a pole gap of 4 cm and at a power consumption of 15 kW. Very heavy magnets of this type were constructed at Leiden, Bellevue and Upsala (the last one has never been used for adiabatic demagnetization work). The Leiden magnet consists of about 10 tons of iron. Using 80 kW a field of 24 kilo oersteds can be obtained in a pole gap of 6 cm.

An improved Weiss magnet was constructed by Bitter [12]. Its weight is only two tons but it produces the same field as the Leiden magnet at an energy consumption of 20 kW. This seems to be due to the facts that the windings are located closer to the field space and the yoke is axially symmetrical around the poles.

The field in the centre of an iron free coil magnet [13, 14] can be expressed by:

$$H = G\sqrt{\frac{Wf}{\varrho r_i}},$$

where W is the power dissipated in the magnet, ϱ the resistivity of the coil material, r_i the inner radius of the coil and f the "filling factor", i.e. the volume occupied by the coil metal divided by the total volume of the winding space. G is a dimensionless factor depending on the shape of the winding space and on the distribution of the current density in it. The higher the value of G is the smaller is the homogeneity of the field. In a practical case the value of G should be adapted to the homogeneity requirements of the experiments.

d. BRIDGES

As we mentioned before the temperature determination depends usually on the measurement of some magnetic quantity of the salt, a so-called "thermometric parameter". Different parameters are used in different temperature regions. The quantities that have been used up to the present are the static susceptibility χ, the real and imaginary parts of the dynamic susceptibility χ' and χ'', and the remanent magnetic moment.

In a bridge method the susceptibility is derived from the self inductance of a coil or from the mutual inductance of two coils surrounding the salt. A self inductance may be determined with the Anderson bridge, mutual inductances are often measured with the Hartshorn bridge. Since at the present time most laboratories use mutual inductances we shall restrict ourselves to a description of the Hartshorn bridge. Both ballistic and a.c. bridges are in use. Giauque gave a description of a nice ballistic bridge [15]; the Leiden [16, 17] group developed a combination of a ballistic and a.c. bridge, which was recently improved by the Oak Ridge workers [18].

The principle of the Hartshorn mutual inductance bridge is the following: The coils surrounding the salt, M_1, are connected in series with another set of coils, M_2, which has a variable coefficient of mutual inductance. The connections are made in such a way that the secondary voltages due to a variation in the primary current have opposite signs. Now the mutual inductance of M_2 is set to such a value that the secondary voltages are exactly or approximately balanced. Either a null detector of a high sensitivity measuring device is used for the recor-

ding, the susceptibility being derived from the bridge setting and, eventually, the residual deflection.

For a ballistic bridge (Fig. 2a) the standard procedure is to equalize M_1 and M_2 approximately and to observe the residual deflection of a ballastic galvanometer. Remanence and hysteresis loops can be derived from a series of subsequent deflections. The swinging time of the galvanometer should be so short that a reasonable number of measurements can be taken in the first few minutes after the demagnetization but, on the other hand, so long that it is not of the same order of magnitude as the characteristic time of some relaxation phenomenon in the salt. The commercial "ballistic" galvanometers are too slow and not sufficiently sensitive. We found that a galvanometer with a full swinging time of five seconds is the fastest that can be read directly. If a faster galvanometer can be used photographic registration of the deflections [19] is a valuable aid.

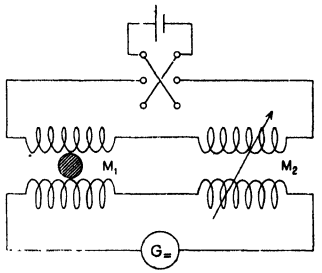

Fig. 2a. Ballistic mutual inductance bridge.

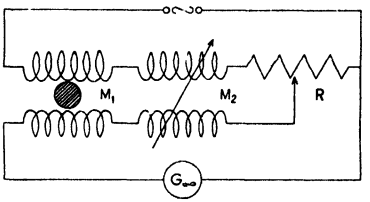

Fig. 2b. Alternating current mutual inductance bridge.

In the case of an a.c. bridge (Fig. 2b) the mutual inductance M_2 is continuously variable and balance is recorded with a null-instrument. Since in most cases the secondary voltages of M_1 and M_2 have not exactly opposite phases it is usually impossible to balance the bridge by varying M_2 alone. In other words, by adjusting M_2 the component in quadrature with the primary current can be balanced, but a small out of phase voltage is left. Since this voltage is in phase with the primary current it can be balanced by admitting a small voltage from the primary into the secondary circuit with the help of a potentiometer, R. The detector only has its zero position if both M_2 and R are set to the correct value. The occurrence of the out of phase component may be due to (1) eddy currents and capacities in the bridge network and the metal parts of the apparatus, (2) relaxation and hystere-

sis effects in the paramagnetic salt. In the latter case the setting of R is significant for the imaginary part of the dynamic susceptibility χ'', hence for the heat absorption per second by the paramagnetic salt from the alternating magnetic field of the primary coil of M_1. If the magnetic field is given by $H = h_o e^{i\omega t}$ the heat supply per unit time is equal to

$$\tfrac{1}{2} h_o^2 \, \omega \, \chi''. \tag{11}$$

For an a.c. bridge of high precision M_1 should consist of at least four decades and a continuous variometer. Since such bridges are not commercially available most experimenters construct their own networks. In the Leiden bridges the secondary coils are made of tenfold stranded wire. This has the advantage that the ten coils of one decade are identical with a high precision (a few parts in 10^4), but the disadvantage is that the capacitive coupling between the ten coils is not negligible, hence the bridge can only be used for low frequencies (up to about 500 Hz). This system was abandoned in the bridge recently constructed in Oak Ridge [18]. In this bridge all the coils were wound separately, the layers of different coils being kept well apart by polysterene sheet of 0.5 mm thick. Small trimming coils were needed for each of the individual coils in order to adjust the exact ratios, but the bridge could be used up to 16 kHz.

As a null detector a vibration galvanometer preceded by an amplifier can be used for the region between 20 and 500 Hz; headphones are useful for somewhat higher frequencies; a selective amplifier with an oscilloscope can be used in almost any frequency range. It might be useful to have the possibility of measuring the values of M_2 and R independently, especially at the lower temperatures where both χ' and χ'' become steep functions of temperature (and hence, during a heating up curve, functions of time). This could be done with two phase sensitive detectors tuned in such a way that one responds only to a variation in M_2 and the other only to a variation in R.

In most adiabatic demagnetization work the a.c. method must be preferred over the ballistic one: it is more surveyable, it works faster and higher precision can be obtained. The main disadvantage is that the whole apparatus inside the cryostat must be made of glass, since all metal parts give rise to eddy currents which influence the bridge settings. At the lowest temperatures, where the salt may have hysteresis effects the method gives valuable data on both χ' and χ'', but some-

times the heat absorption from the measuring field gives rise to a too rapid heating of the sample. In this case the ballistic method must be preferred which, moreover, gives information on the remanent magnetism and the hysteresis loop. The rate at which measurements can be taken may be increased noticeably by using a fast galvanometer with photographic registration as was mentioned before.

3. Absolute Temperature Determination

In § 1 it was pointed out that the salts most suitable for the adiabatic demagnetization process are the ones that obey Curie's law down to the lowest temperatures. For this reason one might be tempted to base the absolute temperature determination on this law. Hence the gas thermometer with the "perfect gas" should be replaced by a "perfect paramagnetic salt" and the temperature should be derived from the measured susceptibility, according to:

$$T = C\frac{H}{M} = \frac{C}{\chi}. \tag{12}$$

As was stated in § 1 no salt can obey Curie's law down to absolute zero and corrections must always be applied, the situation being more or less the same as that of a gas thermometer. In some cases the corrections can be founded on a theoretical basis, but sometimes they are completely empirical.

Thus C/χ is not the absolute temperature, but a quantity related to it by the true magnetic equation of state of the salt under investigation. Since a susceptibility measurement can be easily performed C/χ is a very suitable thermometric parameter (see § 2). It is called the "magnetic temperature" and is denoted [20] by T^*, hence

$$T^* = C\frac{H}{M} = \frac{C}{\chi}. \tag{13}$$

Close to 1°K the magnetic temperature is practically equal to the thermodynamic temperature, the difference becoming more and more pronounced the lower the temperature. At the very lowest temperatures they may become of different orders of magnitude and here T^* looses its meaning as a thermometric parameter for reasons that will be pointed out later.

The magnetic temperature provides only a preliminary scale. We

will discuss a few methods for the determination of the thermodynamic temperatures. For each method we will assume that the relation between the thermometric parameter and the entropy is known. This relation can be determined as follows. If we know how M depends on H and T at the initial temperature, the decrease in entropy during the isothermal magnetization can be calculated from (7). Hence from measurements of the parameter immediately after a number of demagnetizations the relation can be determined.

The first possible method is a theoretical evaluation of the influence of the crystalline electric field and the interactions between the magnetic ions on the magnetic moment of the sample [21, 22]. (It is equivalent to the calculation of the level scheme of the ions (see § 1 and also Chap. XII)). The results of these calculations can be checked experimentally if an expression for the internal energy can also be derived. Suppose we have the relations:

$$M = M\,(H, T) \quad \text{and} \quad U = U\,(H, T).$$

From these we may derive for the case of zero field:

$$\chi = \chi\,(T) \text{ or } T^* = T^*(T) \quad \text{and} \quad S = S\,(T). \tag{14}$$

Elimination of T gives:

$$S = S\,(T^*). \tag{15}$$

From this relation we know the entropy difference of the salt between the initial and final temperatures and this should be equal to the decrease of entropy during the isothermal magnetization. If these entropies check it is plausible that the theoretical considerations are correct, especially the $T^*(T)$ – relation. This method is essentially an application of (10) using T^* as a thermometric parameter. Usually theoretical relations of sufficient accuracy can only be derived if the deviations from Curie's law are relatively small.

A second method for absolute temperature determination is based on the measurement of magnetization curves. If the magnetic moment is measured as a function of the field on a number of isentropics the quantity $(\partial M/\partial H)_S$ can be calculated as a function of H and S. Garrett [23, 24] pointed out that if

$$M = \chi\,(T)\,H + \psi\,(T)\,H^3 + \ \ldots, \tag{16}$$

(where $\psi\,(T)\,H^3 + \ \ldots$ is due to saturation effects) then

$$\left(\frac{\partial M}{\partial H}\right)_S = \left(\frac{\partial M}{\partial H}\right)_{H=0} (1 - pH^2 + \ . \ . \ .). \tag{17}$$

In the case of an external field parallel to the measuring field

$$p = 3\left(\tfrac{1}{2}\,\Xi - \frac{\psi}{\chi}\right) \tag{18}$$

and in the case of the external field perpendicular to the measuring field

$$p = \tfrac{1}{2}\,\Xi - \frac{\psi}{\chi}, \tag{19}$$

where Ξ satisfies the relation

$$\Xi = \frac{1}{\chi}\left(\frac{\partial \chi}{\partial S}\right)_{H=0}\left(\frac{\partial \chi}{\partial T}\right)_{H=0}. \tag{20}$$

In formulae (16) . . (20) χ is defined as $(\partial M/\partial H)_{H=0}$. Now $(\partial M/\partial H)_S$ and $(\partial M/\partial H)_{H=0}$ are derived from the measurements hence, if ψ/χ is small or can be accounted for somehow, Ξ can be calculated. With the help of experimental values for $(\partial\chi/\partial S)_{H=0}$ one can derive $(\partial\chi/\partial T)_{H=0}$. From the relation between $(\partial\chi/\partial T)_{H=0}$ and χ we can integrate T at any point starting from a known temperature.

A third method, also based on the measurement of magnetization curves, is an application of (6). If M is known as a function of H and S the quantity $(\partial M/\partial S)_H$ can also be calculated as a function of H and S. Integration along an isentropic gives the temperature difference between any two points. Hence if T is known for one reference point of the isentropic it can be calculated for any other point.

The most obvious application is [25] the case where the reference temperature is the initial temperature and the temperature in zero field is calculated from the course of $(\partial M/\partial S)_H$ over the whole isentropic. If turns out, however, that the accuracy is only a few hundredths of a degree [6] making the method unsuitable for temperatures well below 0.1°K. Still it has some interesting applications: If the course of an isentropic can be predicted on a theoretical basis it can be checked by the experiment (see § 1). If the temperature in zero field can be derived from one of the other methods the variation of temperature in moderate fields can be determined and this may be of interest, for instance in the case of investigations on other substances where a magnetic field is required (e.g. superconductors).

The last method is based on Kelvin's definition of the absolute temperature:

$$\frac{dQ_1}{T} = \frac{dQ_2}{T}.$$

Since here ratios of temperatures are determined rather than differences the disadvantage of the foregoing method does not apply. If we consider a cycle with two isentropics very close together dQ/T at the high temperature is equal to the difference in entropy, dS, which is known from (7). Then we have

$$dQ = T\,dS, \tag{21}$$

where T is the low temperature and dQ the amount of heat which, if supplied in a reversible way at this temperature, corresponds to dS. Since we suppose that the relation between the entropy and the thermometric parameter is known (see above) the method consists of measuring the variation in the thermometric parameter when a known amount of heat is supplied to the salt. The main difficulty is finding a method of heat supply that is strictly homogeneous over the sample. This is an absolute necessity at the lower temperatures where the heat conductivity of the salt is very poor. A heating coil or an induction heater can be used down to 0.2°K, but below this temperature they are unsatisfactory. Two other methods are available: irradiation with gamma rays [26] and heat absorption from an alternating magnetic field [27]. Both methods have been used independently for many years. In several cases the agreement is not too good and authors have often criticized each other's methods more or less vaguely.

It is only very recently that a critical discussion of the gamma ray method was given. Since the absorption coefficient of a paramagnetic salt is small the penetration depth is large, hence for not too thick samples the absorption is rather homogeneous. This can still be improved by a suitable arrangement of the gamma sources around the sample. If sufficient care is given to this point no after period is found in the heating experiment and this gives at first sight some confidence to the method. Platzman [28] showed, however, that it is quite possible that at very low temperatures an appreciable part of the gamma radiation energy is not converted into heat, but stored in the crystal. But, as was pointed out by Kurti and Simon [29] this does not necessarily mean that the results obtained with the method are wrong. The transfer

of radiation energy into thermal energy can be described with the help of a relaxation time. If this relaxation time is either very short or very long as compared with the times involved in the experiment (e.g. shorter than a second or longer than a day) no error can be caused. If it is of the order of some minutes (hence comparable with a heating period) considerable after effects must be found in the heating. If it is of the order of some hours differences must be found between experiments with a "virgin" specimen and one that has been irradiated during the preceding hour or so. None of these effects were found so far. The absolute value of the heat absorption is derived from measurements in a region where the specific heat of the salt is known. If the gamma ray absorption or the relaxation time is very different at 1°K and at the low temperature similar effects as the above should be noticed, or if the change is very sharp with temperature an actual heat evolution should be found at the transition temperature. The absence of such effects makes it plausible that the results obtained with the method are sufficiently reliable.

The method of heat absorption from an alternating magnetic field has the advantage that no troubles occur involving the homogeneity of the heat supply over the sample. Since in most cases the heat absorption is the stronger the lower the temperature small inhomogeneities will even be decreased automatically. The practical execution of the method is very elegant: χ' and χ'' of the salt are determined simultaneously with an a.c. bridge; the variation of the entropy is derived from the variation of χ' (or: of T^*) and the heat supply per second follows from the value of χ'' (Eq. (11)). Hence in this method the heating field is the same as the measuring field. It requires some experience to obtain a reasonable number of bridge compensations in a short time if both components are steep functions of time, but this is not unsurmountable and the application of two phase sensitive detectors might be of great help.

The method has two main disadvantages. First it can only be applied if actual relaxation or hysteresis effects occur in the salt. This restricts the practical application to the determination of only the lowest temperatures that can be reached with each individual salt. Secondly it is sometimes difficult to discriminate between the contributions in the measured χ'' due to the heat absorption in the salt and to the a.c. losses in the bridge and other parts of the circuit. A correction can be determined from measurements at somewhat higher temperatures

where the heat absorption in the salt is negligible, and from measurements in which the cryostat mutual inductance is replaced by coils with small losses. In the case of a salt with a relatively large χ'' (e.g. chromium potassium alum or manganese ammonium sulphate) the correction can be applied with sufficient precision, but in the case of chromium methylamine alum, for instance, where the χ'' of the salt itself is very small the final accuracy seems to be insufficient.

In the frame of this chapter it is impossible to describe all the temperature determinations that have been made up to the present time. We will restrict ourselves to the discussion of the results obtained with two chromium salts: chromium potassium alum, $CrK(SO_4)_2\ 12H_2O$, and chromium methylamine alum, $Cr(CH_3NH_3)\ (SO_4)_2\ 12H_2O$. In these salts the trivalent chromium ions are located on a face centered cubic lattice, each ion being surrounded by a cube of six water molecules. The chromium ion is in a ^4F-state, but the orbital degeneracy is completely removed by the crystalline Stark splitting leaving the ion effectively in a ^4S-state. This state cannot be split by an electric field of cubic symmetry; a splitting is possible, however, in a field of lower symmetry due to a small distorsion of the water cube. In this case the fourfold spin level is split into two twofold levels not very far apart. Formulae can be given [23] for the specific heat and the magnetic susceptibility in terms of the level splitting parameter δ, defined in such a way that $k\delta$ is the distance between the sublevels. In the salts under consideration δ is of the order of a few tenths of a degree Kelvin.

According to a theorem of Kramers the remaining twofold degeneracy of the lower level cannot be removed by an electric field. The level broadening [22] due to magnetic interactions is small as compared with $k\delta$ so that its influence becomes significant only at still lower temperatures. Since magnetic (dipole and exchange) interactions are essentially many particle problems it is difficult to give exact formulae for the influence on the specific heat and the susceptibility, but approximate relations have been given [23].

The value of δ can be derived from entropy measurements in the region where both the Stark and the magnetic specific heats are proportional to $1/T^2$. Especially in the case of the methylamine alum the results are very nice. De Klerk and Hudson [30] at the National Bureau of Standards found $\delta = 0.275°K$. Unpublished measurements performed at Leiden gave the same value. Gardner and Kurti found [41]

$\delta = 0.265°K$. A more recent value by Hudson, quoted at the Houston low temperature conference is $\delta = 0.270°K$. The only essentially different value is the one given by Bleaney [31], from his microwave resonance experiments: $\delta = 0.245°K$. This was calculated from the separation of the absorption lines in a strong magnetic field directed along the (111) axis, assuming a trigonal electric field with symmetry around this axis as was found in the rubidium and caesium alums. Unpublished measurements by Baker [41], however, show that this assumption cannot be correct. It has not yet been established whether the crystalline field has symmetry about some other axis or whether it has only rhombic symmetry but in either case the splitting as calculated by Bleaney will be too small. In the case of chromium potassium alum the results are somewhat less consistant: the values published until now [33, 34, 35, 36, 37] vary between 0.24°K and 0.27°K and since different samples measured in the same apparatus by the same method even give different results it seems to be plausible that this is due to the salt itself, may be to the method of preparation or to the way in which it is cooled down to liquid helium temperature [38].

When δ is adapted at one temperature (for instance 0.5°K) it turns out that the agreement between the experiments and the theoretical relations mentioned above is rather good down to about 0.1°K. In

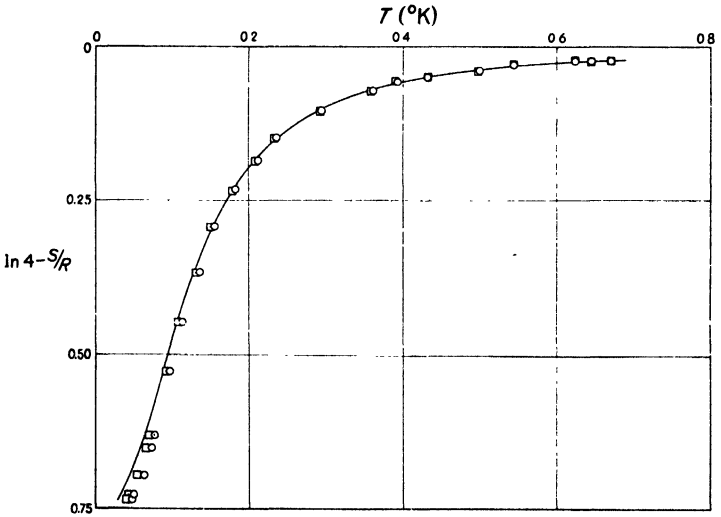

Fig. 3. *S versus T*-diagram for chromium methylamine alum.
⊙ Lorentz approximation. □ Onsager approximation. The curve is calculated for $\delta = 0.275°K$.

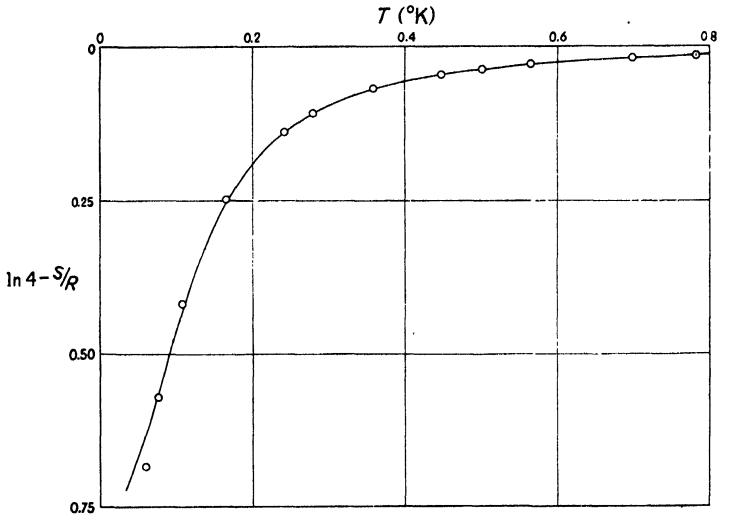

Fig. 4. *S versus T*-diagram for chromium potassium alum.
⊙ Lorentz approximation. The curve is calculated for $\delta = 0.270°K$

the case of the methylamine alum the deviations are within the limits of accuracy (see Fig. 3). For the potassium alum small systematic deviations are found below 0.2°K (see Fig. 4). Also direct specific heat measurements performed by Bleaney with gamma ray heating [37] give a deviation from the theoretical curve (see Fig. 5) and his results are in good numerical agreement with the entropy curve found by Casimir, de Haas and de Klerk [33].

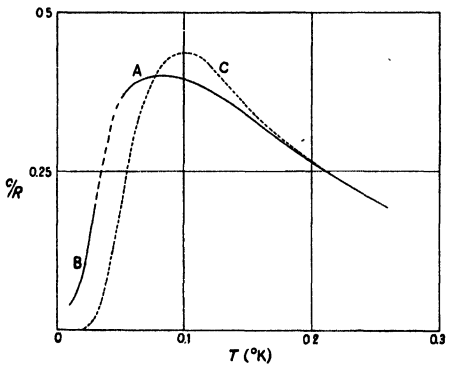

Fig. 5. Specific heat of chromium potassium alum as a function of temperature.
A: experimental curve of Bleaney,
B: experimental curve of de Klerk, Steenland and Gorter,
C: curve calculated for $\delta = 0.245°K$.

The deviations found below 0.1°K for both salts are apparently due to the fact that there the theoretical assumptions for the magnetic interactions don't hold any more. A complication of a different origin may contribute to the deviations for the potassium alum between 0.2 and 0.1°K. It was concluded by Bleaney from his microwave resonance experiments that this salt does not show one but two Stark level splittings of respectively 0.22 and 0.39°K. Hence it seems that there are two

kinds of chromium ions in the lattice, surrounded by water cubes distorted in different ways. This might mean that the specific heat is a superposition of two Schottky curves. Unfortunately the shape of the specific heat curve of Fig. 5 cannot be quantitatively explained by the two level splittings as found by Bleaney. The part of the curve above 0.2°K can be accounted for assuming that 85% of the ions have the smaller δ and 15% have the larger one, but the spectrum intensities suggest equal numbers. The curve below 0.2°K cannot be explained by any distribution of splittings between different percentages of ions. For the methylamine alum where deviations from the theoretical curve did not occur Bleaney showed that there is really only one level splitting [31]. This interesting difference in the magnetic behaviour of the two alums may be due to the fact that they have different crystal structures as was found by Lipson [32].

Measurements in external fields up to 500 oersteds were made at Leiden for both salts. In the region down to 0.1°K and somewhat below they satisfy the general rule that the variation of χ in small fields should be proportional to H^2. The calculation of the Garrett parameter Ξ as introduced in Eq. (18) and (19) is somewhat difficult since for these salts the correction term ψ/χ is not very small. If we use a Brillouin function for the magnetic moment we have:

$$\frac{\psi}{\chi} = -\frac{17}{15}\left(\frac{\mu_B}{k}\right)^2 \frac{1}{T^2}. \tag{22}$$

Using Hudson's formula for the magnetic moment [39] this must be multiplied by an analytical function in $(\delta/T)^2$ which converges slowly for temperatures below 0.2°K. It was found that above 0.2°K the $d\chi/dT$ values (and hence dT^*/dT) calculated from the measured Ξ-data, applying equation (20), are in reasonable agreement with the values derived from the Hebb and Purcell formula [23]. The accuracy, however, is better if the data are obtained from entropy diagrams. This is probably due to the fact that the slopes of two experimental curves are involved in the calculation of dT^*/dT.

If we calculate the variation of temperature on the isentropics with the help of (6) the results look quite reasonable (see Fig. 6 and 7). In low fields the variation of T is proportional to H^2, in higher fields the curves can be extrapolated without difficulties to the initial fields and temperatures of the demagnetizations.

Summarizing we can say that in the region above 0.1°K the results

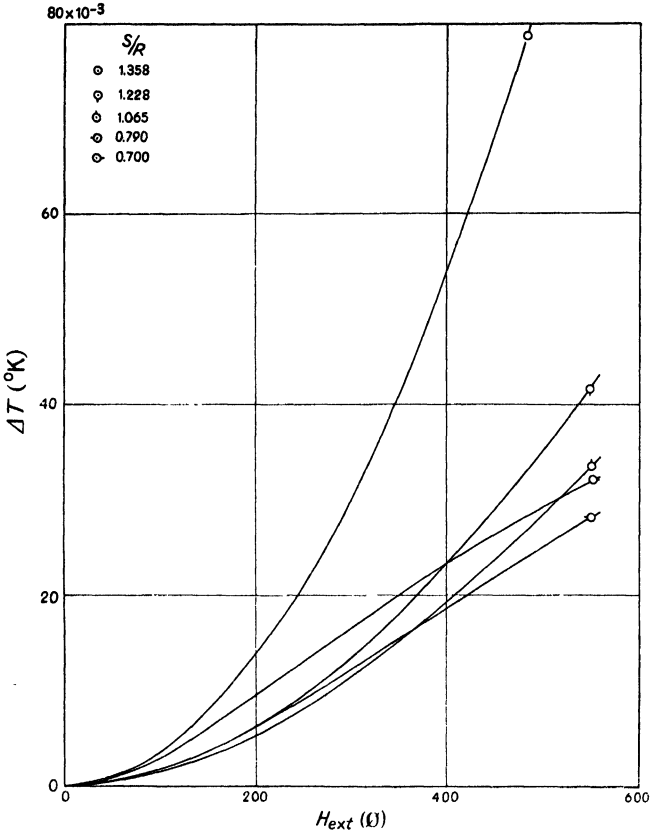

Fig. 6. Variation of temperature with external field on adiabatic magnetization curves for a spherical sample of chromium methylamine alum.

obtained with the chromium methylamine alum are somewhat better understood than those with the potassium alum. Though in the case of the latter salt the deviations from theory are so small that they are not disturbing for most experiments we believe that from the point of view of pure thermometry in this region the methylamine alum is somewhat better as a standard substance than the potassium alum.

The most striking phenomenon in the region of the lowest temperatures is a maximum in the susceptibility. Hysteresis effects occur below this maximum. The magnetic properties near and below the maximum will be discussed in § 4, here we restrict ourselves to the absolute temperature determinations. The situation is less satisfactory than in the

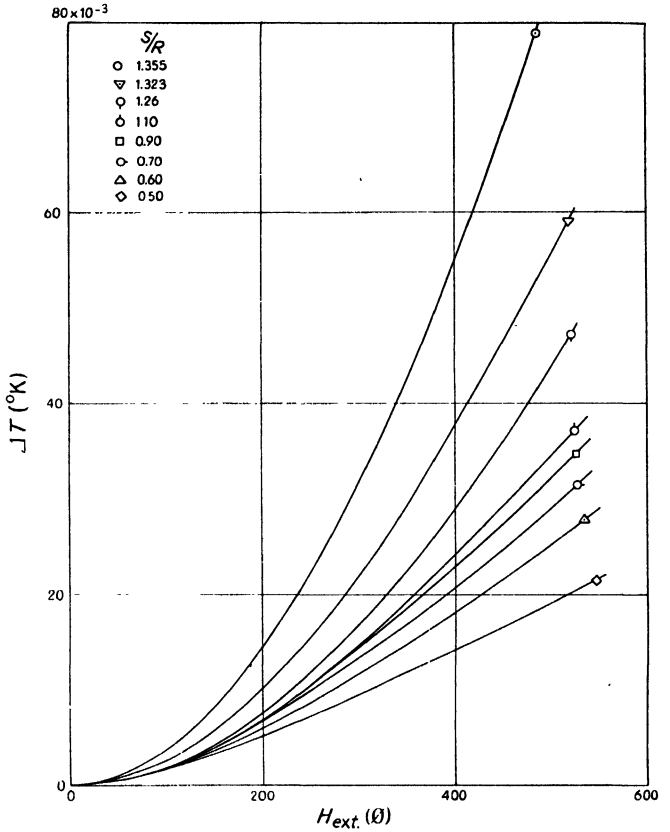

Fig. 7. Variation of temperature with external field on adiabatic magnetization curves for a spherical sample of chromium potassium alum.

region above 0.1°K. Two kinds of investigations have been published until now: the a.c. and hysteresis heating measurements of de Klerk, Steenland and Gorter [35] and the gamma ray heating experiments of Daniels and Kurti [40] and of Gardner and Kurti [41].

In the Leiden experiments the thermometric parameter used down to the susceptibility maximum was T^* or χ' and the measurements were performed as described earlier in this chapter. Near and below this maximum χ' is no more very suited as a thermometric parameter since its variation with T is too slow and it is no single valued function of temperature (or entropy). Measurements can be made with χ'' as a parameter, but since also χ'' shows a maximum somewhat below the maximum of χ' the lowest temperatures can better be measured with

the help of the remanent moment. In this case the measurements are performed in such a way that directly after the demagnetization the remanence is measured ballistically switching the measuring field on and off, then heat is supplied from an a.c. field and finally the remanence is redetermined. The entropy variation is derived from the experimental remanence *versus* entropy curve and the heat supply from the course of χ'' with time during the heating period. In some experiments heat was supplied differently by describing a number of hysteresis loops at such a rate that relaxation heating could be neglected (e.g. one loop per second during some minutes). The area of the loops was determined in separate experiments during the same helium run.

In the case of chromium potassium alum the results of all these investigations were quite consistent. They can be summarized in the statement that in the lowest region the absolute temperatures are much lower than the corresponding T^*-values. The lowest temperature was 0.0029°K, corresponding to $T^* = 0.033$ and $S/R = 0.258$.

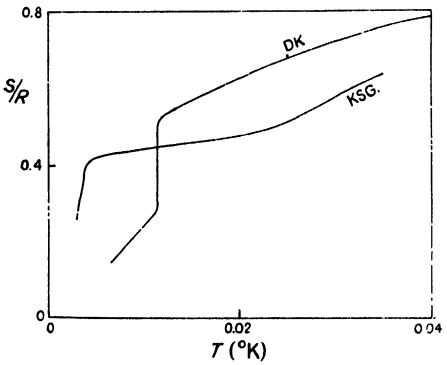

Fig. 8. *S versus T*-diagram for chromium potassium alum. KSG: curve obtained by de Klerk, Steenland and Gorter, DK: curve obtained by Daniels and Kurti.

In the Oxford gamma ray experiments [40], performed on the same salt, T^* was used as a parameter throughout the whole region. The calculated temperatures were widely different from the Leiden ones. The results of both investigations are given in Fig. 8. The point corresponding to the lowest Leiden temperature was 0.010°K.

If we compare the Leiden and Oxford measurements in some detail it follows that the *S versus* T^* curves coincide except in a small region around the maximum, here the Oxford T^*-values are higher than the Leiden ones. Daniels and Kurti's suggestion that this may be due to the fact that in Leiden the T^* was measured with a.c. and in Oxford ballistically cannot be true in general since ballistic measurements give higher susceptibilities than a.c. ones. There are, however, two possible explanations: In the case of chromium potassium alum the susceptibility decreases with increasing measuring field and it may be that a much higher field was

used in the Oxford measurements than in the Leiden ones (1.08 oersted). The other possibility is that, since in the susceptibility maximum the correction for the demagnetizing field becomes extremely high (see § 4), small deviations from the assumed spherical or ellipsoidal shape of the sample may markedly influence the measured susceptibility.

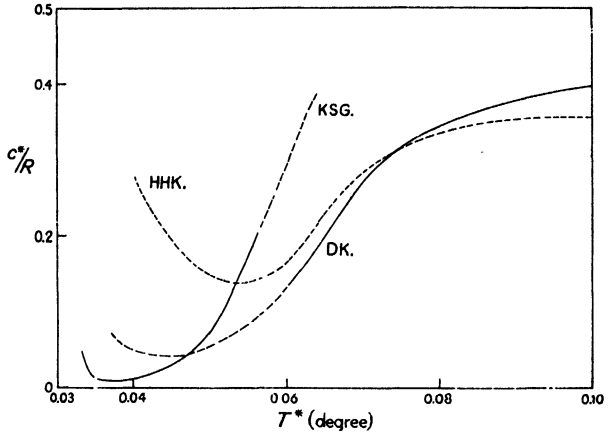

Fig. 9. c^* *versus* T^*-diagram for chromium potassium alum.
KSG: curve obtained by de Klerk, Steenland and Gorter. HHK: curve obtained by Hudson, Hunt and Kurti. DK: curve obtained by Daniels and Kurti.

From the heat supply experiments one can calculate a "specific heat on the T^*-scale", usually denoted as c^*. From Fig. 9 it follows that the values for c^* found in Leiden and Oxford diverge widely. A minimum occurs in all cases, but the Leiden minimum is lower than that of Daniels and Kurti by at least a factor of three. The origin of the discrepancy is not very clear. It might be due to a difference in the properties of the samples themselves (The discrepancy between the results of Daniels and Kurti and measurements of Hudson, Hunt and Kurti, quoted by Daniels and Kurti, is still worse than the deviation given here though they were made by the same method). As Daniels and Kurti remarked, however, it is more likely that this should influence the Stark splitting than the magnetic interactions. Daniels and Kurti suggested that the very low absolute temperature values found by the Leiden workers might be due to a large stray heat influx for which the proper allowance has not been made. The application of a correction for the stray heat is a somewhat difficult problem. It is often supposed that some time after the demagnetization the sample consists of two parts: a fraction $(1 - \alpha)$ still at the original low tem-

perature, while the fraction α is much warmer. This picture was originally given by Cooke and Hull [7]. It was further developed by de Klerk, Steenland and Gorter [41a] for the case of a diluted chromium alum neglecting χ' and χ'' of the warm part of the sample. Daniels and Kurti [40] estimated also the susceptibility of the warm part. A point that has not been taken into account until now is, however, that if some time after the demagnetization the shape of the cold core is not similar to that of the sample as a whole, the demagnetizing field is different and for an undiluted salt this may influence the observed susceptibilities noticeably. An indication that this may actually happen was found in the Leiden measurements of the remanent magnetic moment. It was often observed that after the demagnetization the remanence increased somewhat with time, and the only explanation that we could find is that after some time the shape of the cold core is more prolate than that of the sample as a whole. The influence of this effect on the experiments is difficult to estimate, but since the shapes of the Leiden and Oxford samples and their methods of suspension are widely different it is possible that the shapes of the cold parts of the samples change in different ways. Maybe investigations with both a.c. and gamma ray heating on the same sample during the same helium run will provide new information.

Some measurements were made at Leiden on the absolute temperature scale of chromium methylamine alum using a.c. heating, but it was found that for this salt the χ''-values are much smaller than for the potassium alum. This makes it difficult to correct the measured χ''-values for the a.c. losses in the mutual inductance bridge. Recent measurements by Gardner and Kurti [41] using gamma ray heating gave absolute temperature values of the same order as found by the same method for the potassium alum. The lowest temperature was 0.013°K, corresponding to an entropy $S/R = 0.350$. Below $T = 0.020$°K the susceptibility was found to be independent of temperature, in distinct disagreement with the Leiden and Washington [30] results which show a decrease of susceptibility, both for a.c. and ballistic measurements. We doubt whether this salt will prove to be as suitable as a standard substance for absolute thermometry in this region as it is above 0.1°K.

Measurements in external magnetic fields for chromium methylamine alum were made at Leiden. Below the maximum of χ the $(\partial M/\partial S)_H$ becomes positive, hence, according to (6), T decreases with increasing field. The results have the same general character has those for iron

ammonium alum [42]. The temperature goes down a few thousands of a degree, a minimum occurring at about 140 oersteds. In iron alum the temperature decrease is the stronger the lower the entropy, in the chromium methylamine alum this is not true. At $S/R = 0.3$ the minimum is deeper than at $S/R = 0.2$.

4. Magnetic Behaviour at the lowest Temperatures

The behaviour of the paramagnetic salts at the lowest temperatures that can be reached by demagnetization is mainly determined by the magnetic interactions. In this section we will first summarize this behaviour as it occurs in the alums and Tutton salts of the iron group which have been investigated extensively. Next we discuss in more detail the two salts of § 3, chromium potassium alum and chromium methylamine alum. We give most attention to the experimental data, since an adequate theoretical treatment has not been given until now. A phenomenological comparison with the behaviour of the anhydrous salts of the iron group will give us some indications concerning the character of the magnetic interactions present in the hydrated salts.

All the quantities will be given as functions of the entropy since S generally is better known than the absolute temperature.

a. THE SUSCEPTIBILITIES

With decreasing entropy the susceptibilities often show first a strong increase but then pass through a maximum and decrease again (see Fig. 10). In the neighbourhood of this maximum the ballistic susceptibility χ and the real part of the a.c. susceptibility χ' become different, χ reaching higher values; the imaginary part of the a.c. susceptibility χ'' begins to increase steeply. χ, χ' and χ'' depend upon the amplitude of the measuring field, and χ'' increases with increasing frequency. At the frequencies used (up to 500 Hz) χ'' is very small, a few percents of χ'; only in the case of manganese ammonium Tutton salt does χ''/χ' reach an appreciable value, viz. about $\frac{1}{2}$.

As was stated in § 1 the susceptibilities given in this chapter are defined as M/H_E, where H_E is the external measuring field (usually of the order of 1 oersted). Thus, the values depend upon the shape of the sample used in view of the demagnetizing field. The field inside a sample with demagnetizing factor ε is given by

$$H_I = H_E - \varepsilon M/V, \tag{23}$$

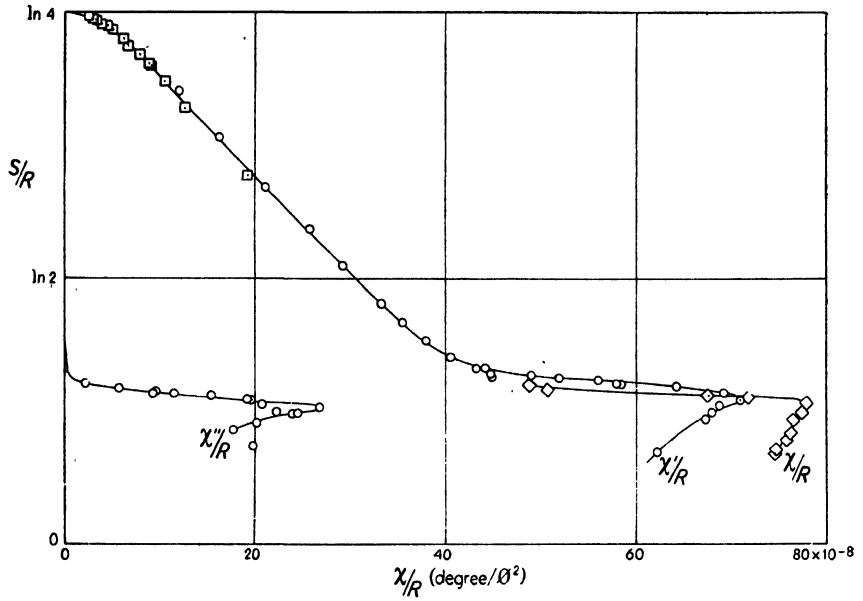

Fig. 10. The entropy S as a function of the susceptibilities, χ, χ' and χ'' for a spherical sample of chromium potassium alum. χ''/R is plotted on a tenfold magnified scale. χ/R: measuring field 1.08 oersted, free period of galvanometer 7 sec, χ'/R and χ''/R: amplitude of measuring field 0.183 oersted, $\nu = 225$ Hz.

where M/V is the magnetization per cm³. In the case of a spherical sample $\varepsilon = 4\pi/3$, in the case of an infinitely long cylinder $\varepsilon = 0$. From (23) it follows that the influence of the external shape on the susceptibility χ can be accounted for by dividing χ by $1 - \varepsilon\,\chi_{cc}$. In the cases of chromium potassium alum and iron ammonium alum the maximum value of $\varepsilon\chi_{cc}$ is almost 1, thus in the neighbourhood of the maximum the correction for the demagnetizing field is extremely large.

b. HYSTERESIS PHENOMENA

Hysteresis effects occur below a certain entropy which is almost the same as the entropy at which the susceptibilities reach a maximum. Table 1 gives a survey of the critical values of the entropies S_c, together with the corresponding temperatures T_c, for all the salts investigated so far.

The values mentioned for the alums indicate the point, at which ballistically determined remanences set in. These values are slightly higher than those corresponding to the maximum of the susceptibility. In the case of the Tutton salts the remanences either were too small to

TABLE 1
Survey of critical temperatures

Substance	$(S/R)_c$	T_c(°K)	Reference
$TiCs(SO_4)_2.12H_2O$	0.22		Kurti, Lainé and Simon[43]
$CrK(SO_4)_2.12H_2O$	0.40	0.004	De Klerk, Steenland and Gorter[35, 44]
	0.46	0.010	Daniels and Kurti [40]
$CrCH_3NH_3(SO_4)_2.12H_2O$	0.50	0.020	Gardner and Kurti[41]
	0.52		Beun, de Klerk, Steenland and Gorter[45]
$Mn(NH_4)_2(SO_4)_2.6H_2O$	1.27	0.15	Cooke[35]
	1.28	0.12	Steenland, v. d. Marel, de Klerk and Gorter[46]
$FeNH_4(SO_4)_2.12H_2O$	0.64	0.03	Steenland, de Klerk, Potters and Gorter[47]
	0.65	0.042	Kurti, Lainé and Simon[43, 36, 42]
$Co(NH_4)_2(SO_4)_2.6H_2O$		0.084	Garrett[48]
		0.125	Malaker[49]
$CuK_2(SO_4)_2.6H_2O$	0.42	0.04	Steenland, de Klerk, v. d. Marel, Beun and Gorter[46, 50]

establish the point of onset accurately or have not been investigated. Hence, for the Tutton salts, those values are quoted where the susceptibility reaches its maximum.

Usually the remanences increase with decreasing temperature. Only in the case of chromium methylamine alum do the remanences show a maximum as a function of temperature.

Complete hysteresis loops can be measured by switching on and off the field in several steps in both directions. Fig. 11 shows some loops measured on chromium potassium alum. One sees, that if the magnetizations are plotted as functions of H_E, the loops are very narrow and the remanences are very small. If, however, the correction for the demagnetizing field is applied, the loops (M *versus* H_I) show a more familiar shape. The remanences in these loops are much larger. If we assume that the corrected loops can not have a negative slope, it follows that the values of the directly measured remanences per cm^3 can never exceed H_c/ε, H_c being the coercitive field. Thus, the smallness of the measured remanences is a consequence of the smallness of the coercitive fields and the use of specimens with a rather high value of ε. It is remarkable that the hysteresis effects have already disappeared in fields of some tens of oersteds. In this respect they are quite different from regular ferromagnetic effects.

We have to keep in mind that all the measurements are made adia-

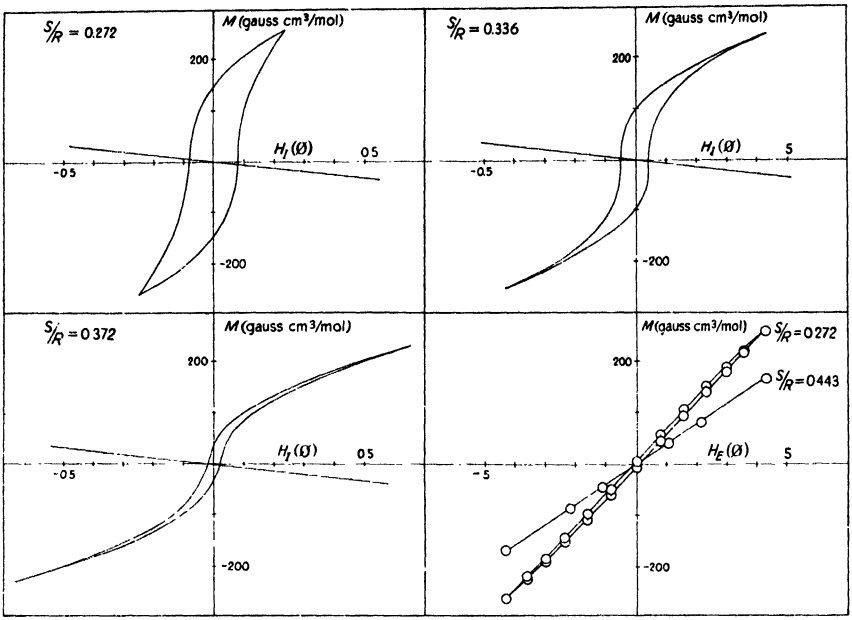

Fig. 11. Hysteresis loops of a spherical sample of chromium potassium alum. $H_E = 4.30$ oersteds. Three loops have been plotted against H_I, the oblique lines represent $H_E = 0$. The lower right hand figure shows the loop at $S/R = 0.272$ plotted against H_E and a magnetization curve just above T_c (at $S/R = 0.443$).

batically and that the shape of an isothermally described loop might differ from that of an adiabatic one. In § 3 we saw, however, that in the case of chromium methylamine alum the changes in temperature along the adiabatic magnetization curves are very small over the first tens of oersteds. It is unlikely that the difference between isothermal and adiabatic loops will be large.

The occurrence of a χ'', mentioned sub (a), is not merely caused by these hysteresis phenomena. The onset of χ'' takes place already somewhat above T_c; and, moreover, χ'' is not frequency independent, as it should be in the case of pure hysteresis losses.

c. THE SPECIFIC HEAT

From the (S, T-)graphs the specific heat can be derived. It always shows a strong increase in the neighbourhood of T_c.

The above mentioned phenomena must be attributed to cooperative effects arising between the spins of the paramagnetic ions. Before

saying more about the kinds of ordering that may exist in these salts, it is interesting to consider some salts in more detail, since we then find rather large differences even between salts which contain the same paramagnetic ion and differ only in the diamagnetic cation. This can be clearly demonstrated by comparing chromium potassium alum and chromium methylamine alum.

Comparison of $CrK(SO_4)_2 \cdot 12\,H_2O$ *and* $CrCH_3NH_3(SO_4)_2 \cdot 12\,H_2O$.

The general description given above applies to both salts, but in the case of the potassium alum the increase in χ before the maximum is steeper and occurs at about $S/R = 0.40$, while in the case of methylamine alum the increase is much less pronounced and is found at about $S/R = \ln 2$. The maximum value of the susceptibility reached by the first alum, corrected for the demagnetizing field, is more than 20 times greater than that for the latter salt. For the methylamine alum is about $C/0.02$, which is equal to C/T_c (see Table 1); for the potassium alum it is much larger than C/T_c, even if we take the lowest value for T_c (0.004°K).

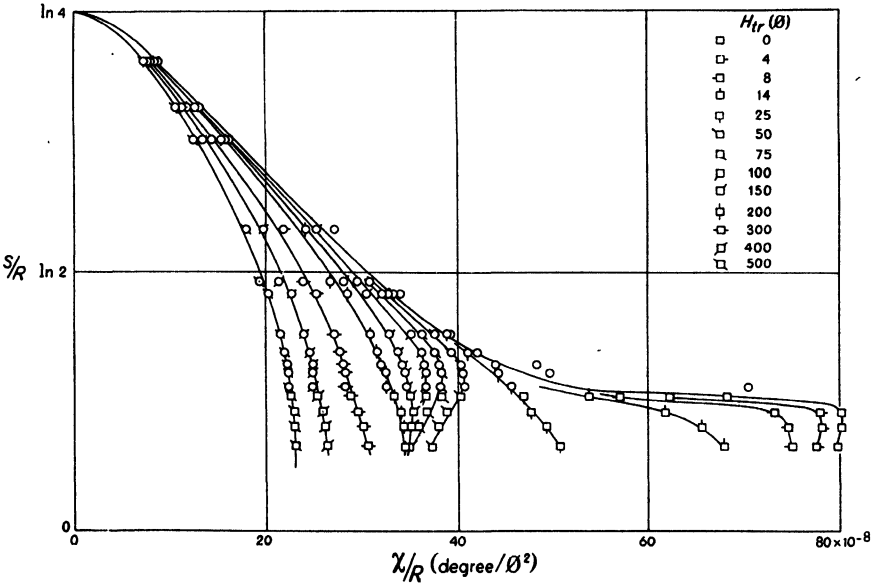

Fig. 12. *S versus* χ-diagram for a spherical sample of chromium potassium alum. Transverse magnetic fields H_{tr} up to 500 oersteds.
⊡: ballistic measurements, measuring field 1.10 oersted, free period of galvanometer 1.3 sec, ⊙: a.c. measurements, amplitude of the measuring field 1.86 oersted, $\nu = 225$ Hz.

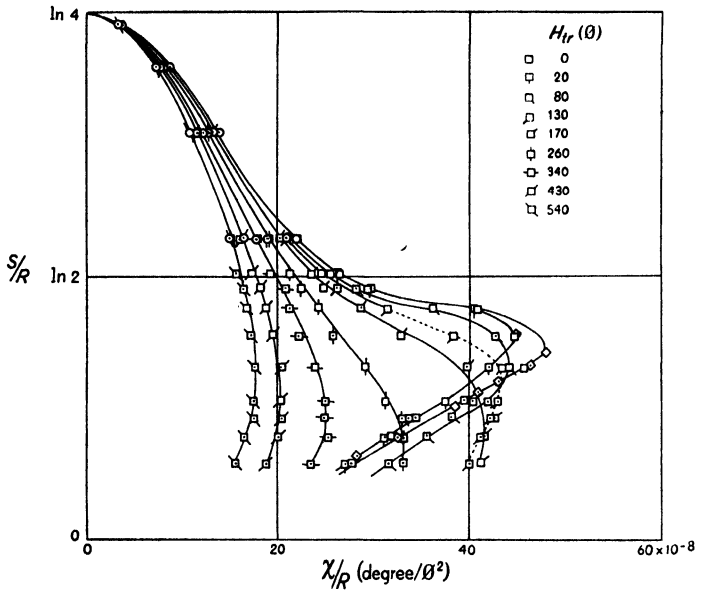

Fig. 13. *S versus* χ-diagram for a spherical sample of chromium methylamine alum. Transverse magnetic fields H_{tr} up to 540 oersteds.
⊡: ballistic measurements, measuring field 1.10 oersted, free period of galvanometer 1.3 sec, ◈: ballistic measurements, measuring field 1.10 oersted, free epriod of galvanometer 7.0 sec, ⊙: a.c. measurements, amplitude of the measuring field 1.86 oersted, $\nu = 225$ Hz.

Moreover, the behaviour of the susceptibilities in constant external fields differs widely. Fig. 12 shows the susceptibilities of CrK-alum with constant transverse fields, H_{tr}, applied. In the region below the maximum of the susceptibility a very strong decrease occurs with increasing H_{tr}, the maximum moves to lower entropies and has already disappeared in fields of 14 oersteds. (A second maximum appears in higher fields; but its origin is completely obscure, and it is not known if this is connected with the cooperative effects under consideration.)

In the case of $CrCH_3NH_3$-alum the behaviour at the lowest entropies is quite different, as shown in Fig. 13. Here the susceptibilities – after a small decrease – increase strongly untill fields of about 200 oersteds are reached.

In both cases the measurements were made on a spherical single crystal. The field used for the demagnetization and the constant transverse field were perpendicular to the measuring field and all were directed along cubic axes. Measurements on chrome methylamine alum showed that in the temperature region below T_c a different susceptibili-

ty was found if the transverse field had a direction other than along a cubic axis. The magnetic behaviour is then no longer isotropic, and even exhibits an axial rather than a cubic symmetry.

In order to determine magnetization curves the susceptibilities were remeasured applying both the constant field and the measuring field in the same direction. In this case the magnetization curves can be derived by integrating the susceptibilities. Fig. 14 shows some results.

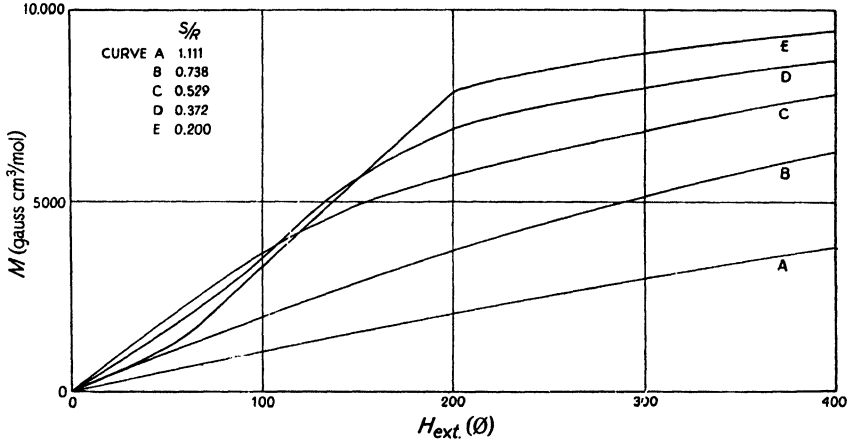

Fig. 14. *M versus* H_{ext}-diagram for a spherical sample of chromium methylamine alum. External field H_{ext} parallel to a cubic axis. The value of the saturation magnetization is 16700 gauss cm³/mol.

At the higher entropies the curves are convex, but at the lowest entropies they start with a concave part. At a field of about 200 oersteds the slope of the curves changes abruptly and the curves become convex. The internal field, H_I, corresponding to this value of 200 oersteds is about 90 oersteds. In the case of chromium potassium alum the magnetization curves are convex over the whole temperature range. Below T_c the curves start almost vertically, if M is plotted against H_I.

Irreproducibilities

As was quoted in § 3, for specimens of the same salt, the measurements give somewhat different results. In the case of CrK-alum four different specimens were investigated, all showed small differences in δ (see § 3). At the lower temperatures the shapes of the susceptibility curves may differ even more (compare Fig. 10 and 12). Also the values of S_c as well as the course of the remanences were somewhat different. It even turned out that the remanences measured on the same specimen increased slightly from one run to the other.

The comparison is made extra difficult by the presence of relaxation times in the spin system which can be so long that even the ballistic measurements are influenced. This influence is the larger, the shorter the free period of the galvanometer, and the greater the fraction of the induction that is compensated with the bridge. Using a galvanometer with a free period of some seconds and compensating 90% of the deflection, it may occur that "double deflections" are observed. The galvanometer – although critically damped – first shows a deflection in one direction, then passes through its zero position and shows a second maximum in the opposite direction. We recorded these double deflections photographically. The shape was analogous to that which is expected theoretically if one relaxation time is assumed to be present, but the exact form could not be fully accounted for. Probably a continuous distribution of relaxation times exists.

The Character of the Magnetic Ordering

It is evident to compare the anomalous behaviour of these magnetically diluted salts at very low temperatures with the behaviour of the more concentrated salts at higher temperatures. Also the latter salts often show a maximum in their susceptibility as a function of temperature; it lies in the helium range or even higher. This may be explained by the hypothesis that below the maximum an antiferromagnetic ordering occurs (see Chap. XIII). The existence of such a type of ordering was proved by the neutron diffraction experiments of Shull and Smart [51] and by Poulis [52] in his proton resonance experiments on $CuCl_2 . 2H_2O$.

Not all the more concentrated salts which show cooperative effects behave in a similar way. Here, too, many individual differences occur, but it appears to be possible to divide these salts according to their magnetic behaviour into two groups. The salts of group A show a maximum in the susceptibility at a well-defined temperature T_N. Usually deviations from the Curie-Weiss law already occur slightly above T_N, but the value of the susceptibility at the maximum is of the order of, or usually somewhat smaller than, the value calculated from the Curie-Weiss law. Below T_N the susceptibility is field dependent, $d\chi/dH_I$ is positive, and thus the magnetization curves are concave.

The salts of group B show no maximum in χ, but at a certain temperature the susceptibility increases strongly. Moreover, since $d\chi/dH_I$ is negative, the magnetization curves are convex. Both groups show,

as far as is known, small hysteresis effects and an increase in the specific heat in the neighbourhood of the critical temperature.

The behaviour of the salts of group A is characteristic for an antiferromagnetic kind of ordering. The salts of group B give the impression of behaving analogous to ferromagnetics.

If we return now to the alums and Tutton salts, we may conclude that they also can be divided into two similar groups. Chromium methylamine alum and cobalt ammonium Tutton salt, investigated thoroughly by Garrett [48], show anomalous properties quite analogous to group A. Thus in these salts an antiferromagnetic ordering is very likely occurring [48a].

The behaviour of chromium potassium alum and iron ammonium alum is more analogous to that of group B, with this difference that χ shows a maximum. But at this maximum the value of χ is much higher than that derived from C/T_c since χ increases sharply in the region somewhat above T_c. And the magnetization curves are always found to be strongly convex.

Manganese ammonium Tutton salt and copper potassium Tutton salt have been studied in the form of powders solely. The manganese salt showed a very pronounced maximum in the susceptibility quite compatible with a behaviour of type A. In the case of copper potassium Tutton salt the maximum was much less pronounced. The rather high positive Weiss-Θ might point to a ferromagnetic interaction.

5. Non Magnetic Investigations in the Region below 1°K

The aim of adiabatic demagnetization work, as was pointed out in § 1, is not only to investigate the thermometric, magnetic and caloric properties of paramagnetic salts, but also to cool down other materials with a salt and to make measurements on them. Since heat transfer takes place through the thermal vibrations of the lattice we must expect that heat contact in general becomes less effective upon lowering the temperature.

Suppose the substance under investigation (for instance a metal wire the resistance of which is to be measured) is connected to a paramagnetic salt by means of a "transfer medium" (e.g. liquid helium or some kind of glue) then the thermal equilibrium is accomplished in the following steps [53]:

1. the heat transfer from the spin system to the lattice of the salt.
2. the establishment of thermal equilibrium in the salt itself.

3. the heat transfer from the lattice of the salt to the transfer medium.
4. the heat conduction of the transfer medium.
5. the heat transfer from this medium to the substance under investigation.
6. the establishment of equilibrium in the substance under investigation.

Little is known theoretically about each of these steps separately and in many cases it is difficult to separate them experimentally. For instance it is often impossible to distinguish between 3, 4 and 5.

Casimir showed that the heat transfer between the spin system and the lattice of the salt takes place in a negligible time (less than 10^{-4} sec) due to the smallness of the lattice specific heat [54].

The heat conductivity of chromium potassium alum below 1°K has been investigated by Kurti, Rollin and Simon [53] and by Garrett [55]. A long single crystal was demagnetized in such a way that the ends were cooled to different temperatures and the approach to temperature equilibrium was derived from susceptibility measurements made with coils placed around the ends of the sample. Kurti, Rollin and Simon made the demagnetization from an inhomogeneous field. Garrett demagnetized from a homogeneous field and set up the temperature gradient separately with a set of coils producing a linearly varying field. It was found that the heat conductivity is a steep function of temperature: above 0.3°K the equilibrium time was too short to be measured, below 0.14°K it was too long. Between 0.14°K and 0.3°K the heat conductivity was found to be proportional to T^3.

Little is known about the heat transfer from one medium to another since in most experiments it is difficult to separate it from the heat conductivities of the media themselves. Heitler and Teller showed the theoretical possibility of direct heat transfer from the spin system of a salt to the free electrons of a metal within a very short time [56].

Not many heat conductivities of other materials have been measured, but some data are available. In the case of metals (excluding superconductors) the heat conductivity is reasonably good down to very low temperatures. The conductivity being mainly due to the free electrons, it is proportional to T. The heat conductivity of liquid helium was measured by Kurti and Simon [57] and by de Klerk [58]. Though the determinations had a very preliminary character and though no correction could be applied for the heat transfer from the salt to the liquid it followed that the heat conductivity decreased strongly with falling

temperature. At about 0.2°K it is of the same order of magnitude as that of He I. Here under normal experimental conditions thermal equilibrium can still be reached in a short time through a thin layer of liquid, but not through a long narrow capillary. Very little is known about the heat conductivities of adhesives and glues. Probably they are not too good, but if a really thin layer is applied the equilibrium time may be not too long. Residual helium gas in a sample may act as a transfer medium as long as the pressure is higher than 10^{-6} mm. Extrapolation of the vapour pressure curve suggests that this may be true above 0.4°K.

From the above it follows that the best transfer media are liquid helium and non superconducting metals, but also that the main source of troubles is the small heat conductivity of the paramagnetic salts themselves at the lower temperatures. If a piece of salt is immersed in liquid helium at 0.1°K only a thin outer layer is active in cooling the liquid. The same is true for a metal to salt contact, even if the heat transfer from one to the other causes no trouble. In some cases this is not serious. If the heat capacity of the substance under investigation is much smaller than that of the salt a reasonably low temperature will still be reached. But if appreciable amounts of heat are developed in the substance (e.g. in the case of experiments on electric or thermal conductivity) a noticeable difference from the temperature of the bulk salt may occur. This is especially unpleasant if the temperature of the substance must be derived from the temperature of the salt.

We shall describe some of the standard arrangements for measurements below 1°K.

If liquid helium, is used as a transfer medium (or if investigations are made on the helium itself) the salt should be used in the form of powder or small crystals. This increases the area of contact and reduces temperature differences in the grains. The main problem of an apparatus containing liquid helium is the heat leak due to film creep. Two solutions to this problem are in use at the present time. One is that a thick walled metal capsule containing some salt is filled at room temperature with say 100 atmospheres of helium and sealed off [53]. At low temperatures the helium is condensed and provides a good contact between the salt and the metal wall. The substance under investigation may be soldered to the outer wall of the capsule. Good results have been obtained with these capsules, but sometimes they leak and under certain circumstances it may be undesirable to have

large amounts of metal in the sample. The second solution is that an open container is used into which the helium is condensed after the cryostat has been cooled to liquid helium temperature. The effect of the film is decreased by applying a long narrow capillary (e.g. 0.2 mm inner diameter) between the sample and the bath [59]. The film creeping through the capillary is pumped off with a diffusion pump, thus preventing recondensation into the sample tube; this condensation is the main source of heat leak. Under these conditions the thermal insulation must be inferior to that of a dry sample. A heat influx of 30 ergs per second, corresponding to a heating time of an hour from 0.05°K to 1°K must be considered as good, and for many investigations this time is quite reasonable. De Klerk, in his heat conductivity experiment on liquid helium, used a metal valve instead of a capillary [58]. The thermal insulation proved to be not much different in either case and for this reason the capillary technique was also applied in later Leiden investigations.

In the case of a metal to salt contact it is essential that the area of contact is large and that nowhere in the sample is the salt far away from the contact surface. Gluing a metal to the outside of a piece of salt is unsatisfactory. A practical solution to this problem has been given by Mendoza [60]. A sample of salt powder containing thin copper vanes or wires is compressed hydraulically into a solid pill, the substance under investigation is then soldered to the vanes or wires. Some investigators mix the salt with some cement before compressing. If the idea of Heitler and Teller [56] is correct that direct heat transfer is possible from the spin system of the salt to the free electrons of the metal it should be better not to use the cement. But there is no experimental evidence that one method is better than the other. Steele and Hein [61] found that the thermal contact deteriorated to some extent once the apparatus was allowed to warm up from liquid helium temperatures to room temperature. They ascribed this to the salt's breaking away from the copper vanes, possibly due to the difference in thermal expansions.

We shall describe some of the investigations on the following subjects:

a. properties of helium.
b. electric conductivity of solids, including superconductors.
c. heat conductivity of solids, including superconductors.
d. the thermal valve and the cascade demagnetization.
e. the magnetic refrigerator.

a. PROPERTIES OF HELIUM

The heat conductivity measurements of Kurti and Simon [57] and of de Klerk [58] have already been quoted. Kurti and Simon used a twin capsule connected by a metal capillary. De Klerk had two glass spheres filled with powdered salt, connected by a glass tube. The results were in reasonable agreement with each other, the conductivity being more or less proportional to T^5. But extrapolation to the region above 1°K gave values too small by about a factor ten. We shall not discuss these measurements further since they were of a preliminary character.

The heat conductivity of solid helium was measured by Wilks [62] using a capsule technique. Above 1°K the conductivity increases with falling temperature, but a maximum occurs somewhat below 1°K. The curve is of the normal type for dielectric crystals.

Hull, Wilkinson and Wilks [8] measured the specific heat of liquid helium using a capsule with iron ammonium alum. Down to 0.6°K their results obeyed the formula $c = 10.0 \times 10^5\, T^{6,2}$ erg/gram degree. Below this temperature the specific heat of the helium was too small as compared with that of the salt. Kramers, Wasscher and Gorter [63] made measurements applying a capillary technique. They used copper potassium sulphate as a paramagnetic salt since its specific heat is about one twentieth of that of iron alum. They found a rather sharp bend in the curve at 0.6°K. Below this temperature proportionality to T^3 was found as was to be expected, since at sufficiently low temperatures only the phonons must make a contribution to the specific heat.

The specific heat of liquid helium three was measured by several investigators down to about 0.5°K. Daunt and de Vries [64] used a calorimeter of the normal type connected to the salt by a "thermal valve" of superconducting material as will be described below. ^{3}He of 96% purity was used and the temperatures were measured with a carbon resistor. Roberts and Sydoriak [65] used ^{3}He of 99.9% purity. The specific heat was derived from warming up rates for different amounts of liquid in the calorimeter. In the measurements of Osborne, Abraham and Weinstock [66] a copper container with ^{3}He was embedded in ferric ammonium alum. Four copper vanes were soldered to the ^{3}He container and one atmosphere of helium gas was admitted to the salt at room temperature in order to improve the heat contact. A strip carbon resistor was fastened to one of the vanes. It served both as a thermometer and as a heater. All the results agreed rather well with

each other. For the discussion we refer to Chap. V where the melting curve measurements of Weinstock, Abraham and Osborne [67] (making use of the blocked capillary technique) are also described.

The velocity of second sound of liquid helium, v_{II}, was measured by several investigators, using a heat pulse technique. Though between 1°K and 2°K the velocity depends little on temperature an appreciable rise was found below 1°K. The theoretical speed limit of Landau (the first sound velocity divided by $\sqrt{3}$) was not confirmed by experiment. De Klerk, Hudson and Pellam [68] as well as Kramers, van den Burg and Gorter [69] found values approaching the velocity of first sound at the lowest temperatures. Kramers, van den Burg and Gorter, who used a single pulse method, found that v_{II} depends on the size of the cavity; for a given temperature it becomes higher the shorter the tube. Moreover all the investigators found a marked pulse broadening at the lower temperatures. A possible explanation is that at the lowest temperatures one has no second sound at all but normal transmission of heat pulses with a phonon free path length of the order of the dimensions of the cavity. Mayper and Herlin [70] measured the second sound velocity of helium under pressure. At the higher temperatures the velocity decreases with increasing pressure, at the lower temperatures it increases; and this also can be explained with the phonon free path hypothesis.

Second sound velocities in mixtures of ^{4}He and ^{3}He were measured by King and Fairbank [71]. The heat contact between the cavity and the salt was made by a copper rod with copper discs connected perpendicular to it. The discs were compressed together with the salt, hence a modified vane technique was used. The second sound velocity was measured with single pulses. It was found that addition of some percents of ^{3}He to the ^{4}He increased v_{II} appreciably at the higher temperatures. A maximum in the v_{II} was found near 0.8°K, below which it falls rapidly below the value for pure ^{4}He. No significant pulse broadening was found down to the lowest temperatures. This checks very well with the phonon free path hypothesis since a small addition of ^{3}He may decrease the free path length appreciably (cf. Chap. VI).

Ambler and Kurti [72] made a very refined experiment on film creep below 1°K. A compressed cylinder of manganous ammonium sulphate split in half longitudinally was mounted in a glass beaker and surrounded by an annulus of the same salt with a slit in line with the first one. Narrow slits were also applied in the silvering of the glass walls

of the cryostat and the vacuum jacket, so that the helium level in the sample could actually be seen with the help of a small mercury lamp (with filters transmitting only the green light). If care was taken that no light fell directly on the salt, and if the slit was only illuminated during the actual time of observation (a few seconds) the total heating up time was about an hour. The results were somewhat different for different runs (probably due to slight contamination of the creep surface), but it was clear that below 1°K the creep rate increased with falling temperature. This was corroborated by measurements of Lesensky and Boorse [73] who derived the variation in the helium level from the variation in the capacity of a condenser caused by the dielectric constant of the helium.

Measurements of the fountain effect were made by Bots and Gorter[74]. A glass capillary in a cryostat of 1.1°K was connected by a tube filled with jeweler's rouge (Fe_2O_3) to a glass sphere containing chrome alum. After demagnetization the integrated fountain effect between the low temperature and 1.1°K could be derived from the level in the capillary. The results were lower than predicted by H. London's formula (see Chap. 1). Measurements are in preparation with two salt samples so that smaller temperature differences can be applied.

Lambda temperatures of mixtures of ^3He and ^4He were determined by Daunt and Heer [75]. The mixture was condensed in a copper reservoir pressed inside a pill of chromium alum. The reservoir was connected thermally to the liquid helium bath by a stainless steel capillary. As long as the temperature of the mixture was below its lambda point the heating was fast due to the film in the capillary, a sharp decrease in the warming rate appearing at the lambda point. It was found that the lambda temperature decreases with increasing ^3He concentration and this is in agreement with the hypothesis that ^3He shows no superfluidity (cf. Chap. VI).

b. ELECTRIC CONDUCTIVITY

In the early years of adiabatic demagnetization some experimenters cooled a phosphorbronze wire with the paramagnetic salt, mainly in order to investigate the possibility of resistance thermometry in the region below 1°K. It was found that the resistance decreased linearly with falling temperature down to 0.25°K (Van Dijk, Keesom and Steller [76]), may be even to much lower temperatures (Allen and Shire [77]).

At present phosphorbronze thermometers have mostly been aban-

doned for this region and replaced by carbon resistors. In 1938 Giauque, Stout and Clark [78] showed that resistors made of lampblack on porous paper have high thermometric sensitivity and are little affected by magnetic fields. In a more recent paper Geballe, Lyon, Whelan and Giauque [79] showed that the sensitivity of a carbon thermometer is larger the smaller is the size of the carbon particles. Sizes between 12×10^{-6} cm and 1.3×10^{-6} cm were investigated and a great variety of sensitivities proved to be possible. It was also found that adsorption of helium gas on the thermometer may influence its resistance somewhat. If the pressure is less than half the saturation pressure, mistakes of the order of some millidegrees may be made.

Clement, Quinnell, Steele, Hein and Dolecek [80] investigated some commercial carbon-composition resistors manufactured by the Allen-Bradley company. The resistor was cemented into a cylindrical copper holder screwed to a brass case to which a copper vane was soldered. The salt was pressed around the vane. The resistance *versus* temperature curves were similar to those found by Giauque *et al.* Between 1°K and 0.3°K the resistance increased by a factor 10^3. The data fitted a formula of the form: $\log R + K/\log R = A + B/T$. The reproducibility from one run to the other was somewhat better than in the case of Giauque's thermometers, but it was not possible to obtain resistors in as wide a range of sensitivities.

Howling, Darnell and Mendoza [81] investigated an Erie "ceramicon" radio resistor, connected thermally to the salt with the vane technique. Between 1°K and 0.1°K the resistance increased by about 50% which is much less than in the case of an Allen-Bradley resistor, but still sufficient for many purposes of thermometry. The authors proposed to use a carbon resistor for absolute temperature determination below 1°K. The resistance of the carbon in this case plays the role of the thermometric parameter: it is measured as a function of the entropy of the salt and its variation is determined by supplying heat (see § 3). Since already at 0.1°K they found a thermal equilibrium time of seven minutes it is not likely that the method will be suited for lower temperatures.

Apart from the thermometrical interest there are two main reasons of investigating the resistance of metals below 1°K. One is the possibility of discovering new superconductors, the other is the desirability of investigating them below the well known resistance minimum.

The classical example of this behaviour is gold and the first measure-

ments below 1°K were made in 1938 by de Haas, Casimir and van den Berg [82]. The heat contact was made by means of some helium gas in the sample. Down to 0.4°K the resistance was found to contain a term proportional to $T^{-\frac{1}{2}}$. Below this temperature the points scattered badly due to lack of thermal equilibrium. Mendoza and Thomas [83], using the vane technique for heat contact, found a much steeper dependence on temperature than could be described by $T^{-\frac{1}{2}}$. Croft, Faulkner, Hatton and Seymour [84] made new measurements using a liquid helium contact down to 0.2°K, and for the lower temperatures (down to 0.006° K) a two stage demagnetization apparatus (see below) in which the second sample was compressed around the gold itself. Here the temperature dependent term was proportional to —log T.

Several other metals were investigated by Mendoza and Thomas [83,85]. Silver samples showed minima like gold. The resistance of copper was constant in the helium range, but below 1°K it increased somewhat. Magnesium wires showed minima located anywhere between 25°K and 0.7°K. No minimum was found in aluminium. Molybdenum showed a minimum, but below 0.1°K the resistance became constant again. A very slight minimum was detected in cobalt, none was found in tungsten. At present the explanation of these minima is difficult. Several theories have been put forth among which that proposed by Korringa and Gerritsen seems most promising [86].

Many investigations below 1°K dealt with the discovery of new superconductors and the establishment of their threshold curves. The simplest technique consists in pressing together grains of the metal under investigation with the salt into a solid pill. After demagnetization the susceptibility of the pill is followed during the warming up. The disappearance of superconductivity is evidenced by a fairly sudden discontinuity in the susceptibility curve, since a superconductor behaves like a completely diamagnetic substance with volume susceptibility $-1/4\pi$, whereas the susceptibility of a normal metal can be neglected. Especially in investigations on threshold curves the heat contact has to be very good because of the caloric effects occurring in the transitions between the normal and the superconductive states. With this method Kurti and Simon [87] discovered the superconductivity of Zr, Cd and Hf. Daunt, Heer and Smith [88, 89, 90] established the transition points and threshold curves of Al, Ti, Zn, Zr, Cd and Hf. They showed the large influence of heat treatment on the threshold curve of Zr. Steele and Hein [91, 61] studied Ti, Zn, Ru and Cd; in the

case of Cd they found a dependance of the threshold curve on the particle size, which can be explained by a penetration depth of the order of 10^{-4} cm. Smith, Gager and Daunt [92] reexamined Ti.

The technique of making direct mechanical contact has some disadvantages:

1. in pressing the pill the metal is subjected to considerable stresses.
2. if particles of large size are used, the thermal contact between metal and salt may become bad owing to the difference in thermal expansion coefficients.
3. the magnetic field inside the pill is different from that outside, the difference being unknown if the particles are of irregular shape and distributed at random.
4. the magnetic field influences the temperature of the salt.

These disadvantages can be avoided by separating metal and salt and using the vane technique of Mendoza described above. In this way Goodman and Shoenberg [93, 94] discovered the superconductivity of Ru, Os and U, Goodman and Mendoza [95] established threshold curves of very pure Al, Zn, Ga and Cd. The threshold curve of Cd was also measured by Samoilov [95a]. Steele and Hein [61] measured a Ti crystal, using a carbon resistor to control their thermal contact.

The results obtained by the various investigators generally are in reasonably good agreement. No systematic differences between the two techniques are revealed. The threshold curves of Al, Zn, Ga, Zr, Ru and Os were found to be very well represented by parabolae. Clement showed [95b] that the threshold curve of Cd could be better expressed by an equation of cubic form. This is also in agreement with specific heat measurements by Samoilov [95c].

Only in the case of titanium a serious discrepancy exists between the results of Smith, Gager and Daunt [92] and Steele and Hein [61]. They investigated Ti crystal bars of similar chemical purity and hardness. The transition temperatures reported are 0.39°K and 0.49°K, the initial slopes of the threshold curves being —89.5 and —400 oersteds per degree respectively. The specimen used by Smith, Gager and Daunt was annealed subsequent to production, that of Steele and Hein was not. Moreover, different cooling techniques were used (see above). Possibly the annealing should be responsible for the differences. It seems to us, however, that in this case of a rather large sample and low transition temperatures the vane technique should be preferred.

The following elements have been investigated and no supercon-

ductivity has been found. Usually temperatures of about 0.1°K were reached [87, 95, 96]: Li, Be, Na, Mg, Si, K, Cr, Mn, Co, Cu, Ge, Y, Mo, Rh, Pd, Ag, Sb, Ba, Ce, Pr, Nd, W, Ir, Pt, Au, Bi.

c. HEAT CONDUCTIVITY

Several experiments on heat transport in metals below 1°K have been reported, all but one relating to superconducting metals. Two techniques were used:

1. A rod is connected with two salt pills, one on each side, which are demagnetized to slightly different temperatures. The connections are made either by high-pressure molding or by the vane technique. Temperatures are derived from the susceptibilities of the salt pills.
2. One pill is used as a heat sink, a heater is connected to the other end of the rod and the temperature difference is measured with two carbon resistors.

The thermal conductivity of copper was measured by Nicol and Tseng [97] using the first technique. They found, that the linear dependence on T which existed in the helium range, also remained valid below 1°K.

Heat conduction of superconductors has been investigated by Heer and Daunt [98] and by Goodman [99], who used the two pill technique, and by Mendelssohn, Olsen and Renton [100, 101] who used the second technique. Well below their transition temperature superconductors show a much smaller thermal conductivity than in the normal state. For further discussion we refer to Chap. X.

d. THERMAL VALVE AND CASCADE DEMAGNETIZATION

The large difference of heat conductivities in superconducting and normal states gives the possibility of using a wire of a superconducting material with a high transition temperature as a "thermal valve". The valve is "closed" if in the superconducting state, it can be easily "opened" by applying a magnetic field stronger than the critical field H_c.

The application of a superconductor as a thermal valve was suggested independently by several investigators (Gorter [102], Heer and Daunt [98], Mendelssohn and Olsen [103]). Also some other proposals for the construction of thermal valves have been made, but until now only superconducting valves have been realized successfully. They were used in the following three types of experiments.

Darby, Hatton, Rollin, Seymour and Silsbee [104] carried out a two

stage demagnetization using an apparatus consisting of a pill of iron alum connected by a pure lead wire to a pill of 1 : 20 diluted chromium alum. First the iron alum was demagnetized, while the chromium alum and the lead wire were kept in the field. After the temperatures of the alums had been equalized, a second demagnetization was carried out, whereby simultaneously the chrome alum was cooled down and the thermal valve was closed. Performing both demagnetizations from a field of 9000 oersteds a temperature was reached that might be obtained in a single demagnetization from a field of about 25000 oersteds.

A second application of a thermal valve was in the experiments on the specific heat of ^{3}He below 1°K of Daunt and de Vries [64], mentioned above. Here the ^{3}He container was cooled down by connecting it to an alum cylinder by means of a lead wire. After the demagnetization the superconducting wire insulated the salt from the container, so that one did not have to take into account the specific heat of the alum.

A third application was made in the construction of the so-called magnetic refrigerator, the principle of which we will describe now.

e. MAGNETIC REFRIGERATOR

A disadvantage of all the experiments below 1°K is the steady rise in temperature during the measurements, a consequence of the unavoidable heat influx. It would be of much importance to be able to maintain a specimen at a constant temperature for some time. Daunt and Heer proposed in 1949 [105] a technique for a cyclic magnetic refrigeration. As working substance a paramagnetic salt P is used (see Fig. 15). P is connected through the thermal valves V_1 and V_2 to the helium bath B (at about 1°K) and to the reservoir R, which is to be kept at a constant low temperature.

The operation procedure is as follows: The substance is magnetized with V_2 closed ($H_2 < H_c$) and V_1 open ($H_1 > H_c$), so that the heat of magnetization is conducted to the helium bath. Now V_1 is closed and P is demagnetized. If then V_2 is opened, heat flows from R to P until the temperatures are equalized. For highest efficiency the valve V_2 must be opened at the time that the temperature of P is equal to the temperature of R and from that moment the field H must be decreased so slowly that P and R remain in thermal equilibrium. From now the process of operation is repeated cyclically switching on and off the three magnetic fields each time in the same order. Finally R reaches

a temperature where the amount of heat that is extracted by P is equal to the heat leaking into R during each cycle.

Recent data on a magnetic refrigerator operating in Columbus (Ohio) [106] were reported at the Houston Low Temperature Conference. As a working substance 15 grams of iron ammonium alum were used compressed in a copper cylinder, thin ribbons of lead were used for the heat valves. Copper posts connected the alum with the valves, which had to be at some distance for practical reasons of magnet design. The initial value of H was 7000 oersteds, the time that each valve was open was about 50 seconds, the total cycle duration was 2 minutes. The final value of H was 1800 oersteds during the first cycles, it was gradually reduced till 300 oersteds. All the fields were automatically controlled. After about 30 minutes the reservoir reached a lowest temperature of 0.23 ± 0.02°K, the final heat extraction rate being 70 ergs per sec.

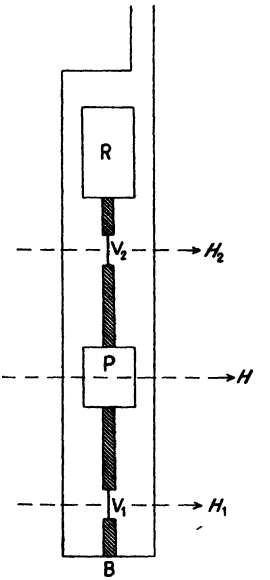

Fig. 15. Schematic diagram of a magnetic refrigerator.

The magnetic refrigerator seems to be most suitable for those experiments in which a rather large amount of energy is dissipated in the substance under investigation. In those cases a single demagnetization has the disadvantage that the temperature of the substance rises rapidly during the measurements, which, moreover, may easily cause an inhomogeneous temperature distribution.

6. Nuclear Orientation

a. METHODS FOR OBTAINING NUCLEAR ORIENTATION, NUCLEAR DEMAGNETIZATION

Many nuclei have a non-zero nuclear spin $I\,\hbar$, and a non-zero magnetic moment μ_n. In consequence, a sufficiently high magnetic field H will split up each electronic energy level into $2I + 1$ sublevels E_m ($m = -I, \ldots, +I$), the energy difference between two subsequent sublevels being $\mu_n H/I$.

In order to obtain a considerable nuclear orientation the populations of the sublevels must differ notably, thus $\mu_n H/I$ must be of the same

order as kT. Since μ_n is always very small (of the order of 10^{-3} times the electron magnetic moment) even in the most favourable cases a value of H/T of about 10^6 oersteds per degree is required to produce a nuclear magnetization of 10 per cent of the saturation value.

Gorter [107] and Kurti and Simon [108] pointed out that it should be necessary to cool down the nuclear sample by thermal contact with a paramagnetic salt which has been demagnetized adiabatically. After cooling there must be a high magnetic field at the place of the nuclear sample, while the field at the paramagnetic sample must be small. Since we saw in § 5 that cooling by thermal contact until now has only been successful down to temperatures which lie certainly not below 0.05°K, the very highest fields available in the laboratory are required to obtain a considerable nuclear orientation.

Originally the possibility of orienting nuclei was only considered in view of the attainment of still lower temperatures [107, 108, 109]. After breaking the heat contact between paramagnetic sample and nuclear sample a nuclear demagnetization could be made. The opening of a temperature region considerably below the region reached so far could be expected, as the interaction energy between the nuclei at equal concentration is a factor of about 10^6 smaller than between electron spins. It seems to be possible even to obtain and appreciable cooling by using a nuclear sample with a high concentration of nuclei (e.g. a metal). This has the advantage of a higher heat capacity.

Besides the possibility of reaching very low temperatures a nuclear demagnetization might also give information about the occurrence of ordering processes in assemblies of nuclei. Fröhlich and Nabarro [110] predicted the possibility of nuclear ferromagnetism, Garrett [111] pointed out that also an antiferromagnetic order might be expected.

Although many suggestions have been made for realizing a nuclear demagnetization [109, 112] no successful experiments have yet been reported. Moreover, during the last few years the interest has shifted from the temperatures to be reached by nuclear demagnetization to the magnetization itself in order to acquire data on nuclear processes involving oriented nuclei.

In 1948 Gorter [113] and Rose [114] independently suggested a new method for obtaining a considerable nuclear orientation. They pointed out that in paramagnetic ions the coupling between the nuclear spin and the surrounding electron spins can give rise to a hyperfine splitting of the order of $0.01 - 0.1\ k$, corresponding to a magnetic field at the

place of the nucleus of 10^5—10^6 oersteds. Thus, if in a salt containing such ions the electron spins are polarized (preferably oriented in one direction) at a temperature of some hundredths of a degree, a considerable nuclear polarization will occur. The polarization of the electron spins can easily be reached at such a low temperature using external fields of a few hundred oersteds. The conditions under which this method can be best applied were discussed by Bleaney [115] who also proposed an important variation (see part c).

The method yielded many interesting results. The orientation of the nuclei was proved by making use of the following nuclear processes:
1. The interaction of slow neutrons with polarized nuclei.
2. The radiation emitted by oriented radioactive nuclei.
The experiments on neutron interaction are given in part b, the investigations on radioactive emission are discussed in part c.

In 1949 Pound [116] suggested another method for nuclear orientation. He pointed out that the interaction of the nuclear electric quadrupole moment with a local electric field gradient could be used. High gradients are needed to give the required level splitting. They can be produced by asymmetric electron clouds as they occur in homopolar bonds. A single crystal or an assembly of single crystals with parallel axes have to be used. Paramagnetic ions are only needed for cooling. Here no resultant nuclear polarization is produced, only a nuclear *alinement*, since the energy levels E_{+m} and E_{-m} remain degenerate.

No successful experiments with this method have been reported. This may be caused by the existence of long relaxation times between nucleus and lattice.

In the following we shall distinguish carefully between nuclear orientation in which the nuclei are alined and orientation in which the nuclei are polarized, thus show a net magnetization.

b. ABSORPTION OF NEUTRONS BY POLARIZED NUCLEI

The cross section for absorption of polarized neutrons is different in the case of unpolarized and polarized nuclei. If σ_o is the resonance cross section in the absence of polarization, the cross sections for partly polarized neutrons (polarization fraction f_n) and partly polarized nuclei (polarization fraction f_N) with spin $I\,\hbar$ are to the first approximation given by [117]:

$$\sigma_+ = \sigma_o \left(1 + \frac{I}{I+1} f_N f_n\right),$$

if the spin of the compound state is $(I + \frac{1}{2})\,\hbar$, and:

$$\sigma_- = \sigma_0\,(1 - f_N f_n),$$

if the spin of the compound state is $(I - \frac{1}{2})\,\hbar$.

Thus the spin value of the resonance level of the compound nucleus can be determined from measurements of the resonance absorption, if the signs of f_N and f_n are known.

De Vries [118] pointed out that also in the case of nonpolarized neutrons a difference in absorption by unpolarized and polarized nuclei must be expected. In that case, however, we are dealing with a second order effect, quadratic in f_N.

Attempts to observe neutron absorption have been made in Leiden and in Oak Ridge. In Leiden no polarized neutron beams were available, a RaBe source of low intensity was used. The neutrons were slowed down by 2 cm of paraffin. A metal cryostat had to be used, because of the strong absorption of the neutrons by the glass dewars. As paramagnetic ions suitable for demonstrating the nuclear polarization gadolinium and samarium were chosen, since ^{155}Gd, ^{157}Gd and ^{149}Sm have large neutron cross sections. A mixture of gadolinium sulphate and chromium potassium alum was highly compressed in a flat container. It was demagnetized from a field of 21 000 oersteds at 1.1°K to fields of 1000, 500 and 0 oersteds. The transmitted neutron intensity (about 25 per cent of the incident intensity) was counted by BF_3-counters. Within the statistical spread of the measurements (about 5%) no effect in the transmission was found [119, 120]. This negative result could later be explained, when resonance measurements had shown that in the Gd-isotopes concerned almost no h.f.s. splitting occurred [121].

The measurements on samarium, carried out by demagnetizing a compressed mixture of samarium sulphate and chromium potassium alum from 21 000 oersteds down to 1200, 500 and 0 oersteds gave inconclusive results (stat. spread $1\frac{1}{2}$%) [120].

The first positive results were obtained in Oak Ridge on ^{55}Mn, irradiated by thermal neutrons [122]. In this case the change in transmission could not be used for the detection of the orientation because only a small fraction of the neutrons is captured. However, the ^{56}Mn compound nucleus formed is γ-radioactive with a half life of 2.6 hours. Therefore after irradiation the amount of ^{56}Mn formed was measured by removing the sample from the cryostat and counting its γ-radioactivity. The sample consisted of a pressed powder of $^{55}Mn(ND_4)_2(SO_4)_2.6D_2O$,

it had been deuterated to avoid incoherent neutron scattering by protons. It was demagnetized to a final field of 2350 oersteds, the final temperature being 0.20°K, as derived from gamma ray heating experiments (cf. § 3). Under these conditions an electron polarization of 85% is reached, from the known h.f.s. splitting [123] a nuclear polarization of 16% can be calculated. The sample was then irradiated by neutrons from a uranium reactor, which were polarized to an extent of 32% by passage through magnetized iron. All activity measurements were made relative to the activity of a Mn metal monitor, which was passed by the same beam of neutrons.

The results showed that at 0.20°K the sample activity with antiparallel neutron and nuclear polarizations was $3.38 \pm 0.34\%$ higher than the activity with parallel polarizations. Unfortunately, the measured effect could not be fully accounted for by theory. Probably this is caused by the fact that more than one resonance level is responsible for the neutron capture, while the place of these levels is not well established.

Preliminary measurements on ^{149}Sm have also been reported by the same group of workers [124]. The transmission of unpolarized neutrons of 0.075 eV by $Sm(C_2H_5SO_4)_3 \cdot 9H_2O$ was observed. The energy of 0.075 eV corresponds almost to the lowest resonance level of ^{149}Sm (0.094 eV), thus the transmission measurements might yield direct information on the spin of this level. Since in samarium ethyl sulphate at low temperatures only one Kramers doublet is occupied and the g-value is 0.60, high fields are required in order to reach a sufficient electron polarization. Therefore the samarium salt was cooled indirectly by a sample of iron ammonium alum the connection being made by a 12 cm long copper bar. The iron alum was demagnetized to a temperature of 0.07°K. Then a field of 11 000 oersteds could be applied to the Sm sample, while the iron alum remained in zero field. This set-up with cooling agent and cooled substance separated in space must be preferred to the Leiden design as described above, where the temperature of the cooling agent is influenced by the field.

The Sm sample was used as neutron polarizer, a single crystal of magnetized magnetite, set to reflect neutrons of 0.075 eV was used as analyzer. A change in counting rate of about 10% was measured, when the neutron polarization was destroyed. From the observed polarization direction of the transmitted neutrons a spin quantum number of $I+\frac{1}{2}$ follows for the 0.094 eV level of ^{149}Sm. From the degree of neutron

polarization the degree of polarization of the samarium nuclei could be calculated (about 12%), from which a sample temperature of 0.12 — 0.15°K could be derived. This is considerably higher than the temperature of the iron alum. Direct susceptibility measurements on the Sm sample were impossible because of the small amount of salt used.

c. GAMMA RADIATION EMITTED BY ORIENTED NUCLEI

In 1948 Spiers [125] remarked that in general the directional distribution of γ-radiation emitted by oriented nuclei should be anisotropic. Later Steenberg [126] and Tolhoek and Cox [127] gave general expressions for many types of transitions. Moreover, they gave formulae for the state of polarization of the emitted radiation.

In the case of dipole radiation, for instance, the directional distribution function is given by

$$W(\vartheta) = 2\,[1 + aP_2\,(\cos\vartheta)], \tag{24}$$

while in the case of quadrupole radiation

$$W(\vartheta) = 2\,[1 + aP_2\,(\cos\vartheta) + bP_4\,(\cos\vartheta)]. \tag{25}$$

ϑ is the angle with the axis of orientation, a and b are functions of the spin of the parent nucleus I_i and of the Boltzmann factor $\beta = \mu_n H/I_i kT$, depending on the kind of transition involved.

In general $W(\vartheta)$ consists only of even powers of $\cos\vartheta$, thus experiments on the radiation anisotropy require no polarization of the nuclei, but only an alinement. In 1951 Bleaney [115] gave an excellent analysis of the way in which such an alinement could be achieved in certain paramagnetic crystals. We shall not go into the details of this analysis, but may explain its results by simple reasoning. In these crystals, at the place of the paramagnetic ions, a strong inhomogeneous electric field is present of predominantly axial symmetry. It causes a splitting of the electronic levels, so that at low temperatures only a Kramers doublet is occupied. This, generally, will lead to an alinement of the electron magnetic moments with respect to the axis of the field. Then, at temperatures of the order of some hundredths of a degree, the magnetic coupling between nuclear spin and electron spins effects that the nuclei are also alined relative to the same axis. Thus, if a single crystal is used, a nuclear orientation occurs without the presence of an external magnetic field. An external field usually causes an undesired rise in temperature.

Information from measurements on oriented radioactive nuclei.

From the shape of the directional distribution of the gamma radiation one can determine the multipole order of the transition, since $W(\vartheta)$ depends strongly upon this multipole character. In special cases it may be possible to obtain the spin values of the nuclear levels involved in the transition from the coefficients a and b in equation (24) or (25). If the decay scheme is well-known, β can be determined from which one of the quantities μ_n, H or T can be found, if the other two are known. For instance, μ_n can be determined, if H and T are known, respectively from paramagnetic resonance measurements on the stable isotope and from caloric measurements. Or the directional distribution can serve as a thermometer, if the nuclear data are known.

By measuring the direction of the linear polarization of the emitted γ-rays one can distinguish between the electric and the magnetic character of the transition.

In the case of *polarized* nuclei circular polarized γ-radiation is emitted. From the sense of this circular polarized radiation the sign of μ_n can be determined.

Suggestions have been made to determine the nuclear gyromagnetic ratio of oriented radioactive nuclei by applying a radiofrequent magnetic field to the nuclei [128, 129]. As soon as the frequency of the field is in resonance, the radiation anisotropy will disappear in consequence of induced transitions among the h.f.s.-levels. The gyromagnetic ratio γ follows from the resonant frequency ν_r and the magnetic field at the nucleus: $2\pi\nu_r = \gamma H$. An experimental problem seems to be avoiding spurious heating by non-resonant electron spin-spin absorption during the search for nuclear resonance.

Several paramagnetic and γ-radioactive isotopes suitable for nuclear orientation are known. A complication, however, arises from the requirement of a reasonably long lifetime for these experiments (preferably more than a month). This means, that almost no direct γ-emitters are available, but only nuclei with a preceding β-emission or K-capture. This preceding transition disturbs the initial orientation. It is possible to account for this desorientation, assuming that between the β-transition and γ-emission no appreciable spin precession occurs nor a reorientation due to the recoil of the nucleus. In the case of K-capture calculations show that the desorientation due to the hole in the K-shell is generally negligible because of the very short lifetime of the hole [129a].

In certain cases it might be possible to obtain information about the character of the β-transition preceding a γ-emission from the measured angular distribution of the γ-radiation [130].

Experimental results

Only a few examples of crystals suitable for the production of an appreciable nuclear alinement are known. Until now merely the cobalt Tutton salts have been used. Here the electric field properties are very favourable; a disadvantage is that the unit cell contains two ions having axes of alinement which make an angle of about 70 degrees [131]. The crystals have to be magnetically diluted, the criterion being that the h.f.s.-splitting must be reasonably resolved in the paramagnetic resonance spectrum.

For the production of nuclear polarization such crystals must be chosen in which the h.f.s.-splittings caused by the crystalline electric field can be easily surpassed by the splittings caused by an external magnetic field. Mixed crystals of cerium magnesium nitrate appeared to be suitable.

The following results have been obtained:

COBALT 60

In Oxford 70 μC of ^{60}Co was included in six crystals of (1% Co, 12%Cu, 87%Zn)$Rb_2(SO_4)_2 \cdot 6H_2O$ [132]. The copper ions acted as cooling agent having a much smaller h.f.s.-splitting. By demagnetizing from an H/T of 30 000 oersteds per degree a temperature of about 0.01°K was reached. The γ-ray intensities in the direction of the bisector of the axes of alinement (K_1-direction) and perpendicular to these axes (K_2-direction) were measured. A maximum anisotropy $(J_{K_2} - J_{K_1})/J_r$ of 35 per cent was obtained, J_r being the intensity at random orientation. Assuming as decay scheme for ^{60}Co:

$$I_i = 5 \xrightarrow{\beta^-} I = 4 \xrightarrow{\gamma_1} I = 2 \xrightarrow{\gamma_2} I = 0$$

and correcting theoretically for the difference in magnetic and thermodynamic temperature a μ_n-value of 3.5 ± 0.5 n.m. was derived.

From measurements of the linear polarization the electric character of the γ-transitions was confirmed [133].

Independently in Leiden experiments were made on a crystal of (3.5%Co, 96.5%Zn) $NH_4)_2 \cdot (SO_4)_2 \cdot 6H_2O$, containing 90 μC of ^{60}Co[134].

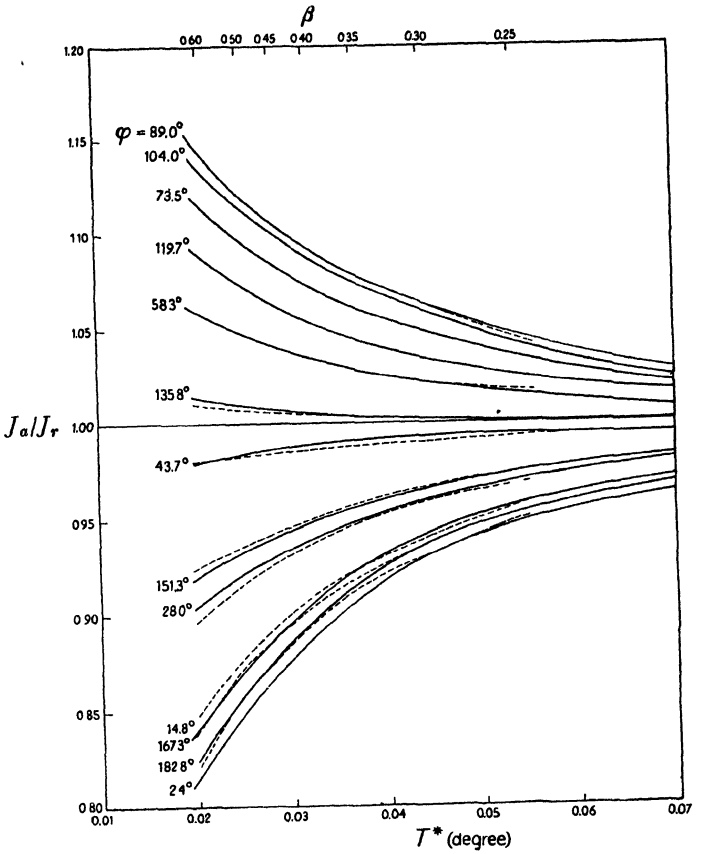

Fig. 16. Normalized intensity J_a/J_r of gamma radiation from ^{60}Co in (1%Co, 20%Cu, 79%Zn) $(NH_4)_2(SO_4)_2 \cdot 6H_2O$ as a function of T^* and of β ($= \mu_n H/I_1 kT$). φ denotes the angle between the K_1-axis and the direction of observation. Solid lines: experimental curves. Dashed lines: theoretical curves ($\alpha = 33°$). The uppermost theoretical curve was fitted to the uppermost experimental curve by a transformation of the β-scale into the T^*-scale. The theoretical curves of $\varphi = 2.4°$ and $\varphi = 182.8°$ almost coincide. The experimental curves of $\varphi = 14.8°$ and $\varphi = 167.3°$ coincide. The statistical spread of the measurements was about 0.2%.

The crystal was embedded in chrome alum to screen it from heat leaking in. An anisotropy of about 15% was found.

Later a stack of six single crystals was used, also containing copper ions as cooling agent [135]. The chrome alum envelope was removed. The heat leakage through the glass support was cut off by inserting a piece of chrome alum, which was also demagnetized. The best results

were obtained with the crystals (1%Co, 20%Cu, 79%Zn) $(NH_4)_2(SO_4)_2 \cdot 6H_2O$, containing 50 μC of ^{60}Co [136]. A complete angular diagram could be measured in the K_1-K_2-plane. It is given in Fig. 16. The best agreement with theory was found if the angle between the axes of alinement, 2α, was taken as 66°.

More accurate measurements on the crystal, containing no copper, (up to a temperature of 0.1°K, where $T^* \approx T$) yielded a value of 4.3 ± 0.2 n.m. for the magnetic moment of ^{60}Co.

Recent experiments in which the anisotropy was measured for both gamma rays separately showed no difference in J_{K_1}/J_{K_2} within the limits of accuracy (slightly better than 1%).

Experiments on polarization of ^{60}Co were made in Oxford by using crystals of $3[(0.5\%Co, 99.5\%Mg)(NO_3)_2]\ 2Ce(NO_3)_3 \cdot 24H_2O$, containing 50 μC of ^{60}Co [137]. Very low temperatures could be reached, because cerium has no nuclear spin. Moreover, the external polarizing field could be applied in the direction in which Ce has a very low g-value (see Chap. XII), so that the resulting rise in temperature is small. Anisotropies up to 50% in an external field of about 400 oersteds were found. A detailed analysis of the results was impossible, because of the unknown influence of the third Co-ion of the unit cell that shows alinement in zero field, while, moreover, the corrections for the magnetic interaction of the Co-ions with the neighbouring Ce-ions are not very well known.

COBALT 58

The directional anisotropy of ^{58}Co was measured by Daniels *et al.*[138] using cobalt rubidium Tutton salt of the same composition as mentioned above. By fitting the theoretical and experimental curves the best agreement was obtained for the decay scheme:

$$I_i = 2 \xrightarrow{85\%K,\ 15\%\beta^+} I = 2 \xrightarrow{\gamma} I = 0.$$

A magnetic moment of 3.5 ± 0.3 n.m. was derived. Measurements on the polarization direction showed the γ-transition to have an electric quadrupole character [133].

COBALT 56

Preliminary measurements on ^{56}Co were made in Leiden. It was alined in the same manner as was ^{60}Co (by including 20 μC of ^{56}Co in a single crystal of (1%Co, 20%Cu, 79%Zn) $(NH_4)_2(SO_4)_2 \cdot 6H_2O$

and cooling to about 0.02°K). Using NaJ-crystal scintillation counters for γ-ray energy discrimination, anisotropies in four of the six gamma rays from the excited states of ^{56}Fe were measured. The results indicate that the 0.84, 1.23 and 3.25 MeV transitions probably are quadrupole in character with a spin change $\Delta I = 2$; and that the 1.74 MeV transition is dipole, $\Delta I = 1$. From the magnitude of the anisotropy it can be concluded that the magnetic moment of ^{56}Co is of about the same order as that of ^{60}Co (or slightly smaller).

MANGANESE 54

Preliminary results on polarization of ^{54}Mn have been reported by Kurti at the Houston Low Temperature Conference. ^{54}Mn decays by K-capture in ^{54}Cr which emits one γ-ray. It was included in crystals of the same type as used for the polarization experiments of ^{60}Co. Using polarizing fields up to 1000 oersteds, anisotropies up to 80% were observed. Of the two possibilities existing for the excited state of ^{54}Cr, $I = 1$ or $I = 2$, the possibility $I = 1$ could be ruled out.

The nuclear information obtained so far in experiments on oriented radioactive nuclei is rather limited. The main reason for this seems to be that until now one has been restricted to nuclei of paramagnetic ions, while the crystals in which the paramagnetic ions are included have to meet very special requirements concerning their electric field properties. Moreover, exact determinations of magnetic moments involve an accurate knowledge of the thermodynamic temperature. In § 3 we saw that the establishment of the precise relation between T and T^* below 1°K usually is not a simple problem.

REFERENCES

[1] P. Debije, Ann. d. Phys. **81**, 1154 (1926).
[2] W. F. Giauque, Journ. Am. Chem. Soc. **49**, 1864, 1870 (1927).
[3] W. J. de Haas, E. C. Wiersma and H. A. Kramers, Physica **1**, 1 (1933—34); Leiden Comm. No. 229a.
[4] W. F. Giauque and D. P. MacDougall, Phys. Rev. **43**, 768 (1933).
[5] N. Kurti and F. Simon, Nature **133**, 907 (1934).
[6] W. F. Giauque, Phys. Rev. **92**, 1339 (1953).
[7] A. H. Cooke, R. A. Hull, Proc. Roy. Soc. London A **181**, 83 (1942).
[8] R. A. Hull, K. R. Wilkinson, J. Wilks, Proc. Phys. Soc. A **64**, 379 (1951).
[9] J. Darby, J. Hatton, B. V. Rollin, E. F. W. Seymour and H. S. Silsbee, Proc. Phys. Soc. A **64**, 861 (1951).
[10] S. Bernstein, L. D. Roberts, C. P. Stanford, J. W. T. Dabbs and T. E. Stephenson, Phys. Rev. **94**, 1243 (1954).

[11] P. Weiss, Journ. de Phys. **6**, 353 (1907).
[12] F. Bitter and F. E. Reed, Rev. Sci. Inst. **22**, 171 (1951).
[13] F. Bitter, Rev. Sci. Inst. **7**, 482 (1936).
[14] F. Bitter, Rev. Sci. Inst. **10**, 373 (1939).
[15] W. F. Giauque and J. W. Stout, Journ. Am. Chem. Soc. **61**, 1384 (1939).
[16] D. de Klerk, Thesis, Leiden 1948, pag. 36.
[17] M. J. Steenland, Thesis, Leiden 1952, pag. 12.
[18] R. A. Erickson, L. D. Roberts and J. W. T. Dabbs, Rev. Sci. Inst. (in the press).
[19] D. de Klerk, Proc. N.B.S. Semicentennial Symposium on Low-Temp. Physics 1951 pag. 211.
[20] N. Kurti and F. Simon, Phil. Mag. **26**, 849 (1938).
[21] J. H. van Vleck, Journ. Chem. Phys. **5**, 320 (1937).
[22] M. H. Hebb and E. M. Purcell, Journ. Chem. Phys. **5**, 338 (1937).
[23] C. G. B. Garrett, Proc. Roy. Soc. London A **203**, 375 (1950).
[24] C. G. B. Garrett, Magnetic Cooling, Harvard University Press, 1954.
[25] W. F. Giauque and D. P. MacDougall, Phys. Rev. **47**, 885 (1935).
[26] N. Kurti and F. Simon, Phil. Mag. **26**, 840 (1938).
[27] H. B. G. Casimir, W. J. de Haas and D. de Klerk, Physica **6**, 255 (1939); Leiden Comm. No. 256b.
[28] R. L. Platzman, Phil. Mag. **44**, 497 (1953).
[29] N. Kurti and F. E. Simon, Phil. Mag. **44**, 501 (1953).
[30] D. de Klerk and R. P. Hudson, Phys. Rev. **91**, 278 (1953).
[31] B. Bleaney, Proc. Roy. Soc. London A **204**, 203 (1950).
[32] H. Lipson, Proc. Roy. Soc. London A **151**, 347 (1935).
[33] H. B. G. Casimir, W. J. de Haas and D. de Klerk, Physica **6**, 365 (1939); Leiden Comm. No. 256c.
[34] H. B. G. Casimir, D. de Klerk and D. Polder, Physica **7**, 737 (1940); Leiden Comm. No. 261a.
[35] D. de Klerk, M. J. Steenland and C. J. Gorter, Physica **15**, 649 (1949); Leiden Comm. No. 278c.
[36] A. H. Cooke, Proc. Phys. Soc. A **62**, 269 (1949).
[37] B. Bleaney, Proc. Roy. Soc. London A **204**, 216 (1950).
[38] D. Bijl, Physica **14**, 684 (1949); Leiden Comm. No. 276b.
[39] R. P. Hudson, Phys. Rev. **88**, 570 (1952).
[40] J. M. Daniels and N. Kurti, Proc. Roy. Soc. London A **221**, 243 (1954).
[41] W. E. Gardner and N. Kurti, Proc. Roy. Soc. London A **223**, 542 (1954).
[41a] D. de Klerk, M. J. Steenland and C. J. Gorter, Physica **16**, 571 (1950); Leiden Comm. No. 282a.
[42] N. Kurti, J. Phys. Radium **12**, 281 (1951).
[43] N. Kurti, P. Lainé and F. Simon, C. R. Acad. Sci. Paris **204**, 675 (1937).
[44] M. J. Steenland, D. de Klerk and C. J. Gorter, Physica **15**, 711 (1949); Leiden Comm. No. 278d.
[45] J. A. Beun, D. de Klerk, M. J. Steenland and C. J. Gorter, in course of publication.
[46] M. J. Steenland, L. C. van der Marel, D. de Klerk and C. J. Gorter, Physica **15**, 906 (1949); Leiden Comm. No. 279c.
[47] M. J. Steenland, D. de Klerk, M. L. Potters and C. J. Gorter, Physica **17**, 149 (1951); Leiden Comm. No. 284b.
[48] C. G. B. Garrett, Proc. Roy. Soc. London A **206**, 242 (1951).
[48a] T. van Peski-Tinbergen and C. J. Gorter, Physica **20**, 592 (1954); Leiden Comm. Suppl. No. 109a.

[49] S. F. Malaker, Phys. Rev. **84, 133** (1951).
[50] M. J. Steenland, D. de Klerk, J. A. Beun and C. J. Gorter, Physica **17, 161** (1951); Leiden Comm. No. 284d.
[51] C. G. Shull and J. S. Smart, Phys. Rev. **76, 1256** (1949).
C. G. Shull, W. A. Strauser and E. O. Wollan, Phys. Rev. **83, 333** (1951).
[52] N. J. Poulis and G. E. G. Hardeman, Physica **18, 201** and **315** (1952); Leiden Comm. No. 287a and 288b.
[53] N. Kurti, B. V. Rollin and F. Simon, Physica **3, 266** (1936).
[54] H. B. G. Casimir, Physica **6, 156** (1939); Leiden Comm. Suppl. No. 85c.
[55] C. G. B. Garrett, Phil. Mag. **41, 621** (1950).
[56] W. Heitler and E. Teller, Proc. Roy. Soc. London A **155, 640** (1936).
[57] N. Kurti and F. Simon, Nature **142, 207** (1938).
[58] D. de Klerk, Physica **12, 513** (1946); Leiden Comm. No. 270c.
[59] R. P. Hudson, B. Hunt and N. Kurti, Proc. Phys. Soc. A **62, 392** (1949).
[60] E. Mendoza, Cérémonies Langevin-Perrin, Paris 1948, pag. 53.
[61] M. C. Steele and R. A. Hein, Phys. Rev. **92, 243** (1953).
[62] J. Wilks, Oxford Low Temp. Conf. Report 1951, pag. 33.
[63] H. C. Kramers, J. D. Wasscher and C. J. Gorter, Physica **18, 329** (1952); Leiden Comm. No. 288c.
[64] J. G. Daunt and G. de Vries, Phys. Rev. **93, 631** (1954).
[65] T. R. Roberts and S. G. Sydoriak, Phys. Rev. **93, 1418** (1954).
[66] D. W. Osborne, B. M. Abraham and B. Weinstock, Phys. Rev. **94, 202** (1954).
[67] B. Weinstock, B. M. Abraham and D. W. Osborne, Phys. Rev. **85, 158** (1952).
[68] D. de Klerk, R. P. Hudson and J. R. Pellam, Phys. Rev. **93, 28** (1954).
[69] H. C. Kramers, F. A. W. van den Burg and C. J. Gorter, Phys. Rev. **90,** 1117 (1953).
[70] V. Mayper and M. A. Herlin, Phys. Rev. **89,** 523 (1953).
[71] J. C. King and H. A. Fairbank, Phys. Rev. **93,** 21 (1954).
[72] E. Ambler and N. Kurti, Phil. Mag. **43, 260** (1952).
[73] L. Lesensky and H. A. Boorse, Schenectady Low Temp. Conf. 1952, pag. 33.
[74] G. J. C. Bots and C. J. Gorter, Phys. Rev. **90,** 1117 (1953).
[75] J. G. Daunt and C. V. Heer, Phys. Rev. **79, 46** (1950).
[76] H. van Dijk, W. H. Keesom and J. P. Steller, Physica **5,** 625 (1938); Leiden Comm. No. 252g.
[77] J. F. Allen and E. S. Shire, Nature **139,** 878 (1937).
[78] W. F. Giauque, J. W. Stout and C. W. Clark, Journ. Am. Chem. Soc. **60,** 1053 (1938).
[79] T. H. Geballe, D. N. Lyon, J. M. Whelan and W. F. Giauque, Rev. Sci. Inst. **23,** 489 (1952).
[80] J. R. Clement, E. H. Quinnell, M. C. Steele, R. A. Hein and R. L. Dolecek, Rev. Sci. Inst. **24,** 545 (1953).
[81] D. H. Howling, F. J. Darnell and E. Mendoza, Phys. Rev. **93,** 1416 (1954).
[82] W. J. de Haas, H. B. G. Casimir and G. J. van den Berg, Physica **5,** 225 (1938); Leiden Comm. No. 251c.
[83] E. Mendoza and J. G. Thomas, Phil. Mag. **42,** 291 (1951).
[84] A. J. Croft, E. A. Faulkner, J. Hatton and E. F. W. Seymour, Phil. Mag. **44,** 298 (1953).
[85] J. G. Thomas and E. Mendoza, Phil. Mag. **43,** 900 (1952).
[86] J. Korringa and A. N. Gerritsen, Physica **19, 457** (1953); Leiden Comm. Suppl. No. 106.
[87] N. Kurti and F. Simon, Proc. Roy. Soc. London A **151,** 610 (1935).
[88] J. G. Daunt and C. V. Heer, Phys. Rev. **76,** 715 (1949).

[89] J. G. Daunt and C. V. Heer, Phys. Rev. **76**, 1324 (1949).
[90] T. S. Smith and J. G. Daunt, Phys. Rev. **88**, 1172 (1952).
[91] M. C. Steele and R. A. Hein, Phys. Rev. **87**, 908 (1952).
[92] T. S. Smith, W. B. Gager and J. G. Daunt, Phys. Rev. **89**, 654 (1953).
[93] B. B. Goodman and D. Shoenberg, Nature, London **165**, 441 (1950).
[94] B. B. Goodman, Nature, London **167**, 111 (1951).
[95] B. B. Goodman and E. Mendoza, Phil. Mag. **42**, 594 (1951).
[95a] B. N. Samoilov, Doklady Akad. Nauk, SSSR **81**, 791 (1951).
[95b] J. R. Clement, Phys. Rev. **92**, 1578 (1953).
[95c] B. N. Samoilov, Doklady Akad. Nauk, SSSR **86**, 281 (1952).
[96] N. E. Alekseyevski and L. Migunov, J. Phys. USSR **11**, 95 (1947).
[97] J. Nicol and T. P. Tseng, Phys. Rev. **92**, 1062 (1953).
[98] C. V. Heer and J. G. Daunt, Phys. Rev. **76**, 854 (1949).
[99] B. B. Goodman, Proc. Phys. Soc. A **66**, 217 (1953).
[100] J. L. Olsen and C. A. Renton, Phil. Mag. **43**, 946 (1952).
[101] K. Mendelssohn and C. A. Renton, Phil. Mag. **44**, 776 (1953).
[102] C. J. Gorter, Cérémonies Langevin-Perrin, Paris 1948, pag. 76.
[103] K. Mendelssohn and J. L. Olsen, Proc. Phys. Soc. A **63**, 2 (1950).
[104] J. Darby, J. Hatton, B. V. Rollin, E. F. W. Seymour and H. S. Silsbee, Proc. Phys. Soc. A **64**, 861 (1951) (see also ref. 84).
[105] J. G. Daunt and C. V. Heer, Phys. Rev. **76**, 985 (1949).
[106] C. V. Heer, C. B. Barnes and J. G. Daunt, Phys. Rev. **91**, 412 (1953).
[107] C. J. Gorter, Phys. Z. **35**, 923 (1934).
[108] N. Kurti and F. E. Simon, Proc. Roy. Soc. London A **149**, 152 (1935).
[109] F. E. Simon, C. R. Congr. Magnétisme, Strasbourg **3**, 1 (1939).
[110] H. Fröhlich and F. R. N. Nabarro, Proc. Roy. Soc. London A **175**, 382 (1940).
[111] C. G. B. Garrett, J. Chem. Phys. **19**, 1154 (1951).
[112] N. Kurti, Cérémonies Langevin-Perrin, Paris, 1948, pag. 29; see also § 5.
[113] C. J. Gorter, Cérémonies Langevin-Perrin, Paris, 1948, pag. 77; Physica **14**, 504 (1948); Leiden Comm. Suppl. No. 97d.
[114] M. E. Rose, U.S. At. En. Comm. Report AECD-2119 (1948); Phys. Rev. **75**, 213 (1949); see also: A. Simon, M. E. Rose and J. M. Jauch, Phys. Rev. **84**, 1155 (1951).
[115] B. Bleaney, Proc. Phys. Soc. A **64**, 315 (1951); Phil. Mag. **42**, 441 (1951).
[116] R. V. Pound, Phys. Rev. **76**, 1410 (1949).
[117] M. E. Rose. Nucleonics **3**, No. 6, 23 (1948); Phys. Rev. **75**, 213 (1949).
[118] See: O. J. Poppema, Thesis, Groningen 1954, Ch. II
[119] C. J. Gorter, D. de Klerk, O. J. Poppema, M. J. Steenland and Hl. de Vries, Physica, **15**, 679 (1949).
[120] O. J. Poppema, Thesis, Groningen 1954, Ch. III.
[121] B. Bleaney, R. J. Elliott, H. E. D. Scovil and R. S. Trenam, Phil. Mag. **42**, 1062 (1951).
[122] S. Bernstein, L. D. Roberts, C. P. Stanford, J. W. T. Dabbs and T. E. Stephenson, Phys. Rev. **94**, 1243 (1954).
[123] B. Bleaney and D. J. E. Ingram, Proc. Roy. Soc. London A **205**, 336 (1951).
[124] L. D. Roberts, S. Bernstein, J. W. T. Dabbs and C. P. Stanford, Phys. Rev. **95**, 105 (1954).
[125] J. A. Spiers, Nature, London **161**, 807 (1948).
[126] N. R. Steenberg, Phys. Rev. **84**, 1051 (1951); Proc. Phys. Soc. A **65**, 791 (1952); Proc. Phys. Soc. A **66**, 391 (1953).
[127] H. A. Tolhoek and J. A. M. Cox, Physica **18**, 357, 359, 1257 and 1262 (1952); Physica **19**, 101 and 673 (1953); J. A. M. Cox, Thesis, Leiden 1952 Survey

articles: S. R. de Groot, Physica **18**, 1201 (1952); S. R. de Groot and H. A. Tolhoek, Beta and gamma spectroscopy. Noord Holl. Publ. Comp., in the press.

[128] H. A. Tolhoek and S. R. de Groot, Physica **17**, 82 (1951).

[129] N. Bloembergen and G. M. Temmer, Phys. Rev. **89**, 883 (1953).

[129a] H. A. Tolhoek, Chr. D. Hartogh and S. R. de Groot, Colloque C.N.R.S. sur le rôle du cortège électronique dans les phénomenès radioactifs. Paris, 1954 in the press.

[130] J. A. M. Cox, S. R. de Groot and Chr. D. Hartogh, Physica **19**, 1119 and 1123 (1953).

[131] B. Bleaney and D. J. E. Ingram, Proc. Roy. Soc. London A **208**, 143 (1951).

[132] B. Bleaney, J. M. Daniels, M. A. Grace, H. Halban, N. Kurti, F. N. H. Robinson and F. E. Simon, Nature, London **168**, 780 (1951); Phys. Rev. **85**, 688 (1952); Physica **18**, 1227 (1952); Proc. Roy. Soc. London A **221**, 170 (1954).

[133] G. R. Bishop, J. M. Daniels, G. Goldschmidt, H. Halban, N. Kurti and F. N. H. Robinson, Phys. Rev. **88**, 1432 (1952).

[134] C. J. Gorter, O. J. Poppema, H. A. Tolhoek, M. J. Steenland and J. A. Beun, Physica **17**, 1050 (1951); Leiden Comm. No. 287b and Physica **18**, 135 (1952); Leiden Comm. Suppl. No. 104a.

[135] O. J. Poppema, J. A. Beun, M. J. Steenland and C. J. Gorter, Physica **18**, 1235 (1952); Leiden Comm. No. 291a.

[136] O. J. Poppema, Thesis, Groningen 1954, Ch. IV.

[137] E. Ambler, M. A. Grace, H. Halban, N. Kurti, H. Durand, C. E. Johnson and H. R. Lemmer, Phil. Mag. **44**, 216 (1953).

[138] J. M. Daniels, M. A. Grace, H. Halban, N. Kurti and F. N. H. Robinson, Phil. Mag. **43**, 1297 (1952).

CHAPTER XV

THEORETICAL REMARKS ON FERROMAGNETISM AT LOW TEMPERATURES

BY

L. NÉEL
UNIVERSITÉ, GRENOBLE

1. Introduction

Among the questions in the domain of ferromagnetism which may be solved by using low temperatures, those that are directly concerned with the thermal fluctuations appear to be the most interesting: their manifestation depends on the ratio of the thermal energy kT to the various anisotropy energies, and this ratio can be varied between wide limits. Unfortunately, the properties involved must be studied in magnetic fields that are smaller than, or comparable to, the coercive force, i.e. in a region where the theoretical description of the phenomena does not yet possess the complete rigour and generality one would desire. No rapid progress can therefore be expected in this field.

There are only two extreme examples for which it is possible to give a clear and satisfactory picture of the magnetization process inside the hysteresis region. On the one hand there is the case of a finely divided substance the grains of which are so small that they contain only a single elementary Weiss domain, and which are sufficiently separated from each other, so that their interactions may be neglected. The other case is that of a solid substance which is sufficiently pure and homogeneous, so that the elementary domains are large and well-formed, and such that the walls that separate them (the Bloch walls) are approximately plane and at a distance from each other that is large compared to their thickness. Incidentally, pure iron is about the only substance for which it will be possible to satisfy these various conditions.

Let us investigate the importance of the thermal fluctuations in these two cases successively.

2. Finely Dispersed Substances

One may either have independent grains, which are usually obtained by chemical means, or ferromagnetic grains that are dispersed in a non-magnetic phase, and which are obtained during segregation by cooling a homogeneous phase that is stable at high temperatures. If the grains are to contain only a single elementary domain, we have shown [1] that their diameter must be smaller than a certain critical diameter D_c given by:

$$D_c = 0.69\, a\, N^{\frac{1}{2}} \left(\mathrm{Log} \frac{D_c}{a} - 0.307 \right)^{\frac{1}{2}},$$

in which N is the coefficient of the molecular field (referred to unit volume) and a the distance between neighbouring atoms: for iron, one thus finds $D_c = 320$ Å. For the ordinary ferromagnetic substances, neither a nor N varies appreciably between room temperature and absolute zero. We may therefore assume that the critical diameter D_c is practically independent of the temperature.

When the diameter is smaller than D_c, the magnetic moment M of a grain of volume V preserves a constant magnitude equal to the product of the spontaneous magnetization J and the volume V. The energy of the grain, on the other hand, depends on the *orientation* of M. Consequently, various factors come into play: the magnetocrystalline and the magnetoelastic energy, the demagnetizing field, and finally the *surface anisotropy*, a new effect which; as we have shown [2], is of importance for the case of very small grains with a diameter smaller than 100 Å. The result is that in each grain the magnetization M has two antiparallel orientations of minimum energy separated by a potential barrier. In the absence of an external magnetic field, the magnetic moment of a grain points in one of these two directions. When the magnetizing field has been reduced to zero after magnetization to saturation in a certain direction Δ, the individual magnetic moments of the grains point in that direction of minimum energy that is closest to Δ: an ensemble of randomly oriented grains thus shows a remanent magnetization equal to one half of the saturation magnetization. To destroy this remanent magnetization, it is necessary to force the individual magnetic moments of the grains over the potential barriers by applying a certain coercive field H_c in the opposite direction. This field is equal [1] to 0.48 H_c, if H_c is the coercive force of an ensemble of grains for which the directions of minimum energy are all parallel

to the direction of magnetization. This field is a measure for the height of the potential barrier separating the two antiparallel directions of minimum energy. Indicating the difference in energy between the top and the minimum of the barrier by E, we have [3]:

$$E = \tfrac{1}{2} V J_s H_c.$$

The details of the theory of the magnetic properties of an ensemble of small grains has been the object of a number of papers [1, 3, 4], and it is unnecessary to reproduce them here. However, it is essential to remember that the theory is applicable only if the thermal energy kT is considerably smaller than the energy E defined above: to fix ideas, kT must be 20 to 30 times smaller than E. Otherwise, the thermal fluctuations are able to force the magnetic moment of a grain over the potential barrier from one direction of minimum energy to the opposite one. In the limit of very small grains with a diameter of say 10 Å, in zero external field a time interval smaller than one millionth of a second is sufficient to go from one equilibrium position to the other. In other words, this ensemble of very small grains can reach the state of thermodynamical equilibrium that corresponds to the imposed external conditions almost instantaneously, and so behaves in first approximation like an ensemble of independent magnetic moments, subjected to the classical statistics, and of individual moment equal to VJ_s: there is no longer any hysteresis. Consequently, the ensemble of grains is paramagnetic, and no longer possesses any ferromagnetic properties, at least in so far as one considers these properties to be bound to the presence of a remanent magnetization and coercive force.

Hence it is necessary to mark the division between the ferro and the paramagnetic grains.

For this it is necessary to know the perturbing forces, or more exactly the perturbing couples perpendicular to M, which are able to turn the magnetic moment of a grain from one direction to the other. A complete list of these couples has not yet been made, but it appears that the couples corresponding to the variations in the demagnetizing field and the magnetocrystalline forces that result from the thermoelastic deformations of the crystal lattice, are the most effective.

Consider a grain with a magnetic symmetry of an ellipsoid of revolution, which is subjected to a magnetic field in the direction of the symmetry axis R. In the absence of any perturbations the magnetic moment M describes a precession around R, keeping the angle φ

between M and R constant. A perturbing couple Γ, perpendicular to R, brings about a change in φ, and can thus overcome a potential barrier for M. In this way, the spontaneous thermoelastic deformations of the grain alter the symmetry and give rise to a perturbing couple of magnetocrystalline origin. The magnitude of the average value of this couple is given by [3] the expression:

$$\bar{\Gamma} = 3\,\lambda(2\,G\,k\,T/\pi\,V)^{\frac{1}{2}}.$$

These same thermoelastic deformations destroy the axial symmetry of the external form of the grain, and thus give rise to a perturbing demagnetizing field, and hence to a couple:

$$\bar{\Gamma} = D\,J_s^2\,(2\,k\,T/\pi\,V\,G)^{\frac{1}{2}}.$$

In these expressions, λ is the longitudinal magnetostriction at saturation (supposed to be isotropic), G is the modulus of shear elasticity, k the Boltzmann constant, and D a numerical coefficient depending on the form of the grain, but being always approximately equal to 3. For small values of the volume V of the grains, these perturbing couples are, of course, more important than for large values of V. Let us now consider an ensemble of identical grains, which at the time $t = 0$ has a certain resultant remanent magnetization M_0 in an external field zero. As a result of the spontaneous reorientations of the magnetic moments, the resultant remanent moment decreases with increasing time, and at the time t its value M_r is given by:

$$M_r = M_0 \exp\,(-t/\tau_0),$$

in which τ_0 is a relaxation time that can be expressed in terms of the perturbing couples by means of the relation [3]:

$$\frac{1}{\tau_0} = (e\,H_c/m)\,\left|\,3\,G\,\lambda + D\,J_s^2\,\right|\left(\frac{2\,V}{\pi\,G\,k\,T}\right)^{\frac{1}{2}} \exp\left(-\frac{V\,H_c\,J_s}{2\,k\,T}\right),$$

where e and m represent respectively the elementary electric charge and the mass of the electron.

The application of this formula to grains of iron with a coercive force $H_c = 1000$ oersteds shows that the relaxation time varies from 10^{-1} to 10^{9} seconds when the ratio V/T increases from 3.2 tot 7.0, which corresponds to an increase of the diameter of the grains of only 30%.

If the relaxation time of a grain is smaller than 10^{-1} second, the grain may be said to be paramagnetic, since it comes to equilibrium in the applied field almost instantaneously. If, on the other hand, the

relaxation time is larger than 10^9 seconds, the grain must be said to be ferromagnetic, since it is able to preserve its remanent magnetization during a practically indefinite time. The numerical values given above show that in an ensemble of grains with different diameters, the division between the two kinds of grains is unambiguous and the transition region relatively small. For iron at room temperature this division corresponds to grains of a diameter of 160 Å, while at 1°K it would correspond to a diameter of 25 Å. By extending the study of the magnetic properties to very low temperatures, it is thus possible to explore the granular structure between the indicated limits.

In spite of the fact that the transition region between the para- and ferromagnetic grains is narrow, it is of importance that the magnetic moment of the grains belonging to the transition region, which may constitute 1 to 10% of the total mass, is a function of the time: there is *magnetic relaxation*. The investigation of this relaxation as a function of the temperature furnishes another means of studying the granular structure. The theory of this relaxation is complicated by the fact that the time constants that govern the rotations of the individual magnetic moments of the grains from one direction of minimum energy to the other, depend on the magnetic field to which the grains are subjected [3].

3. Substances with Bloch walls

It is possible to give a satisfactory description of the influence of the thermal fluctuations on the propagation of the walls that separate the various elementary domains without entering into the details of the exact mechanism of the phenomenon, to which we will return later: we assume [5] that there is a fluctuating field $H_i(t)$, which is an alternating function of the time with an average value equal to zero, which is superimposed algebraically on the external magnetic field applied to the sample. If the substance does not show any hysteresis, a small field of average value zero will not change the average magnetization of the substance. If there is hysteresis, however, this is no longer true: it depends on the magnetic history of the sample, whether the susceptibility in the direction considered will be equal to a or to $a + c$, where a and c represent respectively the reversible and irreversible differential susceptibilities: c depends in fact not only on the field and the magnetization but also on the magnetic history of the sample. The change in the magnetization resulting from the presence

of the alternating field is equal to $cH_i'(t)$, where $H_i'(t)$ is the largest value attained by $H_i(t)$ in the chosen direction up till the time t.

This value $H_i'(t)$ increases of course with time, and one can show that under sufficiently general conditions $H_i'(t)$ is given by the expression

$$H_i'(t) = S\,(Q + \log t)$$

in which S is a constant depending on the nature of the substance and on the temperature, and in which Q is a numerical constant of the order of 40 or 50. In particular it follows that if one subjects a ferromagnetic substance to a magnetic field H, the substance behaves as if one had applied a field $H + S\,(Q + \log t)$.

The amplitude of the magnetic after-effect thus obtained, which we shall call the irreversible after-effect or, better, the thermal after-effect, depends on the value of the constant S which has the dimension of a magnetic field: the experiments show that the order of magnitude of S is equal to one hundredth or one thousandth of the coercive force[7,8].

There are several mechanisms which can give rise to the fluctuating field $H_i(t)$. The most effective one seems to arise from the fluctuations in the internal field that are produced by the thermal ondulations of the spinwaves, i.e. by the thermal oscillations of the elementary moments: it is, in fact, the "fluctuating" aspect of this same mechanism that is responsible for the decrease of the spontaneous magnetization under the influence of an increase in the temperature. A simple calculation shows [5] that.

$$S = r\,(k\,T/V)^{\frac{1}{2}},$$

where r is a numerical coefficient of the order of 0.3, and V the volume affected by an elementary Barkhausen discontinuity. In strongly perturbed materials, as in good permanent magnets, V must be nearly equal to the volume of an elementary Weiss domain; in very soft materials on the contrary, V must be considerably smaller than the volume of the elementary domains.

The study of the thermal variation of S is of great interest and may yield information about the possible dependence of the volume of the Barkhausen discontinuities and the elementary domains on the temperature.

4. Thermal Activation

The thermal fluctuations, or more exactly the *thermal activation*, may

be of importance also for the magnetic relaxation due to diffusion. The best known example is constituted by the interstitial carbon atoms in the crystal lattice of α iron. The carbon atoms can occupy a number of different kinds of sites which are characterized by different energies that depend on the orientation of the spontaneous magnetization relative to the crystal axes, and which are such that a change in the magnetization must be accompanied by a redistribution in the positions of the carbon atoms. This mechanism gives rise to magnetic relaxation and to the disaccomodation of the permeability, as soon as the time during which the variations in the magnetization are produced is of the same order of magnitude as the time constant that characterizes the redistribution of the carbon atoms. This time constant is of the order of magnitude of $\exp(W/kT)$, where W is the height of the potential barrier separating two possible positions of the interstitial atoms. This time constant is therefore extremely sensitive to variations in the temperature. The result is that the relaxation produced by the diffusion of atoms of a definite kind is observable only in a relatively small interval of temperature. Thus the band in carbon iron has a breadth of some hundred degrees and is centered around room temperature.

Besides carbon, the atoms of the elements oxygen, boron, etc., which are able to take up interstitial position in the iron lattice, are known to give rise to "diffusion" relaxation. We must further remark that the ferromagnetic substitution alloys are also able to give rise to diffusion relaxation: as we have shown in a recent paper [3], the relative positions of the atoms A and B in the state of equilibrium of a binary alloy AB depend on the orientation of the spontaneous magnetization. However, in this case the activation energy W is probably much larger than in the interstitial alloys, so that the relaxation band must be shifted to higher temperatures, for the ferro-nickels for instance to about 700°K. The application of low temperatures is therefore of no importance for the study of this question, except in the case of magnetite or substances with a similar structure, which can be considered to be composed of ferrous and ferric ions. These ions can play the role of different atoms, but the interchange of a ferrous and a ferric ion does not require the interchange of the complete atoms but only the simple transfer of an electron from one atom to the other. The activation energy is then much smaller, and the corresponding relaxation band is probably located at about 100°K: interesting problems can then arise in the domain of low temperatures.

REFERENCES

[1] L. Néel, Comptes-rendus Ac. Sc., **224**, 1488, 1550 (1947).
[2] L. Néel, J. Physique et Radium, **15**, 225 (1954).
[3] L. Néel, Ann. Géophysique, **5**, 99 (1949).
[4] E. C. Stoner and E. P. Wohlfahrt, Phil. Trans., **240**, 599 (1948).
[5] L. Néel, J. Physique et Radium, **11**, 49 (1950).
[6] L. Néel, J. Physique et Radium, **12**, 339 (1951).
[7] J. C. Barbier, Ann. Phys., **9**, 84 (1954).
[8] L. Lliboutry, Ann. Phys., **6**, 731 (1951).
[9] J. L. Snoek, Physica, **5**, 663 (1938).

CHAPTER XVI

EXPERIMENTAL RESEARCH ON FERROMAGNETISM AT VERY LOW TEMPERATURES

BY

L. WEIL
GRENOBLE

Measurements on ferromagnetism at very low temperatures, excepting those on the approach towards saturation [1] and some rare determinations of the magnetic anisotropy (the principal results of which are given by Becker [2]) are of a relatively recent date. The object of these measurements has been the study of the fluctuation phenomena, discussed by Néel in Chapter XV, and the properties of the hysteresis loop connected therewith.

The effect of the fluctuations presents itself from the experimental point of view in two ways. On the one hand, an ensemble of very small ferromagnetic grains behaves as a paramagnetic substance: the time required for the spontaneous reduction of the magnetization is smaller than the duration of a measurement, and the remanence and the coercive force are zero. If, on the other hand, the dimensions become a little larger, the τ become of the order of a second, and one can then follow the relaxation process directly. If the changes in the magnetization of a substance are a result of the displacements of Bloch walls (connected ferromagnetics), only the relaxation, with a relatively small time constant, is observable.

While a study of the relaxation gives sufficient information to make a detailed verification of the theory possible, the study of the fine powders has yielded a particularly striking confirmation of the theory. Whether one is dealing with fine grains obtained separately in the course of a preparation (catalyzers), or with grains nucleated in a non-magnetic matrix, as produced during the treatment of the Alnico's or the stainless steels (martensitic precipitation, for instance), one can

always choose the circumstances in such a way that the grains are so small that at sufficiently high temperatures, for example at room temperature, the ensemble of grains is either in part only or as a whole "paramagnetic". The remanence (Ch. XV, § 2) will not be equal to one half of the saturation, but smaller. The coercive force will be smaller than one would expect theoretically for grains consisting of a single domain. The large variations in τ which can be produced by varying the temperature can sometimes make an ensemble of such grains nearly totally "ferromagnetic" in the liquid-helium region.

1. The Methods of Measurement

The measurement of the magnetization and the coercive force has nearly always been made by means of classical methods, in particular the method of extraction of the sample in the Dewar vessel placed in the field of a solenoid or an electromagnet [3, 4, 5]. However, we must mention the original method of Van Itterbeek [6, 7] for the measurement of the coercive force of films. The author and his collaborators remark that the magnetoresistance is an even function of the induction. In particular, if the latter is zero, so that the applied field is equal to the coercive force, one must expect to observe either a minimum or a maximum in the resistance depending on the sign of the magnetoresistance effect.

Fig. 1 refers to films of iron for which the magnetoresistant effect is negative. Unfortunately some films show both a minimum and a maximum in the resistance because of the coexistence of two varie-

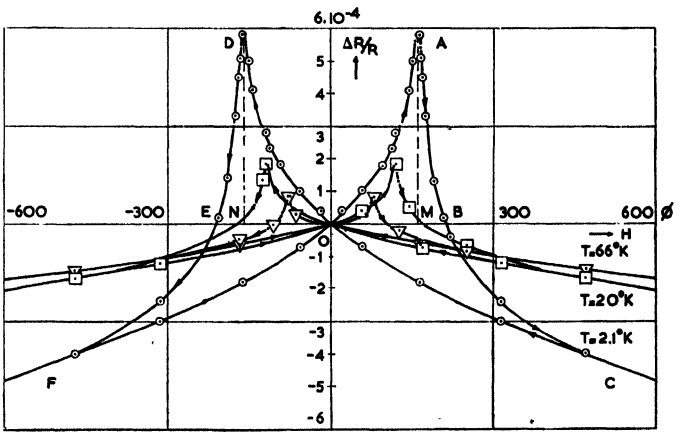

Fig. 1.

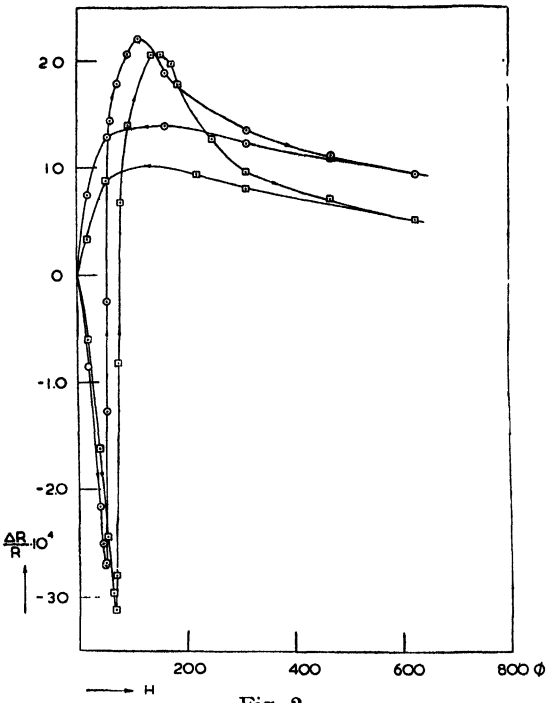

Fig. 2.

ties [8] of film with opposite sign of $\Delta R/R$. The interpretation of the curves, like those of Fig. 2, is then more difficult.

The existence of two varieties of film had already been noticed earlier [9], during measurements at room temperature: the coercive force of the two varieties is appreciably different; one can very well assume that they can exist simultaneously.

For the investigation of the relaxation, Barbier [10] used two different methods. The first method is a classical one: the sample is placed in a Dewar vessel and the evolution of the magnetization of the sample is followed with a magnetometer. This method can be used only if the magnetization changes appreciably during a time of the order of some hours, and its application becomes difficult at very low temperatures. The second method is original, and consists of the direct measurement of the losses in a rotating field. Because of these losses, there appears, in a rotating field h, a phase difference δ between the field h and the magnetization $J = a_0 vh$ of the sample of volume v; the sample then experiences a couple of magnitude $a_0 h^2 v \sin \delta$, which can be measured

by suspending the sample with a torsion wire with a known torsion constant Γ. Fig. 3 and 4 shows the details of the suspension device and in particular of the upper part of the apparatus used by Barbier and Lacaze. When the torsion angle Θ of the sample is known, one can calculate the quantity:

$$a_0 v\, h^2 \sin \delta = \Gamma\, \Theta.$$

On the other hand, we know that the losses in ergs are given by the quantity $W = 2\pi\, a_0 h^2 \sin \delta$.

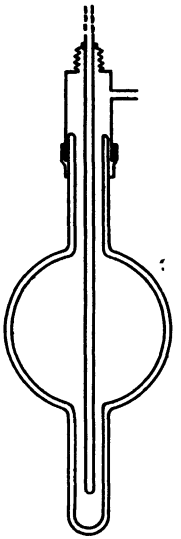

Fig. 3.

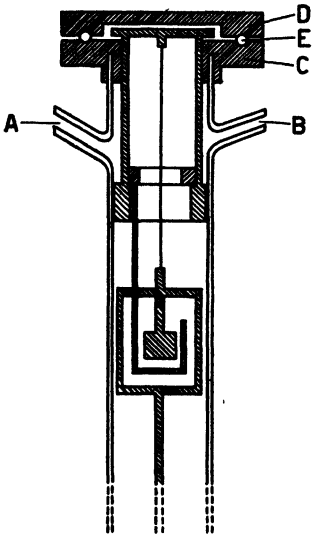

Fig. 4.

We shall show in § 5 how a study of W as a function of h enables one to separate the losses due to relaxation from those due to hysteresis, and how one can then find the quantity S that characterizes the relaxation losses.

2. Results Obtained with Fine Powders

Measurements have been made on fine powders obtained by the methods used in preparing catalyzers (cf. references 11 to 16), and on powders obtained by starting from amalgams [17, 18].

(a) Raney nickel, obtained by dissolving an alloy of aluminium and nickel in a solution of potassium hydroxide, has at room temperature

a coercive force of only a few oersteds. Fig. 5 shows how much H_c increases when the temperature decreases to 2°K. For a nickel like Sabatier nickel, which has larger grains and practically no fluctuations, the increase is much less important, only of the order of a factor 3 (for instance from 150 to 500) instead of a factor 10. In Raney nickel at room temperature, because of the fluctuations a large fraction of the grains has a remanent magnetization that cannot be observed during the time of a normal measurement (some tenths of a second or some seconds). At each point in Fig. 5 we have indicated the value of the ratio of the remanent to the saturation magnetization. We remark (cf. Ch. XV, § 2) that the "ferromagnetic" fraction of the powder, F_T, at the temperature T, is exactly equal to this ratio divided by 0.5. At room temperature one has for instance $F_{293} = 0.196$, and at 2°K one has $F_2 = 0.682$.

With the help of Néel's formula and a hypothesis concerning the value of δ, one can calculate the minimum diameter L_T of the ferromagnetic elements for each temperature T. In Fig. 6 we have taken

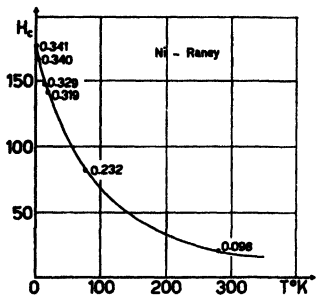

Fig. 5.

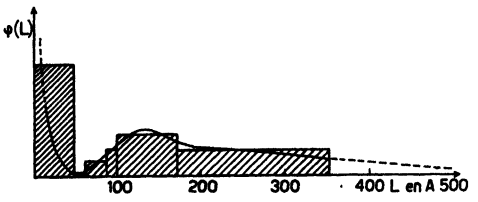

Fig. 6.

$\tau = 10$ sec., but a change of τ by a factor of 10 leads to a change in L of only a few percent. The rectangles represent the number of grains $(F_T)_i - (F_T)_j$ with a diameter between L_i and L_j. The curve that follows the general behaviour of the upper sides of these rectangles thus represents the function $\varphi(L)$ which is defined in such a way, that, except for a multiplicative constant, the mass dm contained in the interval between L and $L + dL$ is given by the relation $dm/m = \varphi(L)dL$.

The information on the granular structure thus obtained is in good agreement with the "mean" dimension of 50 Å determined with x-rays, and so constitutes an indirect verification of Néel's theory.

We must remark that in the above reasoning we have implicitly introduced the following hypothesis: we have assumed that in a field of a few thousand oersteds the whole powder is saturated. However, if the fluctuations are of importance, part of the substance remains "paramagnetic", and in the calculation of F_T one then has divided the remanent magnetization by a quantity that is too small: the ratios given in Fig. 5 are therefore to large. In Fig. 7 we show the magnetization curves to 20000 oersteds for another sample of Raney nickel, and it is seen that a correction is in fact necessary. At 2500 oersteds this correction may be as large as 30% at room temperature, but below 100°K it becomes much smaller. So the right hand part of the curve $\varphi(L)$ in Fig. 6 must be lowered, and the result is a slight decrease of the mean diameter. But the orders of magnitude remain unaltered.

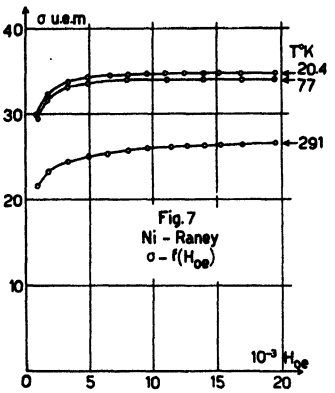

Fig. 7.

(b) Raney iron, obtained by the same method, also shows the fluctuation phenomena. The mean diameter of the grains measured with x-rays is again very small: 72 Å for one of the samples studied. The coercive force changes from 9.6 oersteds at room temperature to 56 oersteds at liquid-air temperature, while for a powder with larger grains (about 300 Å), which does not show the fluctuation phenomena, the coercive force shows a change of only 10% in the same temperature interval. One has been able to determine the "ferromagnetic" proportions in these samples, but the presence of ferromagnetic oxydes makes these determinations much less certain than in the case of nickel.

(c) Ex-amalgam iron has been studied as a function of the temperature, but to liquid-air temperature only, by Meyer and Vogt, who noticed a considerable increase of the coercive force. Their measurements have been extended by Meiklejohn [18] in a more complete fashion and taking into account Néel's theory. This author mentions a sample for which H_c increases from 35 at 20°C to 590 at liquid-air temperature (electron microscope diameter: 75 Å), and another sample for which H_c increases from 400 at — 196°C to 700 at liquid-helium temperature. These variations are due almost entirely to the disappearance of the

fluctuations with decreasing temperature: a sample of reduced iron shows a variation of only about 20% when the temperature drops from room temperature to liquid-helium temperature [15]. We remark that according to Néel's theory the relaxation time for particles with a diameter of 75 Å has a value of 0.9×10^{-7} sec at room temperature, but a value of 1.7×10^{-2} sec at liquid-nitrogen temperature, confirming the result that an appreciable fraction of the particles of the sample become "ferromagnetic" on cooling. Unfortunately, the authors have not published any usable values of the remanence and they do not indicate the way in which the mean value of the diameter has been calculated, which makes a quantitative interpretation hazardous.

3. Results Obtained with Films

In the case of films of nickel [6], it is difficult to separate the effect of the fluctuations from the effect resulting from the increase of the magnetic anisotropy, so that an interpretation of the increase of the coercive force that is observed at low temperatures is difficult. However, the large increase of the coercive force at low temperatures ob-

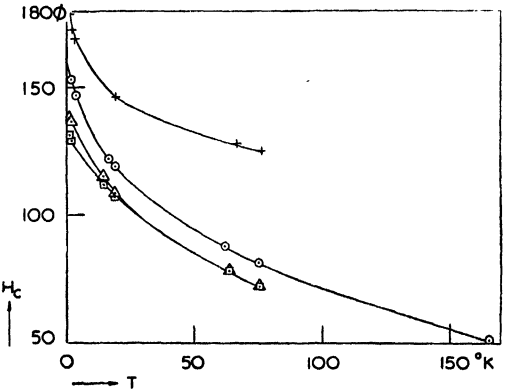

Fig. 8.

served in various films of iron [8] and shown in Fig. 8, must, as we have already pointed out in the case of iron powder, be interpreted as due to the occurrence of the fluctuation phenomena at high temperatures, i.e. to the existence of small elements in the films.

4. The Alloys

Measurements have been made on the Alnico's [3] and on some samples

of stainless steel 18/8. For the Alnico's the results are shown in Fig. 9, and in Table I the values of the coercive force for five samples of stainless steel with different cold working are given in the order of the measurements.

TABLE 1

	E_0	E	E_2	E_3	E_8
Cold Working	0	15.5%	25.5%	33.4%	77.4%
293°K	59.6	78.1	54.1	44	33.6
4°K	64.4	93.9	63.9	54.8	39.7
293°K	58.8	78.3	54.1	45	34.6
77°K	70.6	95.6	65	54.9	40.2
293°K	58.5	78.7	54.2	44.9	33.9

The ratio remanence/saturation for these samples varies but slightly, except for E_8 for which it increases a little.

The increase observed for the Alnico's (a ticonal was used here) below 50°K leads to the assumption that in this alloy there are very fine elements the ferromagnetism of which becomes stable only at liquid-hydrogen temperatures. Because of the fact that the exact constants of this phase are not known, it is not possible to determine the dimensions of these elements accurately with the help of Néel's formula, as we have done for nickel and iron. In analogy with what we found for nickel and iron, one can imagine that they are of the order of a hundred ångströms.

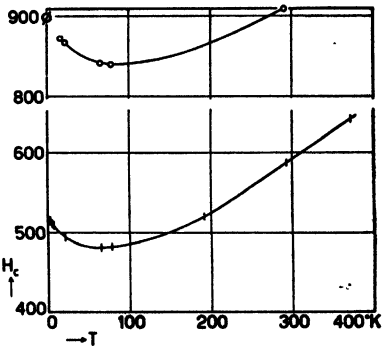

Fig. 9.

It is remarkable that the samples of stainless steel have such a small coercive force, and that the coercive force shows such a slight variation between room temperature and liquid helium: we know that the alloy of which the samples are made is used as magnetic tape because of the large value of its coercive force. By an extensive heat treatment at 500°C, H_c may indeed be made as large as 500 oersteds [20]. However, if the heat treatment is continued too long, H_c begins to decrease again. The explanation of this behaviour is no doubt the following: first the grains begin to grow until their diameter reaches the minimum value for which the fluc-

tuations are no longer of importance; and for still larger dimensions the grains do no longer consist of single domains. The samples we studied had not been treated after the martensitic precipitation (in the case E_o obtained by cooling, in the other cases by cold working), and their grains were too small. The fact that the increase of the coercive force has not yet set in at 4°K shows that the mean dimension of the precipitate is particularly small. One can estimate this dimension to be about twenty ångströms, but as in the case of the Alnico's this value is uncertain.

5. Magnetic Relaxation at very low Temperatures

Measurements have been made on an Alnico sample without a preferred direction [10, 21]. The object of this study was the determination of the quantity S in the expression of Néel for the hypothetical fluctuating field

$$H_i(t) = S\,(Q + \log t)$$

where t is the time and Q a constant of the order of 40.

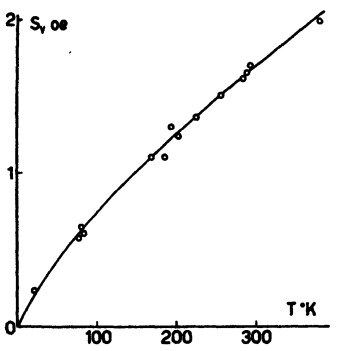

Fig. 10.

With the magnetometric method Barbier has shown that in the Rayleigh domain in the neighbourhood of the remanence, S follows a $T^{3/4}$-law rather than a $T^{\frac{1}{2}}$-law. He attributes the deviation from the $T^{\frac{1}{2}}$-law to the variations with the temperature of the volume v, affected by the discontinuities in the magnetization.

As we have seen above, the use of a rotating field enables one to determine the losses in energy W per cm³ of the substance. The fraction of the losses due to the relaxation is given by the expression $W_t = 2\,\pi^2 b S_v h^2$, while the fraction due to the hysteresis is of the form $W_h = \pi\, b h^3$, where b is Rayleigh's constant. We therefore plot W/h^2 as a function of h (Fig. 11), and the slopes of the straight lines thus obtained then give the values of the constant b. The value of S can then be deduced from the value of the ordinate at the origin. The results have been corrected for the effect of the Foucault currents which were determined by a preliminary study of the dependence on the frequency.

Between 14° and 300° one thus obtains the points shown in Fig. 12, where S is plotted versus $T^{\frac{1}{2}}$. Here too, S varies more rapidly than

required by the law of Néel, in consequence of the variation in v.

It is seen (Fig. 11) that the values measured at helium temperature deviate from the other values: the losses increase suddenly. This increase cannot be ascribed to an increase in the value of b, because the

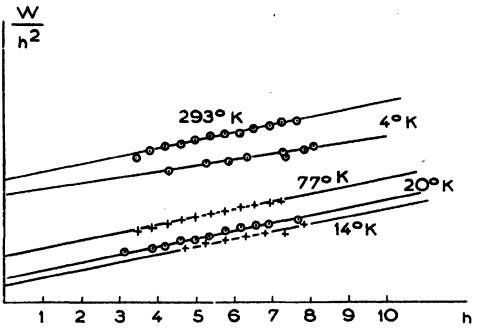

Fig. 11.

slope of the line is not appreciably different. Barbier has verified that the initial permeability a_0 diminishes by only 2.5% between 293 and 4°K. The increase of S may perhaps be attributed to the role played at low temperatures by the very small particles that are precipitated in this type of alloy, which we invoked also for the explanation of the coercive force of Ticonal measured by Van Itterbeek and his collaborators: on the one hand their contribution to the relaxation losses is added to the losses at medium temperatures, and on the other hand they tend to diminish v.

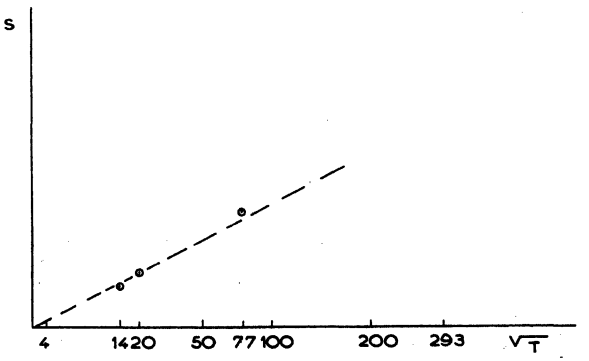

Fig. 12.

Very few relaxation measurements have been carried out on the non-metallic ferromagnetic substances. However, we must mention the investigation of the width of the ferromagnetic resonance lines in iron and nickel ferrite. The breadth of these lines is probably due to the displacements of electrons, and the resulting relaxation is analogous to the diffusion relaxation arising from the effect of the thermal activation (Ch. XV, § 4).

REFERENCES

[1] P. Weiss, Extr. Act. VII, Cong. int. Froid **1**, 508—514 (1937).
[2] R. Becker, Ferromagnetism.
[3] D. A. Lockhorst, A. van Itterbeek and G. J. van den Berg, Appl. Sci. Res., B, **3**, (1954).
[4] L. Weil, Bull. Inst. Int. Froid, 1952-1, p. 131.
[5] L. Weil and S. Marfoure, J. Physique et Radium, **8**, 358 (1947).
[6] A. van Itterbeek, L. de Greeve, L. van Gerven and K. Sable, Physica, **20**, 111—122 (1954).
[7] A. van Itterbeek, R. Lambeir, B. Franken, G. J. van den Berg and D. A. Lockhorst, Physica, **18**, 137 (1952).
[8] B. Franken, A. van Itterbeek, G. J. van den Berg and D. A. Lockhorst, Physica, **18**, 771 (1952).
[9] J. N. Felici, Cahiers de Physique, **21**, 1 (1944).
[10] J. C. Barbier, Thesis, Grenoble, 1953, (Ann. de Phys., 1953).
[11] L. Weil, C. R. Ac. Sci., **229**, 584 (1949).
[12] L. Weil, J. Physique et Radium, **11**, 6S (1950).
[13] L. Weil and R. Pauthenet, J. de Physique et Radium, **12**, 23S (1951).
[14] L. Weil, Proc. Int. Conf. on Low Temperature Physics, Oxford, 1951.
[15] L. Weil, 3rd Int. Conf. on Low Temperature Physics, Houston, 1953.
[16] L. Weil, Réunion de la Société française de Chimie-Physique, 1954.
[17] H. Meyer and F. Vogt, Z. Naturforschung, 7a 302 (1953).
[18] W. H. Meiklejohn, Rev. Mod. Phys. **25**, 302 (1953).
[19] L. Weil, to appear.
[20] W. Sucksmith, The British Electrical and Allied Research Association, 1952.
[21] J. C. Barbier, private communication.
[22] J. K. Galt, W. A. Yager and F. R. Merritt, Phys. Rev.**93**, (1954) 1119.

CHAPTER XVII

VELOCITY AND ATTENUATION OF SOUND AT LOW TEMPERATURES

BY

A. VAN ITTERBEEK
UNIVERSITY, LOUVAIN AND LEIDEN

1. Introduction

During the last twenty years accoustical measurements have been carried out at low temperatures in different fields.

Thus ultrasonic vibrations have been used to study the physical properties of solids, liquefied gases and gases at low temperatures.

As for the solids, the measurements were concerned with the study of the elastic constants of metals and crystals at low temperatures, and their relation to the temperature variation of the specific heat. Furthermore, measurements were carried out on the velocity and the attenuation of sound in superconductors for the purpose of checking whether a discontinuity appears at the transition point.

In connection with the measurements on liquefied gases we must consider the measurements carried out on liquid helium I and II as a separate problem.

Measurements on the other condensed gases were done to obtain experimental data about the equation of state of the liquid and also about the calorimetric and thermodynamic quantities like the isothermal- and the adiabatic compressibility coefficient, the ratio of the specific heats, etc.

Measurements on gases were done at low temperatures for the purpose of determining the virial coefficients appearing in the equation of state. Furthermore, from measurements on the attenuation of sound in gases like hydrogen and deuterium at low temperatures information could be obtained concerning the relaxation time for the transfer of translational- into rotational energy corresponding to the lowest levels.

2. Experimental Techniques

For the detailed description of the existing experimental methods we refer to the textbooks on ultrasonics and to the original publications.

1. THE PULSE TECHNIQUE

This technique was developed during the second world war and is in principle similar to the radar technique. Short ultrasonic pulses of about one microsecond emitted from a quartz transducer travel through the medium. After reflection either the emitter itself or a second quartz crystal can be used as a receiver. Further, the time delay and the attenuation which the sound pulse undergoes when traversing a known path, are measured. The pulse and the echo are observed on an oscilloscope. The frequencies used are rather high, between 1 and 100 MHz.

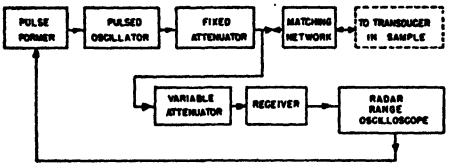

Fig. 1. Block diagram for pulsetechnique

The attenuation coefficient in liquids and solids is very small as compared to that in gases. However, the attenuation being proportional to the square of the frequency ν, it is necessary to use high frequencies for liquids and solids to obtain an appreciable decrease of the amplitude of the pulse after it has traveled through the sample.

Galt [1] was the first to apply this technique to measurements on liquefied gases (argon, oxygen, nitrogen). Later on Pellam and Squire[2] extended this technique to liquid helium. In 1951, Atkins and Chase [3] measured the velocity and the attenuation in liquid helium with the help of two quartz crystals, down to the lowest temperatures obtainable with liquid helium. Later on Chase [4] repeated these measurements with greater accuracy, and Atkins and Stasior [5] carried out measurements on liquid helium under pressure up to 60 atm.

Galt [6], using the experimental technique developed by Huntington [7], was the first to apply the pulse technique to measure the elastic constants and attenuations in solid salts like NaCl, KBr and KCl, down to the boiling point of liquid helium. Later on the same kind of measurements were continued by Overton and Swim [8] on rock salt between room temperature and 60°K. The elastic properties of metals (copper) were studied down to liquid helium temperatures by Overton and Gaffney [9].

The pulse technique has also been used to study the superconductivity. Overton [10] has measured the velocity and the attenuation in a superconducting tin rod. A discontiunity was found at the transition point, which was interpreted as resulting from the change of the specific heat.

Recently, however, measurements were done by Bommel and Olsen[11] on lead and tin.* From their measurements they could conclude that at a frequency of 1 MHz a possible change in the velocity of sound at the transition point must be smaller than 1 part in 20.000.

A new field of investigation has recently been suggested, whereby it is proposed to measure the velocity and attenuation in metals and ferromagnetics. Kornhauser [12] has predicted an attenuation of plane acoustic waves in a conducting medium, caused by the atomic losses of magnetically induced currents.

Special ferromagnetic single crystals have already been investigated by Levy and Truell [13] using the pulsed ultrasonic technique described by Roderick and Truell [14]. For the case of nickel they found that the attenuation as a function of the frequency is much smaller in the magnetized state (saturation) than in the unmagnetized state.

2. ACOUSTICAL INTERFEROMETER METHOD

In this method a single quartz crystal is used as emitter and receiver of the ultrasonic waves. Standing waves are set up between the quartz crystal and the surface of a movable piston. The piston is moved by means of a micrometer, so that the gas column can be set in resonance periodically, which produces a periodic change of the impedance of the quartz crystal. This variation can be measured by means of a circuit similar to that of an autodyne oscillator. This method is also used in nuclear resonance measurements. This last scheme has been used in the Louvain laboratory to measure the attenuation and the velocity of sound in gases at low temperatures.

After detection, this change is observed on a galvanometer, so that a graph like the one shown in Fig. 2 is observed. The distance between the successive maxima and minima corresponds to half a wave-length. This half wave-lentgh is measured on the micrometer. Sometimes also a bridge method [15] is used to measure the change of the impedance

* Since this text has been written new measurements have been published, bij Bommel on the attenuation in monocrystals of tin, a large effect has been found between the normal and the superconductive state (Phys. Rev. **95**, (1954), 220).

of the quartz crystal. This bridge method corresponds to the Purcell-Bloembergen bridge used in nuclear magnetic resonance measurements. As the wave-length is inversely proportional to the frequency, the method is limited to relatively low frequencies (0.1 — 1 MHz). Otherwise the measurement of the wave-length becomes too inaccurate. The absorption coefficient can be determined from the decrease of the galvanometer deflection. The method is particularly useful for gases for which the absorption coefficient is about a hundred times as large as

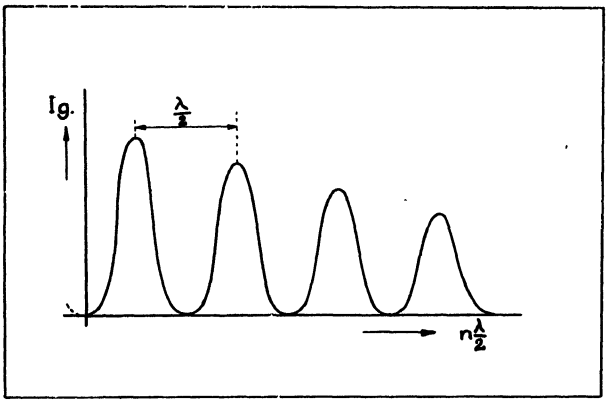

Fig. 2.

the absorption coefficient in liquids. Thus in the case of gases the piston has to be moved only over a small distance, of about 5 cm, to obtain accurate values for the absorption coefficient. Consequently, the interferometer can easily be used at low temperatures. The same type of apparatus can also be used to measure the velocity of sound in condensed gases at low temperatures. At these temperatures the velocity in liquids is of the same order of magnitude as the velocity in gases.

In Fig. 3 is shown one of our types of acoustical interferometers used in Louvain for the measurement of the velocity of sound in gases and condensed gases, and even in liquid helium [16]. The theory of the acoustical interferometer for the measurement of the velocity or the attenuation coefficient has been developed by Hubbard [17].

By using the interferometric method special attention must be paid to the quartz mounting, and particularly to the exact parallelism of the surface of the crystal and the piston. Otherwise so-called satellites may appear which make velocity measurements inaccurate and ab-

sorption measurements rather difficult. This kind of corrections have been dicussed by Krasnooskkin [18] and also by Bell [15].

In order to adjust this parallelism, the piston is fixed to the piston rod by means of a ball raticularion (see Fig. 3). The impedance of the quartz crystal can also be regulated by means of adjustable springs such that no radial motion of the quartz crystal can occur.

Chase [4] has recently combined the pulse technique with the interferometer technique, and he used this method to measure the velocity and the attenuation of sound in liquid helium down to 0.85°K.

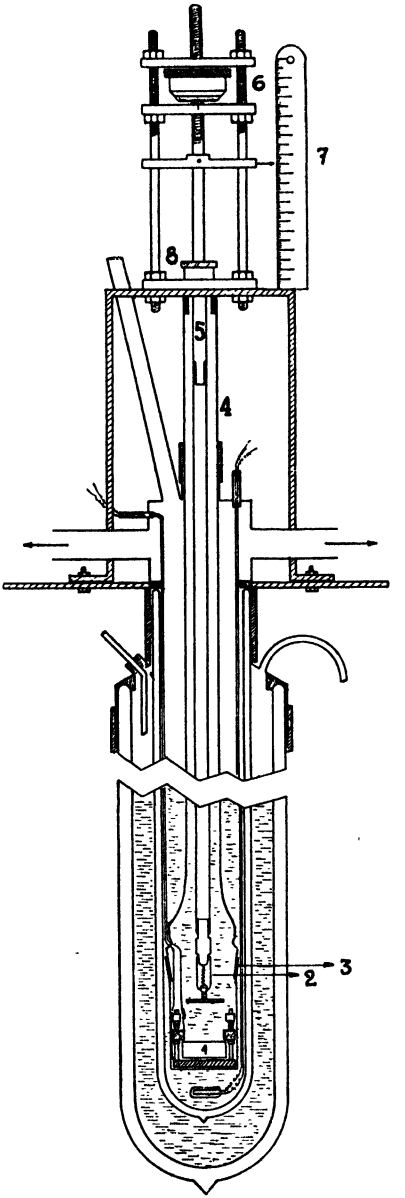

Fig. 3.

3. THE OPTICAL METHOD

Debije and Biquard, starting from the theory of Brillouin for the scattering of X-rays by the thermal waves in crystals, were the first to suggest a new method of measuring the velocity of sound in liquids. The principle of their method is based on the fact that when acoustical waves (standing or progressive) are produced in a liquid, periodic variations in the pressure in the nodes occur. This produces small variations in the refractive index, so that an artificial grating, with a constant equal to the half wave-length, is created within the liquid. When a parallel light beam traverses the medium, diffraction occurs. The velocity of sound in the liquid can then be calculated from the distance between the diffraction lines, the optical constants and the frequency.

Debije and Sears [19], and also Lucas and Biquard [20], were the first to develop the method experimentally.

The principle of the method can be explained by means of Fig. 4. In this figure L represents a monochromatic light source, combined with an optical filter F, which is placed behind the slit S. By means of the lens L_2 a parallel light beam is obtained through the vessel K

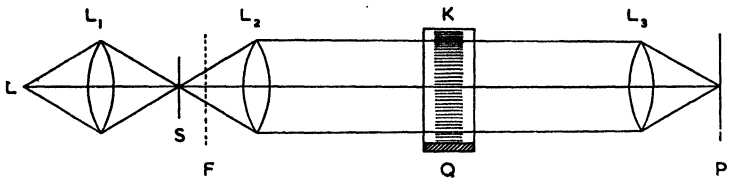

Fig. 4. Optical system

containing the liquid for which the velocity ot sound is to be measured. At the bottom of this vessel the quartz crystal Q is mounted. The diffraction pattern corresponding to the different orders appears in the form of thin parallel lines on the screen P placed in the focus of the lens L_3. The distance between the lines can be measured by means of a comparator.

If d_k is half the distance between the two diffraction maxima of order k, the velocity V in the liquid is given by the expression

$$V = kf\nu\lambda/d_k,$$

in which f is the focus distance of the lens L_2, and ν the ultrasonic frequency. The accuracy of the measurements is determined in first instance by the accuracy of the measurement of d_k. Taking advantage of the possibility to excite the quartz crystal in its odd harmonics, the velocity V can be measured at different frequencies with the help of one and the same crystal.

Another advantage of this method is that the measurement of the velocity takes only a short time, viz. the time necessary to take a photograph of the diffraction picture. The optical method can be developed also for very high frequencies.

The optical method has also been used to measure the absorption coefficient α in liquids, by measuring the light intensity of the diffracted light at two distances x_1 and x_2:

$$\alpha = \frac{1}{2\,(x_1 - x_2)} \ln \frac{I_1}{I_2}.$$

The change of the light intensity as a function of x can be measured by means of a photomultiplier (see Willis [21]). Bär [22] and Liepmann [23] were the first to apply this method to the measurement of the velocity of sound in liquid oxygen, nitrogen and argon.

Recently Van Itterbeek, Van den Berg and Limburg [14] succeeded in developing this method to carry out measurements on liquid hydrogen and liquid helium.

In Fig. 5 the cryostat built for these measurements is shown.

The optical method can be used also to measure the elastic constants of transparent isotropic solids. The method has been developed by E. Hiedemann and K. H. Hoesch [25].

Finally we mention that, when light is diffracted by ultrasonic waves in a crystal, its polarization changes. Measurements in the field were carried out by Galt [6].

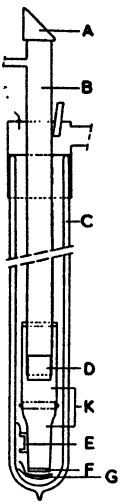

Fig. 5. Apparatus and cryostat for the optical method

4. Recently Barker, Dobbs and Jones [26] measured the velocity of sound in solid argon. To this end argon was slowly deposited from the vapour at temperatures below the triple point on one face of a gold-plated X-cut quartz crystal. The other face of the crystal was in contact with a copper rod kept at the temperature desired for the experiment. When the crystal was covered by a layer of several millimeters of solid argon, a metal piston the surface of which was parallel to that of the quartz crystal was pressed slowly into the argon so as to produce a flat reflecting surface for the ultrasonic waves. To cause the excess solid to evaporate, the piston was kept at a slightly higher temperature. The following preliminary values for the velocity of longitudinal waves were found: 1600 m/sec^{-1} at 60°K and 1300 m/sec^{-1} at 78°K. The velocity in liquid argon at 87.1°K is 849 m/sec^{-1}.

3. Determination of the Thermodynamic Quantities

Measurements on the velocity of sound in gases and liquids can give valuable information about thermodynamic quantities.

1. GASES

If experimental data on the equation of state are available from

measurements on isotherms, it is possible to calculate from measurements on the velocity of sound the ratio of the specific heats, the specific heats themselves and eventually their variation with temperature and pressure.

For the case that no experimental data about the equation of state are available, an indirect method to obtain the second virial coefficient as a function of the temperature has been developed by Van Itterbeek and Keesom. The method consists in measuring the velocity of sound as a function of pressure at different temperatures. When the second virial coefficient and its variation with temperature have thus been measured, the specific heats can then be calculated as functions of pressure and temperature.

The method was first applied to helium gas [27] at liquid helium temperatures and later on also to other gases, like oxygen [28], argon, hydrogen, deuterium [29] and also to mixtures [30].

Starting from the well-known equation for the velocity of sound

$$W = \sqrt{\frac{E}{\varrho}} = \sqrt{-\frac{v^2}{M}\left(\frac{\partial p}{\partial v}\right)_S} = \sqrt{-\frac{C_p}{C_v}\frac{v^2}{M}\left(\frac{\partial p}{\partial v}\right)_T}, \tag{1}$$

and the equation of state

$$pv = R\,T\,(1 + B/v + C/v^2), \tag{2}$$

one can derive the following expression:

$$W^2 = W_o^2\,[1 + (2S/RT)p + f(B, C, T)p^2]. \tag{3}$$

As the terms containing p and p^2 are usually small, we can write

$$W = W_o\left(1 + \frac{S}{RT}p\right),$$

with

$$W_o^2 = \left(\frac{C_p}{C_v}\right)_{p=0}\frac{RT}{M}, \tag{4}$$

so that the change of W as a function of p is linear in first approximation.

For the case of helium gas $(C_p/C_v)_{p=0} = 1.666$. S is a function of the temperature, and can be written as follows:

$$S = B + \frac{T}{\lambda}\frac{dB}{dT} + \frac{T^2}{2\lambda\,(\lambda + 1)}\frac{d^2B}{dT^2}, \tag{5}$$

in which $\lambda = (C_v)_{p=0}/M$. Thus for the case of helium $\lambda = \frac{3}{2}$.

By carrying out measurements at different temperatures, the function $S(T)$ can be determined. By taking for B a series development of the form

$$B = a + \frac{b}{T} + \frac{C}{T^2} + \frac{d}{T^3},$$

the terms a, b, c, . . . can be obtained by integrating equation (5).

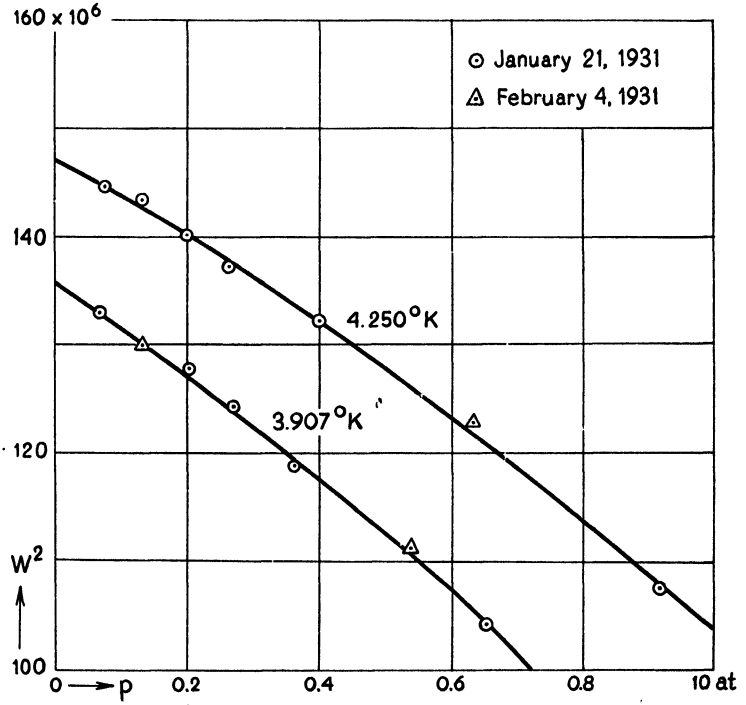

Fig. 6. Velocity of sound measurements in helium gas at liquid helium temperatures

As an example Fig. 6 shows the measurements done on helium gas at liquid helium temperatures.

From these measurements the following series [31] was calculated:

$$10^3 B = 0.7559 - \frac{19.64}{T} - \frac{3.79}{T^2} + \frac{3.94}{T^3}.$$

Later on Walstra [32] checked the values of B deduced from this equation with the results obtained from direct measurements of the isotherms. They were found to be in good agreement with each other.

From these measurements at liquid helium temperatures Van Itterbeek calculated the variation of the ratio of the specific heats and the specific heats themselves as functions of the pressure (see Table I) *.

As we already mentioned above, this method was developed by Van Itterbeek and Van Doninck [30] to determine the interaction term B_{12} in the equation of state of mixtures,

$$B_{12} = B_{11}\, x^2 + B_{12}\, x\,(1 - x) + B_{22}\,(1 - x)^2$$

where x represents the concentration, and B_{11} and B_{22} the second virial coefficients for the components 1 and 2.

TABLE I

T °K	p atm	W^2 $(m/\text{sec})^2$	C_p/C_v	C_v cal/°mol
4.245	0.1	14379	1.71	2.93
	0.2	14010	1.75	2.91
	0.4	13225	1.85	2.87
	0.6	12360	1.94	2.89
	0.75	11748	2.02	2.97

From table I we see that a minimum appears in the specific heat.

2. LIQUIDS AND CONDENSED GASES

In the case of condensed gases the problem is more complicated, since hardly any data about the equation of state are available. However, measurements on the velocity of sound can give information about the compressibility coefficients and also about the ratio of the specific heats and the specific heats themselves if other quantities of the liquid, like the thermal expansion coefficient, are known. In some other cases measurements on the velocity of sound can give direct information about the equation of state.

Firstly, we remark that the propagation of sound in liquefied gases is assumed to be an adiabatic process. Liepmann [33] did calculations about the validity of this supposition. This condition can be expressed by the following equation:

$$2k\omega/C_v\varrho \leqslant W^2,$$

* Since these notes have been written Van Itterbeek and Forrez (Physica 20, (1954), 767) repeated the same kind of measurements but with the use of ultrasonics, so that a better accuracy was obtained. They also calculated the specific heats for different pressures and temperatures. They also find the appearance of minima for the specific heats at different temperatures.

in which k is the coefficient of thermal conduction, $\omega = 2\pi\nu$, and ϱ the density. Liepmann obtained for the case of argon:

$$\omega \leqslant 10^{15}\ \text{sec}^{-1}.$$

Since the frequencies used are usually much smaller, the process can be considered to be adiabatic. Liepmann also considered liquid helium II, and found as limit:

$$\omega < 10^{6} - 10^{7}\ \text{sec}^{-1}.$$

This is of the order of the frequencies generally used.

Groenewold [34], considering the mean free path of the helium molecules, arrives at the same conclusion, viz. that the sound propagation in He II is an adiabatic process. Moreover we mention that for liquid helium Cp/Cv is practically equal to 1.

The Louvain measurements in liquid helium, which were carried out for a large range of frequencies, have shown that there is no correction need be applied to the velocity of sound.

For the velocity of sound in a liquid we can write:

$$W = (\varrho\beta_{ad})^{-\frac{1}{2}} = (\gamma/\varrho\beta_{is})^{\frac{1}{2}}. \tag{6}$$

From this equation we see that the adiabatic compressibility can be calculated from the measured values of the velocity of sound and the density. Furthermore, the isothermal compressibility β_{is} can be calculated when $\gamma = Cp/Cv$ is known. On the other hand, values of γ are usually not available, but this ratio can then be calculated from the equations:

$$C_p/C_v - 1 = -\frac{T(\partial v/\partial T)_p}{C_v(\partial v/\partial p)_T} = -\frac{T\alpha_T^2 W^2}{C_p/M}, \tag{7}$$

with

$$\alpha_T = \frac{1}{v}\left(\frac{\partial v}{\partial T}\right)_p.$$

In Table II are collected the values of the adiabatic and isothermal compressibility coefficients, and of the ratio of the specific heats as they were calculated by Verhaegen [35] from the Louvain measurements on the velocity and from thermodynamic data given in the literature. In the last column are given the values of the isothermal compressibility coefficient as determined by direct static measurements.

Various attempts have been made to overcome the difficulty that the equation of state for the liquid state is not known. Thus for the liquids Schaaffs [36] uses the equation of state of Van der Waals

$$(p + a/v^2)(v - b) = RT.$$

TABLE II

Compressibility coefficients and specific heats

liquid	T °K	V m/sec	ρ gr/cm³	$\beta_{ad} \times 10^{-12}$ cm²/dyne		$\beta_{is} \times 10^{-12}$ cm²/dyne	$\beta_{is} \times 10^{-12}$ cm²/dyne
O_2	90.0	913	1.142	105			
–	85.0	951	1.167	95			
–	80.0	989	1.191	86	1.69	145	169
–	75.0	1027	1.215	78			(S – K)
–	70.0	1065	1.239	71			
–	65.0	1103	1.263	66			
–	61.0	1133	1.282	61			
N_2	77.0	880	0.811	159			
–	74.0	910	0.825	146	2.02	295	247
–	71.0	940	0.839	135			(S – K)
–	68.0	970	0.854	124			
–	65.0	1005	0.868	114			
A	87.1	849	1.404	99	2.17	218	(245) (E,H)
–	86.1	857	1.410	97	2.18	212	(180) (S.K)
–	85.1	866	1.417	94	2.19	205	
–	84.1	874	1.424	92	2.20	200	
CH_4	112.0	1414	0.4232	118			
–	110	1430	0.4262	115			
–	105	1468	0.4337	107			
–	100	1506	0.4412	100			
–	95	1544	0.4487	93			
–	91	1576	0.4548	88			
H_2*	20	1199	0.0712	977	1.57	1534	
–	19	1224	0.0722	924			
–	18	1250	0.0732	874			
–	17	1276	0.0742	828			
–	16	1302	0.0752	784			

(S – K) F. Simon and F. Kippert, Zs. phys. Chem. **135**, 113 (1928).
(E – H) A. Eucken and F. Hauck, Zs. phys. Chem. **134**, 161 (1928).

Further he assumes that the propagation process is an isothermal one, and he then obtains the following expression for b

$$b = \frac{M}{\varrho} - \frac{RT}{\varrho W^2}\left(\sqrt{1 + MW^2/3RT} - 1\right),$$

from which he calculates the radius of the molecule.

* H_2 – normal, but which has already undergone a small transformation. Concerning liquid hydrogen a distinction must be made between the values found for normal- and for para-hydrogen. A. van Itterbeek and L. Verhaegen[35a] found that a rapid transformation occurs of normal-hydrogen into para-hydrogen under the influence of the ultrasonic waves in the presence of small traces of oxygen (see also: A. van Itterbeek, G. J. van den Berg and W. Limburg [24].

A different method of calculation has been followed by Kittel [37]. Kittel postulates that the following relation exists between the velocity in the liquid and that in the gas:

$$W_{liq} = (L/L_f)\, W_{gas},$$

L being equal to the distance between the two centres of gravity of the molecules, and L_f being the free distance between the surface of the molecules, considered as rigid spheres.

$L_f = L - \sigma$, where σ is the diameter of the molecules. In the preceding equation it is assumed that the propagation of the sound waves is short-circuited by the molecules themselves. The ratio L/L_f can again be calculated from the equation of state in the gas and the liquid.

Therefore Kittel starts from the equation of state of Tonks [38]

$$p\, v\, (1 - \delta^{1/3}) = NkT, \tag{8}$$

in which $\delta = v_0/v$; v_0 is the volume corresponding to the closest sphere packing, and $v_a = v - v_0$ is the "available" volume. Using the classical thermodynamic equation, Kittel obtains the following equation:

$$W_{liq} = \left(\frac{v}{v_a}\right)\left(\frac{c_v + 3R}{c_v}\right)^{1/2}\left(\frac{3RT}{M}\right)^{1/2} = \\ = \left(\frac{v}{v_a}\right)\left(\frac{3\gamma_{liq}}{\gamma_{gas}}\right)^{1/2} W_{gas}. \tag{9}$$

W_{liq} can be calculated from this equation when v_a is known. v_a can be written in the form: $v_a = v_1 + v_2 + v_3$, where v_1 = molar volume change on heating the solid from 0°K to the melting point; v_2 = molar volume change on fusion; and v_3 = molar volume change on heating the liquid from the melting point to the temperature concerned.

4. Sound Attenuation

Dissipation of acoustical energy in a gas or a liquid is primarily a result of internal friction and heat conduction. These two effects are incorporated in the Eq. (10) for the classical absorption coefficient. The theory of this absorption was developed by Stokes and Kirchhoff who started from the classical dynamical equation for an elastic, viscous (tensor componants proportional to the velocity gradient) medium, and who also introduced the correction for the heat transfer. The absorption coefficient due to these two factors has been written in the following form by Lebedew [39]:

$$\alpha_{cl} = \frac{4\pi^2}{W_o \varrho \lambda^2}\left(\frac{4}{3}\eta + \frac{\gamma - 1}{c_p}k\right) = \frac{4\pi^2\gamma^2}{\varrho W_o^3}\left(\frac{4}{3}\eta + \frac{\gamma - 1}{c_p}k\right), \quad (10)$$

in which α_{cl} is the absorption coefficient per cm for the acoustical energy, η is the viscosity, k the heat conductivity, and $\gamma = c_p/c_v$. Sometimes the absorption coefficient is expressed per wave-length rather than per cm. This quantity, $a = \alpha_{cl}\,\lambda$ is then independent of the frequency. Since the velocity and the density are larger for liquids than for gases, we see from Eq. (9) that the absorption coefficient in liquids is much smaller than that in gases.

In the laboratory of Louvain various measurements were done in order to check Eq. (9). In Fig. 7 and 8 the measurements on the absorption coefficient in respectively N_2- and He-gas at 90°K are shown.

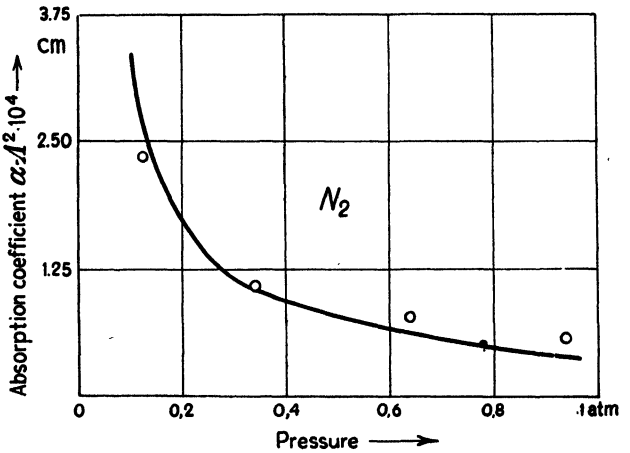

Fig. 7. Absorption coefficient in Nitrogen-gas as a function of pressure at 90°K.

Measurements were carried out also in liquid Helium I by Pellam and Squire, but their results will be discussed in § 6.

Another cause of absorption of acoustical energy may result from a relaxation phenomenon produced by a delay of the transfer of the internal energy (vibrational or rotational) to the translational energy. In the laboratory of Louvain Van Itterbeek and Verhaegen also investigated systematically the rotational absorption in normal- and para-hydrogen. In Fig. 9 is shown the absorption coefficient for the two modifications of hydrogen.

They found a relaxation time for the rotational energy of approxima-

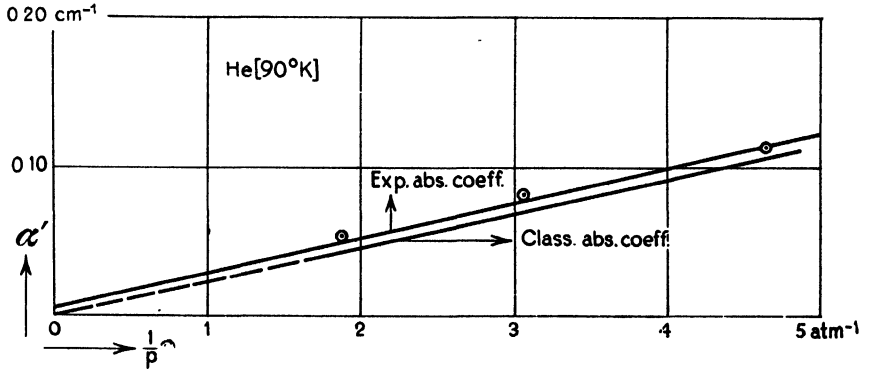

Fig. 8. Absorption coefficient in Helium-gas as a function of $1/p$ at 90°K.

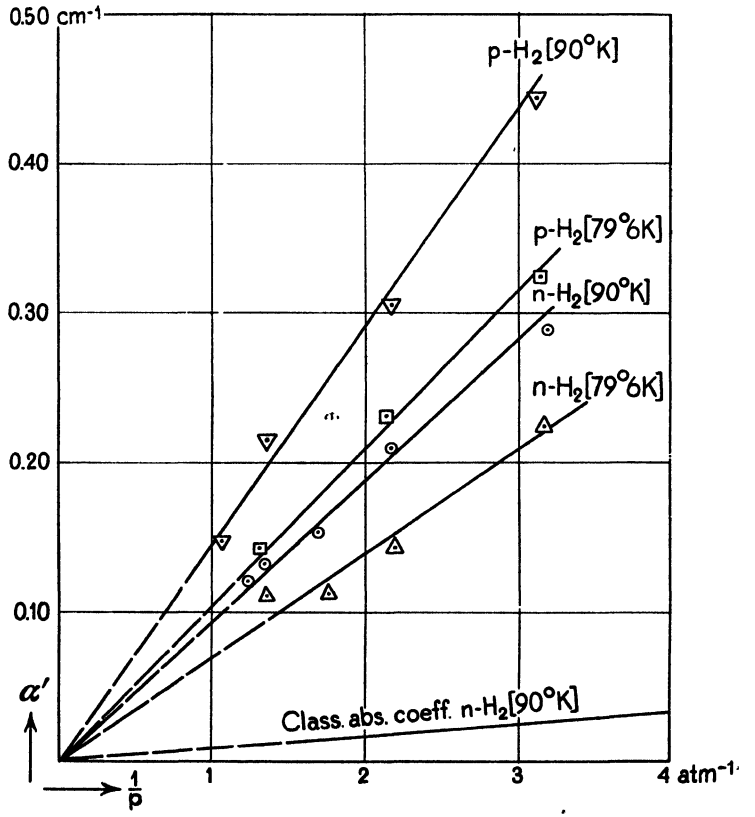

Fig. 9. Absorption coefficient in hydrogen modifications at 90°K. Absorption coefficient in hydrogen modifications at 79.6 and 90°K.

tely 1×10^{-8} sec. In the United States, measurements were done on the dispersion in hydrogen and deuterium by Stewart, Stewart and Hubbard, and by Rhodes [40]. They found that the dispersion region is located between 1 and 50 MHz.

5. Measurements in Liquid Helium

Since liquid helium is a quantum liquid, its physical properties differ essentially from those of other liquids. Therefore we will discuss the experiments on liquid helium in this separate section. The following problems were examined during the last few years:

1. As liquid helium undergoes a second order transition at the λ-point, a discontinuity in the velocity of first sound can, according to the Ehrenfest relation, be expected. This discontinuity would be given by the equation:

$$W_I - W_{II} = \frac{TW^3}{2} \frac{c_I c_{II}}{c_{II} - c_I} \left(\frac{\alpha_I}{c_I} - \frac{\alpha_{II}}{c_{II}} \right)^2, \tag{11}$$

in which W_I and W_{II} are the velocities of first sound in respectively liquid helium I and liquid helium II, c_I and c_{II} the specific heats in the two phases, and α_I and α_{II} the expansion coefficients.

The first attempt in this direction was made by Burton [41], and by Findlay, Pitt, Grayson Smith and Wilhelm [42], who carried out measurements between 4.22 and 1.76°K with the help of the interferometer method. Later on these measurements were repeated by Pellam and Squire [2] with the pulse technique (15 MHz). Within the same temperature range Atkins and Chase [3], in 1950, measured again the velocity between the boiling point and 1.3°K with the pulse technique (14 MHz) and investigated in particular the temperature region near the λ-point. The results obtained are shown in Fig. 10.

As can be seen from Fig. 10, they found a rapid drop in the velocity on either side of the λ-point. However, it was impossible to determine the magnitude of the discontinuity. Pellam and Squire were also unable to measure this magnitude. However, Findlay, Pitt, Grayson Smith and Wilhelm [42] who carried out measurements on helium under pressure (between 1 and 5.55 atm), observed a discontinuity at the λ-point. Recently Atkins and Stasior [5] measured the velocity between 1.2 and 4.2°K at pressures up to 69 atm using the pulse technique (carrier frequency 12 MHz) (see Fig. 11). They found no evidence for a discontinuity in velocity at the λ-point at any of the pressures used.

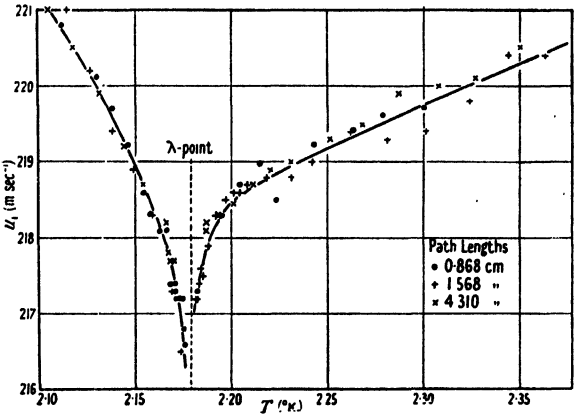

Fig. 10. Velocity of sound in liquid helium in the neighbourhood of the λ-point (Atkins and Chase)

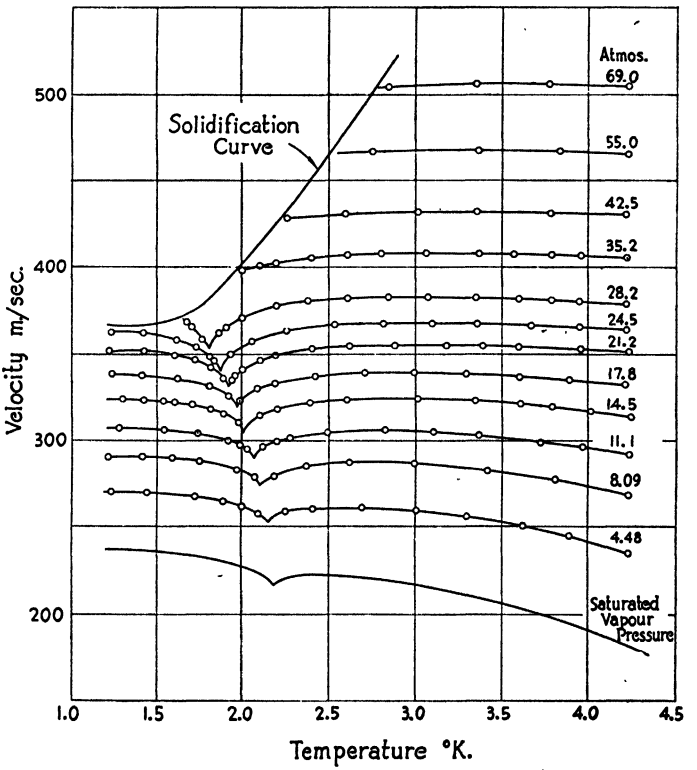

Fig. 11. The velocity as a function of pressure at the very low temperatures (Atkins and Stasior).

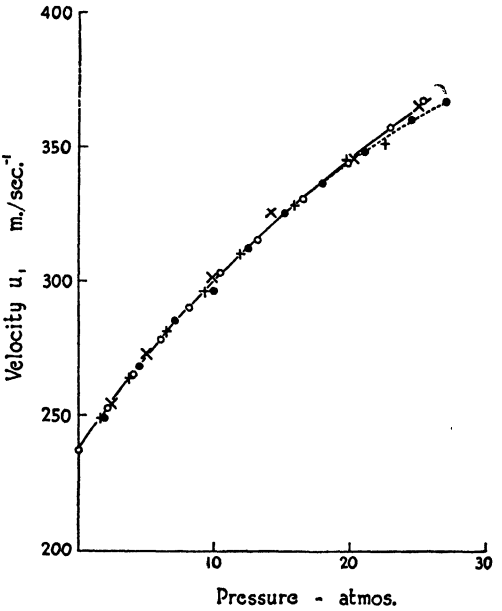

Fig. 12.

Atkins and Stasior have also drawn some interesting theoretical conclusions from their measurements, which we will discuss briefly.

They calculated the velocity of sound at the lowest temperature by means of the equation: $W = (\gamma/\varrho\beta_{isoth})^{\frac{1}{2}}$, in which ϱ and β_{isoth} were taken from the measurements of Keesom and Miss Keesom [43]; $\gamma = c_p/c_v$ was assumed to be approximately equal to 1. The comparison between the theoretical values and the experimental data is shown in Fig. 11. We see that the agreement is rather good, except at the highest pressures. From these measurements they calculated also the ratio γ and its change with pressure. The results obtained are given in table III.

TABLE III

The ratio of the specific heats (Atkins and Stasior)

p / T°K	5	10	15	20	30 atm
2.0				1.00	1.04
2.5	1.06	1.02	1.08	1.02	1.08
3.0	1.17	1.14	1.10	1.05	1.09
3.5	1.31	1.22	1.17	1.10	1.10
4.0	1.47	1.32	1.27	1.27	1.14

For the other condensed gases, as for instance for hydrogen (see Table II), γ is much larger than unity. Atkins and Stasior obtained a more direct evaluation for the quantity $\gamma - 1$ starting from the Eq. (12):

$$\gamma(\gamma - 1) = \frac{TW^2}{c} \frac{1}{\varrho} \left(\frac{\partial p}{\partial T}\right)^2. \tag{12}$$

The calculations were done only for 19 atm, for which all the necessary data are available. The results obtained are shown in Fig. 13.

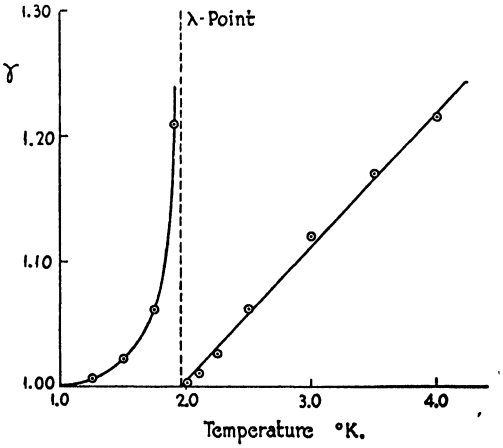

Fig. 13. $\frac{c_p}{c_v} - 1$ as a function of the temperature at a pressure of 19 atm.

2. A second point which has been considered concerns the question whether there is dispersion for the velocity in He II.

This has been investigated by Van Itterbeek and Forrez [16]. Measuring with an accuracy of 0.1% (and in some cases even more accurately) between 4.2°K and 1.1°K, the values obtained for the velocity corresponding to the frequencies 220, 420, 512 and 800 KHz were found to be equal. Moreover, these values agree with the values obtained by other investigators using the pulse technique. In Fig. 14 the values obtained for different frequencies are shown.

The fact that no dispersion is found in the low frequency region agrees with the measurements done by Chase [4] on the attenuation, and also with the recent theory of Khalatnikow [44], who predicted that at the lowest temperatures a dispersion would be found in the very high frequency region only ($>$ 20 MHz), taking into account the value

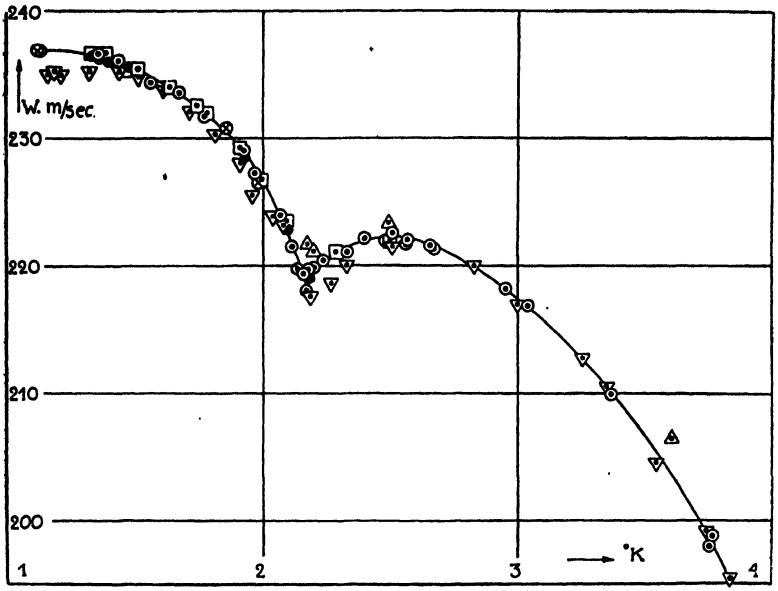

Fig. 14. Velocity of first sound as a function of temperature:

△	Findlay, Pitt, Grayson Smith, Wilhelm	1.338	MHz	⊡	Van Itterbeek and Forrez	218.0	KHz
▽	Atkins and Chase	14	MHz	●	Van Itterbeek and Forrez	423	KHz
⊙	Van Itterbeek and Forrez	520.0	KHz	⊗	Van Itterbeek and Forrez	800	KHz

obtained for the relaxation time deduced from the measurements.

Another aspect of the problem is connected with the extrapolation down to absolute zero of the values obtained for first sound. Landau [45] predicts that at the absolute zero the velocity of second sound should be equal to the velocity of first sound divided by $\sqrt{3}$. It appears, however, that even at the lowest temperatures (see the measurements of Van Itterbeek and Forrez, loc. cit.) the velocity of first sound still increases slightly, and it is therefore impossible to extrapolate accurately down to the absolute zero starting from 1°K.

3. *Attenuation.* The first measurements on the attenuation were done by Pellam and Squire [2]. Above 3.0°K, in the He-I region, they found a deviation from the classical absorption coefficient of about 15%. But this deviation can be ascribed to the inaccuracy of the experimental values of the attenuation, the viscosity and the heat conductivity of liquid helium known at that time. At present much better values are known and it would be worth while to recalculate the classical absorp-

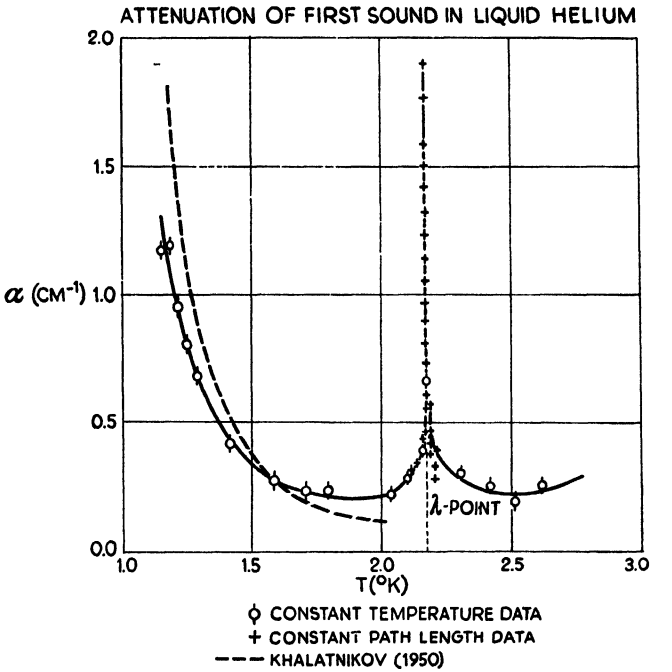

Fig. 15. Attenuation of first sound in liquid helium (full line experimental results, dotted line Khalatnikov's calculations 1950).

tion coefficient. Below 3.0°K, just above the λ-point, Pellam and Squire found a strong increase of the attenuation, and at the λ-point a very sharp increase. Immediately below the λ-point a strong decrease is observed, and below 2.0°K a new increase appears. The measurements were carried out down to 1.5°K.

In 1950 new measurements were carried out by Atkins and Chase [3] (see Fig. 15) down to 1.3°K using the same experimental technique as Pellam and Squire. Above the λ-point approximately the same increase was obtained. However, it must be remarked that when approaching the λ-point the appearance of bubbles in the liquid is always observed, and it is well known that the presence of gas bubbles in the liquid produces a strong attenuation.

The rise in attenuation below 1.5°K was predicted by Khalatnikov [44]. The theoretical curve is shown in Fig. 15. The basis of the theory is a relaxation phenomenon resulting from the fact that the phonons and rotons present in the liquid are unable to follow the instantaneous temperature change produced by the sound waves. However, no con-

clusion could be drawn concerning the frequency region where dispersion appears. As we mentioned already, new measurements were recently carried out by Chase [4], who investigated in particular the attenuation. Thus he measured the attenuation in the neighbourhood of the λ-point and also below 2.19°K down to 0.85°K for three frequencies 2.0 MHz, 6.0 MHz and 12.1 MHz. He found a very pronounced variation of the attenuation with frequency (see Fig. 16, 17 and 18). Chase has plotted α_1/ω^2 (α_1 the residual absorption coefficient: $\alpha_1 = \alpha - \alpha_{cl}$; ω angular frequency) as a function of temperature for the three frequencies used. Above 1.1°K the experimental results obtained for the different frequencies lie on a single curve, so that α_1/ω^2 is essentially independent of the frequency. This would point to a relaxation time the reciprocal of which is much larger than the frequency used. The deviation which appears at the lowest temperatures could be explained by the fact that at those temperatures the reciprocal of the relaxation term does not differ much from the frequency used, and that this relaxation time depends strongly on the temperature. Using the well-known equations for the relaxation absorption [46], this relaxation term can be calculated from the measurements at the lowest temperatures using two frequencies. The third frequency can then be used to check the results. Thus Chase found at 1°K a relaxation time of about 1.2×10^{-8} sec and a temperature dependence proportional to T^{-5}. At lower temperatures, however, a single relaxation term would not be sufficient to explain the observations. A second, shorter one must be considered. The experimental value obtained for the relaxation time is in very good agreement with Khalatnikov's calculations. Khalatnikov considers the various types of collision processes which can lead to a change in the number of phonons and rotons. He also calculated the temperature dependence of the collision probabilities. Thus for the frequencies lower than the reciprocal relaxation times, he obtains for the absorption coefficient α_1 the expression

$$\alpha_1 = \frac{\omega^2}{2\varrho W^3}\left[\Theta_{ph}\left(\frac{\partial p}{\partial \mu_r} + \frac{\partial p}{\partial \mu_{ph}}\right)^2\left(\frac{\partial \mu_{ph}}{\partial N_{ph}}\right) + \Theta_{r.ph}\left(\frac{\partial p}{\partial \mu_r}\right)^2\left(\frac{\partial \mu_r}{\partial N_r} + \frac{\partial \mu_{ph}}{\partial N_{ph}}\right)_{\rho_1\rho}\right]$$

in which W is velocity of sound; μ_r and μ_{ph} are the chemical potentials of rotons and phonons, N_r and N_{ph} the number of rotons and phonons per unit volume; Θ_{ph} and $\Theta_{r.ph}$ are the relaxation times corresponding to the processes. Further Khalatnikov estimated the values of the derivatives of the functions entering in the expression for α_1. He cal-

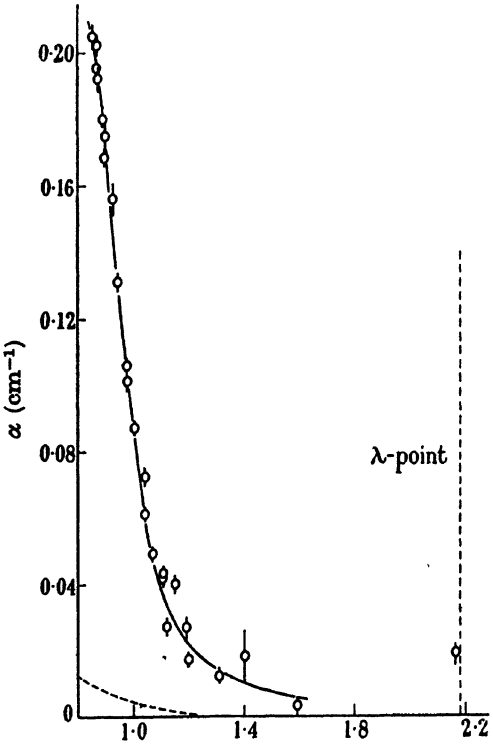

Fig. 16. Attenuation at 2.0 MHz, - - - viscosity attenuation

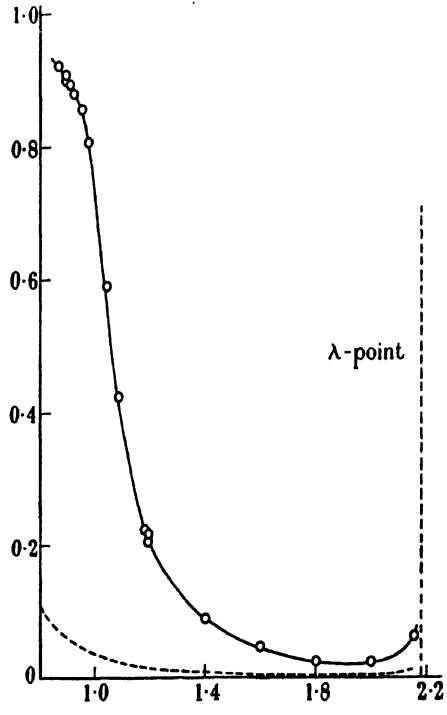

Fig. 17. Attenuation at 6.0 MHz, - - - viscosity attenuation

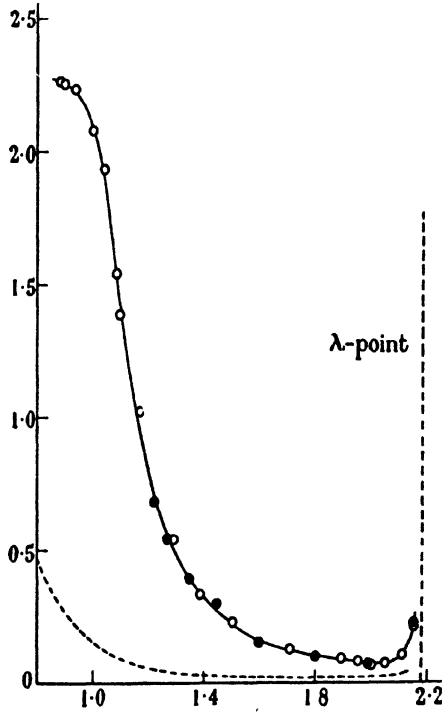

Fig. 18. Attenuation at 12.1 MHz, - - - viscosity attenuation

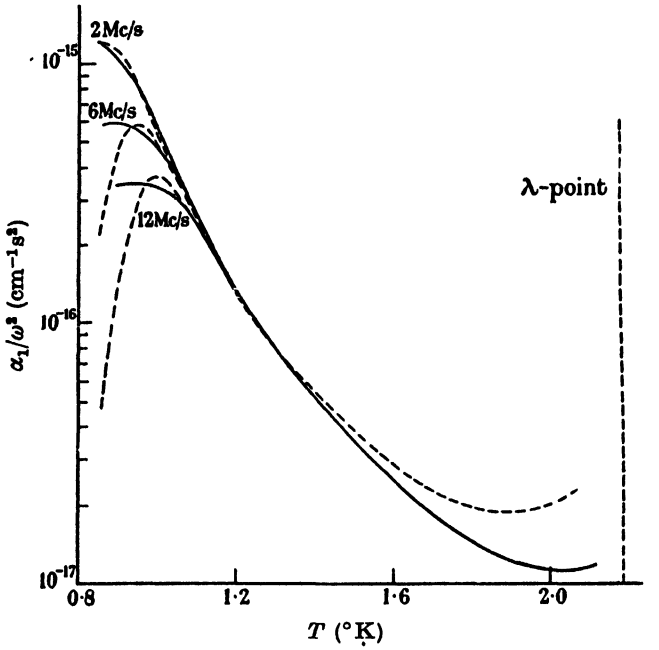

Fig. 19. Comparison with Khalatnikov's theory

culated the relaxation times between 0.85 and 2.00°K. Thus it is found theoretically at 1°K: $\Theta_{rph} = 7.42 \times 10^{-9}$ sec, which agrees very well with the experimental value obtained by Chase. So the agreement appears to be rather good, in spite of the fact that the values of some of the quantities used in Khalatnikov's calculations are only imperfectly known.

Another relaxation process has to be considered just below the λ-point, viz. the relaxation connected with the equilibrium between normal and superfluid helium. Just as Pellam and Squire, and Atkins and Chase, Chase finds a pronounced deviation from the classical absorption coefficient just below the λ-temperature. Kronig and Thellung [47], and Kronig, Thellung and Woldringh [48] calculated the relaxation time connected with the transformation of the two fluids in each other. From the measurements of Pellam and Squire they concluded that this relaxation time must be either smaller than 10^{-12} sec or larger than about 10^{-4} sec. Since Chase found that below the λ-point for his frequencies used (2.6 and 12 MHz) the attenuation is

proportional to ω^2, one can conclude that the relaxation time must be smaller than 10^{-12} sec.

In connection with the existing theories it would be important if in the future velocity and attenuation measurements could be carried out down to demagnetization temperatures.* The velocity measurements with the acoustical interferometer must be extended to much higher frequencies, as this was also done during the earlier measurements. In order to check the relaxation theory measurements must be done also at different pressures.

REFERENCES

[1] J. K. Galt, Mass. Inst. of Technology, Techn. Rep. No. 46 (1947).
[2] J. R. Pellam and C. F. Squire, Phys. Rev. **72**, (1947) 1245.
[3] K. R. Atkins and C. E. Chase, Proc. Phys. Soc. **64**, (1951) 826.
[4] C. E. Chase, Proc. Roy. Soc. **220**, (1953) 116.
[5] K. R. Atkins and R. A. Stasior, Canad. Journ. of Physics, **31**, 1156 (1953).
[6] J. K. Galt, Phys. Rev. **73**, 1460 (1948).
[7] H. B. Huntington, Phys. Rev. **72**, 321 (1947).
[8] W. Overton and R. Swim, Phys. Rev. **84**, 758 (1951).
[9] W. Overton and J. Gaffney, Houston Conf. on low temperatures, December 1953.
[10] W. Overton, Annual Progress Report 1949, Low Temperature Laboratory – Rice Institute, Houston, Texas.
[11] H. Bommel and J. L. Olsen, Phys. Rev. **91**, 1017 (1953).
[12] E. T. Kornhauser, Journ. Accoust. Soc. **25**, 1011 (1953).
[13] S. Levy and R. Truell, Rev. Modern Physics, **25**, 140 (1953).
[14] R. L. Roderick and R. Truell, Journ. Appl. Phys. **23**, 267 (1952).
[15] J. H. W. Bell, Proc. Phys. Soc. *B*, **64**, 958 (1950).
[16] A. van Itterbeek and G. Forrez, Physica **20**, 133 (1954).
[17] J. C. Hubbard, Phys. Rev. **38**, 1011 (1931); **41**, 523 (1932).
[18] P. E. Krasnooskkin, Phys. Rev. **65**, 190 (1944).
[19] P. Debije and F. W. Sears, Proc. Nat. Acad. Sci.; Washington, **18**, 410 (1932).
[20] R. Lucas and P. Biquard, C. R. Acad. Sci., Paris, **194**, 2132 (1932).
[21] F. H. Willis, J. Accous. Soc. Amer. **19**, 242 (1947).
[22] R. Bär, Nature **135**, 153 (1935).
[23] H. W. Liepmann, Helvetica Physica Acta **9**, 507 (1936); **11**, 381 (1938); **12**, 421 (1939).
[24] A.van Itterbeek, G. J. van den Berg and W. Limburg, Physica **20**, 307 (1954).
[25] E. Hiedemann and K. H. Hoesch, Z. f. Phys. **96**, 268 (1935); **98**, 141 (1935).
[26] J. R. Barker, E. R. Dobbs and J. O. Jones, Phil. Mag. **44**, 1182 (1953).
[27] W. H. Keesom and A. van Itterbeek, Comm. Leiden No. 216 c; Proc. Amst. **34**, 996 (1931).

* Since this paper has been written a new report has recently been published by Chase and Herlin [49]) on the absorption in the demagnetization region. Two absorption peaks appear below 1°.

[28] A. van Itterbeek and O. van Paemel, Physica **5**, 593 (1938).
[29] A. van Itterbeek and O. van Paemel, Physica **5**, 845 (1938).
[30] A. van Itterbeek and W. van Doninck, Proc. Phys. Soc. **58**, 615 (1946); **62**, 62 (1949).
[31] A. van Itterbeek, Doctorate Thesis, Ghent, 1932.
[32] W. K. Walstra, Doctorate Thesis, Leiden, 1946.
[33] H. W. Liepmann, Helv. Phys. Acta, **12**, 421 (1939).
[34] H. J. Groenewold, Physica, **6**, 303 (1939).
[35] L. Verhaegen, Doctorate Thesis, Louvain, 1952.
[35a] A. van Itterbeek and L. Verhaegen, Nature 477 (1955).
[36] W. Schaaffs, Z. für Phys. **114**, 110 (1939); **115**, 69 (1940).
[37] C. Kittel, J. Chem. Phys. **50**, 955 (1936).
[38] L. Tonks, Phys. Rev. **50**, 955 (1936).
[39] Lebedew, Ann. de Phys. **35**, 171 (1911).
[40] E. J. Stewart, J. L. Stewart and J. C. Hubbard, Phys. Rev. **68**, 231 (1945); J. E. Rhodes, Phys. Rev. **70**, 932 (1946).
[41] E. F. Burton, Nature, London, **141**, 970 (1938).
[42] J. C. Findlay, A. Pitt, H. Grayson Smith and J. O. Wilhelm, Phys. Rev. **54**, 506 (1938); **56**, 122 (1939).
[43] W. H. Keesom and Miss A. P. Keesom, Comm. Leiden, No. 224e, Proc. Roy. Acad. Amsterdam **36**, 612 (1933).
[44] I. Khalatnikow, J. Exp. Theor. Phys. **20**, 243 (190); **23**, 8 (1952).
[45] L. Landau, Journ. Phys. U.S.S.R. **5**, 71 (1941).
[46] A. van Itterbeek, Med. Kon. Acad., Brussels, 1940, No. 2.
[47] R. Kronig and A. Thellung, Physica **16**, 678 (1950).
[48] R. Kronig, A. Thellung and H. H. Woldringh, Physica **18**, 21 (1952).
[49] C. E. Chase and M. A. Herlin, Phys. Rev. **95**, (1954), 565.

CHAPTER XVIII

TRANSPORT PROPERTIES OF GASEOUS HELIUM AT LOW TEMPERATURES

BY

J. DE BOER

1. Introduction

The investigation of the transport processes in gases at low temperatures has many interesting aspects, mainly because of the fact that at low temperatures remarkable quantum effects which are rather difficult to detect at higher temperatures can be observed. It will therefore be necessary to base the discussion of the transport properties entirely on quantum mechanics.

Unfortunately it is at low temperatures possible to make measurements with only very few gases, namely, the light and heavy isotopes of helium, ^3He and ^4He, and the hydrogenic molecules, H_2, HD, D_2, etc. Of these cases only helium has been observed in more detail, whereas a complete investigation of all the hydrogenic molecules and their ortho- and para-varieties is still in a rather incomplete state. It may be hoped, however, that in the future this gap will be filled up.

In the following we will give a brief sketch of the quantum mechanical theory of the transport phenomena, indicating as far as possible the limitations and applicability of the theoretical results (§ 2, 3). Then we will discuss the results obtained for helium gas in § 4,5 and 6 and compare with the experimental results in so far as these are available.

For the sake of completeness we will start with the definition of the transport coefficients which are discussed in the present survey article.

For a *simple gas of monatomic molecules*, we define the two coefficients:
a) *The viscosity coefficient*: In a gas at constant temperature in which

there is a laminar flow, such that the average velocity, the "bulk velocity," c_x is always in the x-direction and is a linear function of the z-coordinate, the coefficient of viscosity μ is defined as the proportionality coefficient in the expression:

$$p_{xz} \; (= nm\overline{c_x c_z}) = - \mu \, d\overline{c_x}/dz \qquad (1)$$

where p_{xz} is the xz-component of the pressure tensor, being defined as the *average transport of momentum* in the x-direction per unit time through unit surface perpendicular to the z-axis. It should be remembered that for gases at normal pressures and normal temperatures the coefficient of viscosity defined above is a quantity independent of the density, but that at higher as well as at lower densities, this is no longer true. This region of "normal" density is defined by two conditions. On the one hand the density should be high enough so as to make the mean free path small compared to the dimensions of the vessel: *Knudsen phenomena* can then be neglected. On the other hand the density should be so small that effects due to triple collisions are negligible, the mean free path remaining large compared with distances characteristic for the intermolecular interaction: *pressure effects* on the viscosity can then be neglected. The viscosity considered here is by definition the value of the coefficient μ in the density region between the region of the Knudsen phenomena and the region of the pressure effects, in which the viscosity is approximately constant. Neither the Knudsen effects nor the pressure effects will be considered in this treatise.

b) *The coefficient of thermal conduction:* In a gas at constant pressure, in which there is a temperature gradient such that the temperature changes linearly as a function of the z-coordinate, the coefficient of thermal conduction is defined as the proportionality coefficient in the equation:

$$q_z \; (= n \, . \, \tfrac{1}{2} m\overline{c^2 \, . \, c_z}) = - \lambda dT/dz \qquad (2)$$

where q_z is the *average transport of energy* per unit time through unit surface perpendicular to the z-axis. As in the case of the viscosity coefficient, the coefficient of thermal conduction which is considered in this treatise is again by definition the density independent value of the thermal conduction coefficient at normal densities.

For a *mixture of two monatomic gases* the coefficients of viscosity and thermal conduction are defined in the same way as above, but now

they will be functions of the temperature *and* the relative concentrations $x_i = n_i/n$ and $x_j = n_j/n$ ($x_i + x_j = 1$) of the two gases. Moreover there exist in this case the coefficients describing the diffusion phenomena:
c) *The diffusion coefficient*: The diffusion coefficient is defined for a gas mixture of uniform density and temperature in which a concentration gradient in the z-direction exists for each of the components. The diffusion coefficient is then defined as the coefficient of proportionality in the equations:

$$\Gamma_i\ (= n_i\overline{c_i}) = -\,D_{ij}\,dn_i/dz \quad \Gamma_j\ (= n_j\overline{c_j}) = -\,D_{ij}\,dn_j/dz \tag{3}$$

in a frame in which the gas as a whole is at rest. Γ_i is the average transport of molecules i per unit time through unit surface perpendicular to the z-axis. Because $dn_i/dz + dn_j/dz = 0$ and $\Gamma_i + \Gamma_j = 0$, one may write for the relative velocity of the two gases:

$$\overline{c_{zi} - c_{zj}} = -\,(1/x_i x_j)\,D_{ij}\,dx_i/dz \tag{3b}$$

where D_{ij} is the mutual diffusion coefficient of the two gases i and j. In the region of normal densities this diffusion coefficient is inversely proportional to the total density $n = n_i + n_j$ of the mixture.
d) *Thermal diffusion coefficient and thermal diffusion ratio:* When in a gaseous mixture a uniform temperature gradient is maintained along the z-axis, there results a relative velocity of the two components due to the temperature gradient in addition to the relative velocity proportional to the concentration gradient. The expression (3b) should be completed by adding a term:

$$\overline{c_{zi} - c_{zj}} = -\,(1/x_i x_j)\,\{D_{ij}\,dx_i/dz + D_T d\ln T/dz\} \tag{3c}$$

where D_T is the *coefficient of thermal diffusion.*

Usually one introduces the *thermal diffusion ratio* $\varkappa_T$ defined as the ratio of D_{ij} and D_T : $\varkappa_T = D_T/D_{ij}$ giving:

$$\overline{c_{zi} - c_{zj}} = -\,(1/x_i x_j)\,D_{ij}\,\{dx_i/dz + \varkappa_T\, d\ln T/dz\} \tag{3d}$$

The quantities D_{ij}, D_T and $\varkappa_T$ are in general functions of the concentration.

The *theoretical procedure* for calculating these four transport coefficients should be of course to find on the basis of the kinetic gas theory theoretical expressions for the average pressure tensor $nm\overline{c_x c_z}$, for the average heat current $\frac{1}{2}nm\overline{c^2 c_z}$, and for the average relative velocity $\overline{c_{zi} - c_{zj}}$

in a gas mixture, as functions of the gradients of the bulk velocity, temperature, and molecular densities existing in the system.

The elementary procedure of expressing these quantities in terms of a mean free path, which is a function of the collision crosssection of the molecules, has long been abandoned because these "free path theories" did not lead to rigorous theoretical expressions for the coefficients, there being much uncertainty about the physical picture on which these considerations were based.

The modern procedure, which leads to rigorous expressions for the transport coefficients, is based on the solution of the Boltzmann equation, which should determine the complete velocity distribution function in the non-uniform state of the gas. Once this distribution function is known, one can calculate theoretically the appropriate averages, which represent the transport of momentum, energy and molecules, and determine the transport coefficients by using (1), (2) and (3c). This will be shown in § 2 and 3.

2. The Boltzmann Equation. Definition of the Crosssections

The quantum mechanical theory of the transport processes is based on the solution of the quantum mechanical version of the Boltzmann integral equation:

$$\frac{\partial f_i}{\partial t}+\boldsymbol{c}_i\cdot\frac{\partial f_i}{\partial \boldsymbol{r}_i}=\int\int\int\left\{f_i'f_j'\,(1+\Theta_i f_i)\,(1+\Theta_j f_j)-f_i f_j\,(1+\Theta_i f_i')\,(1+\Theta_j f_j')\right\}\cdot$$
$$\cdot\, g\sigma(g,\chi)\sin\chi\, d\chi\, d\varepsilon\, d\boldsymbol{c}_j. \qquad (4)$$

The derivation is based on the following assumptions: (a) the deviations from the uniform equilibrium state should be small, and (b) the density should be so small that effects due to the interaction of more that two molecules at the same time (i.e. triple collisions) can be neglected. The effects due to "triple collisions" would lead to density dependent corrections for the transport coefficients, and will not be considered here. This equation is an integral equation for the velocity distribution function $f_i = f(\boldsymbol{c}_i; \boldsymbol{r}_i)$, which is a function of $\boldsymbol{c}_i$ and may vary slowly as a function of the coordinates $\boldsymbol{r}_i$. The integration is carried out over all velocities c_j of molecules j colliding with the molecule i. The functions $f_i' = f(\boldsymbol{c}_i'; \boldsymbol{r}_i)$ and f_j' are the same distribution functions as above, but have the velocities after the collision, $\boldsymbol{c}_i'$ and $\boldsymbol{c}_j'$, as variables, which thus are functions of the initial velocities, $\boldsymbol{c}_i$ and $\boldsymbol{c}_j$, and the variables specifying the collision. $\sigma(\boldsymbol{g}, \boldsymbol{g}')$ is the quantum

mechanical cross-section for a scattering process in which molecules i and j with a relative velocity $\boldsymbol{g}$ are scattered in a collision in such a way that the relative velocity after the collision is given by the vector $\boldsymbol{g}'$, the direction of which is determined by the polar angles χ and ε relative to the relative velocity vector $\boldsymbol{g}$ before the collision. When no internal degrees of freedom can be excited, one has $\sigma(\boldsymbol{g},\boldsymbol{g}') = \sigma(g, \chi)$, and then the scattering cross-section $\sigma(g, \chi)$ is a function of g and the scattering angle χ only. When the molecules i and j are identical, one has to introduce the factors $1 + \Theta_i f_i = 1 + (\delta/G_i)\ (h/m_i)^3 f_i$, in which G_i is a statistical weight and δ is $+1$ or -1 for molecules obeying Bose-Einstein statistics and Fermi-Dirac statistics, respectively.

This equation was derived for the first time by E. A. Uehling and G. E. Uhlenbeck [1] in an article in which the complete statistical theory of the transport coefficients in quantum mechanics was founded. We see that the "streaming terms" on the left hand side are the same as in classical theory but that the integral expression differs in two respects from the classical expression:

a) The introduction of the factors $1 + \Theta f$ due to symmetry effects,*

b) The introduction of the quantum mechanical cross-section $\sigma(g, \chi)$ instead of the classical one.

Recently it has been shown by H. Mori and S. Ono [2] that this equation can also be derived from the general formulae of quantum statistical mechanics in a way similar to the derivation given by J. G. Kirkwood [3] in the classical case, except for some corrections which, however, do not contribute to the density-independent part of the viscosity and heatconductivity.

The quantum mechanical *expression for the differential scattering crosssection* $\sigma(k, \chi)$ is given, according to the general theory of scattering (see e.g. Chapman and Cowling [3], Ch. 17) by the expression:

$$\sigma(k, \chi) = (1/4k^2) \sum_l (2l + 1)\ (\exp 2i\eta_l(k) - 1)\ P_l(\cos\chi), \qquad (5)$$

where $k = \mu g/\hbar$ is the circular wavenumber of relative motion ($\mu =$

* As we will omit systematically *all* terms which would lead to a density dependence of the transport coefficients, we will omit also at once the factors $(1 + \Theta f)$ in the Boltzmann equation. These terms lead only to density dependent corrections (compare Uehling and Uhlenbeck), and it is not sensible to evaluate these terms without evaluating also the other density dependent corrections which would result from tri- and more molecular collisions.

reduced mass) of two molecules with relative velocity g, $P_l(\cos\chi)$ are zonal spherical harmonics of the scattering angle χ, and l, over whose range the summation is carried out, * is the angular momentum quantum number. The quantity $\eta_l(k)$ is the important quantity which determines the relative contribution of the different spherical harmonics for different values of l to the total differential scattering cross-section. This "phase" or "phase shift" $\eta_l(k)$ is determined by the asymptotic behaviour of the radial wavefunction for the relative motion of two molecules. The asymptotic solution, for large values of the relative separation r, is of the periodic form $r^{-1}\sin\{kr - \frac{1}{2}l\pi + \eta_l(k)\}$ and differs by a phaseshift $\eta_l(k)$ from the corresponding solution in the case in which there is no interaction.

In fact, the solution of the integral equation shows that we do not need the quantity $\sigma(k,\chi)$ itself, but instead a certain weighted average over all scattering angles, the so called "total" crosssection

$$Q^{(r)}(k) = 2\pi \int_0^{\pi} (1 - \cos^r\chi)\,\sigma(k,\chi)\sin\chi\,d\chi \tag{6}$$

with r equal to 1 and to 2. The "weight functions" are proportional to $\sin^2\frac{1}{2}\chi$ and $\sin^2\chi$ in these two cases.

Substitution of the expression (5) for the differential crosssection into (6) and integration over χ leads to the following two expressions **

$$Q^{(1)} = (4\pi/k^2) \sum_{l=0.1....} (l+1)\sin^2(\eta_{l+1} - \eta_l) \tag{6a}$$

$$Q^{(2)} = (2\pi/k^2) \sum_{l=0.1....} \{(l+1)(l+2)/(l+\tfrac{3}{2})\}\sin^2(\eta_{l+2} - \eta_l). \tag{6b}$$

Of course, these "total" crosssections are still functions of the wavenumber k or velocity $g = \hbar k/\mu$ of relative motion of the two molecules.

The determination of the crosssections for the scattering of two molecules is a problem which is in principle determined completely by the internal structure and the quantum numbers characterizing the

* For the case of two identical molecules, these expressions should be multiplied by a factor 2, and one should take all phases equal to zero for odd values of l, when the wavefunction should be symmetrical, and for even values of l, when the wavefunction should be antisymmetrical in the coordinates of the two particles.

** These expressions, which are simpler then those generally used (see [3]) but which are mathematically equivalent with the more complicated expressions, have been used by J. de Boer and R. B. Bird [18] (see also [4]), Ch. 10).

relative motion of the two molecules. We come back to the solution of this *microscopic* problem in section (4), as we want to discuss first in the next section the statistical problem of how to express the transport coefficients in terms of these crosssections. The solution of this problem is identical with finding a solution for the integral equation of Boltzmann.

3. General Expressions for the Transport Coefficients

In the general theory of Chapman and Enskog, as described in a brilliant manner in the book "The mathematical theory of non-uniform gases" by Chapman and Cowling, the distribution function $f(\boldsymbol{c};\boldsymbol{r})$ is developed in a power series $f = f^{(0)} + f^{(1)} + \ldots$ in which $f^{(0)}$ is the Maxwell distribution function:

$$f^{(0)} = n(m/2\pi kT)^{3/2} \exp - \tfrac{1}{2}m(\boldsymbol{c} - \bar{\boldsymbol{c}}_o)^2/kT \tag{7}$$

The number density n, the bulk velocity $\bar{\boldsymbol{c}}_o$, and the temperature T are considered to be the "local" values and functions of the spatial coordinates. The series development is essentially a series in powers of a quantity which may be identified physically with the relative change of these local constants n, $\bar{\boldsymbol{c}}_o$, or T over the distance of one free path.Thus, it is legitimate to neglect terms higher than the second term $f^{(1)}$ in the series expansion, only when the relative change of the local density, bulk velocity, or local temperature over one free path is small. Deviations would occur either when the gradients become extremely large or when the density becomes so small that the free path becomes extremely large. Large gradients should be avoided when one wants to determine the transport coefficients. In the second case Knudsen corrections will become important, and it is well-known that this region also should be avoided when one wants to determine the transport coefficients of a gas. Since the free path is inversely proportional to the density, the series for f is a series in inverse powers of the density; consequently, the second term $f^{(1)}$ is independent of the density. The viscosity and heatconductivity calculated from $f = f^{(0)} + f^{(1)}$ are also independent of the density; consequently this is the proper theoretical counterpart of the density independent part of the experimental transport coefficients.

For the present study of the transport coefficients it is thus essential to take only the first two terms in the distribution function

$$f(\boldsymbol{c}) = f^{(0)}(\boldsymbol{c}) + f^{(1)}(\boldsymbol{c}) = f^{(0)}(\boldsymbol{c})\,\{1 + \Phi(c)\} \qquad (8)$$

as the inclusion of other terms would only lead to density-dependent contributions, which are not considered in principle here. Substitution of (8) in the Boltzmann equation leads to

$$\frac{\partial f^{(0)}}{\partial t} + \boldsymbol{c} \cdot \frac{\partial f^{(0)}}{\partial \boldsymbol{r}} = \int\int f^{(0)} f_1^{(0)} \{\Phi' + \Phi_1' - \Phi - \Phi_1\}\, g\sigma(g,\chi)\, \sin\chi d\chi d\varepsilon d\boldsymbol{c}_1. \qquad (9)$$

It is very fortunate that the solutions of this integral equation can be developed with very much success in terms of the socalled "Sonine-polynomials". The "success" arises from the fact that one can break off the development without serious error even after the first term. The solutions obtained with this first term alone are called the "first order solutions". Thus for a gas of uniform temperature in which a velocity gradient occurs this first order solution has the form

$$f(\boldsymbol{c}) = f^{(0)}(\boldsymbol{c})\,\{1 + \zeta_\mu(T)\, n^{-1}\, (\tfrac{1}{3}C^2 - C_x C_z)\, d\overline{c_x}/dz\}, \qquad (10a)$$

where $\boldsymbol{C} = \boldsymbol{c} - \bar{\boldsymbol{c}}$, and ζ_μ is a function of temperature only whose exact form follows from the solution of the integral equation. Similarly, for a gas at rest which has a temperature gradient in the z-direction the first order solution is

$$f(\boldsymbol{c}) = f^{(0)}(\boldsymbol{c})\,\{1 + \zeta_\lambda(T)\, n^{-1}\, (\tfrac{5}{2} - mC^2/2kT)\, d\ln T/dz\}, \qquad (10b)$$

where ζ_λ is a function of temperature different from ζ_μ above.

We wish to make two remarks about these distribution functions in the non-homogeneous state of the gas.

(1) They are proportional to the quantities $d\overline{c_x}/dz$ and $d\ln T/dz$, respectively, which characterize macroscopically the relative magnitude of the deviation from equilibrium.

(2) As $f^{(0)}(\boldsymbol{c})$ is proportional to the density n and the expression between brackets contains the factor $1/n$, the total correction term is *independent* of the density.

The evaluation of the average momentum transport $nm\overline{c_x c_z}$ or the average energy transport $\frac{1}{2}nm\overline{c^2 c_z}$ thus leads to a result which is proportional to the gradients $d\overline{c_x}/dz$ and $d\ln T/dz$, as is required by (1) and (2), and which is independent of the density! The viscosity and the heat conductivity coefficients are directly proportional to the two quantities ζ_μ and ζ_λ, respectively. The final expressions obtained for these *transport coefficients in first approximation* are[3], ref. 4 Ch. 8

$$[\mu]_1 = 5kT/8\Omega^{(2,2)} \quad [\lambda]_1 = (5c_v/2)\,(5kT/8\Omega^{(2,2)}) \tag{11}$$

where $\Omega^{(r,s)}$ are functions of temperature defined by [3]

$$\Omega^{(r,s)} = (kT/2\pi\mu)^{\frac{1}{2}} \int e^{-\gamma^2}\, \gamma^{2s+3}\, Q^{(r)}\, d\gamma \tag{12}$$

where $\gamma^2 = \mu g^2/2kT$. The quantity $\Omega^{(r,s)}$ might thus be interpreted as a kind of average of the crosssection which is a function of the relative velocity of the molecules over all relative velocities. It is of interest that in this first approximation the relation $[\lambda]_1$, $= (5/2)c_v\,[\mu]_1$, holds *exactly*, where $c_v = 3k/2m$ is the specific heat per unit mass.

In higher approximations one should include subsequent Sonine polynomials in the development of the distribution function. For a complete exposition of this method and the results we refer to Chapman and Cowling's standard work. The *second approximation* may be written as:

$$[\mu]_2 = [\mu]_1\,(1 + \varepsilon_\mu) \quad [\lambda]_2 = [\lambda]_1\,(1 + \varepsilon_\lambda) \tag{13a}$$

where the corrections are given by (comp [4] p. 604—605 and [10])

$$\varepsilon_\mu^{-1} = \frac{4\Omega^{(2,2)}\,(\frac{3\,0\,1}{1\,2}\,\Omega^{(2,2)} - 28\Omega^{(2,3)} + 20\Omega^{(2,4)})}{(7\Omega^{(2,2)} - 8\Omega^{(2,3)})^2} - 1 \tag{13b}$$

$$\varepsilon_\lambda^{-1} = \frac{4\Omega^{(2,2)}\,(\frac{7\,7}{4}\,\Omega^{(2,2)} - 28\Omega^{(2,3)} + 20\Omega^{(2,4)})}{(7\Omega^{(2,2)} - 8\Omega^{(2,3)})^2} - 1$$

It has to be stressed, however, that the first approximation alone already furnishes an excellent approximation in the case of the viscosity and heat conductivity. Thus for a gas of hard spheres one finds that the first approximation for μ and λ is only 1.6 and 2.4% too small and the second approximation 0.1 and 0.2%, respectively. However for the case of the diffusion and thermal diffusion ratio the situation is worse because, again for hard spheres, the first approximation is 11% and 20% too small and the second approximation 4.3 and 12%, respectively.

For *mixtures of two gases* the theory given above can easily be generalised. One should distinguish then between the crosssections $Q_i^{(r)}$ for scattering of molecules of the same species and the crosssections $Q_{ij}^{(r)}$, defined in exactly the same manner, for scattering of molecules

of different type. The same should be done for the average crosssections $\Omega^{(r,s)}$.

The final expression for the *viscosity in first approximation of a mixture of two gases* may be written in the form [10]

$$1/[\mu_{mix}]_1 = \frac{H_i x_i^2/[\mu_i]_1 + 2H_{ij}x_i x_j/[\mu_{ij}]_1 + H_j x_j^2/[\mu_j]_1}{H_i x_i^2 + 2K_{ij}x_i x_j + H_j x_j^2} \tag{14}$$

where x_i and x_j are the relative concentrations of the two components of the mixture. The quantities $[\mu_{ij}]_1$ and $[\mu_i]_1$ are now defined as:

$$[\mu_i]_1 = \frac{5kT}{8\Omega_i^{(2,2)}} \qquad [\mu_{ij}]_1 = \frac{5kT}{8\Omega_{ij}^{(2,2)}} \tag{15}$$

The quantities H_i and K_{ij} are complicated expressions in terms of the $\Omega^{(r,s)}$-functions, for the definition of which we refer to the article of Cohen, Offerhaus and de Boer [10].

The expression for the *thermal conduction in first approximation of a mixture of two gases* becomes [10]

$$1/[\lambda_{mix}]_1 = \frac{L_i x_i^2/[\lambda_i]_1 + 2L_{ij}x_i x_j/[\lambda_{ij}]_1 + L_j x_j^2/[\lambda_j]_1}{L_i x_i^2 + 2M_{ij}x_i x_j + L_j x_j^2} \tag{16}$$

where

$$[\lambda_i]_1 = \frac{5kT}{8\Omega_i^{(2,2)}} \cdot \frac{5c_v'}{4\mu_i} \qquad [\lambda_{ij}]_1 = \frac{5kT}{8\Omega_{ij}^{(2,2)}} \cdot \frac{5c_v'}{4\mu_{ij}}. \tag{17}$$

Again we refer for the definition of the quantities L_i and M_{ij} in terms of the $\Omega^{(r,s)}$ functions to the literature. [10] Here $c_v' = 3k/2$.

For a mixture of two gases we find for the *diffusion coefficient* the expression [3, 4]:

$$[D_{ij}]_1 = 3kT/16\pi\mu_{ij}\,\Omega_{ij}^{(1,1)} \tag{18}$$

where $\mu_{ij} = m_i m_j/(m_i + m_j)$ is the reduced mass. Thus for the diffusion coefficient we have to take an average of the crosssection $Q_{ij}^{(1)}$, but it should be mentioned that this is only true for the first approximation. It has been remarked that in the case of the diffusion coefficient the first approximation is not as good as in the cases of viscosity and thermal conduction and that the correction leading to the second approximation may be appreciable. This correction is given by the formula (comp. [4] p. 605 and [10])

$$[D_{ij}]_2 = [D_{ij}]_1/(1 - \Delta)$$

$$\Delta = \frac{(6\Omega^{(1,2)} - 5\Omega^{(1,1)})^2}{\Omega^{(1,1)}\,(55\Omega^{(1,1)} - 60\Omega^{(1,2)} + 48\Omega^{(1,3)} + 16\Omega^{(2,2)\,2})}. \qquad (19)$$

The *thermal diffusion ratio* $[\varkappa_T]_1$ becomes in *first approximation* (comp. [4] p. 541 and [10])

$$[\varkappa_T]_1 = \tfrac{5}{6}\,(C_{ij} - 1)\,\frac{x_i x_j}{[\lambda_{ij}]_1}\,\frac{S_i x_i - S_j x_j}{L_i x_i^2/[\lambda_i]_1 + 2L_{ij}x_j x_i/[\lambda_{ij}]_1 + L_j x_j^2/[\lambda_j]_1} \qquad (20)$$

where $C_{ij} = 2\Omega_{ij}^{(1,2)}/5\Omega_{ij}^{(1,1)}$ and the quantities L_{ij} and S_i are defined as functions of Ω_{ij} by Cohen, Offerhaus and de Boer [10]. Usually the molecule i is taken as the heavier molecule, so that we will identify i with ^{4}He and j with ^{3}He.

After having evaluated the different crosssections which are needed in § 4, we will use the general expressions as reproduced in this section for the calculation of all the transport coefficients of ^{3}He, ^{4}He and their mixtures in § 5 and 6.

4. Intermolecular Interaction and Crosssections for Helium

The only monatomic substances for which rather complete and detailed calculations of the transport properties at low temperatures have been made are the two isotopes of helium. For the other monatomic substances no measurements are possible at low temperatures and they need not be considered therefore in this article.

After having discussed in the previous section the macroscopic problem, i.e. the problem of deriving formal expressions for the transport coefficients in terms of the crosssections $Q^{(r)}$, we now come to the *microscopic problem*, namely, the evaluation of the crosssection for bimolecular collisions from first principles.

The interaction between two helium atoms, the calculation of which should form the starting point for any calculation of a collision crosssection, could be evaluated in principle on a purely theoretical basis by evaluating the lowest eigenvalue of a system of two helium atoms as a function of their relative reparation. As is well known this interaction curve was obtained several years ago by Slater and Kirkwood[5] in the form of the formula

$$\varphi(r) = b \exp r/a - c/r^6 \qquad (21)$$

with $b = 7.7 \times 10^{-10}$ erg, $c = 1.47 \times 10^{-60}$ erg. cm^6 and $a = 0.217 \times$

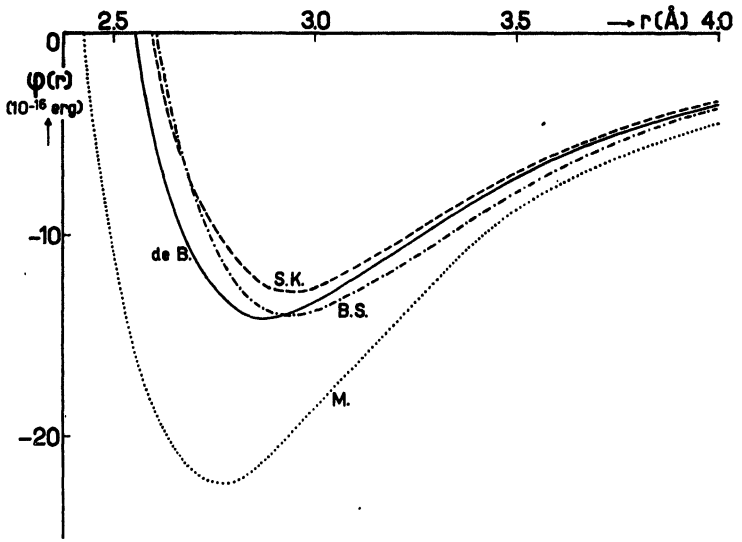

Fig. 1. Interaction potential of two helium atoms:
curve S. K.: Expression (21) of Slater and Kirkwood [5]; curve M.: Corrected curve according to Margenau [6]; curve de B.: Expression (22) used by de Boer and coll. [8, 9, 10]; curve B. S.: Expression (24) with $\epsilon = 14.04 \times 10^{-16}$ erg used by Buckingham and Scriven [14]

10^{-8} cm. The curve, reproduced (S.K.) in figure 1, has been corrected by several investigators [6] to account for higher order terms, particularly additional r^{-8} and r^{-10} attractive terms, in the interaction. The general tendency of these corrections is to make the attraction larger and the minimum deeper, as shown by the typical curve obtained, for instance, by Margenau [7]. Unfortunately the perturbation calculation converges less rapidly as the distance becomes smaller. In addition the position and depth of the minimum are influenced very much by the addition of attractive contributions, which themselves vary so largely with the distance r. Moreover, second order effects in the evaluation of the repulsive field should be taken into account, as has been emphasized in particular by Margenau. One may thus conclude that the interaction curve is not known at this moment with the precision needed for the further calculation.

It is for this reason that one *assumes* in general a curve for the interaction of the general type indicated by the theoretical calculations, but provided with undetermined constants which can be determined in an empirical way.

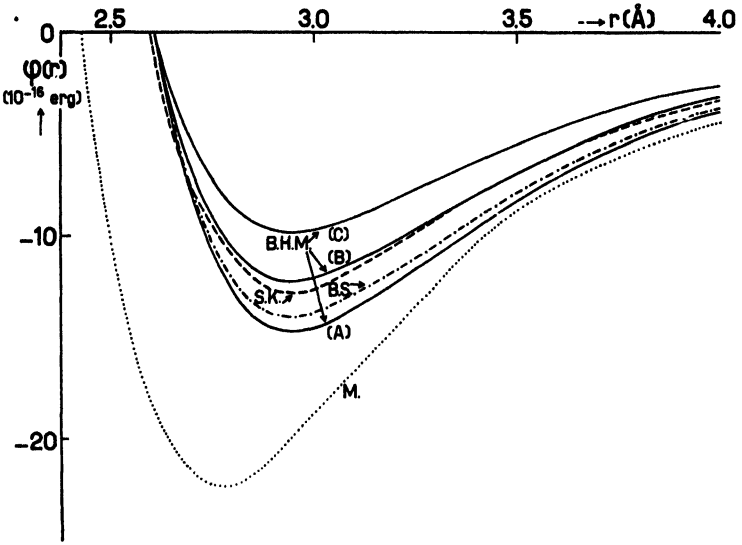

Fig. 2. Interaction potential of two helium atoms:
curve S. K.: Expression (21) of Slater and Kirkwood [5]; curve M.: Corrected curve according to Margenau; curves B.H.M.A.B. and C: Expression (24) with $\epsilon =$ 14.69, 12.24 and 9.80 $\times$ 10^{-16} erg used by Buckingham Hamilton and Massey [13]; curve B.S.: Expression (24) with $\epsilon = 14.04 \times 10^{-16}$ erg used by Buckingham and Scriven

A *potential field of the Lennard-Jones type* with twelve-six-power laws has been proposed by J. de Boer [8]. This may be written in the form

$$\varphi(r) = 4\varepsilon\,[(\sigma/r)^{12} - (\sigma/r)^{6}] = \varepsilon\,[(r_m/r)^{12} - 2(r_m/r)^{6}], \qquad (22)$$

where σ, the "diameter", is the distance where the interaction is equal to zero, and ε is the depth of the potential field. The values $\varepsilon/k = 10.22$ °K and $N\sigma^3 = 10.06$ cm^3, were obtained from a best fit of the second virial coefficient of helium gas. Using the present values for N and k one obtains $\varepsilon = 14.11 \times 10^{-16}$ erg and $\sigma = 2.556$ Å, whereas the distance r_m of the minimum becomes $r_m = 2.869$ Å. Of course, the interaction between two ^{4}He atoms is exactly the same as that between two ^{3}He atoms, because this interaction is determined by the electronic structure and not by the mass of the nuclei. This interaction is compared in Fig. 1 with the theoretical curves.

The crosssection for the case of ^{4}He has been evaluated on a quantum mechanical basis by first calculating the phases and then using

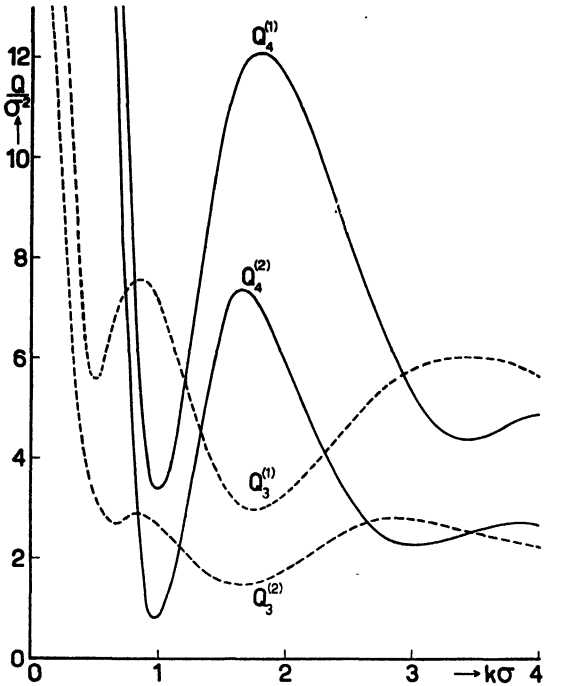

Fig. 3. Crosssections $Q_4^{(r)}$ for ^{4}He according to de Boer [8] and cross sections $Q_3^{(r)}$ for ^{3}He according to de Boer and Cohen [9]

the sum expressions for the crosssections *. The result of this calculation is plotted in Fig. 3 as a function of the wavenumber of relative motion $k^* = k\sigma$.

The crosssections for the case of ^{3}He have been evaluated by de Boer and Cohen [9]. The results of the calculation of these crosssections ** are also given in Fig. 3. As could be expected the crosssections for ^{3}He are smaller than those of ^{4}He, because of the fact that the longer

* ^{4}He atoms follow Bose-Einstein statistics and have no nuclear spin. Hence, according to the principle of the note on page 386, the following formulae for the crosssections:

$$Q^{(1)} = Q_s^{(1)} = (8\pi/k^2) \sum_{l=0,2...} (2l + 1) \sin^2\eta_l,$$

$$Q^{(2)} = Q_s^{(2)} = (4\pi/k^2) \sum_{l=0,2...} [(l + 1)(l + 2)/(l + 3/2)] \sin^2(\eta_{l+2} - \eta_l),$$

have been used in this calculation.

** Since ^{3}He has a nuclear spin $1/2\hbar$, the expressions for the crosssections to be used are now

$$Q = 1/4 Q_s + 3/4 Q_{a.s}$$

where Q_s is given in note * on this page and a similar expression holds for $Q_{a.s}$.

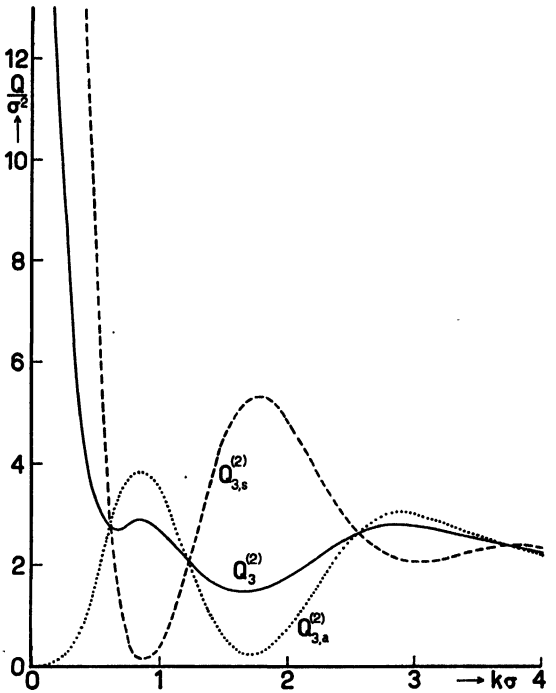

Fig. 4. Influence of the symmetry effects (statistics) on the crosssection $Q_3^{(2)}$ for ^{3}He according to de Boer and Cohen [9]

De Broglie wavelength reduces the influence of the attractive field in the case of the lighter molecules. There is also an important difference at very small relative wavenumbers. As in the case of ^{4}He there happens to be a real or virtual stationary state in the neighbourhood of $E \approx 0$ (most probably virtual), the crosssection nearly goes to infinity, proportional to k^{-2} in this case. For the case of ^{3}He there is no such singularity at $E \approx 0$ and consequently the crosssection goes to a constant value (which is determined by the slope of the curve of the phase $\eta_0(k)$ versus k near $k \approx 0$).

It may be of interest to demonstrate in the case of ^{3}He the rôle of the statistics. In Fig. 4 we have drawn the curves for $Q_s^{(2)}$ and $Q_{a.s}^{(2)}$ which would be valid if ^{3}He had no spin and followed Bose-Einstein statistics and Fermi-Dirac statistics, respectively. This large influence of the statistics disappears at higher relative wavenumbers (or momenta).

The crosssections which are valid for collisions between ^{4}He and

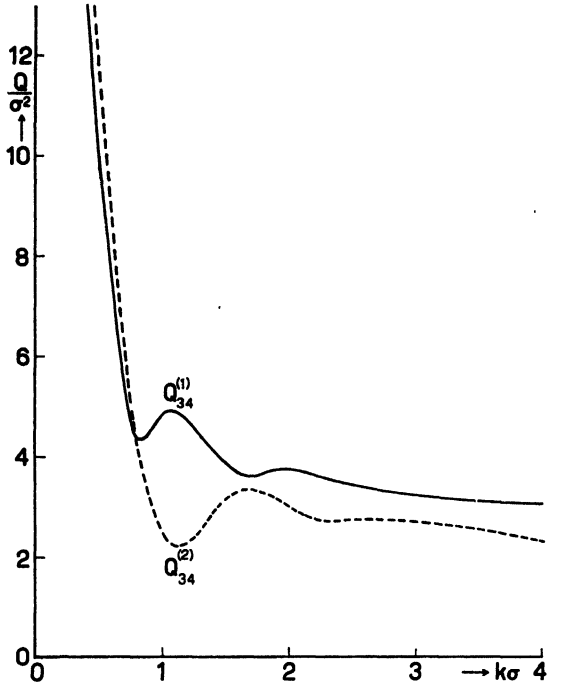

Fig. 5. Crosssections $Q_{34}(r)$ for collisions of ^{4}He and ^{3}He atoms according to Cohen, Offerhaus and de Boer [10]

^{3}He atoms have been evaluated by Cohen, Offerhaus and de Boer [10]. They have been plotted in Fig. 5. In this case symmetry effects do not exist, because ^{4}He and ^{3}He are two different atoms.

A *potential field of the exponential-six type* has been proposed by Massey and Buckingham [12]. We will write this field in the form

$$\varphi(r) = \varepsilon \left[f_1 \exp\left(-\alpha r/r_m\right) - f_2 (r_m/r)^6 \right] \tag{23}$$

When the two factors f_1 and f_2 are taken equal to $(6/(\alpha - 6)) \exp \alpha$ and $\alpha/(\alpha - 6)$, respectively, the constants ε and r_m are again the depth and the value of r at the minimum of the interaction curve. The value $r_m = 2.95$ Å of the field (21), together with Slater and Kirkwood's value of a, leads to $\alpha = r_m/a = 13.6$. Slater and Kirkwood's expression[21] leads to a value:

$$\varepsilon = 12.50 \times 10^{-16} \text{ erg}$$

for the minimum energy. An *extension of this exponential-six potential*

field was proposed later on by Buckingham, Hamilton and Massey [13], who added an eighth power attractive field the potential then being

$$\varphi(r) = \varepsilon\,[f_1 \exp(-\alpha r/r_m) - f_2\,(r_m/r)^6 - \beta f_2\,(r_m/r)^8]. \qquad (24)$$

The constant β was assumed to be equal to 0.2. This assumption finds support in the theoretical data about the relative importance of the high frequency quadrupole-dipole forces as compared with the high frequency dipole-dipole Van der Waals forces. If one now takes $f_1 = (6 + 8\beta)/(\alpha - 6 + \beta(\alpha - 8)) \exp \alpha$ and $f_2 = \alpha/(\alpha - 6 + \beta(\alpha - 8))$ then again ε and r_m are, respectively, the depth of the potential field and the value of r for which this minimum occurs. Fig. 2 gives a comparison between Slater and Kirkwood's expression and the three curves of the type (24) obtained by taking ε equal to three different values (cases A, B and C). According to Buckingham and Scriven the best agreement with the second virial coefficient at low temperatures was obtained by taking $\varepsilon = 14.04 \times 10^{-16}$ erg and $r_m = 2.943$ Å. This potential field (B.S. in fig. 2) is very similar to the twelve-six potential field used by J. de Boer (comp. fig 1) which also gave good agreement at low temperatures. This is a very satisfactory result as it shows that at these very low temperatures only the negative part of the interaction curve is of importance and that, although the mathematical formula for the curve is different (eq. (22) resp. (24)), the effective curve for the interaction is approximately the same. At high temperatures the behaviour is different however, because at distances smaller then 2.5 Å, which then are of importance, the exponential repulsion is weaker then the twelfth power repulsion. The twelve-six potential field *does* represent the second virial coefficient also at relatively high temperatures. The exponential curve however has a maximum at even smaller distances, beyond which the curve approaches minus infinity for $r \to 0$. Buckingham, Hamilton and Massey [13] and Buckingham and Scriven [24] have used these potential fields to calculate the crosssections and transport properties of ^{3}He and ^{4}He, but explicite data for the crosssections have not been published. The results will be discussed in the next section.

5. Viscosity and Heat Conductivity for ^{4}He and ^{3}He

On the basis of the crosssections for collisions between helium atoms obtained in the previous section (§ 4) and the general formulae expressing the transport coefficients in terms of these crosssections which

were obtained in section § 3 on the basis of the general Chapman-Enskog theory, one is able to calculate all the transport coefficients for light and heavy helium gas and their gaseous mixtures. In this section we discuss the viscosity and heat conductivity of the pure gases and their mixtures.

Using the *twelve-six-potential field* (22) calculations have been made by de Boer [8] for ^{4}He with the crossections of Fig. 3. The results for the viscosity in first and second Enskog approximation, according to the formulae (12) and (13), are given in Fig. 6, together with the latest experimental results obtained by Van Itterbeek, Schapink, Van den Berg and Van Beek [15], and by Becker, Misenta and Schmeissner [16]. The experimental data seem to be systematically somewhat higher than the theoretical data even after the second order correction has been applied. This might be an indication that the value of $h^2/m\varepsilon\sigma^2$, which occurs in the Schrödinger equation and thus determines the wavefunctions, the phases, and the crosssections, is somewhat too small. A similar conclusion could be drawn from the comparison of the theoretical data of the second virial coefficient calculated by

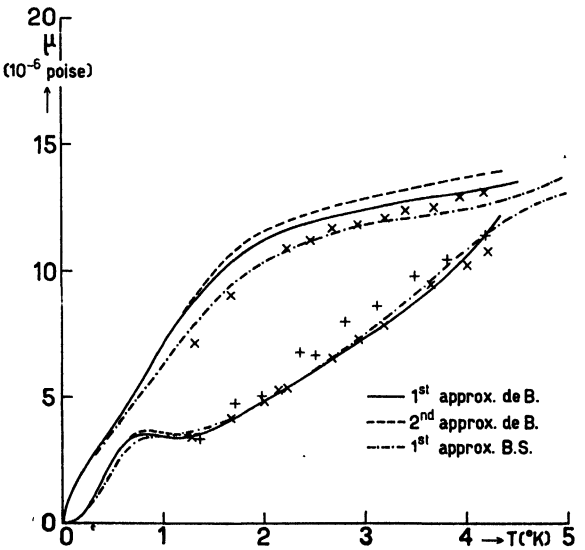

Fig. 6. Viscosity of ^{4}He and ^{3}He in first and second approximation according to de Boer and Cohen [8, 9] (de B.) and to Buckingham and Scriven (B.S.), compared with experimental data of Van Itterbeek, and coll. [15], and Becker and coll.[16]

de Boer [8] with the experimental data, as discussed in detail by the author in a previous report [11], page 354).

Calculations for ^{3}He have been carried out by de Boer and Cohen [9] with the crosssections of fig. 3, and the results for the first and second Enskog approximation are also given in figure 6. The only data which can be used in this case for comparison are the experimental data obtained by Becker, Misenta and Schmeissner [16] for gaseous ^{3}He which however still contained about 6% ^{4}He. It is satisfactory that the theoretical results for pure ^{3}He are still higher than those for the mixture and that linear interpolation shows that fair agreement can be obtained for the experimental concentration, but there still seem to exist small deviations which change systematically with temperature.

It may be of interest to show in a separate figure the effect of the *symmetrization of the wave functions* (or of the *statistics*) on the values for the viscosity of ^{3}He, using the values of the crosssections which were reproduced in Fig. 4. Fig. 8 shows an enormous effect of the statistics. If ^{3}He had no spin, the result would have been entirely different.

Calculations for the mixtures of ^{3}He and ^{4}He have been carried out by Cohen, Offerhaus and de Boer [10], and we refer to this publication for full details. All the results, as far as the first Enskog approximation is concerned, are collected in table I. This contains the values $[\mu_3]_1$

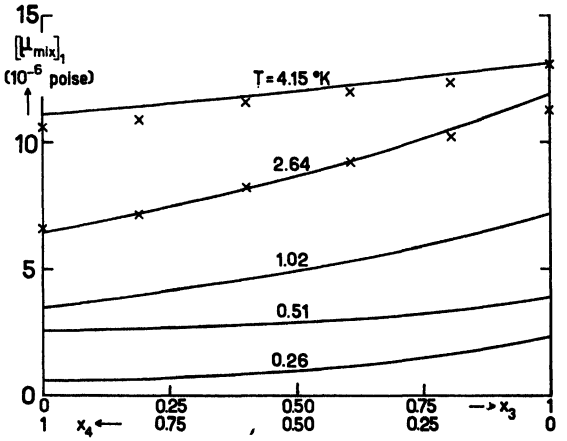

Fig. 7. Viscosity of mixtures of ^{4}He and ^{3}He in first approximation according to Cohen, Offerhaus and de Boer [10] compared with experimental data of Becker and coll. [16]

TABLE I

Data for viscosity of ^{3}He, ^{4}He and mixtures in first approximation

T °K	$[\mu_3]_1$ μP	$[\mu_4]_1$ μP	$[\mu_{34}]_1$ μP	H_3	H_4	H_{34}	K_{34}
0	0	0	0	1.45	1.80	∞	∞
0.256	2.35	0.54	0.98	1.40	1.71	1.41	1.69
0.511	3.87	2.50	2.80	1.41	1.72	1.45	1.48
1.02	7.20	3.44	5.14	1.43	1.77	1.63	1.72
2.04	11.3	5.01	7.49	1.52	1.93	1.69	1.82
3.07	12.4	7.45	9.68	1.53	1.95	1.74	1.80
4.09	13.1	10.9	11.9	1.52	1.92	1.70	1.72

and $[\mu_4]_1$ for the pure substances as well as the coefficients H_3, H_{34}, H_4, K_{34}, and $[\mu_{34}]_1$ which should be used in connection with the theoretical expression (14) giving the viscosity of the mixture as a function of the concentrations.

In Fig. 7 the theoretical curves for the viscosity of ^{4}He—^{3}He mixtures obtained from the data in table I are compared with the experimental data of Becker, Misenta and Schmeissner [16].

The available theoretical data for the *heat conductivity* of pure ^{3}He and ^{4}He and their mixtures are given in Table II, which should be

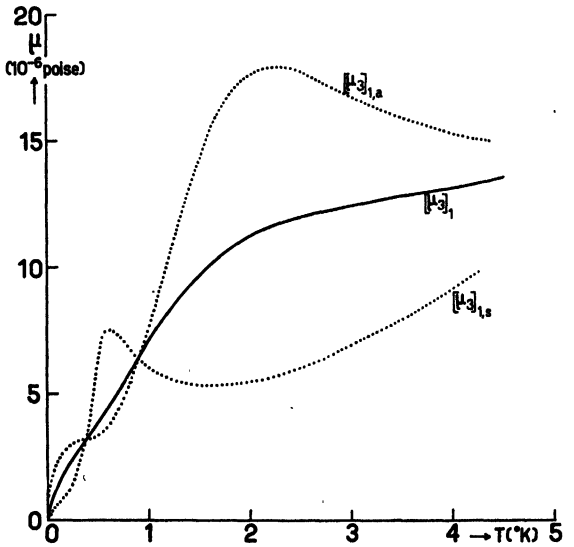

Fig. 8. Effect of statistics on viscosity of ^{3}He according to de Boer and Cohen [9] (Crosssections Fig. 4)

TABLE II

Data for heat conductivity of ^{3}He, ^{4}He and mixtures in first approximation

T °K	$[\lambda_3]_1$	$[\lambda_4]_1$	$[\lambda_{34}]_1$	L_3	L_4	L_{34}	M_{34}
	10^2 erg s^{-1} cm^{-1} deg^{-1}						
0	0	0	0	1.10	0.93	∞	∞
0.256	2.44	0.418	0.888	1.05	0.88	0.92	1.06
0.511	4.02	1.95	2.55	1.08	0.92	0.97	0.97
1.02	7.49	2.69	4.68	1.08	0.91	1.03	1.07
2.04	11.8	3.91	6.75	1.13	0.95	1.04	1.12
3.07	12.9	5.81	8.81	1.13	0.96	1.06	1.09
4.09	13.6	8.51	10.8	1.12	0.95	1.04	1.04

used in connection with the formulae (16). In this case the available experimental data are rather scarce, the only data being, as far as the author is aware, the heat conductivity measurements for ^{4}He by Ubbink and de Haas [17]. These measurements are compared with the theoretical data (first and second approximation) given in Fig. 9.

On the basis of the exponential-six potential field as extended by

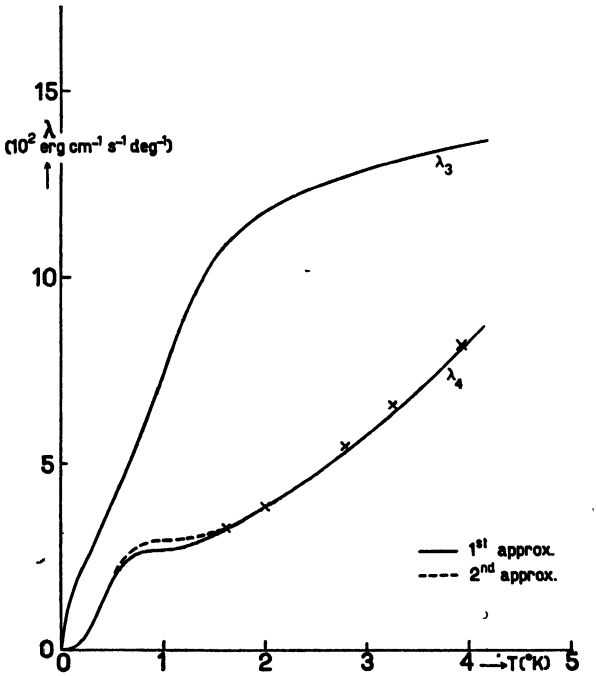

Fig. 9. Heat conductivity of ^{4}He and ^{3}He in first and second approximation, according to de Boer [8] compared with experimental data of Ubbink and de Haas [17]

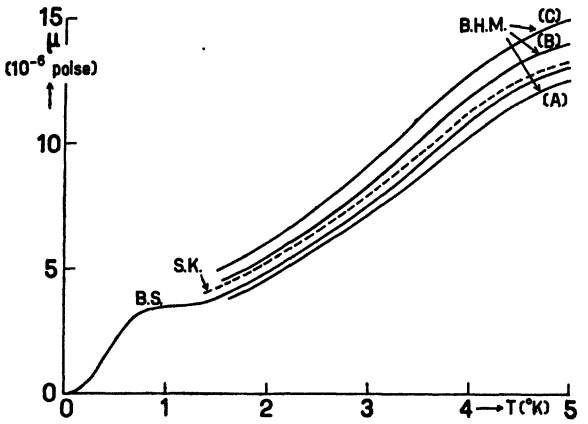

Fig. 10. Viscosity of ^{4}He in first approximation according to Buckingham, Hamilton and Massey [13] and Buckingham and Scriven [14] for the four interactions B.H.M. A, B and C and B.S. of figure 2, showing the effect of changing the value of ϵ

Buckingham, Hamilton and Massey [13], calculations have been carried out by these authors for gaseous ^{4}He using the original exponential-six potential field (23) and the extended exponential-six potential field (24) with three different values of the constants, namely, $\varepsilon = 14.69 \times 10^{-16}$ erg, 12.24×10^{-16} erg and 9.80×10^{-16} erg. For the first Enskog approximation the corresponding curves B.H.M. (A), (B) and (C) are given in Fig. 10, showing the net result of changing the interaction constant on the viscosity. A calculation of the second virial coefficient with the same potential field showed that the best fit could be obtained with the intermediate value $\varepsilon = 14.04 \times 10^{-16}$. This potential field is practically identical with the field used by de Boer and collaborators, as was shown in figure 1 in the previous section. This field was used by Buckingham and Scriven [14] to evaluate the first Enskog approximation for ^{4}He as well as for ^{3}He, and their results for ^{4}He are plotted as a function of temperature in Fig. 10. The two curves obtained by these authors nearly coincide with those of de Boer and Cohen [9], as could be expected.

6. Diffusion and Thermal Diffusion

The coefficients of diffusion for a mixture of ^{3}He and ^{4}He have been evaluated in first and second approximation by Cohen, Offerhaus and de Boer [10] using the crosssections plotted in Fig. 5 which were obtained

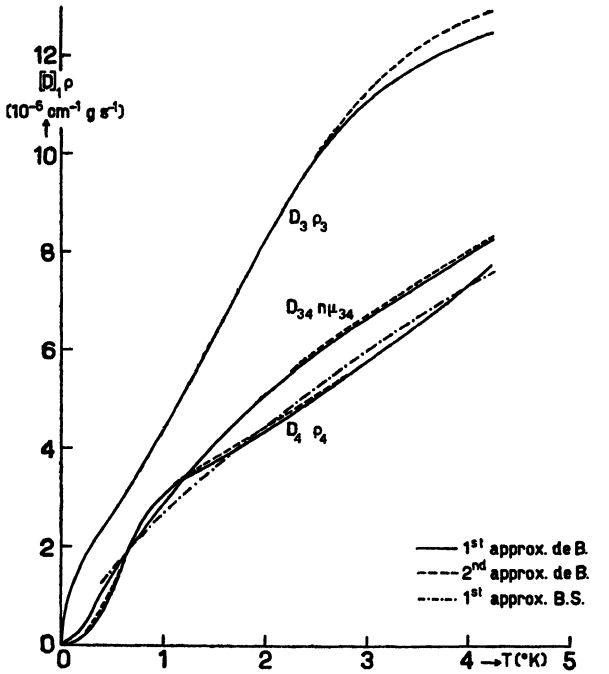

Fig. 11. Diffusion coefficients for ^{3}He and ^{4}He in first and second approximation. Curves ————: Cohen, Offerhaus and de Boer, 1st appr.; Curves – – – – –: Cohen, Offerhaus and de Boer, 2nd appr.; Curves —.—.—.—: Buckingham and Scriven, 1st appr.

on the basis of the twelve-six power interaction, eq. (22). The equations which were used in the evaluation are given in § 4, eq. (18) and (19). In Fig. 11 these data are plotted, together with the coefficients of self-diffusion for ^{3}He and ^{4}He. These coefficients were calculated on the basis of the crosssections of figure 3 with the same formulae, but taking $i = j$, in which case $\mu_{ii} = \frac{1}{2}m_i$ and $\Omega_{ii}^{(r)} = \Omega_i^{(r)}$.

From this figure one may see that the difference between the first and the second approximation is larger in this case than for the case of viscosity and heat conductivity. This could be expected from the behaviour of a gas of hard spheres discussed in § 4. All the relevant data are collected in table III.

Buckingham and Scriven have calculated the diffusion coefficient in first approximation only on the basis of their potential field, which is plotted in Fig. 1 and 2 (curve B.S.), and the results of this calculation are also plotted in Fig. 11.

TABLE III

Data for the diffusion coefficients

T °K	$[D_3]_1 n\mu_{34}$	$[D_4]_1 \rho_3$	$[D_{34}]_1 \rho_4$
	10^{-5} cm^{-1} g s^{-1}		
0	0	0	0
0.256	0.184	0.0293	0.0514
0.511	0.272	0.117	0.149
1.02	0.447	0.311	0.293
2.04	0.842	0.441	0.519
3.07	1.12	0.588	0.673
4.09	1.24	0.750	0.810

The *thermal diffusion coefficient* has also been evaluated in first approximation by Cohen, Offerhaus and de Boer on the basis of the crosssections of Fig. 3 and 5. The coefficients S_3, S_4, and C_{34} which occur in expression (20) for the thermal diffusion ratio are given in table IV together with the thermal diffusion factor $[\alpha]_1 = [\varkappa_T]_1/x_3x_4$ for three different cases. According to the usual practice in investigations on thermal diffusion, we have assumed the species i, corresponding to the *first* term in the numerator $S_ix_i - S_jx_j$ of the expression (20) for the thermal diffusion ratio K_T, to be the heavy isotope, ^{4}He, and the species j to be the light isotope, ^{3}He. For isotopic mixtures the thermal diffusion ratio then turns out to be positive in classical theory, at least when the temperature is not too low. At lower temperatures, however, according to the classical theory the thermal diffusion ratio should change sign at about 9.5°K in the case of He, being negative down to a temperature of about 4°K, where it should change sign again, being positive at still lower temperatures. It is interesting that this same behaviour, although on a different scale, occurs in the results of

TABLE IV

Data for the thermal diffusion factor $[\alpha]_1 = [\varkappa_T]_1/x_3x_4$, equation (20)

T °K	S_3	S_4	C_{34}	$[\alpha]_1 = [\varkappa_T]_1/x_3x_4$		
				$x_3 = 0$ $x_4 = 1$	$x_3 = \frac{1}{2}$ $x_4 = \frac{1}{2}$	$x_3 = 1$ $x_4 = 0$
0	—1.55	∞	1.20	+0.21	+0.39	+2.11
0.256	—1.38	2.00	0.690	—0.28	—0.43	—0.93
0.511	—1.14	1.05	0.865	—0.10	—0.13	—0.20
1.02	—1.10	1.52	1.04	+0.03	+0.04	+0.06
2.04	—1.04	1.42	1.14	+0.10	+0.13	+0.18
3.07	—0.93	1.17	1.14	+0.10	+0.12	+0.14
4.09	—0.85	0.89	1.14	+0.09	+0.10	+0.11

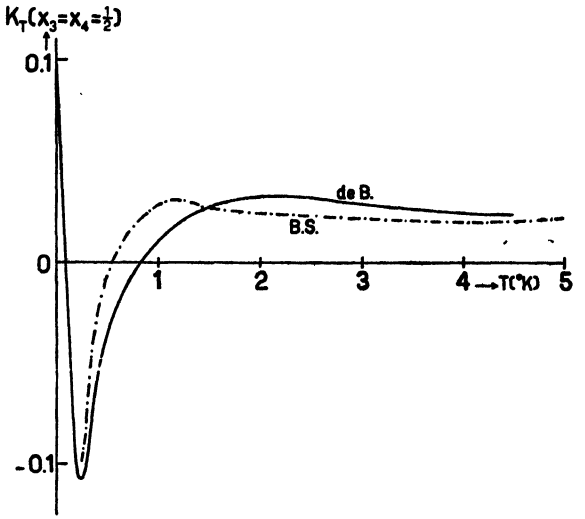

Fig. 12. Thermal diffusion ratio $[\kappa_T]_1$ in first approximation for ^{3}He and ^{4}He mixtures:
curve ——: Cohen, Offerhaus and de Boer [10]; curve —.—.—.—: Buckingham and Scriven [14]

the quantum mechanical calculations. The results obtained with their respective potential fields of the calculations of Cohen, Offerhaus and de Boer have been plotted in Figure 12, together with those of Buckingham and Scriven. These results are rather similar, although they differ in some details, but is should be remembered that the thermal diffusion ratio is, as is well known, extremely sensitive to small differences in the potential field. The two curves show that in the quantum mechanical calculations as well the thermal diffusion factor is positive at high temperatures, indicating that here the ^{4}He atoms diffuse down the temperature gradient and concentrate on the low temperature side. For the quantum mechanical calculations there is also a change of sign at 0.8°K according to de Boer and coll. and at 0.55°K according to Buckingham and Scriven. According to the first there should be a second change of sign at 0.07°K, below which temperature the thermal diffusion ratio becomes positive again. Both the positive as well as the negative values are very much larger in absolute value than in the classical theory. It is hoped that measurements of this thermal diffusion ratio will make it possible to test these calculations with the experimental data.

REFERENCES

[1] E. A. Uehling and G. E. Uhlenbeck, Phys. Rev. **43**, 552 (1933).
E. A. Uehling, Phys. Rev. **46**, 917 (1934).
[2] H. Mori and S. Ono, Progr. Theor. Phys. **8**, 327 (1952); J. G. Kirkwood, J. Chem. Phys. **15**, 72 (1947); J. Ross and J. G. Kirkwood, J. Chem. Phys. **22**, 1094 (1954).
[3] S. Chapman and T. G. Cowling, The mathem. Theory of Non-Uniform Gases.
[4] J. O. Hirschfelder, C. F. Curtiss and R. Byron Bird, Molecular theory of Gases and Liquids.
[5] J. C. Slater and J. G. Kirkwood, Phys. Rev. **37**, 682 (1931).
[6] H. Margenau, Phys. Rev. **38**, 747 (1931); see also for further references: H. Margenau, Rev. Mod. Phys. **11**, 23 (1939).
[7] H. Margenau, Phys. Rev. **90**, 1021 (1953).
[8] J. de Boer and A. Michels, Physica **6**, 409 (1939); J. de Boer, Dissertation Amsterdam; J. de Boer, Physica **10**, 348 (1943).
[9] J. de Boer and E. G. D. Cohen, Physica **17**, 993 (1951).
[10] E. G. D. Cohen, M. J. Offerhaus and J. de Boer, Physica **20**, 501 (1954).
[11] J. de Boer, Reports on Progress in Physics **12**, 305 (1949).
[12] H. S. W. Massey and R. A. Buckingham, Proc. Roy. Soc. A. **168**, 378 (1938); **169**, 205 (1939).
[13] R. A. Buckingham, J. Hamilton and H. S. W. Massey, Proc. Roy. Soc. A **179**, 103 (1941).
[14] R. A. Buckingham and R. A. Scriven, Proc. Phys. Soc. London, B, **65**, 376 (1952).
[15] A. van Itterbeek, F. W. Schapink, G. J. v. d. Berg and H. J. M. van Beek, Physica **19**, 1158 (1953).
[16] E. W. Becker, R. Misenta and F. Schmeissner, Phys. Rev. **93**, 244 (1954).
[17] J. B. Ubbink and W. J. de Haas, Physica **10**, 465 (1943).
[18] J. de Boer and R. Byron Bird, Physica **20**, 185 (1954).

AUTHOR INDEX

SUBJECT INDEX